





### รายงานวิจัยฉบับสมบูรณ์

ผลของการจำกัดปริมาณพลังงานอาหารและการออกกำลังกาย ต่อการทำงานของสมองหนูที่มีภาวะอ้วนร่วมกับการตัดรังไข่

The effects of calorie restriction and exercise training on brain function in ovariectomized obese rats

โดย

ผู้ช่วยศาสตราจารย์ ดร. วาสนา ปรัชญาสกุล และคณะ

เมษายน 2561



### รายงานวิจัยฉบับสมบูรณ์

### โครงการ ผลของการจำกัดปริมาณพลังงานอาหารและการออกกำลังกายต่อ การทำงานของสมองหนูที่มีภาวะอ้วนร่วมกับการตัดรังไข่

The effects of calorie restriction and exercise training on brain function in ovariectomized obese rats

ผู้ช่วยศาสตราจารย์ ดร. วาสนา ปรัชญาสกุล ศูนย์วิจัยและฝึกอบรมสาขาโรคทางไฟฟ้าของหัวใจ คณะแพทยศาสตร์ มหาวิทยาลัยเชียงใหม่

สนับสนุนโดยสำนักงานคณะกรรมการการอุดมศึกษาและสำนักงาน กองทุนสนับสนุนการวิจัย (ความเห็นในรายงานนี้เป็นของผู้วิจัย สกอ. และ สกว. ไม่จำเป็นต้องเห็นด้วยเสมอไป)

### กิตติกรรมประกาศ

I would like to thank with my deepest sense of gratitude to my mentor, Professor Dr. Siriporn Chattipakorn, who afforded the opportunity of my research and provided the continuous useful guidance, understanding, great encouragement and the technical support throughout the period of my research work. I am also deeply grateful to Professor Dr. Nipon Chattipakorn, for his invaluable suggestions and comments that made my manuscript better. My special thanks to Ms. Duangkamol Mantora, Ms. Wanitchaya Minta, Ms. Wissuta Sutham and Dr. Siripong Palee, for helping and cooperation in this experiment.

I would like to acknowledge the Thailand Research Fund MRG5980198 (WP), TRG5980020 (SP) and RTA6080003 (SC), a NSTDA Research Chair Grant from the National Science and Technology Development Agency (NC) and Chiang Mai University Excellent Center Award (NC) for financial support. I also thank Cardic Electrophysiology Research and Training Center, Faculty of Medicine, Chiang Mai University for laboratory facilities. Unforgettably, special thanks to all my friends at Cardiac Electrophysiology Research and Training Center and Department of Physiology for their help, encouragement, friendship and entertainment during my study.

Finally, I wish to express my profound gratitude and appreciation to my family for their love, generous standing and loving support throughout my life.

Wasana Pratchayasakul

### บทคัดย่อ

รหัสโครงการ: MRG5980198

ชื่อโครงการ: ผลของการจำกัดปริมาณพลังงานอาหารและการออกกำลังกายต่อการทำงานของ สมองหนูที่มีภาวะอ้วนร่วมกับการตัดรังไข่

### ชื่อนักวิจัย :

ผศ.ดร. วาสนา ปรัชญาสกุล ศูนย์วิจัยและฝึกอบรมสาขาโรคทางไฟฟ้าของหัวใจ คณะแพทยศาสตร์ มหาวิทยาลัยเชียงใหม่

อีเมล์: wpratchayasakul@gmail.com ระยะเวลาโครงการ: 24 เดือน

บทคัดย่อ:

วัตถุประสงค์/สมมุติฐาน: การศึกษาที่ผ่านมาพบว่า ภาวะอ้วนจะทำให้เกิดภาวะดื้อต่ออินซูลินและเกิด พยาธิสภาพในสมองที่รุนแรงขึ้นในกรณีที่มีการตัดรังไข่ อย่างไรก็ตามผลของภาวะอ้วนตามด้วยการ ขาดฮฮร์โมนเอสโตรเจนต่อการทำงานของสมองยังไม่มีการศึกษามาก่อน นอกเหนือไปจากนั้นการ ปรับเปลี่ยนพฤติกรรมโดยการปรับเปลี่ยนการรับประทานอาหารและการออกกำลังกายจะมีประโยชน์ต่อ อย่างไรก็ตามผลร่วมของการจำกัดอาหาร การลดความรุนแรงของโรคเบาหวานและโรคอัลไซล์เมอร์ และการออกกำลังกายต่อการทำงานของสมองในหนูอัวนที่มีการตัดรังไข่ยังไม่มีการศึกษามาก่อน ดังนั้น งานวิจัยนี้จึงมีสมมุติฐานที่ว่า 1) การขาดฮอร์โมนเอสโตรเจนจะกระตุ้นการสูญเสียภาวะเมตาโบลิซึม การเกิดพยาธิสภาพของสมอง การสูญเสียความจำและการเรียนรู้ (ทั้งชนิดที่ขึ้นอยู่กับสมองส่วนฮิบโป แคมพัสและชนิดที่ไม่ขึ้นอยู่กับสมองส่วนฮิบโปแคมพัส) ให้รุนแรงขึ้นในหนูอ้วนเพศเมียที่มีภาวะดื้อต่อ อินซูลินโดยการเหนี่ยวนำด้วยอาหารไขมันสูง 2) การจำกัดอาหารและการออกกำลังกายช่วยลดการ สูญเสียภาวะเมตาโบลิซึม การเกิดพยาธิสภาพของสมองในหนูอัวนที่มีการตัดรังไข่ วิธีการทดลอง: ในการศึกษาที่ 1 หนูเพศเมียจำนวน 32 ตัว จะถูกแบ่งให้ได้รับอาหารปกติ (ND, n=16) และอาหารไขมันสูง (HFD, n=16) เป็นระยะเวลา 12 สัปดาห์ ในสัปดาห์ที่ 13 หนูในแต่ละกลุ่มจะถูกแบ่ง ออกเป็นกลุ่มที่ผ่าตัดหลอกและกลุ่มผ่าตัดรังไข่ (n=8/กลุ่ม) ในสัปดาห์ที่ 20 หนูทุกตัวจะได้รับการ ทดสอบความความจำและการเรียนรู้ทั้งชนิดที่ขึ้นอยู่กับสมองส่วนฮิบโปแคมพัสและชนิดที่ไม่ขึ้นอยู่กับ สมองส่วนฮิบโปแคมพัส โดยวิธี morris water maze (MWM) และ novel objective recognition (NOR) ตามลำดับ หลังจากนั้นตัวอย่างสมองจะถูกเก็บเพื่อนำไปศึกษาหน้าที่การทำงานของสมอง ในการศึกษาที่ 2 หนูเพศเมียจำนวน 54 ตัว จะถูกแบ่งให้ได้รับอาหารปกติ (ND, n=9) และอาหารไขมัน สูง (HFD, n=48) เป็นระยะเวลา 12 สัปดาห์ หลังจากนั้น หนูที่ได้รับอาหารปกติจะถูกผ่าตัดหลอก หนู ที่ได้รับอาหารไขมันสูงจะถูกแบ่งออกเป็นกลุ่มที่ผ่าตัดหลอกและกลุ่มผ่าตัดรังไข่ หลังจากนั้น 4 สัปดาห์ หนูที่ได้รับอาหารไขมันสูงร่วมกับการผ่าตัดหลอก จะถูกแบ่งออกให้ได้รับตัวทำละลายยา (HFSV), การ จำกัดอาหาร (HFSCR), การออกกำลังกาย (HFSEx), การกำจัดอาหารร่วมกับการออกกำลังกาย (HFSCB) (n=6/กลุ่ม) เป็นระยะเวลา 6 สัปดาห์ หนูที่ได้รับอาหารไขมันสูงร่วมกับการตัดรังไข่ จะถูก แบ่งออกให้ได้รับตัวทำละลายยา (HFOV), การจำกัดอาหาร (HFOCR), การออกกำลังกาย (HFOEx), การกำจัดอาหารร่วมกับการออกกำลังกาย (HFOCB) และการได้รับเอสโตรเจน (HFOE2) (n=6/กลุ่ม) เป็นระยะเวลา 6 สัปดาห์ หลังจากนั้นตัวอย่างสมองจะถูกเก็บเพื่อนำไปศึกษาหน้าที่การทำงานของ สมอง

ผลการทดลอง: เราพบว่าภาวะดื้อต่ออินซูลินโดยการเหนี่ยวนำโดยภาวะอัวนจะปรากฏในกลุ่ม ที่ได้รับ อาหารไขมันสูงร่วมกับการผ่าตัดหลอก (HFS), กลุ่มที่ได้รับอาหารปกติร่วมกับการตัดรังไข่ (NDO), และ กลุ่มที่ได้รับอาหารไขมันสูงร่วมกับการตัดรังไข่ (HFO) การสูญเสียความความจำและการเรียนรู้ชนิด ที่ขึ้นอยู่กับสมองส่วนฮิบโปแคมพัส การเกิดภาวะอนุมูลอิสระ การเกิดการตายของเซลล์ การสูญเสีย การปรับเปลี่ยนที่จุดประสานประสาท การลดลงของเอสโตรเจน จะถูกตรวจพบในสมองส่วนฮิบโปแคมพัส ของหนูกลุ่ม HFS, NDO, และ HFO อย่างไรก็ตามความความจำและการเรียนรู้ชนิดที่ไม่ ขึ้นอยู่กับสมองส่วนฮิบโปแคมพัส ระดับเอสโตรเจน การเกิดภาวะอนุมูลอิสระ การเกิดการตายของ เซลล์ในสมองส่วนคอร์เท็กซ์ ไม่พบความแตกต่างกันทางสถิติระหว่างกลุ่ม นอกเหนือไปจากนั้น การจำกัดอาหาร การออกกำลังกาย และการร่วมระหว่างการจำกัดอาหารและการออกกำลังกายจะให้ผลดีกว่า การจำกัดอาหารในการช่วยรักษาหน้าที่การทำงานของอินซูลินในสมอง การร่วมระหว่างการจำกัด อาหารและการออกกำลังกายจะให้ผลดีกี่สุดในแง่ของการลดการตายของเซลล์ในสมองเมื่อเทียบกับการ จำกัดอาหารหรือการออกกำลังกายจะให้ผลดีที่สุดในแง่ของการลดการตายของเซลล์ในสมองเมื่อเทียบกับการ จำกัดอาหารหรือการออกกำลังกายจะให้ผลดีที่สุดในแง่ของการลดการตายของเซลล์ในสมองเมื่อเทียบกับการ จำกัดอาหารหรือการออกกำลังกายเพียงอย่างเดียว

สรุปผลการทดลอง: การศึกษานี้สามารถสรุปได้ว่าการขาดเอสโตรเจนและความอ้วนจะทำให้สูญเสีย ความความจำและการเรียนรู้ชนิดที่ขึ้นอยู่กับสมองส่วนฮิบโปแคมพัส โดยกลไกผ่านทางการสูญเสียการ ทำงานในสมองส่วนฮิบโปแคมพัส โดยการขาดเอสโตรเจนจะไม่กระตุ้นให้การให้การสูญเสียการทำงาน นี้รุนแรงมากขึ้นในกรณีที่มีภาวะอ้วน นอกเหนือไปจากนั้น การออกกำลังกายจะให้ผลดีกว่าการ จำกัดอาหารในการช่วยรักษาหน้าที่การทำงานของอินซูลินในสมอง การร่วมระหว่างการจำกัดอาหาร และการออกกำลังกายจะให้ผลดีที่สุดในแง่ของการลดการตายของเซลล์ในสมองเมื่อเทียบกับการจำกัด อาหารหรือการออกกำลังกายเพียงอย่างเดียว ดังนั้นการร่วมระหว่างการจำกัดอาหารและการออกกำลัง กายอาจจะเป็นแนวทางที่ดีในการช่วยรักษาและป้องกันอันตรายของสมองจากภาวะดี้อต่ออินซูลินโดย การเหนี่ยวนำโดยอาหารไขมันสูงทั้งที่ร่วมกับการขาดหรือไม่ขาดฮฮร์โมนเอสโตรเจน

คำหลัก: อาหารไขมันสูง, การผ่าตัดรั้งไข่, การเรียนรู้จดจำ, การจำกัดปริมาณพลังงานอาหาร, การออก กำลังกาย

#### **Abstract**

Project Code: MRG5980198

Project Title: The effects of calorie restriction and exercise training on brain function in

ovariectomized obese rats

#### Investigator:

Asst. Prof. Dr. Wasana Pratcahayasakul, PhD.

Cardiac Electrophysiology Research and Training center

Faculty of Medicine Chiang Mai University

E-mail Address: wpratchayasakul@gmail.com

Project Period: 24 months

#### Abstract:

Aim/Hypothesis: Our previous study demonstrated that obesity aggravated peripheral insulin resistance and brain dysfunction in the ovariectomized condition. However, the effect of obesity followed by estrogen deprivation on brain function has not been investigated. Furthermore, lifestyle modification, including dietary intervention or exercise training, has beneficial effects on the improving of diabetes and Alzheimer's disease. However, the effects of combined calorie restriction with exercise training on metabolic and brain functions in ovariectomized-obese rats have not been investigated. Therefore, the hypotheses for this study are that 1) estrogen deprivation exaggerates metabolic impairment, brain pathology and impairment of learning and memory (both hippocampal-dependent and hippocampal-independent) in HFD-induced obeseinsulin resistant female rats, 2) the calorie restriction and exercise training attenuate metabolic impairment and brain pathology in ovariectomized-obese rats.

Methods: In protocol I, thirty-two female rats were fed with either a normal diet (ND, n=16) or a high-fat diet (HFD, n=16) for 12 weeks. At week 13, rats in each group were subdivided into sham and ovariectomized subgroups (n=8/subgroup). At week 20, all rats were tested for hippocampal-dependent and hippocampal-independent memory by using morris water maze (MWM) and novel objective recognition (NOR) tests, respectively. After that, the brain was removed for determining brain function. In protocol II, fifty-four female rats were fed with either a normal diet (ND, n=9) or a high-fat diet (HFD, n=48) for 12 weeks. After that, ND rats were assigned to sham-operated (Sham), HF rats were randomly assigned to either Sham or ovariectomized (OVX) groups. Four weeks after surgery period, HF-fed rats with sham operation (HFS) were subdivided to received either vehicle (HFSV), calorie restriction (HFSCR), exercise training (HFSEx), and combined calorie restriction with exercise training (HFSCB) (n=6 /groups) for 6 weeks. HF-fed rats with ovariectomy were subdivided to received either vehicle (HFOV), calorie restriction (HFOCR), exercise training (HFOEx), combined calorie restriction with exercise training (HFOCB) and estrogen therapy (HFOE2) (n=6 /groups) for 6 weeks. After that, brain was removed for determining brain function.

Results: We found that the obese- insulin resistant condition occurred in sham-HFD-fed rats (HFS), ovariectomized-ND-fed rats (NDO), and ovariectomized-HFD-fed rats (HFO). Increased hippocampal ROS production, increased hippocampal apoptosis, increased hippocampal synaptic dysfunction, decreased hippocampal estrogen level and impaired hippocampal-dependent memory were observed in HFS, NDO, and HFO rats. However, the hippocampal-independent memory, cortical estrogen levels, cortical ROS production, and cortical apoptosis showed no significant difference between groups. Furthermore, calorie restriction, exercise training and combined treatment equally improved metabolic function. Moreover, exercise training had better efficacy than calorie restriction for preserved insulin receptor function. Interestingly, combined treatment had a greater efficacy in reducing brain apoptosis than single treatment.

Conclusions: These findings suggested that estrogen deprivation and obesity exclusively impaired hippocampal-dependent memory, possibly via increased hippocampal dysfunction. Nonetheless, estrogen deprivation did not aggravate these deleterious effects under conditions of obesity. Furthermore, exercise training had better efficacy than calorie restriction for preserved insulin receptor function. Interestingly, combined treatment had a greater efficacy in reducing brain apoptosis than single treatment. Therefore, combined treatment may be the best therapeutic approach for neuroprotection in HFD-induced obese-insulin resistance with or without estrogen deprivation.

Keywords: High-fat diet, Ovariectomy, Cognition, Calorie restriction, Exercise training

### เนื้อหางานวิจัย (Executive summary)

### บทน้ำ (Introduction)

Previous studies demonstrated that the obese-insulin resistant condition can lead to the development of pathophysiological conditions in several organs, including brain. <sup>1-4</sup> In addition to the work of other researchers we have also reported that consumption of a high-fat diet (HFD) over 12-weeks in both male and female rats led, not only to obesity and peripheral insulin resistance, but also brain insulin resistance, <sup>5, 6</sup> brain mitochondrial dysfunction, increased brain oxidative stress and impaired learning and memory. <sup>6, 7</sup> Interestingly, our recent study showed that obesity aggravated peripheral insulin resistance, brain insulin resistance, brain mitochondrial dysfunction, brain oxidative stress and hippocampal synaptic dysfunction and also impaired learning and memory in the estrogen-deprived condition. <sup>8</sup> However, the effect of estrogen deprivation after obesity on metabolic changes and brain functions has not been thoroughly investigated.

The process of learning and memory can be divided into explicit memory (a hippocampal-dependent process) and implicit memory (a hippocampal-independent process). <sup>9, 10</sup> In an animal study, hippocampal-dependent memory can be assessed using the Morris water maze (MWM) test, <sup>11</sup> and hippocampal-independent memory can be assessed using the novel object recognition (NOR) test. <sup>12</sup> Previous studies demonstrated that both HFD-induced obese-insulin resistance and estrogen deprivation caused the impairment of hippocampal-dependent memory, as indicated by increased time to reach the platform and decreased time spent in the target quadrant in the MWM test. <sup>7, 13</sup> However, the impairment of hippocampal-independent memory in the case of HFD-induced obese-insulin resistance or estrogen-deprivation is still unclear. <sup>14-16</sup> In addition, the effect of estrogen deprivation after HFD-induction of an obese-insulin resistant condition on hippocampal-dependent and hippocampal-independent memory and the underlying mechanisms associated with these have not been investigated.

Lifestyle modification, including dietary intervention or exercise training, has beneficial effects on the improving of diabetes and Alzheimer's disease. Several studies found that calorie restriction (CR) had a beneficial impact on the metabolic effects such as reduced visceral adipose tissue deposit, reduced hepatic glucose levels in aging obese-insulin resistant rats, increased IRS-1 and Akt-serine phosphorylation in skeletal muscle, reduced ROS production and oxidative damage of mitochondrial rat liver.

insulin stimulation of IR, IRS, and Akt activity in the skeletal muscle of ovariectomized model.  $^{21}$ Furthermore, the CR not only exerted the effects on metabolic control, but also affected brain function. <sup>22</sup> Previously study demonstrated that CR increased an endogenous apoptosis inhibitor, decreased the rate of mitochondrial H<sub>2</sub>O<sub>2</sub> production via reduced ROS production <sup>24</sup> and prevented aged related deficit synaptic LTP.  $^{25}$ Epidemiological studies have shown that exercise was an effective method to prevent and improve obesity and diabetes. <sup>26</sup> Several studies found that the increased in mitochondria biogenesis 27, 28 and insulin sensitivity were observed following exercise training.  $^{\rm 29,\ 30}$ In addition, exercise training could reduce the white adipose tissue size, which resulted in the attenuation of adipokines and oxidative stress. 31 Furthermore, exercise training also plays an important role in synaptic plasticity. Previous studies found that exercise training increased LTP, dendritic spine density, brain-derived neurotrophic factor (BDNF) level, insulin-like growth factor-1 (IGF-1), angiogenesis and neurotransmitter releasing such as serotonin, noradrenalin and acetylcholine. 32-38 Recently, 8weeks exercise training enhanced synaptic plasticity markers such as BDNF, p38MAPK and pp38MAPK proteins in hippocampus of obese rats. <sup>39</sup> However, the effects of combined calorie restriction with exercise training on metabolic and brain functions in ovariectomized-obese rats have not been investigated. Therefore, the hypotheses for this study are that 1) estrogen deprivation exaggerates metabolic impairment, hippocampal ROS production, hippocampal synaptic dysfunction and impairment of learning and memory (both hippocampal-dependent and hippocampal-independent) in HFD-induced obese-insulin resistant female rats, 2) the calorie restriction and exercise training attenuate metabolic impairment and brain pathology in ovariectomized-obese rats.

### วิธีการทดลอง (Methods)

### Animal models and experimental protocols

# Aim 1: To investigate the effect of estrogen deprivation on metabolic changes and brain function in obese insulin-resistant condition

All experimental protocols were approved by the Faculty of Medicine, Chiang Mai University Institutional Animal Care and Use Committee, in compliance with NIH guidelines. Thirty-two female Wistar rats weighing about 200-220 g (about 6 weeks old) were obtained from the National Animal Center, Salaya Campus, Mahidol University, Thailand. All animals were housed (n=2/cage) in a temperature-controlled room and maintained at a light-dark cycle of 12:12 h (lights on at 6 a.m.). One week after arrival, female rats were randomly assigned to either be fed on a normal diet (ND, n=16) or a high-fat diet (HFD, n=16) for a total of 20 weeks. The normal diet was a standard laboratory chow (Mouse Feed Food No. 082, C.P. Company, Bangkok, Thailand), which had an energy content of 4.02 kcal/g, 19.77% of total energy (%E) of the food being from fat. The high-fat diet had an energy content of 5.35 kcal/g and contained fat mostly from lard (59.28% E). All animals were given ad libitum access to food and water. The daily amount of food intake and weekly body weight were monitored. After 13 weeks of either ND or HFD consumption, rats in each diet group were divided into two subgroups: sham-operated (S) and bilateral ovariectomized (O) subgroups. All animals were finally divided into four subgroups, including sham-ND-fed rats (NDS), ovariectomized-ND-fed rats (NDO), sham-HFD-fed rats (HFS) and ovariectomized-HFD-fed rats (HFO). All animals were continuously fed on either a ND or HFD for 7 weeks. At week 14 and 20 all animals were tested with several behavioral tests, including the locomotive activity with the open-field test (OFT), the hippocampal-independent learning and memory with the novel object recognition test (NOR), and the hippocampal-dependent learning and memory with the Morris water maze test (MWM). Blood samples were collected from each animal at week 13 and 21 to determine the metabolic parameters. At the end of the experiment protocol (21 weeks), animals were decapitated and the brains removed to enable the hippocampal synaptic plasticity to be investigated by electrical induced long-term potentiation (LTP), brain insulin receptor function (insulin-induced long term depression, LTD), hippocampal and cortical ROS production, hippocampal and cortical apoptotic levels and hippocampal and cortical estrogen levels.

# Aim 2: To examine the effects of combined calorie restriction and exercise training on the metabolic changes and brain function in ovariectomized-obese rats

All experiments were conducted with an approved protocol from the Faculty of Medicine, Chiang Mai University Institutional Animal Care and Use Committee, in compliance with NIH quidelines. Female (n=54) Wistar rats were obtained from the National Laboratory Animal Center, Salaya Campus, Mahidol University, Thailand. Animals were individually housed in a temperature-controlled environment with a 12:12 hour light-dark cycle. After one week, female rats were randomly assigned to feed either normal-diet or high-fat diet for 12 weeks. The normal-diet (ND) group was given a standard laboratory chow, which has energy content of 4.02 kcal/q, and 19.77% of total energy (%E) of the food is from fat (Mouse Feed Food No. 082, C.P. Company, Bangkok, Thailand). The high-fat (HF) group was consumed high-fat diet, which has energy content of 5.35 kcal/g and contains fat mostly from lard (57.60% E). Twelve weeks after the dietary period, ND rats were assigned to sham-operated (Sham), HF rats were randomly assigned to either Sham or ovariectomized (OVX) groups. Four weeks after surgery period, HF-fed rats with sham operation (HFS) were subdivided to received either vehicle (HFSV), calorie restriction (HFSCR), exercise training (HFSEx), and combined calorie restriction with exercise training (HFSCB) (n=6 /groups) for 6 weeks. HF-fed rats with ovariectomy were subdivided to received either vehicle (HFOV), calorie restriction (HFOCR), exercise training (HFOEx), combined calorie restriction with exercise training (HFOCB) and estrogen therapy (HFOE2) (n=6 /groups) for 6 weeks. At the end of experimental period, blood samples were collected from the tails after fasting for glucose measurement and oral glucose tolerance test (OGTT). After that, animals were deeply anesthetized and decapitated. For each rat, the brain was rapidly removed for determining brain apoptosis, brain insulin receptor function and brain inflammation.

### Ovariectomized procedure

Ovariectomy was performed following our previous study guidelines. Briefly, female rats were anesthetized with 2-3% isoflurane and oxygen support. The ovariectomized groups received bilateral flank incisions, the ovaries were removed and the incisions were closed.

#### **Determination of metabolic parameters**

Fasting plasma glucose, HDL, LDL, cholesterol and triglyceride levels were determined using commercially available kits (ERBA diagnostic, Mannheim, Germany). The fasting plasma insulin levels were investigated using ELISA kits (LINCO Research, Missouri, USA). Serum

estrogen levels were determined using an EIA kit (Cayman chemical, Ann Arbor, Michigan, USA).

### Calorie restriction (CR) diet

This CR diet will be provided 60% energy high fat caloric intake of mean of basal freely available (ad lib) in the form of normal diet chow. By 1 g of high fat diet is 5.35 kcal and normal diet is 4.02 kcal and feeding for 6 weeks.

### Exercise training protocol

The exercise training, in terms of endurance training, will be performed on a motor-driven rodent treadmill five days/week over a four-week period. The intensity progressively will be increased from 10 min once a day at 22 m/min, 5% upgrade, up to 15 min twice a day at 25 m/min, 5% upgrade, after the first week of practicing. 41

#### Determination of peripheral insulin resistance

Insulin resistance was evaluated by the Homeostasis Model Assessment (HOMA) index and the total area under the curve of the oral glucose tolerance test (OGTT) as described in our previous study. <sup>6</sup>

#### Determination of serum malondialdehyde (MDA) levels

The MDA level was determined using a high performance liquid chromatography method following a previous study protocol.  $^{43}$ 

#### Determination of cell apoptosis by TUNEL assay kit

The brains weres fixed with 4% paraformaldehyde, cryoprotect in 30% sucrose in PBS at 4 °C, and then were frozen in isopentane and dry ice, and store at -80°C. Then brains were cut using cryosection (Leica CM1950, Leica Biosystem Nussloch GmbH, Nussloch, Germany) at 10 µm. Sections were subjected to label immunofluorescence. The brain sections were conducted following commercial protocol of TdT In Situ Apoptosis Detection Kit (TACS, Trevigen, R&D Systems, Minneapolis, MN, USA). The images were taken from confocal microscopy (Olympus flouview FV3000) and apoptotic cell were measured by Imaris software 7.0 (Bitplane, Oxford instrument company, AG, Zurich, Switzerland).

# Extracellular recordings of hippocampal slices for insulin-induced long term depression (LTD) and electrical-induced long term potentiation (LTP)

The brain slices for extracellular recordings of insulin-induced LTD and electrical-induced LTP were prepared following the protocol described in our previous study. <sup>8, 44</sup> In the LTD protocol, hippocampal slices were perfused with aCSF for ten minutes as a baseline measure. After that, the insulin-induced LTD condition was evaluated by perfusion with aCSF plus 500 nM insulin (Humulin R, Eli Lilly, Giessen, Germany) for an additional ten minutes and

then the slices were perfused with aCSF for 50 minutes further. In the LTP protocol, LTP was induced by delivering high-frequency stimulation (HFS: 4 trains at 100 Hz; 0.5 s duration; 20 s interval). Experiments were performed for at least 50 minutes after HFS.

# Protein preparation for hippocampal and cortical reactive oxygen species (ROS) production measurement

The details of protein preparation for hippocampal and cortical ROS have been described in a previous study. <sup>45</sup> Briefly, the hippocampus and cortex were rapidly removed and transferred into 1 ml of ice-cold MSE solution. Then, the supernatant was collected for protein concentration measurement by the bicinchoninic acid assay (BCA assay).

#### Hippocampal and cortical reactive oxygen species (ROS) assay

The details of ROS measurement again have been previously described. <sup>46</sup> Briefly, dichloro-hydrofluoresceindiacetate (DCFH-DA) dye was used to determine hippocampal and cortical ROS production. Fluorescence was used to determine an excitation wavelength of  $\lambda$ 485 nm and emission wavelength of  $\lambda$ 530 nm by a microplate reader (Bio-tek Instrument, Inc. Winooski, Vermont USA). Hippocampal and cortical ROS production were calculated as a percentage change from the following equation: (ROS with  $H_2O_2 - ROS)/ROS \times 100$ 

### **Immunoblotting**

The brain homogenates for immunoblotting were prepared as described in our previous study. <sup>6</sup> Electrophoresis and immunoblotting of Bax, Bcl-2 and pNFkB were carried out with rabbit antibodies for the Bax (1:200, Santa Cruz Biotechnology, CA, USA), Bcl-2 (1:1000, Abcam, MA, USA) and pNFkB (1:1000, Abcam, MA, USA), respectively. All blots were incubated with a horseradish peroxidase conjugated anti-rabbit secondary antibody (1:2000, Cell Signaling Technology, MA, USA). The membranes were exposed to ECL Western blotting substrate, and densitometric analysis was carried out using ChemiDoc Touch Imaging system (Bio-Rad Laboratories, CA, USA).

#### Morris water maze test (MWM)

The assessment of hippocampal-dependent memory was performed by using MWM, as described in previous studies. <sup>11</sup> Before the MWM test, the open-field test (OFT) was used to screen locomotive activity by counting the distance and speed in the area of the open-field during the test. <sup>47, 48</sup> After that, the rats were assessed by the MWM with two different tests, acquisition test (hidden platform) and probe trial test (removal of the platform from the water pool). After testing was completed, times taken to reach the platform, times spent in the target quadrant, and swim speeds were calculated using Smart 3.0 software (Planlab, Harvard Apparatus, Barcelona, Spain).

#### Novel object recognition test (NOR)

The assessment of hippocampal-independent memory was performed using the NOR, as described in previous studies. <sup>49, 50</sup> Briefly, time of exploration was calculated as percentage exploration on the familiarization phase. During the test phase, the animals were allowed 10 minutes for exploration, and the time spent exploring the novel object was calculated and presented as a percentage of index preference. All data were analyzed using Smart 3.0 software (Planlab, Harvard Apparatus, Barcelona, Spain).

#### Statistical analysis

The data for each experiment was presented as mean ± SEM. All statistical analysis was performed using the program SPSS (version 17; SPSS, Chicago, III., USA). For all comparisons, the significant differences between the means were calculated using a three-way ANOVA followed by post-hoc LSD. A two-way ANOVA with repeated measurements was used to compare the training trials of the MWM test. P-value < 0.05 was considered as significant.

### ผลการทดลอง (Results)

### Effects of estrogen deprivation and HFD-induced obese-insulin resistance on metabolic function.

Estrogen-deprivation was confirmed by determining uterine weight and serum estrogen level. The ovariectomized rats had decreased uterine weight and serum estrogen level when compared with those of sham-operated rats. Moreover, we identified metabolic dysfunction in ovariectomized-ND-fed rats (NDO), sham-HFD-fed rats (HFS) and ovariectomized-HFD-fed rats (HFO), as indicated by increased the body weight, visceral fat weight, cholesterol and LDL level, plasma insulin level, HOMA index and total area under the glucose curve (TAUCg) when compared with sham-ND-fed rats (NDS). Interestingly, the most severe metabolic dysfunction, as represented by the highest level of obesity, dyslipidemia, insulin resistance and hyperglycemia, was observed in HFO rats (p<0.05; Table 1). These findings suggest that estrogen deprivation aggravates the severity of the metabolic dysfunction in the obese-insulin resistant condition.

# Effect of estrogen deprivation and HFD-induced obese-insulin resistance on hippocampal-dependent memory and hippocampal-independent memory.

In this study, the hippocampal-dependent and hippocampal-independent learning and memory were determined using the Morris water maze test (MWM) and novel object recognition test (NOR), respectively. During the acquisition test of MWM, both time and distance to the platform of the NDO, HFS and HFO rats were significantly increased, when compared with that of NDS rats (Fig. 1A, B). During the probe test of MWM, both time and distance in the target quadrant of the NDO, HFS and HFO rats were significantly decreased, when compared with that of NDS rats (Fig. 1C, D). These results indicate that estrogen deprivation alone, HFDinduced obese-insulin resistance alone, and a combination of the conditions has equal impact on the impairment of hippocampal-dependent learning and memory. In the NOR test, the percentage exploration time as well as index preference were not significantly different among four groups (Fig. 2A, B). This result suggests that estrogen deprivation alone, HFD-induced obese-insulin resistance alone, and a combination of these conditions does not impair hippocampal-independent learning and memory. All of these findings suggest that both estrogen deprivation alone and HFD-induced obese-insulin resistance alone impair only hippocampal-dependent memory. However, estrogen deprivation does not aggravate the impairment of hippocampal-dependent memory under conditions of HFD-induced obese-insulin resistance.

**TABLE 1.** Effect of estrogen deprivation on metabolic change in obese-insulin resistance rats.

|   | Groups               |                                  |                                    |                                       |
|---|----------------------|----------------------------------|------------------------------------|---------------------------------------|
| Parameters  | NDS                  | NDO                              | HFS                                | HFO                                   |
| Body weight (g)                                       | 279.55±3.90          | 304.21±4.92 <sup>a</sup>         | 325.56±5.33 <sup>a,b</sup>         | 391.19±10.79 <sup>a,b,c</sup>         |
| Visceral fat (g)                                      | 6.82 <u>+</u> 1.42   | 12.29 <u>+</u> 1.53 <sup>a</sup> | 25.98 <u>+</u> 1.30 <sup>a,b</sup> | 33.71 <u>+</u> 2.25 <sup>a,b,c</sup>  |
| Uterus weight (g)                                     | 0.45 <u>+</u> 0.06   | 0.15 <u>+</u> 0.04 <sup>a</sup>  | 0.38 <u>+</u> 0.03                 | 0.13 <u>+</u> 0.02 <sup>a,c</sup>     |
| Plasma glucose (mg/dl)                                | 133.48 <u>+</u> 2.66 | 136.59 <u>+</u> 4.75             | 141.87 <u>+</u> 4.12               | 159.58 <u>+</u> 6.84 <sup>a,b,c</sup> |
| Plasma insulin (ng/ml)                                | 0.99 <u>+</u> 0.12   | 2.38 <u>+</u> 0.31 <sup>a</sup>  | 2.44 <u>+</u> 0.38 <sup>a</sup>    | 3.46 <u>+</u> 0.32 <sup>a,b,c</sup>   |
| HOMA index  | 8.73 <u>+</u> 1.02   | 19.13 <u>+</u> 1.80 <sup>a</sup> | 17.47 <u>+</u> 3.69 <sup>a</sup>   | 29.49 <u>+</u> 3.77 <sup>a,b,c</sup>  |
| Plasma glucose AUC (AUCg)(mg/dl×min×10 <sup>4</sup> ) | 1.85±0.08            | 2.16±0.07 <sup>a</sup>           | 2.26±0.08 <sup>a,b</sup>           | 2.53±0.10 <sup>a,b,c</sup>            |
| Cholesterol (mg/dl)                                   | 77.33 <u>+</u> 4.64  | 95.59 <u>+</u> 7.23              | 106.53 <u>+</u> 6.80 <sup>a</sup>  | 117.57 <u>+</u> 10.50 <sup>a</sup>    |
| HDL (mg/dl)   | 7.72 <u>+</u> 0.21   | 8.34 <u>+</u> 0.25               | 8.12 <u>+</u> 0.39                 | 8.56 <u>+</u> 0.31                    |
| LDL (mg/dl)   | 67.80± 4.82          | 76.36± 3.62                      | 84.63± 8.31 <sup>a</sup>           | 85.74± 5.82 <sup>a</sup>              |
| Triglyceride (mg/dl)                                  | 70.99±5.31           | 72.41±4.64                       | 72.84±6.62                         | 91.07±3.92 <sup>a,b,c</sup>           |
| Calorie intake (Kcal/day)                             | 54.04± 2.06          | 60.83± 0.66 <sup>a</sup>         | 60.35± 1.46 <sup>a</sup>           | 66.71± 1.57 <sup>a,b,c</sup>          |
| Estradiol level (pg/ml)                               | 112.37±17.19         | 31.55±3.92 <sup>a</sup>          | 48.49±2.98 <sup>a</sup>            | 23.97±2.05 <sup>a,c</sup>             |
| Serum MDA (μM)  | 3.51±0.25            | 4.26±0.20 <sup>a</sup>           | 4.58±0.22 <sup>a</sup>             | 5.22±0.24 <sup>a,b,c</sup>            |

<sup>&</sup>lt;sup>a</sup>, p <0.05 compared with NDS, <sup>b</sup>, p <0.05 compared with NDO, <sup>c</sup>, p <0.05 compared with HFS; n = 8/group; NDS = sham-ND-fed rats; NDO = ovariectomized-ND-fed rats; HFS = sham-HFD-fed rats; HFO = ovariectomized-HFD-fed rats; HOMA= homeostasis model assessment; HDL= high-density lipoprotein; LDL= low-density lipoprotein, MDA= malondialdehyde

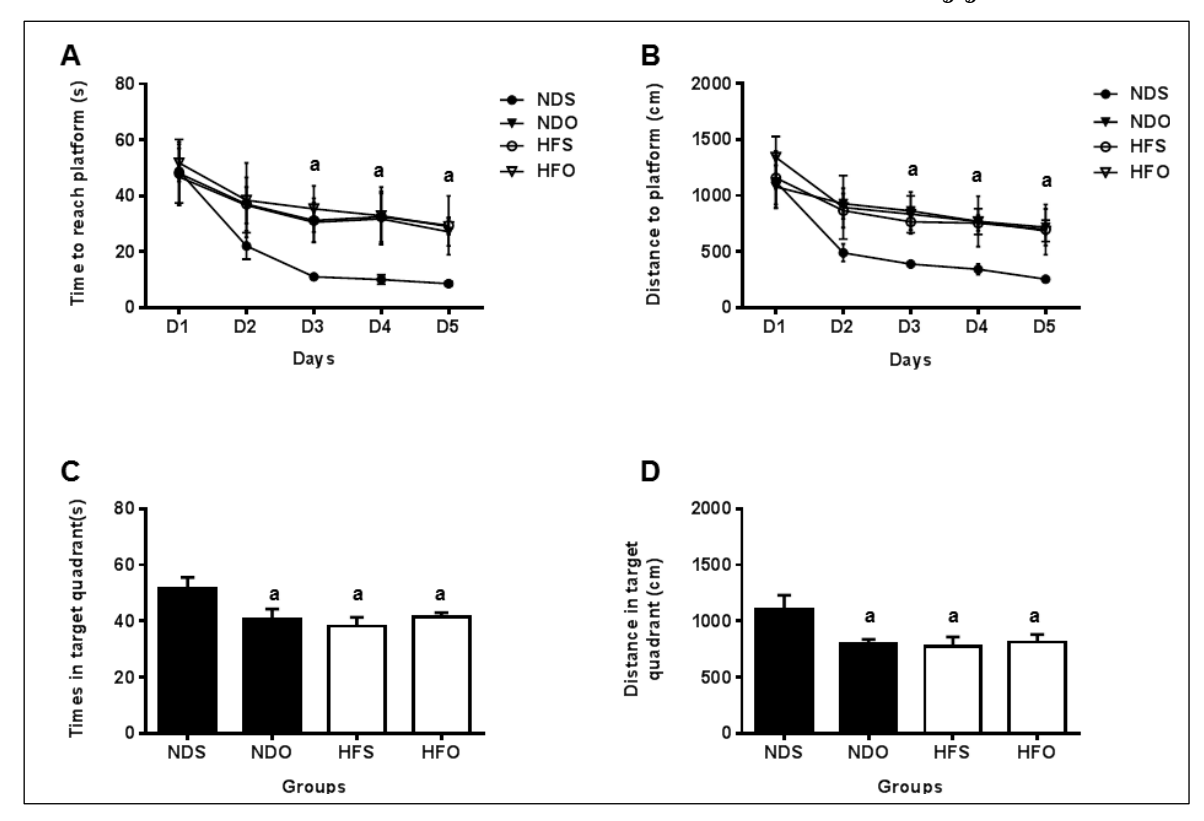


**FIG. 1.** Time to reach platform in acquisition test (A); distance to platform in acquisition test (B); time in target quadrant in probe test (C) and distance in target quadrant in probe test (D) in the NDS, NDO, HFS and HFO rats. <sup>a</sup>, p<0.05 compared with NDS; n=8/group; NDS = sham-ND-fed rats; NDO = ovariectomized-ND-fed rats; HFS = sham-HFD-fed rats; HFO = ovariectomized-HFD-fed rats

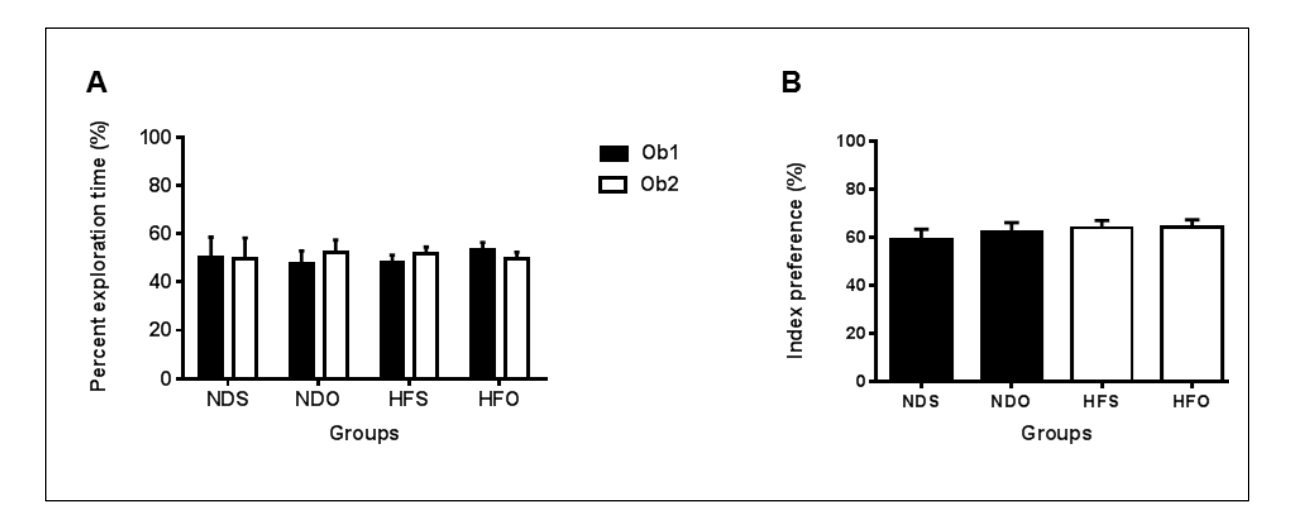


**FIG. 2.** Percentage exploration time (A), and index preference (B) from the NDS, NDO, HFS and HFO rats; n=8/group; NDS = sham-ND-fed rats; NDO = ovariectomized-ND-fed rats; HFS = sham-HFD-fed rats; HFO = ovariectomized-HFD-fed rats; Ob1 = object 1; Ob2 = object 2

# Effect of estrogen deprivation and HFD-induced obese-insulin resistance on hippocampal synaptic plasticity and hippocampal insulin receptor function.

Several studies have demonstrated that both hippocampal synaptic plasticity and hippocampal insulin receptor function are involved in the mechanisms involved in hippocampal-dependent learning and memory. Therefore, hippocampal-synaptic plasticity and hippocampal insulin receptor function were determined by long term potentiation (LTP) and insulin-induced long term depression (LTD), respectively. The electrical-induced LTP observed from hippocampal slices of the NDO, HFS, HFO rats was significantly decreased, when compared with that of NDS rat (p<0.05; Fig. 3A, C). In addition, the levels of insulin-induced LTD observed from the hippocampal slices of the NDO, HFS and HFO rats were significantly reduced, when compared with that of NDS rats (p<0.05, Fig. 3B, D). All of these findings indicate that estrogen deprivation alone and HFD-induced obese-insulin resistance alone impair hippocampal-synaptic plasticity and hippocampal insulin receptor functions. Moreover, estrogen deprivation does not appear to aggravate these impairments under conditions of HFD-induced obese-insulin resistance.

# Effect of estrogen deprivation and HFD-induced obese-insulin resistance on hippocampal and cortical ROS production.

Several studies found that the underlying mechanisms of impaired learning and memory were influenced by increased ROS production. Therefore, both hippocampal and cortical ROS production was determined for investigation of the hippocampal-dependent process and hippocampal-independent process, respectively. Hippocampal ROS production of the NDO, HFS and HFO rats was significantly increased when compared with that of NDS rats (p<0.05, Fig. 4A). However, cortical ROS production was not significantly different between the four groups (Fig. 4B). These findings suggest that estrogen deprivation alone and HFD-induced obese-insulin resistance alone increase hippocampal ROS production alone. Moreover, estrogen deprivation does not aggravate these impairments under conditions of HFD-induced obese-insulin resistance.

# Effect of estrogen deprivation and HFD-induced obese-insulin resistance on hippocampal and cortical apoptosis.

Several studies found that the mechanisms underlying the impairment of learning and memory were influenced by apoptosis. <sup>54, 55</sup> Therefore, the levels of pro-apoptotic protein (Bax), anti-apoptotic protein (Bcl-2) and the Bax/Bcl-2 ratio in both the hippocampus and cortex were determined for investigating the hippocampal-dependent process and hippocampal-independent process, respectively. We found that Bax protein expression in both hippocampus and cortex

was not significantly different between the four groups (Fig. 5A, D). Interestingly, Bcl-2 protein expression in the hippocampus of NDO, HFS and HFO rats were significantly decreased when compared with that of NDS rats (p<0.05, Fig. 5B). In addition, the Bax/Bcl-2 ratios in the hippocampus of NDO, HFS and HFO rats were significantly increased when compared with that of NDS rats (p<0.05, Fig. 5C). However, Bcl-2 protein expression and Bax/Bcl-2 ratio in the cortex was not significantly different among four groups (Fig. 5E, F). These findings suggest that estrogen deprivation alone and HFD-induced obese-insulin resistance alone increase hippocampal apoptosis alone. Moreover, estrogen deprivation dose not aggravate these impairments under conditions of HFD-induced obese-insulin resistance.

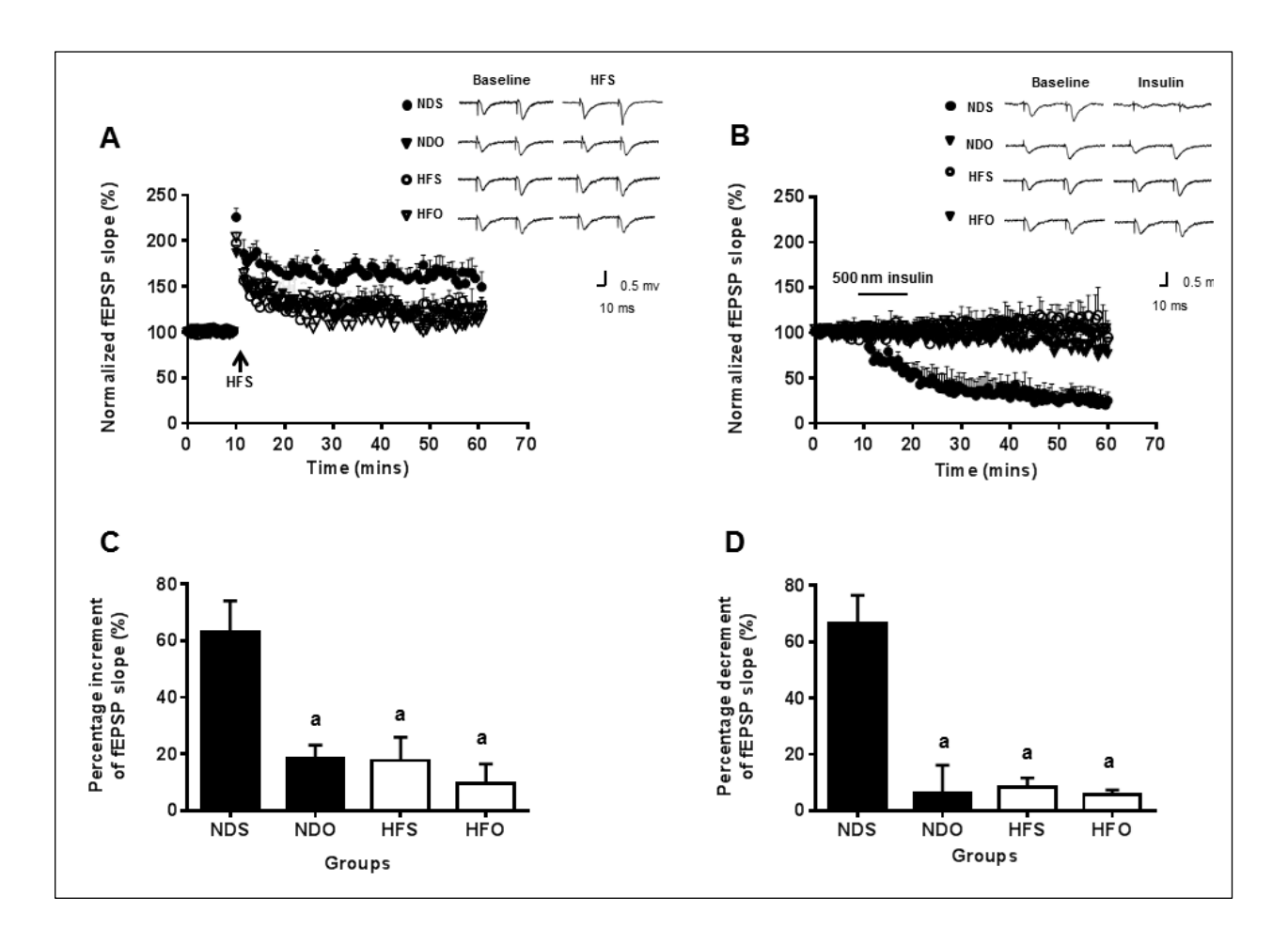


**FIG. 3.** The degree of electrical-mediated LTP (A), the degree of insulin-mediated LTD (B), the percentage increment of fEPSP slope (C) and the percentage decrement of fEPSP slope (D) observed from hippocampal slices of NDS, NDO, HFS and HFO rats; <sup>a</sup>, p<0.05 compared with NDS; (n=7-8 independent slices, n=8 animals/group); NDS = sham-ND-fed rats; NDO = ovariectomized-ND-fed rats; HFS = sham-HFD-fed rats; HFO = ovariectomized-HFD-fed rats; Hfs = high frequency stimulation; fEPSPs = field excitatory post synaptic potential

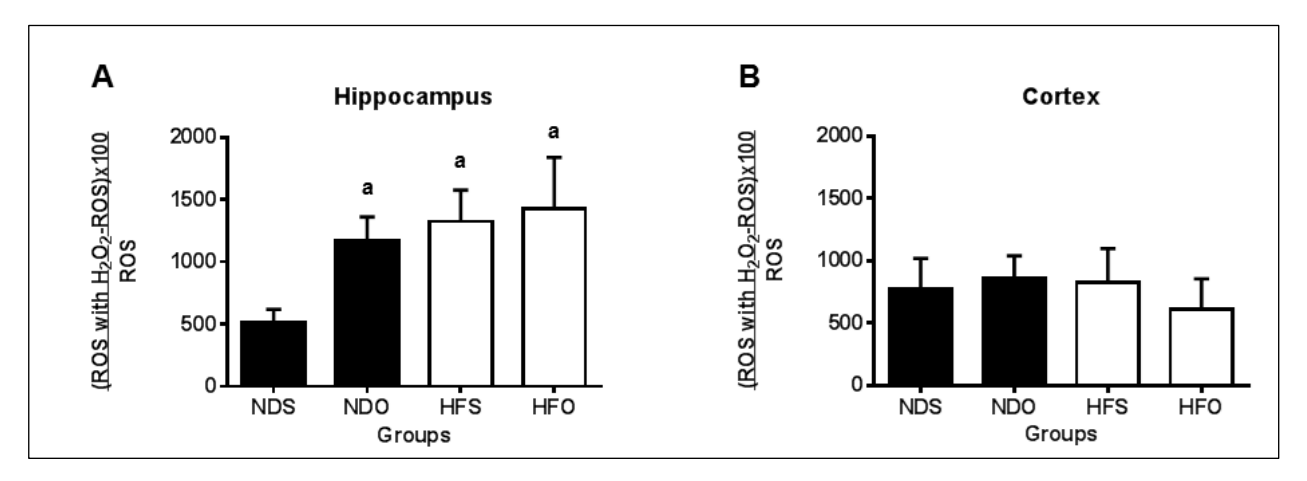


**FIG. 4.** Hippocampal ROS production (**A**) and cortical ROS production from the NDS, NDO, HFS and HFO rats (**B**); <sup>a</sup>, p<0.05 compared with NDS; n=8/group; NDS = sham-ND-fed rats; NDO = ovariectomized-ND-fed rats; HFS = sham-HFD-fed rats; HFO = ovariectomized-HFD-fed rats; ROS = reactive oxygen species

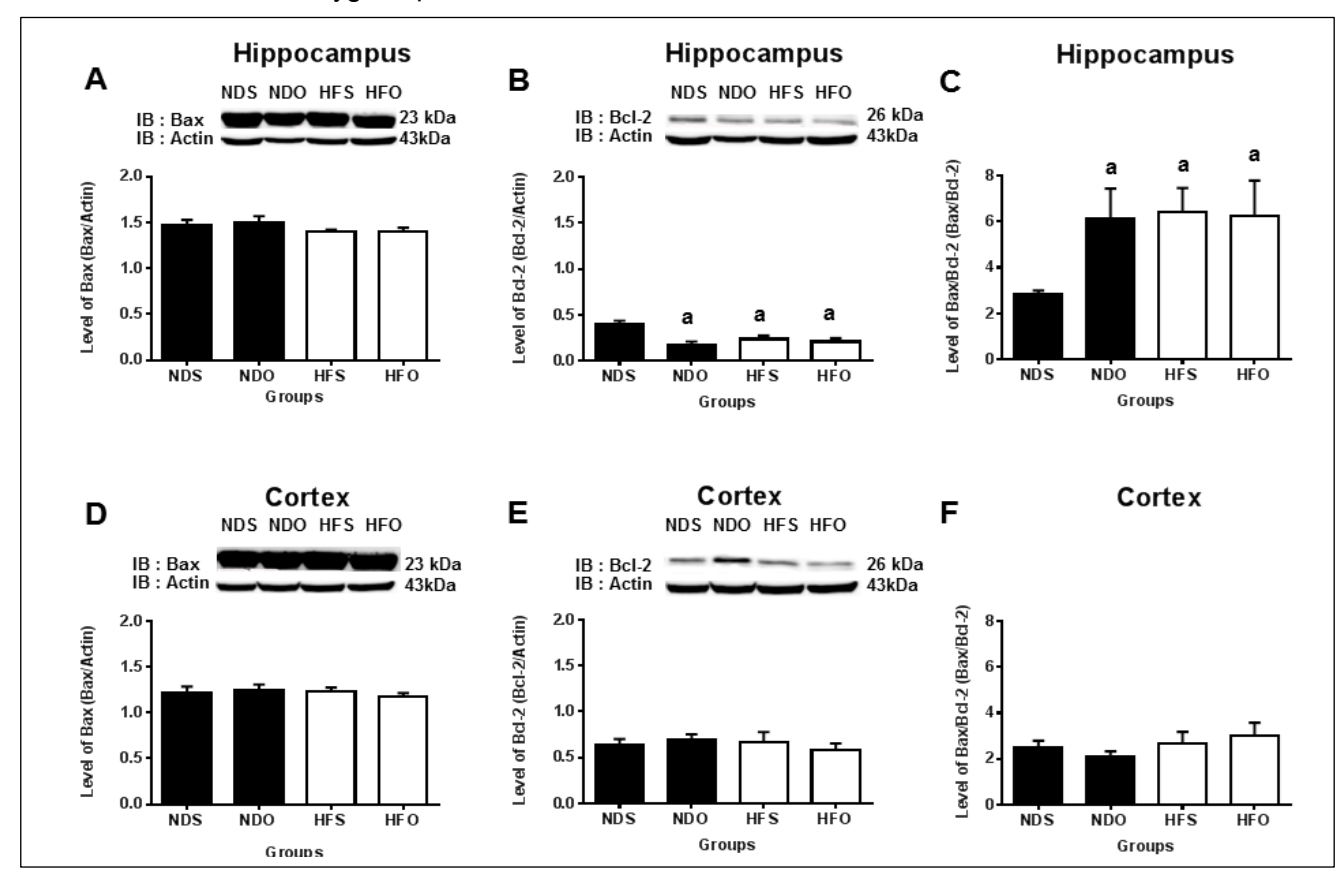


**FIG. 5.** Representative blots of hippocampal Bax protein expression (A), representative blots of hippocampal Bcl-2 protein expression (B), hippocampal Bax/Bcl-2 ratio (C), representative blots of cortical Bax protein expression (D), representative blots of cortical Bcl-2 protein expression (E) and cortical Bax/Bcl-2 ratio (F) from the NDS, NDO, HFS and HFO rats; <sup>a</sup>, p<0.05 compared with NDS; n=8/group; NDS = sham-ND-fed rats; NDO = ovariectomized-ND-fed rats; HFS = sham-HFD-fed rats; HFO = ovariectomized-HFD-fed rats

# Effect of estrogen deprivation and HFD-induced obese-insulin resistance on hippocampal and cortical estrogen levels.

Previous studies found that estrogen could modulate cognitive function. Therefore, hippocampal and cortical estrogen levels were determined. We found that estrogen levels in the hippocampus of NDO, HFS and HFO rats were significantly decreased when compared with that of NDS rats (p<0.05, Fig. 6A). However, estrogen levels in the cortex were not significantly different between the four groups (Fig. 6B). These findings suggest that both estrogen deprivation alone and HFD-induced obese-insulin resistance alone decrease solely the hippocampal estrogen level. Moreover, estrogen deprivation does not aggravate this impairment under conditions of HFD-induced obese-insulin resistance.

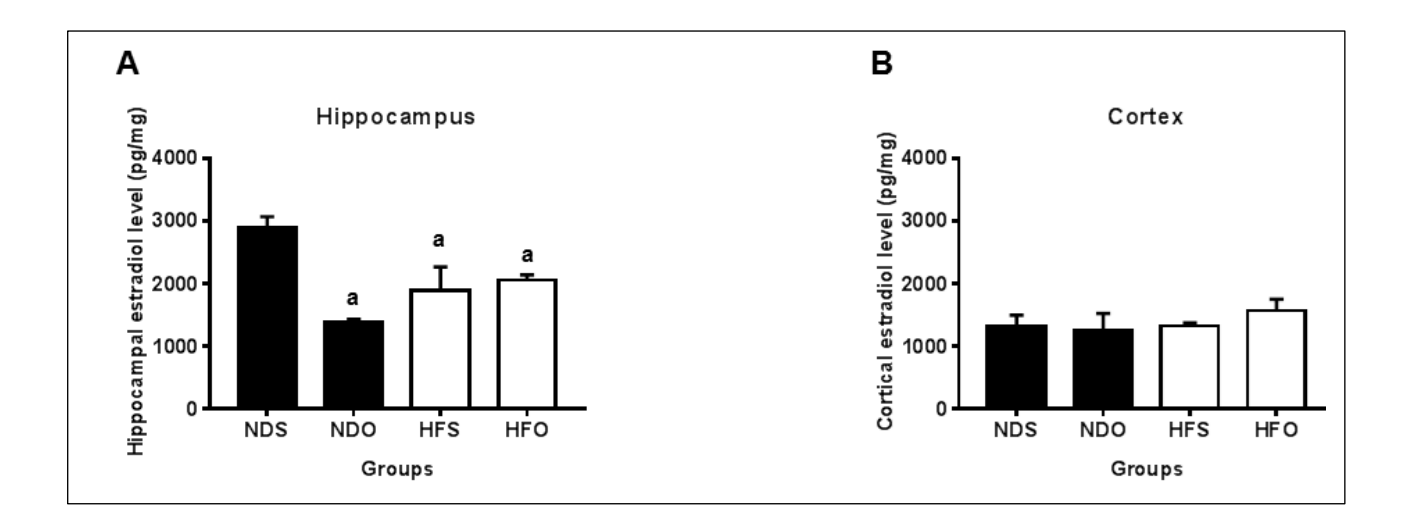


**FIG. 6.** Hippocampal estradiol level (A) and cortical estradiol level (B) from the NDS, NDO, HFS and HFO rats; <sup>a</sup>, p<0.05 from NDS; n=8/group; NDS = sham-ND-fed rats; NDO = ovariectomized-ND-fed rats; HFS = sham-HFD-fed rats; HFO = ovariectomized-HFD-fed rats

### Effect of calorie restriction combined with exercise training on metabolic function in ovariectomized obese rats.

We found that the plasma glucose level and area under the plasma glucose curve (AUCg) of HFSV and HFOV rats were significantly increased when compared with that of NDSV rats (p<0.05, Fig. 7 & 8). Interestingly, calorie restriction, exercise training and combined treatment share similarly effects on the improvement of metabolic function as indicated by decreased plasma glucose level and AUCg in HFS. In addition, calorie restriction, exercise training, combined treatment and estrogen treatment share similarly effects on the improvement of metabolic function as indicated by decreased plasma glucose level and AUCg in HFO rats (p<0.05, Fig. 7 & 8).

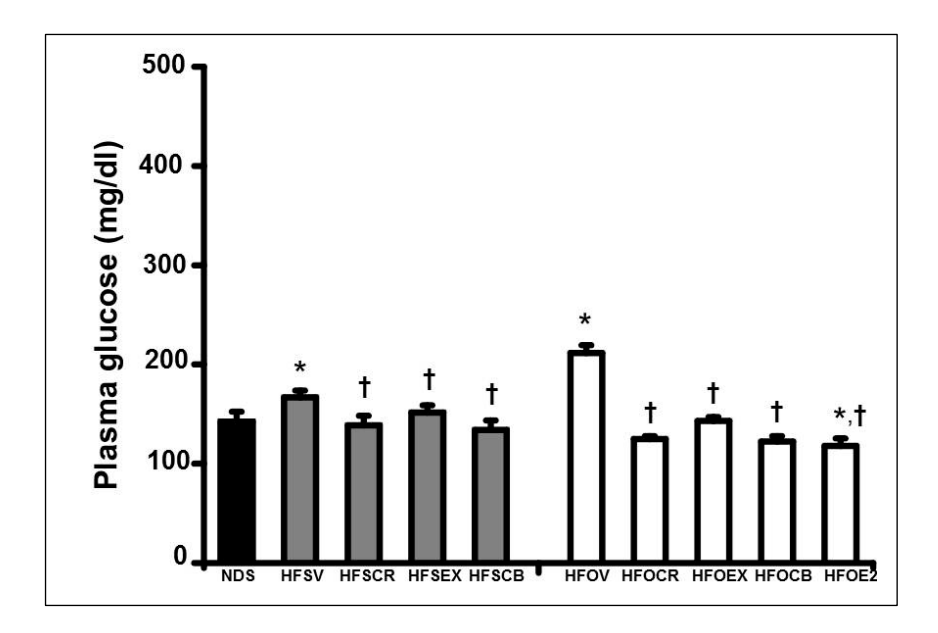


FIG. 7. Fasting plasma glucose level from the NDS, HFSV, HFSCR, HFSEX, HFSCB, HFOV, HFOCR, HFOEX, HFOCB, and HFOE2 rats; \*, p<0.05 from NDS; †, p<0.05 from vehicle in the same group; n=6/group; NDS = sham-ND-fed rats; HFSV = sham-HFD-fed rats with vehicle treatment; HFSCR = sham-HFD-fed rats with calorie restriction; HFSEX = sham-HFD-fed rats with exercise training; HFSCB = sham-HFD-fed rats with calorie restriction combined with exercise training; HFOV = ovariectomized-HFD-fed rats with vehicle treatment; HFOCR = ovariectomized-HFD-fed rats with calorie restriction; HFOEX = ovariectomized-HFD-fed rats with exercise training; HFOCB = ovariectomized-HFD-fed rats with calorie restriction combined with exercise training; HFOE2 = ovariectomized-HFD-fed rats with estradiol treatment

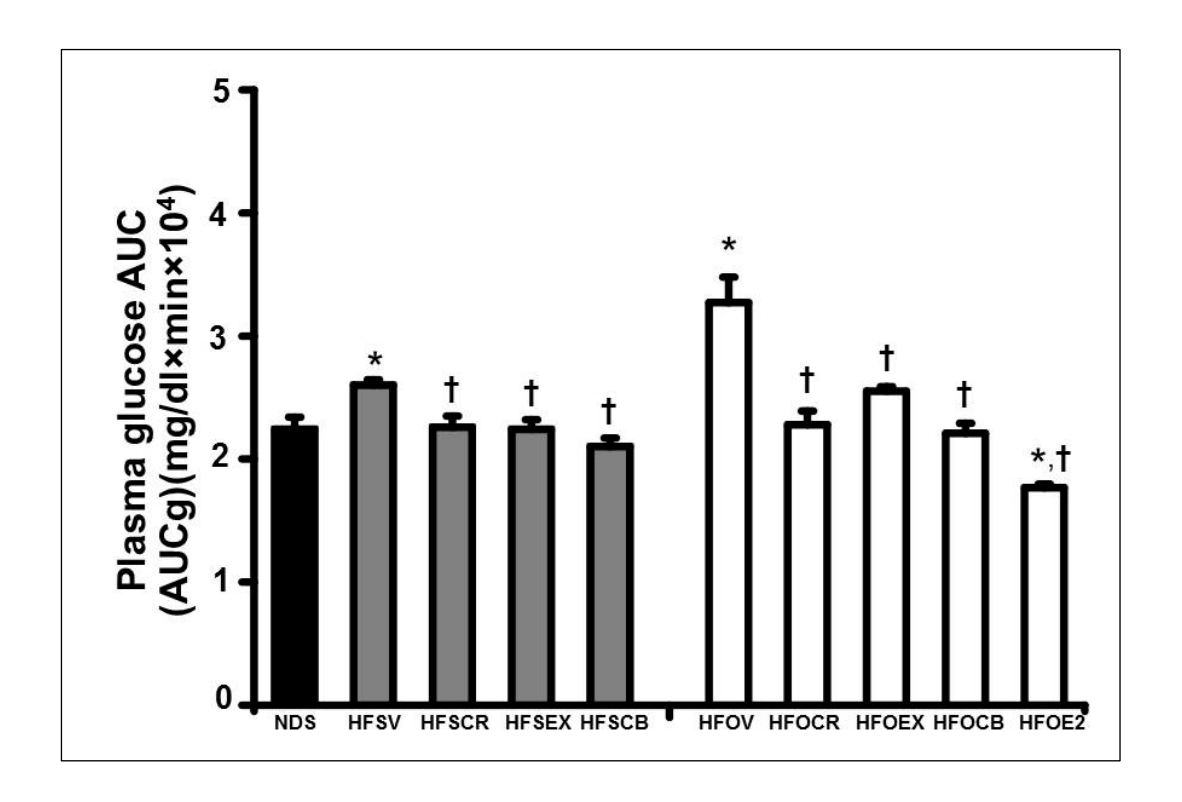
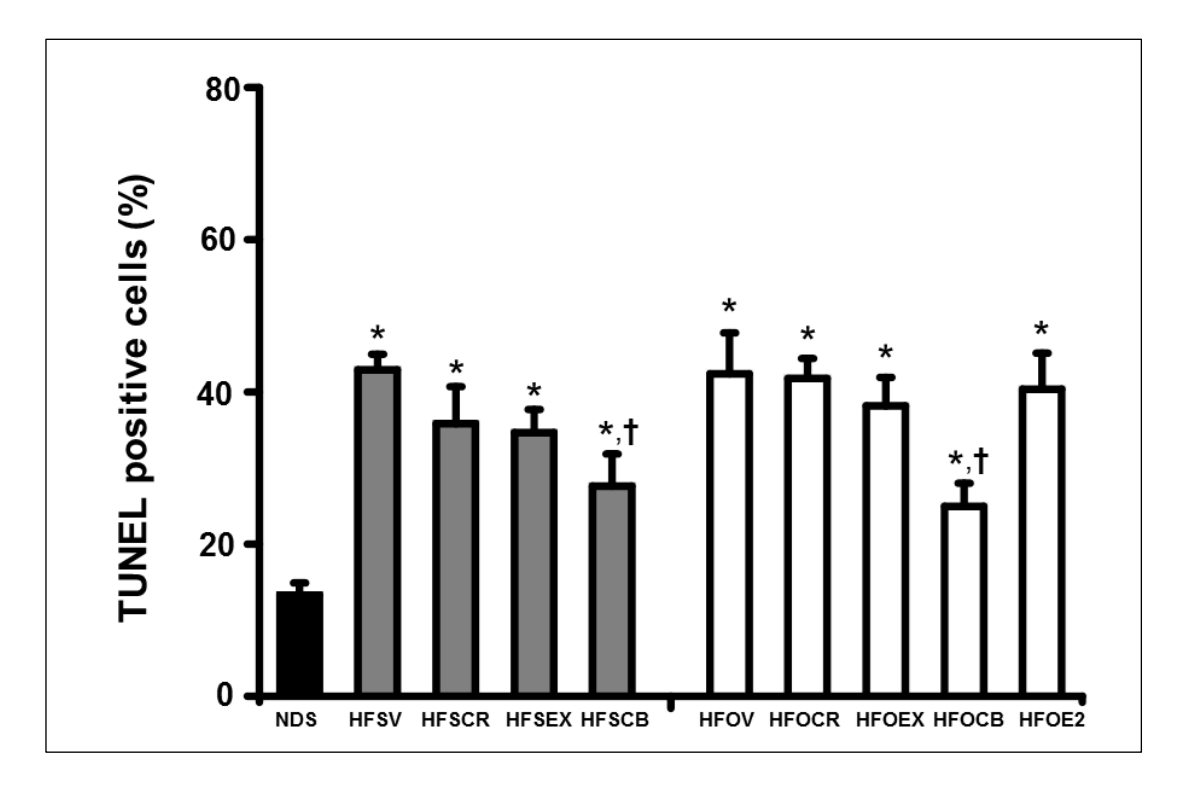


FIG. 8. Area under the plasma glucose curve (AUCg) from the NDS, HFSV, HFSCR, HFSEX, HFSCB, HFOV, HFOCR, HFOEX, HFOCB, and HFOE2 rats; \*, p<0.05 from NDS; †, p<0.05 from vehicle in the same group; n=6/group; NDS = sham-ND-fed rats; HFSV = sham-HFD-fed rats with vehicle treatment; HFSCR = sham-HFD-fed rats with calorie restriction; HFSEX = sham-HFD-fed rats with exercise training; HFSCB = sham-HFD-fed rats with calorie restriction combined with exercise training; HFOV = ovariectomized-HFD-fed rats with vehicle treatment; HFOCR = ovariectomized-HFD-fed rats with calorie restriction; HFOEX = ovariectomized-HFD-fed rats with calorie restriction combined with exercise training; HFOCB = ovariectomized-HFD-fed rats with estradiol treatment

# Effect of calorie restriction combined with exercise training on brain apoptosis in ovariectomized obese rats.

We found that TUNEL positive cell of HFS and HFO rats were significantly decreased when compared with that of NDS rats (p<0.05, Fig. 9). However, either calorie restriction or exercise training did not decrease TUNEL positive cell in HFS and HFO rats. Interestingly, calorie restriction with exercise training decreased TUNEL positive cell in both HFS and HFO rats.



**FIG. 9.** TUNEL positive cell from the NDS, HFSV, HFSCR, HFSEX, HFSCB, HFOV, HFOCR, HFOEX, HFOCB, and HFOE2 rats; \*, p<0.05 from NDS; †, p<0.05 from vehicle in the same group; n=6/group; NDS = sham-ND-fed rats; HFSV = sham-HFD-fed rats with vehicle treatment; HFSCR = sham-HFD-fed rats with calorie restriction; HFSEX = sham-HFD-fed rats with exercise training; HFSCB = sham-HFD-fed rats with calorie restriction combined with exercise training; HFOV = ovariectomized-HFD-fed rats with vehicle treatment; HFOCR = ovariectomized-HFD-fed rats with calorie restriction; HFOEX = ovariectomized-HFD-fed rats with exercise training; HFOCB = ovariectomized-HFD-fed rats with calorie restriction combined with exercise training; HFOE2 = ovariectomized-HFD-fed rats with estradiol treatment

Effect of calorie restriction combined with exercise training on insulin-induced long term depression (LTD) in ovariectomized obese rats.

We found that the ability of insulin-induced LTD of HFS and HFO rats were significantly decreased when compared with that of NDS rats (p<0.05, Fig. 10). Interestingly, exercise training increased the ability of insulin-induced LTD in HFS. In addition, calorie restriction with exercise training increased the ability of insulin-induced LTD in both HFS and HFO rats.

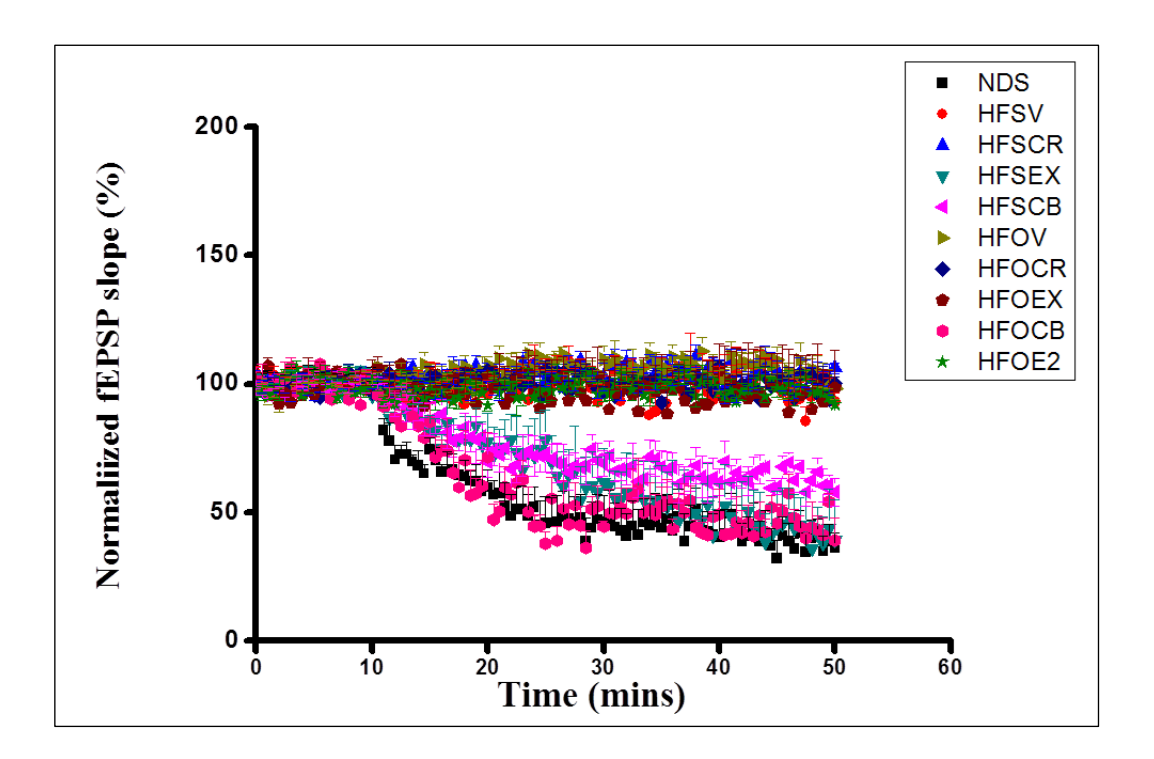


FIG. 10. The ability of insulin-induced LTD from the NDS, HFSV, HFSCR, HFSEX, HFSCB, HFOV, HFOCR, HFOEX, HFOCB, and HFOE2 rats; n=6/group; NDS = sham-ND-fed rats; HFSV = sham-HFD-fed rats with vehicle treatment; HFSCR = sham-HFD-fed rats with calorie restriction; HFSEX = sham-HFD-fed rats with exercise training; HFSCB = sham-HFD-fed rats with calorie restriction combined with exercise training; HFOV = ovariectomized-HFD-fed rats with vehicle treatment; HFOCR = ovariectomized-HFD-fed rats with calorie restriction; HFOEX = ovariectomized-HFD-fed rats with exercise training; HFOCB = ovariectomized-HFD-fed rats with calorie restriction combined with exercise training; HFOE2 = ovariectomized-HFD-fed rats with estradiol treatment

# Effect of calorie restriction combined with exercise training on brain inflammation in ovariectomized obese rats.

We found that the brain inflammation of HFSV and HFOV rats were significantly increased when compared with that of NDSV rats, as indicated by increased brain pNFkB level (p<0.05, Fig. 11). Interestingly, calorie restriction, exercise training and combined treatment share similarly effects on the improvement of brain inflammation as indicated by decreased brain pNFkB level in HFS. In addition, calorie restriction, exercise training, combined treatment and estrogen treatment share similarly effects on the improvement brain inflammation as indicated by decreased in brain pNFkB level HFO rats (p<0.05, Fig. 11).

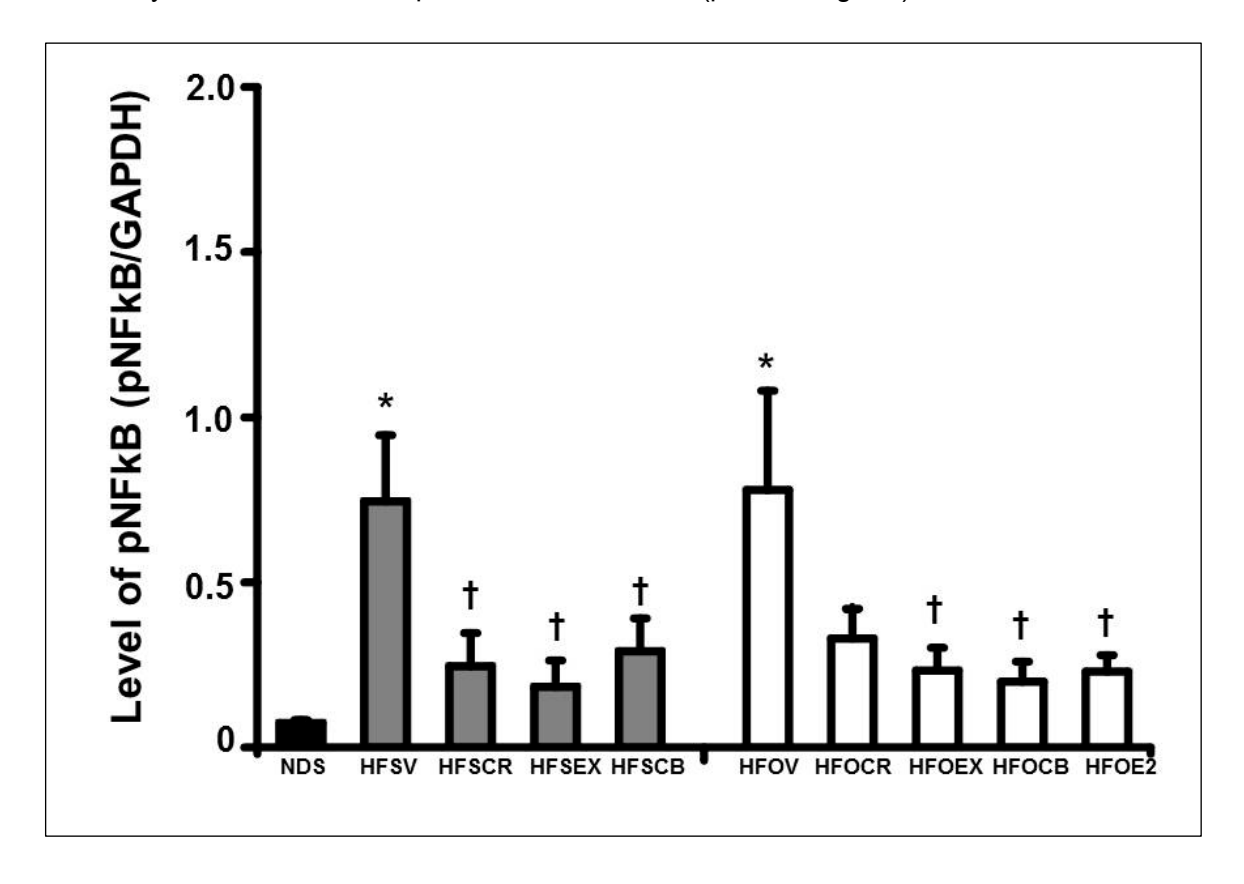


FIG. 11. Brain pNFkB level from the NDS, HFSV, HFSCR, HFSEX, HFSCB, HFOV, HFOCR, HFOEX, HFOCB, and HFOE2 rats; \*, p<0.05 from NDS; †, p<0.05 from vehicle in the same group; n=6/group; NDS = sham-ND-fed rats; HFSV = sham-HFD-fed rats with vehicle treatment; HFSCR = sham-HFD-fed rats with calorie restriction; HFSEX = sham-HFD-fed rats with exercise training; HFSCB = sham-HFD-fed rats with calorie restriction combined with exercise training; HFOV = ovariectomized-HFD-fed rats with vehicle treatment; HFOCR = ovariectomized-HFD-fed rats with calorie restriction; HFOEX = ovariectomized-HFD-fed rats with calorie restriction combined with exercise training; HFOCB = ovariectomized-HFD-fed rats with estradiol treatment

### บทวิจารณ์ (Discussion)

The major findings of the present study are as follows: 1) estrogen deprivation aggravated the severity of metabolic dysfunction in conditions of HFD-induced obese-insulin resistance; 2) estrogen deprivation alone, HFD-induced obese-insulin resistance alone and a combination of these conditions impaired solely hippocampal-dependent memory via increased hippocampal dysfunction; 3) estrogen deprivation did not aggravate these impairments under conditions of HFD-induced obese-insulin resistance; 4) calorie restriction, exercise training and combined treatment equally improved metabolic function; 5) exercise training had better efficacy than calorie restriction for preserved insulin receptor function; and 6) combined treatment had a greater efficacy in reducing brain apoptosis than single treatment.

To study the combined effects of estrogen deprivation and obesity, many previous studies used the model of estrogen-deprived condition followed by obesity. Those studies and our previous study showed that obesity aggravated peripheral insulin resistance in the estrogen-deprived condition, as indicated by increased plasma insulin, increased hyperglycemia, increased HOMA index and impaired glucose tolerance, when compared with HFD-fed rats alone or ovariectomized rats alone. <sup>8, 59-63</sup> In the present study, we used the model of obesity followed by the estrogen-deprived condition and this condition is most likely to occur in menopausal women who suffer from obesity after menopause. We found that not only the highest level of impaired insulin sensitivity, but also the highest level of dyslipidemia was observed in obese-ovariectomized rats, when compared with HFD-fed rats alone or ovariectomized rats alone. These findings suggest that the condition of the obesity followed by estrogen deprivation could aggravate metabolic disturbance to a greater extent than the condition of estrogen deprivation followed by obesity, as indicated by the aggravation of both peripheral insulin resistance and dyslipidemia.

This study was the first to investigate the comparative and cumulative effects of estrogen deprivation and obesity on hippocampal-dependent and hippocampal-independent memory in the same study. We found that both estrogen deprivation and obesity impaired hippocampal-dependent memory, but not hippocampal-independent memory. In addition, both estrogen deprivation and obesity exclusively caused brain pathophysiological changes in the hippocampal region, as indicated by increased synaptic dysfunction, insulin receptor dysfunction, ROS production and apoptosis. Furthermore, we also found that both estrogen deprivation and obesity exclusively decreased estrogen level in the hippocampus. Previous studies found that estrogen is synthesized in the brain, especially in the hippocampus

and also that hippocampal estrogen plays an important role in cognitive function via moderation of synaptic function. 65, 66 In addition, previous studies found that estrogen could have an antioxidant effect, which could reduce brain oxidative stress and apoptosis levels. Therefore, we speculated that both estrogen deprivation and obesity caused a decrease in hippocampal estrogen levels and increased hippocampal ROS production, which led to increased hippocampal apoptosis, and as a consequence led to impaired hippocampal synaptic function and also impaired hippocampal insulin receptor function. All of these mechanisms caused the impairment of hippocampal-dependent memory in rats, as indicated by increased time to reach the platform and decreased time in the target guadrant in the MWM test. However, neither estrogen deprivation nor obesity impaired hippocampal-independent memory and the brain pathophysiological changes in the cortex region. We speculated that neither estrogen deprivation nor obesity would decrease cortical estrogen level and cortical ROS production. Therefore, these situations did not cause cortical apoptosis, which therefore did not lead to impaired hippocampal-independent memory, as indicated by no change of percentage exploration time as well as index preference in the NOR test. However, a previous study found that only long-term estrogen deprivation (12 wks), but not short-term estrogen deprivation in rats (6 wks), caused the impairment of hippocampal-independent memory, as indicated by a decreased time with novel object in the NOR test. 14 Therefore, this short-term estrogen deprivation (7 wks) in our study could only impair hippocampal-dependent memory, and the impairment of hippocampal-independent memory may have occurred later. Furthermore, we found that estrogen deprivation did not aggravate brain pathophysiological changes or cognitive decline in an obese condition. In contrast, our recent studies showed that obesity accelerated and aggravated the increase in brain oxidative stress, hippocampal synaptic dysfunction, brain mitochondrial dysfunction, brain insulin resistance and cognitive impairment in estrogendeprived rats. 8, 69 A possible explanation could be the shorter duration of the estrogen deprivation in this study (7 wks), compared to our previous study (12 wks). As a result, the longer duration of estrogen deprivation may aggravate aforementioned brain pathophysiological changes and cognitive decline in this obese condition. Further studies are needed to give greater evidence to support this possible explanation.

Interestingly, we found that calorie restriction, exercise training and combined treatment equally improved metabolic function in both HFD-induced obese-insulin resistance with or without estrogen deprivation. Furthermore, calorie restriction, exercise training and combined treatment also decreased brain pathology in HFD-induced obese-insulin resistance with or without estrogen deprivation. Surprisingly, combined treatment had a greater efficacy in

reducing brain pathology than single treatment, as indicated by decreased brain apoptosis in both HFD-induced obese-insulin resistance with or without estrogen deprivation. Combined drugs could be the best therapeutic approach for neuroprotection in obese-insulin resistant condition. Therefore, combined drugs may be the best therapeutic approach for neuroprotection in HFD-induced obese-insulin resistance with or without estrogen deprivation.

### CONCLUSION

In summary, our findings demonstrate that estrogen deprivation aggravated the severity of peripheral insulin resistance and dyslipidemia in the obese condition. In addition, both estrogen deprivation and obesity impaired solely hippocampal-dependent memory, hippocampal synaptic function, hippocampal insulin receptor function, hippocampal ROS productions, hippocampal apoptosis and caused decreased hippocampal estrogen levels. However, estrogen deprivation did not aggravate these impairments in an obese condition. Interestingly, calorie restriction, exercise training and combined treatment equally improved metabolic function. Exercise training had better efficacy than calorie restriction for preserved insulin receptor function. Combined treatment had a greater efficacy in reducing brain apoptosis than single treatment. Therefore, combined treatment may be the best therapeutic approach for neuroprotection in HFD-induced obese-insulin resistance with or without estrogen deprivation.

### หนังสืออ้างอิง (References)

- 1. Zhao WQ, Alkon DL. Role of insulin and insulin receptor in learning and memory. Mol Cell Endocrinol. 2001;177(1-2):125-34.
- 2. Craft S, Watson GS. Insulin and neurodegenerative disease: shared and specific mechanisms. Lancet Neurol. 2004;**3**(3):169-78.
- 3. Greenwood CE, Winocur G. High-fat diets, insulin resistance and declining cognitive function. Neurobiology of Aging. 2005;**26**(1, Supplement):42-5.
- 4. Winocur G, Greenwood CE. Studies of the effects of high fat diets on cognitive function in a rat model. Neurobiol Aging. 2005;**26 Suppl 1**:46-9.
- 5. Pratchayasakul W, Chattipakorn N, Chattipakorn SC. Effects of estrogen in preventing neuronal insulin resistance in hippocampus of obese rats are different between genders. Life Sci. 2011;89(19-20):702-7.
- 6. Pratchayasakul W, Kerdphoo S, Petsophonsakul P, Pongchaidecha A, Chattipakorn N, Chattipakorn SC. Effects of high-fat diet on insulin receptor function in rat hippocampus and the level of neuronal corticosterone. Life Sci. 2011;**88**(13-14):619-27.
- 7. Pintana H, Apaijai N, Pratchayasakul W, Chattipakorn N, Chattipakorn SC. Effects of metformin on learning and memory behaviors and brain mitochondrial functions in high fat diet induced insulin resistant rats. Life Sci. 2012;**91**(11-12):409-14.
- 8. Pratchayasakul W, Sa-Nguanmoo P, Sivasinprasasn S, et al. Obesity accelerates cognitive decline by aggravating mitochondrial dysfunction, insulin resistance and synaptic dysfunction under estrogen-deprived conditions. Horm Behav. 2015;**72**:68-77.
- 9. Dew IT, Cabeza R. The porous boundaries between explicit and implicit memory: behavioral and neural evidence. Ann N Y Acad Sci. 2011;**1224**:174-90.
- 10. Bailey CH, Bartsch D, Kandel ER. Toward a molecular definition of long-term memory storage. Proceedings of the National Academy of Sciences of the United States of America. 1996;93(24):13445-52.
- 11. Vorhees CV, Williams MT. Morris water maze: procedures for assessing spatial and related forms of learning and memory. Nature protocols. 2006;**1**(2):848-58.
- 12. Antunes M, Biala G. The novel object recognition memory: neurobiology, test procedure, and its modifications. Cognitive processing. 2012;**13**(2):93-110.
- 13. Stranahan AM, Norman ED, Lee K, et al. Diet-induced insulin resistance impairs hippocampal synaptic plasticity and cognition in middle-aged rats. Hippocampus. 2008;**18**(11):1085-8.

- 14. Bastos CP, Pereira LM, Ferreira-Vieira TH, et al. Object recognition memory deficit and depressive-like behavior caused by chronic ovariectomy can be transitorially recovered by the acute activation of hippocampal estrogen receptors. Psychoneuroendocrinology. 2015;57:14-25.
- 15. Bocarsly ME, Fasolino M, Kane GA, et al. Obesity diminishes synaptic markers, alters microglial morphology, and impairs cognitive function. Proceedings of the National Academy of Sciences of the United States of America. 2015;**112**(51):15731-6.
- 16. Gainey SJ, Kwakwa KA, Bray JK, et al. Short-Term High-Fat Diet (HFD) Induced Anxiety-Like Behaviors and Cognitive Impairment Are Improved with Treatment by Glyburide. Frontiers in behavioral neuroscience. 2016;**10**:156.
- 17. Barzilai N, Banerjee S, Hawkins M, Chen W, Rossetti L. Caloric restriction reverses hepatic insulin resistance in aging rats by decreasing visceral fat. J Clin Invest. 1998;**101**(7):1353-61.
- 18. McCurdy CE, Davidson RT, Cartee GD. Calorie restriction increases the ratio of phosphatidylinositol 3-kinase catalytic to regulatory subunits in rat skeletal muscle. Am J Physiol Endocrinol Metab. 2005;288(5):E996-E1001.
- 19. Ayala V, Naudi A, Sanz A, et al. Dietary protein restriction decreases oxidative protein damage, peroxidizability index, and mitochondrial complex I content in rat liver. J Gerontol A Biol Sci Med Sci. 2007;62(4):352-60.
- 20. Caro P, Gomez J, Lopez-Torres M, et al. Forty percent and eighty percent methionine restriction decrease mitochondrial ROS generation and oxidative stress in rat liver. Biogerontology. 2008;**9**(3):183-96.
- 21. Prasannarong M, Vichaiwong K, Saengsirisuwan V. Calorie restriction prevents the development of insulin resistance and impaired insulin signaling in skeletal muscle of ovariectomized rats. Biochimica et biophysica acta. 2012;**1822**(6):1051-61.
- 22. Yamaoka K, Tango T. Effects of lifestyle modification on metabolic syndrome: a systematic review and meta-analysis. BMC Med. 2012;**10**:138.
- 23. Hiona A, Leeuwenburgh C. Effects of age and caloric restriction on brain neuronal cell death/survival. Ann N Y Acad Sci. 2004;**1019**:96-105.
- 24. Sanz A, Caro P, Ibanez J, Gomez J, Gredilla R, Barja G. Dietary restriction at old age lowers mitochondrial oxygen radical production and leak at complex I and oxidative DNA damage in rat brain. J Bioenerg Biomembr. 2005;37(2):83-90.
- 25. Eckles-Smith K, Clayton D, Bickford P, Browning MD. Caloric restriction prevents agerelated deficits in LTP and in NMDA receptor expression. Brain Res Mol Brain Res. 2000;**78**(1-2):154-62.

- 26. LaMonte MJ, Blair SN, Church TS. Physical activity and diabetes prevention. Journal of applied physiology. 2005;**99**(3):1205-13.
- 27. Hoppeler H, Fluck M. Plasticity of skeletal muscle mitochondria: structure and function. Medicine and science in sports and exercise. 2003;**35**(1):95-104.
- 28. Porter C, Reidy PT, Bhattarai N, Sidossis LS, Rasmussen BB. Resistance Exercise Training Alters Mitochondrial Function in Human Skeletal Muscle. Medicine and science in sports and exercise. 2014.
- 29. Wojtaszewski JF, Hansen BF, Gade, et al. Insulin signaling and insulin sensitivity after exercise in human skeletal muscle. Diabetes. 2000;**49**(3):325-31.
- 30. Wojtaszewski JF, Nielsen JN, Richter EA. Invited review: effect of acute exercise on insulin signaling and action in humans. Journal of applied physiology. 2002;**93**(1):384-92.
- 31. Sakurai T, Ogasawara J, Kizaki T, et al. The effects of exercise training on obesity-induced dysregulated expression of adipokines in white adipose tissue. International journal of endocrinology. 2013;**2013**:801743.
- 32. Stranahan AM, Khalil D, Gould E. Running induces widespread structural alterations in the hippocampus and entorhinal cortex. Hippocampus. 2007;17(11):1017-22.
- 33. van Praag H, Christie BR, Sejnowski TJ, Gage FH. Running enhances neurogenesis, learning, and long-term potentiation in mice. Proceedings of the National Academy of Sciences of the United States of America. 1999;**96**(23):13427-31.
- 34. Lafenetre P, Leske O, Ma-Hogemeie Z, et al. Exercise can rescue recognition memory impairment in a model with reduced adult hippocampal neurogenesis. Frontiers in behavioral neuroscience. 2010;3:34.
- 35. Lista I, Sorrentino G. Biological mechanisms of physical activity in preventing cognitive decline. Cellular and molecular neurobiology. 2010;**30**(4):493-503.
- 36. Rhyu IJ, Bytheway JA, Kohler SJ, et al. Effects of aerobic exercise training on cognitive function and cortical vascularity in monkeys. Neuroscience. 2010;**167**(4):1239-48.
- 37. Trejo JL, Carro E, Torres-Aleman I. Circulating insulin-like growth factor I mediates exercise-induced increases in the number of new neurons in the adult hippocampus. The Journal of neuroscience: the official journal of the Society for Neuroscience. 2001;**21**(5):1628-34.
- 38. Hotting K, Roder B. Beneficial effects of physical exercise on neuroplasticity and cognition. Neuroscience and biobehavioral reviews. 2013;37(9 Pt B):2243-57.

- 39. Woo J, Shin KO, Park SY, Jang KS, Kang S. Effects of exercise and diet change on cognition function and synaptic plasticity in high fat diet induced obese rats. Lipids in health and disease. 2013;**12**:144.
- 40. Wilsey J, Scarpace PJ. Caloric restriction reverses the deficits in leptin receptor protein and leptin signaling capacity associated with diet-induced obesity: role of leptin in the regulation of hypothalamic long-form leptin receptor expression. J Endocrinol. 2004;**181**(2):297-306.
- 41. Zoth N, Weigt C, Zengin S, et al. Metabolic effects of estrogen substitution in combination with targeted exercise training on the therapy of obesity in ovariectomized Wistar rats. J Steroid Biochem Mol Biol. 2012;**130**(1-2):64-72.
- 42. Matthews DR, Hosker JP, Rudenski AS, Naylor BA, Treacher DF, Turner RC. Homeostasis model assessment: insulin resistance and beta-cell function from fasting plasma glucose and insulin concentrations in man. Diabetologia. 1985;28(7):412-9.
- 43. Candan N, Tuzmen N. Very rapid quantification of malondialdehyde (MDA) in rat brain exposed to lead, aluminium and phenolic antioxidants by high-performance liquid chromatography-fluorescence detection. Neurotoxicology. 2008;**29**(4):708-13.
- 44. Chattipakorn SC, McMahon LL. Pharmacological characterization of glycine-gated chloride currents recorded in rat hippocampal slices. J Neurophysiol. 2002;87(3):1515-25.
- 45. Pipatpiboon N, Pratchayasakul W, Chattipakorn N, Chattipakorn SC. PPARgamma agonist improves neuronal insulin receptor function in hippocampus and brain mitochondria function in rats with insulin resistance induced by long term high-fat diets. Endocrinology. 2012;**153**(1):329-38.
- 46. Friedman JM. Obesity: Causes and control of excess body fat. Nature. [10.1038/459340a]. 2009;**459**(7245):340-2.
- 47. Arakawa H. Age dependent effects of space limitation and social tension on open-field behavior in male rats. Physiol Behav. 2005;**84**(3):429-36.
- 48. Pintana H, Apaijai N, Chattipakorn N, Chattipakorn SC. DPP-4 inhibitors improve cognition and brain mitochondrial function of insulin resistant rats. J Endocrinol. 2013;**218**(1):1-11.
- 49. Bryzgalova G, Lundholm L, Portwood N, et al. Mechanisms of antidiabetogenic and body weight-lowering effects of estrogen in high-fat diet-fed mice. American Journal of Physiology Endocrinology and Metabolism. 2008;**295**(4):E904-E12.
- 50. Godsland IF. Oestrogens and insulin secretion. Diabetologia. 2005;48(11):2213-20.
- 51. Akhondzadeh S. Hippocampal synaptic plasticity and cognition. Journal of clinical pharmacy and therapeutics. 1999;**24**(4):241-8.

- 52. Droge W, Schipper HM. Oxidative stress and aberrant signaling in aging and cognitive decline. Aging cell. 2007;**6**(3):361-70.
- 53. Chen X, Guo C, Kong J. Oxidative stress in neurodegenerative diseases. Neural regeneration research. 2012;**7**(5):376-85.
- 54. Guo YJ, Wang SH, Yuan Y, et al. Vulnerability for apoptosis in the hippocampal dentate gyrus of STZ-induced diabetic rats with cognitive impairment. Journal of endocrinological investigation. 2014;**37**(1):87-96.
- 55. Tehranian R, Rose ME, Vagni V, et al. Disruption of Bax protein prevents neuronal cell death but produces cognitive impairment in mice following traumatic brain injury. Journal of neurotrauma. 2008;**25**(7):755-67.
- 56. Brinton RD. Estrogen-induced plasticity from cells to circuits: predictions for cognitive function. Trends Pharmacol Sci. 2009;**30**(4):212-22.
- 57. Daniel JM, Fader AJ, Spencer AL, Dohanich GP. Estrogen enhances performance of female rats during acquisition of a radial arm maze. Horm Behav. 1997;**32**(3):217-25.
- 58. Desmond NL, Zhang DX, Levy WB. Estradiol enhances the induction of homosynaptic long-term depression in the CA1 region of the adult, ovariectomized rat. Neurobiol Learn Mem. 2000;**73**(2):180-7.
- 59. Shen M, Kumar SP, Shi H. Estradiol regulates insulin signaling and inflammation in adipose tissue. Hormone molecular biology and clinical investigation. 2014;**17**(2):99-107.
- 60. Camporez JP, Jornayvaz FR, Lee HY, et al. Cellular mechanism by which estradiol protects female ovariectomized mice from high-fat diet-induced hepatic and muscle insulin resistance. Endocrinology. 2013;**154**(3):1021-8.
- 61. Yonezawa R, Wada T, Matsumoto N, et al. Central versus peripheral impact of estradiol on the impaired glucose metabolism in ovariectomized mice on a high-fat diet. Am J Physiol Endocrinol Metab. 2012;**303**(4):E445-56.
- 62. Feigh M, Andreassen KV, Hjuler ST, et al. Oral salmon calcitonin protects against impaired fasting glycemia, glucose intolerance, and obesity induced by high-fat diet and ovariectomy in rats. Menopause. 2013;**20**(7):785-94.
- 63. Tominaga K, Yamauchi A, Egawa T, et al. Vascular dysfunction and impaired insulin signaling in high-fat diet fed ovariectomized mice. Microvascular research. 2011;82(2):171-6.
- 64. Fester L, Prange-Kiel J, Jarry H, Rune GM. Estrogen synthesis in the hippocampus. Cell and tissue research. 2011;**345**(3):285-94.

- 65. Bian C, Zhu H, Zhao Y, Cai W, Zhang J. Intriguing roles of hippocampus-synthesized 17beta-estradiol in the modulation of hippocampal synaptic plasticity. Journal of molecular neuroscience: MN. 2014;**54**(2):271-81.
- 66. Foy MR, Baudry M, Diaz Brinton R, Thompson RF. Estrogen and hippocampal plasticity in rodent models. Journal of Alzheimer's disease: JAD. 2008;**15**(4):589-603.
- 67. Moosmann B, Behl C. The antioxidant neuroprotective effects of estrogens and phenolic compounds are independent from their estrogenic properties. Proceedings of the National Academy of Sciences of the United States of America. 1999;**96**(16):8867-72.
- 68. Razmara A, Duckles SP, Krause DN, Procaccio V. Estrogen suppresses brain mitochondrial oxidative stress in female and male rats. Brain research. 2007;**1176**:71-81.
- 69. Pratchayasakul W, Chattipakorn N, Chattipakorn SC. Estrogen restores brain insulin sensitivity in ovariectomized non-obese rats, but not in ovariectomized obese rats. Metabolism: clinical and experimental. 2014;**63**(6):851-9.

### Output จากโครงการวิจัยที่ได้รับทุนจาก สกว.

- 1. ผลงานตีพิมพ์ในวารสารวิชาการนานาชาติ (ระบุชื่อผู้แต่ง ชื่อเรื่อง ชื่อวารสาร ปี เล่มที่ เลขที่ และหน้า)
- 1: Pratchayasakul W, Sivasinprasasn S, Sa-Nguanmoo P, Proctor C, Kerdphoo S, Chattipakorn N, Chattipakorn SC. Estrogen and DPP-4 inhibitor share similar efficacy in reducing brain pathology caused by cardiac ischemia-reperfusion injury in both lean and obese estrogendeprived rats. Menopause. 2017 Mar 13. (IF= 2.733)(เอกสารแนบหมายเลขา)
- 2: Sivasinprasasn S, Tanajak P, Pongkan W, **Pratchayasakul W**, Chattipakorn SC, Chattipakorn N. DPP-4 Inhibitor and Estrogen Share Similar Efficacy Against Cardiac Ischemic-Reperfusion Injury in Obese-Insulin Resistant and Estrogen-Deprived Female Rats. Sci Rep. 2017 Mar 10;7:44306. (IF= 5.228) (เอกสารแนบหมายเลข2)
- 3: Pintana H, Tanajak P, **Pratchayasakul W**, Sa-Nguanmoo P, Chunchai T, Satjaritanun P, Leelarphat L, Chattipakorn N, Chattipakorn SC. Energy restriction combined with dipeptidyl peptidase-4 inhibitor exerts neuroprotection in obese male rats. Br J Nutr. 2016 Nov 17:1-9. (IF= 3.706) (เอกสารแนบหมายเลข3)
- 4: Sa-Nguanmoo P, Tanajak P, Kerdphoo S, Satjaritanun P, Wang X, Liang G, Li X, Jiang C, **Pratchayasakul W**, Chattipakorn N, Chattipakorn SC. FGF21 improves cognition by restored synaptic plasticity, dendritic spine density, brain mitochondrial function and cell apoptosis in obese-insulin resistant male rats. Horm Behav. 2016 Sep;85:86-95. (IF= 3.378) (เอกสารแนบ หมายเลข4)
- 5: Sivasinprasasn S, Sa-Nguanmoo P, Pongkan W, **Pratchayasakul W**, Chattipakorn SC, Chattipakorn N. Estrogen and DPP4 inhibitor, but not metformin, exert cardioprotection via attenuating cardiac mitochondrial dysfunction in obese insulin-resistant and estrogen-deprived female rats. Menopause. 2016 Aug;23(8):894-902. (IF= 2.733) (เอกสารแนบหมายเลข5)
- 6: Pintana H, Apaijai N, Kerdphoo S, **Pratchayasakul W**, Sripetchwandee J, Suntornsaratoon P, Charoenphandhu N, Chattipakorn N, Chattipakorn SC. Hyperglycemia induced the Alzheimer's proteins and promoted loss of synaptic proteins in advanced-age female Goto-Kakizaki (GK) rats. Neurosci Lett. 2017 Aug 10;655:41-45. (IF= 2.180) (เอกสารแนบหมายเลข6)
- 7: Sa-Nguanmoo P, Tanajak P, Kerdphoo S, Jaiwongkam T, **Pratchayasakul W**, Chattipakorn N, Chattipakorn SC. SGLT2-inhibitor and DPP-4 inhibitor improve brain function via attenuating

mitochondrial dysfunction, insulin resistance, inflammation, and apoptosis in HFD-induced obese rats. Toxicol Appl Pharmacol. 2017 Oct 15;333:43-50. (IF= 3.791) (เอกสารแนบหมายเลข7)

- 8: Shwe T, **Pratchayasakul W**, Chattipakorn N, Chattipakorn SC. Role of D-galactose-induced brain aging and its potential used for therapeutic interventions. Exp Gerontol. 2018 Jan;101:13-36. (IF= 3.340) (เอกสารแนบหมายเลข8)
- 9: Chunchai T, Thunapong W, Yasom S, Wanchai K, Eaimworawuthikul S, Metzler G, Lungkaphin A, Pongchaidecha A, Sirilun S, Chaiyasut C, **Pratchayasakul W**, Thiennimitr P, Chattipakorn N, Chattipakorn SC. Decreased microglial activation through gut-brain axis by prebiotics, probiotics, or synbiotics effectively restored cognitive function in obese-insulin resistant rats. J Neuroinflammation. 2018 Jan 9;15(1):11. (IF= 5.102) (เอกสารแนบหมายเลข9)
- 10: Minta W, Palee S, Mantor D, Sutham W, Jaiwongkam T, Kerdphoo S, **Pratchayasakul W**, Kumfu S, Chattipakorn SC, Chattipakorn N. Estrogen deprivation aggravates cardiometabolic dysfunction in obese-insulin resistant rats through the impairment of cardiac mitochondrial dynamics. Exp Gerontol. 2018 Mar;103:107-114. (IF= 3.340) (เอกสารแนบหมายเลข10)
- 11: **Pratchayasakul W**, Thongnak LO, Chattipakorn K, Lungaphin A, Pongchaidecha A, Satjaritanun P, Jaiwongkam T, Kerdphoo S, Chattipakorn SC. Atorvastatin and insulin equally mitigate brain pathology in diabetic rats. Toxicol Appl Pharmacol. 2018 Mar 1;342:79-85. (IF= 3.791) (เอกสารแนบหมายเลข11)
- 12: Mantor D, **Pratchayasakul W**, Minta W, Sutham W, Palee S, Sripetchwandee J, Kerdphoo S, Jaiwongkum T, Sriwichaiin S, Krintratun W, Chattipakorn N, Chattipakorn SC. Both oophorectomy and obesity impaired solely hippocampal-dependent memory via increased hippocampal dysfunction. Exp Gerontol. 2018 Apr 17. (IF= 3.340) (co-first author) (เอกสารแนบ หมายเลข12)

# การนำผลงานวิจัยไปใช้ประโยชน์

2.1 เชิงสาธารณะ (มีเครือข่ายความร่วมมือ/สร้างกระแสความสนใจในวงกว้าง)

ในปัจจุบันถือว่าเป็นภาวะอ้วนมีความสำคัญอย่างมากเนื่องจากมีจำนวนประชากรที่ภาวะอ้วน ร่วมกับสภาวะขาดเอสโตรเจนเพิ่มขึ้นในทุกปี ดังนั้นข้อมูลจากงานวิจัยนี้จึงได้มีการนำเสนอผลงานวิจัย ในงานประชุมทั้งในระดับชาติและนานาชาติ โดยได้เผยแพร่ความรู้ว่าการขาดเอสโตรเจนและความอ้วนจะ ทำให้สูญเสียความความจำและการเรียนรู้ชนิดที่ขึ้นอยู่กับสมองส่วนฮิบโปแคมพัส โดยกลไกผ่านทางการ สูญเสียการทำงานในสมองส่วนฮิบโปแคมพัส นอกเหนือไปจากนั้นการออกกำลังกายจะให้ผลดีกว่า การจำกัดอาหารในการช่วยรักษาหน้าที่การทำงานของอินซูลินในสมอง การร่วมระหว่างการจำกัดอาหาร และการออกกำลังกายจะให้ผลดีที่สุดในแง่ของการลดการตายของเซลล์ในสมองเมื่อเทียบกับการจำกัด อาหารหรือการออกกำลังกายเพียงอย่างเดียว ดังนั้นการร่วมระหว่างการจำกัดอาหารและการออกกำลัง

กายอาจจะเป็นแนวทางที่ดีในการช่วยรักษาและป้องกันอันตรายของสมองจากภาวะดื้อต่ออินซูลินโดยการ เหนี่ยวนำโดยอาหารไขมันสูงทั้งที่ร่วมกับการขาดหรือไม่ขาดฮฮร์โมนเอสโตรเจน

- 2.2 เชิงวิชาการ (มีการพัฒนาการเรียนการสอน/สร้างนักวิจัยใหม่) โดยมีการตีพิมพ์เผยแพร่ในวารสารทางวิชาการในระดับนานาชาติแล้ว ดังต่อไปนี้
- 1: Pratchayasakul W, Sivasinprasasn S, Sa-Nguanmoo P, Proctor C, Kerdphoo S, Chattipakorn N, Chattipakorn SC. Estrogen and DPP-4 inhibitor share similar efficacy in reducing brain pathology caused by cardiac ischemia-reperfusion injury in both lean and obese estrogendeprived rats. Menopause. 2017 Mar 13. (IF= 2.733)(เอกสารแนบหมายเลข1)
- 2: Sivasinprasasn S, Tanajak P, Pongkan W, **Pratchayasakul W**, Chattipakorn SC, Chattipakorn N. DPP-4 Inhibitor and Estrogen Share Similar Efficacy Against Cardiac Ischemic-Reperfusion Injury in Obese-Insulin Resistant and Estrogen-Deprived Female Rats. Sci Rep. 2017 Mar 10;7:44306. (IF= 5.228) (เอกสารแนบหมายเลข2)
- 3: Pintana H, Tanajak P, **Pratchayasakul W**, Sa-Nguanmoo P, Chunchai T, Satjaritanun P, Leelarphat L, Chattipakorn N, Chattipakorn SC. Energy restriction combined with dipeptidyl peptidase-4 inhibitor exerts neuroprotection in obese male rats. Br J Nutr. 2016 Nov 17:1-9. (IF= 3.706) (เอกสารแนบหมายเลข3)
- 4: Sa-Nguanmoo P, Tanajak P, Kerdphoo S, Satjaritanun P, Wang X, Liang G, Li X, Jiang C, **Pratchayasakul W**, Chattipakorn N, Chattipakorn SC. FGF21 improves cognition by restored synaptic plasticity, dendritic spine density, brain mitochondrial function and cell apoptosis in obese-insulin resistant male rats. Horm Behav. 2016 Sep;85:86-95. (IF= 3.378) (เอกสารแนบ หมายเลข4)
- 5: Sivasinprasasn S, Sa-Nguanmoo P, Pongkan W, **Pratchayasakul W**, Chattipakorn SC, Chattipakorn N. Estrogen and DPP4 inhibitor, but not metformin, exert cardioprotection via attenuating cardiac mitochondrial dysfunction in obese insulin-resistant and estrogen-deprived female rats. Menopause. 2016 Aug;23(8):894-902. (IF= 2.733) (เอกสารแนบหมายเลข5)
- 6: Pintana H, Apaijai N, Kerdphoo S, **Pratchayasakul W**, Sripetchwandee J, Suntornsaratoon P, Charoenphandhu N, Chattipakorn N, Chattipakorn SC. Hyperglycemia induced the Alzheimer's proteins and promoted loss of synaptic proteins in advanced-age female Goto-Kakizaki (GK) rats. Neurosci Lett. 2017 Aug 10;655:41-45. (IF= 2.180) (เอกสารแนบหมายเลข6)
- 7: Sa-Nguanmoo P, Tanajak P, Kerdphoo S, Jaiwongkam T, **Pratchayasakul W**, Chattipakorn N, Chattipakorn SC. SGLT2-inhibitor and DPP-4 inhibitor improve brain function via attenuating mitochondrial dysfunction, insulin resistance, inflammation, and apoptosis in HFD-induced obese rats. Toxicol Appl Pharmacol. 2017 Oct 15;333:43-50. (IF= 3.791) (เอกสารแนบหมายเลข7)

- 8: Shwe T, **Pratchayasakul W**, Chattipakorn N, Chattipakorn SC. Role of D-galactose-induced brain aging and its potential used for therapeutic interventions. Exp Gerontol. 2018 Jan;101:13-36. (IF= 3.340) (เอกสารแนบหมายเลข8)
- 9: Chunchai T, Thunapong W, Yasom S, Wanchai K, Eaimworawuthikul S, Metzler G, Lungkaphin A, Pongchaidecha A, Sirilun S, Chaiyasut C, **Pratchayasakul W**, Thiennimitr P, Chattipakorn N, Chattipakorn SC. Decreased microglial activation through gut-brain axis by prebiotics, probiotics, or synbiotics effectively restored cognitive function in obese-insulin resistant rats. J Neuroinflammation. 2018 Jan 9;15(1):11. (IF= 5.102) (เอกสารแนบหมายเลข9)
- 10: Minta W, Palee S, Mantor D, Sutham W, Jaiwongkam T, Kerdphoo S, **Pratchayasakul W**, Kumfu S, Chattipakorn SC, Chattipakorn N. Estrogen deprivation aggravates cardiometabolic dysfunction in obese-insulin resistant rats through the impairment of cardiac mitochondrial dynamics. Exp Gerontol. 2018 Mar;103:107-114. (IF= 3.340) (เอกสารแนบหมายเลข10)
- 11: **Pratchayasakul W**, Thongnak LO, Chattipakorn K, Lungaphin A, Pongchaidecha A, Satjaritanun P, Jaiwongkam T, Kerdphoo S, Chattipakorn SC. Atorvastatin and insulin equally mitigate brain pathology in diabetic rats. Toxicol Appl Pharmacol. 2018 Mar 1;342:79-85. (IF= 3.791) (เอกสารแนบหมายเลข11)
- 12: Mantor D, **Pratchayasakul W**, Minta W, Sutham W, Palee S, Sripetchwandee J, Kerdphoo S, Jaiwongkum T, Sriwichaiin S, Krintratun W, Chattipakorn N, Chattipakorn SC. Both oophorectomy and obesity impaired solely hippocampal-dependent memory via increased hippocampal dysfunction. Exp Gerontol. 2018 Apr 17. (IF= 3.340) (co-first author) (เอกสารแนบ หมายเลข12)
- 3. อื่นๆ (เช่น หนังสือ การจดสิทธิบัตร)
- 1. Apaijai N, **Pratchayasakul W**, Chattipakorn N, Chattipakorn SC. Mitochondrial link between metabolic syndrome and pre-Alzheimer's disease: Alzheimer's Disease the 21st Century Challenge. IntechOpen Publishers. (Accepted)

# Estrogen and DPP-4 inhibitor share similar efficacy in reducing brain pathology caused by cardiac ischemia-reperfusion injury in both lean and obese estrogen-deprived rats

Wasana Pratchayasakul, PhD, 1,2 Sivaporn Sivasinprasasn, PhD, 1,3 Piangkwan Sa-Nguanmoo, MSc, 1,2 Cicely Proctor, BSc,<sup>4</sup> Sasiwan Kerdphoo, MSc,<sup>1</sup> Nipon Chattipakorn, MD, PhD,<sup>1,2</sup> and Siriporn C. Chattipakorn, DDS, PhD<sup>1,5</sup>

#### **Abstract**

Objective: Cardiac ischemia-reperfusion injury (I/R) caused an oxidative burst, increased beta-amyloid production, and decreased dendritic spine density in the brain. However, the effect of cardiac I/R in the brain of estrogen-deprived rats who were or were not obese have not been investigated. Moreover, the benefits of estrogen or dipeptidyl peptidase-4 (DDP-4) inhibitor therapies in those conditions have never been determined. We hypothesized that cardiac I/R aggravates brain pathology in estrogen-deprived obese rats, to a greater extent when compared with estrogen-deprived lean rats, and treatment with either estrogen or a DPP-4 inhibitor attenuates those

**Methods:** In protocol 1, rats were divided into sham operation (n = 12) or ovariectomy (n = 24). Sham-operated rats were fed with normal diet (ND) and ovariectomized rats were fed with either ND or high-fat diet (HF) for 12 weeks. Then, rats were subdivided to sham operation or cardiac I/R injury. In protocol 2, ovariectomized rats were given either ND (n = 18) or HF (n = 18). At week 13, ovariectomized rats were subdivided to receive vehicle, estradiol, or DPP-4 inhibitor for 4 weeks. Then, all rats were subjected to cardiac I/R.

Results: Cardiac I/R injury aggravated brain oxidative stress, beta-amyloid production, and decreased dendritic spine density in either sham-operated or ovariectomized ND-fed rats, but not in ovariectomized HF-fed rats. Either estrogen or DPP-4 inhibitor therapies reduced those conditions in all rats with cardiac I/R.

Conclusions: Cardiac I/R aggravates brain toxicity in estrogen-deprived lean rats, but not in the estrogendeprived obese rats. Estrogen and DPP-4 inhibitor treatments attenuate those effects in all groups.

Key Words: DPP-4 inhibitor - Brain - Cardiac ischemia-reperfusion injury - Estrogen - Obesity -Ovariectomy.

ardiac ischemia-reperfusion (cardiac I/R) injury can lead to not only myocardial damage but also increased brain pathology. Previous studies have shown that cardiac I/R injury induced an oxidative burst in many organs, including the brain.<sup>1,2</sup> In addition, the

Received October 20, 2016; revised and accepted December 13, 2016. From the <sup>1</sup>Neurophysiology Unit, Cardiac Electrophysiology Research and Training Center, and <sup>2</sup>Department of Physiology, Faculty of Medicine, Chiang Mai University, Chiang Mai, Thailand; <sup>3</sup>School of Health Science, Mae Fah Luang University, Chiang Rai, Thailand; <sup>4</sup>Faculty of Life Sciences, The University of Manchester, Manchester, UK; and <sup>5</sup>Department of Oral Biology and Diagnostic Sciences, Faculty of Dentistry, Chiang Mai University, Chiang Mai, Thailand.

Funding/support: This work was supported by the Thailand Research Fund BRG5780016 (S.C.C.) and MRG5980198 (W.P.), a NSTDA Research Chair Grant from the National Science and Technology Development Agency Thailand (N.C.), and a Chiang Mai University Center of Excellence Award (N.C.).

Financial disclosure/conflicts of interest: None reported.

Address correspondence to: Siriporn C. Chattipakorn, DDS, PhD, Department of Oral Biology and Diagnostic Sciences, Faculty of Dentistry, Chiang Mai University, Chiang Mai 50200, Thailand. E-mail: scchattipakorn@gmail.com; siriporn.c@cmu.ac.th

deleterious effects of cardiac I/R injury have been demonstrated in the brain of lean male rats as indicated by bloodbrain barrier (BBB) breakdown, increased brain oxidative stress, increased brain mitochondrial dysfunction, and an increased susceptibility to brain apoptosis.3 Furthermore, it has been shown that increased brain oxidative stress could cause Alzheimer's disease via increasing beta-amyloid (Aβ) production and reduced dendritic spine density. 4-6 In addition, recent studies have demonstrated that both obesity and estrogen deprivation significantly aggravated the severity of oxidative stress and myocardial damage in animal models of cardiac I/R injury. This increase in severity was indicated by increased cardiac malondialdehyde (MDA) level, increased cardiac mitochondrial dysfunction and cardiac calcium dysregulation, and impaired left ventricle (LV) function. 7-9 These findings suggest an influential role of female hormones and obesity on the adverse effects of the heart caused by I/R injury. Despite these findings on the heart, the effects of cardiac I/R injury on brain oxidative stress, AB production, and dendritic spine density in estrogen-deprived lean or obese rats have never been investigated.

Several studies have shown that estrogen has beneficial effects on cardiac I/R injury as indicated by reduced myocardial infarction and improved postischemic recovery after estrogen administration in in vitro, in vivo, and clinical studies. 8,10,11 Furthermore, our previous study found that an antidiabetic drug dipeptidyl peptidase-4 (DPP-4) inhibitor (Vildagliptin) attenuated the adverse effects of cardiac I/R injury in obese male rats, as indicated by decreased cardiac oxidative stress levels and improved cardiac mitochondrial function. 9 However, the potential benefits of either estrogen or DPP-4 inhibitor on brain oxidative stress levels, AB production, and dendritic spine density in a cardiac I/R injury model of lean or obese rats with an estrogen-deprived condition have never been determined. In this study, our hypothesis was that incidence of cardiac I/R injury aggravates brain oxidative stress level, increases AB production, and decreases dendritic spine density in both lean and obese rats with estrogen deprivation, and that administration of estrogen or DPP-4 inhibitor leads to an attenuation of these adverse effects in the brain.

#### **METHODS**

#### Animal models and experimental protocols

All experiments were conducted in accordance with the approved protocol from the Faculty of Medicine, Chiang Mai

University Institutional Animal Care and Use Committee, in compliance with NIH guidelines. Seventy-two female Wistar rats weighing 200 to 220 g (aged  ${\sim}6$  weeks old) were obtained from the National Animal Center, Salaya Campus, Mahidol University, Thailand. At baseline, there was no significant difference in weight between all groups. The mean body weights for normal diet (ND)-fed rats and high-fat diet (HF)-fed rats at baseline (week 0) were 213.50  $\pm$  2.98 g and 210.00  $\pm$  3.09 g, respectively. All animals were individually housed in a temperature-controlled environment with a 12:12 light-dark cycle. The experimental protocols were divided into two protocols.

In protocol 1 (Fig. 1A), 36 rats were randomly assigned to either the sham-operated group (S; n = 12) or the ovariectomized group (O; n = 24). One week after the surgery, the sham-operated group was fed with a normal diet (ND; NDS) for 12 weeks, whereas the ovariectomized group was further subdivided into two subgroups. Each of these subgroups received either a ND (NDO; n = 12) or a HF (HFO; n = 12) for 12 weeks. Animals in the HF group were fed a diet containing 59.3% total energy from fat, with the major component being saturated fatty acids from lard, as described in our previous study. <sup>12</sup> The animals were given ad libitum access to food and water. Body weight and food intake were

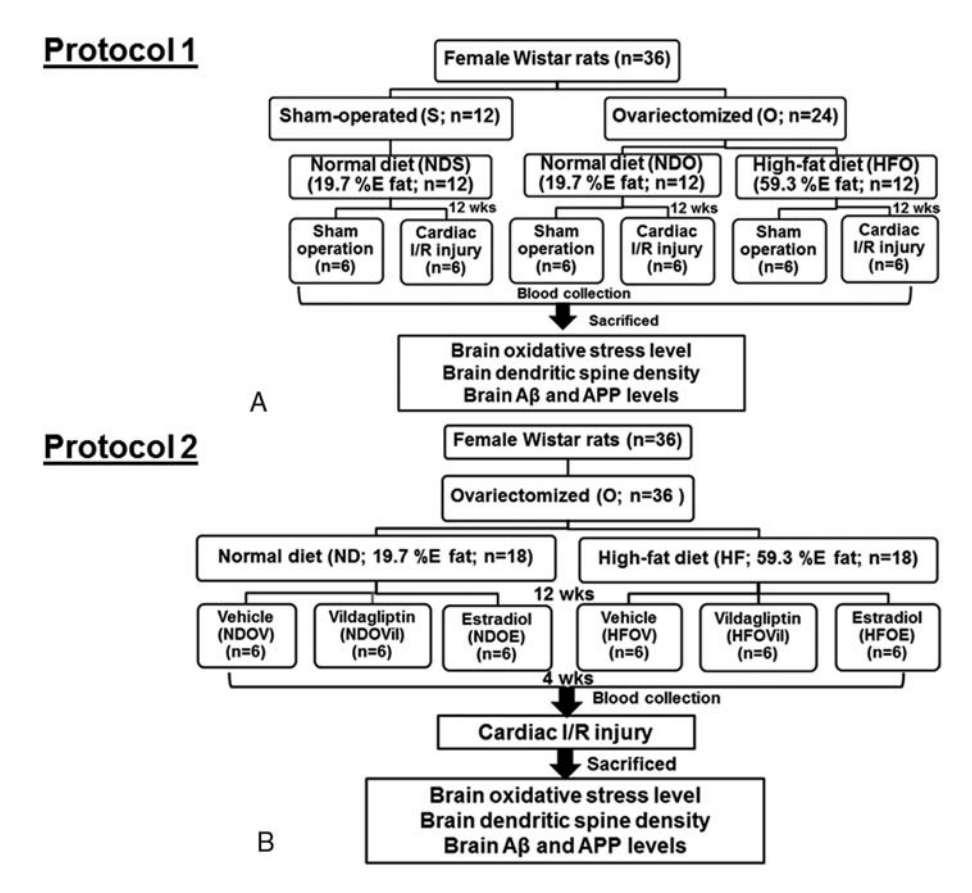


FIG. 1. Experimental protocol 1 (A) and protocol 2 (B) of the study. Aβ, beta-amyloid; APP, amyloid precursor protein; cardiac I/R, cardiac ischemia-reperfusion injury; HF, high-fat diet; HFO, ovariectomized HF-fed rats; HFOE, ovariectomized HF-fed rats with estradiol administration; HFOV, ovariectomized HF-fed rats with vehicle treatment; HFOVil, ovariectomized HF-fed rats with vildagliptin administration; ND, normal diet; NDO, ovariectomized ND-fed rats; NDOE, ovariectomized ND-fed rats with vehicle administration; NDOV, ovariectomized ND-fed rats with vildagliptin administration; NDOS, sham ND-fed rats; O, ovariectomy; S, sham-operated.

2

recorded daily. At the end of the dietary period, the animals were put into deep anesthesia using isoflurane after fasting for at least 5 hours. Blood samples were collected for determining metabolic parameters (glucose, total cholesterol, triglycerides, high-density lipoprotein [HDL], low-density lipoprotein [LDL], insulin), estrogen, and MDA levels. Finally, rats in each dietary group were further subdivided and either received a sham operation or had cardiac I/R injury (n = 6/ subgroup) instigated by left anterior descending (LAD) artery occlusion for 30 minutes, followed by 120-minute reperfusion. At the end of the protocol, animals were sacrificed by decapitation. Their brains were rapidly removed, and all brain tissues from all of the animals in this study were included in the various analyses. The left hemisphere of the brain was used to determine dendritic spine density by using Golgi staining method. The right hemisphere of the brain was used to determine the levels of brain oxidative stress by measuring MDA levels and Aβ protein by using western blot analysis. Total visceral fat, including peritoneal, periovarian, and perirenal fat pads, were removed and weighed.

In protocol 2 (Fig. 1B), 36 ovariectomized (O) rats were subdivided and were given either a ND (NDO; n = 18) or a HF (HFO; n = 18) for 12 weeks. At the end of week 13, the ovariectomized rats in each dietary group were further divided into three subgroups to receive one of the following daily: a vehicle (sesame oil in equal volume with estradiol [E<sub>2</sub>]) via subcutaneous injection (V; NDOV and HFOV; n = 6/subgroup); 50 µg/kg E<sub>2</sub> via subcutaneous injection (NDOE and HFOE; n = 6/subgroup; or 3 mg/kg DPP-4 inhibitor (Vildagliptin) via intragastric gavage (NDOVil and HFOVil; n = 6/subgroup) for 4 weeks. We chose these doses because previous studies have already demonstrated the beneficial effects of these doses on the improvement of peripheral insulin sensitivity, <sup>13,14</sup> brain insulin sensitivity, <sup>15,16</sup> and cardiac function <sup>14,17</sup> in both obese insulin-resistant model and ovariectomized model. In addition, previous studies found that only the highest dose of estrogen, which produced plasma E<sub>2</sub> levels above 250 pg/mL, could enhance dendritic spine density and cognitive function. 18,19 At the end of the experimental period (week 16), the animals were deeply anesthetized with isoflurane after fasting for at least 5 hours. Blood samples were collected to allow the determination of metabolic parameters (glucose, total cholesterol, triglycerides, HDL, LDL, insulin), estrogen and MDA levels. Finally, all of the rats were subjected to cardiac I/R injury by LAD artery occlusion for 30 minutes, followed by 120-minute reperfusion. At the end of the protocol, animals were sacrificed by decapitation. Their brains were rapidly removed, and all brain tissues from all of the animals in this study were included in the various analyses. The left hemisphere of the brain was used to determine dendritic spine density by using Golgi staining method. The right hemisphere of the brain was used to determine the levels of brain oxidative stress by measuring MDA levels and Aβ protein by using western blot analysis. Total visceral fat, including peritoneal, periovarian, and perirenal fat pads, were removed and weighed.

#### Ovariectomy procedure

The details of the ovariectomy procedure have been described previously. 15,20 Briefly, female rats were anesthetized by intramuscular injection with Xylazine (0.15 mg/kg; Laboratorios Calier, Barcelona, Spain) and Zoletil (50 mg/kg; Virbac Laboratories, Carros, France). After that, the bilateral ovariectomy was performed using double dorso-lateral skin incisions.

#### Cardiac ischemia-reperfusion injury protocol

The details of the cardiac I/R injury protocol have been described previously. Briefly, female rats were anesthetized by intramuscular injection with Xylazine (0.15 mg/kg; Laboratorios Calier, Barcelona, Spain) and Zoletil (50 mg/kg; Virbac Laboratories, Carros, France). The LAD coronary artery was ligated using a 5-0 silk suture underneath the LAD, near its origin at the aorta (approximately 2 mm distal to its origin). The end of a ligature was passed through a small vinyl tube, which is used to occlude the LAD by pulling the thread. Ischemia was confirmed by ST elevation. The heart was subjected to ischemia for 30 minutes, followed by 120-min reperfusion.

## Chemical analysis for assessment of insulin, glucose, triglyceride, cholesterol, LDL, HDL, and estrogen levels

Fasting plasma insulin levels were measured using a commercial sandwich ELISA kit (LINCO Research, MO). Fasting plasma glucose, triglyceride, cholesterol, LDL, and HDL concentrations were measured using commercially available colorimetric assay kits (ERBA diagnostic; Mannheim, Germany). Serum estrogen levels were determined using an enzyme immunoassay kit (Cayman chemical, Ann Arbor, MI). All chemical analyses used to identify metabolic parameters were performed in duplicate in the same assay. The coefficient of variation for the intra and inter assays were 6.67% and 12.54% for insulin; 5.31% and 4.54% for glucose; 8.43% and 11.55% for triglycerides; 4.84% and 8.48% for cholesterol; 7.66% and 10.80% for LDL; 3.45% and 5.30% for HDL; and 6.51% and 12.92% for estrogen, respectively.

#### **Determination of insulin resistance**

The Homeostasis Model Assessment (HOMA) index was calculated from fasting plasma insulin and fasting plasma glucose concentrations. <sup>21</sup> A higher HOMA index indicates a higher degree of insulin resistance.

#### Determination of malondialdehyde levels

Malondialdehyde levels were measured using a high-performance liquid chromatography (HPLC) method.<sup>22</sup> Briefly, serum and brain fractions were prepared by trichloroacetic acid (TCA) protein precipitation. The supernatant was mixed with thiobarbituric acid solution (TBA). MDA levels were measured using an HPLC system at 532 nm.

#### **Immunoblotting**

The details of the subsequent brain homogenates for immunoblotting have been described previously. 12 The whole brain in each conditioned group was homogenized. After that, the cytosol fractions were separated and used for further immunoblotting of the Aβ and amyloid precursor protein (APP) expression. Immunoblotting was conducted with rabbit antibodies for Aβ (1:1000; Santa Cruz Biotechnology, Santa Cruz, CA) and APP (1:1000; Merck Millipore Corporation, Darmstadt, Germany). The primary antibody was detected by horseradish peroxidase (HRP) conjugated antirabbit antibody (1:2000; Cell Signaling Technology, Beverly, MA) to measure Aβ expression, and HRP-conjugated antimouse antibody (1:2000; Cell Signaling Technology, MA) to measure APP expression. The protein bands were visualized on Amersham Hyperfilm Enhanced Chemiluminescence (GE Healthcare, Buckinghamshire, UK).

#### Golgi impregnation and analysis

The details of dendritic spine density analysis have been described previously. After decapitation, the brains were processed for Golgi staining using a commercially available kit (FD Neurotechnologies kit, PK 401, Ellicott City, MD). For the dendritic spine density analysis, three segments from a pyramidal cell in the CA1 area of the hippocampus (three slices/animal, n=6 animals/group) were randomly measured using the Xcellence imaging software (Olympus, Tokyo, Japan).

#### Statistical analysis

Data were presented as mean ± SEM. All statistical analyses were performed using the program SPSS (version 16; SPSS, Chicago, IL). In protocol 1, the two-way analysis of variance (ANOVA) (diet × surgery) and post-hoc analysis with Fisher's tests were used to test significant differences for all comparisons. Independent Student's test was used to test between sham operation and cardiac I/R injury condition in the same diet and surgery groups. In protocol 2, a two-way ANOVA (diet × treatment) and post-hoc analysis with

Fisher's tests were used to test significant differences for all comparisons. *P* value less than 0.05 was statistically significant.

#### **RESULTS**

Obesity aggravated the peripheral insulin resistance and dyslipidemia in ovariectomized rats, and both vildagliptin and estradiol administrations attenuated these metabolic impairments

Ovariectomized ND-fed rats displayed peripheral insulin resistance as demonstrated by significantly increased fasting plasma insulin levels, fasting plasma glucose levels, and HOMA index when compared with the sham-operated NDfed rats (Table 1). In addition, HF consumption increased the severity of peripheral insulin resistance and dyslipidemia in the ovariectomized group, as shown by significantly increased fasting plasma glucose levels, HOMA index, body weight, visceral fat, fasting plasma cholesterol, and LDL levels, when compared with ovariectomized ND-fed rats (Table 1). Interestingly, the administration of either vildagliptin or E<sub>2</sub> led to a significant decrease in the severity of peripheral insulin resistance and dyslipidemia in ovariectomized ND-fed rats and ovariectomized HF-fed rats (Table 1). The uterine weight and serum estrogen levels significantly decreased in all ovariectomized rats, confirming the effectiveness of estrogen deprivation via bilateral ovariectomy (Table 1).

# The effects of cardiac I/R injury on brain pathological conditions in both ovariectomized ND-fed rats and HF-fed rats

We found that estrogen deprivation by ovariectomy increased serum and brain oxidative stress levels in the ND-fed rats, as indicated by increased serum and brain MDA levels. In addition, HF-induced obesity showed a correlation with an increase in the severity of serum and brain oxidative stress levels in the ovariectomized group (Table 1, Fig. 2A). Interestingly, we found that cardiac I/R

| <b>TABLE</b> | 1. | Metabolic | parameters | after | vildagliptin | and | estradiol | treatment |
|--------------|----|-----------|------------|-------|--------------|-----|-----------|-----------|
|--------------|----|-----------|------------|-------|--------------|-----|-----------|-----------|

|                        |                   | Norm                | al diet             | High-fat diet       |                         |                       |                       |  |
|------------------------|-------------------|---------------------|---------------------|---------------------|-------------------------|-----------------------|-----------------------|--|
| Parameters             | NDS               | NDOV                | NDOVil              | NDOE                | HFOV                    | HFOVil                | HFOE                  |  |
| Body weight, g         | $290 \pm 13$      | $342 \pm 7^{a}$     | $340 \pm 11^{a}$    | $302 \pm 9^{b}$     | $398 \pm 11^{a,b}$      | $401 \pm 5^{a,b}$     | $346 \pm 4^{a,c}$     |  |
| Visceral fat, g        | $16 \pm 1$        | $16 \pm 2$          | $13 \pm 1$          | $12 \pm 2$          | $31 \pm 2^{a,b}$        | $31 \pm 3^{a,b}$      | $19 \pm 2^{c}$        |  |
| Uterine mass, g        | $0.40\pm0.02$     | $0.08 \pm 0.0^{a}$  | $0.07 \pm 0.0^{a}$  | $0.41 \pm 0.02^{b}$ | $0.06 \pm 0.0^{a}$      | $0.06 \pm 0.0^{a}$    | $0.38 \pm 0.02^{c}$   |  |
| Plasma estrogen, pg/mL | $121 \pm 10$      | $59 \pm 7^{a}$      | $60 \pm 7^{a}$      | $252 \pm 32^{b}$    | $65 \pm 12^{a}$         | $53 \pm 11^{a}$       | $249 \pm 38^{c}$      |  |
| Glucose, mg%           | $132.61 \pm 2.73$ | $185.77 \pm 3.61^a$ | $134.04 \pm 3.97^b$ | $134.43 \pm 3.92^b$ | $239.89 \pm 5.81^{a,b}$ | $151.66 \pm 5.31^{c}$ | $158.32 \pm 6.47^{c}$ |  |
| Insulin, ng/mL         | $1.13 \pm 0.08$   | $2.97 \pm 0.35^a$   | $1.12 \pm 0.06^b$   | $1.17 \pm 0.06^b$   | $3.15 \pm 0.39^a$       | $1.13 \pm 0.10^{c}$   | $1.30 \pm 0.04^{c}$   |  |
| HOMA index             | $9.32 \pm 0.83$   | $32.27 \pm 3.76^a$  | $8.97 \pm 0.62^b$   | $9.13 \pm 0.51^b$   | $43.96 \pm 4.90^{a,b}$  | $10.04 \pm 0.79^{c}$  | $12.15 \pm 0.66^{c}$  |  |
| Triglyceride, mg%      | $56.01 \pm 4.97$  | $54.62 \pm 6.05$    | $54.80 \pm 5.18$    | $51.20 \pm 5.52$    | $56.94 \pm 4.95$        | $52.11 \pm 6.77$      | $52.37 \pm 4.00$      |  |
| Cholesterol, mg%       | $72.95 \pm 3.71$  | $97.98 \pm 4.16^a$  | $81.96 \pm 5.58$    | $83.96 \pm 5.17$    | $154.75 \pm 6.97^{a,b}$ | $145.11 \pm 12.67$    | $140.98 \pm 8.51$     |  |
| LDL, mg/dL             | $29.17 \pm 2.13$  | $55.61 \pm 3.75^a$  | $30.59 \pm 5.95^b$  | $30.96 \pm 6.93^b$  | $118.27 \pm 5.65^{a,b}$ | $90.01 \pm 15.37^{c}$ | $91.38 \pm 7.31^{c}$  |  |
| HDL, mg/dL             | $41.79 \pm 2.78$  | $32.36 \pm 1.74^a$  | $42.04 \pm 1.94^b$  | $39.98 \pm 1.94^b$  | $29.16 \pm 2.53^a$      | $43.78 \pm 3.97^{c}$  | $39.128 \pm 3.45^{c}$ |  |
| Serum MDA, μM          | $5.64 \pm 0.27$   | $6.41 \pm 0.16^a$   | $5.43 \pm 0.27^b$   | $5.94 \pm 0.26^b$   | $7.13 \pm 0.25^{a,b}$   | $5.73 \pm 0.23^{c}$   | $5.42 \pm 0.44^{c}$   |  |

HDL, high-density lipoprotein; HF, high-fat diet; HFOE, ovariectomized HF-fed rats with estradiol administration; HFOV, ovariectomized HF-fed rats with vehicle treatment; HFOVil, ovariectomized HF-fed rats with vildagliptin administration; HOMA, Homeostasis Model Assessment; LDL, low-density lipoprotein; MDA; malondialdehyde; ND, normal diet; NDOE, ovariectomized ND-fed rats with estradiol administration; NDOV, ovariectomized ND-fed rats with vildagliptin administration; NDS, sham ND-fed rats.

 $<sup>^{</sup>a}P < 0.05$  from NDS.

 $<sup>^</sup>bP$  < 0.05 from NDOV.

 $<sup>^{</sup>c}P < 0.05$  from HFOV (n = 6/group).

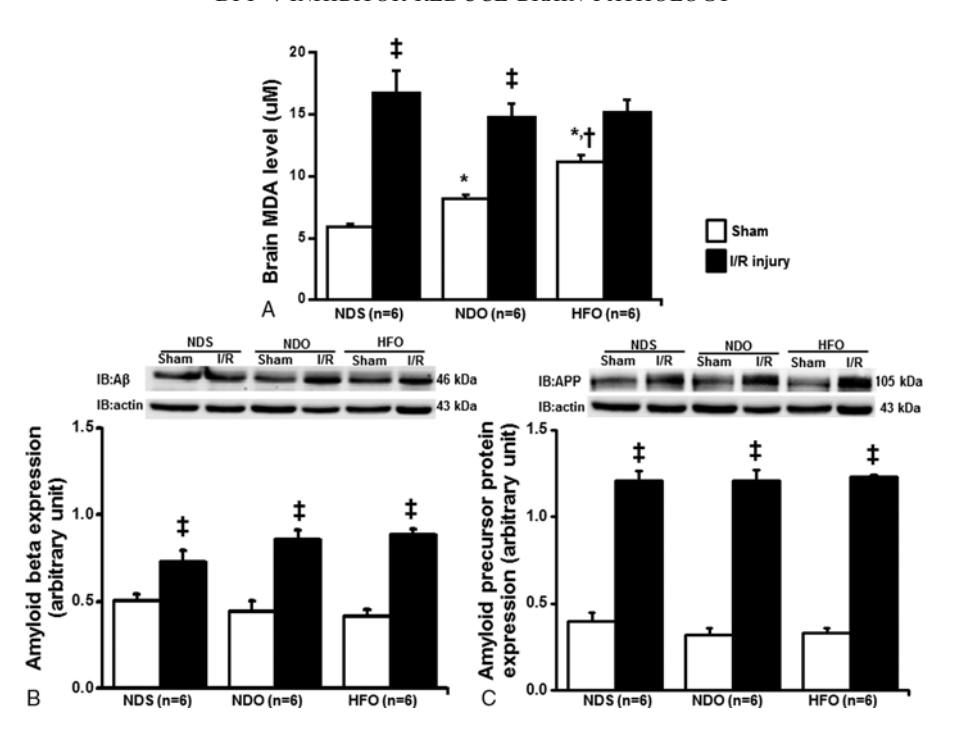
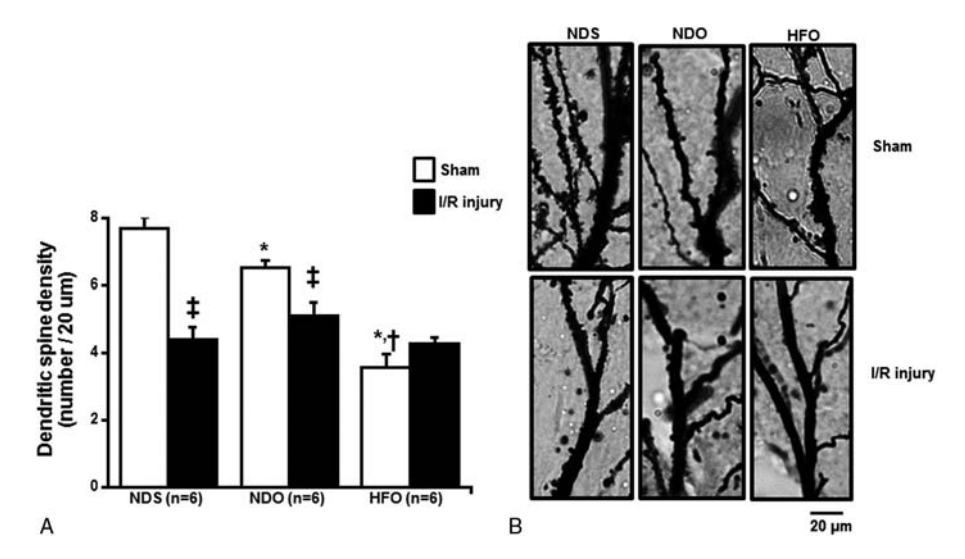


FIG. 2. The effects of cardiac I/R injury on malondialdehyde (MDA) levels (**A**), beta-amyloid (Aβ) levels (**B**), and amyloid precursor protein (APP) levels (**C**) in brains harvested from the NDS, NDO, and HFO rats with sham or cardiac I/R injury.  $^*P < 0.05$  compared with NDO;  $^\dagger P < 0.05$  compared with sham; n = 6/group. HF, high-fat diet; HFO, ovariectomized HF-fed rats; I/R injury, ischemia-reperfusion injury; ND, normal diet; NDO, ovariectomized ND-fed rats; NDS, sham ND-fed rats; Sham, sham operation.

injury alone led to increased brain oxidative stress levels in the ND-fed rats, when compared with ND-fed rats with noncardiac I/R injury (Fig. 2A). Under conditions of estrogen-deprivation, cardiac I/R injury aggravated brain oxidative stress levels in the ND-fed rats, but not in the HF-fed rats, when compared with the sham group (P < 0.05; Fig. 2A).

In addition, we found that estrogen-deprivation in both ND-fed rats and HF-fed rats did not cause the accumulation of  $A\beta$  and APP levels in the brains of noncardiac I/R injury (Fig. 2B and C). However, an increase in the  $A\beta$  and APP protein expression in the brains of all groups occurred to a similar degree after cardiac I/R injury (Fig. 2B and C), indicating that cardiac I/R injury caused the accumulation of  $A\beta$  and APP in



**FIG. 3.** The effects of cardiac I/R injury on (**A**) the number of dendritic spines on tertiary apical dendrites in brains harvested from the NDS, NDO, and HFO rats with sham or cardiac I/R injury; (**B**) a picture of a representative dendritic spines from the NDS, NDO, and HFO rats with sham or cardiac I/R injury. \*P < 0.05 compared with NDS;  $^{\dagger}P < 0.05$  compared with NDO;  $^{\dagger}P < 0.05$  compared with sham; n = 6/group. HF, high-fat diet; HFO, ovariectomized HF-fed rats; I/R injury, ischemia-reperfusion injury; ND, normal diet; NDO, ovariectomized ND-fed rats; NDS, sham ND-fed rats; Sham, sham operation.

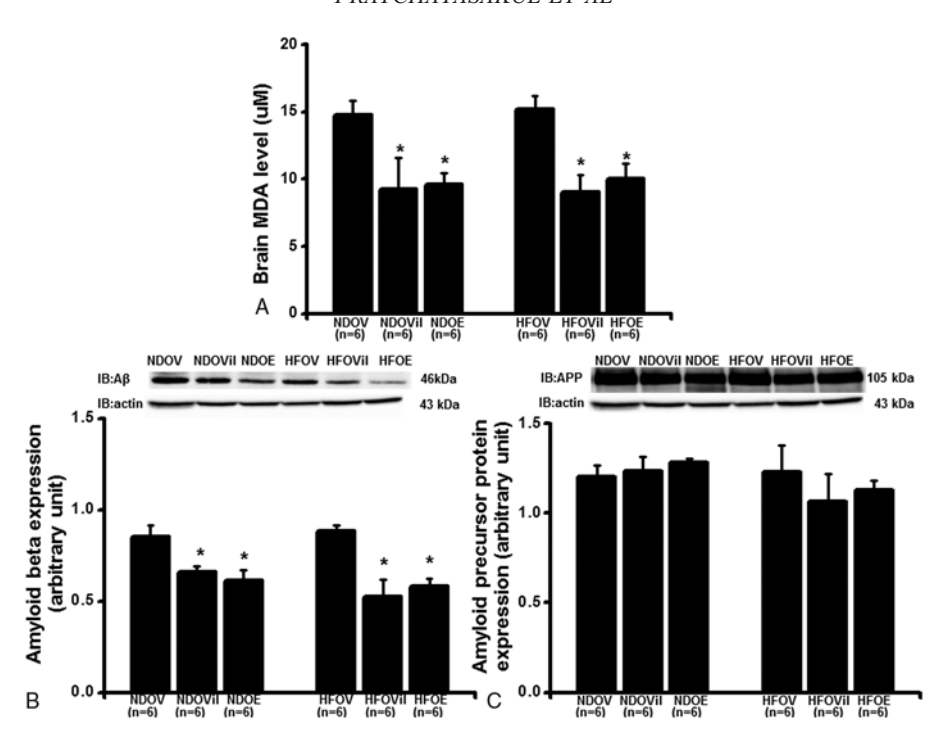


FIG. 4. The effects of vildagliptin and estrogen administration on malondialdehyde (MDA) levels (**A**), the beta-amyloid (Aβ) levels (**B**), and amyloid precursor protein (APP) levels (**C**) in brains harvested from the NDOV, NDOVil, NDOE, HFOV, HFOVil, and HFOE rats.  $^*P < 0.05$  compared with vehicle group; n = 6/group. HF, high-fat diet; HFOE, ovariectomized HF-fed rats with estradiol administration; HFOV, ovariectomized HF-fed rats with vehicle treatment; HFOVil, ovariectomized HF-fed rats with vildagliptin administration; ND, normal diet; NDOE, ovariectomized ND-fed rats with vehicle administration; NDOVil, ovariectomized ND-fed rats with vildagliptin administration.

the sham-operated ND-fed rats, ovariectomized ND-fed rats, and ovariectomized HF-fed rats.

Results also showed that estrogen deprivation decreased the density of dendritic spines in the CA1 area of the hippocampus in the sham-operated ND-fed rats (Fig. 3A and B). In addition, obesity significantly aggravated the reduction of dendritic spine density in the sham-operated ovariectomized group (Fig. 3A and B). Interestingly, we found that cardiac I/R injury alone caused the reduction of dendritic spine density in the ND-fed rats. In the estrogen-deprived condition, cardiac I/R injury aggravated the reduction of dendritic spine density in the ND-fed rats, but not in the HF-fed rats (P < 0.05; Fig. 3A and B).

# The effect of either vildagliptin or estradiol administration on brain oxidative stress, $A\beta$ , and APP expression in both ovariectomized ND-fed rats and HF-fed rats with cardiac I/R injury

Either vildagliptin or  $E_2$  administrations led to an equally reduced brain MDA level in both the ovariectomized ND-fed rats and ovariectomized HF-fed rats with cardiac I/R injury (P < 0.05; Fig. 4A), indicating that either vildagliptin or  $E_2$  led to reduced brain oxidative stress levels in both the ovariectomized ND-fed rats and the ovariectomized HF-fed rats with cardiac I/R injury.

Either vildagliptin or  $E_2$  administration showed a correlation with equally reduced A $\beta$  protein expression in the brains harvested from both ovariectomized ND-fed rats and the ovariectomized HF-fed rats with cardiac I/R injury (P < 0.05; Fig. 4B), indicating that either vildagliptin or  $E_2$ 

reduced A $\beta$  production in both the ovariectomized ND-fed rats and the ovariectomized HF-fed rats with cardiac I/R injury. However, neither treatment reduced APP expression in both the ovariectomized ND-fed rats and the ovariectomized HFD-fed rats with cardiac I/R injury (Fig. 4C).

# The effects of either vildagliptin or estradiol administration on dendritic spine density in both ovariectomized ND-fed rats and HF-fed rats with cardiac I/R injury

Either vildagliptin or  $E_2$  administration led to an equal increase in the number of dendritic spines in the CA1 area of the hippocampus of both ovariectomized ND-fed rats and the ovariectomized HF-fed rats with cardiac I/R injury (P < 0.05; Fig. 5A and B), indicating that either vildagliptin or  $E_2$  treatment led to improved dendritic spine density in both the ovariectomized ND-fed rats and the ovariectomized HF-fed rats with cardiac I/R injury.

#### DISCUSSION

The major findings of the present study are as follows: (1) estrogen deprivation caused the reduction in dendritic spine density and increased brain oxidative stress levels; (2) obesity aggravated the reduction in dendritic spine density and increased brain oxidative stress levels in estrogen-deprived rats; (3) cardiac I/R injury alone caused the reduction of dendritic spines and increased brain oxidative stress levels in sham-operated ND-fed rats; (4) in the estrogen-deprived condition, cardiac I/R injury aggravated dendritic spine loss

**6** M

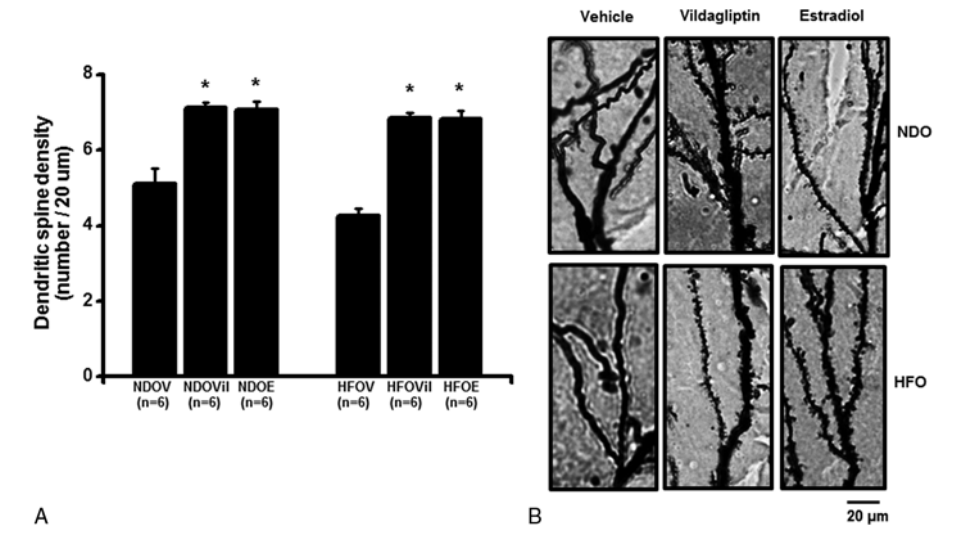


FIG. 5. The effects of vildagliptin and estrogen administration on (A) the number of dendritic spines on tertiary apical dendrites in brains harvested from the NDOV, NDOVII, NDOE, HFOV, HFOVII, and HFOE rats; (B) a picture of a representative dendritic spines from the NDOV, NDOVII, NDOE, HFOV, HFOVil, and HFOE rats. \*P < 0.05 compared with the vehicle group; n = 6/group. HF, high-fat diet; HFOE, ovariectomized HF-fed rats with estradiol administration; HFOV, ovariectomized HF-fed rats with vehicle treatment; HFOVil, ovariectomized HF-fed rats with vildagliptin administration; ND, normal diet; NDOE, ovariectomized ND-fed rats with estradiol administration; NDOV, ovariectomized ND-fed rats with vehicle administration; NDOVil, ovariectomized ND-fed rats with vildagliptin administration; NDO, ovariectomized ND-fed rats; HFO, ovariectomized HF-fed rats.

and the rise in brain oxidative stress levels in ND-fed rats, but not in HF-fed rats; (5) neither obesity or estrogen deprivation without cardiac I/R injury increased Aβ or APP levels; (6) cardiac I/R injury caused the accumulation of Aβ and APP in all groups; (7) and estrogen and DPP-4 inhibitor treatments equally attenuated brain oxidative stress levels, decreased AB production, and increased dendritic spine density in the ovariectomized ND-fed rats and the ovariectomized HF-fed rats with cardiac I/R injury.

Our findings showed that ovariectomy increased peripheral insulin resistance, brain oxidative stress levels, and dendritic spine loss, and obesity aggravated these impairments in ovariectomized rats. Previous studies have demonstrated that peripheral insulin resistance and oxidative stress are known to play an important role in the impairment of dendritic spine density via the reduction of brain-derived neurotrophic factor (BDNF) level and excessive synaptic depression. 5,24 As a result, the highest levels of peripheral insulin resistance and brain oxidative stress found in ovariectomized HF-fed rats in this study could lead to a marked increase in dendritic spine loss, when compared with the sham-operated ND-fed rats and the ovariectomized ND-fed rats.

This is also the first study to demonstrate that cardiac I/R injury aggravated brain oxidative stress, increased AB protein expression, increased APP protein expression, and decreased dendritic spine density as observed in the sham-operated ND-fed rats (Figs. 2 and 3). It has been demonstrated that excessive brain oxidative stress levels cause cognitive decline via increased AB production, which leads to decreased dendritic spine density in Alzheimer's diseases. 4-6 As a result, cardiac I/R injury by itself, in sham-operated ND-fed rats, could cause increased brain oxidative stress levels, leading to

increased AB and APP production, and decreased dendritic spine density, as found in this study. Under conditions of estrogen deprivation, our results showed that cardiac I/R injury aggravates this brain toxicity only in ND-fed rats, but not in HF-fed rats. The possible explanation could be due to the severity of brain toxicity in ovariectomized HF-fed rats, which may have already reached maximum levels, before cardiac I/R injury occurred. This is supported by the findings that the levels of oxidative stress was more severe in ovariectomized HF-fed rats, compared with ovariectomized NDfed rats, even before cardiac I/R injury.

Interestingly, under conditions of cardiac I/R injury, we found that E<sub>2</sub> and vildagliptin treatments significantly reduced brain oxidative stress, Aβ production, and increased dendritic spine density in both ovariectomized ND-fed rats and HF-fed rats (Figs. 4 and 5). Both E<sub>2</sub> and vildagliptin have been shown to exert antioxidant effects in several models including conditions of obesity, ovariectomy, and cardiac I/R injury. 25-27 Therefore, E<sub>2</sub> and vildagliptin could have acted as antioxidant agents, thus decreasing brain oxidative stress levels in ovariectomized NDfed rats and HF-fed rats with cardiac I/R injury. This decrement caused the reduction in AB production in the brain, which ultimately leads to the prevention of dendritic spine loss.

#### Potential clinical value

The objective of this animal model was to understand brain pathology (brain oxidative stress, AB production, and dendritic spine loss) caused by cardiac I/R injury in both lean and obese estrogen-deprived models. Cardiac I/R injury is a common pathological state that occurs in postmenopausal women. This study demonstrated that it can lead to not only myocardial damage but also increased brain pathology. In addition, the severity of brain pathology after cardiac I/R injury is associated with obesity, and also estrogen deprivation. This study is the first to report that pharmacological interventions by either estrogen or DPP-4 inhibitor share a similar efficacy in reducing brain pathology caused by cardiac I/R injury in both lean and obese estrogen-deprived model.

#### Limitations

The limitation of the present study was the lack of investigation into the effects of aged rats on brain pathology caused by cardiac I/R injury in both lean and obese estrogen-deprived model. It is known that ageing affected brain function.<sup>28,29</sup> However, since the main purpose of the present study was to determine the effect of cardiac I/R injury on brain functions in models of estrogen deprivation with or without obesity, we therefore did not use aged rats, so that the ageing-related confounding factors other than estrogen deprivation could be limited. Another limitation of the present study was the lack of investigation into cognitive function. However, previous studies from our group and others already reported the cognitive decline in obesity, and also estrogen-deprived models. 19,20,30

Furthermore, the phytoestrogen-free chow was not used in this study. However, this small amount of phytoestrogen in our rat chow did not affect serum estrogen levels, which was indicated by a decrease in uterine weight and serum estrogen levels in ovariectomized ND-fed rats. In addition, the HF used in our study also contained similar small amount of phytoestrogen as in the normal-diet chow.

#### **CONCLUSIONS**

Our findings demonstrate that cardiac I/R injury itself could cause an increase in brain oxidative burst and a reduction in dendritic spines. In conditions of estrogen deprivation, cardiac I/R injury aggravates brain oxidative stress and increases dendritic spine loss. However, estrogen deprivation with obese-insulin resistance already causes the severest brain toxicity, and therefore is no further affected by the cardiac I/R injury. Since estrogen and DPP-4 inhibitor treatments share similar efficacy on brain protection affected by cardiac I/R injury, DPP-4 inhibitor may be considered as an alternative drug to estrogen replacement in those who have contraindications to the use of estrogen.

#### REFERENCES

- 1. Nour M, Scalzo F, Liebeskind DS. Ischemia-reperfusion injury in stroke. Interv Neurol 2013;1:185-199.
- 2. Kalogeris T, Baines CP, Krenz M, Korthuis RJ. Cell biology of ischemia/ reperfusion injury. Int Rev Cell Mol Biol 2012;298:229-317.
- 3. Kumfu S, Charununtakorn ST, Jaiwongkam T, Chattipakorn N, Chattipakorn SC. Humanin prevents brain mitochondrial dysfunction in a cardiac ischaemia-reperfusion injury model. Exp Physiol 2016; 101:697-707.
- 4. Texel SJ, Mattson MP. Impaired adaptive cellular responses to oxidative stress and the pathogenesis of Alzheimer's disease. Antioxid Redox Signal 2011:14:1519-1534.
- 5. Yu W, Lu B. Synapses and dendritic spines as pathogenic targets in Alzheimer's disease. Neural Plast 2012;2012:247150.

- 6. Butterfield DA, Reed T, Newman SF, Sultana R. Roles of amyloid betapeptide-associated oxidative stress and brain protein modifications in the pathogenesis of Alzheimer's disease and mild cognitive impairment. Free Radic Biol Med 2007;43:658-677.
- 7. Ross JL, Howlett SE. Age and ovariectomy abolish beneficial effects of female sex on rat ventricular myocytes exposed to simulated ischemia and reperfusion. PloS One 2012;7:e38425.
- Sivasinprasasn S, Shinlapawittayatorn K, Chattipakorn SC, Chattipakorn N. Estrogenic impact on cardiac ischemic/reperfusion injury. J Cardiovasc Transl Res 2016;9:23-39.
- 9. Apaijai N, Chinda K, Palee S, Chattipakorn S, Chattipakorn N. Combined vildagliptin and metformin exert better cardioprotection than monotherapy against ischemia-reperfusion injury in obese-insulin resistant rats. PloS One 2014;9:e102374.
- Wang Y, Wang Q, Zhao Y, et al. Protective effects of estrogen against reperfusion arrhythmias following severe myocardial ischemia in rats. Circ J 2010;74:634-643.
- 11. Li WL, Xiang W, Ping Y. Activation of novel estrogen receptor GPER results in inhibition of cardiocyte apoptosis and cardioprotection. Mol Med Rep 2015;12:2425-2430.
- 12. Pratchayasakul W, Kerdphoo S, Petsophonsakul P, Pongchaidecha A, Chattipakorn N, Chattipakorn SC. Effects of high-fat diet on insulin receptor function in rat hippocampus and the level of neuronal corticosterone. Life Sci 2011:88:619-627.
- 13. Bryzgalova G, Lundholm L, Portwood N, et al. Mechanisms of antidiabetogenic and body weight-lowering effects of estrogen in high-fat diet-fed mice. Am J Physiol Endocrinol Metab 2008;295:E904-E912.
- 14. Apaijai N, Inthachai T, Lekawanvijit S, Chattipakorn SC, Chattipakorn N. Effects of dipeptidyl peptidase-4 inhibitor in insulin-resistant rats with myocardial infarction. J Endocrinol 2016;229:245-258.
- 15. Pratchayasakul W, Chattipakorn N, Chattipakorn SC. Estrogen restores brain insulin sensitivity in ovariectomized non-obese rats, but not in ovariectomized obese rats. Metabolism 2014;63:851-859.
- 16. Pintana H, Pongkan W, Pratchayasakul W, Chattipakorn N, Chattipakorn SC. Dipeptidyl peptidase 4 inhibitor improves brain insulin sensitivity, but fails to prevent cognitive impairment in orchiectomy obese rats. J Endocrinol 2015;226:M1-M11.
- 17. Sivasinprasasn S, Sa-Nguanmoo P, Pongkan W, Pratchayasakul W, Chattipakorn SC, Chattipakorn N. Estrogen and DPP4 inhibitor, but not metformin, exert cardioprotection via attenuating cardiac mitochondrial dysfunction in obese insulin-resistant and estrogen-deprived female rats. Menopause 2016;23:894-902.
- 18. Gould E, Woolley CS, Frankfurt M, McEwen BS. Gonadal steroids regulate dendritic spine density in hippocampal pyramidal cells in adulthood. J Neurosci 1990;10:1286-1291.
- 19. Leuner B, Mendolia-Loffredo S, Shors TJ. High levels of estrogen enhance associative memory formation in ovariectomized females. Psychoneuroendocrinology 2004;29:883-890.
- 20. Pratchayasakul W, Sa-Nguanmoo P, Sivasinprasasn S, et al. Obesity accelerates cognitive decline by aggravating mitochondrial dysfunction, insulin resistance and synaptic dysfunction under estrogen-deprived conditions. Horm Behav 2015;72:68-77.
- 21. Matthews DR, Hosker JP, Rudenski AS, Naylor BA, Treacher DF, Turner RC. Homeostasis model assessment: insulin resistance and beta-cell function from fasting plasma glucose and insulin concentrations in man. Diabetologia 1985;28:412-419.
- 22. Candan N, Tuzmen N. Very rapid quantification of malondialdehyde (MDA) in rat brain exposed to lead, aluminium and phenolic antioxidants by high-performance liquid chromatography-fluorescence detection. Neurotoxicology 2008;29:708-713.
- 23. Sripetchwandee J, Pipatpiboon N, Pratchayasakul W, Chattipakorn N, Chattipakorn SC. DPP-4 inhibitor and PPARgamma agonist restore the loss of CA1 dendritic spines in obese insulin-resistant rats. Arch Med Res 2014;45:547-552.
- 24. Stranahan AM, Norman ED, Lee K, et al. Diet-induced insulin resistance impairs hippocampal synaptic plasticity and cognition in middle-aged rats. Hippocampus 2008:18:1085-1088.
- 25. Moosmann B, Behl C. The antioxidant neuroprotective effects of estrogens and phenolic compounds are independent from their estrogenic properties. Proc Natl Acad Sci USA 1999;96:8867-8872.
- 26. Abdelsalam RM, Safar MM. Neuroprotective effects of vildagliptin in rat rotenone Parkinson's disease model: role of RAGE-NFkappaB and Nrf2antioxidant signaling pathways. J Neurochem 2015;133:700-707.

- 27. El Batsh MM, El Batch MM, Shafik NM, Younos IH. Favorable effects of vildagliptin on metabolic and cognitive dysfunctions in streptozotocininduced diabetic rats. Eur J Pharmacol 2015;769:297-305.
- 28. Smith CC, Vedder LC, Nelson AR, Bredemann TM, McMahon LL. Duration of estrogen deprivation, not chronological age, prevents estrogen's ability to enhance hippocampal synaptic physiology. Proc Natl Acad Sci U S A 2010;107:19543-19548.
- 29. Lagunas N, Calmarza-Font I, Diz-Chaves Y, Garcia-Segura LM. Longterm ovariectomy enhances anxiety and depressive-like behaviors in mice submitted to chronic unpredictable stress. *Horm Behav* 2010;58:786-791.
- 30. Pintana H, Apaijai N, Pratchayasakul W, Chattipakorn N, Chattipakorn SC. Effects of metformin on learning and memory behaviors and brain mitochondrial functions in high fat diet induced insulin resistant rats. Life Sci 2012;91:409-414.



Received: 26 September 2016 Accepted: 07 February 2017 Published: 10 March 2017

# **OPEN** DPP-4 Inhibitor and Estrogen **Share Similar Efficacy Against Cardiac Ischemic-Reperfusion Injury** in Obese-Insulin Resistant and **Estrogen-Deprived Female Rats**

Sivaporn Sivasinprasasn<sup>1,2,3,4</sup>, Pongpan Tanajak<sup>1,3,4</sup>, Wanpitak Pongkan<sup>1,3,4</sup>, Wasana Pratchayasakul<sup>1,3,4</sup>, Siriporn C. Chattipakorn<sup>1,4,5</sup> & Nipon Chattipakorn<sup>1,3,4</sup>

Estrogen deprivation aggravates cardiac injury after myocardial ischemia and reperfusion (I/R) injury. Although either estrogen or the dipeptidyl peptidase-4 (DPP-4) inhibitor, vildagliptin, reduces myocardial damage following cardiac I/R, their effects on the heart in obese-insulin resistant and estrogen deprived conditions remain unknown. Ovariectomized (O) rats (n = 36) were divided to receive either normal diet (NDO) or high-fat diet (HFO) for 12 weeks, followed by treatment with a vehicle, estrogen or vildagliptin for 4 weeks. The setting of in vivo cardiac I/R injury, 30-min ischemia and 120min reperfusion, was performed. At 12 weeks after ovariectomy, both NDO and HFO rats exhibited an obese-insulin resistant condition. Both NDO and HFO rats treated with estrogen and vildagliptin showed reduced fasting plasma glucose, insulin and HOMA index. Both treatments improved cardiac function indicated by restoration of heart rate variability and increased %left ventricular ejection fraction (%LVEF). The treatments similarly protected cardiac mitochondrial function against I/R injury, leading to a reduction in the infarct size, oxidative stress and apoptosis in the ischemic myocardium. These findings demonstrate that vildagliptin effectively improves metabolic status, and shares similar efficacy to estrogen in reducing myocardial infarction and protecting cardiac mitochondrial function against I/R injury in estrogen-deprived obese-insulin resistant rats.

Cardiovascular disease (CVD) remains the major cause of mortality in both genders and accounts for 17.3 million deaths per year<sup>1</sup>. Coronary heart disease accounts for the highest percentage of deaths attributes to cardiovascular disease<sup>1</sup>. The incidence of CVD in women is lower than that in men, but this gender disparity is gradually reversed after the onset of menopause<sup>2</sup>. Estrogen deprivation from a bilateral ovariectomy (OVX) in women also causes an increase in mortality from CVD and an estradiol replacement can reduce the mortality risk indicating the impact of female sex hormone deprivation on heart problems<sup>3</sup>. Endogenous estrogen deficiency has been shown to result in more severe cardiac tissue damage and dysfunction after myocardial ischemia and reperfusion (I/R)4. In OVX animals which underwent cardiac I/R, cardiac mitochondria were damaged and disrupted to a greater extent than non-OVX animals, leading to decreased mitochondrial function when compared to intact ones<sup>4</sup>. Moreover, menopause is also associated with an increase in body weight, visceral fat weight, total cholesterol, LDL cholesterol, triglycerides and systolic blood pressure, all factors contributing to an increase in risk of metabolic syndrome<sup>5</sup>. The presence of metabolic syndrome could increase the risk of the development of cardiovascular disease, especially coronary artery disease and myocardial ischemia, which is the leading cause of mortality of women in many countries<sup>6</sup>.

<sup>1</sup>Cardiac Electrophysiology Research and Training Center, Faculty of Medicine, Chiang Mai University, Chiang Mai, 50200, Thailand. <sup>2</sup>School of Medicine, Mae Fah Luang University, Chiang Rai, 57100, Thailand. <sup>3</sup>Cardiac Electrophysiology Unit, Department of Physiology, Faculty of Medicine, Chiang Mai University, Chiang Mai, 50200, Thailand. 4Center of Excellence in Cardiac Electrophysiology Research, Chiang Mai University, Chiang Mai, Thailand. Department of Oral Biology and Diagnostic Science, Faculty of Dentistry, Chiang Mai University, Chiang Mai, 50200, Thailand. Correspondence and requests for materials should be addressed to N.C. (email: nchattip@qmail.com)

|                         |                 |                | NDO                       |                          | НГО                                     |                            |                            |  |  |  |
|-------------------------|-----------------|----------------|---------------------------|--------------------------|---|----------------------------|----------------------------|--|--|--|
| Parameters              | NDS             | Ve             | E                         | Vil                      | Ve                                      | E                          | Vil                        |  |  |  |
| Body weight (g)         | $300\pm14$      | 338 ± 7*       | $304\pm8^{\dagger}$       | 333±11*                  | $393\pm10^{\dagger}$                    | $351 \pm 6^{\ddagger}$     | 394±8                      |  |  |  |
| Visceral fat (g)        | $14.7 \pm 1.4$  | $14.5 \pm 1.7$ | $11.2 \pm 1.8$            | $12.0 \pm 1.0$           | $30.8\pm1.7^{\dagger}$                  | $20.5 \pm 2.3^{\ddagger}$  | 29.1 ± 2.9                 |  |  |  |
| Uterus weight (g)       | $0.38 \pm 0.0$  | 0.07 ± 0.0*    | $0.40\pm0.0^{\dagger}$    | 0.06 ± 0.0*              | $0.06 \pm 0.0$                          | $0.36\pm0.0^{\ddagger}$    | $0.06 \pm 0.0$             |  |  |  |
| Glucose (mg/dl)         | $130.7 \pm 2.3$ | 184.2 ± 3.5*   | $134.4 \pm 3.9^{\dagger}$ | $134.0\pm3.9^{\dagger}$  | $233.4\pm4.5^{\dagger}$                 | $147.1 \pm 4.6^{\ddagger}$ | $148.5 \pm 5.5^{\ddagger}$ |  |  |  |
| Insulin (ng/ml)         | $1.06 \pm 0.0$  | 2.40 ± 0.2*    | $1.17\pm0.0^{\dagger}$    | $1.16\pm0.5^{\dagger}$   | $1.16 \pm 0.5^{\dagger}$ $2.68 \pm 0.2$ |                            | $1.23\pm0.0^{\ddagger}$    |  |  |  |
| HOMA index              | $8.42 \pm 0.4$  | 21.36±1.3*     | $9.13\pm0.5^{\dagger}$    | $8.97\pm0.6^{\dagger}$   | $29.93\pm2.1^{\dagger}$                 | $11.33 \pm 0.4^{\ddagger}$ | $10.04 \pm 0.7^{\ddagger}$ |  |  |  |
| Cholesterol (mg/dl)     | $70.4 \pm 3.1$  | 101.5 ± 4.12*  | $80.6 \pm 4.6$            | $78.4 \pm 4.8$           | $160.0\pm5.0^{\dagger}$                 | $145.9 \pm 8.0$            | $145.1 \pm 12.6$           |  |  |  |
| HDL (mg/dl)             | $41.7 \pm 2.7$  | 32.3 ± 1.7*    | $41.0\pm1.8^{\dagger}$    | $39.9 \pm 1.7^{\dagger}$ | $27.9 \pm 2.4$                          | $41.0 \pm 3.3^{\ddagger}$  | $41.4 \pm 4.1^{\ddagger}$  |  |  |  |
| LDL (mg/dl)             | $29.1 \pm 2.1$  | 53.2 ± 3.3*    | $30.9\pm6.9^{\dagger}$    | $32.9\pm6.1^{\dagger}$   | $114.4\pm4.5^{\dagger}$                 | $86.2 \pm 5.9^{\ddagger}$  | $82.7 \pm 16.8^{\ddagger}$ |  |  |  |
| Triglyceride (mg/dl)    | $50.1 \pm 4.4$  | 57.4±5.9       | 51.2 ± 5.5                | 51.3 ± 4.3               | 59.0 ± 4.9                              | 52.3 ± 3.9                 | 52.1 ± 6.7                 |  |  |  |
| Estradiol level (pg/ml) | 143±5           | 53 ± 3*        | 196 ± 21*†                | 59±6*                    | 56±8                                    | $202\pm24^{\ddagger}$      | 53 ± 11                    |  |  |  |
| Serum MDA (μmol/ml)     | $5.56 \pm 0.2$  | 6.18 ± 0.1*    | $5.42\pm0.3^{\dagger}$    | $5.31\pm0.2^{\dagger}$   | $6.28 \pm 0.1$                          | $5.38 \pm 0.2^{\ddagger}$  | $5.40\pm0.1^{\ddagger}$    |  |  |  |
| Tissue MDA (μmol/ml)    | $4.71 \pm 1.1$  | 7.76 ± 1.1*    | $4.48\pm0.6^{\dagger}$    | $3.85\pm0.58^\dagger$    | $7.94 \pm 1.1$                          | $4.58 \pm 0.4^{\ddagger}$  | $4.63\pm0.8^{\ddagger}$    |  |  |  |
| Food intake (gram/day)  | $15.6 \pm 0.0$  | $15.2 \pm 0.3$ | $14.2\pm0.1$              | $14.3 \pm 0.3$           | $18.6\pm0.2^{\dagger}$                  | $18.6 \pm 0.2$             | $17.9 \pm 0.5$             |  |  |  |

**Table 1. Metabolic parameters of experimental groups at after 4 weeks of treatments.** Values are mean  $\pm$  SEM. \*P < 0.05 vs NDS, †P < 0.05 vs NDOVe, and \*P < 0.05 vs HFOVe. NDS, normal-diet fed shamoperated rats; NDO, normal-diet fed ovariectomized rats; HFO, high-fat-diet fed ovariectomized rats; Ve, vehicle; E, estradiol; Vil, vildagliptin; HOMA, Homeostasis Model Assessment; MDA, Malondialdehyde.

Hormone therapy is an effective remedy for the management of menopausal-related problems such as bone health, reproductive tract symptoms, and vasomotor symptoms<sup>7</sup>. It also exhibited an advantage on prevention against metabolic syndrome and CVDs in estrogen-deprived individuals<sup>8,9</sup>. Although the benefits of estradiol replacement have been reported, its therapeutic effects are still being investigated. The use of hormone therapy is also limited due to the timing effect of hormone initiation<sup>7,10</sup>. Moreover, the hormone therapy is not recommended for menopausal women who have some health considerations such as reproductive cancers, thromboembolic disease, risk of stroke, as well as existent CVD or diabetes<sup>7</sup>. Therefore, alternative strategies for improving cardiometabolic function in estrogen-deprived individuals who have contraindications for estrogen therapy are still needed.

Vildagliptin is a member of the group of dipeptidyl peptidase-4 (DPP-4) inhibitor drugs. It is used for T2DM treatment. DPP-4 is a protease enzyme which inactivates glucagon-like polypeptide-1 (GLP-1) hormone, resulting in decreased insulin secretion. Thus, inhibition of DPP-4 helps in enhancing the GLP-1 level and increasing insulin secretion, thus lowering blood glucose level<sup>11</sup>. It has been shown that treatment with vildagliptin in high-fat-diet induced insulin resistant rats caused decreased cardiovascular oxidative stress in both heart tissues and plasma<sup>12</sup>. Vildagliptin also effectively restored heart rate variability to normal levels in obese-insulin resistant rats, indicating its positive impact in the regulation of cardiac sympathovagal balance. Moreover, cardiac mitochondrial morphology and function were completely restored in vildagliptin-treated insulin resistant rats<sup>12</sup>.

Both estrogen and vildagliptin also exhibited cardioprotective effects in instances of myocardial I/R injury by improving cardiac functional recovery, and reducing myocardial infarction and reactive oxygen species (ROS) production<sup>4,13</sup>. However, their protective roles on cardiometabolic function and I/R conditions had never been examined in obese-insulin resistant estrogen deprived rats. This study aimed to investigate the effects of chronic estrogen and vildagliptin treatments on the condition of obese-insulin resistance with estrogen-deprivation in combination with cardiac I/R injury. We hypothesized that estrogen and vildagliptin could improve metabolic status, cardiac function, cardiac autonomic regulation, and cardiac mitochondrial function and also inhibit oxidative stress and apoptosis in obese-insulin resistant estrogen deprived female rats who had undergone cardiac I/R injury.

#### Results

Efficacy of estrogen and vildagliptin on metabolic status. The estrogen-deprived rats demonstrated several features of obese-insulin resistance as indicated by significantly increased levels of body weight, fasting plasma glucose and insulin, plasma cholesterol and HOMA index in NDO group (Table 1). Plasma HDL level showed a significant reduction in NDO rats. The levels of body weight, visceral fat weight, fasting glucose, cholesterol and HOMA index showed a significant increase, and plasma LDL level was significantly increased in HFO rats, when compared with NDO rats suggesting the higher degree of metabolic disturbance induced by chronic high-fat consumption. Treatment with estrogen and vildagliptin similarly led to improved plasma glucose levels, insulin levels and HOMA index in both NDO and HFO rats. However, only estrogen treatment resulted in significantly reduced body weight in both NDO and HFO rats, and also significantly diminished visceral fat deposition in HFO rats. The levels of MDA were elevated in both serum and tissue samples from NDOVe rats, when compared with NDS rats which is the normal-diet fed sham rats, and these upregulated MDA levels in NDOVe rats were not significant different with HFOVe rats. Estrogen replacement and vildagliptin treatment led to significantly reduced serum and tissue MDA elevation in both NDO and HFO rats.

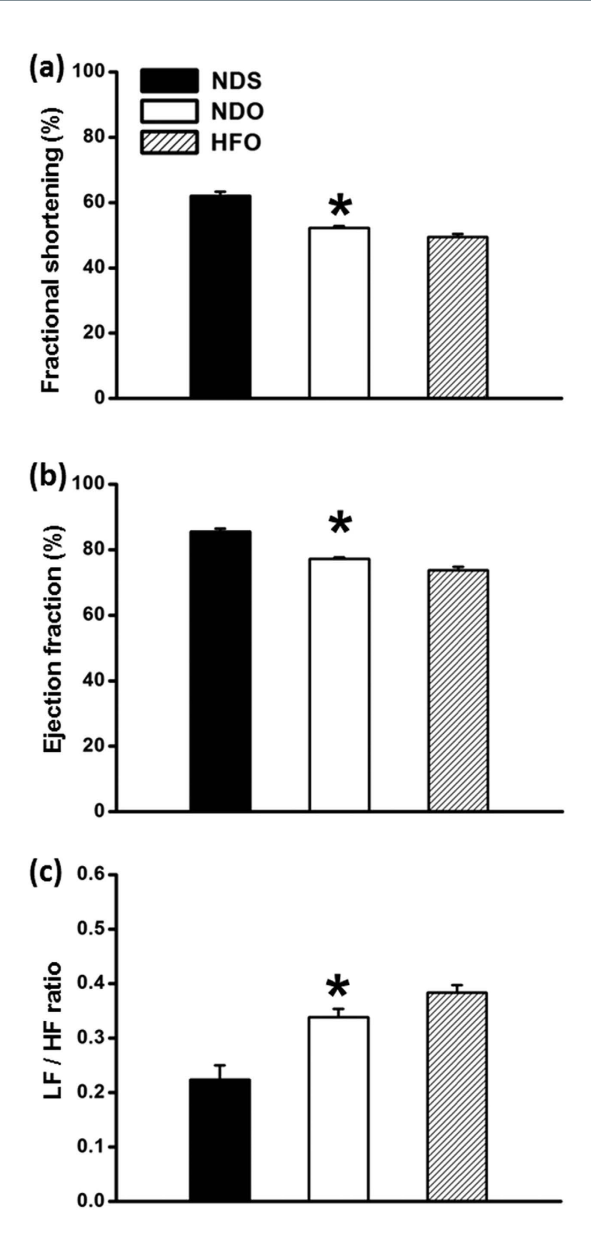


Figure 1. Effect of estrogen deprivation and obese-insulin resistance on left ventricular function and heart rate variability prior to pharmacological interventions. 12 weeks after ovariectomy, normal-diet fed ovariectomized rats (NDO) and high fat-diet fed ovariectomized rats (HFO) had reduced % fractional shortening (a), reduced % ejection fraction (b) and had increased LF/HF ratio (c), when compared with normal-diet fed sham operated (NDS) rats. Values are mean  $\pm$  SEM for 6 rats in each group. \*P< 0.05 vs. NDS.

Effect of estrogen and vildagliptin on cardiac function in the basal condition. Endogenous estrogen deprivation induced the impairment of cardiac function within 12 weeks, as indicated by decreased levels of %FS and %EF as well as depressed HRV in NDO rats (Fig. 1a–c, respectively). These parameters were not significant different between NDO and HFO rats. Both estrogen and vildagliptin treatments led to significantly increased %FS and %EF, and an improved HRV, when compared with vehicle-treated NDO- and HFO rats (Fig. 2a–c, respectively). Data from the P-V loop study indicated that LV function was impaired in vehicle-treated rats according to the lower levels of LVESP,  $\pm$ dP/dt and SV/BW, and the higher level of LVEDP (Table 2). These cardiac function parameters were not different when compared between NDO and HFO rats. Estrogen and vildagliptin protected the heart from functional impairment by maintaining the levels of LVESP, LVEDP,  $\pm$ dP/dt, and also increasing SV/BW ratio in both NDO and HFO rats, when compared with vehicle-treated rats (Table 2).

Cardioprotective effect of estrogen and vildagliptin against cardiac I/R injury. Effects of interventions on LV function. Cardiac LAD occlusion induced a significant reduction in LVESP, -dP/dt and SV/BW in both NDOVe and HFOVe rats, when compared with NDS rats (Table 3). Furthermore, when compared with NDOVe rats, SV/BW ratio was further reduced in HFOVe rats. At the end of 30-minute ischemia, both estrogen- and vildagliptin-treated rats demonstrated a significant improvement in LVESP, LVEDP and SV/BW

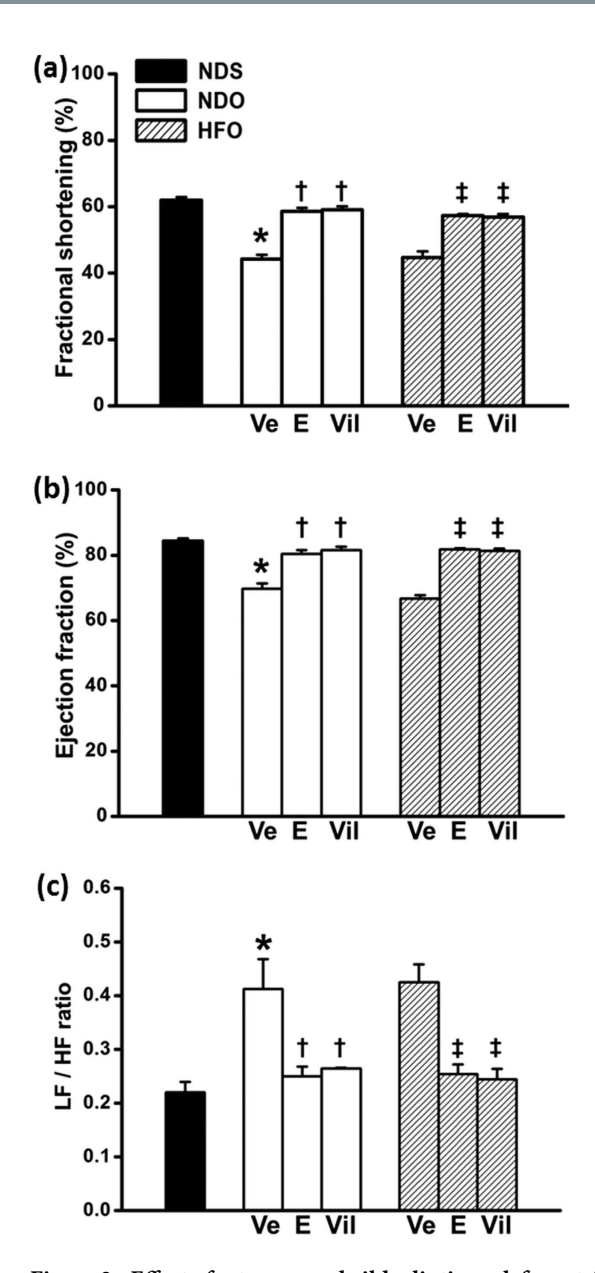


Figure 2. Effect of estrogen and vildagliptin on left ventricular function and heart rate variability of estrogen-deprived rats after treatments. % Fractional shortening (a) and % ejection fraction (b) were increased in estrogen (E)- and vildagliptin (Vil)-treated rats when compared with vehicle-treated rats. LF/HF ratio (c) was increased and restored to the normal level in both E- and Vil-treated groups. Values are mean  $\pm$  SEM for 6 rats per group. \*P<0.05 vs. NDS, †P<0.05 vs. NDOVe and †P<0.05 vs. HFOVe.

in both NDO and HFO rats, when compared with vehicle-treated groups (Table 3). Similarly to the ischemic period, NDOVe rats had significantly reduced LV function at the end of the reperfusion period as demonstrated by significantly decreased LVESP, increased LVEDP and lowered SV/BW ratio, when compared with NDS rats (Table 4). HFOVe rats demonstrated similar impaired cardiac function since there was no significant difference of the cardiac parameters, when compared with NDOVe rats. This impairment of parameters in both NDO and HFO rats was restored after treatment with estrogen and vildagliptin. Both estrogen and vildagliptin treatment led to significantly reduced LVEDP, increased LVESP and improved SV/BW in NDO- and HFO rats, when compared with vehicle-treated rats (Table 4).

Effects of interventions on cardiac arrhythmia and mortality rate. Arrhythmia score was significantly increased (Fig. 3a), and the time to 1st VT/VF was significantly reduced in NDOVe and HFOVe groups (Fig. 3b). Treatment with estrogen and vildagliptin effectively reduced the arrhythmia score in both NDO and HFO rats (Fig. 3a). Both of the treatments also similarly delayed time to 1st VT/VF in HFO rats, when compared with vehicle-treated rats (Fig. 3b). This increased mortality rate in HFO rats was significantly decreased following treatment with estrogen and vildagliptin (Fig. 3c). However, only estrogen treatment led to a significantly reduced mortality rate in the

|                   |                  |                   | NDO                     |                         | НГО             |                          |                            |  |  |
|-------------------|------------------|-------------------|-------------------------|-------------------------|-----------------|--------------------------|----------------------------|--|--|
| Parameters        | NDS              | Ve                | E                       | Vil                     | Ve              | E                        | Vil                        |  |  |
| Heart rate (bpm)  | $231 \pm 23$     | $249\pm16$        | 229 ± 19                | $231\pm27$              | 251 ± 12        | 234±19                   | $234 \pm 26$               |  |  |
| LVESP (mmHg)      | 119±12           | 73 ± 11*          | 99±14                   | 92±8                    | 75 ± 15         | $101\pm18$               | $102 \pm 12$               |  |  |
| LVEDP (mmHg)      | 9±2              | 20±4*             | 7 ± 2                   | 9±3                     | 21±4            | 13±1                     | 15±5                       |  |  |
| +dP/dt (mmHg/sec) | $9328 \pm 1617$  | 4986 ± 1238*      | $6433 \pm 672$          | 6973 ± 791              | $4713 \pm 1061$ | 6391±959                 | $7023 \pm 856$             |  |  |
| -dP/dt (mmHg/sec) | $-6532 \pm 1452$ | $-2749 \pm 216*$  | $-4986 \pm 1095$        | $-4087 \pm 560$         | $-2812 \pm 621$ | $-4099 \pm 688$          | $-4283 \pm 457$            |  |  |
| SV/BW (μl/gram)   | $1.02 \pm 0.13$  | $0.72 \pm 0.10^*$ | $1.21\pm0.05^{\dagger}$ | $1.15\pm0.06^{\dagger}$ | $0.71\pm0.08$   | $1.09\pm0.06^{\ddagger}$ | $1.06 \pm 0.05^{\ddagger}$ |  |  |

Table 2. Effect of estrogen and vildagliptin on cardiac function before I/R injury. Values are mean  $\pm$  SEM (n = 6 per group). \*P < 0.05 vs NDS, †P < 0.05 vs NDOVe, and \*P < 0.05 vs HFOVe. NDS, normal-diet fed sham-operated rats; NDO, normal-diet fed ovariectomized rats; HFO, high-fat-diet fed ovariectomized rats; Ve, vehicle; E, estradiol; Vil, vildagliptin; LVESP, left ventricular end systolic pressure; LVEDP, left ventricular end diastolic pressure; +dP/dt, maximal slope of the systolic pressure increment; -dP/dt, maximal slope of the diastolic pressure decrement; SV/BW, stroke volume/body weight.

|                   |                  |                   | NDO                     |                         | HFO                     |                            |                            |  |  |
|-------------------|------------------|-------------------|-------------------------|-------------------------|-------------------------|----------------------------|----------------------------|--|--|
| Parameters        | arameters NDS    |                   | Ve E                    |                         | Ve                      | E                          | Vil                        |  |  |
| Heart rate (bpm)  | $218 \pm 18$     | $241 \pm 20$      | $205\pm26$              | 221 ± 29                | $236 \pm 11$            | $221\pm12$                 | 224±21                     |  |  |
| LVESP (mmHg)      | 92±5             | 61 ± 9*           | $87\pm4^{\dagger}$      | $79\pm2^{\dagger}$      | 46±5                    | $95\pm5^{\ddagger}$        | $85 \pm 17^{\ddagger}$     |  |  |
| LVEDP (mmHg)      | 17±2             | 27 ± 4            | 20±5                    | 17±5                    | 30±2                    | $16 \pm 1^{\ddagger}$      | $16 \pm 2^{\ddagger}$      |  |  |
| +dP/dt (mmHg/sec) | $5478 \pm 642$   | $4154 \pm 1472$   | $5521\pm1032$           | $5258 \pm 264$          | $3974 \pm 1062$         | $5712 \pm 1174$            | 5544±937                   |  |  |
| -dP/dt (mmHg/sec) | $-4638 \pm 1483$ | $-1521 \pm 522*$  | $-3547 \pm 563$         | $-3126 \pm 111$         | $-1745 \pm 635$         | $-3802 \pm 962$            | $-3926 \pm 850$            |  |  |
| SV/BW (μl/gram)   | $0.90 \pm 0.05$  | $0.48 \pm 0.04^*$ | $1.04\pm0.05^{\dagger}$ | $0.85\pm0.05^{\dagger}$ | $0.30\pm0.05^{\dagger}$ | $0.53 \pm 0.06^{\ddagger}$ | $0.51 \pm 0.09^{\ddagger}$ |  |  |

Table 3. Effect of estrogen and vildagliptin on cardiac function at the end of myocardial ischemia. Values are mean  $\pm$  SEM (n = 6 per group). \*P < 0.05 vs NDS, †P < 0.05 vs NDOVe, and †P < 0.05 vs HFOVe. NDS, normal-diet fed sham-operated rats; NDO, normal-diet fed ovariectomized rats; HFO, high-fat-diet fed ovariectomized rats; Ve, vehicle; E, estradiol; Vil, vildagliptin; LVESP, left ventricular end systolic pressure; LVEDP, left ventricular end diastolic pressure; +dP/dt, maximal slope of the systolic pressure increment; -dP/dt, maximal slope of the diastolic pressure decrement; SV/BW, stroke volume/body weight.

|                   |                  |                 | NDO                     |                         | HFO             |                            |                            |  |
|-------------------|------------------|-----------------|-------------------------|-------------------------|-----------------|----------------------------|----------------------------|--|
| Parameters        | NDS              | Ve              | Е                       | Vil                     | Ve              | E                          | Vil                        |  |
| Heart rate (bpm)  | 233 ± 21         | $273\pm12$      | $213 \pm 33$            | $228 \pm 35$            | 214±5           | $217 \pm 21$               | $205 \pm 26$               |  |
| LVESP (mmHg)      | 85 ± 10          | 48 ± 11*        | $79\pm9^{\dagger}$      | $78\pm9^{\dagger}$      | $41\pm12$       | $81 \pm 12^{\ddagger}$     | $82\pm13^{\ddagger}$       |  |
| LVEDP (mmHg)      | 14±2             | 26±3*           | $12\pm5^{\dagger}$      | $10\pm4^{\dagger}$      | 32±1            | $14\pm2^{\ddagger}$        | $12 \pm 3^{\ddagger}$      |  |
| +dP/dt (mmHg/sec) | $6283 \pm 395$   | $4511 \pm 1311$ | 5889 ± 87               | $5879 \pm 1124$         | 2586 ± 738      | $5682 \pm 1280$            | $5882 \pm 1130$            |  |
| -dP/dt (mmHg/sec) | $-4029 \pm 1826$ | $-2759 \pm 967$ | $-3817 \pm 411$         | $-3313 \pm 506$         | $-2962 \pm 145$ | $-3881 \pm 360$            | $-3967 \pm 884$            |  |
| SV/BW (μl/gram)   | $0.68 \pm 0.10$  | 0.36 ± 0.03*    | $0.88\pm0.04^{\dagger}$ | $0.87\pm0.10^{\dagger}$ | $0.40 \pm 0.07$ | $0.64 \pm 0.11^{\ddagger}$ | $0.70 \pm 0.10^{\ddagger}$ |  |

Table 4. Effect of estrogen and vildagliptin on cardiac function at the end of reperfusion. Values are mean  $\pm$  SEM (n = 6 per group). \*P < 0.05 vs NDS, †P < 0.05 vs NDOVe, and \*P < 0.05 vs HFOVe. NDS, normal-diet fed sham-operated rats; NDO, normal-diet fed ovariectomized rats; HFO, high-fat-diet fed ovariectomized rats; Ve, vehicle; E, estradiol; Vil, vildagliptin; LVESP, left ventricular end systolic pressure; LVEDP, left ventricular end diastolic pressure; +dP/dt, maximal slope of the systolic pressure increment; -dP/dt, maximal slope of the diastolic pressure decrement; SV/BW, stroke volume/body weight.

NDO rats, when compared with NDOVe group (Fig. 3c). The increased incidence of arrhythmia in NDOVe and HFOVe was consistent with the altered level of p-Cx43 in their cardiac tissue. The expression level of p-Cx43/total-Cx43 in ischemic areas/remote areas was significantly lower in NDOVe rats, compared to that in NDS rats (Fig. 3d), and the p-Cx43/total-Cx43 ratio was not significant different between NDOVe and HFOVe rats.

Effects of interventions on myocardial infarct size. The levels of area at risk (AAR) were no different among the experimental groups. Data from the myocardial infarct size analysis showed that the percentage of infarct size per AAR was significantly increased in NDOVe and HFOVe rats, when compared with the NDS rats (Fig. 4a). Representative images of the infarcted myocardia are shown in Fig. 4b. The cardiac expression of apoptotic and anti-apoptotic proteins, Bax and Bcl-2, were investigated to confirm cardiomyocyte cell death, and we found that the expression level of Bax was significantly increased in NDOVe and HFOVe rats, when compared with NDS rats (Fig. 4c). Consistent with infarct size reduction (Fig. 4a), estrogen and vildagliptin treatment showed a significant reduced expression of Bax in the myocardium in both NDO and HFO rats (Fig. 4c). Moreover,

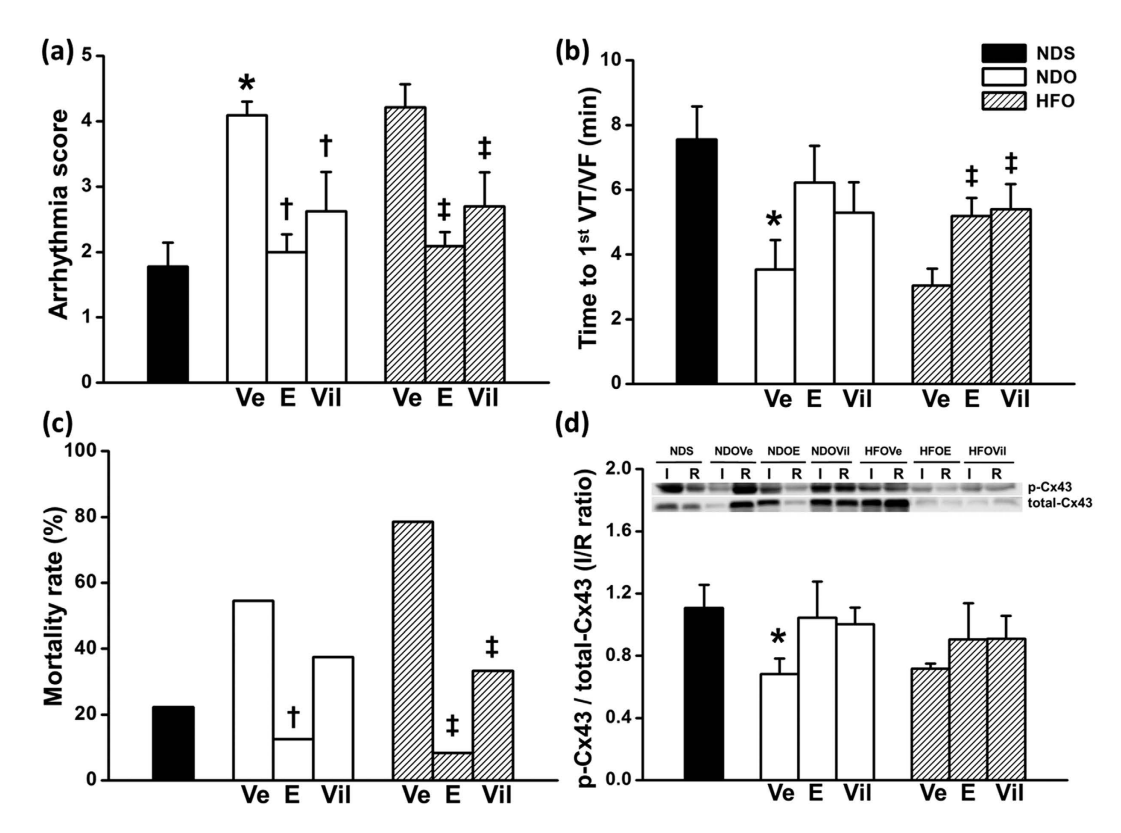


Figure 3. Cardiac arrhythmia, mortality rate and cardiac expression Cx43, after treatment with estrogen or vildagliptin for 4 weeks. Arrhythmia score (a) was decreased, and time to 1st VT/VF (b) was prolonged in both estrogen (E)- and vildagliptin (Vil)-treated groups. Post-ischemia mortality rate (c), presented in % of number of rats in each experimental group was significantly reduced following treatment with E and Vil, when compared with vehicle-treated group. The ratio of p-Cx43/total-Cx43 expressions (d) in ischemic (I) area/remote (R) area, were reduced in NDOVE and HFOVe rats, when compared with those of NDS rats. Values are mean  $\pm$  SEM for 6 rats per group. \* $^*P$ <0.05 vs. NDS,  $^†P$ <0.05 vs. NDOVe and  $^*P$ <0.05 vs. HFOVe.

HFOVe rats additionally demonstrated a significant decrease in Bcl-2 expression, when compared with NDS rats (Fig. 4d). The level of cytochrome C expression was found to be significantly increased in HFOVe hearts (Fig. 4e). Consistent with infarct size reduction, estrogen and vildagliptin treatment showed a significant reduced expression of Bax in the myocardium in both NDO and HFO rats (Fig. 4c), and also reduced cytochrome C expression in HFO rats (Fig. 4e). Plasma level of LDH was significantly increased in NDOVe and HFOVe (Fig. 4f), when compared with NDS rats, consistent with the upregulated Bax expression in these experimental groups.

Effects of interventions on cardiac mitochondrial function. After cardiac I/R, mitochondrial impairment was found in NDOVe and HFOVe groups. The parameters of mitochondrial function were assessed and expressed as an ischemic/remote area ratio. NDOVe rats demonstrated a significant increase in ROS production (Fig. 5a) and a decrease in mitochondrial membrane potential gradient ( $\Delta\Psi$ ) (Fig. 5b), of the cardiac mitochondria in the ischemic/remote area indicating increased oxidative stress and mitochondrial depolarization, respectively. Absorbance intensity of the cardiac mitochondria from NDOVe rats was also lower than those of NDS rats (Fig. 5c), indicating mitochondrial swelling. These impaired mitochondrial parameters were not significance between NDOVe and HFOVe rats. Treatment with estrogen and vildagliptin resulted in a significant reduction in mitochondrial ROS production (Fig. 5a) and also a significantly increased  $\Delta\Psi$  in both NDO and HFO rats (Fig. 5b), when compared with NDOVe and HFOVe groups. The mitochondrial absorbance was restored to the normal level following both estrogen and vildagliptin treatments in HFO rats (Fig. 5c). The representative electron micrographs of cardiac mitochondria from the ischemic area of each experimental group are shown in Fig. 5d.

#### Discussion

This study demonstrates the effect of estrogen deprivation with normal diet- and high-fat diet consumptions, as well as the efficacy of estrogen and vildagliptin, on metabolic status and cardiac function, during basal conditions and under conditions involving cardiac I/R injury. The major findings could be summarized as: (1) both NDO and HFO caused the impairment of cardiometabolic function in the basal condition; (2) when compared with NDS rats, the cardiac contractility and mitochondrial function were more diminished, and myocardial infarction and cardiac arrhythmias were more aggravated in both NDO and HFO rats underwent cardiac I/R injury; (3) chronic high-fat diet consumption aggravated the severity of cardiac I/R injury and increased mortality from

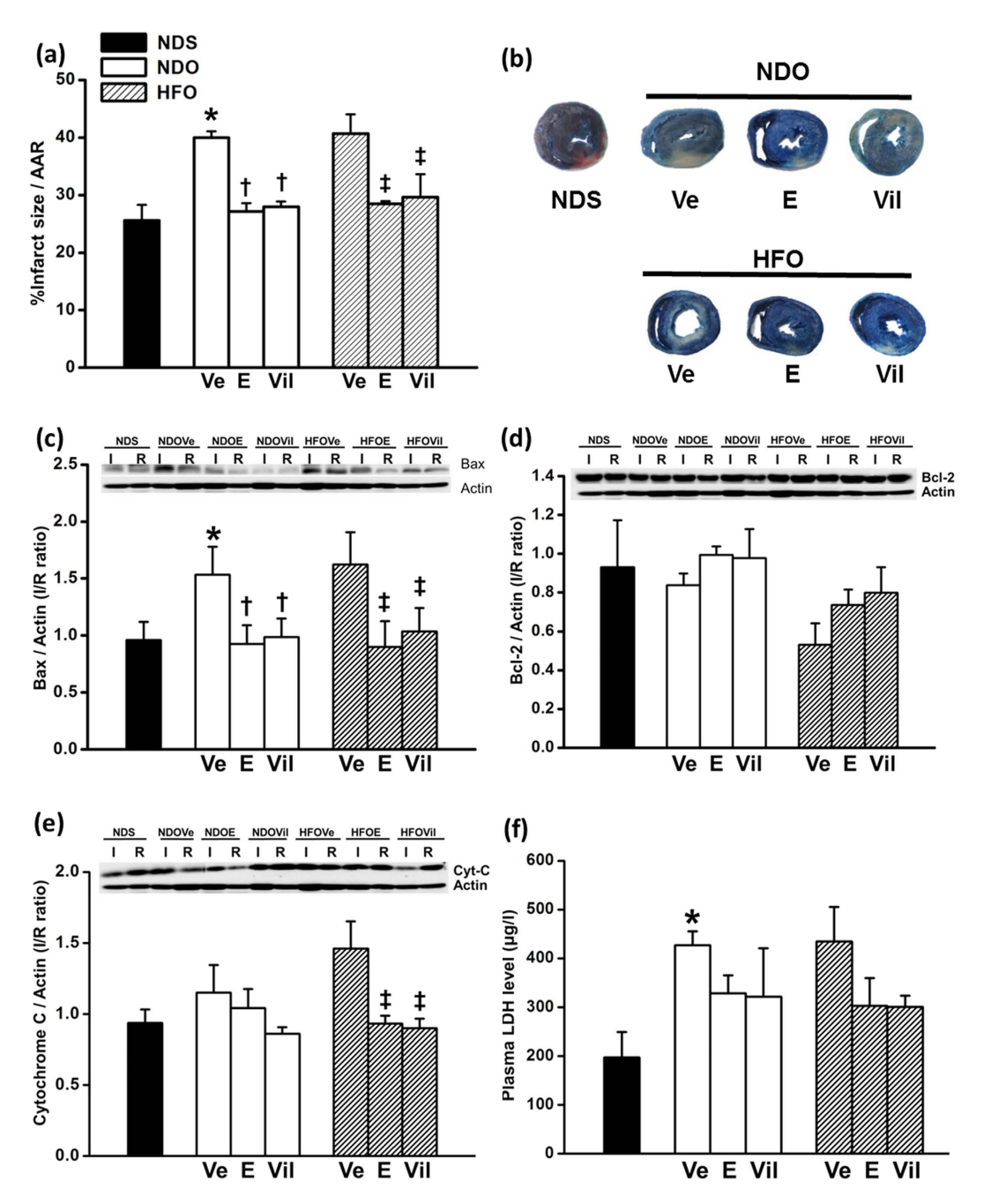


Figure 4. The levels of infarct size and cardiac expression of apoptotic and anti-apoptotic proteins, after treatment with estrogen or vildagliptin for 4 weeks. Both NDOVE and HFOVe had increased level of infarct size (a), and both estrogen (E)- and vildagliptin (Vil)-treatment significantly diminished myocardial infarction. The representative infarcted myocardium was demonstrated in (b). Expression levels of the apoptotic protein Bax (c) were significantly increased in NDOVe and HFOVE rats, whereas the expression levels of anti-apoptotic protein, Bcl-2 (d) were reduced in HFOVe rats. The cardiac level of cytochrome C expression (e) was increased in HFOVe rats and significantly reduced by both E and Vil-treatments. Plasma LDH level (f) was significantly elevated in both NDOVe and HFOVe rats, when compared with NDS rats. The plasma level of LDH in the intervention groups was not significant different from the NDS rats. Values are mean  $\pm$  SEM for 6 rats per group. \*P < 0.05 vs. NDS,  $^{\dagger}P < 0.05$  vs. NDOVe and  $^{\ddagger}P < 0.05$  vs. HFOVe.

cardiac I/R in HFO rats, and (4) an estradiol replacement and vildagliptin exhibited similar efficacy for cardio-protection against I/R injury in NDO and HFO rats.

Both estrogen deprivation and chronic high-fat diet consumption have long been known to be associated with the increased risk of metabolic dysfunction<sup>14–16</sup>. An increased level of oxidative stress has been previously revealed to be an important factor underlying the development of estrogen deprived- and obese-induced metabolic impairment<sup>15,17,18</sup>. In this study, the level of MDA was found to be elevated in both serum and cardiac tissues

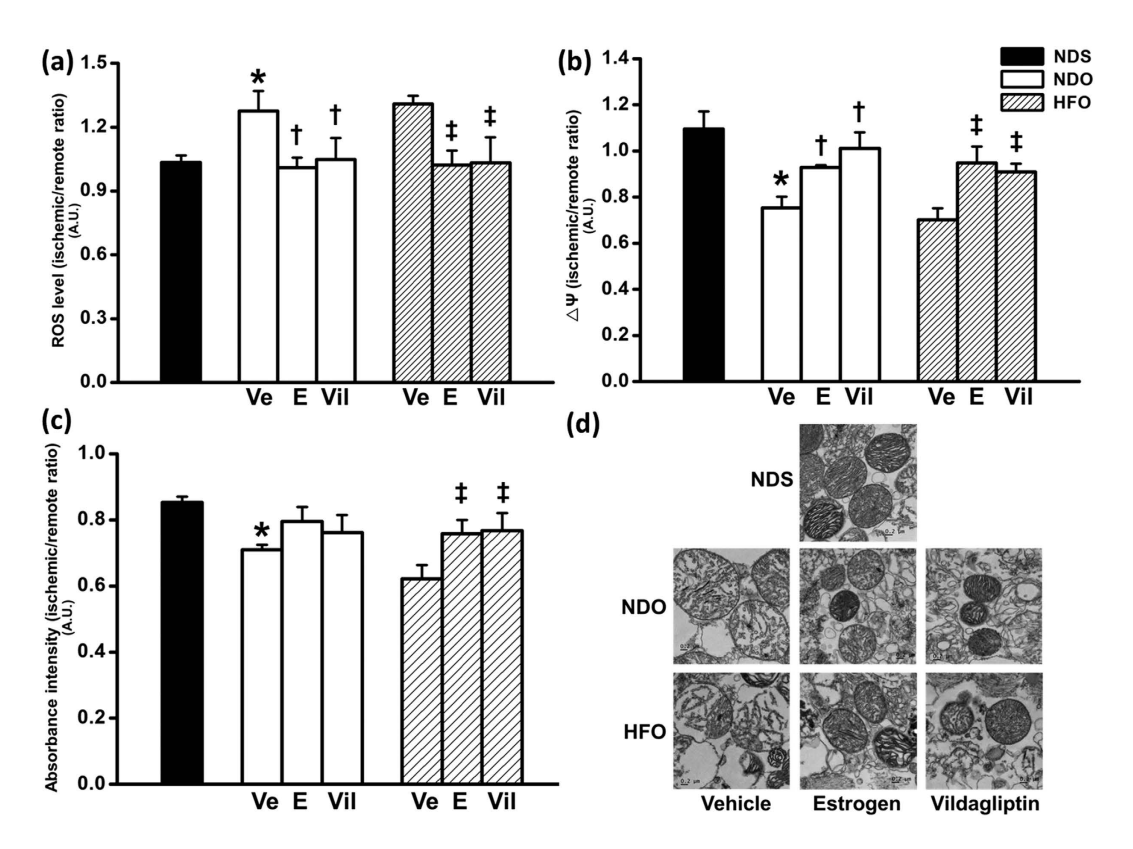


Figure 5. Cardiac mitochondrial function in estrogen-deprived rats after treatment with estrogen or vildagliptin for 4 weeks. All mitochondrial function parameters are represented in the ratio of ischemic/remote area. Mitochondrial ROS level (a) was increased while  $\Delta\Psi$  (mitochondrial membrane potential change, (b) and absorbance intensity (c) were decreased in NDOVe and HFOVe rats. Transmission electron micrographs (d) illustrate cardiac mitochondria morphology of rats in each group. Treatment with estrogen and vildagliptin led to an improvement in all parameters of cardiac mitochondrial function in both NDO and HFO rats. Values are mean  $\pm$  SEM for 6 rats per group. \*P<0.05 vs. NDS, †P<0.05 vs. NDOVe and †P<0.05 vs. HFOVe.

from both NDO and HFO rats indicating an increased level of oxidative stress in both peripheral circulation and the heart<sup>19</sup>. This finding emphasized the association between the elevated level of oxidative stress and metabolic disorders. Estrogen replacement and vildagliptin showed beneficial effects on the reduction of oxidative stress therefore could contribute to improved metabolic function in these rats. Consistent with a study in mice, estrogen provided anti-obese effects as it reduced body weight and visceral fat deposition in female rats<sup>20</sup>. This estrogenic action could be operated via lipogenic and lipolysis gene modulation, as well as may be involving central regulation via brain leptin and insulin sensitivity<sup>21,22</sup>.

Cardiac dysfunction indicated by cardiac autonomic imbalance, decreased levels of %EF and %FS, and impaired LV systolic and diastolic function, manifested itself after 12 weeks in both groups of rats. We have previously reported an association between endogenous estrogen-deprivation and an obese-insulin resistant condition and the development of cardiac dysfunction, involving the progressive increase of oxidative stress and cardiac mitochondrial impairment<sup>15</sup>. In this study, P-V loop analysis confirmed that LV dysfunction was already intensified in both NDO and HFO rats, when compared with NDS rats, in both a basal and I/R period. Moreover, myocardial dysfunction was more aggravated in HFO rats than in the rats that are estrogen-deprived alone. This is concluded from the marked reduction in stroke volume and increased LVEDP and mortality rate. A clinical study previously reported that coronary heart disease patients who had the higher level of homeostasis model assessment of insulin resistance (HOMA) index associated with the increased level of myocardial injury, as well as the higher risk of cardiovascular events and death, after receiving percutaneous coronary interventions<sup>23</sup>. Interestingly, the increased level of glucose intolerance and the higher HOMA index is associated with increased LV mass only in women<sup>24</sup>. This gender disparity may suggest that cardiac dysfunction in women is strongly related to and more amplified by metabolic disturbance.

Estrogen and its receptor activation have been reported as playing a pivotal role in cardioprotection via the regulation of oxidative stress against I/R injury<sup>25–27</sup>. Activation of estrogen receptor by its agonist during 1 week prior to cardiac I/R was demonstrated to reduce ROS production and attenuate inflammation through the reduction of TNF- $\alpha$ , IL-1 $\beta$  and LDH release<sup>28</sup>. Moreover, it has been shown that the expression of estrogen receptor in cardiomyocytes was increased under hypoxia condition suggesting the ischemic-induced upregulation of estrogenic-protective signaling pathway<sup>29</sup>. This cardioprotective effect of estrogen was consistent with the findings in the present study. In this study, depletion of endogenous estrogen initiated by ovariectomy as well as the combination of estrogen deprivation and high-fat diet consumption resulted in a higher level of cardiac oxidative stress

as indicated by increased mitochondrial ROS production and increased myocardial MDA level. Increased mitochondrial ROS production is associated with mitochondrial membrane depolarization and mitochondrial swelling and subsequently triggered apoptosis<sup>30,31</sup>. This was indicated by increased Bax and cytochrome C expression<sup>32,33</sup>. It has been previously reported that consumption of a high-fat diet accelerates cardiac oxidative stress and cardiocyte apoptosis in an estrogen-deprived model without conditions of cardiac I/R<sup>15</sup>. In this study, NDO rats exhibited an increased level of cardiac Bax expression, whereas the HFO rats demonstrated an additional increase in cytochrome C, and decrease in cardiac Bcl-2 expression indicating the reduction of anti-apoptotic protein, therefore predisposing the cardiomyocytes to apoptosis during myocardial I/R injury. The increased level of cardiomyocyte apoptosis in both NDO and HFO rats was consistent with increased infarct size, when compared with NDS rats which had undergone I/R injury.

An estradiol replacement and vildagliptin showed their beneficial effects on the prevention of cardiac dysfunction in both basal conditions and during I/R injury in both NDO and HFO rats, as indicated by the preserved LVESP, LVEDP,  $\pm dP/dt$  and SV. These treatments also decreased cardiomyocyte apoptosis and thus limited the size of myocardial infarction. According to previous studies, both estrogen and vildagliptin have been reported as protecting the cellular redox balance $^{34-36}$ . Treatment with estrogen has been shown to upregulate the level and activity of anti-oxidant enzymes (i.e. GSH/GSSG ratio, CAT, and SOD) in the myocardium, and also to decrease IL-6 and TNF- $\alpha$  level, suggesting it has anti-inflammatory effects in addition to anti-oxidative stress abilities<sup>36</sup>. Similarly, inhibition of DPP-4 activity by vildagliptin has been reported as reducing cardiac mitochondrial ROS production, therefore protecting mitochondrial function during conditions of I/R<sup>37</sup>. This effect of vildagliptin contributed to a decreased level of infarct size and a preservation of cardiac performance, which was diminished by I/R injury<sup>34</sup>. Moreover, treatment with vildagliptin also prevented the dispersion of cardiac electrical activity by inhibiting the shortening of the effective refractory period (ERP) in an I/R heart, resulting in a reduced arrhythmia risk<sup>37</sup>. In this study, the lower incidence of arrhythmia in both estrogen-treated and vildagliptin-treated rats was consistent with the maintained level of p-Cx43 expression in cardiac tissues, whereas the vehicle-treated rats demonstrated higher arrhythmia scores as well as decreased levels of cardiac p-Cx43 expression. This finding indicated that estrogen and vildagliptin provided cardioprotective effects against post-ischemic arrhythmia by maintaining Cx43 expression which contributes to the preservation of gap junction function and anti-arrhythmia effects<sup>35</sup>.

Estrogen and vildagliptin demonstrated similar protective efficacy on cardiometabolic status, mitochondrial function and also protected cardiac performance and prevented arrhythmia during I/R. These results suggested that vildagliptin may be prescribed to menopausal women who have contraindications for estrogen replacement therapy, in order to obtain similar benefits regarding cardiometabolic function. Vildagliptin had been demonstrated the similar therapeutic effects on cardiometabolic function in obese orchiectomized male rats with cardiac I/R injury condition suggesting that its efficiency was not influenced by gender discrepancy<sup>38</sup>. Its safety had been reported in several clinical studies to provide an effective glycemic control and could be used in patients who had renal and cardiovascular diseases, without producing renal risk and cardiovascular event<sup>39-42</sup>. Moreover, vildagliptin did not influence cardiac electrical activity since PR and QRS intervals were not altered during the prescribed treatment for T2DM patients<sup>43</sup>, therefore it could be a feasible alternative to estrogen therapy which had been known to associate with prolonged QT interval and QT dispersion in postmenopausal individuals who received long-term estrogen therapy 44,45. However, our findings showed that estrogen treatment showed a significantly decreased mortality rate in both NDO and HFO rats, suggesting the superior efficacy of estrogen on the reduction of cardiac I/R-related mortality. This result was consistent with clinical reports which have demonstrated that hormone replacement therapy could reduce the incidence of coronary heart disease and total mortality, especially when initiated in recently postmenopausal women (less than 10 years following menopause)<sup>3</sup>. In this study, estradiol replacement was initiated at 12 weeks after endogenous estrogen deprivation, and demonstrated that it could effectively reduce the mortality rate in rats. From clinical studies in humans, the higher mortality rate in coronary artery disease patients and also over-all-cause mortality had been reported to be associated with a higher level of central obesity<sup>46,47</sup>. Therefore, the survival-promoting result of estradiol replacement may be owing to the body weight- and visceral fat-lowering effect, which are not found in the vildagliptin treatment group, in addition to its anti-arrhythmia, anti-oxidative stress and mitochondria protective effects.

In summary, findings from the present study indicate that both endogenous estrogen deprivation alone and combined estrogen deprivation with high-fat diet consumption caused cardiometabolic disorders and induced a higher degree of cardiac dysfunction (i.e. mitochondrial impairment, increased infarct size, contractile dysfunction, cardiac arrhythmia and higher mortality rate) following I/R, when compared with NDS rats. Although high-fat diet consumption aggravated the cardiometabolic status in an estrogen-deprived condition, it did not aggravate these impairments in the estrogen-deprived condition during cardiac I/R injury. The underlying mechanism of these cardiometabolic alterations could be associated with the increased level of oxidative stress caused by estrogen deprivation and metabolic disorders. Estrogen and vildagliptin exerted a similar efficacy on cardiometabolic improvement and also showed protection of the heart against I/R injury and attenuated post-ischemic arrhythmia resulting in a reduced mortality rate in these rats. The reduction of oxidative stress level in the heart and systemic circulation possibly plays an important role contributes to the potential effect of vildagliptin and estradiol treatments. However, further investigation is needed to completely clarify the proposed mechanism of vildagliptin and estradiol. Our findings provide new information for the application of this anti-diabetic drug, which confers cardioprotective benefits to menopausal women who have metabolic disorder and have contraindications for traditional estrogen replacement therapy. Future studies investigating the therapeutic efficacy of estrogen and vildagliptin for different periods and in various dosages are needed in order to warrant its use in a clinical setting in obese-insulin resistant menopausal women under condition of cardiac I/R.

#### **Materials and Methods**

**Animals and ethical approval.** Female Wistar rats (6 weeks of age, weighing 200–220 g) were obtained from the National animal center (Salaya campus, Mahidol University, Bangkok, Thailand). The rats were given time to acclimatize, and were housed in a temperature-controlled room (25 °C) with a 12-hour dark/light cycle setting. All experimental procedures were approved by the Institutional Animal Care and Use Committee at the Faculty of Medicine, Chiang Mai University, in compliance with NIH guidelines.

**Experimental protocol.** Rats were randomly assigned to sham (S) or ovariectomized (OVX) group. The operations were carried out and then the rats were allowed to recover for 1 week. The sham group was fed on a standard normal diet (ND, containing 19.77% energy from fat), whereas the ovariectomized group was randomized and received either a ND or high-fat diet (HFD, containing 59.28% energy from fat) for 12 weeks<sup>15</sup>. At the end of the 12th week, HRV and echocardiography were performed to record the pre-treatment data. OVX rats in both diet groups (NDO and HFO) were randomly subcategorized to be treated with an estradiol replacement (Estradiol, E; 50 µg/kg BW; daily, via subcutaneous injection), vildagliptin (Vil; 3 mg/kg BW; daily, via intragastric gavage) or sesame oil (as a vehicle, Ve; in equal volume with E via subcutaneous injection), daily for 4 weeks (n = 12/group). Estradiol or  $17\beta$ -estradiol is a major circulating estrogen during active reproductive period in female and is the form of estrogen that exerts most potent estrogenic effect<sup>48</sup>. In this study, 17β-estradiol powder (Sigma-Aldrich Co., MO, USA) was dissolved in ethanol (1 mg/ml), then the solution was mixed with sesame oil (Sigma-Aldrich Co., MO, USA) before subcutaneously injected to rats (i.e. NDOE and HFOE rats). The dose of estradiol and vildagliptin used in this study had been demonstrated to improve cardiometabolic function in obese-insulin resistant rats<sup>38,49</sup>. Moreover, these selected doses were also similar to the doses used in clinical setting (transdermal estrogen 25-100 µg/day; vildagliptin 1-2 mg/kgBW/day)<sup>7,50</sup>. Body weight and food intake of all rats were recorded throughout the experimental period. After 4 weeks of treatment, post-treatment data from echocardiography and HRV were examined. Six-hour fasting was assigned to all rats then the fasted blood samples were collected from tail vein, and were centrifuged for plasma preparation. Then, the cardiac I/R procedure was performed. After I/R study, the heart was removed in order to study cardiac mitochondrial function and biochemical activities.

**Ovariectomy.** In the ovariectomized group, rats were anesthetized with Xylazine (0.15 ml/kg) and Zolitil (50 mg/kg)<sup>15</sup>. After hair shaving and skin cleaning, a bilateral ovariectomy was carried out by initially making a midline dorsal skin incision. The incision was centered between the inferior crest of the rib cage and superior base of the thigh. The abdominal-pelvic cavity was accessed then the uterine tubes and ovaries were identified. Both ovaries were removed and uterine horns were returned into the cavity. In a sham group, all rats received the same anesthesia and also the same surgical preparation procedures as OVX rats. Bilateral ovaries of sham rats were identified and exposed, however no excision was done to the ovaries. After the operation, rats were individually housed in a clear box with dry bedding for 1 week before being randomized to be fed on a normal diet or high-fat diet

**Echocardiography protocol.** Echocardiography is a non-invasive method used for the assessment of left ventricular function. Rats were lightly anesthetized (2% Isoflurane with oxygen, via inhalation), then the chest was shaved and they were placed in a supine position. After echocardiography transmission gel was applied, an echocardiography probe (S12, Hewlett Packard) which was connected to an echocardiograph (SONOS4500, Philips), was used for collecting the data from the heart. Signals from M-mode echocardiography at the papillary muscle level were recorded. Parameters obtained from echocardiography were: 1) RVDd = right ventricular dimension during diastole; (2) IVSs,d = systolic and diastolic interventricular septum; (3) LVIDs,d = systolic and diastolic left ventricular internal dimension; and (4) LVPWs,d = left ventricular posterior wall thickness during systole and diastole. Fractional shortening (FS) and ejection fraction (EF) were calculated by the following formula; %FS = ((LVIDd – LVIDs)/LVIDd)\*100, and % EF = ((LVEDV – LVESV)/LVEDV)\*100 $^{51}$ . After investigation, animals were allowed to fully recover and then returned to the cages.

**Heart rate variability (HRV) protocol.** HRV is a non-invasive assessment of cardiac autonomic innervation activity. Rats were anesthetized by using isoflurane inhalation. In the prone position, needle electrodes were subcutaneously placed at the right arm, trunk and left leg of the animal. Electrocardiograms (ECG) were recorded in the animals using a signal transducer (PowerLab 4/25T, ADInstrument) and operated through Chart 5.0 program for 20 minutes consecutively<sup>38,49</sup>. During the recording of the ECG, the rat was in full conscious and was individually confined within a restrainer to limit the mobility. ECG data were then analyzed using the frequency-domain method by the MATLAB program to determine the high-frequency (HF) component (ranging between 0.15–0.40 Hz) and low-frequency (LF) component (ranging between 0.04–0.15 Hz)<sup>15,52</sup>. Cardiac sympathovagal control was reported as LF/HF ratio. Increased LF/HF ratio was used as an indication of cardiac sympathovagal imbalance<sup>15,52</sup>.

Cardiac ischemia/Reperfusion study. After 4-weeks of treatment, a cardiac I/R study was performed on all rats. The rats were anesthetized and ventilated by tracheostomy with a positive pressure ventilator (Harvard rodent ventilator model 683, Harvard apparatus, Massachusetts, USA). ECG limb leads were placed to enable the recording of cardiac electrocardiogram and heart rate using a Powerlab signal transducer (Powerlab 4/25T, ADInsrument)<sup>38</sup>. A left-side thoracotomy incision at the 4<sup>th</sup> intercostal space was made, and then the pericardium was incised to expose the pumping heart. The left anterior descending coronary artery (LAD) was identified and ligated at 2-mm distally to the origin using 5–0 silk suture. Cardiac ischemia was induced for 30 minutes and then followed by 120-minute reperfusion. Myocardial ischemia was indicated by the presence of ST elevation on ECG and the color changes at

the ischemic area of myocardium. The time to  $1^{st}$  VT/VF and mortality rate were investigated. Arrhythmia score was evaluated during the reperfusion period, using the previously described criteria<sup>53,54</sup>.

Pressure-volume (P-V) loop study during cardiac I/R. Prior to the I/R protocol, rats were anesthetized by intramuscular injection with Zoletil (50 mg/kg, Vibbac Laboratories, Carros, France) and Xylazine (0.15 mg/kg, Laboratories Carlier, SA, Barcelona, Spain), then placed in the supine position 13,38,54. Rats were ventilated with room air via a tracheostomy tube. The right carotid artery was identified and ligated, and then a pressure-volume (P-V) loop catheter (Scisence, Ontario, Canada) was inserted. The catheter tip was directed into the left ventricular chamber to record LV pressure and volume. After allowing 5 minutes for stabilization, the signaling data from the P-V loop catheter was recorded while the cardiac I/R protocol was performed. After I/R study, rats were sacrificed and their hearts were removed and prepared for further mitochondrial and biochemical studies. The investigated parameters obtained from the P-V loop study consisted of end-systolic pressure (ESP), end-diastolic pressure (EDP), maximum and minimum dP/dt (+dP/dt and -dP/dt), stroke volume (SV) and heart rate (HR). All P-V loop parameters were analyzed using Labscribe analytical software (Labscribe, Dover, NH, USA).

**Determination of myocardial infarct size in rat.** At the end of the cardiac I/R experiment, blood sample was collected from the abdominal aorta for the examination of post I/R lactate dehydrogenase (LDH) level to identify the level of myocardial injury<sup>55</sup>. The plasma LDH level determination was performed by the clinical chemistry laboratory of the central diagnostic laboratory, Maharajnakorn Chiang Mai hospital, Chiang Mai University, Thailand. The heart was removed and irrigated with normal saline solution. LAD was re-occluded at the same site which had been previously ligated. Evan blue dye was infused into the heart through the catheter inserted at right and left coronary ostria. Non-blue-dyed areas were defined as no-blood flow areas or areas at risk (AAR). The heart was frozen and sliced horizontally from the base to the occluded area, into1-mm thick tissue slices. The tissue slices were immersed in Triphenyltetrazolium chloride (TTC) for about 12–15 minutes in order to turn the non-infarct or viable tissues to red color. Therefore, the area which exhibited neither blue nor red was identified as showing myocardial infarction <sup>13,38,54</sup>. Then myocardial infarct size was evaluated using Image tool software version 3.0.

**Cardiac mitochondrial function study.** The protocols for cardiac mitochondrial function study, i.e. the mitochondrial ROS production, mitochondrial membrane potential changes and mitochondrial swelling, have been previously described<sup>56,57</sup>. The removed heart was re-occluded at LAD and perfused with cold normal saline, then cardiac tissue from non-ischemic (remote area, R) and ischemic areas (I) were identified. Both I and R tissue were separately homogenized and centrifuged to isolate the cardiac mitochondria<sup>38,58</sup>. The isolated cardiac mitochondria were stained using Dichlorohydrofluorescein diacetate (DCFDA) dye, and then the mitochondrial ROS level was measured using a fluorescent microplate reader (BioTek, Winooski, VT), set at an excitation wavelength of 485 nm with an emission wavelength of 530 nm<sup>56,57</sup>. The dye 5,5',6,6'-tetrachloro-1,1',3,3'tetraethylbenzimidazolcarbocyanine iodide (JC-1) was utilized for the detection of mitochondrial membrane potential change. The monomer form of JC-1 was excited at the wavelength of 485 nm and the emission detected at 590 nm (green fluorescence), whereas the JC-1 aggregate form was excited at the wavelength of 485 nm and the emission detected at 530 nm (red fluorescence)<sup>56,57</sup>. The depolarization of the mitochondrial membrane was indicated by a decreased ratio of red/green fluorescence intensity<sup>56,57</sup>. Cardiac mitochondrial swelling was detected using a spectrophotometer at 540 nm, continuously for 30 minutes. The swelling of mitochondria was indicated by a decrease in the absorbance of a mitochondrial suspension. A transmission electron microscope (TEM; JEM-1200 EX II, JEOL Ltd., Japan) was used for projection the mitochondrial morphology, according to the previously described procedure<sup>34</sup>.

**Determination of oxidative stress.** Oxidative stress levels in cardiac issue and serum were indicated by increased malondialdehyde (MDA) concentrations, which were measured using a high performance liquid chromatography (HPLC) system (Thermo Scientific, Bangkok, Thailand) as previously described<sup>12</sup>. Proteins from cardiac tissues, and serum were mixed with 10% trichloroacetic acid (TCA). The mixture was centrifuged and the supernatant was mixed with 0.44 M H3PO4 and 0.6% thiobabituric acid (TBA) solution to generate thiobarbituric acid reactive substances (TBARS), which were further measured by the HPLC system using BDS software (BarSpec Ltd., Rehovot, Israel). The concentration of TBARS was determined directly from a standard curve and reported as a MDA equivalent concentration<sup>12</sup>.

Cardiac expression of Bax, Bcl-2, Cytochrome C and Connexin 43. The expressions of studied proteins, i.e. Bax, Bcl-2, cytochrome C and Connexin 43 (Cx43, in both phospho- and total forms) were determined by western blot analysis. After cardiac I/R protocol were completed, the unstained heart was identified for ischemic (I) area and remote (R) area, and then myocardial tissues were processed for protein extraction. The myocardial tissues from I and R areas were separately homogenized in a lysis buffer (containing 1% Nonidet P-40, 0.5% sodium deoxycholate, 0.1% sodium dodecyl sulfate (SDS) in 1xPBS) and were centrifuged at 13,000 rpm for 10 minutes. Myocardial protein was mixed with the loading buffer (consisting of 5% mercaptoethanol, 0.05% bromophenol blue, 75 nM Tris-HCl, 2% SDS and 10% glycerol with pH 6.8) at 1 mg/ml concentration and boiled at 95 °C for 5 minutes. The protein was loaded into a 10% SDS-polyacrylamide gel, and then transferred to a polyvinyldene difluoride (PVDF) membrane in a transfer system (Bio-Rad). The protein-containing membranes were incubated in 5% skimmed milk in 1xTBS-T buffer for 1 hour, and then exposed to anti-Bax, anti-Bcl-2, anti-phospho-Cn43 (Cell Signaling Technology, Danvers, MA, USA), anti-total-Cn43 (Santa Cruz Biotechnology, Santa Cruz, CA, USA), anti-cytochrome C and anti-actin (Sigma-Aldrich, St. Louis, MO, USA). Horseradish peroxidase conjugated with anti-rabbit or anti-mouse IgG (Santa Cruz Biotechnology, Inc., CA, USA) was administered to induce a peroxidase reaction, which further developed the signal by enhanced chemiluminescence (ECL)

detection reagents. Finally, autoradiography was performed, and the immune-blotted films were investigated to examine the protein band density using the ImageJ analysis program (NIH image)<sup>34</sup>.

**Determination of metabolic parameters and hormone levels.** Plasma was prepared from fasted blood samples and was kept frozen at  $-80\,^{\circ}$ C until analysis of glucose, cholesterol, triglyceride, insulin, estradiol and malondialdehyde (MDA) levels. Plasma estrogen concentration was measured by using a competitive enzyme immunoassay (EIA) kit (Cayman Chemical Company, MI, USA). Plasma insulin level was detected by sandwich ELISA kit (Millipore, MI, USA). Plasma glucose and triglyceride levels were determined by colorimetric assay from a commercially available kit (Biotech, Bangkok, Thailand). Fasting plasma HDL and LDL were determined using commercially available kits (ERBA diagnostic, Mannheim, Germany)<sup>59</sup>. Plasma lactate dehydrogenase (LDH) was determined by the clinical chemistry laboratory of the central diagnostic laboratory, Maharajnakorn Chiang Mai hospital, Chiang Mai University, Thailand.

Chemicals and antibodies. Estradiol and sesame oil were obtained from Sigma-Aldrich (MO, USA). Vildagliptin was from Novartis (Thailand). Colorimetric assay kits for the determination of plasma glucose, cholesterol and triglycerides were from Biotech (Bangkok, Thailand). ELISA kit for the measurement of plasma insulin level was from Millipore (MI, USA). EIA kit for serum estradiol level detection was from Cayman Chemical Company (MI, USA). The antibodies against Bax, Bcl-2, cytochrome C and p-Cx43 were from Cell Signaling Technology (Danvers, MA, USA), total-Cx43 was from Santa Cruz Biotechnology (Santa Cruz, CA, USA), and anti-actin was from Sigma-Aldrich (MO, USA). The horseradish peroxidase conjugated with anti-rabbit and anti-mouse IgG was from Santa Cruz Biotechnology (Santa Cruz, CA, USA).

**Statistical analysis.** All data is presented as mean  $\pm$  standard error of mean (SEM). A one-way ANOVA followed by post-hoc Tukey's test carried out using the SPSS program (SPSS version 16, SPSS Inc.) was used to determine the differences between the means. P value of less than 0.05 (P < 0.05) is considered as statistically significant.

Limitation of the study. Since the treatments were delivered via different routes, different levels of stress and pharmacokinetic differences with different routes of administration could have affected metabolic outcomes. In this study, myocardial apoptosis markers were investigated (i.e. cardiac Bax expression, cardiac cytochrome C and plasma LDH level) and indicated the increased apoptosis in this study, however TUNEL assay was not performed. It has been known that high-fat diet consumption and estrogen deprivation cause an increased oxidative stress and cardiometabolic dysfunction<sup>12,15</sup>. We previously compared the effect of high-fat diet consumption (a high-fat diet sham group; HFS) and estrogen deprivation (normal-diet fed rats with ovariectomy; NDO) on plasma and cardiac oxidative stress, and our results indicated that both HFS and NDO had similar degree of oxidative stress and cardiometabolic dysfunction<sup>15</sup>. In that study, we also further demonstrated that plasma and cardiac oxidative stress levels were higher in high-fat fed rats with estrogen deprivation (HFO), compared to HFS and NDO rats<sup>15</sup>. In this study, we aimed to focus on the therapeutic strategy that could attenuate oxidative stress and cardiometabolic dysfunction only in estrogen deprived model subjected to ischemia/reperfusion injury. Since HFS and NDO exhibited similar effects on oxidative stress and cardiometabolic function, a non-estrogen deprived obese-insulin resistant (HFS) group was not included in this study. Although the reduction of oxidative stress level was proposed as an important mechanism of vildagliptin and estradiol in cardiometabolic function improvement, its impact was not directly measured in this study. The complete mechanisms regarding the potential effect of vildagliptin and estradiol still need the further investigation.

#### References

- 1. D. Mozaffarian *et al.* Heart disease and stroke statistics-2015 update: a report from the American Heart Association. *Circulation* **131(4)**, e29 (2015).
- T. F. Whayne Jr. & D. Mukherjee. Women, the menopause, hormone replacement therapy and coronary heart disease. Curr. Opin. Cardiol. 30(4), 432 (2015).
- H. N. Hodis & W. J. Mack. Hormone replacement therapy and the association with coronary heart disease and overall mortality: clinical application of the timing hypothesis. J. Steroid Biochem. Mol. Biol. 142, 68 (2014).
- 4. P. Zhai et al. Effect of estrogen on global myocardial ischemia-reperfusion injury in female rats. Am. J. Physiol Heart Circ. Physiol 279(6), H2766–H2775 (2000).
- 5. K. Auro et al. A metabolic view on menopause and ageing. Nat. Commun. 5, 4708 (2014).
- 6. S. M. Grundy. Obesity, metabolic syndrome, and cardiovascular disease. J. Clin. Endocrinol. Metab 89(6), 2595 (2004).
- 7. C. A. Stuenkel *et al.* Treatment of Symptoms of the Menopause: An Endocrine Society Clinical Practice Guideline. *J. Clin. Endocrinol. Metab* **100(11)**, 3975 (2015).
- 8. S. Liu & F. Mauvais-Jarvis. Minireview: Estrogenic protection of beta-cell failure in metabolic diseases. *Endocrinology* **151(3)**, 859 (2010).
- L. Mosca et al. Hormone replacement therapy and cardiovascular disease: a statement for healthcare professionals from the American Heart Association. Circulation 104(4), 499 (2001).
- 10. S. M. Harman *et al.* Timing and duration of menopausal hormone treatment may affect cardiovascular outcomes. *Am. J. Med.* **124(3),** 199 (2011).
- 11. M. Banerjee, N. Younis & H. Soran. Vildagliptin in clinical practice: a review of literature. Expert. Opin. Pharmacother. 10(16), 2745 (2009).
- 12. N. Apaijai *et al.* Cardioprotective effects of metformin and vildagliptin in adult rats with insulin resistance induced by a high-fat diet. *Endocrinology* **153(8)**, 3878 (2012).
- 13. N. Apaijai et al. Combined vildagliptin and metformin exert better cardioprotection than monotherapy against ischemia-reperfusion injury in obese-insulin resistant rats. PLoS. One. 9(7), e102374 (2014).
- 14. C. Roberts-Toler, B. T. O'Neill & A. M. Cypess. Diet-induced obesity causes insulin resistance in mouse brown adipose tissue. *Obesity. (Silver. Spring)* **23(9)**, *1765* (2015).
- 15. S. Sivasinprasasn *et al.* Obese-insulin resistance accelerates and aggravates cardiometabolic disorders and cardiac mitochondrial dysfunction in estrogen-deprived female rats. *Age* (*Dordr.*) **37(2**), 28 (2015).

- H. Vogel et al. Estrogen deficiency aggravates insulin resistance and induces beta-cell loss and diabetes in female New Zealand obese mice. Horm. Metab Res. 45(6), 430 (2013).
- 17. S. Paglialunga *et al.* In adipose tissue, increased mitochondrial emission of reactive oxygen species is important for short-term high-fat diet-induced insulin resistance in mice. *Diabetologia* **58(5)**, 1071 (2015).
- 18. P. Sankar *et al.* Amelioration of oxidative stress and insulin resistance by soy isoflavones (from Glycine max) in ovariectomized Wistar rats fed with high fat diet: the molecular mechanisms. *Exp. Gerontol.* **63**, 67 (2015).
- 19. E. Ho et al. Biological markers of oxidative stress: Applications to cardiovascular research and practice. Redox. Biol. 1, 483 (2013).
- 20. L. Zhu *et al.* Estrogen treatment after ovariectomy protects against fatty liver and may improve pathway-selective insulin resistance. *Diabetes* **62(2)**, 424 (2013).
- L. M. Brown & D. J. Clegg. Central effects of estradiol in the regulation of food intake, body weight, and adiposity. J. Steroid Biochem. Mol. Biol. 122(1-3), 65 (2010).
- 22. R. E. Stubbins *et al.* Estrogen modulates abdominal adiposity and protects female mice from obesity and impaired glucose tolerance. *Eur. J. Nutr.* **51**(7), 861 (2012).
- 23. T. Uetani et al. Impact of insulin resistance on post-procedural myocardial injury and clinical outcomes in patients who underwent elective coronary interventions with drug-eluting stents. *JACC. Cardiovasc. Interv.* 5(11), 1159 (2012).
- 24. M. K. Rutter *et al.* Impact of glucose intolerance and insulin resistance on cardiac structure and function: sex-related differences in the Framingham Heart Study. *Circulation* **107(3)**, 448 (2003).
- R. O. Ek et al. Effects of tamoxifen on myocardial ischemia-reperfusion injury model in ovariectomized rats. Mol. Cell Biochem. 308(1-2), 227 (2008).
- 26. J. Favre et al. Endothelial estrogen receptor {alpha} plays an essential role in the coronary and myocardial protective effects of estradiol in ischemia/reperfusion. Arterioscler. Thromb. Vasc. Biol. 30(12), 2562 (2010).
- 27. W. L. Li, W. Xiang & Y. Ping. Activation of novel estrogen receptor GPER results in inhibition of cardiocyte apoptosis and cardioprotection. *Mol. Med. Rep.* 12(2), 2425 (2015).
- 28. E. M. De Francesco et al. Protective role of GPER agonist g-1 on cardiotoxicity induced by doxorubicin. J. Cell Physiol (2016).
- 29. A. G. Recchia *et al.* The G protein-coupled receptor 30 is up-regulated by hypoxia-inducible factor-1alpha (HIF-1alpha) in breast cancer cells and cardiomyocytes. *J. Biol. Chem.* **286(12)**, 10773 (2011).
- M. A. Aon, S. Cortassa & B. O'Rourke. Percolation and criticality in a mitochondrial network. Proc. Natl. Acad. Sci. USA 101(13), 4447 (2004).
- 31. D. B. Zorov *et al.* Reactive oxygen species (ROS)-induced ROS release: a new phenomenon accompanying induction of the mitochondrial permeability transition in cardiac myocytes. *J. Exp. Med.* **192(7)**, 1001 (2000).
- 32. V. Borutaite *et al*. Nitric oxide protects the heart from ischemia-induced apoptosis and mitochondrial damage via protein kinase G mediated blockage of permeability transition and cytochrome c release. *J. Biomed. Sci.* 16, 70 (2009).
- M. Capano & M. Crompton. Bax translocates to mitochondria of heart cells during simulated ischaemia: involvement of AMP-activated and p38 mitogen-activated protein kinases. *Biochem. J.* 395(1), 57 (2006).
- K. Chinda et al. Dipeptidyl peptidase-4 inhibitor reduces infarct size and preserves cardiac function via mitochondrial protection in ischaemia-reperfusion rat heart. Diab. Vasc. Dis. Res. 11(2), 75 (2014).
- 35. Y. Wang *et al.* Protective effects of estrogen against reperfusion arrhythmias following severe myocardial ischemia in rats. *Circ. J.*
- **74(4)**, 634 (2010).

  36. X. Zhu *et al.* Estrogens increase cystathionine-gamma-lyase expression and decrease inflammation and oxidative stress in the
- myocardium of ovariectomized rats. *Menopause*. **20(10)**, 1084 (2013).

  37. K. Chinda *et al.* Cardioprotective effect of dipeptidyl peptidase-4 inhibitor during ischemia-reperfusion injury. *Int. J. Cardiol*.
- 167(2), 451 (2013).
  38. W. Pongkan *et al.* Vildagliptin reduces cardiac ischemic-reperfusion injury in obese orchiectomized rats. *J. Endocrinol.* 231(1), 81 (2016).
- 39. J. Mera *et al.* Long-term efficacy of vildagliptin in patients with type 2 diabetes undergoing hemodialysis. *J. Diabetes Metab Disord.* **14.** 83 (2015).
- 40. G. McInnes *et al.* Cardiovascular and heart failure safety profile of vildagliptin: a meta-analysis of 17 000 patients. *Diabetes Obes. Metab* 17(11), 1085 (2015).
- 41. I. Gueler et al. Effects of vildagliptin (Galvus(R)) therapy in patients with type 2 diabetes mellitus after heart transplantation. Drug Des Devel. Ther. 7, 297 (2013).
- 42. R. M. Rahmi *et al.* Effect of hypoglycemic agents on ischemic preconditioning in patients with type 2 diabetes and symptomatic coronary artery disease. *Diabetes Care* **36(6)**, 1654 (2013).
- 43. Y. L. He *et al.* Thorough QT study of the effects of vildagliptin, a dipeptidyl peptidase IV inhibitor, on cardiac repolarization and conduction in healthy volunteers. *Curr. Med. Res. Opin.* 27(7), 1453 (2011).
- 44. M. Gokce et al. Long term effects of hormone replacement therapy on heart rate variability, QT interval, QT dispersion and frequencies of arrhythmia. Int. J. Cardiol. 99(3), 373 (2005).
- 45. A. H. Kadish *et al.* Estrogen and progestin use and the QT interval in postmenopausal women. *Ann. Noninvasive. Electrocardiol.* **9(4)**, 366 (2004).
- 46. K. A. Ammar *et al.* Central obesity: association with left ventricular dysfunction and mortality in the community. *Am. Heart J.* 156(5), 975 (2008).
- 47. T. Coutinho *et al.* Central obesity and survival in subjects with coronary artery disease: a systematic review of the literature and collaborative analysis with individual subject data. *J. Am. Coll. Cardiol.* **57(19)**, 1877 (2011).
- 48. J. R. Rettberg, J. Yao & R. D. Brinton. Estrogen: a master regulator of bioenergetic systems in the brain and body. Front Neuroendocrinol. 35(1), 8 (2014).
- 49. S. Sivasinprasasn et al. Estrogen and DPP4 inhibitor, but not metformin, exert cardioprotection via attenuating cardiac mitochondrial dysfunction in obese insulin-resistant and estrogen-deprived female rats. *Menopause*. 23(8), 894 (2016).
- 50. D. M. Nathan *et al.* Medical management of hyperglycemia in type 2 diabetes: a consensus algorithm for the initiation and adjustment of therapy: a consensus statement of the American Diabetes Association and the European Association for the Study of Diabetes. *Diabetes Care* **32(1)**, 193 (2009).
- 51. The Terminology and Diagnostic Criteria Committee of The Japan Society of Ultrasonics in Medicine, "Standard measurement of cardiac function indexes". J. Med. Ultrason 33(2), 123 (2006).
- 52. N. Apaijai *et al.* Effects of vildagliptin versus sitagliptin, on cardiac function, heart rate variability and mitochondrial function in obese insulin-resistant rats. *Br. J. Pharmacol.* **169(5)**, 1048 (2013).
- 53. M. J. Curtis & M. J. Walker. Quantification of arrhythmias using scoring systems: an examination of seven scores in an *in vivo* model of regional myocardial ischaemia. *Cardiovasc. Res.* **22(9)**, 656 (1988).
- W. Pongkan, S. C. Chattipakorn & N. Chattipakorn. Chronic testosterone replacement exerts cardioprotection against cardiac ischemia-reperfusion injury by attenuating mitochondrial dysfunction in testosterone-deprived rats. *PLoS. One.* 10(3), e0122503 (2015).
- 55. M. Kemp et al. Biochemical markers of myocardial injury. Br. J. Anaesth. 93(1), 63 (2004).
- 56. Y. Semaming et al. Protocatechuic acid exerts a cardioprotective effect in type 1 diabetic rats. J. Endocrinol. 223(1), 13 (2014).

- 57. S. Thummasorn *et al.* Granulocyte-colony stimulating factor attenuates mitochondrial dysfunction induced by oxidative stress in cardiac mitochondria. *Mitochondrion.* **11(3),** 457 (2011).
- 58. S. Palee *et al.* Mechanisms responsible for beneficial and adverse effects of rosiglitazone in a rat model of acute cardiac ischaemia-reperfusion. *Exp. Physiol* **98**(5), 1028 (2013).
- 59. W. Pratchayasakul *et al.* Obesity accelerates cognitive decline by aggravating mitochondrial dysfunction, insulin resistance and synaptic dysfunction under estrogen-deprived conditions. *Horm. Behav.* **72**, 68 (2015).

#### Acknowledgements

This work was supported by a NSTDA Research Chair Grant from the National Science and Technology Development Agency (NC), the Thailand Research Fund (WPr and SC), and by a Chiang Mai University Center of Excellence Award (NC).

#### **Author Contributions**

N.C. and S.C. designed the study. S.S., P.T., W.Po. and W.Pr. performed experiments. N.C., S.C., S.S., and W.Pr. performed data analysis and drafted the manuscript. N.C., S.C., and S.S. revised the manuscript. All authors reviewed the final manuscript.

#### **Additional Information**

**Supplementary information** accompanies this paper at http://www.nature.com/srep

**Competing Interests:** The authors declare no competing financial interests.

How to cite this article: Sivasinprasasn, S. et al. DPP-4 Inhibitor and Estrogen Share Similar Efficacy Against Cardiac Ischemic-Reperfusion Injury in Obese-Insulin Resistant and Estrogen-Deprived Female Rats. Sci. Rep. 7, 44306; doi: 10.1038/srep44306 (2017).

**Publisher's note:** Springer Nature remains neutral with regard to jurisdictional claims in published maps and institutional affiliations.

This work is licensed under a Creative Commons Attribution 4.0 International License. The images or other third party material in this article are included in the article's Creative Commons license, unless indicated otherwise in the credit line; if the material is not included under the Creative Commons license, users will need to obtain permission from the license holder to reproduce the material. To view a copy of this license, visit http://creativecommons.org/licenses/by/4.0/

© The Author(s) 2017



# Energy restriction combined with dipeptidyl peptidase-4 inhibitor exerts neuroprotection in obese male rats

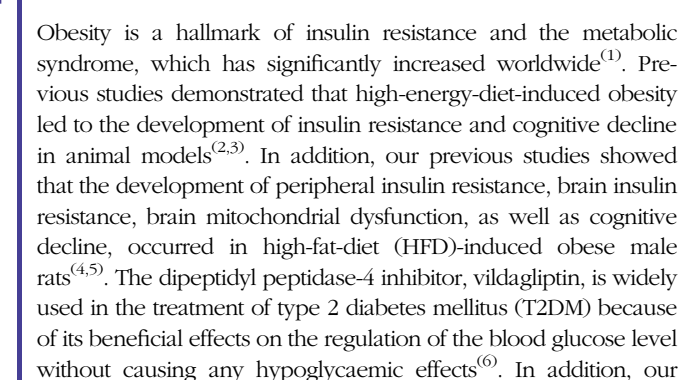
Hiranya Pintana<sup>1,2</sup>, Pongpan Tanajak<sup>1,2</sup>, Wasana Pratchayasakul<sup>1,2</sup>, Piangkwan Sa-nguanmoo<sup>1,2</sup>, Titikorn Chunchai<sup>1,2</sup>, Pattarapong Satjaritanun<sup>1,2</sup>, Linlada Leelarphat<sup>1,2</sup>, Nipon Chattipakorn<sup>1,2</sup> and Siriporn C. Chattipakorn<sup>1,3</sup>\*

(Submitted 25 May 2016 – Final revision received 19 August 2016 – Accepted 10 October 2016 – First publisbed online 17 November 2016)

#### Abstract

Dipeptidyl peptidase-4 (DDP-4) inhibitors and energy restriction (ER) are widely used to treat insulin resistance and type 2 diabetes mellitus. However, the effects of ER or the combination with vildagliptin on brain insulin sensitivity, brain mitochondrial function, hippocampal synaptic plasticity and cognitive function in obese insulin-resistant rats have never been investigated. We hypothesised that ER with DDP-4 inhibitor exerts better efficacy than ER alone in improving cognition in obese insulin-resistant male rats by restoring brain insulin sensitivity, brain mitochondrial function and hippocampal synaptic plasticity. A total of twenty-four male Wistar rats were divided into two groups and fed either a normal diet or a high-fat diet (HFD) for 12 weeks. At week 13, the HFD rats were divided into three subgroups (n 6/subgroup) to receive one of the following treatments: vehicle, ER (60% of energy received during the previous 12 weeks) or ER plus vildagliptin (3 mg/kg per d, p.o.) for 4 weeks. At the end of the treatment, cognitive function, metabolic parameters, brain insulin sensitivity, hippocampal synaptic plasticity and brain mitochondrial function were determined. We found that HFD-fed rats demonstrated weight gain with peripheral insulin resistance, dyslipidaemia, oxidative stress, brain insulin resistance, impaired brain mitochondrial function and cognitive dysfunction. Although HFD-fed rats treated with ER and ER plus vildagliptin showed restored peripheral insulin sensitivity and improved lipid profiles, only ER plus vildagliptin rats had restored brain insulin sensitivity, brain mitochondrial function, hippocampal synaptic plasticity and cognitive function. These findings suggest that only a combination of ER with DPP-4 inhibitor provides neuroprotective effects in obese insulin-resistant male rats.

Key words: Energy restriction: Vildagliptin: Obese insulin-resistant rats: Brain mitochondrial functions: Hippocampal synaptic plasticity: Cognitive functions



previous studies reported that vildagliptin improved not only peripheral insulin resistance but also brain insulin resistance, as indicated by improved brain insulin receptor function in obese insulin-resistant rats<sup>(4)</sup>. Furthermore, the enhancement of hippocampal neurogenesis and improvement in cognition were found in HFD-fed rodents treated with vildagliptin (4,7,8). All of those findings suggest that vildagliptin exerts beneficial effects on metabolic control and cognitive function.

Although several types of medication have been prescribed for the treatment of T2DM or the obese insulin-resistant condition, several side effects of medication have been observed. Therefore, a lifestyle modification, including energy restriction

Abbreviations: aCSF, artificial cerebrospinal fluid; Akt/PKB, serine/threonine-specific protein kinase B; ER, energy restriction; HFD, high-fat diet; HFRV, HFDfed rats on a restricted diet and vehicle; HFRVil, HFD-fed rats on a restricted diet and vildaglptin; HFV, HFD-fed rats treated with the vehicle; IR, insulin receptor; LTD, long-term depression; LTP, long-term potentiation; MDA, malondialdehyde; MWM, Morris Water Maze; ND, normal diet; NDV, ND-fed rats treated with vehicle; ROS, reactive oxygen species.

\* Corresponding author: S. C. Chattipakorn, fax +011 66 53 222 844, email scchattipakorn@gmail.com



 $<sup>^1</sup>$ Neurophysiology Unit, Cardiac Electrophysiology Research and Training Center, Faculty of Medicine, Chiang Mai University, Chiang Mai 50200, Thailand

 $<sup>^2</sup>$ Department of Physiology, Faculty of Medicine, Chiang Mai University, Chiang Mai 50200, Thailand

<sup>&</sup>lt;sup>3</sup>Department of Oral Biology and Diagnostic Science, Faculty of Dentistry, Chiang Mai University, Chiang Mai 50200, Thailand



(ER), has been used as an alternative therapy in the obese insulin-resistant condition and T2DM. A previous study showed that ER in older animals led to improved metabolic parameters and also an extended lifespan<sup>(9)</sup>. Although adverse effects of ER such as promoting bone loss<sup>(10)</sup> and decreasing wound healing rate<sup>(11)</sup>, in rats have been reported, several studies have shown that ER mimetics conferred the benefits of ER without its side effects<sup>(12,13)</sup>. Moderate ER had a beneficial impact on metabolic parameters, and improved insulin sensitivity in in vitro and in vivo studies (14-17). In addition, a previous study reported that ER not only exerts a positive effect on metabolic control but also leads to improved brain function (18,19). Several studies demonstrated that ER caused an increase in an endogenous apoptosis inhibitor in the neuronal cells<sup>(20)</sup>, induced neuroprotection<sup>(21)</sup>, decreased mitochondrial reactive oxygen species (ROS) production in aged rat brains (22) and preserved cognitive function in aged male rats<sup>(23)</sup>. All of those findings suggest that ER has beneficial effects in neuroprotection and the preservation of cognitive function.

However, the effects of either ER or the combination of ER plus vildagliptin on brain function, including brain insulin sensitivity, brain mitochondrial function, hippocampal synaptic plasticity and cognitive function in obese insulin-resistant rats have never been investigated. This study tests the hypothesis that the combination of ER plus vildagliptin has greater beneficial effects on the brain function of obese insulin-resistant rats than ER alone.

#### Methods

#### Animal models and experimental protocols

In total, twenty-four male Wistar rats weighing 180-200 g (approximately aged 5-6 weeks old), obtained from the National Animal Center, Salaya Campus, Mahidol University, Bangkok, Thailand, were used. All experiments were conducted in accordance with the approved protocol from the Faculty of Medicine, Chiang Mai University's Institutional Animal Care and Use Committee, in compliance with NIH guidelines (protocol number: 31/2557). All animals were housed in environmentally controlled conditions  $(25 \pm 0.5$ °C and a 12 h light–12 h dark cycle) and were allowed to acclimate for 1 week. Rats were randomly divided into two groups and fed on either a normal diet (ND: 19.77% energy (%E) from fat, n 6) or a HFD (59.28%E from fat, n 18) for 12 weeks<sup>(24)</sup>. At the end of the 12th week, rats in the ND group received normal saline solution (NSS) via intra-gastric gavage, as indicated, and were designated the control group (ND-fed rats treated with the vehicle (NDV)), and rats in the HFD group were subdivided into three subgroups: (1) 12-week HFD-fed rats continued with HFD and in addition were given NSS via intra-gastric gavage for 4 weeks (HFD-fed rats treated with the vehicle (HFV)); (2) 12-week HFD-fed rats were switched to a restricted diet (ND, containing only 60% energy intake compared with the energy intake of HFD), as described in a previous study<sup>(17)</sup>, and were also given NSS via intra-gastric gavage for 4 weeks (HFD-fed rats on a restricted diet and vehicle (HFRV)); and (3) 12-week HFD-fed rats were switched to a restricted diet and in addition were given 3 mg/kg per d vildagliptin (Novartis, Thailand) via intra-gastric gavage for

4 weeks<sup>(6,8)</sup>. The rats' cognitive function was subsequently determined by the Morris Water Maze (MWM) test. Blood samples were collected from a tail vein at weeks 0, 12 and 16 for further plasma analysis. At the end of the experimental period, rats were deeply anesthetised with 2-3% isoflurane and killed by decapitation. The brain of each rat was rapidly removed after death and carefully sliced in preparation for extracellular recording (insulin-induced long-term depression (LTD) and hippocampal synaptic long-term potentiation (LTP)), immunoblot and brain mitochondrial functions. The experimental protocol is shown in Fig. 1.

#### Blood sample assays

Plasma glucose and cholesterol levels were determined via colorimetric assay (Biotech). Plasma HDL and LDL levels were determined using a commercial colorimetric assay kit (Biovision). Plasma insulin levels were determined using the Sandwich ELISA kit (Millipore). Peripheral insulin resistance was assessed using the homoeostasis model assessment (HOMA), as previously described<sup>(5)</sup>.

#### Oral glucose tolerance test

Oral glucose tolerance test (OGTT) was performed as described previously<sup>(4,8)</sup>. In brief, rats were starved overnight before the test and received 2 g/kg glucose solution via oral gavage, and then blood samples were collected at different time points. AUC were calculated to evaluate glucose tolerance.

#### Brain-slice preparation

The brain-slice preparation was performed as described previously<sup>(4,5,24)</sup>. In brief, the whole brain was rapidly removed after decapitation and then immersed in ice-cold high-sucrose artificial cerebrospinal fluid (aCSF). The hippocampal slices were cut using a vibratome (Vibratome Company). Following a 30-min post-slice incubation in high-sucrose aCSF, the slices were transferred to a standard aCSF for an additional 30 min at room temperature (22–24°C).

#### Extracellular recordings of hippocampal slices for insulin-induced long-term depression

An extracellular recording of hippocampal slices for insulininduced LTD was performed as described in previous studies<sup>(4,5,24)</sup>. Hippocampal slices were perfused with aCSF (as a baseline condition) for 10 min, and then perfused with aCSF plus 500 nm-insulin (as an insulin-induced LTD) for an additional 10 min. After this, the slices were perfused with aCSF for an additional 50 min and readings recorded.

### Extracellular recordings of hippocampal slices for synaptic long-term potentiation

The examination of electrical-induced hippocampal synaptic LTP was performed as described in a previous study<sup>(25)</sup>. In brief, LTP was induced by delivering high-frequency



1702



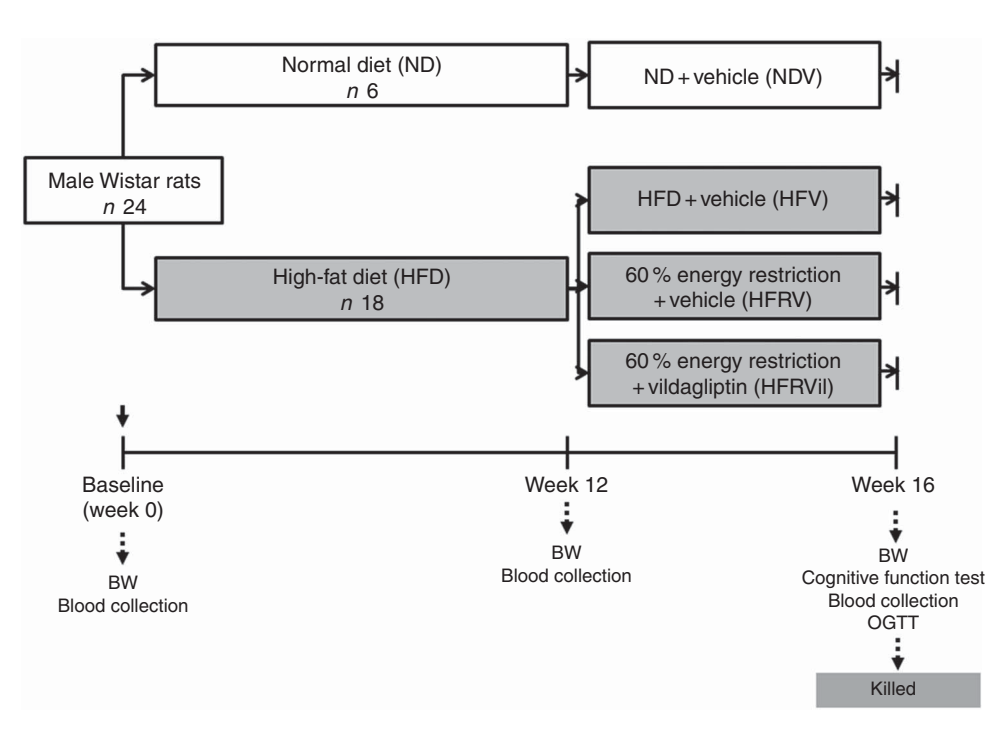


Fig. 1. The experimental protocol of the study. OGTT, oral glucose tolerance test.

stimulation (HFS; four trains at 100 Hz; 0.5-s duration; 20-s interval). Experiments were performed for 40 min after HFS.

#### Immunoblotting for brain insulin signalling

To investigate the expression of insulin receptor phosphorylation (p-IR), insulin receptors (IR), serine/threonine-specific protein kinase B (Akt/PKB) and insulin-mediated Akt Ser473 phosphorylation, homogenated brain slices from each subgroup were used as described in our previous study<sup>(4,5,24)</sup>. The p-IR, IR, Akt/PKB at serine 473 kinase phosphorylation and Akt/PKB were electrophoresed and immunoblotted with rabbit anti-IR at tyrosine phosphorylation (p-IR<sup>tyr1162/1163</sup>) (1:1000, sc-25103-R; Santa Cruz Biotechnology), IR (1:1000, sc-711; Santa Cruz Biotechnology), Akt/PKB at serine 473 kinase phosphorylation (1:1000, no. 9271; Cell Signaling Technology) and Akt/PKB (1:1000, no. 9272; Cell Signaling Technology). For a loading control, the immunoblot for each membrane was incubated with anti- $\beta$ -actin (1:4000, no. 4967; Cell Signaling Technology). All membranes enabling the visualisation of the phosphorylation and the protein levels of IR and Akt/ PKB expression were incubated with secondary goat anti-rabbit antibody conjugated with horseradish peroxidase (1:2000, no. 7074; Cell Signaling Technology). Band densities of phosphorylated IR or Akt/PKB at serine 473 kinase phosphorylation were represented as a ratio of insulin stimulation (+):no insulin stimulation (-) and were normalised to total IR or Akt/PKB. Band intensities were quantified using Scion Imaging, and the results were shown as average signal intensity (arbitrary) units.

#### Serum and brain malondialdehyde levels

HPLC method was used to evaluate the concentrations of serum and brain malondialdehyde (MDA), as described previously (8,26-28).

#### Brain mitochondrial function study

Brain mitochondria were isolated using the method described previously  $^{(4)}$ . Brain mitochondrial function including brain mitochondrial ROS, mitochondrial membrane potential change ( $\Delta\Psi$ m) and mitochondrial swelling were determined. Brain mitochondrial ROS were measured using dichloro-hydrofluorescein diacetate fluorescent dye. The change in mitochondrial membrane potential ( $\Delta\Psi$ m) was measured using the fluorescent dye 5, 52, 6, 62-tetrachloro-1, 12, 3, 32-tetraethyl benzimidazol carbocyanine iodide (JC-1) and brain mitochondrial swelling was determined by measuring the change in the absorbance of brain mitochondrial suspension at 540 nm. All were determined by following the methods described previously  $^{(4,8)}$ .

#### Cognitive function test

The open-field test (OFT) was used to screen locomotor activity, as described in previous studies  $^{(8,29)}$ . The assessment of cognitive function was performed using the MWM test with two assessments including the acquisition test, which was carried out for 5 consecutive days, and the probe test, which was performed on day  $6^{(8,30)}$ . Data analysis of the MWM test was done manually from video tape recordings by the investigators, who were blinded to experimental groups.

# Golgi staining and morphological analysis of dendritic spines

Golgi staining and morphological analysis were carried out using the method described previously<sup>(31)</sup>. After decapitation, brains were removed and rinsed with double-distilled water and were processed for Golgi staining using a commercially



available kit (FD Rapid GolgiStain™ Kit #PK401; FD Neurotechnologies, Inc.). For analysis of dendritic spine density, the secondary and tertiary dendrites of three neurons in the CA1 hippocampus area were counted. Dendritic segments were viewed through an inverted microscope (IX-81; Olympus).

#### Statistical analysis

Data were expressed as mean values with their standard errors. For all comparisons, the significance of the differences in peripheral biochemical parameters was calculated using the Mann–Whitney U test. The comparisons in the percentage of insulin-induced LTD, the percentage of LTP, brain mitochondrial function, immunoblot, the OFT tests and the MWM tests for the probe test between groups were performed using the one-way ANOVA test, followed by post boc Fisher's least significant difference (LSD) analysis. As the acquisition phase of the MWM test has two independent factors (treatment and time), we used the two-way ANOVA followed by post boc Fisher's LSD analysis to analyse the data. P < 0.05 was considered as a measure of statistical significance.

#### Results

Energy restriction and the combination of energy restriction plus vildagliptin in obese insulin-resistant rats equally restored peripheral insulin sensitivity

At baseline levels (week 0), the metabolic parameters were not significantly different between the ND-fed rats and the HFD-fed rats (Table 1). After 12 weeks of diet regimens, the HFD group had significantly increased body weight, plasma insulin, HOMA index, total cholesterol levels and LDL-cholesterol levels, when compared with the ND group (Table 1). However, plasma glucose levels were not significantly different between the groups (Table 1).

After 4 weeks of the treatment, HFV had significantly increased body weight, visceral fat, plasma insulin levels, HOMA index, plasma glucose AUC of OGTT (AUCg), total cholesterol and plasma LDL-cholesterol levels, but had decreased plasma HDL-cholesterol levels, when compared with NDV (Table 2). These findings indicated that peripheral insulin resistance was still observed in HFV rats after 16 weeks. Interestingly, HFRV and HFD-fed rats on a restricted diet and vildaglptin (HFRVil) had significantly decreased body weight, visceral fat, plasma insulin, HOMA index, plasma glucose AUCg, total plasma cholesterol and LDL-cholesterol levels, but increased plasma HDL-cholesterol levels, when compared with HFV rats (Table 2). However, there was no significant difference in plasma glucose and plasma TAG levels between all groups (Table 2).

## Obesity caused the impairment of brain insulin receptor function, which was only restored by the combination of energy restriction plus vildagliptin

After 4 weeks of the treatment, the degree of insulin-induced LTD in HFV rats was significantly reduced, when compared with that in NDV rats (n 2–3 independent slices/animal, n 6 animals/ group, Fig. 2(a)). Interestingly, the degree of insulin-induced LTD in only HFRVil rats showed a significant increase, when compared with that of HFV rats and HFR rats (n 2-3 independent slices/animal, n 6 animals/group, Fig. 2(a)). Regarding brain insulin signalling, the levels of IR and Akt/PKB proteins expression showed no difference between the groups (Fig. 2(d) and (e)). The p-IR and Akt/PKB at the serine 473 site in both HFV and HFRV rats showed a significant decrease, when compared with that of NDV rats (Fig. 2(b) and (c)). However, the p-IR levels and Akt/PKB at the serine 473 site of only HFRVil rats showed a significant increase when compared with those of HFV rats (Fig. 2(b) and (c)).

## Obesity led to brain mitochondrial dysfunction, which improved following treatment with the combination of energy restriction plus vildagliptin

After 4 weeks of treatment, brain mitochondrial dysfunction was observed in HFV rats as indicated by increased brain mitochondrial ROS production, brain mitochondrial membrane depolarisation and brain mitochondrial swelling (Fig. 3(a), (b) and (c)). HFRV rats also had a significant increase in brain mitochondrial ROS production, brain mitochondrial depolarisation

Table 1. Metabolic parameters at week 0 (baseline) and the end of week 12 (before treatment) (Mean values with their standard errors)

|                                  |       | Bas | eline | Week 12 |       |     |       |       |  |
|----------------------------------|-------|-----|-------|---------|-------|-----|-------|-------|--|
|                                  | ND    |     | HFD   |         | ND    |     | HFD   |       |  |
| Metabolic parameters             | Mean  | SEM | Mean  | SEM     | Mean  | SEM | Mean  | SEM   |  |
| Body weight (g)                  | 199-6 | 2.7 | 206.9 | 2.4     | 476-3 | 6.0 | 560.8 | 12.5* |  |
| Plasma glucose (mg/dl)           | 139.0 | 5.4 | 130.5 | 4.5     | 144.6 | 5⋅1 | 143.3 | 9.0   |  |
| Plasma insulin (ng/ml)           | 2.4   | 0.6 | 2.4   | 0.5     | 2.9   | 0.4 | 4.7   | 0.6*  |  |
| HOMA index                       | 12.0  | 2.8 | 10.9  | 2.5     | 24.5  | 3.9 | 38.6  | 3.9*  |  |
| Plasma total cholesterol (mg/dl) | 68.0  | 3.4 | 67.8  | 3.8     | 66.9  | 3.9 | 81.5  | 4.2*  |  |
| Plasma TAG (mg/dl)               | 51.9  | 3.7 | 48.1  | 4.5     | 60.2  | 7.6 | 62.0  | 8.7   |  |
| HDL-cholesterol (mg/dl)          | 32.5  | 1⋅5 | 29.7  | 1.3     | 30.1  | 1.6 | 28.0  | 3.3   |  |
| LDL-cholesterol (mg/dl)          | 23.6  | 3.5 | 28.9  | 4.0     | 23.7  | 2.7 | 39.9  | 3.0*  |  |

ND, normal-diet-fed rats; HFD, high-fat-diet-fed rats; HOMA, homoeostasis model assessment



Compared with ND at the same time interval.

1704 H. Pintana et al.

Table 2. Metabolic parameters after energy restriction and energy restriction plus vildagliptin treatment (Mean values with their standard errors)

|  | Groups |      |       |       |       |       |        |       |  |  |  |
|--|--------|------|-------|-------|-------|-------|--------|-------|--|--|--|
|  | NDV    |      | HFV   |       | HFRV  |       | HFRVil |       |  |  |  |
| Metabolic parameters                                   | Mean   | SEM  | Mean  | SEM   | Mean  | SEM   | Mean   | SEM   |  |  |  |
| Body weight (g)  | 490.7  | 9.4  | 597.9 | 15*   | 519.1 | 10.1† | 511.3  | 10.5† |  |  |  |
| Visceral fat (g)                                       | 24.6   | 1.3  | 52.7  | 2.9*  | 30.0  | 1.3†  | 28.5   | 2.3†  |  |  |  |
| Plasma glucose (mg/dl)                                 | 153.5  | 16.8 | 163-2 | 7.1   | 152.7 | 3.2   | 157.5  | 5.6   |  |  |  |
| Plasma insulin (ng/ml)                                 | 4.2    | 0.2  | 6.4   | 0.8*  | 3.6   | 0.5†  | 4.0    | 0.6†  |  |  |  |
| HOMA index   | 34.6   | 5.3  | 59.2  | 8.8*  | 32.7  | 4.4†  | 34.5   | 6.1†  |  |  |  |
| Plasma glucose AUC (AUCg) (mg/dlxminx10 <sup>4</sup> ) | 4.8    | 0.2  | 6.0   | 0.3*  | 4.8   | 0.3†  | 4.9    | 0.2†  |  |  |  |
| Plasma total cholesterol (mg/dl)                       | 70.5   | 4.2  | 97.3  | 6.0*  | 76.5  | 2.4†  | 75.4   | 3.8†  |  |  |  |
| Plasma TAG (mg/dl)                                     | 52.1   | 7.2  | 54.7  | 5.0   | 51.8  | 5.3   | 53.3   | 7.2   |  |  |  |
| HDL-cholesterol (mg/dl)                                | 33.9   | 1.9  | 24.5  | 1.9*  | 35.9  | 2.2†  | 34.7   | 2.0†  |  |  |  |
| LDL-cholesterol (mg/dl)                                | 26.9   | 3.1  | 52.8  | 6.0*  | 31.8  | 6.5†  | 28.3   | 4.3†  |  |  |  |
| Serum MDA (µmol/ml)                                    | 1.42   | 0.05 | 5.30  | 1.33* | 1.63  | 0.12† | 1.54   | 0.11† |  |  |  |
| Brain MDA (μmol/mg protein)                            | 0.47   | 0.05 | 0.68  | 0.07* | 0.57  | 0.04  | 0.50   | 0.02† |  |  |  |

NDV, normal-diet-fed rats treated with vehicle; HFV, high-fat-diet-fed rats treated with vehicle; HFRV, high-fat-diet-fed rats reversed to normal diet with 60% energy restriction treated with vehicle; HFRVil, high-fat-diet-fed rats reversed to normal diet with 60% energy restriction treated with vildagliptin; HOMA, homoeostasis model assessment; MDA,

and brain mitochondrial swelling, when compared with NDV rats (Fig. 3(a), (b) and (c)). Interestingly, only HFRVil rats showed a significant decrease in brain ROS production, and improvement in brain mitochondrial depolarisation and brain mitochondrial swelling, when compared with HFV rats (Fig. 3(a), (b) and (c)).

Furthermore, there were morphological changes in brain mitochondria; representatives from all groups are shown in Fig. 3(d). Brain mitochondrial swelling was observed in both the HFV and HFRV rats, as indicated by markedly unfolded cristae (Fig. 3(d)). Interestingly, brain mitochondrial morphology with apparent folded cristae was observed in only HFRVil rats (Fig. 3(d)).

### Obesity led to increased brain oxidative stress levels, which was attenuated by the combination of energy restriction plus vildagliptin

After 4 weeks of treatment, both circulating MDA and brain MDA levels significantly increased in HFV rats compared with NDV rats (Table 2). HFRV rats only showed a significant decrease in circulating MDA, when compared with HFV rats (Table 2). Interestingly, HFRVil rats showed a significant decrease in both circulating MDA and brain MDA levels, when compared with HFV rats (Table 2).

Obesity caused impaired hippocampal synaptic plasticity and cognitive decline, which only showed restoration with the combination of energy restriction plus vildagliptin

After 4 weeks of treatment, the results demonstrated that the degrees of electrical-induced LTP significantly decreased in both HFV and HFRV rats, when compared with NDV rats (n 2–3 independent slices/animal, n 6 animals/group, Fig. 4(a)). The reduction of electrical-induced LTP in both HFV and HFRV rats was not significantly different (n 2-3 independent slices/ animal, n 6 animals/group, Fig. 4(a)). However, the degree of electrical-induced LTP of HFRVil rats significantly increased. when compared with that of HFV rats (n 2-3 independent slices/animal, n 6 animals/group, Fig. 4(a)).

The density of hippocampal dendritic spines was determined at the secondary and tertiary dendrites in the apical dendrite of the CA1 hippocampus to investigate the underlying mechanism of memory function. It was found that the dendritic spine density of HFV and HFRV rats decreased significantly, when compared with that of NDV rats (Fig. 4(b)). After treatment regimens, the dendritic spine density of both HFRV and HFRVil rats showed a significant increase, when compared with that of HFV rats (Fig. 4(b)). However, dendritic spine density of HFRVil rats was significantly greater than that of HFRV rats (Fig. 4(b)).

The OFT was used to screen locomotor activity. The results showed that there was no significant difference between all groups, indicating that the locomotor activity did not differ in all groups. In addition, the study determined cognitive function by using the MWM test after 4 weeks of the treatment regimens. For the acquisition test, it was found that both HFV and HFRV rats showed a significantly increased time to reach the platform, when compared with NDV rats (Fig. 4(c)). However, HFRVil rats showed a significantly decreased time to reach the platform, when compared with HFV rats (Fig. 4(c)). For the probe test, both HFV and HFRV rats had a significantly decreased time spent in the target quadrant, when compared with NDV rats (Fig. 4(d)). In contrast, HFRVil rats had a significantly increased time spent in the target quadrant, when compared with HFV rats (Fig. 4(d)).

#### Discussion

The major findings of this study are as follows: (1) obesity induced by HFD consumption leads to the development of peripheral insulin resistance, impairment of brain insulin sensitivity, brain mitochondrial dysfunction, impaired hippocampal synaptic



Compared with NDV.

<sup>†</sup> Compared with HFV.



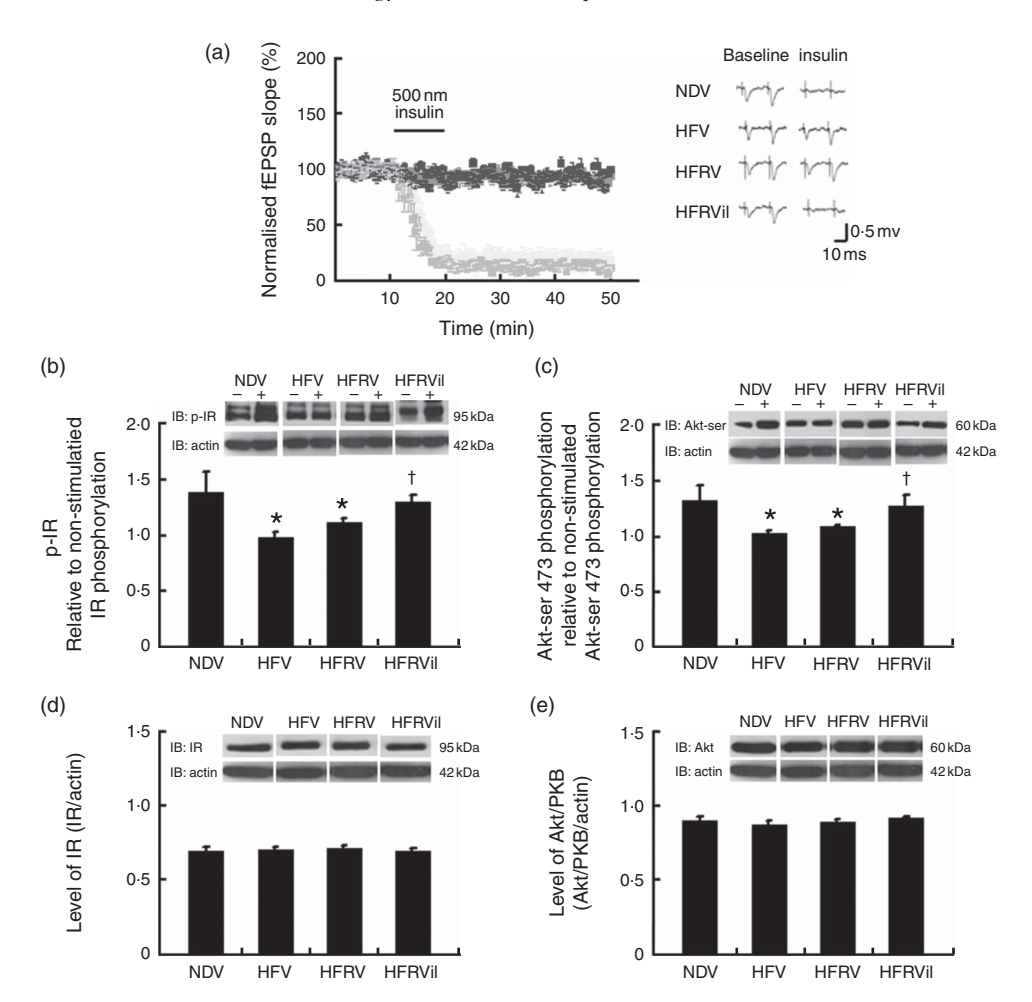


Fig. 2. The effects of energy restriction (ER) and the combination of ER plus vildagliptin on brain insulin receptor function (insulin-induced long-term depression (LTD)) and brain insulin signalling, including the phosphorylation of insulin receptors (p-IR), Akt-Ser 473, insulin receptors (IR) and serine/threonine-specific protein kinase B (Akt/PKB) protein expression in obese insulin-resistant rats. The combination of ER plus vildagliptin improves the ability of insulin-induced LTD in high-fat-diet-fed rats reversed to normal diet with 60% ER treated with vildagliptin (HFRVil), when compared with high-fat-diet-fed rats treated with vehicle (HFV) (a). After 4 weeks of treatment, both p-IR and Akt-Ser 473 expression levels were significantly decreased in HFV and high-fat-diet-fed rats reversed to normal diet with 60 % ER treated with vehicle (HFRV) when compared with normal-diet-fed rats treated with vehicle (NDV) ((b) and (c)). Both p-IR and Akt-Ser 473 expression increased significantly after the combination of ER plus vildagliptin when compared with HFV rats ((b) and (c)). However, there was no difference in IR and Akt/PKB protein expression between all groups ((d) and (e)). \*P<0.05 v. NDV and † P<0.05 v. HFV. 🔄 NDV; 📺 HFV; 📺 HFRV; 📺 HFRVi 🖽 HFRVil. fEPSP, field excitatory postsynaptic potential.

plasticity, decreased dendritic spine density and cognitive decline; (2) both ER and the combination of ER plus vildagliptin showed equally improved peripheral insulin sensitivity and lipid profiles; (3) ER alone showed a decrease only in circulating oxidative stress, whereas the combination of ER plus vildagliptin showed a decrease in both circulating and brain oxidative stress levels; and (4) only the combination of ER plus vildagliptin showed a correlation with restored brain insulin sensitivity, brain mitochondrial function, hippocampal synaptic plasticity and cognitive function in obese insulin-resistant rats.

This study has demonstrated that diet-induced obesity led to the development of the peripheral insulin resistance via impaired peripheral insulin sensitivity, impaired lipid profiles and an increase in both circulating and brain oxidative stress. These findings confirmed other studies and our previous studies that diet-induced obesity not only caused peripheral insulin resistance but also brain insulin resistance (24,32). The present findings indicated that obesity increased oxidative stress and impaired brain mitochondrial function, resulting in brain insulin resistance and cognitive decline.

This study demonstrates that ER enhanced peripheral insulin sensitivity and improved lipid profiles in obese insulin-resistant rats. A possible explanation of these findings may be that ER decreased visceral fat and dyslipidaemia. Decreased fat has been shown to reduce systemic inflammation (33), as well as oxidative stress, as shown in Table 2 and in a previous study (34). An increase in inflammation and oxidative stress led to the impairment of peripheral insulin sensitivity (35,36). Therefore, ER in the present study led to improved peripheral insulin sensitivity, possibly via the reduction of oxidative stress.

Although ER led to the restoration of peripheral insulin sensitivity and decreased circulating oxidative stress, ER alone failed to cause improvement in brain insulin sensitivity and brain mitochondrial dysfunction, as well as failed to restore hippocampal synaptic plasticity and cognitive decline in obese insulin-resistant rats. This may be because of our finding that ER





H. Pintana et al. 1706

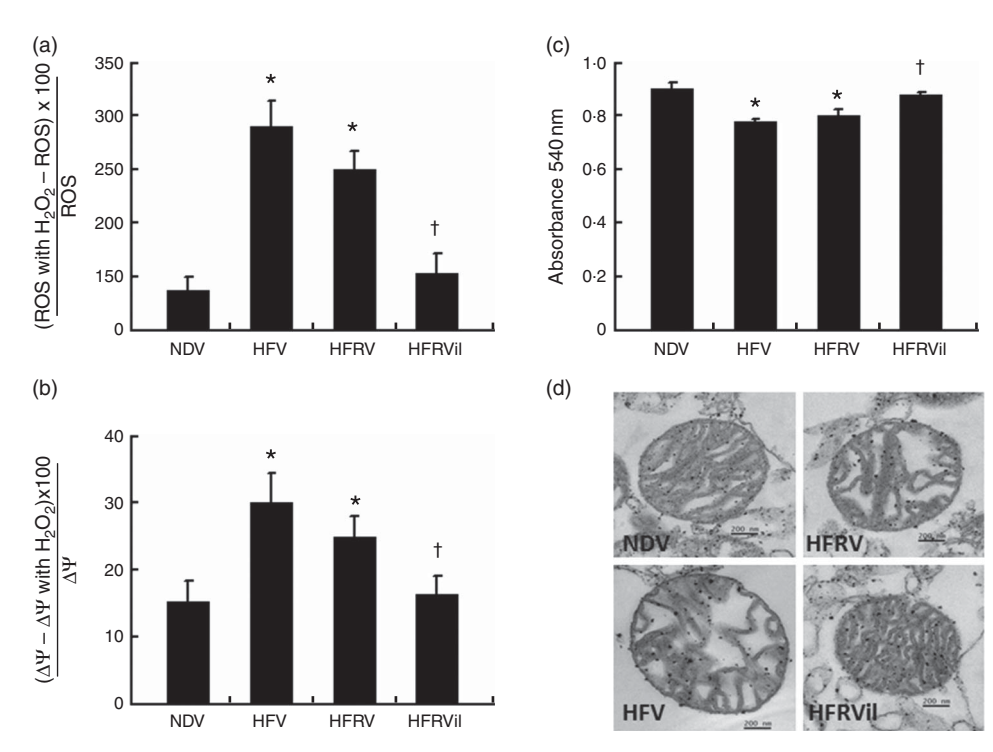


Fig. 3. The effects of energy restriction (ER) and the combination of ER plus vildagliptin on brain mitochondrial function and representative images of brain mitochondrial morphology by transmission electron microscopy (JEM-2200FS field emission electron microscope, original magnification 20000x) in obese insulinresistant rats. High-fat-diet-fed rats treated with vehicle (HFV) and high-fat-diet-fed rats reversed to normal diet with 60 % ER treated with vehicle (HFRV) demonstrated brain mitochondrial dysfunction when compared with normal-diet-fed rats treated with vehicle (NDV), as indicated by increased brain mitochondrial reactive oxygen species (ROS) production following H<sub>2</sub>O<sub>2</sub> application (a), increased brain mitochondrial membrane potential change following H<sub>2</sub>O<sub>2</sub> application (b) and decreased absorbance values, indicating brain mitochondrial swelling (c). The combination of ER plus vildagliptin in high-fat-diet-fed rats reversed to normal diet with 60 % ER treated with vildagliptin (HFRVil) showed improved brain mitochondrial function when compared with HFV rats, as indicated by significantly decreased brain mitochondrial ROS production (a), decreased brain mitochondrial membrane potential change (b) and increased absorbance values (c). Furthermore, normal folding of cristae in brain mitochondrial morphology was shown in both NDV and HFRVil rats (d). However, brain mitochondrial swelling, as indicated by unfolded cristae in both HFV and HFRV rats, was observed (d).  $^*P < 0.05 \ v$ . NDV and  $^+P < 0.05 \ v$ . HFV.

alone could neither decrease brain oxidative stress levels nor brain mitochondrial dysfunction, whereas treatment with combined ER and vildagliptin effectively improved both parameters in obese insulin-resistant rats (Table 2).

Unlike this study, previous studies showed that ER had beneficial effects on neuroprotection and preservation of cognition. For example, (1) a previous study demonstrated that 40% of ER for 24 months reduced the rate of mitochondrial H<sub>2</sub>O<sub>2</sub> production via reduced brain ROS production in aged rats<sup>(22)</sup>. (2) The study involving 40% ER for 22–29 months also reported that ER prevented age-related deficit synaptic LTP and the preservation of the NR1-subunit of N-methyl-D-aspartate (NMDA) receptors in aged Fisher 344 rats<sup>(37)</sup>. (3) The study of 60 % ER for 4 weeks in male rats demonstrated that ER stabilised synaptophysin expression and preserved cognitive function (23). (4) A recent study demonstrated that 70 % ER for 28 d improved metabolic effects and cognitive decline via up-regulation of brain-derived neurotrophic factor and decreased hippocampal oxidative stress in the obese-metabolic syndrome male rats induced by a moderated HFD (35 %E from fat)(19). The different findings between previous studies and the present study could be dependent on the percentage of HFD feeding and the duration of ER. Future studies are needed to verify this issue.

One important finding from this study is that ER combined with vildagliptin restored peripheral insulin sensitivity, brain insulin sensitivity, brain mitochondrial function, synaptic plasticity and cognitive function in obese insulin-resistant rats. This means of intervention provided better efficacy than ER alone in this model. These findings suggest that the beneficial effects on brain function in this group could be because of the action of vildagliptin. This is consistent with our previous studies, which showed that vildagliptin led to the restoration of cognitive function in the obese model, via improved brain insulin sensitivity and reduced brain oxidative stress<sup>(4,8)</sup>. As demonstrated in this study, the combined ER with vildagliptin improved/restored both brain insulin resistance and brain oxidative stress better than ER alone. These findings indicated that ER in combination with the vildagliptin treatment provided more beneficial effects than ER alone in our study model. However, other ER feeding regimens and delivery could have given similar or different results as observed in the present study and require further investigation.

#### Limitations of the study

The two-factorial design study was not conducted in the present study; therefore, the effects of ER or its combination with vildagliptin in ND-fed rats (lean rats) were not known. However, our previous studies showed that the administration of vildagliptin in ND-fed rats has no effect on the metabolic parameters or brain function, when compared with vehicle-treated ND-fed rats<sup>(4,8)</sup>.





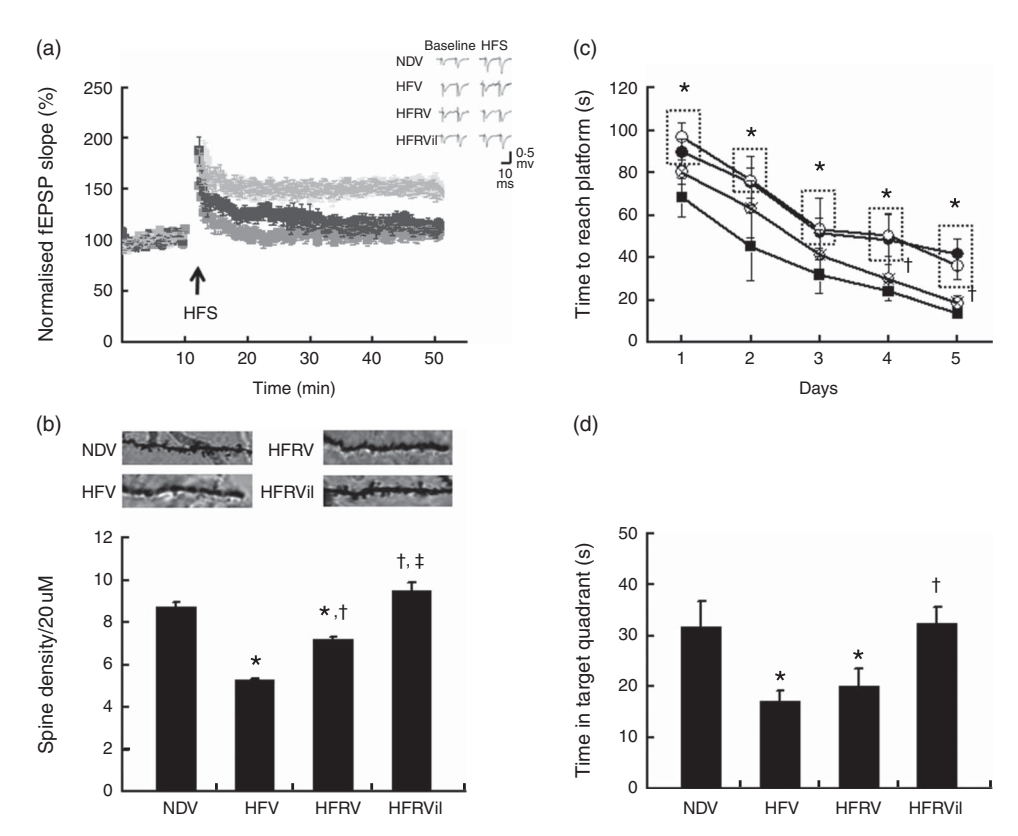


Fig. 4. The effects of energy restriction (ER) and the combination of ER plus vildagliptin on hippocampal synaptic long-term potentiation (LTP) and the number of dendritic spines on tertiary dendrites on apical dendrites, as well as cognitive function, in obese insulin-resistant rats. Both high-fat-diet-fed rats treated with vehicle (HFV) and highfat-diet-fed rats reversed to normal diet with 60 % ER treated with vehicle (HFRV) showed a significantly reduced degree of LTP, when compared with normal-diet-fed rats treated with vehicle (NDV) (a). The degree of LTP showed improvement after a combination of ER plus vildagliptin when compared with HFV rats (a). The number of dendritic spines on secondary or tertiary dendrites in hippocampal apical dendrites was decreased in HFV rats (b). Both HFRV and high-fat-diet-fed rats reversed to normal diet with 60 % ER treated with vildagliptin (HFRVil) showed significantly increased numbers of dendritic spines after the treatment regimen (b). HFV and HFRV rats showed a significantly increased time to reach the platform in the acquisition test, as well as having a decreased time spent in the target quadrant in the probe test, when compared with NDV rats ((c) and (d)). HFRVil rats showed a significantly decreased time to reach the platform in the acquisition test, as well as an increased time spent in the target quadrant in the probe test, when compared with HFV rats ((c) and (d)). HFS, high-frequency stimulation. \*P<0.05 v. NDV, † P<0·05 v. HFV and ‡ P<0·05 v. HFRV. (a) 🖂, NDV; 🗐, HFV; 🗐, HFRV; 📋, HFRViI; (c) 🔳, NDV; 🌒, HFV; 🔘, HFRV; 🚫, HFRViI. fEPSP, field excitatory postsynaptic potential.



In addition, ER had been shown to exert benefits in attenuating cognitive decline via an up-regulation of the brain-derived neurotrophic factor and tropomyosin-related kinase B in obese, hypertensive rats<sup>(19)</sup>; these markers were not investigated in this study.

#### Conclusion

This study indicates that although ER restored peripheral insulin sensitivity and decreased circulating oxidative stress levels regardless of the addition of vildagliptin, only ER plus vildagliptin exerted the best efficacy in effectively decreasing brain oxidative stress levels, as well as the restoration of brain insulin sensitivity, brain mitochondrial function, hippocampal synaptic plasticity and cognition. All of these findings suggest that the addition of vildagliptin to ER provides greater therapeutic benefits on brain function than ER alone in obesity.

#### **Acknowledgements**

This work was supported by grants from the Thailand Research Fund (TRF-BRG5780016 (SC), TRF-MRG5980198 (WP)), the Royal Golden Jubilee PhD programme (PHD/0025/2555 HP&SC), National Research Council of Thailand (SC), a NSTDA Research Chair Grant from the National Science and Technology Development Agency (NC) and Chiang Mai University Excellent Center Award (NC).

H. P., N. C., S. C. C. performed the experiments, analysed the data and wrote the manuscript. P. T., W. P., P. Sa-nguanmoo, T. C. performed the experiments and analysed the data. P. Satjaritanun, L. L. analysed the data.

The authors have no conflicts of interest to disclose.

#### References

- Kitzinger H & Karle B (2013) The epidemiology of obesity. Eur Surg 45, 80-82.
- Stranahan AM, Norman ED, Lee K, et al. (2008) Diet-induced insulin resistance impairs hippocampal synaptic plasticity and cognition in middle-aged rats. Hippocampus 18, 1085-1088.
- Pistell PJ, Morrison CD, Gupta S, et al. (2010) Cognitive impairment following high fat diet consumption is associated with brain inflammation. J Neuroimmunol 219, 25-32.





- Pipatpiboon N, Pintana H, Pratchayasakul W, et al. (2013) DPP4-inhibitor improves neuronal insulin receptor function, brain mitochondrial function and cognitive function in rats with insulin resistance induced by high-fat diet consumption. Eur J Neurosci 37, 839-849.
- Pipatpiboon N, Pratchayasakul W, Chattipakorn N, et al. (2012) PPARgamma agonist improves neuronal insulin receptor function in hippocampus and brain mitochondria function in rats with insulin resistance induced by long term high-fat diets. Endocrinology 153, 329-338.
- Burkey BF, Li X, Bolognese L, et al. (2005) Acute and chronic effects of the incretin enhancer vildagliptin in insulinresistant rats. J Pharmacol Exp Ther 315, 688-695.
- Gault VA, Lennox R & Flatt PR (2015) Sitagliptin, a dipeptidyl peptidase-4 inhibitor, improves recognition memory, oxidative stress and hippocampal neurogenesis and upregulates key genes involved in cognitive decline. Diabetes Obes Metab **17**, 403–413.
- Pintana H, Apaijai N, Chattipakorn N, et al. (2013) DPP-4 inhibitors improve cognition and brain mitochondrial function of insulin resistant rats. J Endocrinol 218, 1–11.
- Speakman JR & Mitchell SE (2011) Caloric restriction. Mol Aspects Med 32, 159-221.
- Baek K, Barlow AA, Allen MR, et al. (2008) Food restriction and simulated microgravity: effects on bone and serum leptin. I Appl Physiol 104, 1086-1093.
- 11. Reiser K, McGee C, Rucker R, et al. (1995) Effects of aging and caloric restriction on extracellular matrix biosynthesis in a model of injury repair in rats. J Gerontol A Biol Sci Med Sci **50A**, B40-B47.
- de Magalhaes JP, Wuttke D, Wood SH, et al. (2012) Genomeenvironment interactions that modulate aging: powerful targets for drug discovery. Pharmacol Rev 64, 88-101.
- Ingram DK, Zhu M, Mamczarz J, et al. (2006) Calorie restriction mimetics: an emerging research field. Aging cell 5, 97-108.
- McCurdy CE, Davidson RT & Cartee GD (2005) Calorie restriction increases the ratio of phosphatidylinositol 3-kinase catalytic to regulatory subunits in rat skeletal muscle. Am J Physiol Endocrinol Metab 288, E996-E1001.
- Dean DJ, Brozinick JT Jr, Cushman SW, et al. (1998) Calorie restriction increases cell surface GLUT-4 in insulin-stimulated skeletal muscle. Am J Physiol 275, E957-E964.
- Sharma N, Castorena CM & Cartee GD (2012) Greater insulin sensitivity in calorie restricted rats occurs with unaltered circulating levels of several important myokines and cytokines. Nutr Metab (Lond) 9, 90.
- Wilsey J & Scarpace PJ (2004) Caloric restriction reverses the deficits in leptin receptor protein and leptin signaling capacity associated with diet-induced obesity: role of leptin in the regulation of hypothalamic long-form leptin receptor expression. J Endocrinol 181, 297-306.
- Yamaoka K & Tango T (2012) Effects of lifestyle modification on metabolic syndrome: a systematic review and meta-analysis. BMC Med 10, 138.
- Kishi T, Hirooka Y, Nagayama T, et al. (2015) Calorie restriction improves cognitive decline via up-regulation of brain-derived neurotrophic factor: tropomyosin-related kinase B in hippocampus of obesity-induced hypertensive rats. Int Heart J 56, 110-115.
- Hiona A & Leeuwenburgh C (2004) Effects of age and caloric restriction on brain neuronal cell death/survival. Ann N Y Acad Sci 1019, 96-105.

- 21. Wood SH, van Dam S, Craig T, et al. (2015) Transcriptome analysis in calorie-restricted rats implicates epigenetic and post-translational mechanisms in neuroprotection and aging. Genome Biol 16, 285.
- 22. Sanz A, Caro P, Ibanez J, et al. (2005) Dietary restriction at old age lowers mitochondrial oxygen radical production and leak at complex I and oxidative DNA damage in rat brain. J Bioenerg Biomembr 37, 83-90.
- 23. Adams MM, Shi L, Linville MC, et al. (2008) Caloric restriction and age affect synaptic proteins in hippocampal CA3 and spatial learning ability. Exp Neurol 211, 141-149.
- 24. Pratchayasakul W, Kerdphoo S, Petsophonsakul P, et al. (2011) Effects of high-fat diet on insulin receptor function in rat hippocampus and the level of neuronal corticosterone. Life Sci 88, 619-627.
- 25. Sripetchwandee J, Pipatpiboon N, Chattipakorn N, et al. (2014) Combined therapy of iron chelator and antioxidant completely restores brain dysfunction induced by iron toxicity. PLOS ONE 9, e85115.
- 26. Candan N & Tuzmen N (2008) Very rapid quantification of malondialdehyde (MDA) in rat brain exposed to lead, aluminium and phenolic antioxidants by high-performance liquid chromatography-fluorescence detection. Neurotoxicology 29, 708-713.
- 27. Mateos R, Lecumberri E, Ramos S, et al. (2005) Determination of malondialdehyde (MDA) by high-performance liquid chromatography in serum and liver as a biomarker for oxidative stress. Application to a rat model for hypercholesterolemia and evaluation of the effect of diets rich in phenolic antioxidants from fruits. J Chromatogr B Analyt Technol Biomed Life Sci 827, 76-82.
- Pintana H, Sripetchwandee J, Supakul L, et al. (2014) Garlic extract attenuates brain mitochondrial dysfunction and cognitive deficit in obese-insulin resistant rats. Appl Physiol Nutr Metab 39, 1373-1379.
- Arakawa H (2005) Age dependent effects of space limitation and social tension on open-field behavior in male rats. Physiol Behav 84, 429-436.
- Vorhees CV & Williams MT (2006) Morris water maze: procedures for assessing spatial and related forms of learning and memory. Nat Protoc 1, 848-858.
- 31. Sripetchwandee J, Pipatpiboon N, Pratchayasakul W, et al. (2014) DPP-4 inhibitor and PPARgamma agonist restore the loss of CA1 dendritic spines in obese insulin-resistant rats. Arch Med Res 45, 547-552.
- 32. Greenwood CE & Winocur G (2005) High-fat diets, insulin resistance and declining cognitive function. Neurobiol Aging 26, Suppl. 1, 42-45.
- Hatori M, Vollmers C, Zarrinpar A, et al. (2012) Time-restricted feeding without reducing caloric intake prevents metabolic diseases in mice fed a high-fat diet. Cell Metab 15, 848-860.
- Jeon BT, Jeong EA, Shin HJ, et al. (2012) Resveratrol attenuates obesity-associated peripheral and central inflammation and improves memory deficit in mice fed a high-fat diet. Diabetes 61, 1444-1454.
- 35. Rains JL & Jain SK (2011) Oxidative stress, insulin signaling, and diabetes. Free Radic Biol Med 50, 567-575
- Glass CK & Olefsky JM (2012) Inflammation and lipid signaling in the etiology of insulin resistance. Cell Metab 15, 635-645.
- 37. Eckles-Smith K, Clayton D, Bickford P, et al. (2000) Caloric restriction prevents age-related deficits in LTP and in NMDA receptor expression. Brain Res Mol Brain Res 78, 154-162.



EI SEVIER

Contents lists available at ScienceDirect

## Hormones and Behavior

journal homepage: www.elsevier.com/locate/yhbeh



# FGF21 improves cognition by restored synaptic plasticity, dendritic spine density, brain mitochondrial function and cell apoptosis in obese-insulin resistant male rats



Piangkwan Sa-nguanmoo <sup>a,b</sup>, Pongpan Tanajak <sup>a,b</sup>, Sasiwan Kerdphoo <sup>a,b</sup>, Pattarapong Satjaritanun <sup>a,b</sup>, Xiaojie Wang <sup>c</sup>, Guang Liang <sup>c</sup>, Xiaokun Li <sup>c</sup>, Chao Jiang <sup>c</sup>, Wasana Pratchayasakul <sup>a,b</sup>, Nipon Chattipakorn <sup>a,b</sup>, Siriporn C. Chattipakorn <sup>a,d,\*</sup>

- a Neurophysiology Unit, Cardiac Electrophysiology Research and Training Center Faculty of Medicine, Chiang Mai University, Chiang Mai, Thailand
- <sup>b</sup> Department of Physiology, Faculty of Medicine, Chiang Mai University, Chiang Mai, Thailand
- <sup>c</sup> School of Pharmaceutical Sciences, Wenzhou Medical University, University-Town, Wenzhou, Zhejiang, China
- <sup>d</sup> Department of Oral Biology and Diagnostic Science, Faculty of Dentistry, Chiang Mai University, Chiang Mai, Thailand

#### ARTICLE INFO

#### Article history: Received 11 March 2016 Revised 13 August 2016 Accepted 19 August 2016 Available online 24 August 2016

Keywords: FGF21 Obese Insulin resistance Cognition Brain mitochondria

#### ABSTRACT

Fibroblast growth factor 21 (FGF21) is an endocrine hormone which exerts beneficial effects on metabolic regulation in obese and diabetic models. However, the effect of FGF21 on cognition in obese-insulin resistant rats has not been investigated. We hypothesized that FGF21 prevented cognitive decline in obese-insulin resistant rats by improving hippocampal synaptic plasticity, dendritic spine density, brain mitochondrial function and brain FGF21 signaling as well as decreasing brain cell apoptosis. Eighteen male Wistar rats were divided into two groups, and received either a normal diet (ND) (n = 6) or a high fat diet (HFD) (n = 12) for 12 weeks. At week 13, the HFD-fed rats were subdivided into two subgroups (n = 6/subgroup) to receive either vehicle or recombinant human FGF21 (0.1 mg/kg/day) for four weeks. ND-fed rats were given vehicle for four weeks. At the end of the treatment, cognitive function, metabolic parameters, pro-inflammatory markers, brain mitochondrial function, cell apoptosis, hippocampal synaptic plasticity, dendritic spine density and brain FGF21 signaling were determined. The results showed that vehicle-treated HFD-fed rats developed obese-insulin resistance and cognitive decline with impaired hippocampal synaptic plasticity, decreased dendritic spine density, brain mitochondrial dysfunction and increased brain cell apoptosis. Impaired brain FGF 21 signaling was found in these obeseinsulin resistant rats. FGF21-treated obese-insulin resistant rats had improved peripheral insulin sensitivity, increased hippocampal synaptic plasticity, increased dendritic spine density, restored brain mitochondrial function, attenuated brain cells apoptosis and increased brain FGF21 signaling, leading to a prevention of cognitive decline. These findings suggest that FGF21 treatment exerts neuroprotection in obese-insulin resistant rats.

© 2016 Elsevier Inc. All rights reserved.

#### 1. Introduction

Long term consumption of a high fat diet (HFD) has been shown to result in obesity, which then causes insulin resistance (Fung et al., 2001; Riccardi et al., 2004). We previously found that male rats fed with a 12-week HFD not only developed peripheral insulin resistance, but also brain insulin resistance indicated by the impairment of brain insulin signaling and insulin-induced long-term depression (LTD)

E-mail addresses: scchattipakorn@gmail.com, siriporn.c@cmu.ac.th (S.C. Chattipakorn).

(Pipatpiboon et al., 2012; Pratchayasakul et al., 2011). In addition, we found that those rats had increased brain oxidative stress, brain mitochondrial dysfunction, decreased synaptic plasticity as well as dendritic spine density in the CA1 region of the hippocampus (Pintana et al., 2013, 2012; Pratchayasakul et al., 2015), which is the region of the brain that involves the learning and memory process. The dysfunction of hippocampal neurons has been shown to cause a loss of learning and memory (Winocur et al., 2005). Furthermore, other previous studies also demonstrated that long-term HFD consumption significantly increased brain damage, leading to impaired long-term potentiation (LTP), decreased dendritic spine at apical CA1 hippocampus region and resulting in impaired learning and memory (Beilharz et al., 2015; Stranahan et al., 2008).

Several clinical studies demonstrated that overweight or higher body mass index (BMI) is correlated with poor cognition and learning

<sup>\*</sup> Corresponding author at: Neurophysiology Unit, Cardiac Electrophysiology Research and Training Center, Faculty of Medicine, Chiang Mai University, Department of Oral Biology and Diagnostic Sciences, Faculty of Dentistry Chiang Mai University, Chiang Mai 50200, Thailand.

and memory deficits including impaired executive function performance in middle aged adults (Cournot et al., 2006; Elias et al., 2003; Sabia et al., 2009). In addition, longitudinal studies have shown that higher body composition and central obesity are related with cognitive decline, particularly in global cognitive function, executive function, and memory over time (Gunstad et al., 2010). Raji and colleagues also demonstrated that a higher BMI can cause brain atrophy in various regions including the frontal lobe, anterior cingulate gyrus, hippocampus and thalamus, when compared with people with normal BMI (Raji et al., 2010). Furthermore, the impaired memory and executive functioning has been reported in patients with type 1 and type 2 diabetes (Munshi et al., 2006; Northam et al., 2001; Reaven et al., 1990). In addition, Den and colleagues demonstrated that subjects with type 2 diabetes also had hippocampal and amygdala atrophy when compared with control subjects (den Heijer et al., 2003). All of these findings from clinical studies suggest that the implication of hippocampus occur following obese-insulin resistant condition.

Fibroblast growth factor 21 (FGF21) is an endocrine hormone and is mainly expressed in the liver, adipose tissues and pancreas (Kharitonenkov and Shanafelt, 2009; Nishimura et al., 2000). Previous studies found that FGF21 exerts beneficial effects on metabolic regulation such as the controlling of glucose levels and lipid homeostasis (Kharitonenkov et al., 2007; Kim et al., 2013; Lin et al., 2013; Xu et al., 2009a, 2009b). FGF21 activity is mediated by the fibroblast growth factor receptor (FGFR) and β-klotho (KLB), which is an essential co-receptor for FGF21 activity; therefore the cells lacking β-Klotho are unable to respond to FGF21 (Adams et al., 2012; Ogawa et al., 2007). When FGF21 binds with those receptors, it causes the activation of downstream targets, including the phosphorylation of fibroblast growth factor receptor substrate 2 (FRS2) and extracellular-signal-regulated kinases (ERK1/2). Previous studies found that administration of FGF21 into ob/ob mice, db/db mice, diet-induced obese (DIO) mice and diabetic monkeys led to improved metabolic parameters such as weight loss promotion, improved insulin sensitivity and lipid profile, reduced blood glucose without hypoglycemia and decreased insulin levels (Kharitonenkov et al., 2007; Kim et al., 2013; Lin et al., 2013; Xu et al., 2009a, 2009b). It has been shown that FGF21 levels were also increased under several pathological conditions including obesity, metabolic syndrome and diabetes (Bobbert et al., 2013; Mashili et al., 2011; Novotny et al., 2014; Zhang et al., 2008). A recent study investigated the effect of LY2405319, an FGF21 analog, in obese humans with type 2 diabetic subjects, and found that FGF21 could improve dyslipidemia, reduce body weight gain, reduce fasting plasma insulin levels and increase adiponectin levels (Gaich et al., 2013).

FGF21 is expressed in the brain and can be produced by glia cells and neurons (Johanna Mäkelä et al., 2014). In addition, FGF21 can cross the blood brain barrier following exogenous application and it has been detected in human cerebrospinal fluid (Hsuchou et al., 2007; Tan et al., 2011). FGF21 exerted neuroprotective effects, which were mediated by an increase in the levels of peroxisome proliferator activated receptor  $\gamma$  coactivator  $1\alpha$  (PGC1- $\alpha$ ) and its activity (Johanna Mäkelä et al., 2014). Those events subsequently increased the levels of mitochondrial antioxidant enzymes and improved mitochondrial biogenesis and cell viability (Johanna Mäkelä et al., 2014). Moreover, FGF21 has been shown to preserve cognitive function in D-galactose-induced aging mice (Yu et al., 2015). Despite these beneficial effects of FGF21 on improving metabolic function in obese and diabetic animal models, little is known about its effect on brain function under an obese-insulin resistant condition.

However, the effects of FGF21 on cognitive function, which associated with brain oxidative stress, brain mitochondrial function, brain apoptosis, hippocampal synaptic plasticity and dendritic spine density in obese-insulin resistant male rats have not been investigated. Therefore, in this study, we hypothesized that the prevention of cognitive decline by FGF 21 in the obese-insulin resistant male rats is associated with its ability to improve peripheral insulin sensitivity, reduce systemic inflammation, restore brain mitochondrial function, decrease brain oxidative

stress, decrease brain cell apoptosis and restore hippocampal synaptic plasticity.

#### 2. Materials and methods

#### 2.1. Animal models and experimental protocols

All experimental protocols were approved by the Faculty of Medicine, Chiang Mai University Institutional Animal Care and Use Committee, in compliance with NIH guidelines. Eighteen male Wistar rats weighing 200–220 g were purchased from the National Animal Center, Salaya Campus, Mahidol University, Thailand. All animals were housed individually in a temperature-controlled environment under a lightdark cycle of 12:12 h. After the rats were acclimatized for one week, they were divided into two groups, one to receive a normal diet (ND; 19.77% E fat), which was a standard laboratory pellet diet (Mouse Feed Food No. 082, C.P. Company, Bangkok, Thailand) (n = 6), or a high fat diet (HFD; 59.28% E fat) group (n = 12). The HFD contained 59.3% total energy from fat with the major composition of fat being saturated fatty acid from lard as described in our previous study (Pratchayasakul et al., 2011). These diets were given for 12 weeks. At week 13, the HFD-fed rats were subdivided into two subgroups to receive either 0.9% normal saline solution (0.9% NSS; 0.1 mg/kg/day; i.p) as a vehicle (HFV) (n = 6) or recombinant human FGF21 (FGF21, 0.1 mg/kg/day; i.p) (HFF) (n = 6) for four weeks. We used 0.1 mg/kg/ day of FGF 21 in the present study because this dose has been shown to improve peripheral insulin sensitivity in previous studies (Coskun et al., 2008; Zhang et al., 2013). Recombinant human FGF21 (rhFGF21) was obtained from Prof. Dr. Xiaokun Li, Zhejiang Provincial Key Laboratory of Biopharmaceuticals, Wenzhou Medical College, Wenzhou, Zhejiang 325,035, P.R. China. Recombinant human FGF21 (rhFGF21) was produced using Escherichia coli and purified to be endotoxin free (Wang et al., 2010). All animals were given ad libitum access to food and water. At the end of protocol, the locomotor activity of each rat was tested by an open field test (OFT). After that, the spatial learning and memory was determined by the Morris water maze (MWM) test. An oral glucose tolerance test (OGTT) was also carried out before the animals were sacrificed by decapitation. Blood samples were collected for determining metabolic parameters. The brain was rapidly removed for electrophysiological and biochemical analysis. For the sample size, we used n = 6/group for investigation of metabolic parameters, open field test, Morris water maze test, brain mitochondrial function, LTP and western blot analysis. We also used the separated animals

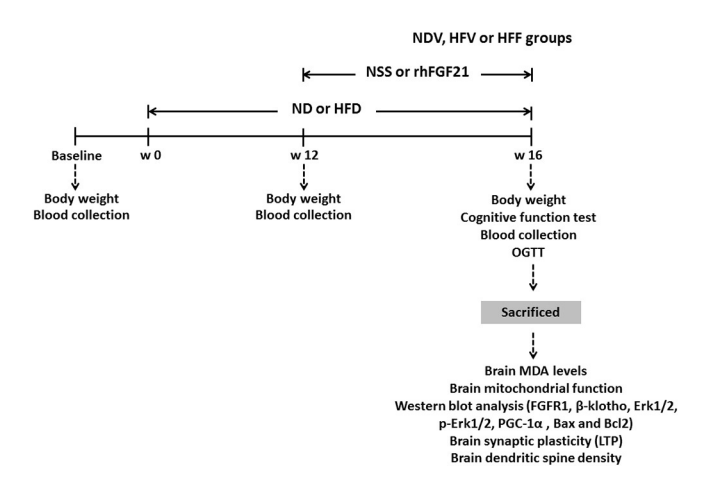


**Fig. 1.** The experimental protocol of the study. NDV; vehicle-treated normal diet fed rats, HFV; vehicle-treated high fat diet fed rats, HFF; FGF21-treated high fat diet fed rats, w; week, OGTT; oral glucose tolerance test, MDA; malondyaldehyde, FGFR1; fibroblast growth factor receptor 1, Erk1/2; extracellular-signal-regulated kinases, PCG-1 $\alpha$ ; peroxisome proliferator activated receptor  $\gamma$  coactivator  $1\alpha$ , LTP; Long-term potentiation.

(n = 6/group) for investigation of the dendritic spine density. The experimental protocol is shown in Fig. 1.

#### 2.2. Chemical analysis for metabolic parameters

Fasting plasma glucose, cholesterol and triglyceride levels were determined by a colorimetric assay (ERBA diagnostic, Mannheim, Germany). Fasting plasma high-density lipoprotein (HDL) levels were determined by a commercial colorimetric assay kit (Biovision, CA, USA). The plasma low-density lipoproteins (LDL) levels were estimated from Friedewald's equation (Friedewald et al., 1972). Previous studies demonstrated that both HDL and LDL levels affected spatial learning and memory in several models such as rats fed with saturated fat, high fat, high cholesterol diet and obese-insulin resistant rats (Granholm et al., 2008; Pratchayasakul et al., 2015; Thirumangalakudi et al., 2008) by increased brain oxidative stress, activated brain microglia and proinflammatory cytokine as well as increased amyloid precursor protein (APP) processing enzyme. Therefore, the present study investigated the effect of a FGF21 on HDL and LDL in obese insulin resistant condition. Fasting plasma insulin levels were evaluated using a sandwich enzyme-linked immunosorbent assay (ELISA) kit (Millipore, MI, USA). The severity of peripheral insulin resistance was assessed by the homeostasis model assessment (HOMA) as described previously (Matthews et al., 1985). An oral glucose tolerance test (OGTT) was performed as described previously (Pratchayasakul et al., 2015). Areas under the curves (AUCs) were calculated to evaluate glucose tolerance.

#### 2.3. Serum TNF- $\alpha$ , adiponectin and plasma FGF21 levels

Serum tumor necrosis factor alpha (TNF- $\alpha$ ) levels were determined by a rat TNF- $\alpha$  enzyme-linked immunosorbent assay (ELISA) kit (GE Healthcare, UK). Serum adiponectin levels were determined by a rat adiponectin enzyme-linked immunosorbent assay (ELISA) (Invitrogen, life technologies, Carlsbad, CA, USA). Plasma FGF21 levels were determined by a Mouse/Rat FGF21 enzyme-linked immunosorbent assay (ELISA) kit (R&D systems Inc., Minneapolis, MN, USA).

#### 2.4. Serum and brain malondyaldehylde (MDA) levels

Serum and brain MDA levels are markers of lipid peroxidation levels (Gulbahar et al., 2009). The levels of MDA were determined by high-performance liquid chromatography (HPLC) as described previously (Pintana et al., 2013).

#### 2.5. Cognitive tests

In this study, the open-field test (OFT) was used to evaluate the locomotor activity of the.

rats. This method was modified from a previous study (Arakawa, 2005). The apparatus consisted of a square-based box opened from above (75  $\times$  75 cm base, 40 cm height). The base was divided into 25 equal squares, each of them sized  $15 \times 15$  cm. Lighting in the testing room was bright (1155 lx). Briefly, the rat was placed into a box, which consisted of white lines, and was observed for 2 min. The numbers of lines that the animals crossed was interpreted as activity (Pintana et al., 2013). To evaluate cognitive function, the protocol of the Morris Water Maze test was used as described previously (Pintana et al., 2012). The MWM set up was a round water pool (diameter 170 cm and height 60 cm) which was assigned with four cardinal points (N = north, S = south, E = east and W = west) and separated into four quadrants (NE = north east, NW = north west, SW = south west and SE = south east). Rats were given four different starting points per day. The round platform (diameter 10 cm) was located in the middle of one of the four quadrants (target quadrant). This protocol evaluated spatial learning and memory ability by two assessments: an acquisition test (hidden platform) and a probe test (removal of the platform from the water pool). Different shaped makers were pasted in the middle of each four quadrants higher than the edge of the pool by about 10 cm. For the acquisition test, rats were tested for five executive days at the same time on each day. The animals rested in the testing room 30 min before the experiment. After 30 min, the animals were placed in the water at one of the randomized starting points, and their time taken to reach the platform was recorded. The rats were left on the platform for 15 s after finding it. After that, the rats were removed from the water and allowed to rest for 15 s before being placed at the other three starting points. In the probe test, at day six, the hidden platform was removed and time spent in the target quadrant was recorded. Data analysis of the MWM test was performed using Smart 3.0 software (Panlab, Harvard Apparatus, Barcelona, Spain).

## 2.6. Extracellular recordings of hippocampal slices for electrical-induced long-term potentiation (LTP)

At the end of the experiment, animals were anesthetized and decapitated. The hippocampal slices were prepared as previously described (Chattipakorn and McMahon, 2002). Briefly, field excitatory postsynaptic potentials (fEPSPs) were evoked by stimulating the Schaffer collateral-commissural pathway with a bipolar tungsten electrode, whereas fEPSPs recordings were taken from the stratum radiatum of the hippocampal CA1 region with micropipettes (3 M $\Omega$ ) filled with 2 M NaCl. The LTP protocol is described in a previous study (Sripetchwandee et al., 2014a). Data were filtered at 3 kHz, digitized at 10 kHz, and stored in a computer using pClamp9.2 software (Axon Instruments, CA, USA). The initial slope of the fEPSPs were measured and plotted against time.

#### 2.7. Golgi impregnation and analysis

Previous studies reported that dendritic spine density was related to synaptic plasticity, LTP (Pratchayasakul et al., 2015), therefore we investigated the dendritic spine density in this experimental protocol. After sacrifice by decapitation, brains were removed and rinsed with double distilled water. After that, brain tissue was processed for Golgi staining using a commercially available kit (FD Neurotechnologies kit, PK 401, Ellicott City, USA) as described previously (Pratchayasakul et al., 2015; Sripetchwandee et al., 2016). Briefly, the area of the hippocampus and two segments of pyramidal cell in the CA1 region were randomly examined. Both segments were located on the tertiary apical dendrites. The dendritic spines were viewed through an inverted microscope (IX-81, Olympus, Tokyo, Japan). For the dendritic spine density analysis, two segments from pyramidal cells in the CA1 hippocampus area were randomly measured with 100-200 µm apart from soma and 20 µm in dendritic length. Three neuronal cells per brain slices were chosen for quantitative analysis (3 slices/animals, n = 6 animals/group). Therefore, nine neurons from each animal were analyzed. The number of spines was counted using a hand counter, and the dendritic lengths were measured using Xcellence imaging software (Olympus, Tokyo, Japan).

#### 2.8. Immunoblotting

To investigate the expression of fibroblast growth factor receptor 1 (FGFR1),  $\beta$ -klotho, ERK1/2, ERK1/2 phosphorylation (p-Erk1/2), PGC- $1\alpha$ , and brain cells apoptosis markers; Bax and Bcl2, homogenated brain tissues from each subgroup were boiled at 95 °C for 5 min. Then, the proteins were separated by electrophoresis and transferred onto nitrocellulose membranes as previously described (Pipatpiboon et al., 2013). Immunoblotting was conducted with FGFR1,  $\beta$ -klotho, PGC- $1\alpha$  (1:200, Santa Cruz Biotechnology, Inc., Texas, USA), Erk1/2, p-Erk1/2, BAX (1: 1000, Santa Cruz Biotechnology, Inc., Texas, USA) and BCL- $2\alpha$  (1:1000, Cell Signaling Technology, Danvers, Massachusetts, USA) overnight. The primary antibody was detected by horse anti-mouse IgG conjugate HRP-linked antibody (1:2000 dilution, Cell Signaling Technology, Danvers, Massachusetts, USA) for  $\beta$ -Actin. Moreover,  $\beta$ -klotho was

detected by rabbit anti goat IgG conjugate HRP-linked antibody (1:2000 Santa Cruz Biotechnology, Inc., Texas, USA). FGFR1, Erk1/2, p-Erk1/2, PGC1- $\alpha$ , Bax and BCL-2 was detected by goat anti-rabbit IgG conjugate HRP-linked antibody (1:2000, Cell Signaling Technology, Danvers, Massachusetts, USA). The protein bands were visualized on Amersham hyperfilm ECL using the Amersham ECL western blotting detection reagents system (GE Healthcare, Buckinghamshire, UK). The membranes were developed using the ChemiDoc touch imaging system (Bio-Rad Laboratories, Hercules, California, USA) on chemiluminescence mode and the densitometric analysis was determined by using an image J program. The results are shown as average signal intensity (arbitrary units).

#### 2.9. Brain mitochondrial function

Isolated mitochondria were prepared by using the same method as described in our previous studies (Pintana et al., 2012; Pipatpiboon et al., 2013). To determine brain mitochondrial function, we evaluated brain mitochondrial reactive oxygen species (ROS) production, brain mitochondrial membrane potential ( $\Delta\Psi m$ ) and brain mitochondrial swelling. The mitochondrial function was determined by following the method in our previous studies (Pintana et al., 2012; Pipatpiboon et al., 2013).

#### 2.10. Brain mitochondrial ROS assay

Brain mitochondrial reactive oxygen species (ROS) were determined using dichloro-hydrofluoresceindiacetate (DCFHDA) fluorescent dye. Brain mitochondria (0.4 mg/ml) were incubated with 2-µM DCFHDA at 25 °C for 20 min. The fluorescence was determined using a fluorescent microplate reader at the excitation wavelength of 485 nm and emission wavelength of 530 nm (Pipatpiboon et al., 2012). Increased fluorescent intensity indicates increased ROS production.

#### 2.11. Brain mitochondrial membrane potential ( $\Delta \Psi m$ ) assay

Mitochondrial membrane potential changes ( $\Delta\Psi$ m) were determined using the fluorescent dye 5,5′,6,6′-tetrachloro-1,1′,3,3′-tetraethyl benzimidazolcarbocyanine iodide (JC-1). JC-1 monomer form, green fluorescence, was excited at a wavelength of 485 nm and detected at the emission wavelength of 590 nm. JC-1 aggregate form, red fluorescence, was excited at a wavelength of 485 nm and detected at the emission wavelength of 530 nm. Brain mitochondria (0.4 mg/ml) were incubated with JC-1 dye at 37 °C for 15 min. Mitochondrial membrane potential changes were determined by measuring the fluorescent intensity using a fluorescent microplate reader. The change in mitochondrial membrane potential was calculated as the ratio of red to green fluorescent intensity (Pipatpiboon et al., 2012). Decreased red/green fluorescent intensity ratio indicates mitochondrial depolarization.

#### 2.12. Brain mitochondria swelling assay

Brain mitochondrial swelling was determined by measuring the change in the absorbance of the brain mitochondrial suspension. Brain mitochondria (0.4 mg/ml) were incubated in 2-ml respiration buffer. The suspension was read at 540 nm using a microplate reader. Decreased absorbance indicates mitochondria swelling (Pipatpiboon et al., 2012).

#### 2.13. Statistical analysis

Data was expressed as mean  $\pm$  SEM. Statistical analysis was assessed by using SPSS program (version17; SPSS, Chicago, III., USA). The significance of the differences in all parameters was calculated using one-way ANOVA followed by Tukey's post-hoc test. For the MWM acquisition test, a two-way ANOVA followed by Tukey's post-hoc test was used. For all comparisons, p < 0.05 was considered as statistically significant.

#### 3. Results

3.1. Twelve weeks of high-fat diet (HFD) consumption caused obesity and peripheral insulin resistance

After 12 weeks of HFD consumption, 12-week HFD-fed rats had significantly increased body mass, plasma total cholesterol level, plasma LDL level, plasma insulin level, HOMA index and increased plasma glucose area under the curve (AUCg) with no change in plasma glucose level, when compared with 12-week ND-fed rats (for body mass: F(1,10) = 28.592, p < 0.001,  $\eta^2 = 0.74$ ; for plasma total cholesterol level: F(1,10) = 40.902, p < 0.001,  $\eta^2 = 0.804$ ; for plasma LDL level: F(1,10) = 8.621, p = 0.015,  $\eta^2 = 0.463$ ; for plasma insulin level: F(1,10) = 5.953, p = 0.035,  $\eta^2 = 0.373$ ; for HOMA index: F(1,8) = 25.261, p = 0.001,  $\eta^2 = 0.759$ ; for plasma AUCg: F(1,8) = 9.405, p = 0.015,  $\eta^2 = 0.540$ ; Table 1). These findings indicated that 12 weeks of HFD consumption caused obesity and peripheral insulin resistance.

3.2. FGF21 treatment attenuated peripheral insulin resistance, oxidative stress and pro-inflammatory cytokine caused by obesity

After 28 days of vehicle treatment, these HFD-fed rats (HFV) had significantly increased body mass, visceral fat, plasma total cholesterol levels, plasma LDL levels, plasma insulin levels, HOMA index and plasma glucose AUCg without hyperglycemia when compared with vehicle treated ND-fed rats (NDV) (for body mass: F(2,15) = 61.725, p < 0.001,  $\eta^2 = 0.892$ ; for visceral fat: F(2,15) = 93.733, p < 0.001,  $\eta^2 = 0.926$ ; for plasma total cholesterol level: F(2,15) = 16.639,  $p < 0.01 \, \eta^2 = 0.689$ ; for plasma LDL level: F(2,15) = 7.857, p = 0.005,  $\eta^2 = 0.512$ ; for plasma insulin level: F(2,15) = 4.653, p = 0.027,  $\eta^2 = 0.383$ ; for HOMA index: F(2,15) = 3.224, p = 0.05,  $\eta^2 = 0.301$ ; for plasma AUCg: F(2,22) = 3.684, p = 0.042,  $\eta^2 = 0.251$ ; Table 2). Moreover, these HFV rats also had significantly increased serum MDA levels when compared with NDV rats (F(2,15) = 5.379, p = 0.017, $\eta^2 = 0.418$ ; Table 2). Additionally, HFV rats significantly increased TNF- $\alpha$  level with decreased serum adiponectin level when compared with NDV rats (F(2,15) = 5.374, p = 0.017,  $\eta^2$  = 0.417; Table 2). These findings indicated that the long-term HFD consumption caused peripheral insulin resistance and the occurrence of peripheral insulin resistance was accompanied by an increase in the oxidative stress and pro-inflammatory cytokine in HFV.

After treatment with FGF21 for 28 days, FGF21 treated HFD-fed rats (HFF) showed significantly decreased body mass, visceral fat, plasma total cholesterol levels, plasma LDL levels, decreased plasma insulin levels, HOMA index, plasma glucose AUCg with increased plasma HDL levels when compared with the vehicle treated HFD-fed rats (HFV). Moreover, the HFF rats had significantly decreased serum MDA levels, decreased serum TNF- $\alpha$  and increased adiponectin levels when compared with HFV rats (p < 0.05, Table 2). Malondialdehyde (MDA) is the end product of lipid peroxidation levels and is widely used as a

**Table 1**Metabolic parameters in rats fed with normal or high fat diet for 12 weeks.

| Parameters   | ND                | HFD                |
|--|-------------------|--------------------|
| Body mass (kg)   | $468.33 \pm 8.33$ | 580.00 ± 19.15*    |
| Food intake (g/day)  | $24.36 \pm 4.45$  | $26.56 \pm 8.44$   |
| Plasma glucose (mg%)                                       | $128.48 \pm 4.01$ | $130.10 \pm 6.65$  |
| Plasma total cholesterol (mg/dl)                           | $67.16 \pm 2.55$  | $88.00 \pm 2.17^*$ |
| Plasma triglyceride (mg/dl)                                | $55.63 \pm 6.20$  | $59.44 \pm 7.09$   |
| Plasma HDL (mg/dl)   | $29.79 \pm 2.02$  | $30.40 \pm 3.90$   |
| Plasma LDL (mg/dl)   | $47.95 \pm 3.98$  | $62.83 \pm 3.14^*$ |
| Plasma insulin (ng/ml)                                     | $2.87 \pm 0.61$   | $4.99 \pm 0.62^*$  |
| HOMA index   | $17.24 \pm 1.90$  | $36.31 \pm 3.73^*$ |
| Plasma Glucose AUC (AUCg) $(mg/dl \times min \times 10^4)$ | $4.63 \pm 0.71$   | $6.18 \pm 0.40^*$  |

ND; normal diet fed rats, HFD; high fat diet fed rats.

<sup>\*</sup> p < 0.05 vs ND.

**Table 2**Effects of FGF21 administration on peripheral insulin sensitivity parameters and MDA levels in HFD-fed rats.

| Parameters   | NDV               | HFV                  | HFF                             |
|--|-------------------|----------------------|---------------------------------|
| Body mass (kg)   | 520.83 ± 10.83    | 678.33 ± 11.38*      | 556.67 ± 9.19*,†                |
| Visceral fat (g)   | $23.87 \pm 1.94$  | $63.94 \pm 1.42^*$   | $50.51 \pm 2.74^*$ ,†           |
| Food intake (g/day)  | $23.87 \pm 1.94$  | $25.78 \pm 3.56$     | $23.97 \pm 2.95$                |
| Plasma glucose (mg%)   | $127.62 \pm 4.05$ | $130.49 \pm 6.54$    | $130.03 \pm 3.67$               |
| Plasma total cholesterol (mg/dl)   | $77.34 \pm 2.25$  | $114.51 \pm 7.55^*$  | $81.51 \pm 3.57^{\dagger}$      |
| Plasma triglyceride (mg/dl)  | $59.15 \pm 4.60$  | $54.62 \pm 2.40$     | $56.65 \pm 2.58$                |
| Plasma HDL (mg/dl)   | $32.82 \pm 1.94$  | $24.52 \pm 1.99^*$   | $31.10 \pm 1.71^{\dagger}$      |
| Plasma LDL (mg/dl)   | $51.38 \pm 2.99$  | $74.39 \pm 5.85^*$   | $55.59 \pm 3.75^{\dagger}$      |
| Plasma insulin (ng/ml)   | $2.69 \pm 0.86$   | $4.96 \pm 1.00^*$    | $2.82 \pm 1.98^{\dagger}$       |
| HOMA index   | $16.13 \pm 1.22$  | $32.82 \pm 8.73^*$   | $17.29 \pm 1.76^{\dagger}$      |
| Plasma glucose AUC (AUCg) (mg/dl $\times$ min $\times$ 10 <sup>4</sup> ) | $5.29 \pm 0.29$   | $7.23 \pm 0.65^*$    | $5.50 \pm 0.36^{\dagger}$       |
| Plasma adiponectin (ng/ml)   | $23.00 \pm 3.38$  | $14.67 \pm 2.94^*$   | $24.50 \pm 1.69^{\dagger}$      |
| Plasma TNF-α (pg/ml)   | $1.11 \pm 0.16$   | $3.05 \pm 0.67^*$    | $1.58 \pm 3.07^{\dagger}$       |
| Serum MDA (μmol/ml)  | $1.14 \pm 0.17$   | $2.99 \pm 0.76^*$    | $1.13 \pm 0.18^{\dagger}$       |
| Brain MDA (μmol/mg protein)  | $0.67 \pm 1.25$   | $1.68 \pm 0.22^*$    | $0.96\pm0.22^{\dagger}$         |
| Plasma FGF21 levels (pg/ml)  | $47.94 \pm 8.43$  | $265.69 \pm 30.74^*$ | $573.70 \pm 131.10^{*,\dagger}$ |

NDV; vehicle-treated normal diet fed rats, HFV; vehicle-treated high fat diet fed rats, HFF; FGF21-treated high fat diet fed rats.

biomarker of oxidative stress (Yagi, 1998). Previous studies demonstrated that the increased brain lipid peroxidation caused cell degeneration and cell death. This lead to impaired cognitive function in several models such as patients with amnestic mild cognitive impairment (MCI) (Markesbery et al., 2005) and obese-insulin resistant rats (Pintana et al., 2013). Therefore, the present study investigated the effect of a FGF21 on MDA in rats under an obese-insulin resistant condition. These findings suggested that FGF21 increased peripheral insulin

sensitivity, decreased oxidative stress levels as well as reduced systemic inflammation.

3.3. Obesity caused impaired cognitive function, and FGF21 prevented cognitive decline in obese-insulin resistant rats

The open field test was used to determine the locomotor activity of each rat before the MWM test. The number of lines that the rats crossed

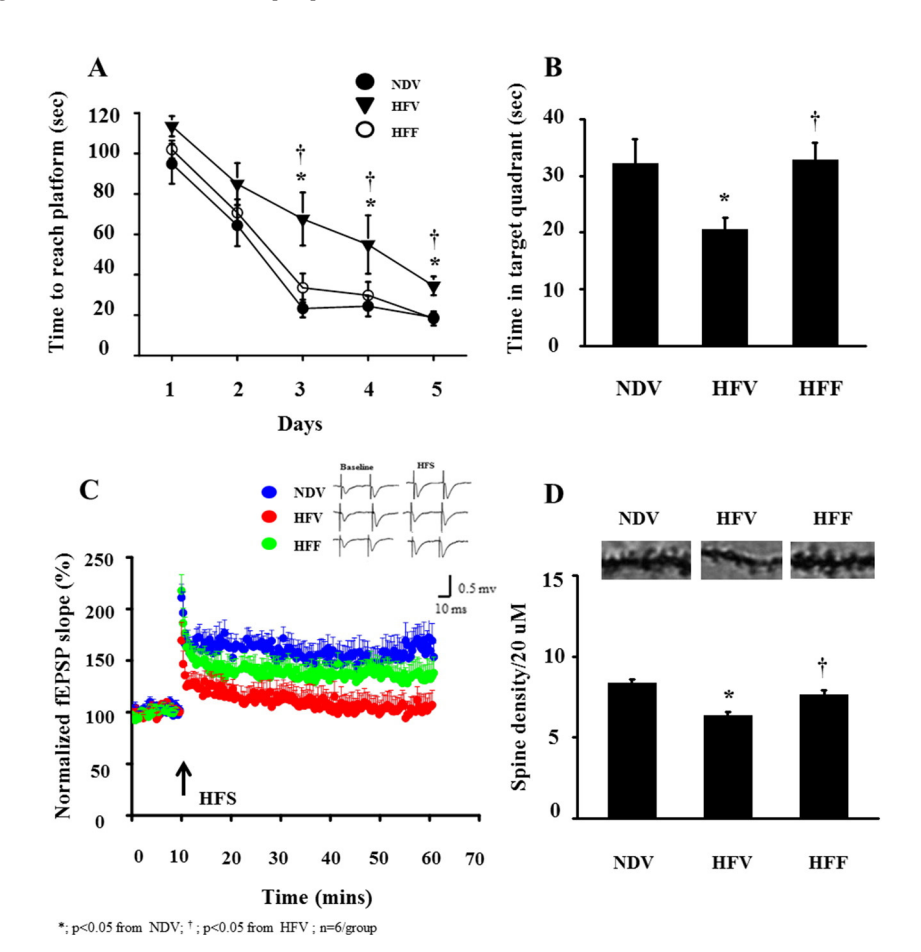


**Fig. 2.** Effects of FGF21 administration on Morris water maze test and hippocampal synaptic plasticity in obese-insulin resistant rats (A) Time to reach the platform in acquisition test and (B) time spent in target quadrant in probe test. (C) The degree of electrical-mediated LTP observed from hippocampal slices and (D) number of dendritic spines on tertiary dendrites in apical dendrite. NDV; vehicle-treated normal diet fed rats, HFV; vehicle-treated high fat diet fed rats, HFF; FGF21-treated high fat diet fed rats. \*p < 0.05 vs. NDV, †p < 0.05 vs. HFV.

<sup>\*</sup> p < 0.05 vs NDV.

 $<sup>\</sup>dot{\bar{p}} < 0.05$  vs HFV.

during the test was not significantly different between groups, indicating that the locomotor activity of all rats after treatment with either the vehicle or FGF21 was similar.

In the MWM test, the time to reach the platform during the acquisition test (day 3 to day 5) in HFV rats was significantly increased, when compared with that of NDV rats (F(4,22) = 57.719,  $\eta^2$  = 0.340; Fig. 2A). Moreover, the mean time spent in the target quadrant during the probe test (day 6) in HFV rats was significantly decreased, when compared with that of NDV rats (F(2,21) = 5.404, p = 0.013,  $\eta^2$  = 0.340; Fig. 2B). These results suggested that obese-insulin resistant rats exhibited cognitive decline. After treatment with FGF21 for 28 days, HFF rats had a decreased time to reach the platform during the acquisition test (day 3 to day 5) (F(4,22) = 57.719,  $\eta^2$  = 0.340; Fig. 2A) and an increased mean time spent in the target quadrant during the probe test (day 6) when compared with HFV rats (F(2,21) = 5.404, p = 0.013, $\eta^2 = 0.340$ ; Fig. 2B). Moreover, we also found the swim speeds were not significantly different between groups (26.33  $\pm$  3.86, 26.73  $\pm$  3.82 and  $30.85 \pm 2.63$  cm/s, in NDV, HFV and HFF, respectively). Meanwhile, the distance to reach the hidden platform in HFV rats was significantly increased when compared with that of the NDV rats (F(2,13) = 10.42,p = 0.002,  $\eta^2 = 0.616$ ). Moreover, HFF rats had decreased the distance to reach the hidden platform when compared with that of HFV rats  $(F(2,13) = 10.42, p = 0.002, \eta^2 = 0.616) (349.40 \pm 87.00,$  $1102.00 \pm 226.60$  and  $347.50 \pm 85.51$  cm, in NDV, HFV and HFF, respectively). These findings confirmed that the impairment of cognitive function in HFD rats was due to spatial memory deficit, not because of movement related deficits following obesity, and FGF21 attenuated the cognitive impairment.

## 3.4. Obesity caused the impairment of hippocampal synaptic plasticity, and FGF21 restored this impairment in obese-insulin resistant rats

The degree of electrical-induced LTP of HFV rats significantly decreased when compared with that of NDV rats  $(F(2,23)=3.033,\,p=0.05,\,\eta^2=0.209;\,Fig.\,2B).$  In addition, the number of dendritic spines in the CA1 hippocampus of HFV rats was significantly less than that of NDV rats  $(F(2,13)=15.901,\,p<0.001,\,\eta^2=0.710;\,Fig.\,2D).$  These findings suggested that obese-insulin resistant rats had impaired hippocampal synaptic plasticity.

After FGF21 treatment for 28 days, HFF rats had an increase in the degree of electrical-induced LTP when compared with HFV rats (F(2,23) = 3.033, p = 0.05,  $\eta^2$  = 0.209; Fig. 2B).

In addition, the dendritic spine density in CA1 hippocampus of HFF rats significantly increased when compared with that of HFV rats (F(2,13) = 15.901, p < 0.001,  $\eta^2$  = 0.710; Fig. 2D). These findings suggested that FGF21 treatment restored hippocampal synaptic plasticity in obese-insulin resistant rats.

## 3.5. Obesity caused increased plasma FGF21 levels and impaired brain FGF21 signaling

The present study investigated the circulating FGF21 level, the expression of brain FGF21 receptors, including FGFR1 and  $\beta$ -klotho, and brain FGF21 signaling such as Erk1/2, phosphorylated-Erk1/2 (p-Erk1/2) and PGC-1 $\alpha$  protein expression. We found that the HFV rats had higher circulating FGF21 levels when compared with NDV rats (F(2,16) = 12.029, p = 0.001,  $\eta^2$  = 0.601; Table 2). The expression of  $\beta$ -klotho and FGFR1 in brain of HFV rats was not significantly different to that of NDV rats (Fig. 3A, B). Interestingly, the level of phosphorylated-FGFR1 (p-FGFR1) expression significantly reduced in HFV rats when compared with NDV rats (F(2,7) = 18.658, p = 0.002,  $\eta^2$  = 0.842; Fig. 3C). Although the expression of total Erk1/2 (t-Erk1/2) expression did not differ between all groups (Fig. 3D) and p-Erk1/2 of HFV rats significantly decreased when compared with those of NDV rats (F(2,19) = 4.127, p = 0.032,  $\eta^2$  = 0.303; Fig. 3E). Moreover, PGC1- $\alpha$  protein expression of HFV was significantly less than that of NDV rats

 $(F(2,11)=7.354,p=0.009,\eta^2=0.512;Fig.\,3F)$ . These findings suggested that the impairment of brain FGF21 signaling occurred in obese-insulin resistant rats.

After FGF21 treatment for 28 days, the highest circulating levels of FGF21 levels were observed in HFF rats when compared with NDV and HFV rats (F(2,16) = 12.029, p = 0.001,  $\eta^2$  = 0.601; Table 2). We did not find a statistically significant difference in  $\beta$ -klotho and FGFR1 expression among all groups (Fig. 3A, B). Moreover, HFF rats had an increase in the expression of p-FGFR1, and p-Erk1/2 protein expression when compared with those of HFV rats (for p-FGFR1: F(2,7) = 18.658, p = 0.002,  $\eta^2$  = 0.842; for p-Erk1/2: F(2,19) = 4.127, p = 0.032,  $\eta^2$  = 0.303; Fig. 3C, E). FGF21-treated HFD-fed rats also showed a significant increase in brain PGC-1 $\alpha$  expression when compared with NDV and HFV rats (F(2,11) = 7.354, p = 0.009,  $\eta^2$  = 0.512; Fig. 3F). These findings suggested that FGF21 treatment enhanced FGF21 mediated signaling indicated by the increased p-FGFR1, p-ERK1/2 and PGC1- $\alpha$  levels in obese-insulin resistant rats.

## 3.6. Obesity caused impaired brain mitochondrial function and increased brain oxidative stress which were attenuated by FGF21 treatment

HFV rats had an increase in brain mitochondrial ROS production, brain mitochondrial membrane potential change (i.e. depolarization) as well as brain mitochondrial swelling when compared with NDV rats (for brain mitochondrial ROS production: F(2,17)=3.611, p=0.049,  $\eta^2=0.298$ ; for brain mitochondrial membrane potential change: F(2,20)=3.308, p=0.05,  $\eta^2=0.249$ ; for brain mitochondrial swelling: F(2,17)=5.419, p=0.015,  $\eta^2=0.389$ ; Fig. 4A, B, C).

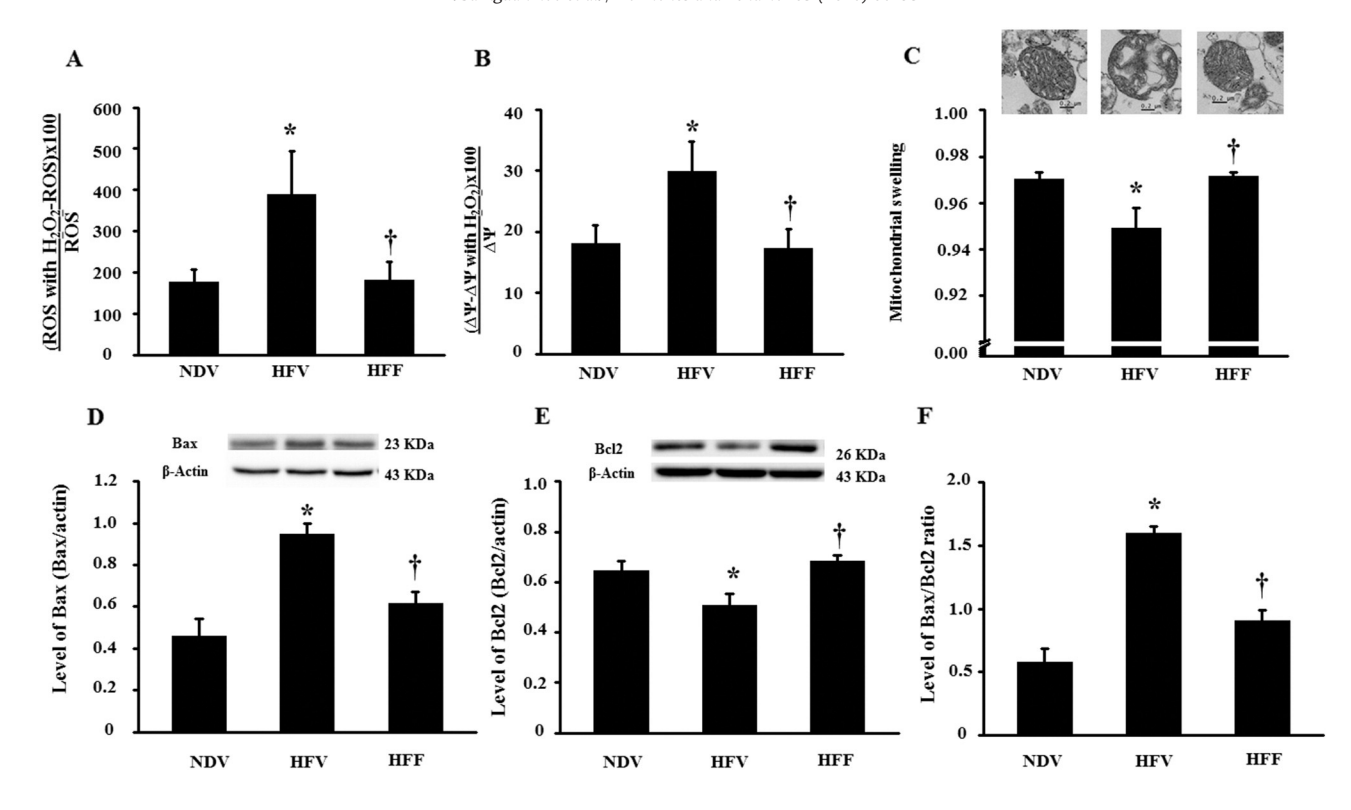
We also found that the brain MDA level of HFV rats significantly increased when compared with that of NDV rats (F(2,15) = 7.159, p = 0.007,  $\eta^2$  = 0.488; Table 2). These findings suggested that obese-insulin resistant rats had brain mitochondrial dysfunction with an increase in brain lipid peroxidation levels.

After FGF21 treatment for 28 days, brain mitochondrial ROS production, brain mitochondrial membrane potential change and brain mitochondrial swelling significantly decreased in HFF rats when compared with HFV rats (for brain mitochondrial ROS production: F(2,17) =3.611, p = 0.049,  $\eta^2$  = 0.298; for brain mitochondrial membrane potential change: F(2,20) = 3.308, p = 0.05,  $\eta^2 = 0.249$ ; for brain mitochondrial swelling: F(2,17) = 5.419, p = 0.015,  $\eta^2 = 0.389$ ; Fig. 4A, B, C). Moreover, brain MDA level of HFF rats was lower than that of HFV rats  $(F(2,15) = 7.159, p = 0.007, \eta^2 = 0.488; Table 2)$ . In addition, the morphological changes of brain mitochondria were demonstrated by transmission electron microscopy (TEM), and were shown in Fig. 4C. Brain mitochondrial swelling was observed in HFV rats indicated by remarkably unfolded cristae. Brain mitochondrial morphology showed obvious folded cristae in NDV and HFF rats. These findings suggested that FGF21 treatment restored brain mitochondrial function and decreased brain oxidative stress levels in obese-insulin resistant rats.

#### 3.7. Obesity caused brain cell apoptosis and FGF21 prevented it

Cells apoptosis in the brain was determined by the expression of Bcl-2 and Bax. The results demonstrated that HFV rats had an increase in the expression of a pro-apoptotic marker (Bax), decreased anti-apoptotic marker (Bcl2) and an increase in Bax/Bcl2 ratio when compared with those of NDV rats (for Bax: F(2,17) = 13.022, p < 0.001,  $\eta^2 = 0.605;$  for Bcl2: F(2,12) = 7.610, p = 0.007,  $\eta^2 = 0.559;$  for Bax/Bcl2: F(2,16) = 36.571, p < 0.001,  $\eta^2 = 0.821;$  Fig. 4D, E, F). These findings suggested that increased brain cell apoptosis was observed in obese-insulin resistant rats.

After FGF21 treatment for 28 days, the reduction in Bax protein expression, increased Bcl2 protein expression and a decrease in Bax/Bcl2 ratio were observed in HFF rats when compared with HFV rats (for Bax: F(2,17) = 13.022, p < 0.001,  $\eta^2$  = 0.605; for Bcl2: F(2,12) = 7.610, p = 0.007,  $\eta^2$  = 0.559; for Bax/Bcl2: F(2,16) = 36.571,



<sup>\*;</sup> p<0.05 from NDV;  $^{\dagger}$ ; p<0.05 from HFV; n=6/group

Fig. 4. Effects of FGF21 administration on brain mitochondrial function and cell apoptosis in obese-insulin resistant rats (A) Brain mitochondrial ROS production, (B) brain mitochondrial membrane potential change and (C) brain mitochondrial swelling and transmission electron microscopy (original magnification  $\times$  25,000), (D) Bax, (E) Bcl2 and (F) Bax/Bcl2 ratio. NDV; vehicle-treated normal diet fed rats, HFV; vehicle-treated high fat diet fed rats, HFF; FGF21-treated high fat diet fed rats. \*p < 0.05 vs. NDV, †p < 0.05 vs. HFV.

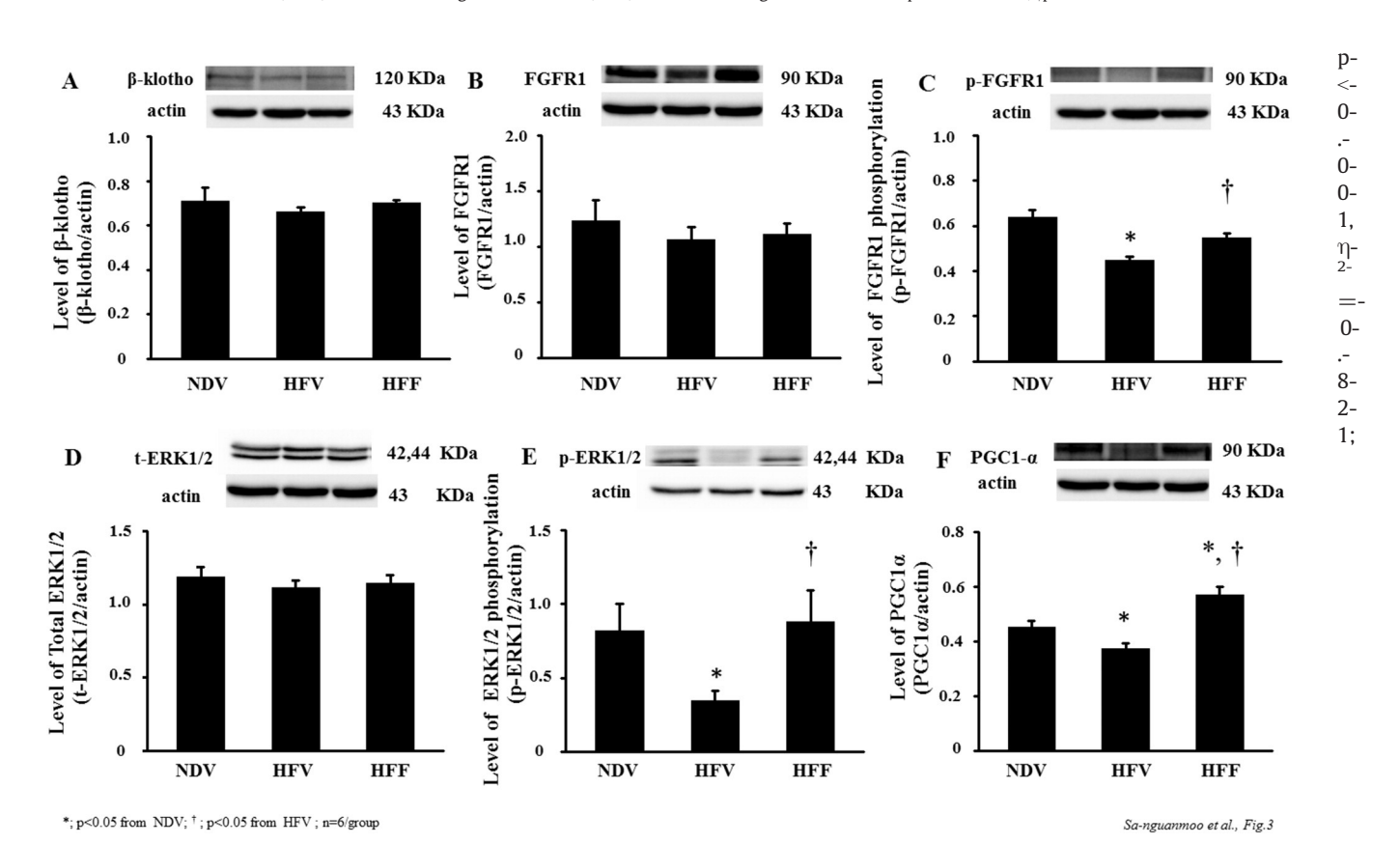


Fig. 3. Effects of FGF21 administration on FGF21 receptor, co-receptor and FGF21 signaling in the brain of obese-insulin resistant rats (A)  $\beta$ -klotho (B) FGFR1 (C) p-FGFR1 (D) t-Erk12 (E) p-Erk1/2 and (D) PGC-1 $\alpha$ . NDV; vehicle-treated normal diet fed rats, HFV; vehicle-treated high fat diet fed rats, HFF; FGF21-treated high fat diet fed rats. \*p < 0.05 vs. NDV, †p < 0.05 vs. HFV.

Fig. 4D, E, F). These findings indicated that FGF21 reduced brain cell apoptosis in obese-insulin resistant rats.

#### 4. Discussion

The major findings of the present study demonstrated that FGF21 treated obese-insulin resistant male rats 1) improved metabolic parameters, decreased circulating pro-inflammatory cytokine and serum oxidative stress levels; 2) prevented cognitive decline; 3) restored hippocampal synaptic plasticity; 4) enhanced brain FGF21-mediated signaling; and 5) restored brain mitochondrial function, decreased brain oxidative stress levels as well as brain cell apoptosis.

In this present study, we demonstrated that obesity induced by HFD consumption caused the development of peripheral insulin resistance, which was indicated by increased body mass, plasma insulin levels, HOMA index, total area under the curve (TAUCg) and euglycemia (Table 1). These findings on metabolic parameters are consistent with our previous reports for this model (Pintana et al., 2013; Pipatpiboon et al., 2013; Pratchayasakul et al., 2011). Moreover, the present study demonstrated that long-term HFD consumption increased systemic inflammation indicated by increased pro-inflammatory cytokine level (TNF- $\alpha$ ) and decreased adipokine level (adiponectin). Previous studies reported that obesity and adipocyte hypertrophy led to an increased level of pro-inflammatory cytokines and impaired the expression and secretion of adiponectin (Ouchi et al., 2011). Hypo-adiponectinemia can cause insulin resistance and diabetes (Kim et al., 2013; Lin et al., 2013). In addition, previous studies reported that low levels of adiponectin found in obesity and the administration of adiponectin in an animal model of obesity improved peripheral insulin sensitivity (Berg et al., 2001; Diez and Iglesias, 2010). All of those findings and our present findings indicated that HFD consumption led to not only obesity, but also systemic inflammation and hypo-adiponectinemia, in which finally resulted the impairment of peripheral insulin sensitivity.

We previously found that the obese-insulin resistant condition led to impaired brain functions (Pintana et al., 2013; Pratchayasakul et al., 2015; Sripetchwandee et al., 2014b). Those findings were confirmed in this study, where we found that long-term HFD consumption caused increased brain oxidative stress, brain mitochondrial dysfunction, impaired hippocampal synaptic plasticity, decreased dendritic spine density as well as impaired cognitive function. Moreover, we found that male rats with long-term HFD consumption had increased brain cell apoptosis which was indicated by an increase in Bax levels, decreased Bcl2 levels and an increased mitochondrial dysfunction in the brain of obese-insulin resistant male rats could lead to impaired cognition found in this study.

Our results also showed that obese-insulin resistant male rats had increased serum FGF21 levels. Serum FGF21 levels have been shown to increase in several pathological conditions such as obesity, metabolic syndrome and diabetes (Bobbert et al., 2013; Mashili et al., 2011; Novotny et al., 2014; Zhang et al., 2008), and that this increased level of FGF21 in the obese model cannot restore or improve metabolic function. It has been suggested that when a state of high endogenous level of a metabolic regulator does not have any effects on the physiological function, but can lead to an improvement of metabolic function if under a high pharmacological level, this suggests a state of hormone resistance (Yang et al., 2012). In addition, the study by Fisher and colleagues demonstrated that diet-induced obese (DIO) mice fed with a high fat/high sucrose diet showed increased serum FGF21, decreased FGFR1 mRNA expression in both the liver and white adipose tissue (WAT), decreased  $\beta\text{-klotho}$  mRNA expression in the WAT but not in the liver (Fisher et al., 2010). These findings suggested that obese-insulin resistance may lead to FGF21 resistance and may alter the FGF21 receptor expression in liver and WAT.

This present study is the first study that has investigated the FGFR1 phosphorylation and  $\beta$ -klotho level in the brain of obese-insulin

resistant male rats. Our results showed that, although there was no change in the protein expression of the receptor, the FGFR1 function was impaired in the brain of obese-insulin resistant male rats. All of the findings from our study suggested that obese-insulin resistant male rats had impaired brain FGF21 signaling.

In this study, FGF21 treatment in obese-insulin resistant male rats improved peripheral insulin sensitivity and decreased systemic inflammation which is possibly due to decreased body mass gain and decreased visceral fat. FGF21 reduced body mass gain in obese-insulin resistant male rats without the reduction of food intake. The possible explanations of this observation may be that 1) FGF21 level could induce an increase in the sympathetic activity as shown in a previous study (Douris et al., 2015; Owen et al., 2014) and 2) FGF 21 could up regulate thermogenesis gene (UCP-1) in adipocytes as demonstrated in a previous study (Douris et al., 2015; Owen et al., 2014). These two possible explanations could increase energy expenditure, which caused body weight loss (Douris et al., 2015; Owen et al., 2014). Moreover, the effect of FGF21 on the improvement of peripheral insulin resistance could be due to the following mechanisms 1) increased rate of glucose uptake in adipocytes, increased insulin synthesis and reduced hepatic gluconeogenesis (Kharitonenkov et al., 2008; Kong et al., 2013; Kralisch et al., 2013; Liu et al., 2012; Xu et al., 2009b) and 2) reduced levels of pro-inflammatory cytokines such as TNF- $\alpha$ , MCP-1 and PAI-1, and 3) increased adiponectin biosynthesis in adipocytes, as shown in Table 2 and other previous studies (Kim et al., 2013; Lin et al., 2013).

Moreover, FGF21 treatment also improved brain FGF21 signaling, as indicated by an increased p-Erk1/2 level and subsequently to increased PGC-1 $\alpha$  expression in obese-insulin resistant male rats (Fig. 3). FGF21 has been shown to improve mitochondrial function in human dopaminergic neurons, by increasing mitochondrial anti-oxidant levels and enhancing mitochondrial respiratory capacity, mediated by sirtuin-1 (SIRT1) and PGC-1 $\alpha$  which leads to improved mitochondrial biogenesis and cell viability (Houten and Auwerx, 2004; Johanna Mäkelä et al., 2014; Lin et al., 2005; Wu et al., 1999). Moreover, increasing the activity of PGC-1 $\alpha$  has been shown to protect oxidative stress-induced cell death and prevent neurodegeneration in Parkinson's disease (Pacelli et al., 2011; St-Pierre et al., 2006). It is known that oxidative stress caused increased neuronal apoptosis and impaired hippocampal synaptic plasticity as indicated by a decrease in the LTP amplitude and the reduction in dendritic spine density (Avila-Costa et al., 1999; Rivas-Arancibia et al., 2010). Additionally, a recent study found that FGF21 treatment improved behavioral performance in the MWM test and in the step-down test by reducing brain cell damage in the hippocampus and suppressing brain oxidative stress in D-galatactose-induced aging model (Yu et al., 2015). The present study showed for the first time that FGF21 treatment in obese-insulin resistant male rats could restore brain mitochondrial function by reducing ROS production, brain oxidative stress levels and these events led to reduced brain cell apoptosis, restored hippocampal synaptic plasticity, restored dendritic spine density as well as prevented cognitive decline.

In conclusion, the present study demonstrated that the effects of FGF21 on the prevention of cognitive decline in obese-insulin resistant condition is associated with its ability to improve peripheral insulin sensitivity, reduce systemic inflammation, restore brain mitochondrial function, decrease brain oxidative stress, decreased brain cell apoptosis and restore hippocampal synaptic plasticity. These beneficial effects of FGF21 in the brain were mediated by the FGF21 signaling pathway.

#### Limitation of the study

Although our results showed that FGF21 treatment for 4 weeks effectively improved cognitive function, it is not known whether a 4-week treatment of FGF21 is the optimal duration to see its beneficial effects. The sample size was also small in the present study. Future studies with larger sample size are needed to investigate the time course effects of FGF21 on the cognition in obese-insulin resistant rats.

#### **Conflict of interest**

The authors declare that there is no conflict of interest.

#### Acknowledgements

This work was supported by Thailand Research Fund grants: TRF-BRG 5780016 (SC) and MRG5980198 (WP), a CMU 50th Anniversary grant by Chiang Mai University (PHD/023/2556 PS&NC), a NSTDA Research Chair Grant from the National Science and Technology Development Agency Thailand (NC) and Chiang Mai University Center of Excellence Award (NC). The authors would like to thank Ms. Cicely Proctor and Ms. Gabrielle Metzler for their editorial assistance.

#### References

- Adams, A.C., Cheng, C.C., Coskun, T., Kharitonenkov, A., 2012. FGF21 requires betaklotho to act in vivo. PLoS One 7, e49977.
- Arakawa, H., 2005. Age dependent effects of space limitation and social tension on openfieldbehavior in male rats. Physiol. Behav. 84, 429–436.
- Avila-Costa, M.R., Colin-Barenque, L., Fortoul, T.I., Machado-Salas, P., Espinosa-Villanueva, J., Rugerio-Vargas, C., Rivas-Arancibia, S., 1999. Memory deterioration in an oxidative stress model and its correlation with cytological changes on rat hippocampus CA1. Neurosci. Lett. 270. 107–109.
- Beilharz, J.E., Maniam, J., Morris, M.J., 2015. Diet-induced cognitive deficits: the role of fat and sugar, potential mechanisms and nutritional interventions. Nutrients 7, 6719–6738.
- Berg, A.H., Combs, T.P., Du, X., Brownlee, M., Scherer, P.E., 2001. The adipocyte-secreted protein Acrp30 enhances hepatic insulin action. Nat. Med. 7, 947–953.
- Bobbert, T., Schwarz, F., Fischer-Rosinsky, A., Pfeiffer, A.F., Mohlig, M., Mai, K., Spranger, J., 2013. Fibroblast growth factor 21 predicts the metabolic syndrome and type 2 diabetes in Caucasians. Diabetes Care 36, 145–149.
- Chattipakorn, S.C., McMahon, L.L., 2002. Pharmacological characterization of glycinegated chloride currents recorded in rat hippocampal slices. J. Neurophysiol. 87, 1515–1525.
- Coskun, T., Bina, H.A., Schneider, M.A., Dunbar, J.D., Hu, C.C., Chen, Y., Moller, D.E., Kharitonenkov, A., 2008. Fibroblast growth factor 21 corrects obesity in mice. Endocrinology 149, 6018–6027.
- Cournot, M., Marquie, J.C., Ansiau, D., Martinaud, C., Fonds, H., Ferrieres, J., Ruidavets, J.B., 2006. Relation between body mass index and cognitive function in healthy middleaged men and women. Neurology 67, 1208–1214.
- den Heijer, T., Vermeer, S.E., van Dijk, E.J., Prins, N.D., Koudstaal, P.J., Hofman, A., Breteler, M.M., 2003. Type 2 diabetes and atrophy of medial temporal lobe structures on brain MRI. Diabetologia 46, 1604–1610.
- Diez, J.J., Iglesias, P., 2010. The role of the novel adipocyte-derived protein adiponectin in human disease: an update. Mini-Rev. Med. Chem. 10, 856–869.
- Douris, N., Stevanovic, D.M., Fisher, F.M., Cisu, T.I., Chee, M.J., Nguyen, N.L., Zarebidaki, E., Adams, A.C., Kharitonenkov, A., Flier, J.S., Bartness, T.J., Maratos-Flier, E., 2015. Central fibroblast growth factor 21 browns white fat via sympathetic action in male mice. Endocrinology 156, 2470–2481.
- Elias, M.F., Elias, P.K., Sullivan, L.M., Wolf, P.A., D'Agostino, R.B., 2003. Lower cognitive function in the presence of obesity and hypertension: the Framingham heart study. Int. J. Obes. Relat. Metab. Disord. 27, 260–268.
- Fisher, F.M., Chui, P.C., Antonellis, P.J., Bina, H.A., Kharitonenkov, A., Flier, J.S., Maratos-Flier, E., 2010. Obesity is a fibroblast growth factor 21 (FGF21)-resistant state. Diabetes 59, 2781–2789.
- Friedewald, W.T., Levy, R.I., Fredrickson, D.S., 1972. Estimation of the concentration of low-density lipoprotein cholesterol in plasma, without use of the preparative ultracentrifuge. Clin. Chem. 18, 499–502.
- Fung, T.T., Rimm, E.B., Spiegelman, D., Rifai, N., Tofler, G.H., Willett, W.C., Hu, F.B., 2001. Association between dietary patterns and plasma biomarkers of obesity and cardiovascular disease risk. Am. J. Clin. Nutr. 73, 61–67.
- Gaich, G., Chien, J.Y., Fu, H., Glass, L.C., Deeg, M.A., Holland, W.L., Kharitonenkov, A., Bumol, T., Schilske, H.K., Moller, D.E., 2013. The effects of LY2405319, an FGF21 analog, in obese human subjects with type 2 diabetes. Cell Metab. 18, 333–340.
- Granholm, A.C., Bimonte-Nelson, H.A., Moore, A.B., Nelson, M.E., Freeman, L.R., Sambamurti, K., 2008. Effects of a saturated fat and high cholesterol diet on memory and hippocampal morphology in the middle-aged rat. J. Alzheimers Dis. 14, 133–145.
- Gulbahar, O., Aricioglu, A., Akmansu, M., Turkozer, Z., 2009. Effects of radiation on protein oxidation and lipid peroxidation in the brain tissue. Transplant. Proc. 41, 4394–4396.
- Gunstad, J., Lhotsky, A., Wendell, C.R., Ferrucci, L., Zonderman, A.B., 2010. Longitudinal examination of obesity and cognitive function: results from the Baltimore longitudinal study of aging. Neuroepidemiology 34, 222–229.
- Houten, S.M., Auwerx, J., 2004. PGC-1alpha: turbocharging mitochondria. Cell 119, 5–7.
   Hsuchou, H., Pan, W., Kastin, A.J., 2007. The fasting polypeptide FGF21 can enter brain from blood. Peptides 28, 2382–2386.
- Johanna Mäkelä, T.V.T., Maiorana, F., Eriksson, O., Do, H.T., Mudò, G., Korhonen, L.T., Belluardo3, N., Lindholm, D., 2014. Fibroblast growth factor-21 enhances mitochondrial functions and increases the activity of PGC-1α in human dopaminergic neurons via Sirtuin-1. SpringerPlus 3, 1-12.

- Kharitonenkov, A., Shanafelt, A.B., 2009. FGF21: a novel prospect for the treatment of metabolic diseases. Curr. Opin. Investig. Drugs 10, 359–364.
- Kharitonenkov, A., Dunbar, J.D., Bina, H.A., Bright, S., Moyers, J.S., Zhang, C., Ding, L., Micanovic, R., Mehrbod, S.F., Knierman, M.D., Hale, J.E., Coskun, T., Shanafelt, A.B., 2008. FGF-21/FGF-21 receptor interaction and activation is determined by betaKlotho, I. Cell. Physiol. 215, 1–7.
- Kharitonenkov, A., Wroblewski, V.J., Koester, A., Chen, Y.F., Clutinger, C.K., Tigno, X.T., Hansen, B.C., Shanafelt, A.B., Etgen, G.J., 2007. The metabolic state of diabetic monkeys is regulated by fibroblast growth factor-21. Endocrinology 148, 774–781.
- Kim, H.W., Lee, J.E., Cha, J.J., Hyun, Y.Y., Kim, J.E., Lee, M.H., Song, H.K., Nam, D.H., Han, J.Y., Han, S.Y., Han, K.H., Kang, Y.S., Cha, D.R., 2013. Fibroblast growth factor 21 improves insulin resistance and ameliorates renal injury in db/db mice. Endocrinology 154, 3366–3376.
- Kong, L.J., Feng, W., Wright, M., Chen, Y., Dallas-yang, Q., Zhou, Y.P., Berger, J.P., 2013. FGF21suppresses hepatic glucose production through the activation of atypical protein kinase Ciota/Jambda. Eur. J. Pharmacol. 702. 302–308.
- Kralisch, S., Tonjes, A., Krause, K., Richter, J., Lossner, U., Kovacs, P., Ebert, T., Bluher, M., Stumvoll, M., Fasshauer, M., 2013. Fibroblast growth factor-21 serum concentrations are associated with metabolic and hepatic markers in humans. J. Endocrinol. 216, 135–143
- Lin, J., Handschin, C., Spiegelman, B.M., 2005. Metabolic control through the PGC-1 family of transcription coactivators. Cell Metab. 1, 361–370.
- Lin, Z., Tian, H., Lam, K.S., Lin, S., Hoo, R.C., Konishi, M., Itoh, N., Wang, Y., Bornstein, S.R., Xu, A., Li, X., 2013. Adiponectin mediates the metabolic effects of FGF21 on glucose homeostasis and insulin sensitivity in mice. Cell Metab. 17, 779–789.
- Liu, M.Y., Wang, W.F., Hou, Y.T., Yu, Y.X., Ren, G.P., Kern, T.S., Sun, G.P., Li, D.S., 2012. Fibroblast growth factor (FGF)-21 regulates glucose uptake through GLUT1 translocation. Afr. J. Microbiol. Res. 6, 2504–2511.
- Markesbery, W.R., Kryscio, R.J., Lovell, M.A., Morrow, J.D., 2005. Lipid peroxidation is an early event in the brain in amnestic mild cognitive impairment. Ann. Neurol. 58, 730–735.
- Mashili, F.L., Austin, R.L., Deshmukh, A.S., Fritz, T., Caidahl, K., Bergdahl, K., Zierath, J.R., Chibalin, A.V., Moller, D.E., Kharitonenkov, A., Krook, A., 2011. Direct effects of FGF21 on glucose uptake in human skeletal muscle: implications for type 2 diabetes and obesity. Diabetes Metab. Res. Rev. 27, 286–297.
- Matthews, D.R., Hosker, J.P., Rudenski, A.S., Naylor, B.A., Treacher, D.F., Turner, R.C., 1985. Homeostasis model assessment: insulin resistance and beta-cell function from fasting plasma glucose and insulin concentrations in man. Diabetologia 28, 412–419.
- Munshi, M., Grande, L., Hayes, M., Ayres, D., Suhl, E., Capelson, R., Lin, S., Milberg, W., Weinger, K., 2006. Cognitive dysfunction is associated with poor diabetes control in older adults. Diabetes Care 29, 1794–1799.
- Nishimura, T., Nakatake, Y., Konishi, M., Itoh, N., 2000. Identification of a novel FGF, FGF-21 preferentially expressed in the liver. Biochim. Biophys. Acta 1492, 203–206.
- Northam, E.A., Anderson, P.J., Jacobs, R., Hughes, M., Warne, G.L., Werther, G.A., 2001. Neuropsychological profiles of children with type 1 diabetes 6 years after disease onset. Diabetes Care 24, 1541–1546.
- Novotny, D., Vaverkova, H., Karasek, D., Lukes, J., Slavik, L., Malina, P., Orsag, J., 2014. Evaluation of total adiponectin, adipocyte fatty acid binding protein and fibroblast growth factor 21 levels in individuals with metabolic syndrome. Physiol. Res. 63, 219–228.
- Ogawa, Y., Kurosu, H., Yamamoto, M., Nandi, A., Rosenblatt, K.P., Goetz, R., Eliseenkova, A.V., Mohammadi, M., Kuro-o, M., 2007. BetaKlotho is required for metabolic activity of fibroblast growth factor 21. Proc. Natl. Acad. Sci. U. S. A. 104, 7432–7437.
- Ouchi, N., Parker, J.L., Lugus, J.J., Walsh, K., 2011. Adipokines in inflammation and metabolic disease. Nat. Rev. Immunol. 11, 85–97.
- Owen, B.M., Ding, X., Morgan, D.A., Coate, K.C., Bookout, A.L., Rahmouni, K., Kliewer, S.A., Mangelsdorf, D.J., 2014. FGF21 acts centrally to induce sympathetic nerve activity, energy expenditure, and weight loss. Cell Metab. 20, 670–677.
- Pacelli, C., De Rasmo, D., Signorile, A., Grattagliano, I., di Tullio, G., D'Orazio, A., Nico, B., Comi, G.P., Ronchi, D., Ferranini, E., Pirolo, D., Seibel, P., Schubert, S., Gaballo, A., Villani, G., Cocco, T., 2011. Mitochondrial defect and PGC-1alpha dysfunction in parkin-associated familial Parkinson's disease. Biochim. Biophys. Acta 1812, 1041-1053.
- Pintana, H., Apaijai, N., Pratchayasakul, W., Chattipakorn, N., Chattipakorn, S.C., 2012. Effects of metformin on learning and memory behaviors and brain mitochondrial functions in high fat diet induced insulin resistant rats. Life Sci. 91, 409–414.
- Pintana, H., Apaijai, N., Chattipakorn, N., Chattipakorn, S.C., 2013. DPP-4 inhibitors improve cognition and brain mitochondrial function of insulin-resistant rats. J. Endocrinol. 218, 1–11.
- Pipatpiboon, N., Pratchayasakul, W., Chattipakorn, N., Chattipakorn, S.C., 2012. PPARgamma agonist improves neuronal insulin receptor function in hippocampus and brain mitochondria function in rats with insulin resistance induced by long term high-fat diets. Endocrinology 153, 329–338.
- Pipatpiboon, N., Pintana, H., Pratchayasakul, W., Chattipakorn, N., Chattipakorn, S.C., 2013. DPP4-inhibitor improves neuronal insulin receptor function, brain mitochondrial function and cognitive function in rats with insulin resistance induced by high-fat diet consumption. Eur. J. Neurosci. 37, 839–849.
- Pratchayasakul, W., Kerdphoo, S., Petsophonsakul, P., Pongchaidecha, A., Chattipakorn, N., Chattipakorn, S.C., 2011. Effects of high-fat diet on insulin receptor function in rat hippocampus and the level of neuronal corticosterone. Life Sci. 88, 619–627.
- Pratchayasakul, W., Sa-Nguanmoo, P., Sivasinprasasn, S., Pintana, H., Tawinvisan, R., Sripetchwandee, J., Kumfu, S., Chattipakorn, N., Chattipakorn, S.C., 2015. Obesity accelerates cognitive decline by aggravating mitochondrial dysfunction, insulin resistance and synaptic dysfunction under estrogen-deprived conditions. Horm. Behav. 72, 68–77.

- Raji, C.A., Ho, A.J., Parikshak, N.N., Becker, J.T., Lopez, O.L., Kuller, L.H., Hua, X., Leow, A.D., Toga, A.W., Thompson, P.M., 2010. Brain structure and obesity. Hum. Brain Mapp. 31, 353–364.
- Reaven, G.M., Thompson, L.W., Nahum, D., Haskins, E., 1990. Relationship between hyperglycemia and cognitive function in older NIDDM patients. Diabetes Care 13, 16–21.
- Riccardi, G., Giacco, R., Rivellese, A.A., 2004. Dietary fat, insulin sensitivity and the metabolic syndrome. Clin. Nutr. 23, 447–456.
- Rivas-Arancibia, S., Guevara-Guzman, R., Lopez-Vidal, Y., Rodriguez-Martinez, E., Zanardo-Gomes, M., Angoa-Perez, M., Raisman-Vozari, R., 2010. Oxidative stress caused by ozone exposure induces loss of brain repair in the hippocampus of adult rats. Toxicol. Sci. 113. 187–197.
- Sabia, S., Kivimaki, M., Shipley, M.J., Marmot, M.G., Singh-Manoux, A., 2009. Body mass index over the adult life course and cognition in late midlife: the Whitehall II Cohort Study. Am. I. Clin. Nutr. 89, 601–607.
- Sripetchwandee, J., Pipatpiboon, N., Chattipakorn, N., Chattipakorn, S., 2014a. Combined therapy of iron chelator and antioxidant completely restores brain dysfunction induced by iron toxicity. PLoS One 9, e85115.
- Sripetchwandee, J., Pipatpiboon, N., Pratchayasakul, W., Chattipakorn, N., Chattipakorn, S.C., 2014b. DPP-4 inhibitor and PPARgamma agonist restore the loss of CA1 dendritic spines in obese insulin-resistant rats. Arch. Med. Res. 45, 547–552.
- Sripetchwandee, J., Wongjaikam, S., Krintratun, W., Chattipakorn, N., Chattipakorn, S.C., 2016. A combination of an iron chelator with an antioxidant effectively diminishes the dendritic loss, tau-hyperphosphorylation, amyloids-beta accumulation and brain mitochondrial dynamic disruption in rats with chronic iron-overload. Neuroscience 332, 191–202.
- St-Pierre, J., Drori, S., Uldry, M., Silvaggi, J.M., Rhee, J., Jager, S., Handschin, C., Zheng, K., Lin, J., Yang, W., Simon, D.K., Bachoo, R., Spiegelman, B.M., 2006. Suppression of reactive oxygen species and neurodegeneration by the PGC-1 transcriptional coactivators. Cell 127, 397–408.
- Stranahan, A.M., Norman, E.D., Lee, K., Cutler, R.G., Telljohann, R.S., Egan, J.M., Mattson, M.P., 2008. Diet-induced insulin resistance impairs hippocampal synaptic plasticity and cognition in middle-aged rats. Hippocampus 18, 1085–1088.
- Tan, B.K., Hallschmid, M., Adya, R., Kern, W., Lehnert, H., Randeva, H.S., 2011. Fibroblast growth factor 21 (FGF21) in human cerebrospinal fluid: relationship with plasma FGF21 and body adiposity. Diabetes 60, 2758–2762.
- Thirumangalakudi, L., Prakasam, A., Zhang, R., Bimonte-Nelson, H., Sambamurti, K., Kindy, M.S., Bhat, N.R., 2008. High cholesterol-induced neuroinflammation and amyloid precursor protein processing correlate with loss of working memory in mice. J. Neurochem. 106, 475–485.

- Wang, H., Xiao, Y., Fu, L., Zhao, H., Zhang, Y., Wan, X., Qin, Y., Huang, Y., Gao, H., Li, X., 2010.
  High-level expression and purification of soluble recombinant FGF21 protein by
  SUMO fusion in *Escherichia coli*. BMC Biotechnol. 10, 14.
- Winocur, G., Greenwood, C.E., Piroli, G.G., Grillo, C.A., Reznikov, L.R., Reagan, L.P., McEwen, B.S., 2005. Memory impairment in obese Zucker rats: an investigation of cognitive function in an animal model of insulin resistance and obesity. Behav. Neurosci. 119, 1389–1395
- Wu, Z., Puigserver, P., Andersson, U., Zhang, C., Adelmant, G., Mootha, V., Troy, A., Cinti, S., Lowell, B., Scarpulla, R.C., Spiegelman, B.M., 1999. Mechanisms controlling mitochondrial biogenesis and respiration through the thermogenic coactivator PGC-1. Cell 98, 115–124
- Xu, J., Lloyd, D.J., Hale, C., Stanislaus, S., Chen, M., Sivits, G., Vonderfecht, S., Hecht, R., Li, Y.S., Lindberg, R.A., Chen, J.L., Jung, D.Y., Zhang, Z., Ko, H.J., Kim, J.K., Veniant, M.M., 2009a. Fibroblast growth factor 21 reverses hepatic steatosis, increases energy expenditure, and improves insulin sensitivity in diet-induced obese mice. Diabetes 58, 250–259
- Xu, J., Stanislaus, S., Chinookoswong, N., Lau, Y.Y., Hager, T., Patel, J., Ge, H., Weiszmann, J., Lu, S.C., Graham, M., Busby, J., Hecht, R., Li, Y.S., Li, Y., Lindberg, R., Veniant, M.M., 2009b. Acute glucose-lowering and insulin-sensitizing action of FGF21 in insulin-resistant mouse models-association with liver and adipose tissue effects. Am. J. Physiol. Endocrinol. Metab. 297, E1105–E1114.
- Yagi, K., 1998. Simple assay for the level of total lipid peroxides in serum or plasma. Methods Mol. Biol. 108, 101–106.
- Yang, M., Zhang, L., Wang, C., Liu, H., Boden, G., Yang, G., Li, L., 2012. Liraglutide increases FGF-21 activity and insulin sensitivity in high fat diet and adiponectin knockdown induced insulin resistance. PLoS One 7, e48392.
- Yu, Y., Bai, F., Wang, W., Liu, Y., Yuan, Q., Qu, S., Zhang, T., Tian, G., Li, S., Li, D., Ren, G., 2015. Fibroblast growth factor 21 protects mouse brain against d-galactose induced aging via suppression of oxidative stress response and advanced glycation end products formation. Pharmacol. Biochem. Behav. 133, 122–131.
- Zhang, X., Yeung, D.C., Karpisek, M., Stejskal, D., Zhou, Z.G., Liu, F., Wong, R.L., Chow, W.S., Tso, A.W., Lam, K.S., Xu, A., 2008. Serum FGF21 levels are increased in obesity and are independently associated with the metabolic syndrome in humans. Diabetes 57, 1246–1253.
- Zhang, C., Shao, M., Yang, H., Chen, L., Yu, L., Cong, W., Tian, H., Zhang, F., Cheng, P., Jin, L., Tan, Y., Li, X., Cai, L., Lu, X., 2013. Attenuation of hyperlipidemia- and diabetes-induced early-stage apoptosis and late-stage renal dysfunction via administration of fibroblast growth factor-21 is associated with suppression of renal inflammation. PLoS One 8, e82275.

# Estrogen and DPP4 inhibitor, but not metformin, exert cardioprotection via attenuating cardiac mitochondrial dysfunction in obese insulin-resistant and estrogen-deprived female rats

Sivaporn Sivasinprasasn, PhD,  $^{1,2,4,5}$  Piangkwan Sa-nguanmoo, MSc,  $^{1,2,4}$  Wanpitak Pongkan, DVM,  $^{1,2,4}$  Wasana Pratchayasakul, PhD,  $^{1,2,4}$  Siriporn C. Chattipakorn, DDS, PhD,  $^{1,3,4}$  and Nipon Chattipakorn, MD, PhD,  $^{1,2,4}$ 

#### Abstract

**Objective:** Cardiac function was markedly compromised in obese insulin-resistant and estrogen-deprived rats. Metformin and dipeptidyl peptidase-4 inhibitor (vildagliptin) were reported to improve cardiac function in insulin-resistant rats. Their effects on the heart under estrogen-deprived conditions are, however, unknown. Therefore, the effects of metformin, vildagliptin, and estrogen on the cardiac function in estrogen-deprived insulin-resistant female rats were investigated.

*Methods:* Bilateral ovariectomized female rats (n = 48) were divided to be fed with either a normal diet (ND) or a high-fat diet (HFD) for 12 weeks. Then, both ND- and HFD-fed groups were subdivided to receive a vehicle, estrogen (50  $\mu$ g/kg), metformin (30 mg/kg), or vildagliptin (3 mg/kg) for 4 weeks (n = 6/group). Heart rate variability, echocardiography, metabolic and biochemical parameters, cardiac function, and mitochondrial function were determined. Sham-operated female rats (n = 6) were used as a control.

**Results:** Both ND- and HFD-fed ovariectomized rats developed insulin resistance, depressed heart rate variability, and decreased cardiac contractility. Although treatment with metformin, vildagliptin, and estrogen improved metabolic status and cardiac function, only estrogen and vildagliptin improved diastolic blood pressure and left ventricular  $\pm dP/dt$ , and also reduced mitochondrial impairment, apoptosis, and oxidative stress in HD-fed ovariectomized rats.

**Conclusions:** Treatment with estrogen and vildagliptin provided more beneficial effects in the inhibition of oxidative stress, apoptosis, and cardiac mitochondrial dysfunction, and preserved cardiac contractile performance in estrogen-deprived insulin-resistant female rats.

*Key Words:* Cardiac function – DPP4 inhibitor – Estrogen – Insulin resistance – Metformin – Mitochondria.

ardiovascular diseases (CVDs) are the leading cause of mortality and morbidity, accounting for 30% of all global deaths. <sup>1,2</sup> Metabolic disorders such as obesity,

Received November 10, 2015; revised and accepted January 25, 2016. From the <sup>1</sup>Cardiac Electrophysiology Research and Training Center, <sup>2</sup>Cardiac Electrophysiology Unit, Department of Physiology, Faculty of Medicine, <sup>3</sup>Department of Oral Biology and Diagnostic Science, Faculty of Dentistry, and <sup>4</sup>Center of Excellence in Cardiac Electrophysiology Research, Chiang Mai University, Chiang Mai, Thailand; and <sup>5</sup>School of Medicine, Mae Fah Luang University, Chiang Rai, Thailand.

Funding/support: This work was supported by an NSTDA Research Chair Grant from the National Science and Technology Development Agency (NC), the Thailand Research Fund, BRG5780016 (SCC), TRG (WPr), and the Chiang Mai University Center of Excellence Award (NC).

Financial disclosure/conflicts of interest: None reported.

Supplemental digital content is available for this article. Direct URL citations appear in the printed text and are provided in the HTML and PDF versions of this article on the journal's Website (www.menopause.org).

Address correspondence to: Nipon Chattipakorn, MD, PhD, Cardiac Electrophysiology Research and Training Center, Faculty of Medicine, Chiang Mai University, Chiang Mai 50200, Thailand. E-mail: nchattip@gmail.com

dyslipidemia, and diabetes are known to be the major risk factors of CVD.<sup>2</sup> Gender is also considered a CVD risk factor, as the prevalence of CVD is higher in men than in women.<sup>3,4</sup> The risk of CVD in women has, however, been found to increase after endogenous estrogen deprivation, by both bilateral ovariectomy (OVX) and natural menopause.<sup>5,6</sup> Owing to the cardiometabolic protective effects of estrogen, estrogen withdrawal has been shown to induce both cardiac and metabolic dysfunction, such as hypertension and impaired glucose tolerance, therefore resulting in an increased risk of developing CVD. Estrogen hormone therapy has been shown to decrease fat accumulation, increase energy expenditure, suppress gluconeogenesis and lipogenesis, and enhance muscular insulin sensitivity, therefore resulting in improved metabolic syndrome conditions in OVX rats.<sup>8,9</sup> Moreover, estrogen helped in improving cardiac autonomic balance in the OVX model through the reduction of oxidative stress. 10,11 Oxidative stress is also considered as a factor responsible for the development of insulin resistance and cardiac dysfunction. 12,13 A recent study confirmed the positive effect of estrogen on antioxidative stress, due to the finding that cardiac reactive oxygen species (ROS) production was inhibited in OVX rats after receiving an estrogen supplement, resulting in an improved mitochondrial function. 14 The effect of the estrogen supplement on the cardiac mitochondrial function in estrogen-deprived rats with an obese insulin-resistant condition has, however, not yet been identified.

Metformin and dipeptidyl peptidase-4 (DPP4) inhibitor (vildagliptin) have been used for the treatment of type 2 diabetes mellitus. Metformin is an antihyperglycemic drug which has been shown to reduce hepatic glucose and lipid production, improve hepatic beta-cell function, and improve insulin sensitivity. 15 Vildagliptin exerts its antidiabetic action by inhibiting the DPP4 enzyme, resulting in increased insulin secretion and lower blood glucose levels. 16 In addition to the therapeutic effects on metabolic disorders, both metformin and vildagliptin were reported to be beneficial to the heart in both diabetic and nondiabetic rats. 17,18 Metformin and vildagliptin enhanced heart rate variability (HRV), and increased mitochondrial and myocardial function in an obese insulinresistant rat model.<sup>17</sup> Their effects as therapeutic agents in obese insulin-resistant rats with estrogen deprivation have, however, not yet been investigated. Owing to the increasing prevalence of metabolic syndrome and CVD in postmenopausal women, together with the increased use of metformin and vildagliptin, we aimed to investigate the roles of these drugs on metabolic status and cardiac function. In addition, this study aimed to investigate the underlying mechanisms acting in estrogen-deprived, obese insulin-resistant rats. We hypothesized that estradiol, metformin, and vildagliptin improve the metabolic function, cardiac performance, and mitochondrial function in estrogen-deprived, obese insulin-resistant rats.

#### **METHODS**

#### Animals and ethical approval

A total of 54 female Wistar rats (weighing 200-220 g) were obtained from the National animal center (Salaya Campus, Mahidol University, Bangkok, Thailand). The rats were given time to acclimatize, and were housed in a temperature-controlled room (25°C) with a 12-hour dark/light cycle setting. All experimental procedures were approved by the Institutional Animal Care and Use Committee at the Faculty of Medicine, Chiang Mai University, in compliance with National Institutes of Health (NIH) guidelines.

#### **Experimental protocol**

Rats were randomly assigned to receive either a sham operation (S; n = 6) or a bilateral OVX (O; n = 48), and then allowed to recover for 1 week. Sham rats were fed a normal diet (ND: containing 19.77% energy from fat), whereas ovariectomized rats were further subdivided to be fed with either a ND or a high-fat diet (HFD: containing 59.28% energy from fat) for 12 weeks. At the end of the 12th week, HRV and echocardiography were examined and recorded as the pretreatment data. Rats in both the ND-fed ovariectomized (NDO) and the HFD-fed ovariectomized (HFO) groups were randomly subcategorized to be treated with either estradiol (E: 50 μg/kg body weight [BW] via subcutaneous injection, once daily [17ß-estradiol; Sigma-Aldrich, St. Louis, MO]), metformin (M: 15 mg/kg BW, b.i.d., via gavage feeding [Glucophage; Merck Serono, Bangkok, Thailand]), vildagliptin (Vil: 3 mg/kg BW, daily, via gavage feeding [Galvus; Novartis, Bangkok, Thailand]), or vehicle (Ve: sesame oil, via subcutaneous injection in equal volumes with the estrogen treatment) for 4 weeks (n = 6/group; see supplement figure,Supplemental Digital Content 1, http://links.lww.com/ MENO/A164). After 4 weeks of treatment, HRV and echocardiography were examined again as the posttreatment data. Blood samples were collected to investigate metabolic parameters. Left ventricular (LV) function was determined using an intraventricular pressure recording system. At the end, rats were terminated by decapitation, and the heart was removed to study cardiac mitochondrial function and biochemical activities.

#### Surgical procedure of OVX

The bilateral OVX was performed according to the protocol which has been previously described. 19 Rats were anesthetized with zoletil (50 mg/kg) and xylazine (1 mg/kg), and ventilated with room air. 19 The abdominal-pelvic cavity was accessed through a skin incision between the inferior crest of the rib cage and superior base. After the uterine tube and ovary were identified, both ovaries were excised and uterine horns were returned into the pelvic cavity. The abdominal wall and the skin incision were closed and cleaned. After the operation, rats were observed for respiratory status and the recovery, and then individually housed in a clear box for 1 week before being fed with ND or HFD diets.

#### Metabolic function and estrogen-level determination

Metabolic parameters were investigated from blood samples (n = 6/group), which were collected at pre- and posttreatment time points. Fasting plasma glucose, cholesterol, and triglyceride levels were determined by colorimetric assay using a commercial kit (Biotech, Bangkok, Thailand). Fasting plasma insulin levels were measured using a sandwich enzyme-linked immunosorbent assay (ELISA) kit (Millipore, Ann Arbor, MI). Homeostasis Model Assessment (HOMA) was calculated to evaluate the degree of insulin resistance. 19 Serum estradiol levels were determined using a competitive enzyme immunoassay kit (Cayman Chemical Company, Ann Arbor, MI).

#### **Echocardiography**

Echocardiography was performed to evaluate the LV function before and after treatment. This test was performed while the animal was unconscious (lightly anesthetized with 2% isoflurane with oxygen [2 L/min] via inhalation) by using an echocardiograph (SONOS4500; Agilent Technologies, Santa Clara, CA).<sup>20</sup> Data from M-mode echocardiography were recorded to determine LV internal diameter at the end of diastole and LV internal diameter at the end of systole. Fractional shortening (%FS) and the ejection fraction (%EF) were calculated to estimate the contractile function (n = 6/group).<sup>21</sup>

#### **HRV** test

HRV measures were derived from electrocardiograms (lead II), which were recorded using a signal transducer (PowerLab 4/25T; ADInstruments, New South Wales, Australia) operated through the Chart 5.0 program for 20 minutes (n = 6/group). The frequency-domain method in the MATLAB program was used for electrocardiogram analysis. The high-frequency (HF) component (ranging between 0.15 and 0.40 Hz) is considered to be a marker of parasympathetic tone, whereas the low-frequency (LF) component (ranging between 0.04 and 0.15 Hz) is considered to be a marker of parasympathetic and sympathetic tone. The LF/HF ratio is considered to be an index of the cardiac sympathetic/parasympathetic balance. An increased LF/HF ratio indicates a suppressed HRV and cardiac sympathovagal imbalance. 20,23

#### LV pressure determination

Rats were anesthetized by intramuscular injections with zoletil ( $50 \, \text{mg/kg}$ ) and xylazine ( $0.15 \, \text{mg/kg}$ ), <sup>17</sup> and were then ventilated with room air via a tracheostomy tube. A pressure catheter (Scisence, Ontario, Canada) was inserted into the right carotid artery, and the catheter tip was directed into the LV chamber. After a 5-minute stabilization period, the signaling data from the catheter were recorded for 20 minutes. Then, rats were terminated and their hearts were removed for further mitochondrial and biochemical studies (n = 6/group). LV end-systolic pressure, LV end-diastolic pressure, maximum and minimum dP/dt (+dP/dt and -dP/dt), and heart rate were recorded. All parameters were analyzed using Labscribe analytical software (Labscribe, Dover, NH).

#### Cardiac mitochondrial function study

The methods for studying cardiac mitochondrial function. that is the mitochondrial ROS production, mitochondrial membrane potential changes, and mitochondrial swelling, have previously been described. 20,24 The removed heart was cut into small sections, and then homogenized and centrifuged to isolate the cardiac mitochondria. Dichlorohydrofluorescein diacetate dye was used to stain the isolated cardiac mitochondria, and then the ROS level was measured using a fluorescent microplate reader (BioTek, Winooski, VT), set at an excitation wavelength of 485 nm and an emission wavelength of 530 nm. 20,24 Mitochondrial membrane potential change was detected by using the dve 5,5',6,6'-tetrachloro-1,1',3,3'-tetraethylbenzimidazolcarbocyanine iodide (JC-1). The monomer form of JC-1 was excited at the wavelength of 485 nm and the emission detected at 590 nm (green fluorescence), whereas the JC-1 aggregate form was excited at the wavelength of 485 nm and the emission detected at 530 nm (red fluorescence).<sup>24</sup> Depolarization of the mitochondrial membrane was indicated by a decreased red/green fluorescence intensity ratio.<sup>24</sup> Cardiac

mitochondrial swelling was detected using a spectrophotometer at 540 nm, continuously for 30 minutes, swelling being indicated by a decrease in the absorbance of a mitochondrial suspension. A transmission electron microscope (JEM-1200 EX II; JEOL Ltd, Tokyo, Japan) was also used to observe the mitochondrial morphology, according to the previously described procedure. <sup>18</sup>

#### **Determination of oxidative stress**

Oxidative stress levels were indicated by the increased malondialdehyde (MDA) concentrations, which were measured by a high-performance liquid chromatography system (Thermo Scientific, Bangkok, Thailand), as previously described. Serum and protein from cardiac tissues were mixed with 10% trichloroacetic acid. The mixture was centrifuged, and the supernatant was mixed with 0.44 M H<sub>3</sub>PO<sub>4</sub> and 0.6% thiobabituric acid solution to generate thiobarbituric acid reactive substances, which were further measured by the high-performance liquid chromatography system with BDS software (BarSpec Ltd, Rehovot, Israel). The concentration of thiobarbituric acid reactive substances was determined directly from a standard curve and reported as an MDA equivalent concentration.

#### Cardiac expression of Bax and Bcl-2

The expressions of Bax and Bcl-2 were determined by western blot analysis. Briefly, myocardial tissues were homogenized in a lysis buffer (containing 1% Nonidet P-40, 0.5% sodium deoxycholate, 0.1% sodium dodecyl sulfate [SDS] in 1 × phosphate buffered saline) and were then centrifuged at 13,000 rpm for 10 minutes. Myocardial protein was mixed with the loading buffer (consisting of 5% mercaptoethanol, 0.05% bromophenol blue, 75 nM Tris-HCl, 2% SDS, and 10% glycerol with pH 6.8) at 1 mg/mL concentration and boiled for 5 minutes. The protein was loaded into a 10% gradient SDSpolyacrylamide gel, and then transferred to a polyvinyldene difluoride membrane in a transfer system (Bio-Rad, Hercules, CA). The protein-contained membranes were incubated in 5% skimmed milk in 1 × Tris-buffered saline and Tween 20 solution-T buffer for 1 hour, and then exposed to anti-Bax, anti-Bcl-2 (Cell Signaling Technology, Danvers, MA) and anti-actin (Sigma-Aldrich). Horseradish peroxidase conjugated with antirabbit or antimouse IgG (Santa Cruz Biotechnology, Inc. Dallas, TX) was administered to produce a peroxidase reaction, which further developed the signal by enhanced chemiluminescence detection reagents. Finally, autoradiography was performed, and the immune-blotted films were investigated to examine the protein band density using the ImageJ program (NIH image).<sup>18</sup>

#### Chemicals and antibodies

Estradiol and sesame oil were obtained from Sigma-Aldrich. Metformin was from Merck Serono, and vildagliptin was from Novartis. Colorimetric assay kits for the determination of plasma glucose, cholesterol, and triglyceride were from Biotech. ELISA kit for the measurement of plasma

insulin level was from Millipore. Enzyme immunoassay kit for serum estradiol-level detection was from Cayman Chemical Company. The antibodies against Bax and Bcl-2 were from Cell Signaling Technology and antiactin was from Sigma-Aldrich. The horseradish peroxidase conjugated with antirabbit and antimouse IgG were from Santa Cruz Biotechnology.

#### Statistical analysis

Data were derived from all rats in each experimental group (n = 6/group) in all experiments. All data were included in the statistical analysis and was presented as mean ± standard error of mean. A one-way analysis of variance followed by post-hoc least significant difference test, which was carried out using the SPSS program (SPSS version 16; SPSS Inc, Chicago, IL), was used to determine the differences between the means. P < 0.05 was considered statistically significant.

#### RESULTS

#### Effects of estrogen, metformin, and vildagliptin on metabolic function in obese insulin-resistant and estrogendeprived rats

Metabolic parameters measured after 4 weeks of treatment are shown in Table 1. Both NDOVe and HFOVe rats exhibited metabolic disorders, shown by an increased BW, increased plasma cholesterol, and decreased plasma high-density lipoprotein level. NDOVe and HFOVe rats also had increased plasma insulin and glucose levels and a higher HOMA index, indicating insulin resistance. All interventions except the vehicle could reverse the insulin-resistant status in both NDO and HFO rats, as indicated by the decreased HOMA index and decreased plasma insulin and glucose levels, to the same level as those of ND-fed sham-operated (NDS) rats. BW was reduced in NDO and HFO rats that were treated with E and M, but not Vil, when compared with those who received the vehicle. HFO rats had a greater visceral fat mass when compared with NDS rats, and only E significantly reduced both BW and visceral fat accumulation. None of the treatments could decrease plasma cholesterol levels in HFO rats.

#### Effects of estrogen, metformin, and vildagliptin on cardiac function and autonomic regulation in estrogen-deprived, obese insulin-resistant rats

Before treatment, echocardiography data showed that both the %FS and %EF had declined, and HRV was suppressed in both NDO and HFO rats when compared with NDS rats (Fig. 1A-C). This indicated that NDO and HFO rats had cardiac contractile dysfunction and autonomic imbalance. All treatment groups except those in the vehicle-only group showed improvements in %FS (Fig. 2A) and corrections in the %EF (Fig. 2B) and LF/HF ratio (Fig. 2C), bringing them back to normal levels.

Heart rate was increased in both NDOVe and HFOVe rats compared with NDS rats, but this increase in heart rate was not seen in all drug-treated groups (Table 2). NDOVe and HFOVe rats had increased systolic and diastolic blood pressures (Table 2). Treatment with E, M, and Vil reduced systolic blood pressure in both NDO and HFO rats. Diastolic blood pressure was improved only in HFOE and HFOVil rats, not in HFOM rats. There were no differences in diastolic blood pressure among treated NDO rats. In HFO rats, there was a reduction in ±dP/dt in HFOVe and HFOM compared with NDS rats, but  $\pm dP/dt$  was maintained in HFOE and HFOVil rats (Table 2). Moreover, LVESP was markedly decreased in HFOVe, HFOM, and HFOVil rats, but it was preserved only in HFOE rats (Table 2), suggesting that only estrogen and vildagliptin improved LV function to a greater extent compared with the other treatments in HFD-fed rats.

**TABLE 1.** Metabolic parameters after 4 weeks of treatment

|                        |                  |                     | ND                   | О                    |                    |                    | Н                    | FO                   |                     |
|------------------------|------------------|---------------------|----------------------|----------------------|--------------------|--------------------|----------------------|----------------------|---------------------|
| Parameters             | NDS              | Ve                  | Е                    | M                    | Vil                | Ve                 | E                    | M                    | Vil                 |
| Body weight, g         | $294.2 \pm 3$    | $356.0 \pm 8^a$     | $308.3 \pm 9^b$      | $321.6 \pm 7^b$      | $331.6 \pm 11^a$   | $414.0 \pm 17^a$   | $340.0 \pm 13^{a,c}$ | $377.5 \pm 6^{a,c}$  | $396.6 \pm 17^a$    |
| Visceral fat, g        | $14.9 \pm 1.4$   | $15.9 \pm 1.6$      | $13.3 \pm 1.6$       | $11.6 \pm 1.3$       | $14.9 \pm 1.1$     | $32.3 \pm 3.2^a$   | $18.2 \pm 1.3^{c}$   | $30.8 \pm 2.1^{a}$   | $31.6 \pm 4.6^a$    |
| Uterus weight, g       | $0.50 \pm 0.1$   | $0.08 \pm 0.0^{a}$  | $0.39 \pm 0.0^{b}$   | $0.07 \pm 0.0^{a}$   | $0.07 \pm 0.0^{a}$ | $0.08 \pm 0.0^{a}$ | $0.47 \pm 0.0^{c}$   | $0.08 \pm 0.0^{a}$   | $0.08 \pm 0.0^{a}$  |
| Glucose, mg%           | $125.8 \pm 7.0$  | $150.3 \pm 8.8^{a}$ | $120.48 \pm 7.2^{b}$ | $111.7 \pm 2.7^b$    | $126.1 \pm 9.2^b$  | $170.6 \pm 11.0^a$ | $142.1 \pm 8.6^{c}$  | $139.8 \pm 11.3^{c}$ | $136.4 \pm 7.8^{c}$ |
| Cholesterol, mg%       | $71.3 \pm 1.9$   | $104.3 \pm 1.5^a$   | $87.6 \pm 8.4$       | $78.8 \pm 3.2^{b}$   | $88.3 \pm 4.0$     | $125.0 \pm 5.7^a$  | $122.0 \pm 10.6^a$   | $120.9 \pm 1.9^a$    | $120.1 \pm 5.43^a$  |
| HDL, µg/µL             | $0.34 \pm 0.0$   | $0.30 \pm 0.0^{a}$  | $0.31 \pm 0.0$       | $0.33 \pm 0.0$       | $0.33 \pm 0.0$     | $0.28 \pm 0.0^{a}$ | $0.33 \pm 0.0^{c}$   | $0.37 \pm 0.0^{c}$   | $0.37 \pm 0.0^{c}$  |
| Triglyceride, mg%      | $30.5 \pm 2.46$  | $33.9 \pm 1.5$      | $32.3 \pm 5.1$       | $32.3 \pm 4.5$       | $32.5 \pm 3.77$    | $37.3 \pm 1.9$     | $32.0 \pm 5.0$       | $31.4 \pm 1.5$       | $33.4 \pm 4.2$      |
| Insulin, ng/mL         | $0.92 \pm 0.1$   | $1.75 \pm 0.1^a$    | $0.81 \pm 0.1^{b}$   | $0.90 \pm 0.4^{b}$   | $1.10 \pm 0.1^{b}$ | $1.93 \pm 0.1^a$   | $1.03 \pm 0.0^{c}$   | $0.90 \pm 0.0^{c}$   | $1.23 \pm 0.3^{c}$  |
| HOMA index             | $6.90 \pm 1.4$   | $16.28 \pm 1.2^a$   | $5.72 \pm 1.1^{b}$   | $6.13 \pm 2.8^b$     | $8.99 \pm 1.2^{b}$ | $20.43 \pm 1.6^a$  | $8.11 \pm 0.9^{c}$   | $7.70 \pm 0.4^{c}$   | $7.08 \pm 1.7^{c}$  |
| Estradiol level, pg/mL | $174.5 \pm 24.4$ | $78.6 \pm 11.3^a$   | $195.7 \pm 51.1^b$   | $88.6 \pm 6.2^{a}$   | $71.1 \pm 8.0^{a}$ | $80.3 \pm 18.9^a$  | $224.9 \pm 27.5^{c}$ | $97.6 \pm 21.1^a$    | $77.7 \pm 19.0^a$   |
| Serum MDA, µmol/mL     | $2.02 \pm 0.0$   | $3.06 \pm 0.1^a$    | $2.40 \pm 0.1^{b}$   | $2.69 \pm 0.0^{a,b}$ | $2.38 \pm 0.0^{b}$ | $3.48 \pm 0.1^{a}$ | $2.37 \pm 0.0^{c}$   | $3.15 \pm 0.0^{a}$   | $2.33 \pm 0.0^{c}$  |
| Tissue MDA, µmol/mL    | $1.72\pm0.2$     | $4.31 \pm 0.5^a$    | $2.53 \pm 0.2^{b}$   | $3.46 \pm 0.2^{a}$   | $2.52 \pm 0.2^{b}$ | $4.16 \pm 0.4^{a}$ | $2.16 \pm 0.4^{c}$   | $3.23 \pm 0.3^{a}$   | $2.38 \pm 0.0^{c}$  |
| Food intake, g/d       | $12.5 \pm 0.7$   | $14.1\pm1.8$        | $12.8 \pm 0.5$       | $13.7 \pm 0.4$       | $12.9 \pm 0.6$     | $18.6 \pm 0.0^{a}$ | $18.3 \pm 0.5^{a}$   | $18.5 \pm 0.5^a$     | $20.5 \pm 1.2^a$    |

Values are mean  $\pm$  SEM for six rats per group.

E, estradiol; HDL, high-density lipoprotein; HFO, high-fat diet-fed ovariectomized rats; HOMA, Homeostasis Model Assessment; M, metformin; MDA, malondialdehyde; NDO, normal diet-fed ovariectomized rats; NDS, normal diet-fed sham-operated rats; Ve, vehicle; Vil, vildagliptin.

 $<sup>^{</sup>a}P < 0.05$  versus NDS.

 $<sup>^{</sup>b}P < 0.05$  versus NDOVe.

 $<sup>^{</sup>c}P < 0.05$  versus HFOVe.

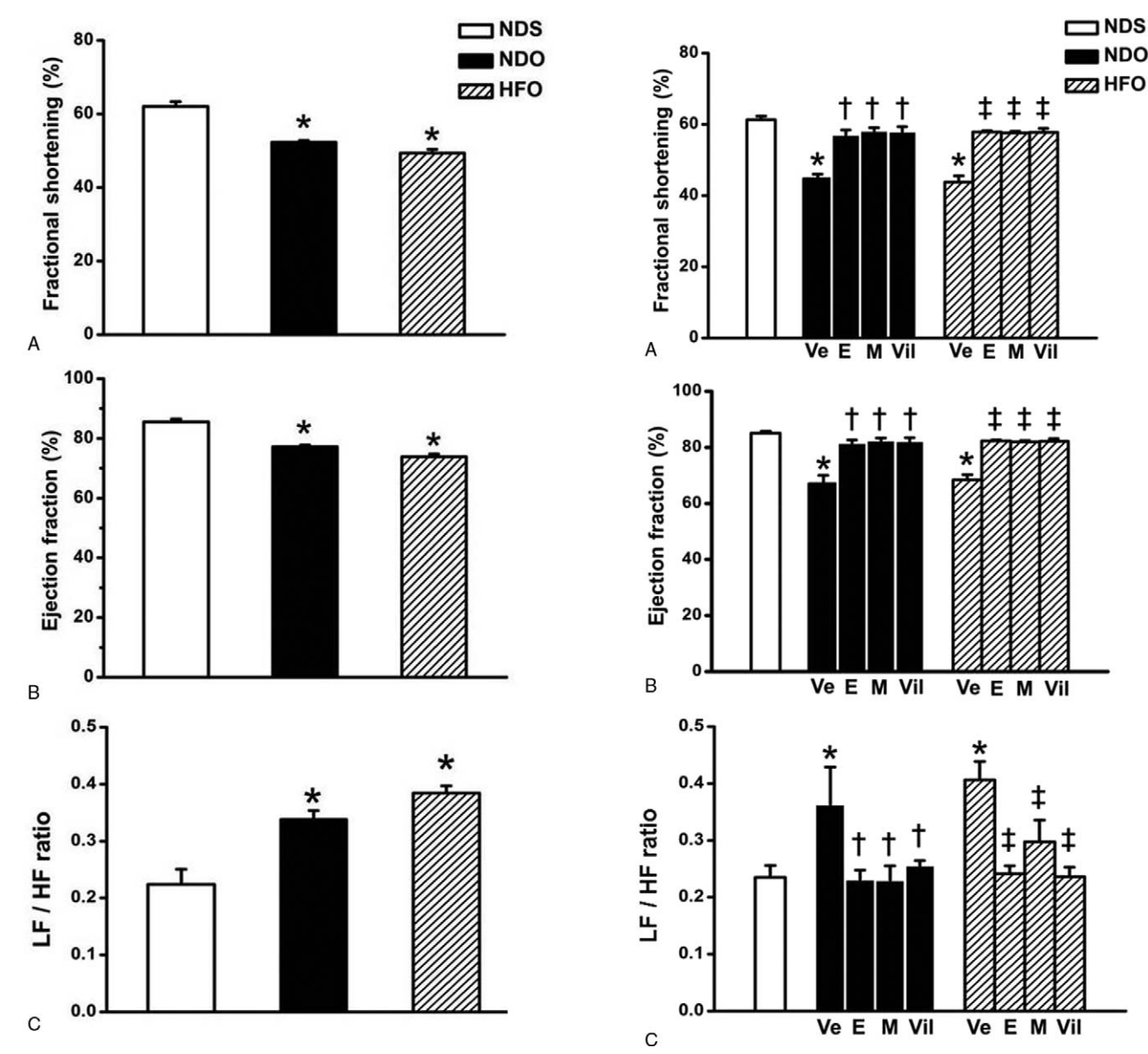


FIG. 1. Effects of estrogen deprivation and obese insulin resistance on left ventricular function and heart rate variability. At week 12 after ovariectomy, both estrogen-deprived rats who fed with NDO and those who fed with HFO had reduced fractional shortening (A), ejection fraction (B), and increased LF/HF ratio (C) when compared with NDS rats. Values are mean  $\pm$  SEM (n = 6 rats/group). \*P < 0.05 versus NDS. HF, high frequency; HFO, high-fat diet-fed ovariectomized rats; LF, low frequency; NDO, normal diet-fed ovariectomized rats; NDS, normal diet-fed sham-operated rats; SEM, standard error of mean.

FIG. 2. Effects of E, M, and Vil on left ventricular function and heart rate variability of estrogen-deprived rats. After 4 weeks of treatment, fractional shortening (A) and ejection fraction (B) were improved, and LF/HF ratio (C) was restored in estrogen (E)-, metformin (M)-, and vildagliptin (Vil)-treated groups when compared with vehicle-treated NDO or HFO rats. Values are mean  $\pm$  SEM (n = 6 rats/group). \*P < 0.05versus NDS;  ${}^{\dagger}P < 0.05$  versus NDOVe; and  ${}^{\ddagger}P < 0.05$  versus HFOVe. E, estradiol; HF, high frequency; HFO, high-fat diet-fed ovariectomized rats; LF, low frequency; M, metformin; NDO, normal diet-fed ovariectomized rats; NDS, normal diet-fed sham-operated rats; SEM, standard error of mean; Ve, vehicle; Vil, vildagliptin.

#### Effects of estrogen, metformin, and vildagliptin on cardiac expression of Bax and Bcl-2 in estrogen-deprived, obese insulin-resistant rats

There were significant increases in the expression of the apoptotic protein Bax in NDOVe, HFOVe, and HFOM groups (Fig. 3A). The expression of the antiapoptotic protein Bcl-2 was significantly decreased in HFOVe and HFOM rats (Fig. 3B). The ratio of cardiac Bax/Bcl-2 was significantly higher in NDOVe, HFOVe, and HFOM rats compared with the NDS rats (Fig. 3C), whereas this ratio was lower in the HFOE and HFOVil groups, suggesting that only estrogen and vildagliptin could attenuate apoptosis in an obese insulinresistant and estrogen-deprived rat model. A significant change in Bax and Bcl-2 expression was not observed in any NDO rats.

■ NDO

 TABLE 2. Cardiac function after 4 weeks of treatment

|                     |                    |                    | NDO                | 00                 |                    |                    | HFO               | 0.                 |                    |
|---------------------|--------------------|--------------------|--------------------|--------------------|--------------------|--------------------|-------------------|--------------------|--------------------|
| Parameters          | NDS                | Ve                 | E                  | M                  | Vil                | Ve                 | E                 | M                  | Vil                |
| Heart rate, bpm     | $238 \pm 18$       | $306 \pm 5^a$      | 266 ± 8            | 275 ± 19           | 266±9              | $307 \pm 21^a$     | $273 \pm 24$      | $285 \pm 28$       | 286±11             |
| Systolic BP, mm Hg  | $118.5\pm4$        | $139.7\pm10^a$     | $117.6 \pm 5^b$    | $112.3 \pm 5^b$    | $113.3 \pm 3^{b}$  | $140.7 \pm 6^{a}$  | $112.9 \pm 3^{c}$ | $111.5 \pm 6^c$    | $112.3 \pm 5^c$    |
| Diastolic BP, mm Hg | $86.7 \pm 4$       | $108.9\pm10^a$     | $89.1 \pm 5$       | $93.5 \pm 7$       | $93.8 \pm 5$       | $107.7 \pm 5^a$    | $77.9 \pm 7^c$    | $91.8\pm6$         | $87.1\pm6^c$       |
| LVESP, mm Hg        | $127.3 \pm 7$      | $99.7 \pm 5^{a}$   | $113.7 \pm 4$      | $115.1\pm4$        | $111.9 \pm 4$      | $100.7 \pm 2^{a}$  | $116.5 \pm 3$     | $111.6 \pm 7^{a}$  | $108.9 \pm 5^{a}$  |
| LVEDP, mm Hg        | $12.0 \pm 2$       | $19.9 \pm 2$       | $15.2 \pm 1$       | $15.8 \pm 4$       | $15.5 \pm 2$       | $18.8 \pm 2$       | $16.2 \pm 2$      | $14.2 \pm 1$       | $13.7 \pm 1$       |
| +dP/dt, mm Hg/s     | $11,339 \pm 1,228$ | $5,877 \pm 458^a$  | $10,758 \pm 4,949$ | $10,427 \pm 2,948$ | $10,048 \pm 3,858$ | $5,894 \pm 341^a$  | $6,555 \pm 1,440$ | $5,872 \pm 286^a$  | $7,227 \pm 932$    |
| -dP/dt, mm Hg/s     | $-7,677 \pm 847$   | $-4,397 \pm 707^a$ | $-5,886 \pm 1,005$ | $-5,914 \pm 997$   | $-5,797 \pm 1,284$ | $-4,839 \pm 623^a$ | $-5,626 \pm 423$  | $-4,706 \pm 179^a$ | $-6,079 \pm 1,218$ |

Values are mean  $\pm$  SEM (n = 6 per group).

ovariectomized rats; LVEDP, left ventricular end-diastolic pressure; LVESP, left ventricular end-systolic pressure; M, metformin; NDO, normal diet-fed ovariectomized rats; NDS, normal diet-fed sham--dP/dt, maximal slope of the diastolic pressure decrement; E, estradiol; HFO, high-fat diet-fed blood pressure; bpm, beats per minute; +dP/dt, maximal slope of the systolic pressure increment; operated rats; Ve, vehicle; Vil, vildagliptin.

< 0.05 versus NDS. < 0.05 versus NDOVe. P < 0.05 versus HFOVe.

#### Effects of estrogen, metformin, and vildagliptin on cardiac mitochondrial function and oxidative stress in estrogendeprived, obese insulin-resistant rats

Both NDOVe and HFOVe rats exhibited cardiac mitochondrial impairment, which was identified by the increased mitochondrial ROS level, decreased  $\Delta\Psi$  indicating mitochondrial depolarization, and decreased absorbance intensity indicating mitochondrial swelling (Fig. 4A–D, respectively). In NDO rats, treatment with E completely halted mitochondrial dysfunction by markedly reducing ROS production, increasing  $\Delta\Psi$ , and attenuating mitochondrial swelling to normal levels. In HFOE rats, all mitochondrial parameters showed significant improvement, especially ROS production and  $\Delta\Psi$ , which were reversed to normal levels. Treatment with Vil also improved all mitochondrial parameters in both NDOVil and HFOVil when compared with vehicle-treated groups; however, it did not bring parameters back to normal levels (Fig. 4). Treatment with M could improve all mitochondrial parameters in NDOM rats; however, it failed to enhance any mitochondrial parameters in HFOM rats when compared with NDOVe rats.

#### DISCUSSION

The major findings from this study are as follows: (1) estrogen, metformin, and vildagliptin can attenuate insulin resistance in both ND- and HFD-fed estrogen-deprived rats; (2) although estrogen, metformin, and vildagliptin similarly attenuated cardiac autonomic dysfunction, estrogen and vildagliptin provided superior advantages through their ability to restore blood pressure and cardiac contractile performance in estrogen-deprived insulin-resistant rats; and (3) oxidative stress, apoptosis, and cardiac mitochondrial dysfunction were effectively decreased by estrogen and vildagliptin, but not by metformin.

Although the impairments of LV function in obese insulinresistant rats and the benefits from the results may be subtle, these impairments as well as the efficacy of treatments by estrogen, metformin, or vildagliptin were demonstrated to be consistent and significant throughout the experiments. This subtle difference could also be due to the fact that we used the obese insulin-resistant model which was a prediabetic state model in which the severity is not high. Investigation in a model of type 2 diabetes with estrogen deprivation may reveal even larger benefits. Future studies are needed to evaluate this issue. Nevertheless, we believe that our findings indicated potential therapeutic efficacy of these antidiabetic drugs in menopause with obese insulin-resistant condition.

All therapeutic agents in this study, that is estrogen, vildagliptin, and metformin, clearly ameliorated insulin resistance, as indicated by the decreased levels of fasting insulin and glucose, and thus resulting in a reduced HOMA index. These results are consistent with a previous study which similarly showed that metformin and vildagliptin decreased insulin levels and the HOMA index in HFD-fed rats. 17 Estrogen supplements also exhibited similar beneficial effects, consistent with the results from a previous study, in

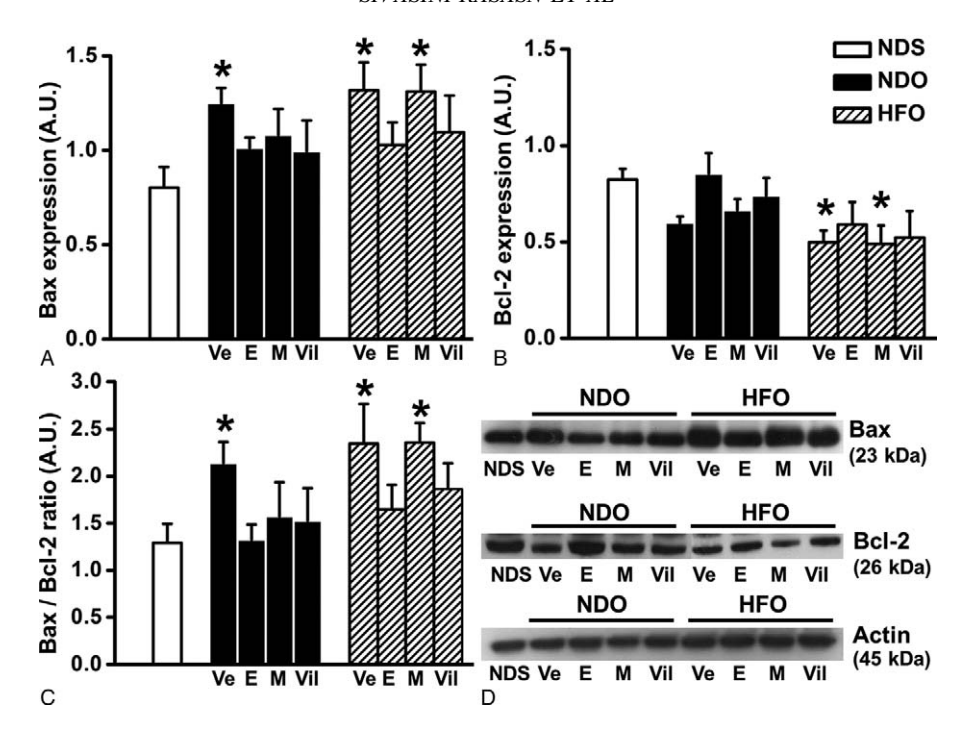


**FIG. 3.** Cardiac expression of apoptotic and antiapoptotic proteins after treatment with E, M, or Vil for 4 weeks. Expression levels of the apoptotic protein Bax (**A**) were significantly increased, whereas the expression levels of antiapoptotic protein, Bcl-2 (**B**), were reduced in HFOVe and HFOM rats. The Bax/Bcl-2 ratio (**C**) was significantly increased in NDOVe, HFOVe, and HFOM rats when compared with NDS rats. The represented protein expressions are in panel **D**. Values are mean  $\pm$  SEM (n = 6 rats per group). \*P < 0.05 versus NDS. E, estradiol; HFO, high-fat diet-fed ovariectomized rats; M, metformin; NDO, normal diet-fed ovariectomized rats; NDS, normal diet-fed sham-operated rats; SEM, standard error of mean; Ve, vehicle; Vil, vildagliptin.

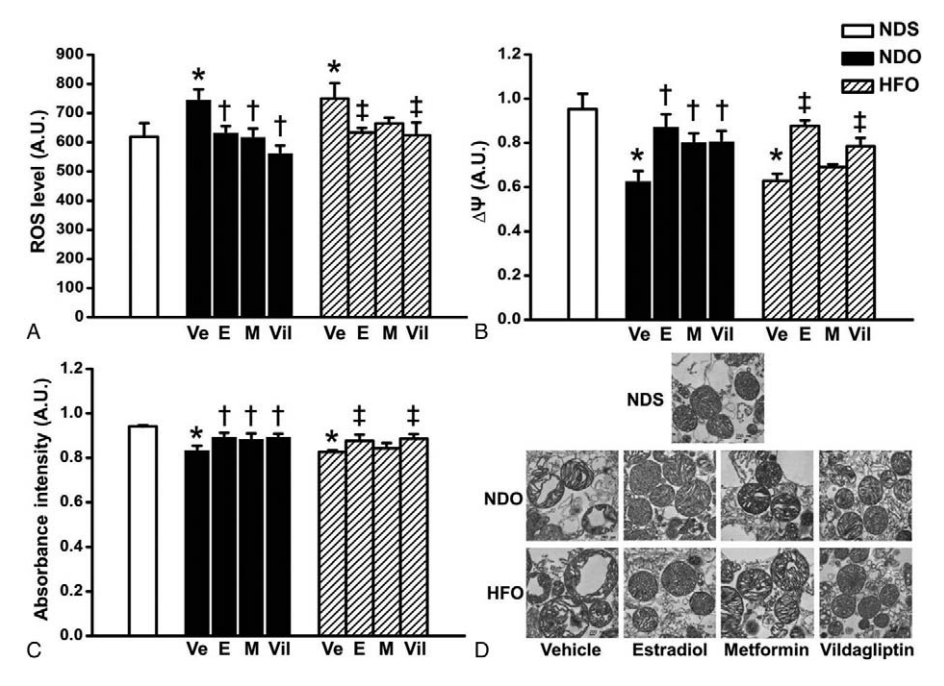


FIG. 4. Cardiac mitochondrial function in estrogen-deprived rats after treatment with E, M, or Vil for 4 weeks. Mitochondrial ROS level (A) was increased, whereas  $\Delta\Psi$  (B) and absorbance intensity (C) were decreased in NDOVe and HFOVe rats. Transmission electron micrographs (D) illustrate cardiac mitochondria morphology from rats in each group. Treatments with E and Vil improved all parameters of cardiac mitochondrial function in both NDO and HFO rats. Treatment with M, however, showed effective effects on mitochondrial function only in NDO, not in HFO rats. Values are mean  $\pm$  SEM (n = 6 rats per group). \* $^{*}P$  < 0.05 versus NDS;  $^{\dagger}P$  < 0.05 versus NDOVe; and  $^{\dagger}P$  < 0.05 versus HFOVe. E, estradiol; HFO, high-fat diet-fed ovariectomized rats; M, metformin; NDO, normal diet-fed ovariectomized rats; NDS, normal diet-fed sham-operated rats; ROS, reactive oxygen species; SEM, standard error of mean; Ve, vehicle; Vil, vildagliptin.

which insulin resistance was reversed after just 1 month of estrogen treatment. 19 Estrogen and metformin also efficiently inhibited BW gain in both ND- and HFD-fed rats. Estrogen had been previously reported to protect female mice from adipocyte hypertrophy, body fat accumulation, and weight gain, and the results of this study are consistent with these findings.<sup>25</sup> Likewise, metformin has previously been reported to increase fatty acid oxidation and decrease weight gain.<sup>26</sup> The ability of metformin to increase fatty acid oxidation, however, could be responsible for the high level of cytotoxicity and oxidative stress in metformin-treated rats, which was indicated by the elevated MDA levels and mitochondrial impairment. Metformin had been shown to decrease cholesterol synthesis and content; however, it has also been shown to increase ROS production in a macrophage cell line.<sup>27</sup> These results are similar to the findings in this study, in which cholesterol levels were reduced, whereas mitochondrial ROS levels were enhanced in metformin-treated rats.

In the present study, estrogen and vildagliptin had measurably enhanced effects on oxidative stress reduction, as they completely attenuated mitochondrial ROS production, decreased mitochondrial depolarization, decreased mitochondrial swelling, and restored serum and tissue MDA levels. Although metformin was able to reverse hyperglycemia, which is a condition linked to increased oxidative stress and inflammation,<sup>28</sup> it failed to improve mitochondrial function and decrease MDA concentrations, therefore could not effectively protect the heart from oxidative stress. This increased oxidative stress could subsequently induce cellular apoptosis,<sup>29</sup> which was indicated by the reduced Bcl-2 level and the upregulated levels of the Bax and Bax/Bcl-2 ratio in the myocardium of metformin-treated rats. Cardiomyocyte apoptosis is known to be associated with the pathogenesis of heart disease and heart failure. 30,31 This oxidative stressinduced cardiomyocyte apoptosis may contribute to decreased myocardium performance as observed in the metformin-treatment group. Moreover, a higher level of ROS. which was found in metformin-treated obese rats, is also harmful to endothelial membranes and nitric oxide function,<sup>32</sup> thus resulting in increased diastolic blood pressure. Estrogen has been reported to inhibit ROS production, decrease lipid peroxidation, and reduce oxidative stress in several cell types such as cardiomyocytes, fibroblasts, and hepatocytes. 33-35 Vildagliptin is also effective in the reduction of oxidative stress and mitochondrial dysfunction.<sup>36</sup> The antioxidant and antiapoptotic effects of estrogen and vildagliptin may play an important role in the attenuation of cardiometabolic disorders in obese insulin-resistant and estrogen-deprived rats.

Moreover, previous studies reported the similar effects of estrogen and vildagliptin regarding the reduction of oxidative stress and inflammatory markers.<sup>37,38</sup> Vildagliptin was also reported to enhance endothelial cell function and blood flow, through the upregulation of Akt and eNOS phosphorylation.<sup>39</sup> The activation of Akt and eNOS pathway had been demonstrated as the common mechanisms underlying estrogen cardioprotection<sup>40,41</sup>; therefore, the benefits of vildagliptin

may share a similar pathway, and thus provide a similar effect as estrogen treatment, as observed in this study.

#### Potential clinical value

Previous studies from both basic and clinical reports demonstrated the adverse effects of estrogen therapy such as increased atrial fibrillation incidence, increased QT interval and dispersion. The use of estrogen supplement has been contraindicated in individuals with the conditions of thromboembolism and migraine. Moreover, estrogen supplement was reported to increase risks of glioma, meningioma, and all tumors of the central nervous system. The findings in the present study, which demonstrated that the cardioprotective effects and efficacy of vildagliptin and metformin are similar to estrogen supplement in ovariectomized rats under normal and obese insulin-resistant conditions, provided important information for future clinical use of these drugs in obese insulin resistance particularly under menopause condition.

#### **CONCLUSIONS**

In summary, this study demonstrated that although metformin exerted similar effects to estrogen and vildagliptin on metabolic regulation, estrogen and vildagliptin offer greater advantage in terms of cardiac mitochondrial protection and LV performance, in obese insulin-resistant and estrogendeprived rats. This study is the first to report the comparative efficacy of estrogen, metformin, and vildagliptin on the cardiometabolic and cardiac mitochondrial function in obese insulin-resistant ovariectomized rats. Treatment with vildagliptin and estrogen therapy similarly provided the cardioprotective benefits in obese insulin-resistant ovariectomized rats. Because estrogen supplement was reported to associate with increased venous thromboembolism and cancer risks, vildagliptin could be considered as an alternative therapy for those who have contraindication for female sex hormone therapy. Vildagliptin was reported as the medication that did not affect the cardiac conduction system and repolarization, and also exerted beneficial effect on ischemic heart. 18,47 The cardioprotective effects under myocardial ischemia of vildagliptin treatment in estrogen-deprived and insulin-resistant conditions still need to be investigated.

#### REFERENCES

- Mendis S, Thygesen K, Kuulasmaa K, et al. World Health Organization definition of myocardial infarction: 2008-09 revision. *Int J Epidemiol* 2011;40:139-146.
- Mendis S. The contribution of the Framingham Heart Study to the prevention of cardiovascular disease: a global perspective. *Prog Cardiovasc Dis* 2010:53:10-14.
- Penno G, Solini A, Bonora E, et al. Gender differences in cardiovascular disease risk factors, treatments and complications in patients with type 2 diabetes: the RIACE Italian multicentre study. *J Intern Med* 2013;274: 176-191.
- Mendis S, Puska P, Norrving B. Global Atlas on Cardiovascular Disease Prevention and Control. Geneva, Switzerland: World Health Organization; 2011.
- Giardina EG. Heart disease in women. Int J Fertil Womens Med 2000;45: 350-357.

- Stampfer MJ, Colditz GA, Willett WC. Menopause and heart disease. A review. Ann N Y Acad Sci 1990;592:193-203.
- Rosano GM, Vitale C, Marazzi G, Volterrani M. Menopause and cardiovascular disease: the evidence. Climacteric 2007;10(suppl 1):19-24.
- Jelenik T, Roden M. How estrogens prevent from lipid-induced insulin resistance. *Endocrinology* 2013;154:989-992.
- Xu J, Xiang Q, Lin G, et al. Estrogen improved metabolic syndrome through down-regulation of VEGF and HIF-1alpha to inhibit hypoxia of periaortic and intra-abdominal fat in ovariectomized female rats. *Mol Biol Rep* 2012;39:8177-8185.
- Campos C, Casali KR, Baraldi D, et al. Efficacy of a low dose of estrogen on antioxidant defenses and heart rate variability. Oxid Med Cell Longev 2014;2014:218749; Available at: http://www.hindawi.com/journals/ omcl/2014/218749/. Accessed May 15, 2016.
- Hernandez I, Delgado JL, Diaz J, et al. 17beta-estradiol prevents oxidative stress and decreases blood pressure in ovariectomized rats. Am J Physiol Regul Integr Comp Physiol 2000;279:R1599-R1605.
- Brownlee M. Biochemistry and molecular cell biology of diabetic complications. *Nature* 2001;414:813-820.
- Dhalla NS, Temsah RM, Netticadan T. Role of oxidative stress in cardiovascular diseases. J Hypertens 2000;18:655-673.
- Rattanasopa C, Phungphong S, Wattanapermpool J, Bupha-Intr T. Significant role of estrogen in maintaining cardiac mitochondrial functions. *J Steroid Biochem Mol Biol* 2014;147C:1-9.
- 15. Bi Y, Tong GY, Yang HJ, et al. The beneficial effect of metformin on beta-cell function in non-obese Chinese subjects with newly diagnosed type 2 diabetes. *Diabetes Metab Res Rev* 2013;29:664-672.
- Banerjee M, Younis N, Soran H. Vildagliptin in clinical practice: a review of literature. Expert Opin Pharmacother 2009;10:2745-2757.
- Apaijai N, Pintana H, Chattipakorn SC, Chattipakorn N. Cardioprotective effects of metformin and vildagliptin in adult rats with insulin resistance induced by a high-fat diet. *Endocrinology* 2012;153:3878-3885.
- Chinda K, Sanit J, Chattipakorn S, Chattipakorn N. Dipeptidyl peptidase-4 inhibitor reduces infarct size and preserves cardiac function via mitochondrial protection in ischaemia-reperfusion rat heart. *Diab Vasc Dis Res* 2014;11:75-83.
- Pratchayasakul W, Chattipakorn N, Chattipakorn SC. Estrogen restores brain insulin sensitivity in ovariectomized non-obese rats, but not in ovariectomized obese rats. *Metabolism* 2014;63:851-859.
- Semaming Y, Kumfu S, Pannangpetch P, Chattipakorn SC, Chattipakorn N. Protocatechuic acid exerts a cardioprotective effect in type 1 diabetic rats. *J Endocrinol* 2014;223:13-23.
- Morgan EE, Faulx MD, McElfresh TA, et al. Validation of echocardiographic methods for assessing left ventricular dysfunction in rats with myocardial infarction. *Am J Physiol Heart Circ Physiol* 2004;287:H2049-H2053.
- Apaijai N, Pintana H, Chattipakorn SC, Chattipakorn N. Effects of vildagliptin versus sitagliptin, on cardiac function, heart rate variability and mitochondrial function in obese insulin-resistant rats. *Br J Pharmacol* 2013;169:1048-1057.
- Incharoen T, Thephinlap C, Srichairatanakool S, et al. Heart rate variability in beta-thalassemic mice. Int J Cardiol 2007;121:203-204.
- Thummasorn S, Kumfu S, Chattipakorn S, Chattipakorn N. Granulocytecolony stimulating factor attenuates mitochondrial dysfunction induced by oxidative stress in cardiac mitochondria. *Mitochondrion* 2011;11:457-466.
- Stubbins RE, Najjar K, Holcomb VB, Hong J, Nunez NP. Oestrogen alters adipocyte biology and protects female mice from adipocyte inflammation and insulin resistance. *Diabetes Obes Metab* 2012;14:58-66.
- Wang C, Liu F, Yuan Y, et al. Metformin suppresses lipid accumulation in skeletal muscle by promoting fatty acid oxidation. *Clin Lab* 2014;60: 887-896.
- Koren-Gluzer M, Aviram M, Hayek T. Metformin inhibits macrophage cholesterol biosynthesis rate: possible role for metformin-induced oxidative stress. *Biochem Biophys Res Commun* 2013;439:396-400.

- Esposito K, Nappo F, Marfella R, et al. Inflammatory cytokine concentrations are acutely increased by hyperglycemia in humans: role of oxidative stress. Circulation 2002;106:2067-2072.
- Cook SA, Sugden PH, Clerk A. Regulation of bcl-2 family proteins during development and in response to oxidative stress in cardiac myocytes: association with changes in mitochondrial membrane potential. *Circ Res* 1999;85:940-949.
- 30. Gill C, Mestril R, Samali A. Losing heart: the role of apoptosis in heart disease-a novel therapeutic target? *FASEB J* 2002;16:135-146.
- Takemura G, Kanoh M, Minatoguchi S, Fujiwara H. Cardiomyocyte apoptosis in the failing heart-a critical review from definition and classification of cell death. *Int J Cardiol* 2013;167:2373-2386.
- Annuk M, Zilmer M, Fellstrom B. Endothelium-dependent vasodilation and oxidative stress in chronic renal failure: impact on cardiovascular disease. Kidney Int Suppl 2003;84:S50-S53.
- Hamden K, Carreau S, Ellouz F, Masmoudi H, El FA. Protective effect of 17beta-estradiol on oxidative stress and liver dysfunction in aged male rats. J Physiol Biochem 2007;63:195-201.
- Richardson TE, Yu AE, Wen Y, Yang SH, Simpkins JW. Estrogen prevents oxidative damage to the mitochondria in Friedreich's ataxia skin fibroblasts. *PLoS One* 2012;7:e34600.
- Urata Y, Ihara Y, Murata H, et al. 17Beta-estradiol protects against oxidative stress-induced cell death through the glutathione/glutaredoxindependent redox regulation of Akt in myocardiac H9c2 cells. *J Biol Chem* 2006;281:13092-13102.
- Scheen AJ. Cardiovascular effects of gliptins. Nat Rev Cardiol 2013; 10:73-84.
- Lamas AZ, Caliman IF, Dalpiaz PL, et al. Comparative effects of estrogen, raloxifene and tamoxifen on endothelial dysfunction, inflammatory markers and oxidative stress in ovariectomized rats. *Life Sci* 2015;124:101-109.
- 38. Rizzo MR, Barbieri M, Marfella R, Paolisso G. Reduction of oxidative stress and inflammation by blunting daily acute glucose fluctuations in patients with type 2 diabetes: role of dipeptidyl peptidase-IV inhibition. *Diabetes Care* 2012;35:2076-2082.
- Ishii M, Shibata R, Kondo K, et al. Vildagliptin stimulates endothelial cell network formation and ischemia-induced revascularization via an endothelial nitric-oxide synthase-dependent mechanism. *J Biol Chem* 2014;289:27235-27245.
- 40. Kim KH, Bender JR. Membrane-initiated actions of estrogen on the endothelium. *Mol Cell Endocrinol* 2009;308:3-8.
- Murphy E, Steenbergen C. Cardioprotection in females: a role for nitric oxide and altered gene expression. Heart Fail Rev 2007;12:293-300.
- Gokce M, Karahan B, Yilmaz R, Orem C, Erdol C, Ozdemir S. Long term effects of hormone replacement therapy on heart rate variability, QT interval, QT dispersion and frequencies of arrhythmia. *Int J Cardiol* 2005;99:373-379.
- Perez MV, Wang PJ, Larson JC, et al. Effects of postmenopausal hormone therapy on incident atrial fibrillation: the Women's Health Initiative randomized controlled trials. Circ Arrhythm Electrophysiol 2012;5: 1108-1116.
- Tremollieres F, Brincat M, Erel CT, et al. EMAS position statement: managing menopausal women with a personal or family history of VTE. *Maturitas* 2011;69:195-198.
- 45. Vermeer LM, Gregory E, Winter MK, McCarson KE, Berman NE. Behavioral effects and mechanisms of migraine pathogenesis following estradiol exposure in a multibehavioral model of migraine in rat. *Exp Neurol* 2015;263:8-16.
- Benson VS, Kirichek O, Beral V, Green J. Menopausal hormone therapy and central nervous system tumor risk: large UK prospective study and meta-analysis. *Int J Cancer* 2015;136:2369-2377.
- 47. He YL, Zhang Y, Serra D, Wang Y, Ligueros-Saylan M, Dole WP. Thorough QT study of the effects of vildagliptin, a dipeptidyl peptidase IV inhibitor, on cardiac repolarization and conduction in healthy volunteers. *Curr Med Res Opin* 2011;27:1453-1463.

ELSEVIER

Contents lists available at ScienceDirect

#### **Neuroscience Letters**

journal homepage: www.elsevier.com/locate/neulet



#### Research article

### Hyperglycemia induced the Alzheimer's proteins and promoted loss of synaptic proteins in advanced-age female Goto-Kakizaki (GK) rats



Hiranya Pintana<sup>a,b,c,1</sup>, Nattayaporn Apaijai<sup>a,c,1</sup>, Sasiwan Kerdphoo<sup>a,c</sup>, Wasana Pratchayasakul<sup>a,b,c</sup>, Jirapas Sripetchwandee<sup>a,b,c</sup>, Panan Suntornsaratoon<sup>d,e</sup>, Narattaphol Charoenphandhu<sup>d,e,f</sup>, Nipon Chattipakorn<sup>a,b,c</sup>, Siriporn C. Chattipakorn<sup>a,c,g,\*</sup>

- a Neurophysiology Unit, Cardiac Electrophysiology Research and Training Center, Faculty of Medicine, Chiang Mai University, Chiang Mai, 50200, Thailand
- <sup>b</sup> Department of Physiology, Faculty of Medicine, Chiang Mai University, Chiang Mai, 50200, Thailand
- <sup>c</sup> Center of Excellence in Cardiac Electrophysiology Research, Chiang Mai University, Chiang Mai, 50200, Thailand
- d Center of Calcium and Bone Research (COCAB), Faculty of Science, Mahidol University, Bangkok, 10400, Thailand
- <sup>e</sup> Department of Physiology, Faculty of Science, Mahidol University, Bangkok, 10400, Thailand
- f Institute of Molecular Biosciences, Mahidol University, Nakhon Pathom, 73170, Thailand
- <sup>g</sup> Department of Oral Biology and Diagnostic Sciences, Faculty of Dentistry, Chiang Mai University, Chiang Mai, 50200, Thailand

#### HIGHLIGHTS

- Although advanced-age contributed to the pathogenesis of AD, only advanced-age with diabetes exhibited Aβ accumulation.
- Tau function was increased by age, independent of plasma glucose levels.
- Synaptic protein loss was observed only in advanced-age T2DM rats.

#### ARTICLE INFO

Article history:
Received 16 April 2017
Received in revised form 8 June 2017
Accepted 23 June 2017
Available online 24 June 2017

Keywords: Goto-Kakizaki (GK) rat Type 2 diabetes mellitus (T2DM) Advanced-age Alzheimer's protein Synaptic proteins

#### ABSTRACT

Although both type 2 diabetes mellitus (T2DM) and aging are related with Alzheimer's disease (AD), the effects of aging on the Alzheimer's proteins and the synaptic markers in T2DM have not been investigated. This study, we hypothesized that T2DM rats with advanced-age, aggravates the reduction of synaptic proteins and an increase in the Alzheimer's protein markers. Goto-Kakizaki rats (GK) were used as a T2DM group and wild-type rats (WT) were used as a control group. Rats in each group were categorized by age into young-adult (7 months) and advanced-age rats (12.5 months). Blood was collected in all rats to determine plasma glucose and insulin levels. The brains were used for determining the level of Alzheimer's and synaptic proteins. Our data demonstrated that GK rats had a decreased body weight and increased blood glucose levels, compared to their age-matched WT. p-Tau was increased in both advanced-age WT and GK, compared to their young-adult rats. Moreover, amyloid-beta (A $\beta$ ) level was higher in advanced-age GK than their age-matched WT. The synaptic proteins were decreased in advanced-age GK, compared to young-adult GK rats. However, no difference in the level of Alzheimer's proteins and synaptic proteins in the brains of young-adult GK compared to age-matched WT was found. Our data suggested that aging contributes to the pathogenesis of AD and the reduction of synaptic proteins to greater extent in a diabetic than in a healthy condition.

© 2017 Elsevier B.V. All rights reserved.

#### 1. Introduction

The number of type 2 diabetes mellitus (T2DM) patients has dramatically risen around the world [32]. T2DM itself causes damage in several vital organs, including the brain [11,27]. Previous studies reported that cognitive deficit and neurodegenerative changes were observed in T2DM patients and animal models [14,33]. Furthermore, previous clinical studies demonstrated that metabolic

<sup>\*</sup> Corresponding author at: Neurophysiology Unit, Cardiac Electrophysiology Research and Training Center, Faculty of Medicine, Chiang Mai University Department of Oral Biology and Diagnostic Sciences, Faculty of Dentistry Chiang Mai University, Chiang Mai, 50200, Thailand.

*E-mail addresses*: scchattipakorn@gmail.com, siriporn.c@cmu.ac.th (S.C. Chattipakorn).

<sup>&</sup>lt;sup>1</sup> Equally contributed to this manuscript.

disturbance decreased cognitive function in elderly [3,6], and also caused worsen cognitive performance in elderly with dementia and Alzheimer's disease (AD) [4,24]. Those findings suggested that T2DM could worsen the effects of aging in both normal brain and pathological brain. Moreover, aging is also considered as an important risk factor for neurodegeneration [13] and cognitive decline [7]. It has been shown previously that Tau and amyloid beta  $(A\beta)$ proteins expression could be detected in the normal brain, however both proteins expression are increased in the brains of AD patients [17,20,30]. These findings suggest that both Tau and AB could be classified as Alzheimer's protein biomarkers. The formation of Alzheimer's proteins, including phosphorylated Tau (p-Tau) and Aβ protein as well as the alteration of the synaptic site level, including synaptophysin (SYN) and postsynaptic density-95 (PSD-95), have been associated with the underlying mechanisms of cognitive decline [31].

Previous studies demonstrated that the increased level of these Alzheimer's proteins and the decrease of the synaptic site proteins were found in the brain of T2DM rodents [5,16,35]. It has been proposed that the increasing of AB level and hyperphosphorylated tau (p-tau), are key pathogenic determinants of AD [23]. Moreover, previous studies suggested that both SYN and PSD-95 could be used as the indication of activity at the presynaptic and postsynaptic sites in the brain [8,29], and the alteration of these proteins influence cognitive decline [10]. Although the influences of both T2DM and aging on neurodegeneration have been demonstrated, the effects of aging on the level of Alzheimer's proteins and the synaptic markers in T2DM are still unclear. In the present study, we aimed to investigate the level of Alzheimer's proteins and synaptic site proteins in T2DM at 2 different ages. Since the Goto-Kakizaki (GK) rat is a spontaneous T2DM animal model, and it is characterized by non-obesity with hyperglycemia [15], we used GK rats as a study model to demonstrate the pathophysiology of the brain in this T2DM model at 2 different age-periods, young-adult rats and advanced-age rats. We hypothesize that under T2DM condition, advanced-aging aggravates the reduction of synaptic proteins as well as increases the Alzheimer's protein markers in the brain of GK rats.

#### 2. Materials and methods

All experiments in this study were approved by the Laboratory Animal Ethics Committee of Faculty of Science, and the National Laboratory Animal Center, Mahidol University, Thailand, in compliance with NIH guidelines, and in accordance with ARRIVE guidelines for reporting experiments involving animals. Twelve female GK rats at the age of 4 weeks old were purchased from the Center for Laboratory Experimental Animals (CLEA), Japan. Twelve female Wistar rats (WT) were used as control. All rats were housed in a 12/12: dark/light cycle in a controlled temperature and humidity room with access to food and water ad libitum. Rats in each group were subdivided into a young-adult group (7 months) and an advanced-age group (12.5 months). The rat is considered an adolescent at 7 months old, whereas at 12.5 months old, it represents a middle-age of human life [28]. In addition, 12.5 month-old rats had decreased alveolar bone turnover [21], low endosteal layers in the tibia, and developed the reproductive senescence [28], when compared with 7 month-old rats [2]. Blood samples were collected from the tail vein at the age of 7 months, and 12.5 months. Rats were then sacrificed at the age of 7 and 12.5 months (n = 6/agegroup/strain) and the brains were removed and used to determine the Alzheimer's proteins and synaptic site proteins level.

An additional experiment has been performed in order to confirm whether p-Tau, A $\beta$ , synaptophysin, and PSD-95 changes are dependent upon DM. Streptotozotocin-induced DM rats were used

to confirm whether p-Tau, A $\beta$ , synaptophysin, and PSD-95 changes are dependent upon DM. Six week-old Wistar rats were injected with 50 mg/kg of streptozotocin for 1 week to induce T1DM. After animals developed diabetic condition, as indicated by hyperglycemia (>250 mg/dL), they were sacrificed at the age of 12 week old, and brains were removed for further analysis.

#### 2.1. Metabolic profiles

At the end of each time point, the body weight and fasting blood glucose were determined. Rats were fasted for 6 h after which the fasting blood glucose levels were determined using the Accu-Chek active blood glucose meter (Roche Diagnostics, Germany).

#### 2.2. Western blot analysis

A snap-frozen whole brain including the hippocampus, a specific area involved in cognition and subjected to plasticity changes, was homogenized in the extraction buffer containing 10 mM Tris, 25 mM EDTA, 100 mM NaCl, 1% (v/v) Trion X-100, 1% (v/v) NP-40, and a protease inhibitor (Calbiochem, Darmstadt, Germany). The brain was centrifuged at 10,000 rpm for 10 min, and the supernatant was kept. Then, the protein concentration assay was performed using Bradford technique (Bio-Rad Laboratories, CA, USA). Forty µg of total protein was loaded onto 10% SDS-Acrylamide gels and transferred to a 0.45 µm pore size nitrocellulose membrane (GE Healthcare, MA, USA) in a glycine/methanol-transfer buffer using a Wet/Tank blotting system (Bio-Rad Laboratories, CA, USA). Membranes were blocked in 5% skim milk in a TBS-tween (TBST) buffer. After that, membranes were incubated with rabbit polyclonal p-Tau (1:1000 dilution in 5% BSA in TBST, Cell signaling Technology, MA, USA), total Tau (1:1000 dilution in 5% BSA in TBST, Cell signaling Technology, MA, USA), Aβ (1:1000 dilution in 5% skim milk in TBST, Santa Cruz technology, MA, USA), SYN (1:1000 dilution in 5% BSA in TBST, Cell signaling Technology, MA, USA) and PSD-95 (1:1000 dilution in 5% BSA in TBST, Cell signaling Technology, MA, USA). SYN:PSD-95 represented pre-: post-synaptic marker in the brain. The reduction of SYN/PSD-95 ratio demonstrated the reduction of the brain synaptic protein between pre- and post-synaptic sites [29]. Beta actin was used as a reference protein (1:2000 dilution in 5% skim milk in TBST, Santa Cruz technology, MA, USA). Bound antibodies were detected using HRP-conjugated with either anti-rabbit or anti-mouse IgG (1:2000 dilution in 5% skim milk in TBST, Cell signaling technology, CA, USA). The membranes were exposed to ECL Western blotting substrate, and densitometric analysis was carried out using ChemiDoc Touch Imaging system (Bio-Rad Laboratories, CA, USA).

#### 2.3. Statistical analysis

Data were presented as mean  $\pm$  SE. Two-way ANOVA followed by Tukey's post-hoc test was performed to determine the difference among groups. p-value < 0.05 was considered as statistically significant.

#### 3. Results

Both the body weight and the fasting blood glucose levels were not significantly altered with age in both WT and GK rats (Fig. 1A and B). However, GK rats at both age groups had significantly lower body weight, when compared to age-matched WT rats (Fig. 1A), whereas fasting blood glucose levels of GK rats at both age groups were significantly higher, when compared to that of age-matched WT rats (Fig. 1B). These findings indicated that it was the diabetic condition, but not aging, that caused weight loss with hyperglycemia. In addition, estradiol levels were ranging between 5 and

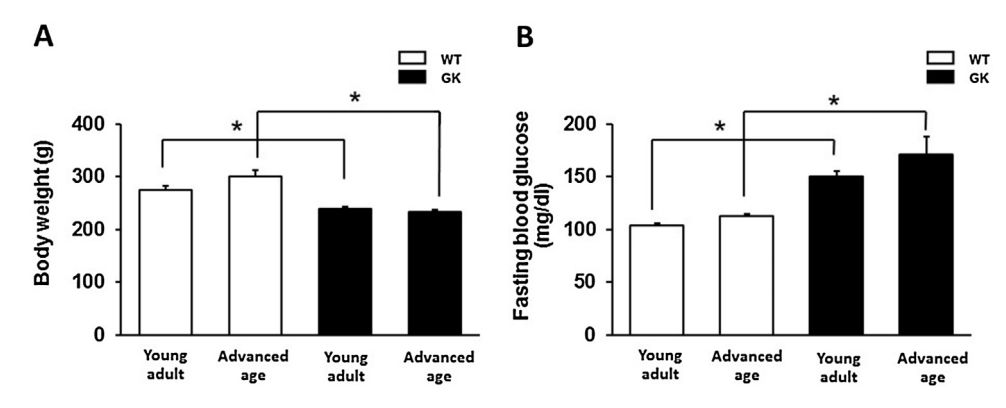


Fig. 1. The effect of T2DM on body weight (A) and fasting plasma blood glucose (B) in young-adult or advanced-age rats. WT, wild-type rats; GK, Goto-Kakizaki rats; T2DM, type 2 diabetes mellitus. p < 0.05 compared between groups.

24 pg/ml in WT rats, and 9–49.3 pg/ml in GK rats. There were no differences for the estradiol levels between WT and GK rats, suggesting that T2DM did not affect sexual cycle in advanced-age GK rats.

Regarding the Alzheimer's protein, p-Tau: total Tau ratio was not significantly different between WT rats and GK rats in aged-match groups (Fig. 2A). Both WT rats and GK rats with advanced-age had a significant increase in p-Tau: total Tau ratio, when compared to their young-adult of same-strained group (Fig. 2A). These findings suggested that aging plays an important role in the Alzheimer's protein level, p-Tau: total Tau ratio. For another Alzheimer's protein, AB level, our results showed that there was no difference in its level in the brain between young-adult and advanced-age rats in both strains. However, at advanced age our results demonstrated that GK rats had higher Aβ level than the WT rats (Fig. 2B). These findings suggest that although aging increased p-Tau level in both WT and GK rats, AB level was increased only in the T2DM with aging group. Furthermore, we found that the ratio of SYN:PSD-95 was not significantly different between young-adult and advanced-age WT rats (Fig. 3A and B). However, the ratio of SYN:PSD-95 was significantly decreased in advanced-age GK rats, when compared to that of young-adult GK rats (Fig. 3A and B). These findings suggest that aging decreased SYN:PSD-95 ratio, suggesting decreased brain synaptic proteins in T2DM rats. Furthermore, there was no correlation between plasma glucose levels and AB levels ( $r^2 = 0.049$ , p = 0.35), or plasma glucose levels and ratio of SYN/PSD-95 ( $r^2 = 0.1353$ , p = 0.11). These findings suggested that hyperglycemia alone did not play a significant role in the reduction of synaptic protein levels nor the increased AB levels.

For STZ-induced T1DM model, our results showed that STZinduced DM young rats developed diabetes as indicated by weight loss and hyperglycemia. However, p-Tau/Tau level was not different between STZ-induced DM young rats and control young rats. This is consistent with the finding in the GK rats. Therefore, our findings suggested that T1DM in young-aged rats was not correlated with increased tau phosphorylation. For AB, AB level was increased in STZ-induced DM young rats, compared to control rats. Although  $A\beta$  level was not different in young GK rats,  $A\beta$  level was increased in advance-aged GK rats, compared to WT rats. These data indicated that AB level is dependent upon hyperglycemia in T1DM, whereas Aβ level in T2DM is dependent upon hyperglycemia and advanced aging. For SYN/PSD-95 in T1DM, we found that SYN/PSD-95 ratio was not different between STZ-induced DM young rats and control young rats. On the other hand, SYN/PSD-95 ratio was reduced in advance-aged GK rats. Therefore, these data indicated that although synaptic proteins are not associated individually with either hyperglycemia or advanced aging, the combination of both

**Table 1**The metabolic parameters, Alzheimer's proteins, and Synaptic proteins in STZ-induced T1DM rats.

| Parameter                         | Control rats                 | STZ rats                  |
|-----------------------------------|------------------------------|---------------------------|
| Body weight (g)                   | $436.00\pm6.00$              | $229.00 \pm 16.38^*$      |
| Glucose (mg%)                     | $147.10 \pm 14.18$           | $459.33 \pm 20.63^{\ast}$ |
| pTau/Tau (a.u.)                   | $0.95 \pm 0.04$              | $0.90\pm0.09$             |
| Amyloid beta level(pg/mg protein) | $\boldsymbol{0.65 \pm 0.07}$ | $1.38 \pm 0.17^*$         |
| SYN:PSD-95 (a.u.)                 | $0.11 \pm 0.06$              | $0.10\pm0.04$             |

\*p < 0.05 compared with control rats, STZ rats: streptozotocin induced-Type 1 Diabetic rats.

hyperglycemia and advanced aging reduced synaptic protein levels (Table 1).

#### 4. Discussion

Major findings of the present study are as follows: 1) T2DM but not aging, caused weight loss with hyperglycemia, 2) aging promoted increased Alzheimer's protein level, p-Tau: total Tau ratio, 3) aging promoted increased Alzheimer's protein level, A $\beta$  level in T2DM, and 4) aging accelerated the decrease in synaptic proteins in the T2DM.

GK rat is widely known as a non-obese T2DM rat model, which is characterized by non-obesity with hyperglycemia [1,15]. This present study demonstrated that GK rats at the age of 7 months developed diabetes, characterized by weight loss with hyperglycemia. In contrast to the previous study [34], our findings demonstrated that the severity of hyperglycemia in GK rats did not increase in proportion to aging. This difference could be due to the insufficient advanced aging (i.e. at 12.5 months) of the GK rats used in the present study to show the aggressiveness of the diabetic condition. Despite the severity of T2DM was not aggravated by advanced-aging in this study, the level of Alzheimer's proteins such as p-Tau in the advanced-age group of both WT and T2DM rats significantly increased, when compared to the youngadult group of same strain (Fig. 2). These findings indicate that aging dominates the increased level of p-Tau proteins in the brain rather than the diabetic condition. Moreover, although the diabetic condition did not affect the level of p-Tau, it is interesting that AB level was markedly increased only in the non-obese T2DM with advanced-age group. All of these findings suggested that aging directly contributed to the level of p-Tau proteins, whilst hyperglycemia influenced the regulation of the level of  $A\beta$  protein only in during advanced-aging. Moreover, our results are inconsistent with previous studies, in which noticed that T2DM do not associated with neither increase cerebrospinal fluid A $\beta$  [22] nor increase brain Aβ accumulation [26] in elderly human. Since our study using 12.5 months old rats, it represents a middle-age of human life [28]. This

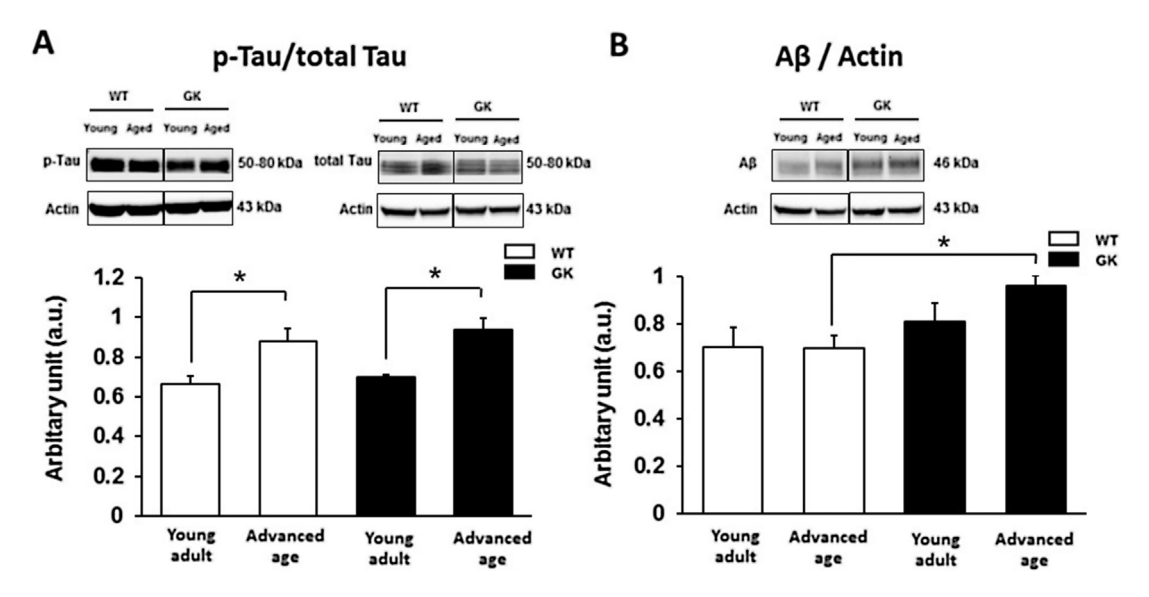


**Fig. 2.** The effect of T2DM on Alzheimers-like proteins, *p*-Tau:total Tau (A) and Aβ, in young-adult or advanced-age rats. WT, wild-type rats; GK, Goto-Kakizaki rats; T2DM, type 2 diabetes mellitus; *p*-Tau, phosphorylation of Tau; Aβ, amyloid beta. p < 0.05 compared between groups.

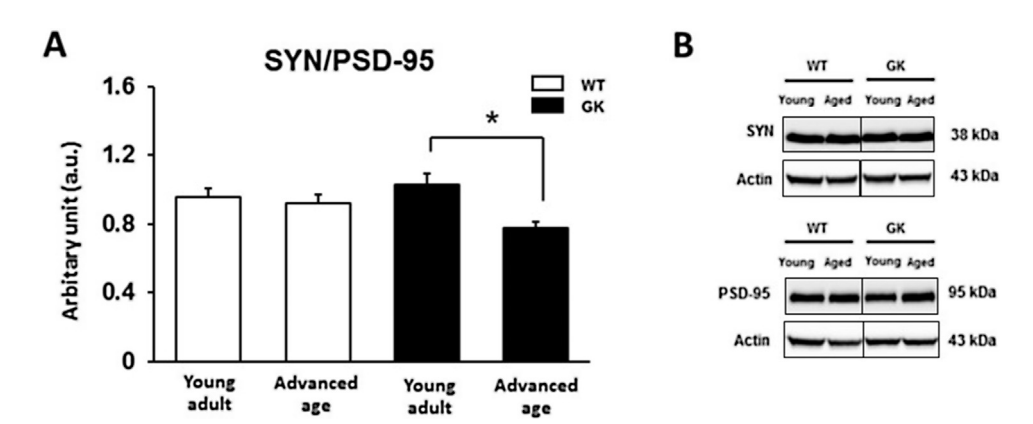


Fig. 3. The effect of T2DM on brain synaptic protein in young-adult or advanced-age rats. WT, wild-type rats; GK, Goto-Kakizaki rats; T2DM, type 2 diabetes mellitus. p < 0.05 compared between groups.

indicated that Aβ accumulation might be depending on longevity. Previous studies reported that not only an increase in Alzheimer's proteins was found in T2DM rodent, but also alterations in the synaptic site protein in the brain was discovered [5,16,35]. We therefore further investigated the synaptic site protein markers (Fig. 3), which are the underlying mechanisms of cognitive processes. The results show that aging accelerated the decreasing of synaptic proteins in T2DM rats. Inconsistent with previous studies [12,19], our findings demonstrated that aging alone does not increase AB protein level or alter synaptic site protein markers. These findings indicated that it was hyperglycemia with aging that significantly decreased the synaptic proteins. Although the effect of T2DM influenced the reduction of brain synaptic plasticity and increased the risk of dementia in elderly with or without AD condition have been reported, several studies demonstrated that the impairment of neurogenesis [9], spinogenesis and dendritogenesis [18], as well as neuronal transmission [25,36] got worse under the T2DM condition. These could be the mechanisms responsible for the effect of T2DM on the alteration of Alzheimer's protein level and brain synaptic proteins in the young-adults and advanced-age rats in the present study.

The present study demonstrated that aging contributes to the pathogenesis of AD and the reduction of synaptic level to greater extent in a diabetic than in a healthy condition, however the limitation of the present study is that the whole brain was used. Future study is needed to determine the effects of T2DM on the pathogenesis of AD and synaptic level in the specific brain areas. Moreover, it has been proposed that the increasing of A $\beta$  level as well as the alteration of SYN and PSD-95 proteins influence cognitive decline [10]. Future studies are needed to perform the behavioral tests of cognitive function and to further investigate the correlation of A $\beta$  level ratio SYN: PSD-95 proteins and cognitive behaviors in advanced-age T2DM model.

In conclusion, our findings report that the level of phosphorylation of Tau is associated with advanced-aging, whereas hyperglycemia accelerates both the increase in A $\beta$  level and decrease in synaptic proteins in advanced-age rats.

#### **Declaration of interest**

The authors declare that they have no conflict of interest.

#### Acknowledgement

This work was supported by grants from the Thailand Research Fund TRF Senior Research Scholar Grant (RTA 60 to SCC and RTA5780001 to N. Charoenphandhu), TRF-TRG 6080005 (NA), TRF-MRG5980198 (WP), TRF-MRG6080226 (JS), a NSTDA Research

Chair Grant from the National Science and Technology Development Agency (N Chattipakorn), and Chiang Mai University Excellent Center Award (N Chattipakorn).

#### References

- M.S. Akash, K. Rehman, S. Chen, Goto-Kakizaki rats: its suitability as non-obese diabetic animal model for spontaneous type 2 diabetes mellitus, Curr. Diabetes Rev. 9 (2013) 387–396.
- [2] J. Aronson, G.G. Gao, X.C. Shen, S.G. McLaren, R.A. Skinner, T.M. Badger, C.K. Lumpkin Jr., The effect of aging on distraction osteogenesis in the rat, J. Orthop. Res. 19 (2001) 421–427.
- [3] Z. Arvanitakis, D.A. Bennett, R.S. Wilson, L.L. Barnes, Diabetes and cognitive systems in older black and white persons, Alzheimer Dis. Assoc. Disord. 24 (2010) 37–42.
- [4] M. Barbagallo, L.J. Dominguez, Type 2 diabetes mellitus and Alzheimer's disease, World J. Diabetes 5 (2014) 889–893.
- [5] C. Carvalho, M.S. Santos, C.R. Oliveira, P.I. Moreira, Alzheimer's disease and type 2 diabetes-related alterations in brain mitochondria, autophagy and synaptic markers, Biochim. Biophys. Acta 1852 (2015) 1665–1675.
- [6] A. Convit, O.T. Wolf, C. Tarshish, M.J. de Leon, Reduced glucose tolerance is associated with poor memory performance and hippocampal atrophy among normal elderly, Proc. Natl. Acad. Sci. U. S. A. 100 (2003) 2019–2022.
- [7] M.M. Corrada, R. Brookmeyer, A. Paganini-Hill, D. Berlau, C.H. Kawas, Dementia incidence continues to increase with age in the oldest old: the 90+ study, Ann. Neurol. 67 (2010) 114–121.
- [8] S.E. Craven, A.E. El-Husseini, D.S. Bredt, Synaptic targeting of the postsynaptic density protein PSD-95 mediated by lipid and protein motifs, Neuron 22 (1999) 497–509.
- [9] A.C. Dorsemans, D. Couret, A. Hoarau, O. Meilhac, C. Lefebvre d'Hellencourt, N. Diotel, Diabetes, adult neurogenesis and brain remodeling: new insights from rodent and zebrafish models, Neurogenesis (Austin) 4 (2017) e1281862.
- [10] D.A. Gimbel, H.B. Nygaard, E.E. Coffey, E.C. Gunther, J. Laurén, Z.A. Gimbel, S.M. Strittmatter, Memory impairment in transgenic alzheimer mice requires cellular prion protein, J. Neurosci. 30 (2010) 6367–6374.
- [11] R. Hempel, R. Onopa, A. Convit, Type 2 diabetes affects hippocampus volume differentially in men and women, Diabetes Metab. Res. Rev. 28 (2012) 76–83.
- [12] H. Huang, S. Nie, M. Cao, C. Marshall, J. Gao, N. Xiao, G. Hu, M. Xiao, Characterization of AD-like phenotype in aged APPSwe/PS1dE9 mice, Age (Dordr) 38 (2016) 303–322.
- [13] C.W. Hung, Y.C. Chen, W.L. Hsieh, S.H. Chiou, C.L. Kao, Ageing and neurodegenerative diseases, Ageing Res. Rev. 9 (2010) S36–46.
- [14] I.K. Hwang, S.S. Yi, Y.N. Kim, I.Y. Kim, I.S. Lee, Y.S. Yoon, J.K. Seong, Reduced hippocampal cell differentiation in the subgranular zone of the dentate gyrus in a rat model of type II diabetes, Neurochem. Res. 33 (2008) 394–400.
- [15] U. Janssen, A. Vassiliadou, S.G. Riley, A.O. Phillips, J. Floege, The quest for a model of type II diabetes with nephropathy: the Goto Kakizaki rat, J. Nephrol. 17 (2004) 769–773.
- [16] B. Kim, C. Backus, S. Oh, J.M. Hayes, E.L. Feldman, Increased tau phosphorylation and cleavage in mouse models of type 1 and type 2 diabetes, Endocrinology 150 (2009) 5294–5301.
- [17] D.H. Lau, M. Hogseth, E.C. Phillips, M.J. O'Neill, A.M. Pooler, W. Noble, D.P. Hanger, Critical residues involved in tau binding to fyn: implications for tau phosphorylation in Alzheimer's disease, Acta Neuropathol. Commun. 4 (2016) 49
- [18] Z. Lazcano, O. Solis, M.E. Bringas, D. Limon, A. Diaz, B. Espinosa, I. Garcia-Pelaez, G. Flores, J. Guevara, Unilateral injection of Abeta 25-35 in the hippocampus reduces the number of dendritic spines in hyperglycemic rats, Synapse (July 22) (2014), http://dx.doi.org/10.1002/syn.21770 (Epub ahead of print).
- [19] L.N. Lu, Z.M. Qian, K.C. Wu, W.H. Yung, Y. Ke, Expression of iron transporters and pathological hallmarks of parkinson's and alzheimer's diseases in the brain of young, adult, and aged rats, Mol. Neurobiol. (August 30) (2016) (Epub ahead of print).

- [20] M. Maftei, F. Thurm, C. Schnack, H. Tumani, M. Otto, T. Elbert, I.T. Kolassa, M. Przybylski, M. Manea, C.A. von Arnim, Increased levels of antigen-bound beta-amyloid autoantibodies in serum and cerebrospinal fluid of Alzheimer's disease patients, PLoS One 8 (2013) e68996.
- [21] Y. Misawa, T. Kageyama, K. Moriyama, S. Kurihara, H. Yagasaki, T. Deguchi, H. Ozawa, N. Sahara, Effect of age on alveolar bone turnover adjacent to maxillary molar roots in male rats: a histomorphometric study, Arch. Oral Biol. 52 (2007) 44–50.
- [22] C. Moran, R. Beare, T.G. Phan, D.G. Bruce, M.L. Callisaya, V. Srikanth, I. Alzheimer's Disease Neuroimaging, Type 2 diabetes mellitus and biomarkers of neurodegeneration, Neurology 85 (2015) 1123–1130.
- [23] R.M. Nisbet, J.C. Polanco, L.M. Ittner, J. Gotz, Tau aggregation and its interplay with amyloid-beta, Acta Neuropathol. 129 (2015) 207–220.
- [24] A. Ott, R.P. Stolk, F. van Harskamp, H.A. Pols, A. Hofman, M.M. Breteler, Diabetes mellitus and the risk of dementia: the Rotterdam Study, Neurology 53 (1999) 1937–1942.
- [25] J.J. Ramos-Rodriguez, T. Spires-Jones, A.M. Pooler, A.M. Lechuga-Sancho, B.J. Bacskai, M. Garcia-Alloza, Progressive neuronal pathology and synaptic loss induced by prediabetes and type 2 diabetes in a mouse model of alzheimer's disease, Mol. Neurobiol. 54 (2017) 3428–3438.
- [26] R.O. Roberts, D.S. Knopman, R.H. Cha, M.M. Mielke, V.S. Pankratz, B.F. Boeve, K. Kantarci, Y.E. Geda, C.R. Jack Jr., R.C. Petersen, V.J. Lowe, Diabetes and elevated hemoglobin A1c levels are associated with brain hypometabolism but not amyloid accumulation, J. Nucl. Med. 55 (2014) 759–764.
- [27] R.O. Roberts, D.S. Knopman, S.A. Przybelski, M.M. Mielke, K. Kantarci, G.M. Preboske, M.L. Senjem, V.S. Pankratz, Y.E. Geda, B.F. Boeve, R.J. Ivnik, W.A. Rocca, R.C. Petersen, C.R. Jack Jr., Association of type 2 diabetes with brain atrophy and cognitive impairment, Neurology 82 (2014) 1132–1141.
- [28] P. Sengupta, The laboratory rat: relating its age with human's, Int. J. Prev. Med. 4 (2013) 624–630.
- [29] L.K. Siew, S. Love, D. Dawbarn, G.K. Wilcock, S.J. Allen, Measurement of preand post-synaptic proteins in cerebral cortex: effects of post-mortem delay, J. Neurosci. Methods 139 (2004) 153–159.
- [30] R.A. Sperling, P.S. Aisen, L.A. Beckett, D.A. Bennett, S. Craft, A.M. Fagan, T. Iwatsubo, C.R. Jack Jr., J. Kaye, T.J. Montine, D.C. Park, E.M. Reiman, C.C. Rowe, E. Siemers, Y. Stern, K. Yaffe, M.C. Carrillo, B. Thies, M. Morrison-Bogorad, M.V. Wagster, C.H. Phelps, Toward defining the preclinical stages of Alzheimer's disease: recommendations from the National Institute on Aging-Alzheimer's Association workgroups on diagnostic guidelines for Alzheimer's disease, Alzheimers Dement 7 (2011) 280–292.
- [31] C. Tapia-Rojas, C.B. Lindsay, C. Montecinos-Oliva, M.S. Arrazola, R.M. Retamales, D. Bunout, S. Hirsch, N.C. Inestrosa, Is L-methionine a trigger factor for Alzheimer's-like neurodegeneration?: Changes in Abeta oligomers, tau phosphorylation, synaptic proteins, Wnt signaling and behavioral impairment in wild-type mice, Mol. Neurodegener. 10 (2015) 62.
- [32] S. Wild, G. Roglic, A. Green, R. Sicree, H. King, Global prevalence of diabetes: estimates for the year 2000 and projections for 2030, Diabetes Care 27 (2004) 1047–1053.
- [33] G. Winocur, C.E. Greenwood, G.G. Piroli, C.A. Grillo, L.R. Reznikov, L.P. Reagan, B.S. McEwen, Memory impairment in obese Zucker rats: an investigation of cognitive function in an animal model of insulin resistance and obesity, Behav. Neurosci. 119 (2005) 1389–1395.
- [34] M. Wu, D.H. Desai, S.K. Kakarla, A. Katta, S. Paturi, A.K. Gutta, K.M. Rice, E.M. Walker Jr., E.R. Blough, Acetaminophen prevents aging-associated hyperglycemia in aged rats: effect of aging-associated hyperactivation of p38-MAPK and ERK1/2, Diabetes Metab. Res. Rev. 25 (2009) 279–286.
- [35] Y. Yang, J. Zhang, D. Ma, M. Zhang, S. Hu, S. Shao, C.X. Gong, Subcutaneous administration of liraglutide ameliorates Alzheimer-associated tau hyperphosphorylation in rats with type 2 diabetes, J. Alzheimers Dis. 37 (2013) 637–648.
- [36] H. Yin, W. Wang, W. Yu, J. Li, N. Feng, L. Wang, X. Wang, Changes in synaptic plasticity and glutamate receptors in type 2 diabetic KK-Ay mice, J. Alzheimers Dis. 57 (2017) 1207–1220.

FISEVIER

Contents lists available at ScienceDirect

#### Toxicology and Applied Pharmacology

journal homepage: www.elsevier.com/locate/taap



## SGLT2-inhibitor and DPP-4 inhibitor improve brain function via attenuating mitochondrial dysfunction, insulin resistance, inflammation, and apoptosis in HFD-induced obese rats



Piangkwan Sa-nguanmoo<sup>a,b</sup>, Pongpan Tanajak<sup>a,b</sup>, Sasiwan Kerdphoo<sup>a,b</sup>, Thidarat Jaiwongkam<sup>a,b</sup>, Wasana Pratchayasakul<sup>a,b</sup>, Nipon Chattipakorn<sup>a,b,c</sup>, Siriporn C. Chattipakorn<sup>a,c,d,\*</sup>

- a Neurophysiology Unit, Cardiac Electrophysiology Research and Training Center, Faculty of Medicine, Chiang Mai University, Chiang Mai, Thailand
- <sup>b</sup> Department of Physiology, Faculty of Medicine, Chiang Mai University, Chiang Mai, Thailand
- Center of Excellence in Cardiac Electrophysiology Research, Chiang Mai University, Chiang Mai, Thailand
- <sup>d</sup> Department of Oral Biology and Diagnostic Sciences, Faculty of Dentistry, Chiang Mai University, Chiang Mai, Thailand

#### ARTICLE INFO

# Keywords: Obese-insulin resistance Cognitive function Mitochondrial function Synaptic plasticity Dapagliflozin Vildagliptin

#### ABSTRACT

Dipeptidyl peptidase-4 inhibitor (vildagliptin) has been shown to exert beneficial effects on insulin sensitivity and neuroprotection in obese-insulin resistance. Recent studies demonstrated the neuroprotection of the sodiumglucose co-transporter 2 inhibitor (dapagliflozin) in diabetes. However, the comparative effects of both drugs and a combination of two drugs on metabolic dysfunction and brain dysfunction impaired by the obese-insulin resistance have never been investigated. Forty male Wistar rats were divided into two groups, and received either a normal-diet (ND, n = 8) or a high-fat diet (HFD, n = 32) for 16 weeks. At week 13, the HFD-fed rats were divided into four subgroups (n = 8/subgroup) to receive either a vehicle, vildagliptin (3 mg/kg/day) dapagliflozin (1 mg/kg/day) or combined drugs for four weeks. ND rats were given a vehicle for four weeks. Metabolic parameters and brain function were investigated. The results demonstrated that HFD rats developed obese-insulin resistance and cognitive decline. Dapagliflozin had greater efficacy on improved peripheral insulin sensitivity and reduced weight gain than vildagliptin. Single therapy resulted in equally improved brain mitochondrial function, insulin signaling, apoptosis and prevented cognitive decline. However, only dapagliflozin improved hippocampal synaptic plasticity. A combination of the drugs had greater efficacy in improving brain insulin sensitivity and reducing brain oxidative stress than the single drug therapy. These findings suggested that dapagliflozin and vildagliptin equally prevented cognitive decline in the obese-insulin resistance, possibly through some similar mechanisms. Dapagliflozin had greater efficacy than vildagliptin for preserving synaptic plasticity, thus combined drugs could be the best therapeutic approach for neuroprotection in the obese-insulin resistance.

#### 1. Introduction

Obesity induced by long-term high fat diet consumption caused not only impaired peripheral insulin sensitivity (Pratchayasakul et al., 2011; Pipatpiboon et al., 2012), but also led to brain dysfunction, as indicated by brain mitochondrial dysfunction, increased brain oxidative stress, impaired brain insulin receptor function, impaired synaptic plasticity, and cognitive decline (Pintana et al., 2012; Sripetchwandee et al., 2014b; Pratchayasakul et al., 2015).

Vildagliptin is one of the group of incretin-based drugs, using for treating type 2 diabetes (T2DM). It inhibits dipeptidyl peptidase-4 (DPP-4), which is an enzyme that catalyses the rapidly degradation of the hormone glucagon-like-peptide-1(GLP-1). It has been shown that on treatment of vildagliptin in rats active GLP-1 levels increased, which led to increased glucose stimulating insulin secretion by enhancing  $\beta$ -cell function, improving insulin sensitivity, and reducing fasting and prandial glucose levels (MacDonald et al., 2002). In addition, our previous studies have shown that vildagliptin ameliorated peripheral insulin

E-mail addresses: scchattipakorn@gmail.com, siriporn.c@cmu.ac.th (S.C. Chattipakorn).

Abbreviation: HFD, high fat diet; GLP1, glucagon-like peptide 1; OFT, open field test; OGTT, oral glucose tolerance test; MWM, Morris water maze; HDL-C, fasting plasma high-density lipoprotein; LDL-C, low-density lipoprotein; HOMA, homeostasis model assessment; AUCs, area under the curves; TNF-α, tumor necrosis factor alpha; MDA, malondialdehyde; HPLC, high-performance liquid chromatography; LTP, long-term potentialion; LTD, long-term depression; ROS, reactive oxygen species; ΔΨm, mitochondrial membrane potential

<sup>\*</sup> Corresponding author at: Neurophysiology Unit, Cardiac Electrophysiology Research and Training Center, Faculty of Medicine, Chiang Mai University, Department of Oral Biology and Diagnostic Sciences, Faculty of Dentistry, Chiang Mai University, Chiang

resistance and prevented cognitive decline by reducing brain oxidative stress, improving brain insulin sensitivity and also improving brain mitochondrial function in obese-insulin resistant rats (Pintana et al., 2013; Pipatpiboon et al., 2013). Although vildagliptin has beneficial effects on the improvement of peripheral and brain insulin sensitivity, it cannot reduce the propensity to weight gain and brain synaptic dysfunction (Pipatpiboon et al., 2013; Pintana et al., 2015).

To date, a new class of anti-diabetic drug: sodium glucose cotransporter 2 (SGLT2) inhibitor, has been approved for the treatment of T2DM. SGLT2 is a glucose transporter and is expressed profusely in segments 1 and 2 of the proximal convoluted tubule (PCT) in the kidney (Jabbour and Goldstein, 2008; Mather and Pollock, 2011). It plays an important role in the reabsorption of urinary glucose, which is dependent on a sodium concentration gradient. Dapagliflozin, a selective and potent SGLT2 inhibitor, has been shown to provide an insulin-independent glucose lowering effect with a low risk of hypoglycemia, by blocking renal glucose reabsorption through SGLT2, leading to enhanced urinary glucose excretion (UGE) (Jabbour and Goldstein, 2008). A previous study demonstrated that dapagliflozin could lead to a decrease in body weight and improve glycemic control in Zucker fatty diabetic (ZDF) rats (Han et al., 2008) and in patients with T2DM (Wilding et al., 2012; Bailey et al., 2013). Moreover, previous study have been shown that SGLT2 inhibitor had better glycemic control and reduction of weight gain than DPP-4 inhibitors in patients with T2DM (Min et al., 2017). This finding suggests that SGLT2 inhibitor may exert better benefit than DPP-4 inhibitor on improving hyperglycemia under diabetic condition. Moreover, a recent study demonstrated that combined SGLT2 inhibitor and DPP-4 inhibitors treatment in diabetic rats could improve glucose tolerance than single therapy (Oguma et al., 2015), suggesting that the combination of these 2 drugs might exert better glycemic control than single regimen in T2DM. Interestingly, recent studies demonstrated that SGLT2 inhibitor exerted not only glycemic control effects, but also led to improve cognitive function in db/db mice (Lin et al., 2014) and high fat diet (HFD)-fed mice (Naznin et al., 2017). The underlying mechanisms of the beneficial effect of the SGLT2 inhibitor on cognition in those models were associated with the reduction in cerebral oxidative stress (Lin et al., 2014) and the suppression of obesity-related inflammation in the nervous system (Naznin et al., 2017). However, the effects of dapagliflozin on brain function, in particular brain insulin sensitivity, synaptic plasticity, brain mitochondrial function, brain inflammation, brain apoptosis and cognitive function in HFD-induced obese rats have not been investigated. Furthermore, the comparative effects of dapagliflozin, vildagliptin and their combined therapeutic use on peripheral insulin sensitivity, brain insulin sensitivity, hippocampal synaptic plasticity, brain mitochondrial function, brain inflammation, brain apoptosis and cognitive function in the obese-insulin resistant condition have never been investigated. Therefore, the present study tested the following hypotheses: 1) Dapaglifozin exerts a better efficacy than vildagliptin on improving peripheral insulin sensitivity and neuroprotective effects in HFD-induced obese rats, and 2) the combination of both drugs provides the greatest efficacy in this model.

#### 2. Material and methods

#### 2.1. Animal models and experimental protocols

Forty male Wistar rats weighing 200–220 g were used in this study and purchased from the National Animal Center, Salaya Campus, Mahidol University, Thailand. All rats were housed in environment-controlled condition in a light-dark cycle of 12:12 h. All rats were acclimatized for a week, then the rats were randomized into two groups to be fed with either a normal diet (ND; 19.77% E fat) (n=8) or a high-fat diet (HFD; 59.28% E fat) (n=32) for 16 weeks. At the beginning of week 13, the HFD-fed rats were further subdivided into four subgroups and were given either a vehicle (0.9%NSS, 0.1 mg/kg/day; intragastric

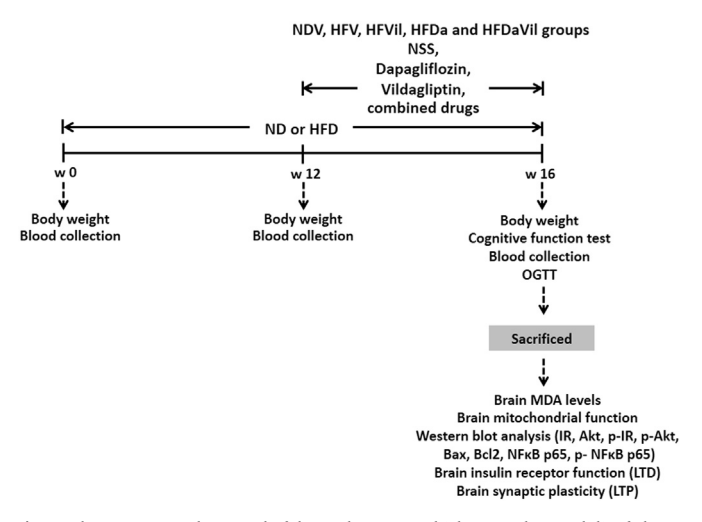


Fig. 1. The experimental protocol of the study. NDV: Vehicle-treated normal diet fed rats; HFV: Vehicle-treated high fat diet fed rats; HFVil: Vildagliptin-treated high fat diet fed rats; HFDa: Dapagliflozin-treated high fat diet fed rats; HFDaVil: Combined dapagliflozin and vildagliptin-treated high fat diet fed rats; w: Week; OGTT: Oral glucose tolerance test; MDA: malondialdehyde; LTP: Long-term potentiation.

gavage) (HFV, n=8); vildagliptin (3 mg/kg/day; intragastric gavage) (HFVil, n=8), dapagliflozin (1 mg/kg/day; intragastric gavage) (HFDa, n=8) or a combination of the two drugs (HFDaVil, n=8) for another four weeks. At the end of 4-week treatment, blood samples were collected to determine metabolic parameters. An oral glucose tolerance test (OGTT), open field test (OFT), Morris water maze test was performed. Then, animals were decapitated, brain was removed rapidly for electrophysiological studies and biochemical analysis. The experimental protocol is shown in Fig. 1.

## 2.2. Chemical analysis for metabolic parameters, serum and brain MDA levels

Fasting plasma glucose, cholesterol and triglyceride levels determine using a colorimetric assay kit (ERBA diagnostic, Mannheim, Germany). A colorimetric assay kit (Biovision, CA, USA) was used to determine fasting plasma high-density lipoprotein levels (HDL-C). The plasma low-density lipoprotein (LDL-C) levels were estimated from Friedewald's equation (Friedewald et al., 1972). Fasting plasma insulin levels were determined by a sandwich enzyme-linked immunosorbent assay (ELISA) kit (Millipore, MI, USA). The severity of peripheral insulin resistance was assessed by the homeostasis model assessment (HOMA) index as described previously (Matthews et al., 1985). Area under the curves (AUCs) were calculated from an oral glucose tolerance test (OGTT) were used to evaluate glucose tolerance (Pratchayasakul et al., 2015). Serum and brain MDA levels, which are lipid peroxidation markers were determined using high-performance liquid chromatography (HPLC) as described previously (Pintana et al., 2013).

#### 2.3. Cognitive tests

The open-field test was performed to measure the locomotor activity of all rats before the learning and memory test. The apparatus consisted of a square box open from above (90  $\times$  90 cm base, 50 cm height). Lighting in the test room was bright. Briefly, the rats were placed into the box and were observed for 10 min. The distance moved by the rat was interpreted as activity. A Morris water maze test was performed as a method of measuring spatial learning activity. Briefly, rats under a dim light were trained to find the hidden platform (diameter 10 cm) in one of four quadrants of the circular pool (diameter 200 cm) from day 1 to day 5. The rats were placed in the opaque water and allowed to find the hidden platform for 2 min. After that, the rats were removed from

the pool and allowed to rest for 15 min before being placed into another quadrant (4 trials/day) and the time to reach the platform was recorded. On day 6, we removed the hidden platform from the pool. Then, the rats were challenged to find the hidden platform and the time to spent in target quadrant was recorded. Data analysis of the MWM test was performed using Smart 3.0 software (Panlab, Harvard Apparatus, Barcelona, Spain).

## 2.4. Extracellular recordings of hippocampal slices for measurement of electrical-induced long-term potentiation (LTP)

The LTP protocol has been described in a previous study (Sripetchwandee et al., 2014a). Briefly, the Schaffer collateral-commissural pathway were stimulated with a bipolar tungsten electrode to evoke field excitatory postsynaptic potentials (fEPSPs), while fEPSPs were recorded from the stratum radiatum of the hippocampal CA1 region with micropipettes filled with 2 M NaCl, whereas fEPSPs recordings LTP was stimulated by high-frequency stimulation (HFS; four trains at 100 Hz; 0.5 s duration; 20 s interval). The experiments were performed for at least 50 min after HFS. The level of potentiation was calculated at 40–50 min after HFS. Data were filtered at 3 kHz, digitized at 10 kHz, and stored in a computer using pClamp9.2 software (Axon Instruments, CA, USA). The initial slope of the fEPSPs were measured and plotted against time using GraphPad prism 6.0.

## 2.5. Extracellular recordings of hippocampal slices for measurement of insulin-induced long term depression (LTD)

To investigate insulin-induced long-term depression (LTD), field excitatory postsynaptic potentials (fEPSPs) were evoked by stimulating the Schaffer collateral–commissural pathway with a bipolar tungsten electrode, whereas fEPSP slope were recorded from stratum radiatum of the hippocampal CA1 with micropipettes filled with 2 M NaCl. The stimulus frequency was 0.033 Hz. For baseline condition, aCSF perfused to hippocampal slices for 10 min. For insulin stimulation condition, aCSF plus 500 nM insulin was perfused for 10 min, after that the hippocampal slices were perfused with aCSF again to wash out and recordings were taken for the next 40 min. All data were analyzed using pClamp 9.2 software (Axon Instruments, Foster City, CA, USA). The initial slope of the fEPSPs was measured and plotted versus time using GraphPad prism 6.0.

#### 2.6. Immunoblotting

Western blot analysis was used to determine insulin signaling including insulin receptor phosphorylation (p-IR), insulin receptors (IR), Akt/PKB at serine 473 kinases phosphorylation (p-Akt/PKB) and Akt/ PKB. The brain homogenates were prepared as described previously (Pipatpiboon et al., 2013). In addition, we determined Bax, Bcl2, NFκB p65 and NFκB p65 phosphorylation (p-NFκB p65) levels from another set of whole brain slices which were homogenized. Briefly, the p-IR, IR, Akt/PKB, p-Akt/PKB, Bax, Bcl2, NFκB p65 and p-NFκB p65 were immunoblotted with rabbit anti-IR tyrosine phosphorylation (1:200, Santa Cruz Biotechnology, Inc., Texas, USA), IR (1:200, Santa Cruz Biotechnology, Inc., Texas, USA), Akt/PKB (1:500, Cell Signaling Technology, Danvers, Massachusetts, USA) and p-Akt/PKB (1:500, Cell Signaling Technology, Danvers, Massachusetts, USA), Bax (1: 200, Santa Cruz Biotechnology, Inc., Texas, USA), Bcl2 (1: 1000, Cell Signaling Technology, Danvers, Massachusetts, USA), NFkB p65 (1: 1000, Cell Signaling Technology, Danvers, Massachusetts, USA) and p-NFκB p65 (1: 500, Cell Signaling Technology, Danvers, Massachusetts, USA). For loading controls, each membrane was incubated with anti-β actin (1: 2000, Santa Cruz Biotechnology, Inc., Texas, USA) and anti-GAPDH (1: 10,000, Abcam, Cambridge, Massachusetts, USA) for immunoblotting. The ChemiDoc touch imaging system (Bio-Rad Laboratories, Hercules, California, USA) were used to develop the membrane. All data were analyze using an image J program. The results are shown as average signal intensity (arbitrary units).

#### 2.7. Brain mitochondrial function

Isolated mitochondria were prepared using the same method as described in our previous studies. In this study we evaluated brain mitochondrial function by determine brain mitochondrial reactive oxygen species (ROS) production, brain mitochondrial membrane potential ( $\Delta\Psi$ m) and brain mitochondrial swelling. The mitochondrial function was determined by following the method stated in our previous studies (Pintana et al., 2012; Pipatpiboon et al., 2013).

#### 2.8. Statistical analysis

All data were expressed as mean  $\pm$  SEM. Statistical analysis was carried out using the SPSS program (version 17: SPSS, Chicago, III., USA). The significant differences in all parameters were calculated using a one-way ANOVA followed by post-hoc LSD. For the MWM test and the acquisition test, a two-way ANOVA followed by an LSD test was used. For all comparisons, p < 0.05 was considered as statistically significant.

#### 3. Results

## 3.1. Dapagliflozin and combined drugs exerted greater efficacy on weight reduction and greater improved peripheral insulin sensitivity than vildagliptin in cases of HFD-induced obese rats

Vehicle-treated HFD-fed rats (HFV) developed obesity and peripheral insulin resistance, indicated by significantly increased body weight, visceral fat, plasma insulin, HOMA index, plasma glucose area under the curve (AUCg), plasma total cholesterol level and plasma LDL level, when compared with vehicle-treated ND-fed rats (NDV) (Table 1).

Vildagliptin-treated HFD-fed rats (HFVil) effectively improved peripheral insulin sensitivity and lipid profiles, as indicated by decreased HOMA index, decreased plasma total cholesterol, plasma LDL-C level and AUCg levels, when compared with HFV rats. Interestingly, dapagliflozin therapy in HFD-fed rats restored peripheral insulin sensitivity to the same levels as that of the NDV rats (Table 1). In addition, dapagliflozin-treated HFD-fed rats (HFDa) and combined drug-treated HFD-fed rats (HFDaVil) had significantly increased glucose urinary excretion (UGE) and reduced body weight gain, as indicated by decreased body weight and visceral fat, when compared with HFV and HFVil rats (p < 0.05, Table 1). These findings suggest that dapagliflozin exerted a greater efficacy on reducing body weight gain and improving metabolic profiles in HFD-induced obese rats.

## 3.2. Dapagliflozin, vildagliptin and a combination of the 2 drugs exerted a similar efficacy on ameliorating cognitive decline in HFD-induced obese rats

At the end of the experimental period, locomotor activities of all rats were tested using an open field test (OFT) before the MWM test. The data demonstrated that all rats did not show a significant difference in locomotor activity, which was determined by the distance that the rats moved during the test. To assess spatial learning and memory, a MWM test was used and we found that the swim speed was not significantly different among all groups (27.17  $\pm$  0.62, 27.12  $\pm$  0.99, 25.95  $\pm$  2.92, 26.99  $\pm$  1.72, 25.79  $\pm$  1.42 cm/s, in NDV, HFV, HFVil, HFDa and HFDaVil rats, respectively). Moreover, HFV rats showed cognitive decline, as indicated by a significantly increased time to reach the platform (p < 0.05, Fig. 2A) and decreased mean time spent in the target quadrant, when compared with NDV rats (p < 0.05, Fig. 2B).

HFVil rats, HFDa rats and HFDaVil rats showed significantly reduced time to reach the platform (p < 0.05, Fig. 2A) and reduced

The effects of dapagliflozin, vildagliptin, and combined drug treatment on metabolic parameters in HFD-induced obese rats (n = 8/group).

| Parameters  | Groups          |                         |                           |                                      |                                     |
|---|-----------------|-------------------------|---------------------------|--------------------------------------|-------------------------------------|
|   | NDV             | HFV                     | HFVil                     | HFDa                                 | HFDaVil                             |
| Body weight (g)                                     | 504 ± 9         | 693 ± 13*               | 667 ± 13*                 | 589 ± 19*, <sup>†,‡</sup>            | 578 ± 20**,†,‡                      |
| Visceral fat (g)                                    | $28 \pm 2$      | 64 ± 3*                 | 61 ± 3*                   | 48 ± 3*, <sup>†</sup> , <sup>‡</sup> | $48 \pm 4^{*,\uparrow,\ddagger}$    |
| Food intake (g/day)                                 | $20 \pm 2$      | $20 \pm 1$              | $18 \pm 1$                | $20 \pm 1$                           | $21 \pm 2$                          |
| Water intake (ml/day)                               | $32 \pm 3$      | $33 \pm 2$              | $34 \pm 2$                | 52 ± 3*, <sup>†,‡</sup>              | $52 \pm 4^{*,\dagger,\ddagger}$     |
| Urine glucose excretion (UGE; mg/dL)                | $1.6 \pm 0.2$   | $1.4 \pm 0.2$           | $1.5 \pm 0.4$             | $683 \pm 28.4^{*,\uparrow,\ddagger}$ | 711 ± 15.6*, <sup>†,‡</sup>         |
| Plasma insulin (ng/ml)                              | $2.3 \pm 0.2$   | 5.5 ± 0.3*              | $4.3 \pm 0.2^{*,\dagger}$ | $2.5 \pm 0.2^{\uparrow, *}$          | $2.6 \pm 0.2^{\dagger, *}$          |
| Plasma glucose (mg/dl)                              | $112 \pm 3$     | $115 \pm 4$             | $117 \pm 3$               | 100 ± 3*,†,‡                         | $100 \pm 4^{*},^{\dagger,*}$        |
| HOMA index  | $14.4 \pm 1.3$  | 37.4 ± 2.6*             | 28.6 ± 1.9** <sup>†</sup> | $15.4 \pm 1.3^{\dagger, \ddagger}$   | $15.8 \pm 1.7^{\dagger,*}$          |
| AUCg (mg/dl $\times$ min $\times$ 10 <sup>4</sup> ) | $2.3 \pm 0.2$   | $3.8 \pm 0.2^{*}$       | $3.0 \pm 0.1^{*,\dagger}$ | $2.2 \pm 0.2^{\dagger,\ddagger}$     | $2.4 \pm 0.1^{\dagger, *}$          |
| Plasma TC (mg/dl)                                   | $101 \pm 3$     | 131 ± 6*                | $108 \pm 4^{\dagger}$     | $107 \pm 2^{\dagger}$                | $102 \pm 4^{\dagger}$               |
| Plasma TG (mg/dl)                                   | 89 ± 5          | 89 ± 7                  | 93 ± 6                    | 88 ± 7                               | 91 ± 5                              |
| Plasma HDL-c (mg/dl)                                | $30 \pm 2$      | $32 \pm 2$              | $30 \pm 2$                | $30 \pm 2$                           | $29 \pm 1$                          |
| Plasma LDL-c (mg/dl)                                | $55 \pm 4$      | 86 ± 5*                 | 58 ± 4 <sup>†</sup>       | $60 \pm 4^{\dagger}$                 | $60 \pm 6^{\dagger}$                |
| Serum MDA (μmol/ml)                                 | $9.67 \pm 0.02$ | 11.35 ± 0.75*           | $9.91 \pm 0.06^{\dagger}$ | $10.03 \pm 0.21^{\dagger}$           | $9.87 \pm 0.08^{\dagger}$           |
| Brain MDA (µmol/mg protein)                         | $0.22 \pm 0.02$ | $0.37 \pm 0.02^{\circ}$ | $0.25~\pm~0.03^{\dagger}$ | $0.26~\pm~0.02^{\dagger}$            | $0.16 \pm 0.02^{\uparrow,\ddagger}$ |

NDV: Vehicle-treated normal diet fed rats; HFV: Vehicle-treated high fat diet fed rats; HFVil: Vildagliptin-treated high fat diet fed rats; HFDa: Dapaglifozin-treated high fat diet fed rats; HFDaVil: Combined drug-treated high fat diet fed rats.

<sup>\*</sup> p < 0.05 vs. HFDa.

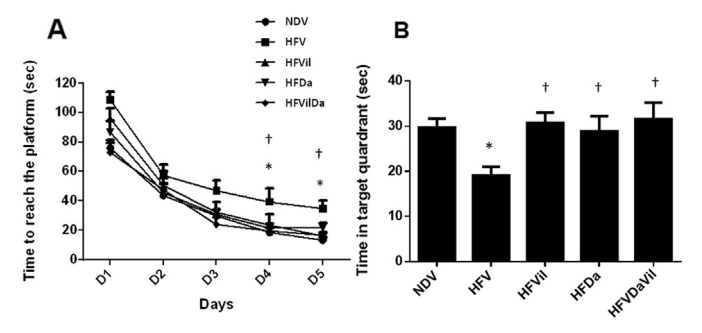
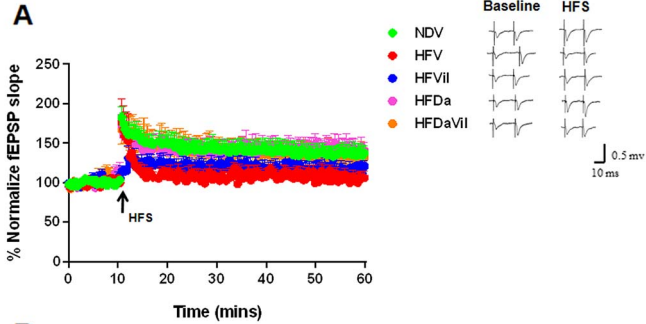


Fig. 2. Effects of vildagliptin, dapagliflozin and combined drug treatment on Morris water maze test in HFD-induced obese rats. (A) Time to reach the platform in acquisition test and (B) time spent in target quadrant in probe test. NDV: Vehicle-treated normal diet fed rats; HFV: Vehicle-treated high fat diet fed rats; HFVil: Vildagliptin-treated high fat diet fed rats; HFDa: Dapagliflozin-treated high fat diet fed rats; HFDaVil: Combined dapagliflozin and vildagliptin-treated high fat diet fed rats. \*p  $\,<\,0.05$  vs. NDV, †p  $\,<\,0.05$ vs. HFV, n = 8/group.

mean time spent in the target quadrant (p < 0.05, Fig. 2B) when compared with HFV rats (p < 0.05, Fig. 2B), indicating that vildagliptin, dapagliflozin and the combined drugs shared a similar efficacy in preventing cognitive decline in HFD-induced obese rats. These findings suggested that vildagliptin, dapagliflozin and the combined drugs effectively prevented cognitive decline in HFD-induced obese rats.

#### 3.3. Dapagliflozin, but not vildagliptin, attenuated the impairment of hippocampal synaptic plasticity in HFD-induced obese rats

In the present study, hippocampal synaptic plasticity was determined by electrically induced-LTP. We found that HFV rats showed a significantly decreased degree of electrical induced-LTP when compared with NDV rats (p < 0.05, Fig. 3A-B). Interestingly, HFDa rats and HFDaVil rats showed a significantly increased degree of electrically induced-LTP when compared with HFV rats (p < 0.05, Fig. 3A-B). Meanwhile, HFVil rats did not increase the degree of electrically induced-LTP when compared with HFV rats (p < 0.05, Fig. 3A-B). These findings suggested that dapagliflozin therapy led to improved hippocampal synaptic plasticity in HFD-induced obese rats, but vildagliptin did not.



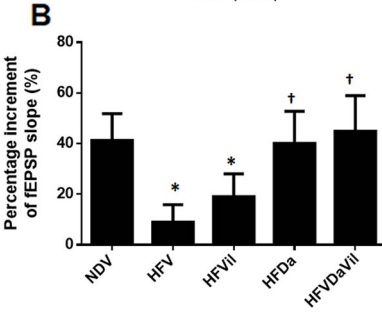


Fig. 3. Effects of vildagliptin, dapagliflozin and combined drug treatment on hippocampal synaptic plasticity in HFD-induced obese rats. (A) The degree of electricalmediated LTP observed from hippocampal slices and (B) Percentage increment of fEPSP slope. NDV: Vehicle-treated normal diet fed rats; HFV: Vehicle-treated high fat diet fed rats; HFVil: Vildagliptin-treated high fat diet fed rats; HFDa: Dapagliflozin-treated high fat diet fed rats; HFDaVil: Combined dapagliflozin and vildagliptin-treated high fat diet fed rats. \*p < 0.05 vs. NDV, †p < 0.05 vs. HFV, ‡p < 0.05 vs. HFDa; n = 8/group.

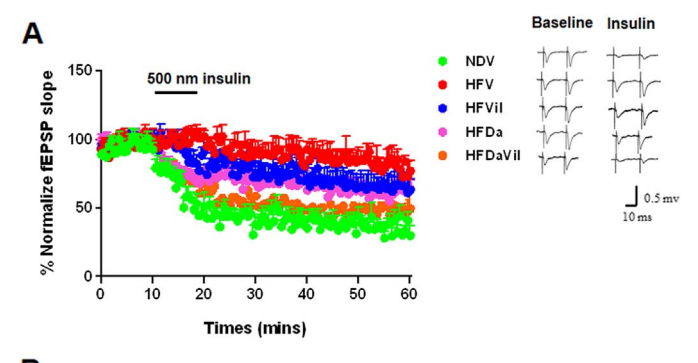
#### 3.4. The effects of vildagliptin, dapagliflozin and combined drugs on improving brain insulin sensitivity of the HFD-induced obese rats

In this study, brain insulin sensitivity was determined by insulininduced long term depression (LTD) and brain insulin signaling. We found that HFV rats showed impairment of brain insulin sensitivity, as indicated by the reduction of the degree of insulin-induced LTD when compared with NDV rats (p < 0.05, Fig. 4A-B). Meanwhile, an increase in the degree of insulin-induced LTD was observed in both vildagliptin and dapagliflozin-treated HFD-fed rats when compared with

n = 8/group.

<sup>\*</sup> p < 0.05 vs. NDV.

p < 0.05 vs. HFV.



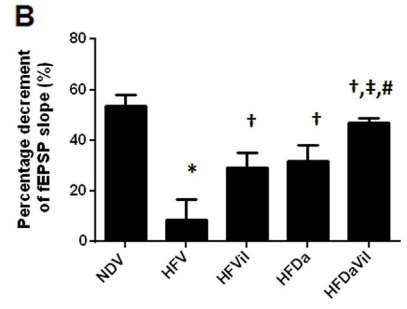


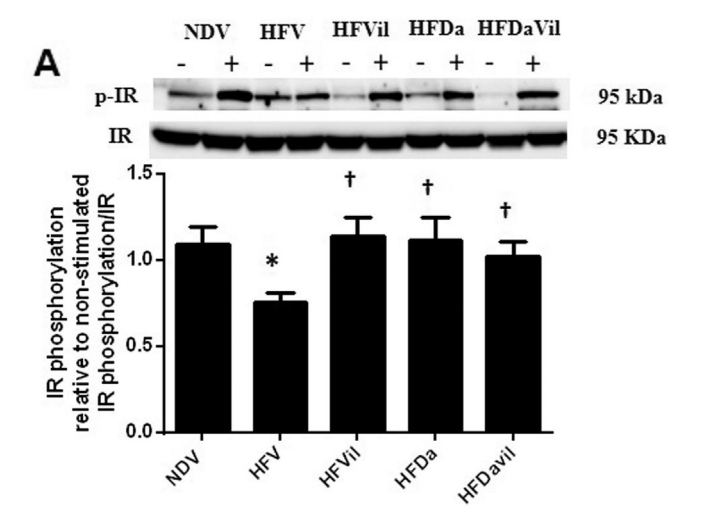
Fig. 4. Effects of vildagliptin, dapagliflozin and combined drug treatment on brain insulin sensitivity in HFD-induced obese rats. (A) The degree of insulin-induced LTD observed in hippocampal slices and (B) Percentage decrement of fEPSP slope. NDV: Vehicle-treated normal diet fed rats; HFV: Vehicle-treated high fat diet fed rats; HFVil: Vildagliptin-treated high fat diet fed rats; HFDa: Dapagliflozin-treated high fat diet fed rats; HFDaVil: Combined dapagliflozin and vildagliptin-treated high fat diet fed rats. \*p < 0.05 vs. NDV, †p < 0.05 vs. HFV, ‡p < 0.05 vs. HFDa; n = 8/group.

HFV rats (p < 0.05, Fig. 4A–B). Interestingly, the combined drug treatment greatly increased the degree of insulin-induced LTD in obeseinsulin resistant rats, when compared with HFV, HFVil and HFDa rats (p < 0.05, Fig. 4A–B). These findings suggested that a greater efficacy on brain insulin sensitivity was observed as a result of the combined drug therapy, as indicated by the restoration of insulin-induced LTD in the HFD-induced obese condition.

Brain insulin signaling was determined by western blot analysis. We found that levels of IR tyrosine phosphorylation/IR and Akt/PKB phosphorylation at serine 473 site (Akt-ser)/Akt/PKB were significantly decreased in HFV rats when compared with NDV rats (p < 0.05, Fig. 5A, B). Dapalifozin, vildagliptin and a combination of the drugs led to equally increased levels of IR tyrosine phosphorylation/IR and Akt/PKB phosphorylation at the serine 473 site (Akt-ser)/Akt/PKB in HFD-induced obese rats, when compared with HFV rats (p < 0.05, Fig. 5A, B). These findings suggested that both dapagliflozin and vildagliptin restored brain insulin signaling in HFD-induced obese rats.

## 3.5. Effects of dapagliflozin, vildagliptin and combined drug therapy on brain mitochondrial function, brain mitochondrial morphology and brain oxidative stress levels in HFD-induced obese rats

In this study we demonstrated that HFV rats showed brain mitochondrial dysfunction, as indicated by significantly increased brain mitochondrial ROS production, increased brain mitochondrial membrane potential change (depolarization) and increased brain mitochondrial swelling, when compared with NDV rats (p < 0.05, Fig. 6A–C). Moreover, HFV rats showed brain mitochondrial swelling with unfolded cristae, as shown by brain mitochondrial morphology from transmission electron microscopy (TEM), when compared with NDV rats (p < 0.05, Fig. 6D). In addition to brain mitochondrial function, brain MDA level, a marker of oxidative stress, was determined. We found that HFV rats showed significantly increased MDA levels and hence higher brain oxidative stress levels, when compared with NDV rats (Table 1). HFVil, HFDa and HFDaVil, rats showed



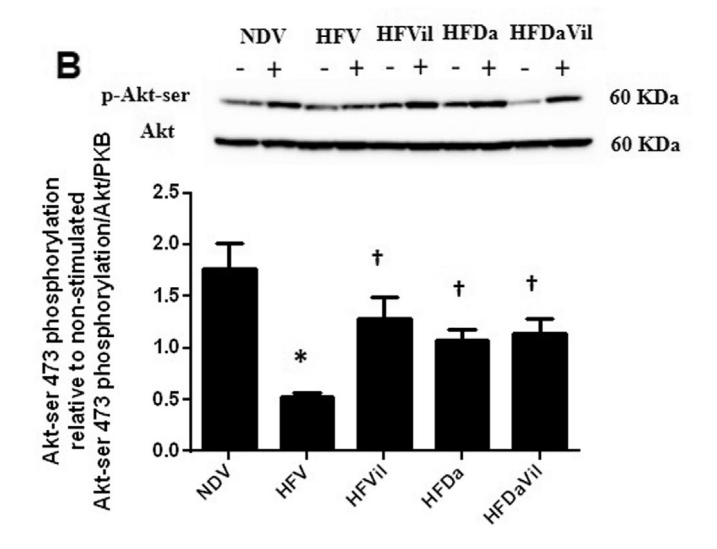


**Fig. 5.** Effects of vildagliptin, dapagliflozin and combined drug treatment on brain insulin signaling in HFD-induced obese rats. (A) IR tyrosine phosphorylation/IR, (B) Akt/PKB phosphorylation at the serine 473 site/Akt/PKB. NDV: Vehicle-treated normal diet fed rats; HFV: Vehicle-treated high fat diet fed rats; HFVi: Vildagliptin-treated high fat diet fed rats; HFDa: Dapagliflozin-treated high fat diet fed rats; HFDaVil: Combined dapagliflozin and vildagliptin-treated high fat diet fed rats. \*p < 0.05 vs. NDV,  $\uparrow p < 0.05$  vs. HFV,  $\ddag p < 0.05$  vs. HFDa; n = 8/group.

significantly decreased brain mitochondrial ROS production, brain mitochondrial membrane potential change (depolarization) and brain mitochondrial swelling, when compared with HFV rats (p < 0.05, Fig. 6A–C). Moreover, HFVil and HFDa rats showed significantly reduced brain MDA levels, when compared with HFV rats (p < 0.05, Table 1). Interestingly, the combined drug therapy led to a greater decrease in brain MDA levels, when compared with all treatments (p < 0.05, Table 1). These findings suggested that dapaglipflozin, vildagliptin and the 2 drugs combined prevented brain mitochondrial dysfunction and exerted anti-oxidant effects in HFD-induced obese rats. Interestingly, combined drug therapy showed a potent effect on the reduction of brain oxidative stress in this model, as indicated by a greater decrease in brain MDA levels, compared to a single therapy.

## 3.6. Dapagliflozin, vildagliptin and the combined drugs attenuated brain apoptosis and brain inflammation in HFD-induced obese rats

To investigate brain apoptosis, pro-apoptotic markers (Bax) and anti-apoptotic markers (Bcl2) were determined. We found that HFV rats increased Bax protein expression, decreased Bcl2 protein expression

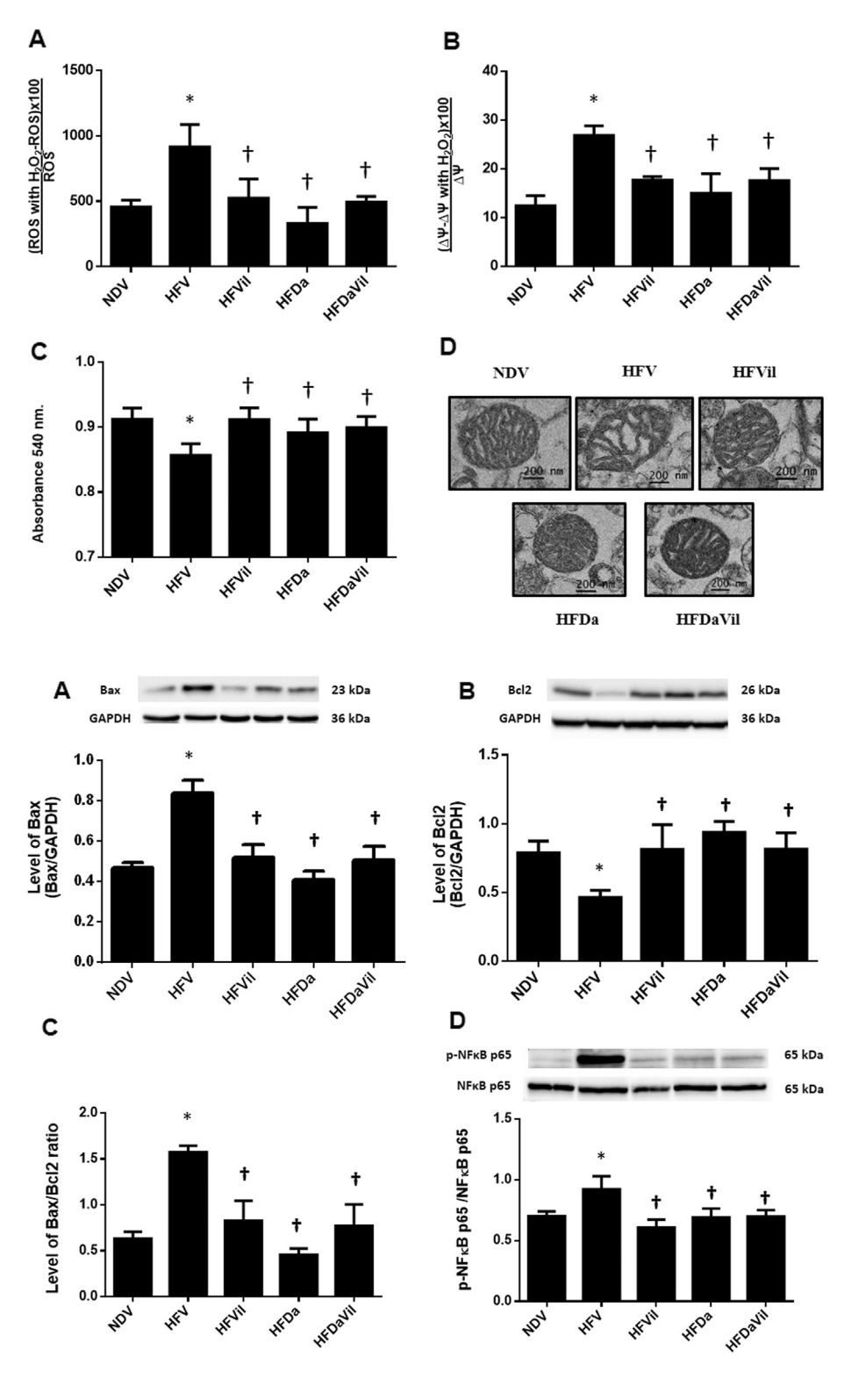


Fig. 6. Effects of vildagliptin, dapagliflozin and combined drug treatment on brain mitochondrial function and morphology in HFD-induced obese rats. (A) Brain mitochondrial ROS production, (B) brain mitochondrial membrane potential change, (C) brain mitochondrial swelling and (D) transmission electron microscopy (original magnification  $\times$  25,000). NDV: Vehicle-treated normal diet fed rats; HFV: Vehicle-treated high fat diet fed rats; HFVil: Vildagliptin-treated high fat diet fed rats; HFDa: Dapagliflozin-treated high fat diet fed rats; HFDavil: Combined dapagliflozin and vildagliptin-treated high fat diet fed rats.  $^*p < 0.05$  vs. NDV,  $^*p < 0.05$  vs. HFV,  $^*p < 0.05$  vs. HFDa; n = 8/group.

Fig. 7. Effects of vildagliptin, dapagliflozin and combined drug treatment on brain apoptosis markers and brain inflammation markers in HFD-induced obese rats. (A) Bax, (B) Bcl2, (C) Bax/Bcl2 ratio and (D) p-NFkB p65/NFkB p65 ratio. NDV: Vehicle-treated normal diet fed rats; HFVi: Vehicle-treated high fat diet fed rats; HFVii: Vildagliptin-treated high fat diet fed rats; HFDa: Dapagliflozin-treated high fat diet fed rats; HFDa: Dapagliflozin and vildagliptin-treated high fat diet fed rats. \*p < 0.05 vs. NDV, †p < 0.05 vs. HFV, ‡p < 0.05 vs. HFDa; n = 8/group.

and also increased Bax/Bcl2 ratio, when compared with NDV rats (p < 0.05, Fig. 7A–C). We also investigated brain inflammation by determining the p-NF $\kappa$ B p-65/NF $\kappa$ B p-65 ratio. We found that HFV rats also had significantly increased p-NF $\kappa$ B p65/NF $\kappa$ B p65 protein expression, when compared with NDV rats (p < 0.05, Fig. 7D). In HFVil, HFDa and HFDaVil rats, there was a decreased level of Bax expression, Bcl2 expression and Bax/Bcl2 ratio (p < 0.05, Fig. 7A–C), and also decreased brain inflammation, as indicated by decreased p-NF $\kappa$ B p-65/NF $\kappa$ B p-65 protein expression, when compared with HFV rats

(p < 0.05, Fig. 7D). These findings suggested that dapaglifozin, vildagliptin and the 2 drugs combined exerted anti-apoptotic effects and anti-inflammatory effects in the brains of HFD-induced obese rats.

#### 4. Discussion

The major findings from this study are as follows: 1) vildagliptin effectively attenuated peripheral insulin resistance, but dapagliflozin exerted a greater efficacy in improving peripheral insulin sensitivity, as

**Table 2**Summary effects of vildagliptin, dapaglifozin and combined drug administration in HFD-induced obese rats.

| Parameters                            | HFV | HFVil | HFDa | HFDaVil |
|---------------------------------------|-----|-------|------|---------|
| Body weight                           | 1   | 1     | ţ    | 1       |
| Visceral fat                          | 1   | 1     | 1    | 1       |
| Insulin sensitivity                   | ↓   | Ť     | 11   | ††      |
| Serum MDA level                       | 1   | 1     | 1    | 1       |
| Brain MDA level                       | 1   | 1     | 1    | 111     |
| Brain mitochondrial function          | 1   | 1     | 1    | 1       |
| Brian insulin signaling               | į   | t     | t    | t       |
| Brain insulin receptor function (LTD) | į   | t     | t    | 111     |
| Bax                                   | Ť   | 1     | 1    | 1       |
| Bcl2                                  | į   | t     | t    | t       |
| Bax/Bcl2 ratio                        | 1   | 1     | 1    | 1       |
| p-NFκB p65/NFκB p65 ratio             | 1   | Ţ     | 1    | 1       |
| LTP                                   | į   | 1     | t    | t       |
| Cognition                             | į   | Ì     | 1    | t       |

Abbreviation: NDV: vehicle-treated normal diet fed rats; HFV: vehicle-treated high fat diet fed rats; HFVil: vildagliptin-treated high fat diet fed rats; HFDa: dapagliflozin-treated high fat diet fed rats; HFDaVil: combined drug-treated high fat diet fed rats; MDA: malondialdehyde; LTP: long-term potentiation.

 $\downarrow$ : decrease/impairment vs NDV;  $\uparrow$ : increase/improvement vs NDV;  $\downarrow$ : decrease/impairment vs HFV;  $\uparrow$ : increase/improvement vs HFV;  $\downarrow$ 11: decrease/impairment vs HFVil and HFDa;  $\uparrow$ 1: increase/improvement vs HFVil;  $\uparrow$ 11: increase/improvement vs HFVil and HFDa

indicated by reduced body weight gain and restored insulin sensitivity; 2) dapagliflozin and vildagliptin therapy led to equally improved brain mitochondrial function, brain insulin signaling and prevented cognitive decline, but only dapagliflozin improved hippocampal synaptic plasticity, and 3) surprisingly, the combined drugs had a greater efficacy in increasing brain insulin sensitivity and reducing brain oxidative stress than did the single therapies.

In this study, long-term HFD consumption led to the development of obese-insulin resistance, impaired brain function, and resulting cognitive decline. These findings are consistent with our previous reports (Pintana et al., 2013; Sa-Nguanmoo et al., 2016). Although vildagliptin effectively improved peripheral insulin sensitivity, dapaglipflozin restored peripheral insulin sensitivity and reduced body weight gain in this model. These effects could be due to the: 1) inhibition of SGLT2 which promotes urinary glucose excretion (as shown in Table 1), leading to loss of calories through urine (Poudel 2013), and 2) reduction of visceral fat in HFD-induced obese rats. Increased brain oxidative stress, brain mitochondrial dysfunction, decreased brain insulin sensitivity, impaired hippocampal synaptic plasticity, and cognitive decline occurred in these HFD-induced obese rats. We also demonstrated for the first time that these rats had an increase in brain inflammation, as indicated by an increase in the p-NFκB p65/NFκB p65 ratio. It has been known that mitochondrial dysfunction, increased oxidative damage and brain inflammation exacerbate neuronal dysfunction (Dias et al., 2013; Verdile et al., 2015). We found that dapaglipflozin, vildagliptin and the 2 drugs combined effectively improved brain mitochondrial function due to a decrease in brain mitochondrial ROS production, decreased brain mitochondrial membrane potential change and brain mitochondrial swelling, decreased brain inflammation, as indicated by the reduction of p-NFκB p65/NFκB p65 ratio and decreased brain apoptosis, as indicated by a decrease in the apoptotic protein (Bax) and antiapoptotic protein (Bcl2) in HFD-induced obese rats. Interestingly, the combined drugs therapy decreased brain oxidative stress levels to a much greater extent than either of the single therapies. These findings suggest that a combination of dapaglipflozin and vildagiptin provide the more potent anti-oxidative effects than the single therapies.

We also determined brain insulin signaling and found that each single therapy and the combined drugs improved brain insulin signaling by increasing p-IR and p-Akt/PKB ser473 in HFD-induced obese rats. Although vildagliptin, dapagliflozin, and combined drugs equally

improved brain insulin sensitivity in HFD-induced obese rats, combined drug had the greatest benefit on improving brain insulin-induced LTD. The possible explanation could be that combined drugs had synergistically enhance the protective effects on brain insulin-induced LTD via greatly decreased brain oxidative stress than single therapy.

Furthermore, a previous study reported that a SGLT2 inhibitor could increase brain-derived neurotrophic factor (BDNF) levels in the brains of db/db mice (Lin et al., 2014). Previous evidence established that BDNF is a major regulator of synaptogenesis and synaptic plasticity mechanisms, which play key roles in learning and memory (Chao and Henry, 2010). In this study, we demonstrated for the first time that dapaglipflozin, but not vildagliptin, enhanced hippocampal synaptic plasticity, indicated by an increased degree of electrical-induced LTP in HFD-induced obese rats. The beneficial effect of dapaglipflozin on hippocampal synaptic plasticity in this model could occur via the BDNF pathways.

The possible underlying mechanisms of dapagliflozin in restoring cognitive function in HFD-induced obese rats could be through 1) restoring peripheral insulin sensitivity, 2) greatly decreasing brain oxidative stress, which led to improve brain mitochondrial function, 3) decreased brain inflammation and subsequently restored brain insulin signaling as well as increased brain insulin sensitivity, and 4) decreased brain apoptosis, leading to increased hippocampal synaptic plasticity. Meanwhile, vildagliptin can restore cognitive decline in the HFD-induced obese rats, possibly through improved peripheral insulin sensitivity, the reduction of brain oxidative stress, brain inflammation and brain apoptosis, resulting in improved brain mitochondrial function and brain insulin sensitivity. In addition, the combined drugs provided the synergistic effects observed from each single therapy by restoring the cognitive decline in obese-insulin resistant rats via better efficacy in restoring peripheral insulin sensitivity, more potent anti-oxidative effects, and greater improved brain insulin-induced LTD than monotherapy.

#### 5. Conclusions

In summary, dapagliflozin exerts a greater efficacy in improving peripheral insulin sensitivity than vildagliptin. However, dapagliflozin and vildagliptin share a similar efficacy in reducing oxidative stress, attenuating brain mitochondrial dysfunction, brain apoptosis, and brain inflammation, and preventing cognitive decline. However, only dapagliflozin treatment led to a decrease in body weight gain and reduced visceral fat mass. The combined drugs therapy in the HFD-induced obese condition exerted greater anti-oxidative effects and improved brain insulin sensitivity to a greater degree than the single therapy. The summarized effects of vildagliptin, dapaglifloin and the combination of these drugs in HFD-induced obese rats are shown in Table 2.

#### Limitation of the study

The limitation of the study is that GLP-1 levels in the plasma and the brain were not determined. However, our previous study already demonstrated that 1) the administration of vildagliptin for 21 days significantly increased not only the plasma level of active GLP-1, but also brain levels of active GLP-1 in obese-insulin resistant rats (Pipatpiboon et al., 2013 Eur J Neurosci. 2013 Mar; 37(5):839–49), and 2) vildagliptin decreased cognitive decline in obese-insulin resistant rats (Pintana et al., 2013 J Endocrinol. May 28; 218(1):1–11). Altogether, our findings suggest that increased GLP1 levels in plasma and brain are associated with improved cognitive function, which is consistent with a previous report (Bomfim et al., 2012).

#### Acknowledgements

The authors would like to thank Dr. Nattayaporn Apaijai for her technical assistance and Ms. Maria Love for her editorial assistance in

the completion of this manuscript.

#### **Funding sources**

This work was supported by Thailand Research Fund grants: TRF-RTA6080003 (SC) and MRG5980198 (WP), a CMU50th Anniversary grant from Chiang Mai University (PHD/023/2556 PS & NC), a NSTDA Research Chair Grant from the National Science and Technology Development Agency Thailand (NC) and a Chiang Mai University Center of Excellence Award (NC).

#### Conflict of interest

There is no conflict of interest to report.

#### References

- Bailey, C.J., Gross, J.L., Hennicken, D., Iqbal, N., Mansfield, T.A., List, J.F., 2013. Dapagliflozin add-on to metformin in type 2 diabetes inadequately controlled with metformin: a randomized, double-blind, placebo-controlled 102-week trial. BMC Med. 11, 43.
- Bomfim, T.R., Forny-Germano, L., Sathler, L.B., Brito-Moreira, J., Houzel, J.C., Decker, H., Silverman, M.A., Kazi, H., Melo, H.M., McClean, P.L., Holscher, C., Arnold, S.E., Talbot, K., Klein, W.L., Munoz, D.P., Ferreira, S.T., De Felice, F.G., 2012. An anti-diabetes agent protects the mouse brain from defective insulin signaling caused by Alzheimer's disease-associated Abeta oligomers. J. Clin. Invest. 122, 1339–1353.
- Chao, E.C., Henry, R.R., 2010. SGLT2 inhibition—a novel strategy for diabetes treatment. Nat. Rev. Drug Discov. 9, 551–559.
- Dias, V., Junn, E., Mouradian, M.M., 2013. The role of oxidative stress in Parkinson's disease. J. Parkinsons Dis. 3, 461–491.
- Friedewald, W.T., Levy, R.I., Fredrickson, D.S., 1972. Estimation of the concentration of low-density lipoprotein cholesterol in plasma, without use of the preparative ultracentrifuge. Clin. Chem. 18, 499–502.
- Han, S., Hagan, D.L., Taylor, J.R., Xin, L., Meng, W., Biller, S.A., Wetterau, J.R., Washburn, W.N., Whaley, J.M., 2008. Dapagliflozin, a selective SGLT2 inhibitor, improves glucose homeostasis in normal and diabetic rats. Diabetes 57, 1723–1729.
- Jabbour, S.A., Goldstein, B.J., 2008. Sodium glucose co-transporter 2 inhibitors: blocking renal tubular reabsorption of glucose to improve glycaemic control in patients with diabetes. Int. J. Clin. Pract. 62, 1279–1284.
- Lin, B., Koibuchi, N., Hasegawa, Y., Sueta, D., Toyama, K., Uekawa, K., Ma, M., Nakagawa, T., Kusaka, H., Kim-Mitsuyama, S., 2014. Glycemic control with empagliflozin, a novel selective SGLT2 inhibitor, ameliorates cardiovascular injury and cognitive dysfunction in obese and type 2 diabetic mice. Cardiovasc. Diabetol. 13, 148
- MacDonald, P.E., El-Kholy, W., Riedel, M.J., Salapatek, A.M., Light, P.E., Wheeler, M.B., 2002. The multiple actions of GLP-1 on the process of glucose-stimulated insulin secretion. Diabetes 51 (Suppl. 3), S434–442.
- Mather, A., Pollock, C., 2011. Glucose handling by the kidney. Kidney Int. Suppl. S1–6. Matthews, D.R., Hosker, J.P., Rudenski, A.S., Naylor, B.A., Treacher, D.F., Turner, R.C., 1985. Homeostasis model assessment: insulin resistance and beta-cell function from fasting plasma glucose and insulin concentrations in man. Diabetologia 28, 412–419. Min, S.H., Yoon, J.H., Hahn, S., Cho, Y.M., 2017. Comparison between SGLT2 inhibitors

- and DPP4 inhibitors added to insulin therapy in type 2 diabetes: a systematic review with indirect comparison meta-analysis. Diabetes Metab. Res. Rev. 33.
- Naznin, F., Sakoda, H., Okada, T., Tsubouchi, H., Waise, T.M., Arakawa, K., Nakazato, M., 2017. Canagliflozin, a sodium glucose cotransporter 2 inhibitor, attenuates obesityinduced inflammation in the nodose ganglion, hypothalamus, and skeletal muscle of mice. Eur. J. Pharmacol. 794, 37–44.
- Oguma, T., Kuriyama, C., Nakayama, K., Matsushita, Y., Yoshida, K., Kiuchi, S., Ikenaga, Y., Nakamaru, Y., Hikida, K., Saito, A., Arakawa, K., Oka, K., Ueta, K., Shiotani, M., 2015. The effect of combined treatment with canagliflozin and teneligliptin on glucose intolerance in Zucker diabetic fatty rats. J. Pharmacol. Sci. 127, 456–461.
- Pintana, H., Apaijai, N., Pratchayasakul, W., Chattipakorn, N., Chattipakorn, S.C., 2012. Effects of metformin on learning and memory behaviors and brain mitochondrial functions in high fat diet induced insulin resistant rats. Life Sci. 91, 409–414.
- Pintana, H., Apaijai, N., Chattipakorn, N., Chattipakorn, S.C., 2013. DPP-4 inhibitors improve cognition and brain mitochondrial function of insulin-resistant rats. J. Endocrinol. 218, 1–11.
- Pintana, H., Pongkan, W., Pratchayasakul, W., Chattipakorn, N., Chattipakorn, S.C., 2015. Dipeptidyl peptidase 4 inhibitor improves brain insulin sensitivity, but fails to prevent cognitive impairment in orchiectomy obese rats. J. Endocrinol. 226, M1–M11.
- Pipatpiboon, N., Pratchayasakul, W., Chattipakorn, N., Chattipakorn, S.C., 2012.
  PPARgamma agonist improves neuronal insulin receptor function in hippocampus and brain mitochondria function in rats with insulin resistance induced by long term high-fat diets. Endocrinology 153, 329–338.
- Pipatpiboon, N., Pintana, H., Pratchayasakul, W., Chattipakorn, N., Chattipakorn, S.C., 2013. DPP4-inhibitor improves neuronal insulin receptor function, brain mitochondrial function and cognitive function in rats with insulin resistance induced by highfat diet consumption. Eur. J. Neurosci. 37, 839–849.
- Poudel, R.R., 2013. Renal glucose handling in diabetes and sodium glucose cotransporter 2 inhibition. Indian J. Endocrinol. Metab. 17, 588–593.
- Pratchayasakul, W., Kerdphoo, S., Petsophonsakul, P., Pongchaidecha, A., Chattipakorn, N., Chattipakorn, S.C., 2011. Effects of high-fat diet on insulin receptor function in rat hippocampus and the level of neuronal corticosterone. Life Sci. 88, 619–627.
- Pratchayasakul, W., Sa-Nguanmoo, P., Sivasinprasasn, S., Pintana, H., Tawinvisan, R., Sripetchwandee, J., Kumfu, S., Chattipakorn, N., Chattipakorn, S.C., 2015. Obesity accelerates cognitive decline by aggravating mitochondrial dysfunction, insulin resistance and synaptic dysfunction under estrogen-deprived conditions. Horm. Behav. 72. 68–77.
- Sa-Nguanmoo, P., Tanajak, P., Kerdphoo, S., Satjaritanun, P., Wang, X., Liang, G., Li, X., Jiang, C., Pratchayasakul, W., Chattipakorn, N., Chattipakorn, S.C., 2016. FGF21 improves cognition by restored synaptic plasticity, dendritic spine density, brain mitochondrial function and cell apoptosis in obese-insulin resistant male rats. Horm. Behav. 85. 86–95.
- Sripetchwandee, J., Pipatpiboon, N., Chattipakorn, N., Chattipakorn, S., 2014a.

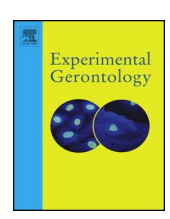
  Combined therapy of iron chelator and antioxidant completely restores brain dysfunction induced by iron toxicity. PLoS One 9, e85115.
- Sripetchwandee, J., Pipatpiboon, N., Pratchayasakul, W., Chattipakorn, N., Chattipakorn, S.C., 2014b. DPP-4 inhibitor and PPARgamma agonist restore the loss of CA1 dendritic spines in obese insulin-resistant rats. Arch. Med. Res. 45, 547–552.
- Verdile, G., Keane, K.N., Cruzat, V.F., Medic, S., Sabale, M., Rowles, J., Wijesekara, N., Martins, R.N., Fraser, P.E., Newsholme, P., 2015. Inflammation and oxidative stress: the molecular connectivity between insulin resistance, obesity, and Alzheimer's disease. Mediat. Inflamm. 2015, 105828.
- Wilding, J.P., Woo, V., Soler, N.G., Pahor, A., Sugg, J., Rohwedder, K., Parikh, S., Dapagliflozin 006 Study, G, 2012. Long-term efficacy of dapagliflozin in patients with type 2 diabetes mellitus receiving high doses of insulin: a randomized trial. Ann. Intern. Med. 156, 405–415.

FISEVIER

#### Contents lists available at ScienceDirect

#### **Experimental Gerontology**

journal homepage: www.elsevier.com/locate/expgero



#### Review

### Role of D-galactose-induced brain aging and its potential used for therapeutic interventions



Thazin Shwe $^{a,b,c}$ , Wasana Pratchayasakul $^{a,b,c}$ , Nipon Chattipakorn $^{a,b,c}$ , Siriporn C. Chattipakorn $^{a,b,c,d,*}$ 

- a Neurophysiology unit, Cardiac Electrophysiology Research and Training Center, Faculty of Medicine, Chiang Mai University, Chiang Mai 50200, Thailand
- b Cardiac Electrophysiology Unit, Department of Physiology, Faculty of Medicine, Chiang Mai University, Chiang Mai 50200, Thailand
- <sup>c</sup> Center of Excellence in Cardiac Electrophysiology, Chiang Mai University, Chiang Mai 50200, Thailand
- d Department of Oral Biology and Diagnostic Sciences, Faculty of Dentistry, Chiang Mai University, Chiang Mai, 50200, Thailand

#### ARTICLE INFO

#### Section Editor: Christian Humpel

Keywords:
D-galactose
Brain aging
Mitochondria
Cognitive function
Therapeutic

#### ABSTRACT

Aging is a phenomenon that all living organisms inevitably face. Every year, 9.9 million people, globally, suffer from dementia, an indicator of the aging brain. Brain aging is significantly associated with mitochondrial dysfunction. This is characterized by a decrease in the activity of respiratory chain enzymes and ATP production, and increased free radical generation, mitochondrial deoxyribonucleic acid (DNA) mutations, and impaired mitochondrial structures. To get a better understanding of aging and to prevent its effects on many organs, chronic systemic administration of D-galactose was used to artificially create brain senescence in animal models and established to be beneficial for studies of anti-aging therapeutic interventions. Several studies have shown that D-galactose-induced brain aging which does so not only by causing mitochondrial dysfunction, but also by increasing oxidative stress, inflammation, and apoptosis, as well as lowering brain-derived neurotrophic factors. All of these defects finally lead to cognitive decline. Various therapeutic approaches which act on mitochondria and cognition were evaluated to assess their effectiveness in the battle to reverse brain aging. The aim of this article is to comprehensively summarize and discuss the underlying mechanisms involved in D-galactose-induced brain aging, particularly as regards alterations in brain mitochondria and cognitive function. In addition, the aim is to summarize the different therapeutic approaches which have been utilized to address D-galactose-induced brain aging.

#### 1. Introduction

The world's population is becoming increasingly aged. According to the United Nations' World Population Prospects, the percentage of people aged 60 or over was reported to be 12.3% in 2015 and it is projected to rise to 21.5% of the global population by 2050 (Sander et al., 2015). Due to the falling fertility rates and remarkable increases in life expectancy around the world, age-related problems have come to the forefront of current attention (Sander et al., 2015). Dementia or cognitive impairment is the major cause of disability and dependency among elderly people worldwide, which is why WHO have reported dementia as being a public health priority (Wortmann, 2012). It is forecasted that the number of people affected by dementia will double every 20 years and it is acknowledged that no one is immune to brain aging disorders (Gillum et al., 2011).

Mitochondrial dysfunction plays an important role in brain aging or

brain senescence, and several aspects of age-associated neurodegeneration (Ames, 2004; Grimm and Eckert, 2017; Sanz and Stefanatos, 2008; Schriner et al., 2005; Wright et al., 2004). Increased production of reactive oxygen species (ROS) following mitochondrial dysfunction induces brain oxidative stress via a vicious cycle of ROS-induced ROS release in mitochondria, and this possibly leads to brain aging or brain senescence (Pak et al., 2003). The senescence of the brain finally leads to cognitive impairment, which is the primary symptom of several neurodegenerative diseases in elderly people. To investigate the underlying mechanisms of brain aging, several animal models have been used. The D-galactose accelerated brain-aging process in animal models is the most common model used for investigating the brain aging process (Haider et al., 2015; Lu et al., 2007; Lu et al., 2010b; Xian et al., 2014; Zhang et al., 2011; Zhu et al., 2014). The administration of Dgalactose into animals can induce aspects of brain aging similar in many ways to human brain aging, including memory deficit, neuronal

<sup>\*</sup> Corresponding author at: Neurophysiology Unit, Cardiac Electrophysiology Research and Training Center, Faculty of Medicine, Chiang Mai University; Department of Oral Biology and Diagnostic Sciences, Faculty of Dentistry, Chiang Mai University, Chiang Mai 50200, Thailand.

E-mail address: siriporn.c@cmu.ac.th (S.C. Chattipakorn).

Table 1 D-galactose-induced brain aging.

| Study model   | Methods   | Brain area        | Aging markers  | Interpretation  | Ref                   |
|---|---|-------------------|--|---|-----------------------|
| 10-week-old Kunming mice<br>Groups:<br>(1) control (0.9% saline,<br>s.c)<br>(2) D-gal (50 mg/kg/d,<br>s.c)            | - AGEs, RAGE by immunosorbent assay   | Prefrontal cortex | • † AGES   | D-gal-induced brain aging by increasing advanced glycation end products and its receptors.  | (Lu et al., 2010b)    |
| Duration: 8 weeks 3-month-old Kumming mice Groups: (1) control (0.9% saline, s.c) (2) D-gal (180 mg/kg/d, inj)        | - AGE by ELISA<br>- AR, SDH, RAGE by PCR  | Whole brain       | • ↑ AGE<br>• ↑ RAGE<br>• ↑ AR<br>• ↑ SDH   | D-gal-induced brain aging by increasing advanced glycation end products, its receptors, aldose reductase and sorbitol dehydrogenase.    | (Yu et al., 2015)     |
| Duration: 8 weeks 3-month-old Sprague-Dawley rats Groups: (1) control (0.9% saline, s.c) (2) D-gal (120 mg/kg/d, s.c) | <ul> <li>- SA-β-gal (Senescence associated β-galactosidase cytochemical staining)</li> <li>- telomere length by Southern blot</li> <li>- telomerase by TRAP-PCR</li> <li>- p53, p19<sup>Arf</sup>, p21<sup>Gp1/Wafl</sup> by qRT-PCR</li> </ul> | Hippocampus       | - Senescence-associated genes:  • ↑ p53  • ↑ p19^Arf  • ↑ p21 <sup>CIP1/Waf1</sup> | D-galactose-induced hippocampus senescence by regulating telomere length, senescence-associated genes, and function of lysosomes.       | (Zhu et al., 2014)    |
| Duration: 6 weeks   |   |                   | - Function of the lysosomes:  • ↑ SA-β-gal staining  • ↓ telomere lengths          |   |                       |
| 3-month-old Sprague-Dawley rats Groups: (1) control (0.9% saline, s.c) (2) D-gal (100 mg/kg/d, i.p.)                  | - Aβ, BACE-1, RAGE by Western Blot<br>- Aβ by Immunofluorescence Analysis   | Whole brain       | - ↓ telomerase activity - Amyloid protein: • ↑ BACE-1 • ↑ Aβ • ↑ RAGE              | D-galactose induced brain aging by increasing amyloid protein, beta-secretase 1 and advanced glycation end products receptor.           | (Rehman et al., 2017) |
| Duration: 7 weeks 3- month-old Kunning mice Groups: (1) Control (2) D-gal (200 mg/kg/d, i.p)                          | - p21, p53, $A\beta_{1-42}$ by Western Blot   | Hippocampus       | • † AGE<br>• † p16, p21, p53<br>• † Aβ <sub>1-42</sub>                             | D-galactose induced hippocampal senescence by increasing advanced glycation end products, its receptor and senescence-associated genes. | (Chen et al., 2016)   |
| Duration: 8 weeks   |   |                   |  |   |                       |

s.c. subcutaneous; AGEs: advanced glycation endproducts; RAGE: AGE receptors; inj: injection; ELISA: enzyme-linked immunosorbent assay; AR: aldose reductase; SDH: sorbitol dehydrogenase; PCR: polymerase chain reaction; SA-β-gal: senescence-associated β-galactosidase; TRAP-PCR: qualitative real time PCR; Aβ: amyloid beta protein; BACE-1: β-site amyloid precursor protein cleaving enzyme 1; i.p.: intraperitoneal.

 Table 2

 D-galactose-induced mitochondrial dysfunction in aging models.

| Study model   | Methods  | Brain area       | Major finding  |  | Interpretation  | Ref                          |
|---|--|------------------|--|--|---|------------------------------|
|   |  |                  | Mitochondrial findings   | Related findings   |   |                              |
| 2-month-old Shanghai C57BL/   | - Mitochondrial respiration by Clark oxygen  | Whole brain      | - Oxidative phosphorylation:   | (-)  | D-galactose induced mitochondrial   | (Long et al.,                |
| o J nite<br>Groups:<br>(1) control (0.9% saline,<br>s.c)<br>(2) D-gal (100 mg/kg/d, | erectroue<br>- Assay of mitochondrial enzyme activities and<br>kinetics by spectrophotometer   |                  | ↓ state 3 respiration     ↓ respiratory control ratio (RCR)     ↓ ADP/O ratio     ← maximum                      |  | dysunction by decreasing oxidative phosphorylation enzyme activity in the mitochondria of senescence mice brain.  | 2007)                        |
| s.c)  |  |                  | velocity (Vmax) and substrate binding affinity (Km) of the complexes   |  |   |                              |
| 2–3 month-old Male Swiss albino mice  | - NADH dehydrogenase, succinate<br>dehydrosenase activity, cytochrome oxidase.   | Whole Brain      | - Oxidative phosphorylation:   | - Antioxidant enzymes:   | D-galactose induced mitochondrial dvsfunction and biochemical changes by  | (Kumar et al., 2009: Prakash |
| Groups: (1) Naive (0.5% sodium  | activity MDA and glutathione, catalase, superoxide dismutase, and glutathione-S-transferase activity MDA and nitrite lavel reseased by   | cerebellum)      | • \understand NADH dehydrogenase, succinate dehydrogenase activity,  | • \ \precedent \ glutathione, catalase, superoxide dismutase,  | ayamacos and social and subject of accessing antioxidant enzymes, oxidative accessing antioxidant enzymes, oxidative absorbed stime and cell viability in | and Kumar,<br>2013)          |
| 0.5 ml/100 g/d, p.o)<br>(2) D-gal (100 mg/kg/d,                                     | spectrophotometer  |                  | - Cell viability:  | transferase activity   | senescence mice.  |                              |
| s.c)<br>Duration: 6 weeks   |  |                  | • ↓MTT ability   | <ul> <li>Oxidative stress:</li> <li>↑ MDA, and nitrite level</li> <li>Apoptosis:</li> </ul>                              |   |                              |
| 3-month-old Kunming mice  | - Complex I, II, III, IV activity by   | Cerebral cortex  | - Oxidative phosphorylation:   | • † caspase 3<br>- Oxidative stress:   | D-galactose decreased the activity of   | (Zhang et al.,               |
| Groups: (1) control (0.9% saline, s.c) (2) model (D-gal, 150 mg/                    | spectrophotometer - Changes in MMP, ROS by fluorescent plate reader - TNOS, iNOS by commercially available kits.   | and hippocampus  | • \$\psi\$ complex I, II, III, IV activity - Function:   | <ul><li>↑ ROS,</li><li>↑ TNOS and iNOS</li></ul>   | mitochondria respiratory chain/oxidative phosphorylation system and cell viability by causing oxidative stress.   | 2010)                        |
| kg/d, s.c)  |  |                  | • ↓ MMP  |  |   |                              |
| Duration: 6 weeks<br>1-month-old male   | - Serum $H_2O_2$ , T-SOD activity and MDA assay by   | Ventral          | - Structural changes:  | - Oxidative stress:  | D-galactose induced the accumulation of   | (Du et al.,                  |
| Sprague–Dawley rats Groups: (1) control (0.9% saline,                               | colonmetric kits  - Tissue H <sub>2</sub> O <sub>2</sub> assay by an Enhanced BCA  Protein Assay Kit  - NOX2 - 0.29plox - 447phox - 467phox by RT-PCR                                    | cocniear nucleus | <ul> <li>† mtDNA common deletion (CD),</li> <li>Swollen with a reduced electron density in the matrix</li> </ul> | <ul> <li>↑ H<sub>2</sub>O<sub>2</sub></li> <li>↑ MDA, 8-OHdG</li> <li>↑ n<sub>2</sub>2phox n<sub>4</sub>7phox</li> </ul> | mtDNA mutations, the decline of A1P and MMP and the activation of caspase-3-dependent apoptosis in the central auditory exerem via increasine NOX2        | 2015)                        |
| (2) D-gal (L) 150 mg/kg/d,s.c,  | - NOX2 and 8-OHdG by immunohistochemical analysis  |                  | - Oxidative, phosphorylation:  | p67 <sup>phox</sup> of NOX2  | expression.   |                              |
| (3) D-sat (m) 300 mg/kg/<br>d, s.c.<br>(4) D-gal (H) 500 mg/kg/                     | - p.z. , p.t. , p.o. , caspase s, cyc. by Western blot - DNA isolation and determination of the  |                  | ● ↓ ATP  | • T-SOD  |   |                              |
| d, s.c,   | mtDNA common deletion by Genomic DNA<br>Purification Kit   |                  | - Function:  | - Apoptosis:   |   |                              |
| Duration: 8 weeks   | <ul> <li>ultrastructure of mitochondria by TEM</li> <li>Detection of ATP levels by BCA assay kit</li> <li>Measurement of MMP by fluorescent</li> <li>anontosis by TIMFI assay</li> </ul> |                  | UMMP     Note: All doses of D-galactose show the same effects  | • † cyt. c and cleaved caspase-3   |   |                              |
| 1-month-old Sprague–Dawley  | - DNA isolation and determination of mtDNA   | Auditory cortex  | - Structure:   | <ul> <li>↑ TUNEL-positive cells</li> <li>DNA repair enzymes:</li> </ul>  | D-galactose induced mtDNA damage  | (Chen et al.,                |
| rats<br>Groups:<br>(1) control (0.9% saline,  | 4834 bp deletion by Genomic DNA Purification<br>Kit<br>- RNA preparation and quantitative RT-PCR   |                  | ullet mtDNA common deletion (CD)   | $ullet$ $\downarrow$ OGG1, pol $_{\scriptscriptstyle \gamma}$  | resulted from decreased DNA repair<br>enzymes and increased apoptosis leading<br>to presbycusis in aging rats.  | 2011)                        |
| s.c)  |  |                  |  | - $\uparrow$ TUNEL-positive cells  |   | (continued on next page)     |

(continued on next page)

| _         |
|-----------|
| $\sim$    |
| . 2       |
| 2         |
| -         |
| =         |
| 'n        |
| 7         |
| =         |
| $\approx$ |
| $\sim$    |
| _         |
| 2         |
| ٠.        |
| a)        |
| _         |
| Φ         |
|           |

| Study model  | Methods   | Brain area      | Major finding  |  | Interpretation   | Ref                     |
|--|---|-----------------|--|--|--|-------------------------|
|  |   |                 | Mitochondrial findings   | Related findings   |  |                         |
| (2) D-gal (150 mg/kg/d, s.c) (3) D-gal (300 mg/kg/d, s.c) (4) D-gal (500 mg/kg/d, s.c)   | - OGG1, pol $_{\nu}$ by Western blot - apoptosis by TUNEL staining  |                 | - Note: All doses of D.galactose show<br>the same effects.   |  |  |                         |
| Duration: 8 weeks 5-week-old male Sprague- Dawley rats Groups: (1) the control group (0.9% saline, s.c) (2) D-gal group (500 mg/kg/d, s.c) | <ul> <li>quantity of the mtDNA CD by TaqMan real-<br/>time PCR</li> <li>ultrastructure of the hippocampal<br/>mitochondria was observed under Transmission<br/>Electron Microscopy</li> <li>NOX and UCP2 by Western Blot</li> </ul> | Hippocampus     | <ul> <li>Structural changes:</li> <li> <ul> <li>↑ mtDNA common deletion (CD),</li> <li>◆ Significant swelling of all mitochondrial spaces, including cristae with a reduced electron density in the matrix.</li> </ul> </li> </ul> | - Oxidative stress:  • ↑ p91 phox, p22phox, p47phox, p67phox of NOX in hippocampus | D-galactose induced brain mitochondria dysfunction, as indicated by common deletion of mitochondria DNA, impaired mitochondria structures in the hippocampus and increased oxidative stress, which mechanism may partly be related to NOX-dependent pathway. | (Du et al., 2012)       |
| Duration: 8 weeks  |   |                 | -Oxidative stress:   |  |  |                         |
| 2-month-old Sprague Dawley rats<br>Grouns:   | - SOD, MDA by spectrophotometer<br>- ultrastructure of mitochondria by<br>Transmission electron microscopy  | Auditory cortex | • † UCP2<br>- Structure changes:<br>• † mtDNA CD. swollen mitochondria   | - Antioxidant enz:   | D-galactose induced oxidative stress accumulated with aging, mitochondria dysfunction, abnormal ultrastructural  | (Zeng et al.,<br>2014)  |
| (1) control (0.9% saline, s.c)   | - DNA extraction and cDNA generation by Genomic DNA  Purification Kit   |                 | - Mitochondrial protein acetylation  | - Oxidative stress:  | changes and auditory cortex cell apoptosis   |                         |
| S.C)   | - Quantification of mtDNA 4834 bp deletion by<br>TaqMan real-time PCR assay   | ٨               | • ↓ mRNA expression of Sirt3   | ● ↑MDA   |  |                         |
| Duration: 8 weeks  | - Gene expression analysis using real-time PCR - Sirt and SOD by Western blot and immunofluorescence - apoptosis by TUNEL staining  |                 |  | - enlarged endoplasmic reticulum and disrupted myelin                              |  |                         |
| 4-month-old Wistar rats<br>Groups:<br>(1) control (methyl  | - GSH, GPx, MDA, protein thiol ( - SH) groups, AOPP (Advanced oxidation protein products), Acotinase, complex I, II, IV by  | ;, Whole brain  | <ul> <li>Oxidative phosphorylation:</li> <li>↓ NADH-co Q oxidoreductase (I),</li> </ul>  | - Antioxidant enz:  • ↓ GSH, GPx   | D-galactose induced mitochondrial oxidative phosphorylation, tricarboxylic acid cycle enzymes, biochemical changes   | (Banji et al.,<br>2014) |
| cellulose, 2%, in distilled water, p.o) (2) D-gal (150 mg/kg/d, s.c)   | spectrophotometer -caspase 3 by western blot - succinate dehydrogenase by spectroscopic techniques  |                 | succinate-co Q oxidoreductase (II), co Q-cytochrome C oxidoreductase (III), cytochrome C oxidase (IV)  | <ul> <li>Oxidative stress:</li> <li>↑ MDA, AOPP and</li> </ul>                     | and histological alterations.  |                         |
| Duration: 7 weeks  | - complex III chromatography  |                 | <ul> <li>Tricarboxylic acid cycle enzymes:</li> <li></li></ul>   | protein carbonyls<br>- Apoptosis:  |  |                         |
|  |   |                 |  | • † caspase-3  |  |                         |
|  |   |                 |  | - damage to neurons in CA1 region  | ***************************************  | (continued on next name |

| Methods Methods Brain area Major findings Related findings  Mitochondrial findings Related findings  Mitochondrial findings (−)  Mitochondrial findings (−)  Mitochondrial findings (−)  Antioxidant (−)  ability:  ability:  ability:  ability:  pripheral benzodiazepine receptors  group  group  gg/d, | rapic = (continued)             |  |                 |                                     |                  |   |                        |
|---|---------------------------------|--|-----------------|-------------------------------------|------------------|---|------------------------|
| Mitochondrial findings Related findings - Antioxidant (−) ability:  • ↓ mitochondrial peripheral benzodiazepine receptors   | Study model                     | Methods  | Brain area      | Major finding                       |                  | Interpretation  | Ref                    |
| - Antioxidant ability:  • ↓ mitochondrial peripheral benzodiazepine receptors   |                                 |  |                 | Mitochondrial findings              | Related findings |   |                        |
|   | Middle-aged Sprague-Dawley rats | - Peripheral-type benzodiazepine binding sites<br>by autoradiographic localization | Cerebral cortex | - Antioxidant<br>ability:           | (-)              | D-galactose decreased the antioxidant ability in mitochondria from cerebral | (Chen et al.,<br>2008) |
| group<br>kg/d,  | (1) control (0.9% saline,       |  |                 | • \underset mitochondrial           |                  | Correction  |                        |
| (2) Mimetic aging group (10% D-gal, 1 ml/kg/d, s.c)   | s.c)                            |  |                 | peripheral benzodiazepine receptors |                  |   |                        |
| (10% D-gal, 1 ml/kg/d, s.c) S.c.  | (2) Mimetic aging group         |  |                 |                                     |                  |   |                        |
| S.C.) Demotions of models   | (10% D-gal, 1 ml/kg/d,          |  |                 |                                     |                  |   |                        |
| Demostrace O consults   | s.c)                            |  |                 |                                     |                  |   |                        |
|   | Duration: 0 wooled              |  |                 |                                     |                  |   |                        |

s.c. subcutaneous, ADP/O: Phosphate/Oxygen Ratio; p.o.: per oral; NADH: Nicotinamide adenine dinucleotide; MTT: tetrazolium dye; MDA: malondialdehyde; MMP: mitochondrial membrane potential; ROS: reactive oxygen species; TNOS: total nitric oxide synthase; iNOS: inducible nitric oxide synthase; H<sub>2</sub>O<sub>2</sub>, hydrogen peroxide; T-SOD: total superoxide dismutase; BCA: bicinchoninic acid; 8-OHdG = 8-hydroxy-2'-deoxyguanosine; ATP: Adenosine triphosphate; NOX: NADPH oxidase; mtDNA: mitochondria DNA; TEM: transmission electron microscopy; TUNEL: terminal deoxynucleotidyl transferase dUTP nick end labeling, UCP2: GPx: glutathione peroxidase; co Q: coenzyme uncoupling protein 2; cDNA: complementary DNA; bp: base pair; PCR: polymerase chain reaction; GSH: glutathione;

degeneration and apoptosis, raised oxidative stress, decreased ATP production, increased mitochondrial DNA mutation, impaired mitochondrial structure and control of abnormal gene expression in the brain (Banji et al., 2014; Kumar et al., 2009; Lei et al., 2008; Prakash and Kumar, 2013; Ullah et al., 2015).

D-galactose is an aldohexose that occurs naturally in the body, including in the brain (Nagy and Pohl, 2015). However, it is known that when an exogenous dose of D-galactose is given beyond normal concentration, this can induce aging effects in several organs by increasing oxidative stress, apoptosis and inflammation (Ou et al., 2016; Rehman et al., 2017; Ullah et al., 2015). Among the various organs in the body. the brain is the organ most vulnerable to oxidative stress due to its high metabolic activity, high lipid content and limited antioxidant defense mechanisms (Çakatay, 2010). In addition, several studies have described that brain aging is attributed to mitochondrial functions (Banji et al., 2014; Chen et al., 2011; Du et al., 2012; Du et al., 2015; Kumar et al., 2009; Long et al., 2007; Prakash and Kumar, 2013; Zeng et al., 2014). The underlying mechanisms of D-galactose-induced brain aging have yet to be discovered. The aim of this article is to comprehensively summarize and discuss the underlying mechanisms of D-galactose-induced brain aging, particularly via alterations in brain mitochondria and cognitive function as well as to summarize the different therapeutic approaches on D-galactose-induced brain aging. The article also discusses the findings that elucidate mitochondrial DNA mutations, respiratory chain enzymes, antioxidant ability and structural changes in the aging brain. It additionally outlines mitochondria-targeted therapies in D-galactose-induced brain senescence models.

#### 1.1. D-galactose metabolism

D-galactose is a reducing sugar and it occurs in many foods such as honey, beets, cheese, yoghurt, butter, milk, kiwi fruit, soy sauce, plums, dry figs, cherries, and celery (Acosta and Gross, 1995). When D-galactose rich food is eaten, the sugar reaches the intestinal lumen and it is transported by sodium-dependent glucose cotransporters type 1 (SGLT-1) into the cells and leaves the cells by glucose transport type 2 (GLUT-2), then enters the blood stream (Bjelakovic et al., 2011). Normally, two enzymes, galactokinase and uridyl transferase, metabolize D-galactose into glucose, which enters the glycolysis pathway or is stored as glycogen in liver, muscle and adipose tissue (Coelho et al., 2015). The mediation of the uptake of D-galactose into the brain through blood brain barrier is by glucose transport type 1 (GLUT-1) (Cura and Carruthers, 2012). The normal concentration of D-galactose in the blood is less than 10 mg/dL (Berry, 1993). For a healthy adult, the maximal recommended daily dose is 50 g of galactose and most of it can be eliminated from the body within about 8 h after ingestion (Morava, 2014).

However, oversupply of D-galactose can give rise to the generation of ROS causing mitochondrial dysfunction, oxidative stress, inflammation and apoptosis in neuronal cells (Kumar et al., 2009; Prakash and Kumar, 2013; Qu et al., 2016; Rehman et al., 2017; Ullah et al., 2015). Therefore, the use of long-term injections of D-galactose is a well-known method in the study of aging, as indicated by increased aging markers such as advanced glycation end products (AGE), receptors for advanced glycation end product (RAGE), aldose reductase (AR), sorbitol dehydrogenase (SDH), telomere length shortening, telomerase activity, beta-site amyloid precursor protein cleaving enzyme 1 (BACE-1), amyloid beta protein  $(A\beta_{1-42})$ , senescence-associated genes (p $^{16}$ , p $^{21}$ , p $^{53}$ , p $^{19Arf}$ , p $^{21Cip1/Waf1}$ ) and senescence-associated beta-galactosidase (SA- $\beta$ -gal) staining. All of these findings are summarized in Table 1.

In addition to aging markers, several previous studies have demonstrated that a chronic supply of D-galactose causes a deterioration in cognitive function that is correlated to symptoms of brain aging and thus, is used as the model of an accelerated aging brain in rodents (Haider et al., 2015; Lu et al., 2007; Lu et al., 2010b; Xian et al., 2014;

 $\label{eq:total_condition} \textbf{Table 3}$  The rapeutic approach on brain mitochondrial aging induced by D-galactose.

| Study model   | Methods  | Brain area                               | Major finding  |   | Interpretation   | Ref                       |
|---|--|--|--|---|--|---------------------------|
|   |  |  | Mitochondrial findings   | Related findings  |  |                           |
| 2-month-old Shanghai C57BL/   | - Mitochondrial respiration by Clark oxygen  | Whole brain                              | - Oxidative phosphorylation:   | (-)   | R-alpha-lipoic acid treatment ameliorated the  | (Long et al.,             |
| 6.5 mice<br>Groups:<br>(1) control (0.9% saline, s.c.)<br>(2) normal treated with R-alpha-lipoic acid<br>(1A),100 mg/kg/d, i.p<br>(3) D-gal (100 mg/kg/d, s.c.)<br>+ LA treatment (100 mg/kg/d, s.c.)<br>kg/d, i.p)   | electrode<br>- Assay of mitochondrial enzyme activities and<br>kinetics by spectrophotometer   |  |  |   | D-gal-induced mitochondrial dystunction by restoring the oxidative phosphorylation enzyme activity.  | C2007                     |
| Duration: 6 weeks.  2-3 month-old Male Swiss albino mice Groups:  (1) Naive (0.5% sodium carboxymethyl cellulose, 0.5 m./100 %, p. o)   | - NADH dehydrogenase, succinate dehydrogenase activity, MTT ability, glutathione, catalase, superoxide dismutase, and glutathione-S-transferase activity, MDA, and nitrite level by spectrophotometer                                | Whole brain<br>(excluding<br>cerebellum) | <ul> <li>Oxidative phosphorylation:</li> <li>↑ NADH dehydrogenase,<br/>succinate dehydrogenase activity</li> <li>Cell viability:</li> </ul>  | <ul> <li>Oxidative stress:</li> <li>↓ MDA, and nitrite level</li> <li>Antioxidant enz:</li> </ul>   | Carvidilol (CAR) attenuate D-galactose-<br>induced mitochondrial dysfunction,<br>biochemical changes by increasing antioxidant<br>enzymes, oxidative phosphorylation, and cell<br>viability in senescence mice.  | (Kumar et al., 2009)      |
| (2) CAR (5 mg/kg/d, 5.C)<br>(4) CAR (5 mg/kg/d, p.o)<br>(4) CAR (2.5 mg/kg/d, p.o)<br>+ D-gal (100 mg/kg/d, s.c)<br>(5) CAR (5 mg/kg/d, p.o)<br>+ D-gal (100 mg/kg/d, s.c)  |  |  | <ul> <li>↑ MTT ability</li> <li>Note: High dose CAR (5 mg/kg/d) was more effective than low dose CAR (2.5 mg/kg/d) in all parameters.</li> </ul>   | † glutathione, catalase,<br>superoxide dismutase,<br>and glutathione-S-<br>transferase activity   |  |                           |
| Duration: 6 weeks 3-month-old Male Laca mice Groups:  (1) Naïve (0.5% sodium carboxymethyl cellulose, 1 ml/100 g/d, p.o.) (2) D-gal (100 mg/kg/d, p.o.) (3) PlO (10 mg/kg/d, p.o.) (4) PlO (30 mg/kg/d, p.o.) (5) PlO (10 mg/kg/d, p.o.) (6) PlO (30 mg/kg/d, p.o.) (6) PlO (30 mg/kg/d, p.o.) (7) Pisphenol A digycidyl ether (BADGE) (PPAR, antagonist) (15 mg/kg/d, p.o.) + PlO (30 mg/kg/d, p.o.) + PlO (30 mg/kg/d, p.o.) + PlO (30 mg/kg/d, | - NADH dehydrogenase, succinate dehydrogenase activity, cytochrome oxidase, MTT ability, glutathione, catalase, superoxide dismutase, and glutathione-S-transferase activity, MDA, and nitrite level, caspase 3 by spectrophotometer | Whole brain (excluding cerebellum)       | - Oxidative phosphorylation:  • ↑NADH dehydrogenase, succinate dehydrogenase, cytochrome oxidase  - Cell viability:  • ↑ MTT ability  - BADGE treatment blocked the protective effect of pioglitazone.  - Note: High dose - PIO (30 mg/kg/d) was more effective than low dose PIO (10 mg/kg/d) in all parameters except in caspase 3 activity. | - Antioxidant enz.  • † glutathione, catalase, superoxide dismutase, and glutathione-5-transferase activity  - Oxidative stress:  • ↓ MDA, nitrite level  - Apoptosis:  • ↓ caspase-3 | Pioglitazone (PIO) attenuates D-galactose-induced mitochondrial dysfunction, oxidative stress and apoptosis by increasing antioxidant enzymes, oxidative phosphorylation, and cell viability in senescence mice through activation of PPARy receptors. | (Prakash and Kumar, 2013) |
| Duration: 6 weeks 3-month-old Kunming mice Groups: (1) control (0.9% saline, s.c) (2) model (D-gal,150 mg/  | - Complex IV activity by spectrophotometer<br>- Changes in MMP, ROS by fluorescent plate<br>reader<br>- TNOS, iNOS by commercially available kits.   | Cerebral cortex<br>and<br>hippocampus    | <ul> <li>Oxidative phosphorylation:</li> <li>↑ complex I, II, III, IV activity</li> </ul>  | <ul> <li>Oxidative stress:</li> <li>↓ ROS</li> <li>↓ TNOS and iNOS</li> </ul>   | Catalpol could ameliorate D-galactose induced mitochondrial dysfunction and biochemical changes by decreasing oxidative stress.  | (Zhang et al., 2010)      |
| kg/d, s.c)  |  |  |  |   | (conti   | (continued on next page)  |

| (continued) |  |
|-------------|--|
| ble 3       |  |
| Ta          |  |

| Study model  | Methods   | Brain area      | Major finding                                       |  | Interpretation  | Ref                      |
|--|---|-----------------|---|--|---|--------------------------|
|  |   |                 | Mitochondrial findings                              | Related findings   |   |                          |
| (3) catalpol (2.5 mg/kg/d, s.c) + D gal (150 mg/kg/d,  |   |                 | - Cell viability:                                   |  |   |                          |
| s.c)<br>(4) catalnol (5 mg/kg/d  |   |                 | • MMP   |  |   |                          |
| (c) canapa $(C)$ |   |                 | 770777  |  |   |                          |
| s.c)   |   |                 | - Note: All doses of Catapol show the               |  |   |                          |
| (5) catapol (10 mg/kg/d,<br>s.c) + D gal (150 mg/kg/d,   |   |                 | same enects.  |  |   |                          |
| s.c)   |   |                 |   |  |   |                          |
| Duration: 6 weeks  |   |                 |   |  |   |                          |
| Adult male BALB/c mice<br>Groups:  | - Active mitochondria levels by MitoTracker<br>Green staining                               | Whole brain     | - † Active mitochondrial levels                     | - Oxidative stress:  | Transcranial low level laser therapy (LLLT) increased active mitochondria levels            | (Salehpour               |
| (1) control (0.9% saline, s.c)   |   |                 | - Oxidative phosphorylation:                        | •   ROS  | membrane potential, ATP production and  |                          |
| (2) D-gal + snam (500 mg/<br>kg/d, s.c)  | determination by Miltochondria Staining Kit - Mitochondrial cytochrome $c$ oxidase activity |                 | • † cytochrome C oxidase (IV)                       | - Apoptosis:   | abrogated oxidative stress, apoptosis leading<br>to restore mitochondrial dysfunction in D- |                          |
| (3) D-gal + red 4 (D-gal   | by commercial kits  |                 | • † ATP   |  | galactose-induced aging mice.   |                          |
| $+4 \text{ J/cm}^2 \text{ of red laser}$   | - Bax/Bcl-2, Caspase 3 by western blot  |                 | T   | • \ Bax/Bcl-2 ratio  |   |                          |
| (4) $D$ -gal + MK 4 ( $D$ -gal + $4 \text{ J/cm}^2$ of MR laser)   | - ATP levels by Colorinlettic assay kit<br>- ROS by Fluorescent dve                         |                 | - ruiction:   | ^ casbase-o  |   |                          |
| (5) D-gal + red 8 (D-gal   | dichlorohydrofluorescein diacetate  |                 | • † MMP   | - Note: Higher dose of                                     |   |                          |
| + 8 J/cm² ot red laser)<br>(6) D-gal + NIR 8 (D-gal  | - Barnes Maze test<br>- What-Where-Which task   |                 |   | LLLT exerted a better<br>response than low dose            |   |                          |
| + 8 J/cm <sup>2</sup> of NIR laser)  |   |                 |   | (4 J/cm2).   |   |                          |
| Duration: 6 weeks  |   |                 |   |  |   |                          |
| 4-month-old Wistar rats  | - GSH, GPx, MDA, protein thiol (- SH) groups,   | Whole brain     | - Oxidative phosphorylation:                        | - Antioxidant enz:   | Curcumin and hesperidin (HES) attenuated D-   | O- (Banji et al.,        |
| (1) Control (methyl  | Acotinase, complex I. II. IV by   |                 | ● ↑ NADH-co O oxidoreductase (I).                   | • ↑ GSH. GPx   | and apoptosis by increasing oxidative   |                          |
| cellulose, 2%, in distilled  | spectrophotometer   |                 | succinate-co Qoxidoreductase                        |  | phosphorylation enzymes and tricarboxylic   |                          |
| water, p.o)  |   |                 | (II), co Q-cytochrome C                             | - Oxidative stress:  | acid cycle enzymes and improve the functional   | T .                      |
| (2) D-gal (150 mg/kg/d, s.c)   | - succinate dehydrogenase by spectroscopic  |                 | oxidoreductase (III), cytochrome                    | bee and AdM  | capacity of neurons.  |                          |
| (s) Curcunin (so mg/ kg/ d,<br>p.o) + D-gal (150 mg/kg/ d,   | reciniques-<br>- complex III by chromatography- techniques                                  |                 | C Oxidase (IV)                                      | <ul> <li>↓ IMDA, AOPP and<br/>protein carbonyls</li> </ul> |   |                          |
| s.c)   |   |                 | - Tricarboxylic acid cycle enzymes:                 |  |   |                          |
| (4) HES $(10 \text{ mg/kg/d}) + \text{D-}$   |   |                 |   | - Apoptosis:   |   |                          |
| gal (150 mg/kg/d, s.c)   |   |                 | <ul> <li>† succinate dehydrogenase &amp;</li> </ul> |  |   |                          |
| (5) Curcumin (50 mg/kg/d)<br>+ HES (10 mg/kg/d) + D-   |   |                 | aconitase   | • ↓ caspase-3  |   |                          |
| gal (150 mg/kg/d, s.c)   |   |                 | - Note: Higher dose of the                          |  |   |                          |
| (6) Curcumin (100 mg/kg/   |   |                 | combination of curcumin with HES                    |  |   |                          |
| gal (150 mg/kg/d, s.c)   |   |                 | dose combination and individual                     |  |   |                          |
| Duration: 7 weeks  |   |                 | tnerapy.  |  |   |                          |
| Middle-aged Sprague-Dawley   | - Peripheral-benzodiazepine Binding by autoradiographic localization                        | Cerebral cortex |   | (-)  | Dehydroepiandrosterone (DHEA) attenuated<br>D-galactose induced mitochondrial               | (Chen et al., 2008)      |
|  |   |                 |   |  |   | (continued on next page) |

| Table 3 (continued)              |         |            |                                     |                  |  |     |
|----------------------------------|---------|------------|-------------------------------------|------------------|--|-----|
| Study model                      | Methods | Brain area | Major finding                       |                  | Interpretation                               | Ref |
|                                  |         |            | Mitochondrial findings              | Related findings |  |     |
| Groups:                          |         |            | - Antioxidant                       |                  | dysfunction by strengthening the antioxidant |     |
| (1) control (0.9% saline, s.c)   |         |            | ability:                            |                  | ability.                                     |     |
| (2) Mimetic aging group          |         |            |                                     |                  |  |     |
| (10% D-gal, 1 ml/kg/d, s.c)      |         |            | • ↑ mitochondrial                   |                  |  |     |
| (3) 2% DHEA-treated normal       |         |            | peripheral benzodiazepine receptors |                  |  |     |
| group $(1 \text{ ml/kg/d, i.p})$ |         |            |                                     |                  |  |     |
| (4) Vehicle control group        |         |            |                                     |                  |  |     |
| (2%  DMSO, i.p) + 10%  D         |         |            |                                     |                  |  |     |
| gal (1 ml/kg/d, s.c)             |         |            |                                     |                  |  |     |
| (5) 2% DHEA-treated              |         |            |                                     |                  |  |     |
| senescent group (1 ml/kg/d,      |         |            |                                     |                  |  |     |
| i.p) + 10% D-gal, (1 ml/kg/      |         |            |                                     |                  |  |     |
| d, s.c)                          |         |            |                                     |                  |  |     |
| Duration: 8 weeks                |         |            |                                     |                  |  |     |

D.gal: D.galactocs; s.c. subcutaneous; i.p.: intraperitoneal; ADP/O: Phosphate/Oxygen Ratio; p.o.: per oral; NADH: Nicotinamide adenine dinucleotide; MTT: tetrazolium dye; MDA: malondialdehyde; MMP: mitochondrial membrane potential; ROS: triphosphate; NOX: NADPH oxidase; p22phox, p47phox, p67phox: subunit of NOX; cyt c: cytochrome c; DNA: Deoxyribonucleic acid; mtDNA: mitochondria DNA; TEM: transmission electron microscopy; TUNEL: terminal deoxynucleotidyl bicinchoninic acid; 8-OHdG: 8-hydroxy-2'-deoxyguanosine; ATP: Adenosine reactive oxygen species; TNOS: total nitric oxide synthase; iNOS: inducible nitric oxide synthase; H2O2: hydrogen peroxide; T-SOD: total superoxide dismutase; BCA: transferase dUTP nick end labeling; UCP2:

Zhang et al., 2011; Zhu et al., 2014). The important underlying mechanisms of brain aging are related to increased oxidative stress and mitochondrial dysfunction. The effect of D-galactose-induced brain aging on oxidative stress and mitochondrial dysfunction are crucial to the understanding of the aging process and are presented and discussed in the following paragraph.

### 1.2. The effects of D-galactose-induced mitochondrial dysfunction and oxidative stress in the brain

There is a growing body of evidence which indicates that the mechanism of D-galactose-induced oxidative stress is occurring at a subcellular level, specifically in the brain mitochondria (Banji et al., 2014; Kumar et al., 2009; Prakash and Kumar, 2013; Zhang et al., 2010). When there is increase in D-galactose concentration, it is oxidized by galactose oxidase to form hydrogen peroxide (H2O2), leading to decrease in superoxide dismutase (SOD) (Hsieh et al., 2009). Increased H<sub>2</sub>O<sub>2</sub> reacts with a reduced form of iron (Fe) to form hydroxide ions (OH<sup>-</sup>). The H<sub>2</sub>O<sub>2</sub> and OH<sup>-</sup> are both types of reactive oxygen species (ROS) and along with others can cause lipid peroxidation in the cell membranes and impair redox homeostasis, leading to neuronal damage (Hsieh et al., 2009). In addition, D-galactose reacts with amines to form an unstable compound (called Schiff's base product) which undergoes several reactions over a period of days to form a more stable compound known as the Amadori product (Ansari and Dash, 2013; Golubev et al., 2017). This Amadori product converts irreversibly to a compound known as an advanced glycation end product (AGE) over months/years (Hsieh et al., 2009). When AGE binds with its receptor RAGE, an increase in nicotinamide adenine dinucleotide phosphate (NADPH) oxidase and ROS production occurs, resulting in neuronal damage and cognitive dysfunction (Hsieh et al., 2009). Additionally, a high level of D-galactose is reduced by galactose reductase to form galactitol which results in osmotic stress and reduces the activity of the electron transport chain (ETC) in the mitochondria with resulting increased ROS production, finally causing mitochondrial dysfunction (Hsieh et al., 2009). Other oxidative stress markers in D-galactose-induced brain aging assessed in those studies were malondialdehyde (MDA), nitrite level, H<sub>2</sub>O<sub>2</sub>, 8-oxoguanine, p91<sup>phox</sup>, p22<sup>phox</sup>, p47<sup>phox</sup>, p67<sup>phox</sup> of NADPH oxidase (NOX) 2, total nitric oxide synthase (TNOS), inducible nitric oxide synthase (iNOS), ROS, protein carbonyl and AOPP.

As regards D-galactose reduced respiratory chain enzymes, four studies pointed out that all respiratory chain complexes enzymes such as NADH-co Q oxidoreductase (I), succinate-co Q oxidoreductase (II), co Q-cytochrome C oxidoreductase (III), cytochrome C oxidase (IV) were damaged as a result of D-galactose injection (Banji et al., 2014; Kumar et al., 2009; Prakash and Kumar, 2013; Zhang et al., 2010). However, Long and colleagues found that only succinate-co Q oxidoreductase activity was affected by D-galactose (Long et al., 2007). The differences in those findings might be due to differing methods being used to measure respiration enzyme activity. D-galactose not only reduced the activity of respiratory enzymes, but also the levels of tricarboxylic acid cycle enzymes (Banji et al., 2014). Chen and colleagues also showed that D-galactose decreased the antioxidant ability of mitochondria from the cerebral cortex via benzodiazepine receptors (Chen et al., 2008). These findings suggested that benzodiazepine receptors might be part of the mechanisms controlling mitochondrial respiration to protect against damage from ROS (Carayon et al., 1996).

In addition, several studies described that D-galactose induced the accumulation of brain mitochondrial DNA mutation (Chen et al., 2011; Du et al., 2012; Du et al., 2015; Zeng et al., 2014) through: 1) decreasing DNA-repairing enzymes (OGG1, pol,) (Chen et al., 2011), and 2) common deletion of mitochondrial DNA and impairing mitochondrial structures via the NOX-dependent pathway (Du et al., 2015).

Accumulating evidence indicates that D-galactose could induce brain aging by causing oxidative stress and mitochondrial dysfunction in different brain regions such as the hippocampus, cerebral cortex,

 $\begin{tabular}{ll} \textbf{Table 4} \\ \textbf{Cognitive function and related findings in $D$-galactose-induced aging models}. \\ \end{tabular}$ 

| Study model  | Methods   | Brain area                               | Major finding   |  | Interpretation  | Ref  |
|--|---|--|---|--|---|--|
|  |   |  | Cognitive function  | Related findings   |   |  |
| 8–10-week-old Kunming mice Groups: (1) control (0.9% saline, s.c) (2) D-gal (150 mg/kg/d, s.c) Duration: 8 weeks   | - Morris water maze test - Open field test - MDA, NO, GSH, SOD, AChE by commercial kit - IL-1β, NF-κB by ELISA - H&E and Nissl staining - Immunohistochemistry  | Whole brain                              | - Morris water maze:  • ↑ Escape latency • ↓Number of crossing • ↓ Time spent in the target quadrant • ⇔ Swimming speed                                       | - Oxidative stress:  • ↑ MDA • ↑ NO levels  - Antioxidant enz: • ↓ GSH, SOD  -Neuromodulation: • ↑ AChE  | D-galactose induced spatial<br>learning and memory<br>impairment, reduced<br>exploratory ability and<br>neuronal cell damage through<br>oxidative damage, dysfunction<br>of the cholinergic system,<br>increased inflammation and<br>apoptosis. | (Yang et a 2016)                                       |
|  |   |  | - Open field test:  | - Apoptosis:  • ↑ Caspase-3  - Inflammatory markers:  • ↑ NF-κB, IL-1β  - neuronal cell damage to  |   |  |
| 10-week-old Kunming mice Groups: (1) control (0.9% saline, s.c) (2) D-gal (50 mg/kg/d, s.c) Duration: 8 weeks  | - Morris Water Maze Test - Step-through passive avoidance task - NF-κB, COX-2, iNOS, TNFα, IL-<br>1β, IL-6 by Western Blot - AGEs, RAGE by Immunosorbent Assay - GFAP, CD11b by Immunofluorescence Staining - ROS, protein carbonyl by chromatography   | Prefrontal cortex                        | - Morris water maze:  • ↑ Escape latency • ↓ Number of crossing • ↓ Time spent in the target quadrant - Step-through passive avoidance task: • ↓ Latency time | the hippocampus  Oxidative stress:  ↑ Protein Carbonyl ↑ ROS  Inflammatory markers:  ↑ COX-2, iNOS, TNFα, IL-1β, IL-6, NF-κB  Aging marker:  ↑ AGEs, RAGE  - Activated astrocytes & microglia cells:   | D-galactose induced spatial learning and memory impairment via increasing oxidative stress, inflammation, aging process, and activated astrocytes and microglial cells.   | (Lu et al., 2010b)                                     |
| 2–3 month-old Male Swiss albino mice Groups: (1) Naive (0.5% sodium carboxymethyl cellulose, 0.5 ml/ 100 g/d, p.o) (2) D-gal (100 mg/ kg/d, s.c) Duration: 6 weeks | - Spatial navigation task (Morris water maze task) - Maze acquisition phase (training) - Maze retention phase (testing for retention of the learned task) - Elevated plus maze paradigm - Assessment of gross behavioral activity - glutathione, catalase, superoxide dismutase, and glutathione-S-transferase activity, MDA, and nitrite level, caspase3, AchE activity by spectrophotometer | Whole brain<br>(excluding<br>cerebellum) | - Morris water maze:  | ↑ GFAP, CD11b     Antioxidant enzymes:     ↓ glutathione, catalase, superoxide dismutase, and glutathione-S-transferase activity  -Oxidative stress:     ↑ MDA, and nitrite level  -Neuromodulation:     ↑ AchE     - Apoptosis:     ↑ caspase 3 | D-galactose induced spatial learning and memory impairment, oxidative stress and apoptosis by decreasing antioxidant enzymes, oxidative phosphorylation, and cell viability in senescence mice.   | (Kumar<br>et al., 200<br>Prakash ar<br>Kumar,<br>2013) |
| 3-month-old Kumming<br>mice<br>Groups:   | - Water-maze test<br>- Step-down test<br>- ROS by spectroflurometer   | Whole brain                              | - ↔ locomotor<br>activity<br>- Water maze test:   | - Oxidative stress:  • ↑ MDA   | D-gal-induced spatial learning<br>and memory impairment by<br>causing oxidative stress,   | (Yu et al.,<br>2015)<br>ued on next p                  |

Table 4 (continued)

| Study model   | Methods  | Brain area  | Major finding  |  | Interpretation  | Ref               |
|---|--|-------------|--|--|---|-------------------|
|   |  |             | Cognitive function   | Related findings   |   |                   |
| (1) control (0.9%<br>NaCl, s.c)<br>(2) D-gal (180 mg/<br>kg/d, s.c)       | - AGE by ELISA - MDA, SOD, GPx, CAT, T-AOC by spectrophotometer - T-ChE by commercial kit - AR, SDH, RAGE, TNF-α, IL-6         |             | <ul> <li>↑ Escape<br/>latency</li> <li>↓ Number of<br/>touching the<br/>blind</li> </ul> | - Inflammatory markers:  • ↑ NF-KB, TNF-α & IL-6   | inflammation and reducing the<br>activities of antioxidant<br>enzymes and increasing AGE<br>formation, TChE activity.                           |                   |
| Duration: 8 weeks   | by PCR<br>- NF-KB by Western Blot  |             | - Step-down test:  | - Antioxidant enz:   |   |                   |
|   |  |             | • ↑ number of errors   | ● ↓ SOD, GPx, CAT, T-AOC   |   |                   |
|   |  |             | • ↓ step down latency  | - Aging marker:  |   |                   |
|   |  |             |  | • † AGE, AR, SDH,<br>RAGE  |   |                   |
|   |  |             |  | - Neuromodulation:   |   |                   |
|   |  |             |  | • ↑ T-chE  |   |                   |
|   |  |             |  | - Histopathological changes  |   |                   |
|   |  |             |  | <ul> <li>intracellular oedema,<br/>degeneration and<br/>necrosis of neurons,<br/>and hyperplasia in<br/>hippocampus</li> </ul> |   |                   |
| 3-month-old Male<br>Sprague-Dawley<br>rats<br>Groups:<br>1. control (0.9% | - Morris water maze test - Step-down type passive avoidance test - IL-1β, TNF-α, IL-6 by ELISA - Txnip, p-NF-κΒρ65, p-ΙκΒα, p- | Hippocampus | - Morris water maze:  • † Escape latency   | Inflammatory markers:  • ↑ TNF-α, IL-6, IL-1β • ↓ Txnip • ↑ p-NF-κΒρ65, p-   | D-gal-induced spatial learning and memory impairment by causing inflammation and apoptosis.   | (Gao et al. 2015) |
| saline, s.c) 2. D-gal (120 mg/kg/d, s.c)                                  | IKKα, p-IKKβ, Bax/Bcl-2 ratio, caspase-9 by Western blot   |             | <ul><li>↓Number of crossing</li><li>↓ Time spent in</li></ul>                            | IκΒα, p-IKΚα, p-IKΚβ - Apoptosis:  |   |                   |
| Duration: 6 weeks   |  |             | the target<br>quadrant   | • ↑ Bax/Bcl-2 ratio • ↑ Caspase-9  |   |                   |
|   |  |             | - Step-down test:  | † Gaspase 5  |   |                   |
|   |  |             | <ul><li>↑ number of errors</li><li>↓ step down</li></ul>                                 |  |   |                   |
| B- month-old Kunming mice   | - Morris water Maze test - p21, p53, $A\beta_{1-42}$ by Western  | Hippocampus | latency - Morris water maze:   | - Oxidative stress:  | D-galactose impaired the spatial learning and memory  | (Chen et a 2016)  |
| Groups:<br>(1) Control<br>(2) D-gal (200 mg/kg/d, i.p)                    | Blot - AGEs, TNF-α, IL-6, SOD, GSH-<br>Px, MDA, CAT, T-AOC, NO and<br>NOS by commercial kits - TNF-α, IL-6, AGEs by ELISA      |             | ↑ Escape     latency     ↓ Time spent in     the target                                  | <ul> <li>↑ MDA</li> <li>↑ NO levels</li> <li>↑ NOS</li> <li>Antioxidant enz:</li> </ul>  | and hippocampal senescence<br>by reducing the hippocampal<br>BDNF expression, anti-<br>oxidation, anti-inflammation<br>and modulation of aging- |                   |
| Duration: 8 weeks   | - p16, p21, p53 by RT-PCR<br>- immunoreactive cells for<br>BDNF by Immunohistochemical<br>analysis                             |             | quadrant  • ↓ Number of crossing   | <ul> <li>↓ SOD,</li> <li>↓ GSH-Px</li> <li>↓ CAT</li> <li>↓ T-AOC</li> <li>Inflammatory markers:</li> </ul>                    | related gene expression in hippocampus of mice.   |                   |
|   |  |             |  | • ↑ TNF-α, IL-6<br>- Aging marker:   |   |                   |
|   |  |             |  | <ul> <li>↑ AGE</li> <li>↑ p16, p21, p53</li> <li>↑ Aβ<sub>1-42</sub></li> </ul>  |   |                   |
| 3-month-old Sprague-<br>Dawley rats                                       | - Morris Water Maze Test<br>- GSH-px activity and GSH  | Hippocampus | - Morris water<br>maze:  | <ul> <li>↓ BDNF positive cells</li> <li>↓ surviving neurones</li> <li>Oxidative stress:</li> </ul>                             | D-galactose induced spatial<br>learning and memory  | (Zhu et al. 2014) |
| Groups:<br>(1) control (0.9%<br>saline, s.c)                              | content, SOD activity and MDA<br>by spectrophotometer<br>- Detection of proinflammatory  |             | • ↑ Escape<br>latency  | <ul><li>↑ MDA</li><li>- Antioxidant enz:</li></ul>   | impairment through effecting<br>oxidative stress, antioxidant<br>enzymes, inflammatory  |                   |

Table 4 (continued)

| Study model   | Methods  | Brain area  | Major finding   |  | Interpretation  | Ref                  |
|---|--|-------------|---|--|---|----------------------|
|   |  |             | Cognitive function  | Related findings   |   |                      |
| kg/d, s.c) Duration: 6 weeks  3-month-old Sprague- Dawley rats Groups: (1) control (0.9% saline, s.c) (2) D-gal (100 mg/ kg/d, i.p.)  Duration: 7 weeks | - SA-β-gal (Senescence associated β -galactosidase cytochemical staining) - SOX2 by Western blot - telomere length by Southern blot - telomerase by TRAP-PCR - p53, p19 <sup>Arf</sup> , p21 <sup>Cip1/Waf1</sup> by qRT-PCR  - Morris Water Maze Test - Y-Maze Test - Aβ, BACE-1, RAGE, TNFα, NF-κb, iNOS, Bax, Bcl-2, PARP-1, synaptophysin, syntaxin, SNAP-23, p-CREB by Western Blot - ROS by spectrofluorometer - MDA by fluorometric assay kit - 8-OxoG, p-JNK, GFAP, lba-1, Aβ by Immunofluorescence Analysis | Whole brain | Osgnitive function  ↓ Number of crossing  ↓ Time spent in the target quadrant  - Morris water maze:  ↑ Escape latency  ↓ Number of crossing  ↓ Time spent in the target quadrant  ↓ Swimming speed  - Y-Maze Test  ↓ The percentage of spontaneous alteration | Related findings   | neurogenesis, senescence- associated genes, function of lysosomes, neuronal marker, activation of astrocytes, telomere length and telomerase activity.  D-galactose induced spatial learning and memory impairment through oxidative stress, neuroinflammation, apoptosis, reducing synaptic proteins, increasing amyloid protein and activation of astrocytes, microglial cells. | (Rehman et al., 2017 |
| 4-month-old Wistar rats<br>Groups:<br>(1) control (methyl<br>cellulose, 2%, in<br>distilled water, p.o)   | - Morris water maze task - GSH, GPx, MDA, protein thiol ( – SH) groups, AOPP (Advanced oxidation protein products) by spectrophotometer  | Whole brain | - Morris water maze:  • ↓ Number of crossing  | <ul> <li>↑ RAGE</li> <li>- Activated astrocytes &amp; microglia cells:</li> <li>↑ ↑ GFAP, Iba-1</li> <li>- Antioxidant enz:</li> <li>↓ GSH, GPx</li> </ul> | D-galactose induced significant spatial learning and memory deficits via increasing oxidative stress, apoptosis and histological alterations.   | (Banji et al. 2014)  |

Table 4 (continued)

| Study model                                    | Methods  | Brain area             | Major finding  |  | Interpretation  | Ref                   |
|--|--|------------------------|--|--|---|-----------------------|
|  |  |                        | Cognitive function   | Related findings   |   |                       |
| (2) D-gal (150 mg/kg/d, s.c)                   | - caspase 3 by Electrophoresis and western blot  |                        | • \ Time spent in the target quadrant  | - Oxidative stress:  |   |                       |
| Duration: 9 weeks                              |  |                        |  | <ul> <li>MDA, AOPP and protein carbonyls</li> </ul>  |   |                       |
|  |  |                        |  | - Apoptosis:   |   |                       |
|  |  |                        |  | • ↑ caspase-3  |   |                       |
| Adult Sprague Dawley rats                      | - Y-maze task<br>- PJNK, COX-2, NOS 2, IL-1β,  | Hippocampus,<br>Cortex | - Y-Maze Test  | <ul><li>damage to neurons in<br/>CA1 region</li><li>Synaptic proteins:</li></ul>           | D-galactose induced spatial learning and memory   | (Ullah et al<br>2015) |
| Groups (1) control (0.9% saline, s.c)          | TNF-α, Cyt.C, PARP-1, Bax/Bcl-2, Caspase3, Caspase9, synaptophysin and PSD95 by Western Blot |                        | <ul> <li>         \[         \] The         percentage of         spontaneous         alteration     </li> </ul> | • \ synaptophysin, PSD95   | impairment via increasing<br>synaptic dysfunction, oxidative<br>stress, apoptosis,            |                       |
| (2) D-gal 120 mg/<br>kg/d, i.p)                | - PJNK, Caspase3, 8-oxoguanine<br>by immunofluorescence                                      |                        | alteration   | <ul> <li>Oxidative stress:</li> <li>         ↑ 8-oxoguanine     </li> </ul>                | neuroinflammation and neurodegeneration.  |                       |
| Duration: 60D                                  | analysis - Degenerating neurons by   |                        |  | - Inflammatory markers:  |   |                       |
|  | Fluoro-Jade B staining - Survival neurons by Cresyl violet staining                          |                        |  | • ↑ COX-2, NOS-2,<br>TNFα & IL-1β  |   |                       |
|  |  |                        |  | - Apoptosis:   |   |                       |
|  |  |                        |  | <ul> <li>↓ anti-apoptotic Bcl2</li> <li>↑ ap Bax</li> <li>↑ Caspase-9, Caspase-</li> </ul> |   |                       |
|  |  |                        |  | 3  • ↑ PARP-1 • ↑ p-JNK  |   |                       |
|  |  |                        |  | - Degenerating neurons:  |   |                       |
|  |  |                        |  | • † FJB + neuronal cells   |   |                       |
|  |  |                        |  | - Survival neurons:  |   |                       |
|  |  |                        |  | <ul> <li>\( \text{Cresyl violet} \)     neurones</li> </ul>                                |   |                       |
| Adult Male Wistar rats<br>Groups:              | <ul><li> Morris water maze test</li><li> Open field test</li></ul>                           | Whole brain            | <ul> <li>Morris water maze:</li> </ul>   | - Oxidative stress:  | D-galactose induced significant spatial learning and memory                                   | (Qu et al.,<br>2016)  |
| (1) control group<br>(0.9% saline, s.c)        | - MDA, NO, GSH, ACh, GPx,<br>SOD, CAT, AChE by commercial                                    |                        | • ↑ Escape   | <ul><li>↑ MDA</li><li>↑ NO levels</li></ul>  | and locomotor and behavioral activity impairment,   |                       |
| (2) D-gal (100 mg/<br>kg/d, s.c)               | kit - NF-κB, caspase-3, GFAP by  |                        | latency  ■ Number of   | - Antioxidant enz:   | neurochemical deficits through<br>oxidative damage, dysfunction<br>of the cholinergic system, |                       |
| Duration: 8 weeks.                             | Immunohistochemical analysis - Histopathological analysis                                    |                        | • ↓ Time spent in the target   | $ullet$ $\downarrow$ GSH, SOD, CAT and GPx   | inflammatory markers and activation of astrocytes.  |                       |
|  |  |                        | quadrant  • ↔ Swimming speed   | - Neuromodulation:   |   |                       |
|  |  |                        | - Open field test:   | <ul><li>↑ AChE</li><li>↓ ACh</li></ul>   |   |                       |
|  |  |                        | • ↓ Number of  | - Apoptosis:   |   |                       |
|  |  |                        | grid crossing  ● ↓ Number of   | ● ↑ Caspase-3  |   |                       |
|  |  |                        | rearing and<br>learning  | - Inflammatory markers:  |   |                       |
|  |  |                        |  | ● ↑ NF-κB  |   |                       |
|  |  |                        |  | - extensively damaged<br>neurons in the<br>hippocampus CA1 region                          |   |                       |
| Middle-aged Sprague-<br>Dawley rats<br>Groups: | - Morris water maze test<br>- Peripheral-type  | Cerebral cortex        | - Morris water<br>maze:  | - Antioxidant<br>ability:  | D-galactose impaired the<br>spatial learning and memory<br>impairment by decreasing the       | (Chen et al., 2008)   |

Table 4 (continued)

| Study model  | Methods  | Brain area | Major finding  |                  | Interpretation  | Ref |
|--|--|------------|--|------------------|---|-----|
|  |  |            | Cognitive function   | Related findings |   |     |
| (1) control (0.9% saline, s.c) (2) Mimetic aging group (D-gal, 10% for stock solution, 1 ml/kg/d, s.c) | benzodiazepine binding sites<br>byutoradiographic localization |            | ↑ Escape latency     ↓ Time spent in the target quadrant     ↓ Swimming distance |                  | antioxidant ability in mitochondria from cerebral cortex. |     |

s.c: subcutaneous; p.o.: per oral; NADH: Nicotinamide adenine dinucleotide; MDA: malondialdehyde; NO: nitric oxide; SOD: superoxide dismutase; AchE: acetyl choline esterase; IL: interleukin; NF-κB: nuclear factor kappa-light-chain-enhancer of activated B cells; ELISA: enzyme-linked immunosorbent assay; COX: Cyclooxygenase; TNF: tumor necrosis factor alpha; GFAP: Glial fibrillary acidic protein; ROS: reactive oxygen species; TNOS: total nitric oxide synthase; iNOS: inducible nitric oxide synthase; 8-OHdG: 8-hydroxy-2'-deoxyguanosine; Ach E: acetylcholinesterase; NOX: NADPH oxidase; p22<sup>phox</sup>, p47<sup>phox</sup>, p67<sup>phox</sup>; subunit of NOX; cyt c: cytochrome c; bp: base pair; PCR: polymerase chain reaction; TRAP-PCR: Telomeric repeat amplification protocol; GSH: glutathione; GPx: glutathione peroxidase; CAT: catalase; T-AOC: total antioxidant capacity; AGEs: advanced glycation endproducts; RAGE: AGE receptors; PCR: polymerase chain reaction; SA-β-gal: senescence-associated β-galactosidase; Txnip: thioredoxin-interacting protein; p-IKKα, p-IKKβ phosphorylated IkB kinase α, β; Bcl: B-cell lymphoma; Bax: bcl-2-like protein 4; SOX: SRY (sex determining region Y)-box 2; p53, p19<sup>Arf</sup>, p21<sup>Cip1/Waf1</sup>: senescence-associated genes; BrdU: Bromodeoxyuridine; Gal-c: galactosylceramidase; Aeg1: astrocyte elevated gene-1; Aβ: amyloid beta protein; BACE-1: β-site amyloid precursor protein cleaving enzyme 1; PARP: poly (ADP-ribose) polymerase; SNAP-23: synaptosomal-associated protein 23; p-CREB: cAMP response elements binding; p-JNK: phosphorylated c-Jun N-terminal kinases; Iba-1: ionized calcium-binding adapter molecule 1; PSD95: postsynaptic density-95.

auditory cortex and ventral cochlear nucleus (as shown in Table 2). D-galactose-induced brain aging, as indicated by brain mitochondrial dysfunction and structural change in these studies was in the dose-in-dependent manner, starting from 100 mg/kg/day to 500 mg/kg/day following 6–8 weeks of the administration (Banji et al., 2014; Chen et al., 2011; Du et al., 2012; Du et al., 2015; Kumar et al., 2009; Long et al., 2007; Prakash and Kumar, 2013; Zeng et al., 2014).

Interestingly, D-galactose also led to a decrease in the antioxidant enzymes such as glutathione, catalase, superoxide dismutase, glutathione-S-transferase activity, glutathione peroxidase and total antioxidant capacity. Therefore, the imbalance between reactive oxygen species and antioxidant activities in D-galactose-induced aging models leads to increased oxidative stress and mitochondrial dysfunction, which are significant in the aging process.

All of those studies suggest that D-galactose-induced mitochondrial dysfunction as indicated by a reduction in respiratory chain enzymes and antioxidant activity, go on to increase oxidative stress, mitochondria DNA mutations, the decline of ATP synthesis, mitochondrial membrane potential changes and cause impairment of mitochondrial structures. D-galactose not only caused mitochondrial dysfunction and oxidative stress, but also induced neuronal apoptosis. All of these findings are summarized in Table 2. The following paragraph will discuss the effect of D-galactose-induced apoptosis in the brain.

#### 1.3. Effect of D-galactose-induced apoptosis in the brain

D-galactose activates both extrinsic and intrinsic pathways of apoptosis (as shown in Table 2). The extrinsic 'death receptor' pathway directly activates effector caspases via JNK (c-Jun-N-terminal kinase) and converges with the intrinsic apoptotic pathway at the mitochondrion (Benn and Woolf, 2004). It was found that D-galactose activated p-JNK and enhanced the level of the cytochrome complex (cyt c) which stimulated the activation of caspase-3, caspases-9 and cleaved poly ADP ribose polymerase (PARP-1) (Ali et al., 2015). In addition, D-galactose triggered the mitochondria to release cyt c, reduced anti-apoptotic Bcl2 expression level and increased apoptotic Bax. All of those events suggested that D-galactose promoted the apoptotic process (Qian et al., 2008). In addition to apoptosis, D-galactose promoted neuro-inflammation and neurodegeneration (Cui et al., 2006). The dosage from which D-galactose started inducing apoptosis was 100 mg-500 mg/kg/day, duration was from 6 weeks to 9 weeks. (as shown in Table 2)

#### 1.4. Effect of D-galactose-induced brain inflammation

Inflammatory markers used for monitoring in D-galactose-induced aging models are cyclooxygenase (COX-2), iNOS, NOS-2, tumor necrosis factor alpha (TNF- $\alpha$ ), interleukin (IL-1 $\beta$ ), IL-6, nuclear factor (NF- $\kappa$ B) thioredoxin-interacting protein (Txnip), p-NF- $\kappa$ Bp65, p-I $\kappa$ B $\alpha$ , p-IKK $\alpha$ , p-IKK $\beta$  as shown in Table 2. All of these studies suggested that D-galactose increased the inflammatory markers and induced neuro-inflammation via the activation of the transcription factor NF $\kappa$ -B through Ras and redox–sensitive signaling pathways, resulting in memory impairment. D-galactose started inducing inflammation at a dosage of 50 mg–180 mg/kg/day and duration was from 6 weeks to 60 days.

### 1.5. Therapeutic approaches to brain mitochondrial aging induced by D-galactose

There are 6 therapeutic studies which focused on the mitochondria in D-galactose-induced brain aging as shown in Table 3. The first one used R-alpha-lipoic acid which is an antioxidant abundant in yeast, liver, kidney, spinach, broccoli, and potatoes, to treat mitochondrial dysfunction (Long et al., 2007). R-alpha-lipoic acid increased state 3 respiration which represents succinate-linked respiration and respiratory control ratio (state 3/state 4), but did not increase the ADP/O ratio (Long et al., 2007). However other therapeutic treatments helped to improve the activity of all respiratory enzyme complexes in the mitochondria as summarized in Table 3. (Banji et al., 2014; Kumar et al., 2009; Prakash and Kumar, 2013; Zhang et al., 2010). The possible reason may be due to inadequate dosages of R-alpha-lipoic acid. One of the studies stated that 100 mg/kg/day of R-alpha-lipoic acid is used for prevention but not for intervention, dosage should be increased up to 180 mg/kg/day (Inman et al., 2013).

Carvidilol, pioglitazone, curcumin and hesperidin have an antioxidant effect. These drugs have been used as an intervention to reverse D-galactose-induced mitochondrial dysfunction in a dose dependent manner. The possible underlying mechanisms of these drugs may be by increasing antioxidant enzymes, oxidative phosphorylation, and cell viability in senescence models (Banji et al., 2014; Kumar et al., 2009; Prakash and Kumar, 2013). In addition, catalpol alleviated oxidative stress and improved D-galactose-induced mitochondrial dysfunction in a dose independent manner, as indicated by a decrease in oxidative stress (Zhang et al., 2010). Chen and colleagues also showed that dehydroepiandrosterone (DHEA) attenuated D-

 Table 5

 Therapeutic approach on cognitive function in D-galactose-induced aging models.

| Study model  | Methods   | Brain area                               | Major finding   |   | Interpretation  | Ref  |
|--|---|--|---|---|---|--|
|  |   |  | Cognitive function  | Related findings  |   |  |
| 8–10-week-old Kunming mice Groups: (1) control (0.9% saline, s.c.) (2) D-gal (150 mg/kg/d, s.c.) (3) D-gal (150 mg/kg/d, s.c.) + FA (50 mg/kg/d, i.g) (4) D-gal (150 mg/kg/d, i.g.) + FA (100 mg/kg/d, i.g.) Duration: 8 weeks | - Morris water maze test - Open field test - MDA, NO, GSH, SOD, AChE by commercial kit - II-1β, NF-κΒ by ELISA - H&E and Nissl staining - Immunohistochemistry  | Whole brain                              | Morris water maze:     ↓ Escape latency     ↑ Number of crossing     ↑ Time spent in the target quadrant     ← Swimming speed     · Open field test:     ↑ Number of grid crossing     ↑ Number of grid crossing  | - Oxidative stress:  • ↓ MDA  • ↓ NO levels  - Antioxidant enz:  • ↑ GSH, SOD  - Neuromodulation:   | Ferulic acid (FA) ameliorated D-galactose induced spatial learning and memory impairment, reduced exploratory ability through attenuating oxidative stress, inhibiting AChE activity and suppressing neuroinflammation and neurodegeneration. | (Yang et al., 2016)                              |
| 10-week-old Kunming mice Groups: (1) control (0.9% saline, s.c.) (2) D-gal (50 mg/kg/d, s.c.) + UA (10 mg/kg/d, p.o.) (4) UA (10 mg/kg/d, p.o.) Duration: 8 weeks  | - Step-through Test - Morris Water Maze Test - NF-kB, COX-2, iNOS, TNFG, IL-1ß, IL-6 by Western Blot - AGEs, RAGE by Immunosorbent Assay - GFAP, CD11b by Immunofluorescence Staining - ROS, protein carbonyl by chromatography | Prefrontal cortex                        | - Note: High dose FA (100 mg/kg/d) was more effective than low dose FA (50 mg/kg/d) in all parameters.  - Morris water maze:  - ↓ Escape latency  - ↑ Number of crossing  - ↑ Time spent in the target quadrant  - Step-through passive avoidance task:  - ↓ Latency time | • ↓ Caspase-3 - Inflammatory markers: • ↓ NF-κB, IL-1β - Prevent neuronal cell damage to the hippocampus - Oxidative stress: • ↓ Protein Carbonyl • ↓ ROS - Inflammatory markers: • ↓ COX-2, iNOS, TNFα, IL-1β, IL-6, NF-κB - Aging marker: • ↓ AGES, RAGE - Arrivated astrocyres & | Ursolic acid (UA) could attenuate D-galinduced spatial learning and memory impairment via decreasing oxidative stress, inflammatory markers, aging marker, activation of astrocytes and microglial cells.                                     | (Lu et al., 2010b)                               |
| 2–3 month-old Male Swiss albino mice Groups:  (1) Naive (0.5% sodium carboxymethyl cellulose, 0.5 ml/100 g/d, p.o)   | - Spatial navigation task (Morris water maze task) - Maze acquisition phase (training) - Maze retention phase (testing for retention of the learned task) - Elevated plus maze paradigm   | Whole brain<br>(excluding<br>cerebellum) | <ul> <li>Morris water maze:</li> <li></li></ul>   |   | Carvidilol (CAR) attenuated D-galactose-induced spatial learning and memory impairment, oxidative stress and apoptosis by increasing antioxidant enzymes, oxidative phosphorylation, and cell viability.                                      | (Kumar et al., 2009) by (continued on next page) |

(continued on next page)

| (continued) |
|-------------|
| Ŋ           |
| Table       |

| (2000)   |   |                        |   |  |   |                         |
|--|---|------------------------|---|--|---|-------------------------|
| Study model  | Methods   | Brain area             | Major finding   |  | Interpretation  | Ref                     |
|  |   |                        | Cognitive function  | Related findings   |   |                         |
| (2) D-Gal (100 mg/kg/d, s.c)<br>(3) CAR (5 mg/kg/d, p.o)   | - Assessment of gross behavioral activity - Glutathione, catalase, superoxide                                 |                        | - Elevated plus maze paradigm   | - Oxidative stress:  |   |                         |
| (4) CAR (Z.5 mg kg/d, p.o)<br>+ D-gal (100 mg/kg/d, s.c)<br>(5) CAR (5 mg/kg/d, p.o)<br>+ D-gal (100 mg/kg/d, s.c) | dismutase, and guitathione-5-transferase activity, MDA, and nitrite level, AchE activity by spectrophotometer |                        |   | <ul> <li>         ↓ MDA, and nitrite levelNeuromodulation:     </li> </ul>   |   |                         |
| Duration: 6 weeks  |   |                        | <ul> <li>↓ second retention transfer<br/>latency</li> <li>→ locomotor activity</li> </ul>               | • ↓ AchE   |   |                         |
|  |   |                        | - Note: High dose CAR (5 mg/kg/d) was more effective than low dose CAR (2.5 mg/kg/d) in all parameters. |  |   |                         |
| 3-month-old Male Laca mice   | - Morris water maze task  | Whole brain            | - Morris water maze:  | - Antioxidant enz:   | Pioglitazone (PIO) attenuated D-galactose-  | (Prakash and            |
| Groups:<br>(1) Naïve (0.5% sodium  | - Maze acquisition phase (training) - Maze retention phase (retention of the                                  | (excluding cerebellum) | • ⇔initial acquisition latency  | • † glutathione, catalase,   | induced spatial rearming and memory impairment, oxidative stress and apoptosis by                                     | Kumar, 2013)<br>y       |
| carboxymetnyi cenulose, 1 mi/<br>100 g/d, p.o)   | learned task)<br>- glutathione, catalase, superoxide  |                        | <ul> <li>         urst retention latency         <ul> <li></li></ul></li></ul>                          | superoxide dismutase,<br>and glutathione-S-  | increasing antioxidant enzymes, oxidative phosphorylation, and cell viability in                                      |                         |
| (2) D-gal (100 mg/kg/d, s.c)   | dismutase, and glutathione-S-transferase  |                        | :   | transferase activity   | senescence mice through activation of PPAR $\!$ | ~                       |
| (3) PIO (10 mg/kg/d, p.o)<br>(4) PIO (30 mg/kg/d, p.o)   | activity, MDA, and nitrite level, caspase3 by spectrophotometer   |                        | - ↔ locomotor activity  | -Oxidative stress:   | receptors.  |                         |
| (5) PIO (10 mg/kg/d, p.o)  |   |                        | - BADGE treatment blocked the   | Contract of the contract of th |   |                         |
| + D-gal (100 mg/kg/d, s.c)   |   |                        | protective effect of pioglitazone.  | <ul> <li>\(\psi\) MDA, nitrite level</li> </ul>  |   |                         |
| (6) PIO (30 mg/kg/d, p.o)  |   |                        | - Note: High dose PIO (30 mg/kg/  |  |   |                         |
| + D-gal (100 mg/kg/d, s.c)   |   |                        | d) was more effective than low  | -Apoptosis:  |   |                         |
| (/) Displicator A digiscidyl<br>ether (PPAR antagonist)  |   |                        | dose PiO (10 mg/kg/d) in an   | • L caspase-3  |   |                         |
| (15 mg/kg/d, p.o) + PIO  |   |                        | activity.   |  |   |                         |
| (30 mg/kg/d, p.o) + D-gal  |   |                        | •   |  |   |                         |
| (100 mg/kg/d, s.c)   |   |                        |   |  |   |                         |
| Duration: 6 weeks  | ;   |                        | ;   |  |   |                         |
| 3-month-old Kumming mice<br>Groups:  | - Water-maze test<br>- Step-down test   | Whole brain            | - Water maze test:  | - Oxidative stress:  | FGF21 protected the aging mice brain from D-<br>gal-induced spatial learning and memory                               | )- (Yu et al.,<br>2015) |
| (1) control (0.9% saline, s.c)   | - ROS by spectroflurometer  |                        | • ↓ Escape latency  | ● ↓ MDA  | impairment by attenuating oxidative stress,   |                         |
| (2) D-gal (180 mg/kg/d, s.c)   | - AGE by ELISA  |                        | • ↑ Number of touching the  |  | inflammatory markers and renewing the   |                         |
| (3) D-gal (180 mg/kg/d, s.c)   | - MDA, SOD, GPx, CAT, T-AOC by  |                        | blind   | - Inflammatory markers:  | activities of antioxidant enzymes and   |                         |
| + FGF21<br>(1 mg/kg/d s.c.)  | spectrophotometer<br>- T-ChF by commercial kit  |                        | - Sten-down test:   | • I NF-KR TNF-α & II-6   | decreasing AGE formation, 1ChE activity.  |                         |
| (4) D-gal (180 mg/kg/d, s.c)   | - AR, SDH, RAGE, TNF-α, IL-6 by PCR   |                        | Josephanna Cat.   | - Antioxidant enz:   |   |                         |
| + FGF21 (2 mg/kg/d, s.c)   | - NF-KB by Western Blot   |                        | • \upspreammetrian number of errors   |  |   |                         |
| (5) D-gal (180 mg/kg/d, s.c)<br>+ FGF21 (5 mg/kg/d ini)  |   |                        | • † step down latency   | • † SOD, GPx, CAT, T-AOC   |   |                         |
| 6. FGF21 (5 mg/kg/d, s.c)  |   |                        | - Note: All doses of FGF21 show   | - Aging marker:  |   |                         |
| Duration: 8 weeks  |   |                        | me same enects.   | • ↓ AGE, AR, SDH, RAGE   |   |                         |
|  |   |                        |   | - Neuromodulation:   |   |                         |
|  |   |                        |   | • J T-chE  |   |                         |

| (continued) |  |
|-------------|--|
| 2           |  |
| <u>e</u>    |  |
| ā           |  |

| Study model   | Methods  | Brain area  | Major finding   |  | Interpretation  | Ref                      |
|---|--|-------------|---|--|---|--------------------------|
|   |  |             | Cognitive function  | Related findings   |   |                          |
| 3- month-old Kunming mice   | - Morris water Maze test   | Hippocampus | - Morris water maze:  | - Oxidative stress:  | Hyperbaric treatment (HBOT) can prevent   | (Chen et al.,            |
| (1) Control<br>(2) D-gal (200 mg/kg/d, i.p)<br>(3) D-gal (200 mg/kg/d, i.p) | - F21, P.5, API-42 by Western Blot<br>- AGEs, TNF-c, IL-6, SOD, GSH-Px, MDA,<br>CAT, T-AOC, NO and NOS by commercial<br>kits |             | <ul> <li> ↓ Escape latency</li> <li> ↑ Number of crossing</li> <li> ↑ Time spent in the target</li> </ul> | <ul><li>\(\psi\) MDA</li><li>\(\psi\) NO levels</li><li>\(\psi\) NOS</li></ul> | Cognitive impairment and implocating sensecence by retaining the hippocampal BDNF expression, anti-oxidation, anti-inflammation and modulation of agine-related |                          |
| + Vit E (0.2 g/kg/d, i.g)<br>(4) D-gal (200 mg/kg/d, i.p)                   |  |             | quadrant  | - Antioxidant enz:   | gene expression in a mouse model of D-galactose-induced aging.  |                          |
| + HBOT (0.25 MPa at a rate of<br>100 kPa/min)                               | - immunoreactive cells for BDNF by<br>Immunohistochemical analysis   |             |   | • † GSH-Px, SOD, CAT,<br>TAOC  |   |                          |
| Duration: 8 weeks   |  |             |   | - Inflammatory markers:  |   |                          |
|   |  |             |   | <ul> <li>† TNF-α, IL-6</li> </ul>  |   |                          |
|   |  |             |   | - Aging marker:  |   |                          |
|   |  |             |   | •   AGE<br>•   p16, p21, p53<br>•   Aβ1-42                                     |   |                          |
|   |  |             |   | <ul> <li>↑ BDNF positive cells</li> <li>↑ surviving neurones</li> </ul>        |   |                          |
| Adult male BALB/c mice  | - Active mitochondria levels by  | Whole brain | - Barnes Maze test  | - Oxidative stress:  | Transcranial low level laser therapy (LLLT)   |                          |
| Groups: (1) control (0.9% saline, s.c)                                      | Mitolracker Green staining<br>- Mitochondrial membrane potential   |             | • \ Escape latency  | • ¢ ROS  | abrogated oxidative stress, apoptosis leading to reverse cognitive impairment in D-galactose-   | to et al., 2017)         |
| (2) D-gal + sham (500 mg/kg/d, s.c)   | determination by Mitochondria Staining<br>Kit  |             | <ul> <li>Time spent in error holes</li> <li>Time spent in the target</li> </ul>                           | - Apoptosis:   | ınduced agıng mice.   |                          |
| (3) D-gal + red 4 (D-gal + $4 \text{ J}$ / cm <sup>2</sup> of red laser)    | <ul> <li>Mitochondrial cytochrome c oxidase<br/>activity by commercial kits</li> </ul>                                       |             | quadrant • ↑ Relative error time  | • J. Bax/Bcl-2 ratio   |   |                          |
| (4) D-gal + NIR 4 (D-gal + $4.1 \text{ cm}^2$ of NID locar)                 | - Bax/Bcl-2, Caspase 3 by western blot   |             | Myhat Whama Which tach  | • ¢ Caspase-3  |   |                          |
| + 4 J/CIII OI MIN IASEL) (5) D-gal + red 8 (D-gal + 8 J/cm² of red laser)   | - A.F. revels, by Colombeut assay Kit<br>- ROS by Fluorescent dye<br>dichlorohydrofluorescein diacetate                      |             | <ul> <li>What-Where-Which task</li> <li>◆ Locomotor activity</li> </ul>                                   | - Note: Higher dose of LLLT exerted a better response than                     |   |                          |
| (6) D-gal + NIR 8 (D-gal<br>+ 8 J/cm <sup>2</sup> of NIR laser)             | - Barnes Maze test<br>- What-Where-Which task  |             | A Total observation time     Displacement index   | low dose (4 J/cm2).  |   |                          |
| Duration: 6 weeks<br>3-month-old Male Sprague-Dawley                        | - Morris water maze test   | Hippocampus | - Morris water maze:  | - Inflammatory markers:  | Salidroside (sal) prevented D-gal-induced   |                          |
| rats<br>Groups:   | - Step-down type passive avoidance test - IL-1 $\beta$ , TNF- $\alpha$ , IL-6 by ELISA                                       |             | • ↓ Escape latency  | • $\downarrow$ TNF- $\alpha$ , IL-6, IL-1 $\beta$                              | spatial learning and memory impairment by<br>the effect of anti-inflammatory and anti-  | 2015)                    |
| (1) control (0.9% saline, s.c)<br>(2) D-gal (120 mg/kg/d, s.c)              | - Txnip, p-NF-κΒρ65, p-IκΒα, p-IKKα, p-IKKβ, Bax/Bcl-2 ratio, caspase-9 by   |             | <ul> <li>Number of crossing</li> <li>Time spent in the target</li> </ul>                                  | <ul> <li>† Txnip</li> <li>↓ p-NF-κBp65, p-IκBα, p-</li> </ul>                  | apoptotic responses in the hippocampus.   |                          |
| (3) D-gal (120 mg/kg/d, s.c)<br>+ sal treatment (20 mg/kg/d                 | Western blot   |             | quadrant  | IKKα, p-IKKβ   |   |                          |
| p.o) (4) D and (120 ma./kg/d s.o.)  |  |             | - Step-down test:   | - Apoptosis:   |   |                          |
| (4) D-8al (120 mg/ng/u, 3.c)  |  |             |   |  | (02)  | (continued on next page) |

Table 5 (continued)

| Study model  | Methods  | Brain area  | Major finding  |  | Interpretation   | Ref                    |
|--|--|-------------|--|--|--|------------------------|
|  |  |             | Cognitive function   | Related findings   |  |                        |
| + sal treatment (40 mg/kg/d, p.o).   |  |             | <ul> <li></li></ul>  | • ↓ Bax/Bcl-2 ratio<br>• ↓ Caspase-9   |  |                        |
| Duration: 6 weeks  |  |             | - Note: All doses of sal show the  |  |  |                        |
| 3-month-old Sprague-Dawley rats  | - Morris Water Maze Test   | Hippocampus | same enects.<br>- Morris water maze:   | - Oxidative stress:  | Ginsenoiside (Rg1) treatment can improve D-  | (Zhu et al.,           |
| (1) control (0.9% saline, s.c)   | activity and MDA by spectrophotometer  |             | • J Escape latency   | ● ↓ MDA  | galactose-maucea spatial tearning and memory impairment and hippocampus  | 2014)                  |
| (2) D-gal (120 mg/kg/d, s.c)<br>(3) Rg1 (20 mg/kg/d, i.p)                  | - Detection of proinfiammatory cytokines by ELISA  |             | <ul> <li>↑ Number of crossing</li> <li>↑ Time spent in the target</li> </ul>           | - Antioxidant enz:   | senescence by involving in the anti-oxidation and antiinflammation regulating telomere                             |                        |
| (4) D-gal (120 mg/kg/d, s.c)<br>(5) D-gal + Rg1 (20 mg/kg/d,               | - 5A-j5-gal (Senescence associated j5 -galactosidase cytochemical staining)  |             | quadrant   | • † GSH, SOD   | length, hippocampus neurogenesis, senescence-associated genes, and function of                                     |                        |
|  | - SOX2 by Western blot<br>- telomere length by Southern blot   |             |  | - Inflammatory markers:  | lysosomes, neuronal marker and activation of astrocytes.   |                        |
| Duration: 6 weeks  | - telomerase by TRAP-PCR<br>- p53, p19 <sup>Arr</sup> , p21 <sup>Gp1/Waf1</sup>                                      |             |  | • $\downarrow$ TNF- $\alpha$ , IL-6, IL-1 $\beta$  |  |                        |
|  | by qki-Pck   |             |  | - Hippocampal neurogenesis:  |  |                        |
|  |  |             |  | <ul><li> ⇔ SOX2</li><li> ↑ BrdU cells</li></ul>  |  |                        |
|  |  |             |  | - Senescence-associated genes:   |  |                        |
|  |  |             |  | $ullet$ $\downarrow$ p53, p19 <sup>Arf</sup> , p21 $^{\mathrm{Cip1/Wafl}}$   |  |                        |
|  |  |             |  | - Function of the lysosomes:   |  |                        |
|  |  |             |  | <ul> <li>↓ SA-β-gal staining</li> </ul>  |  |                        |
|  |  |             |  | - Neuronal marker:   |  |                        |
|  |  |             |  | • † ß-tubulin III  |  |                        |
|  |  |             |  | - Activated astrocytes:  |  |                        |
|  |  |             |  | <ul> <li> \$\int \text{Gal-c and GFAP}\$ </li> <li> \$\int \text{Nestin and Aeg1}\$ </li> <li> astrocyte elevated gene-1 </li> </ul> |  |                        |
| 3-month-old Sprague-Dawley rats  | - Morris Water Maze Test   | Whole brain | - Morris water maze:   | <ul> <li>† telomere lengths,<br/>telomerase activity</li> <li>Oxidative stress:</li> </ul>   | Anthocyanins (Anth) effectively attenuate D-   |                        |
| Groups:<br>(1) control (0.9% saline, s.c)<br>(2) D-gal (100 mg/kg/d. i.n.) | <ul> <li>Y-Maze Test</li> <li>Aβ, BACE-1, RAGE, TNFα, NF-κb, iNOS,<br/>Bax, Bcl-2, PARP-1, synaptophysin.</li> </ul> |             | <ul> <li>\$\bigsep\$ Escape latency</li> <li>\$\bigsep\$ Number of crossing</li> </ul> | • UMDA   | galactose induced spatial learning and memory impairment, oxidative stress, neuroinflammation and reverse synaptic | 2017)                  |
| .8tm (100 m8/ v8/ v, n.p.)   | bas, ber-z, rrau -1, synapropnysm,   |             | Since of Commit  |  |  | (continued on next pag |

(continued on next page)

| Study model  | Methods  | Brain area  | Major finding   |  | Interpretation   | Ref                      |
|--|--|-------------|---|--|--|--------------------------|
|  |  |             | Cognitive function  | Related findings   |  |                          |
| (3) Anth (100 mg/kg/d, i.p)<br>(4) D-gal (100 mg/kg/d, I·P)                  | syntaxin, SNAP-23, p-CREB by Western<br>Blot   |             | <ul> <li>↑ Time spent in the target<br/>quadrant</li> </ul> | • ↓ ROS  | dysfunction, reducing amyloid protein and activation of astrocytes, microglia cells.     |                          |
| + Anth (100 mg/kg/d, i.p)  | - ROS by spectrofluorometer  |             | • ↑ Swimming speed  | - Inflammatory markers:  |  |                          |
| Duration: 7 weeks  | - MDA by involution assay kit - 8-OxoG, p-JNK, GFAP, Iba-1, A $\beta$ by Imminofluescence Anglesis |             | - Y-Maze Test   | <ul> <li>↓ iNOS, TNFα, NF-κB</li> </ul>                            |  |                          |
|  | minimionationescence Analysis  |             | alteration  | - Apoptosis:   |  |                          |
|  |  |             |   | <ul> <li>↓ Bax/Bcl-2</li> <li>↓ p-JNK</li> <li>↓ PARP-1</li> </ul> |  |                          |
|  |  |             |   | - Synaptic proteins:   |  |                          |
|  |  |             |   | • † synaptophysin,<br>syntaxin, SNAP-23, p-<br>CREB                |  |                          |
|  |  |             |   | - Amyloid protein:   |  |                          |
|  |  |             |   | $ullet$ \$\ \text{BACE-1, A}\$                                     |  |                          |
|  |  |             |   | - Aging marker:  |  |                          |
|  |  |             |   | • ↓ RAGE   |  |                          |
|  |  |             |   | - Activated astrocytes & microglia cells:                          |  |                          |
| 4-month-old Wistar rats  | - Morris water maze task   | Whole brain | - Morris water maze:  | • ↓ GFAP, Iba-1<br>- Antioxidant enz:                              | Curcumin and hesperidin (HES) were found to  |                          |
| Groups: (1) control (methyl cellulose,                                       | - GSH, GPx, MDA, protein thiol ( – SH) groups, AOPP (Advanced oxidation protein                    |             | • ↑ Number of crossing                                      | • ↑ GSH, GPx   | improve D-galactose induced spatial learning<br>and memory impairment and the functional | 2014)                    |
| 2%, in distilled water, p.o) (2) D-gal (150 mg/kg/d, s.c)                    | products) by spectrophotometer - caspase 3 by Electrophoresis and western                          |             | <ul> <li>↑ Time spent in the target<br/>quadrant</li> </ul> | - Oxidative stress:  | capacity of neurons, reducing the probability of apoptosis and oxidative stress.         |                          |
| (5) Curcumin (50 mg/kg/d,<br>p.o) + D-gal (150 mg/kg/d,<br>s.c)              |  |             | - Note: Higher dose of the combination of curcumin with     | <ul> <li>JMDA, AOPP and protein carbonyls</li> </ul>               |  |                          |
| (4) HES (10 mg/kg/d) + D-gal<br>(150 mg/kg/d, s.c)                           |  |             | HES exerted a better response than low dose combination and | - Apoptosis:   |  |                          |
| (5) Curcumin (50 mg/kg/d)<br>+ HES (10 mg/kg/d) + D-gal                      |  |             | individual therapy.   | • ↓ caspase-3  |  |                          |
| (150 mg/kg/d, s.c)<br>(6) Curcumin (100 mg/kg/d)<br>+ HES (25 mg/kg) + D-gal |  |             |   | - Improved architecture of<br>neurons in CA1 region                |  |                          |
| (150 mg/kg/d, s.c)   |  |             |   |  | шоэ)   | (continued on next page) |

| Table 5 (continued)  |   |                                 |  |  |   |  |
|--|---|---------------------------------|--|--|---|--|
| Study model  | Methods   | Brain area                      | Major finding  |  | Interpretation  | Ref                                    |
|  |   |                                 | Cognitive function   | Related findings   |   |  |
| Duration: 9 weeks Adult Sprague Dawley rats Groups:  (1) 0.9% saline control (2) D-gal (120 mg/kg/d, i.p) + Caffeine (3 mg/kg/d, i.p) + Caffeine (3 mg/kg/d, i.p) + Caffeine (3 mg/kg/d, i.p) (4) Caffeine (3 mg/kg/d, i.p)  Duration: 60D  Adult Male Wistar rats Groups: (1) Control group (0.9% saline, s.c) + THP (20 mg/kg/d, s.c) + THP (20 mg/kg/d, s.c) + THP (40 mg/kg/d, p.o) (4) D-gal (100 mg/kg/d, p.o) + THP (40 mg/kg/d, p.o) (5) D-gal (100 mg/kg/d, p.o) + THP (80 mg/kg/d, p.o) (5) D-gal (100 mg/kg/d, p.o) | - Y-maze task - PJNK, COX-2, NOS 2, IL-1β, TNF-α, Cyt.C, PARP-1, Bax/Bcl-2, Caspase3, Caspase9, synaptophysin and PSD95 by Western Blot - PJNK, Caspase3, 8-oxoguanine by immunofluorescence analysis - Degenerating neurons by Fluoro-Jade B staining - Survival neurons by Cresyl violet staining - Morris water maze test - Open field test - MDA, NO, GSH, ACh, GPx, SOD, CAT, AChe by commercial kit - NF-κB, caspase-3, GFAP by Immunohistochemical analysis - Histopathological analysis | Hippocampus, Cortex Whole brain | - Y-Maze Test  ↓ The percentage of spontaneous alteration  - Morris water maze:  • ↓ Escape latency  • ↑ Number of crossing  • ↑ Time spent in the target quadrant  - Open field test:  • ↑ Number of grid crossing  • ↑ Number of rearing and learning  • ↑ Number of rearing and learning  - Note: All doses of THP show the same effects. | - Synaptic proteins:  • ↑ synaptic proteins:  • ↓ Soxoguanine  - Inflammatory markers:  • ↓ COX-2, NOS-2, TNFα & IL-1β  - Apoptosis:  • ↑ anti-apoptotic Bcl2  • ↓ Bax  • ↓ Caspase-9, Caspase-3  • ↓ PARP-1  • ↓ PARP-1  • ↓ PJNK  - Degenerating neurons:  • ↓ FJB + neuronal cells  - Survival neurons:  • ↓ MDA  - ↓ NO levels  - ↓ NO levels  - ↓ NO levels  - ↑ AChE  • ↓ AChE  • ↑ AChE | Caffeine attenuated D-galactose induced spatial learning and memory impairment, synaptic dysfunction, oxidative stress, apoptosis, neuroinflammation and neurodegeneration.  Tetrahydropalmatine (THP) attenuated D-galactose induced spatial learning and memory and locomotor and behavioral activity impairment, neurochemical deficits through decreasing oxidative damage, dysfunction of the cholinergic system, inflammatory markers and activation of astrocytes. | (Ullah et al., 2015) (Qu et al., 2016) |
|  |   |                                 |  |  | (201  | (continued on next page)               |

| P             |
|---------------|
| ā             |
| 2             |
| ÷             |
| 7             |
| Ö             |
| ಲ             |
|               |
| L)            |
| e             |
| $\overline{}$ |
| 7             |
| - 25          |

| Study model  | Methods  | Brain area      | Major finding  |   | Interpretation   | Ref                 |
|--|--|-----------------|--|---|--|---------------------|
|  |  |                 | Cognitive function   | Related findings  |  |                     |
| Middle-aged Sprague-Dawley rats Groups:  (1) control (0.9% saline, s.c.) (2) Mimetic aging group (10% D-ga, 1 ml/kg/d, s.c.) (3) DHEA-treated normal group (1 ml/kg/d, i.p.) (4) Vehicle control group (2% DMSO, i.p + 10% D-gai, 1 ml/kg/d, s.c.) (5) 2% DHEA-treated senescent group (1 ml/kg/d, s.c.) | - Morris water maze test<br>- Peripheral-type benzodiazepine binding<br>sites by autoradiographic localization | Cerebral cortex | <ul> <li>Morris water maze:</li> <li>↓ Escape latency</li> <li>↑ Time spent in the target quadrant</li> <li>↑ Swimming distance</li> </ul> | - Inflammatory markers:  • ↓ NF-κB  - Improved damaged neurons in the hippocampus CA1 region - region - Antioxidant ability:  • ↑ mitochondrial Peripheral benzodiazepine receptors | Dehydroepiandrosterone (DHEA) could improve spatial learning and memory in d-galactose-induced senescent rats, perhaps due to its ability to physiologically strengthen the antioxidant ability in mitochondria. | (Chen et al., 2008) |
| 1.p) + 10% D -gal, 1 ml/kg/d,<br>s.c   |  |                 |  |   |  |                     |
| Duranon: 8 weeks   |  |                 |  |   |  |                     |

activated B cells, ELISA: enzyme-linked immunosorbent assay; COX: Cyclooxygenase; TNP: tumor necrosis factor alpha; GFAP: Glial fibrillary acidic protein; ROS: reactive oxygen species; TNOS: total nitric oxide synthase; iNOS: inducible nitric s.c.: subcutaneous; p.o.: per oral; NADH: Nicotinamide adenine dinucleotide; MDA: malondialdehyde; NO: nitric oxide; SOD: superoxide dismutase; AchE: acetyl choline esterase; IL: interleukin; NF-xB: nuclear factor kappa-light-chain-enhancer of oxide synthase; 8-OHdG: 8-hydroxy-2'-deoxyguanosine; Ach E: acetylcholinesterase; NOX: NADPH oxidase; p22p<sup>plox</sup>, p67p<sup>plox</sup>, p67p<sup>plox</sup>, gbCnbuilt of NOX; cyt c: cytochrome c; bp: base pair; PCR: polymerase chain reaction; TRAP-PCR: Telomeric repeat associated β-galactosidase; Txnip: thioredoxin-interacting protein; p-IKKα, p-IKKβ phosphorylated IκB kinase α, β; Bcl: B-cell lymphoma; Bax: bcl-2-like protein 4; SOX: SRY (sex determining region Y)-box 2; p53, p19<sup>λrf</sup>, p21<sup>Cp1/Wafl</sup>, senescenceassociated genes; BrdU: Bromodeoxyuridine; Gal-c; galactosylceramidase; Aeg1: astrocyte elevated gene-1; Aß: amyloid beta protein; BACE-1: [b-site amyloid precursor protein cleaving enzyme 1; PARP: poly (ADP-ribose) polymerase; SNAP-23: synaptosomal-associated protein 23; p-CRBE: cAMP response elements binding; p-JNK: phosphorylated c-Jun N-terminal kinases; Iba-1: ionized calcium-binding adapter molecule 1; PSD95: postsynaptic density-95; FGF21: fibroblast growth factor amplification protocol, GSH: glutathione, GPx: glutathione peroxidase; CAT: catalase; T-AOC: total antioxidant capacity; AGEs: advanced glycation endproducts; RAGE: AGE receptons; PCR: polymerase chain reaction; SA-β-gal: senescence-21; BDNF: Brain-derived neurotrophic factor. galactose-induced mitochondrial dysfunction by strengthening the antioxidant ability via mitochondrial peripheral benzodiazepine receptors (Chen et al., 2008).

#### 1.6. Effect of D-galactose on cognitive function

Numerous studies found that systemic long-term administration of D-galactose has been used extensively to mediate the deterioration of cognitive function correlated to symptoms of aging (Lu et al., 2010b; Rehman et al., 2017; Yu et al., 2015; Zhu et al., 2014). Dosage of D-galactose impairment of cognitive function started from 50 mg to 180 mg/kg/day within a duration of 6–9 weeks. The tests used to detect the cognitive functions which monitor the effect of D-galactose-induced aging models were the following tests: Morris water maze, open field, step-through passive avoidance task, step-down, elevated plus maze paradigm and Y-maze as summarized in Table 4. Cognitive impairment in the D-galactose model has been shown to be caused by mitochondrial dysfunction, oxidative stress, apoptosis, inflammation and aging (Lu et al., 2010b; Rehman et al., 2017; Yu et al., 2015; Zhu et al., 2014).

It is known that the learning and memory deficit occurring in agerelated neurodegenerative disorders is associated with cholinergic decline (Lu et al., 2010a). Therefore, the acetylcholinesterase (AChE) activity and acetylcholine (ACh) level were estimated after behavioral tests. According to previous studies, D-galactose exerted a significant increase in AChE activity and a decrease in ACh level compared with

the controls (Kumar et al., 2009; Qu et al., 2016; Yang et al., 2016; Yu et al., 2015).

Three types of glial cells such as astrocytes, oligodendrocytes, and microglia are seen in the brain. The most abundant cells in the central nervous system are astrocytes (Ronaldson and Bendayan, 2008). Previous studies revealed that the activation of microglia cells and astrocytes plays pivotal roles in neurodegenerative disorders (Benner et al., 2004; Dauer and Przedborski, 2003; Lu et al., 2010a; Wu et al., 2002). Glial fibrillary acidic protein (GFAP) and CD11b are specific markers for activated microglia cells and astrocytes, respectively. When D-galactose was given, activated microglial cells and astrocytes in hippocampus, prefrontal cortex and whole brain were observed (Lu et al., 2010b; Rehman et al., 2017; Zhu et al., 2014).

Brain-derived neurotrophic factor (BDNF) is essential for neuronal proliferation, excitability, synaptic transmission and plasticity. In addition, BDNF plays a crucial role in supporting the survival and growth of sensory and motor neurons, all of which have major roles in cognitive function (Takeda et al., 2014). D-galactose caused BDNF deficit, subsequently leading to cognitive impairment (Chen et al., 2016).

These findings suggested that D-galactose impaired cognitive function via the mechanisms involved in the increase in oxidative stress, apoptosis, inflammation, and neuromodulation, the activation of astrocytes, microglia, BDNF deficiency and the decrease in antioxidant enzymes. All of these findings are summarized in Table 4.

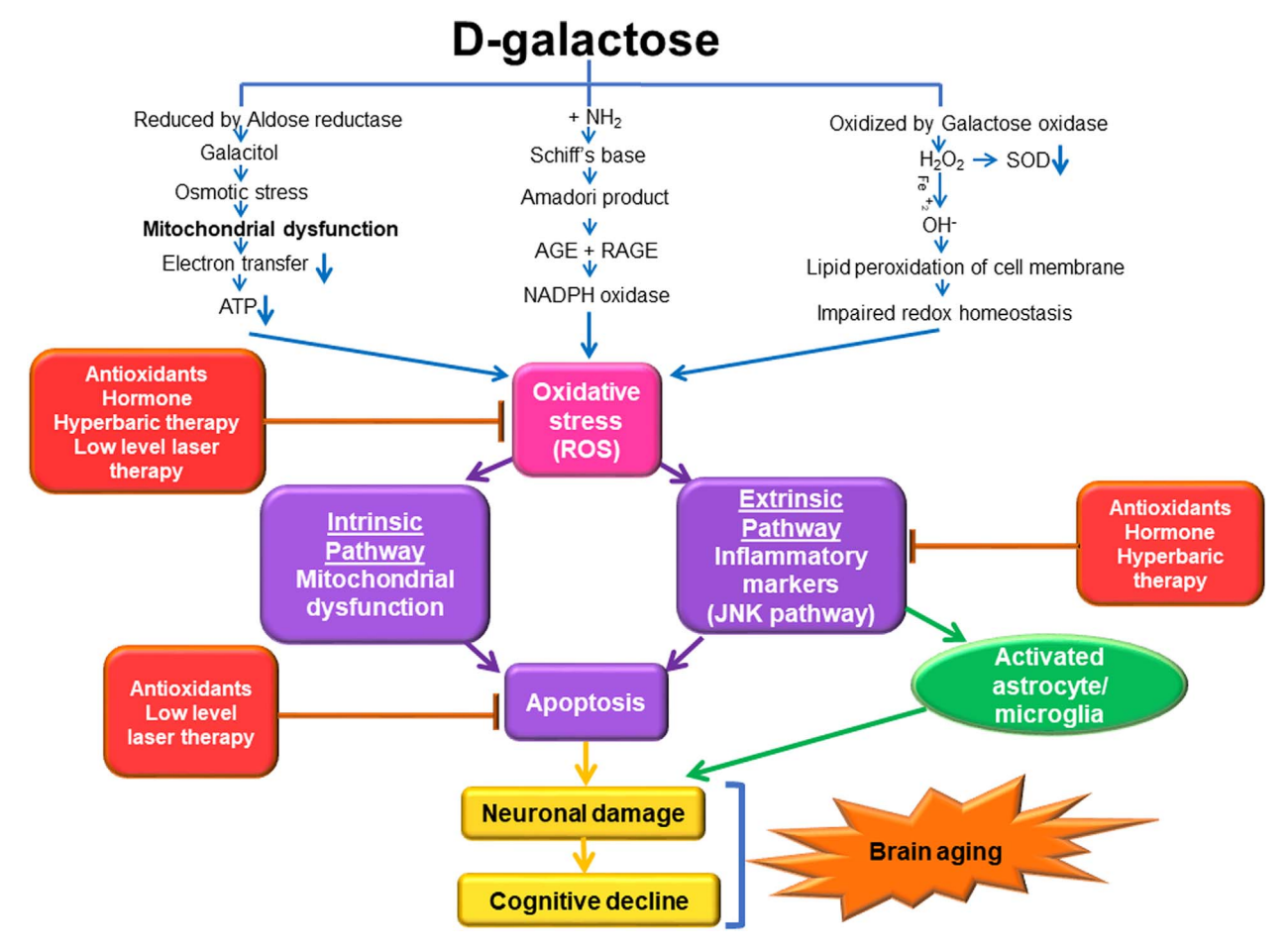


Fig. 1. The possible outcomes of D-galactose-induced brain aging and the therapeutic approaches available for its treatment. SOD: superoxide dismutase;  $H_2O_2$ : hydrogen peroxide; OH $^-$ : hydroxide ion; NH $_2$ : amino group; Fe $^+$ 2: ferrous oxide; AGE: advanced glycation end products; RAGE: receptors for advanced glycation end products; NADPH: Nicotinamide adenine dinucleotide phosphate; ROS: reactive oxygen species; ATP: Adenosine triphosphate; Cyt C: cytochrome c; JNK: phosphorylated c-Jun N-terminal kinase.

### 1.7. Therapeutic approaches addressing cognitive function in D-galactose-induced aging models

Various pharmacological anti-aging agents have been used to reverse the D-galactose-induced cognitive impairment. Among them, the most frequently used interventions are potent antioxidants, including ferulic acid, carvidilol, pioglitazone, curcumin and hesperidin. Those antioxidants improved cognitive function in a dose-dependent manner. In addition, anthocyanin, ursolic acid and ginsenoiside are antioxidants that have been shown to improve cognitive function in the D-galactose model (Lu et al., 2010b; Rehman et al., 2017; Zhu et al., 2014). The other therapeutic approaches to improve cognition with a dose-in-dependent manner in the D-galactose model were fibroblast growth factor 21 (FGF21), salidroside, and tetrahydropalmatine (Banji et al., 2014; Gao et al., 2015; Kumar et al., 2009; Prakash and Kumar, 2013; Qu et al., 2016; Yang et al., 2016; Yu et al., 2015). The dose-in-dependent manner may be due to limitations of their receptors in the brain, while the activity of antioxidants depends on dosage.

FGF21 acts on its receptors and prevents D-galactose-induced spatial learning and memory impairment by attenuating oxidative stress, inflammatory markers and renovating the activities of antioxidant enzymes and decreasing AGE formation, and TChE activity (Yu et al., 2015). While salidroside combines with numerous receptors and regulates several signaling pathways such as those for axonal guidance, glutamate reception, G-protein coupled reception, cAMP-mediation, endothelial nitric oxide synthase (eNOS), ephrin reception, and atherosclerosis signaling pathways, which all were important in the prevention of D-galactose-induced cognitive decline (Panossian et al., 2014). Tetrahydropalmatine is a dopamine receptor antagonist that can prevent D-galactose-induced spatial learning and memory impairment through decreasing oxidative damage, dysfunction of the cholinergic system, inflammatory markers and activation of astrocytes (Qu et al., 2016). Hyperbaric oxygen therapy, also known as HBOT, is a medical treatment which delivers oxygen to patients inside a compressed air chamber (Chen et al., 2016; Lu et al., 2010b; Zhu et al., 2014). HBO treatment can protect against cognitive impairment and hippocampal senescence by retaining the hippocampal BDNF expression and levels of antioxidants, reducing inflammation and modulating the aging-related gene expression in the D-galactose-induced aging mouse (Chen et al., 2016). Caffeine is 1, 3, 7-trimethylxanthine and is well known as the world's most famous psychoactive drug. Many studies have proved that a daily intake of caffeine ameliorated cognitive decline in "non-demented" elderly men and women by the mechanism of reducing synaptic dysfunction, and the reduction in oxidative stress, apoptosis, neuro-inflammation and neurodegeneration (Ritchie et al., 2007; van Gelder et al., 2007). Transcranial low-level laser therapy increased active mitochondrial levels, membrane potential, ATP production and abrogated oxidative stress and apoptosis, leading to a reversal in cognitive impairment in D-galactose-induced aging mice (Salehpour et al., 2017). All of these findings are summarized in Table 5.

#### 1.8. Future applications of D-galactose-induced brain aging model

There are several types of aging models used in anti-aging studies such as X-ray induced aging, jet lag induced aging, naturally aging models and D-galactose-induced aging models (Yanar et al., 2011). Among these aging models, D-galactose-induced aging model has the least side effects and take shorter time than naturally aging. D-galactose can accelerate the aging process, and can be used in research which can be faster to induce aging and easily accessible to induce brain senescence (Aydin et al., 2012; Cebe et al., 2014; Chen et al., 2010; Cui et al., 2006; Lu et al., 2007; Qu et al., 2016). For example: 1) Aydin and colleagues demonstrated that D-galactose-induced aging rats had significant similarities with the naturally aged rats in comparison of oxidative stress biomarkers in renal tissues (Aydin et al., 2012). 2) Cebe and colleagues also suggested that myocardial redox homeostasis in D-

galactose-induced aging rats was similar to that in naturally aging rats (Cebe et al., 2014). 3) Chen and colleagues observed that age-related central auditory dysfunction and its corresponding pathological changes are also present in both naturally aging rats and the D-galactose mimetic aging model (Chen et al., 2010). 4) Moreover, D-galactose has been shown to effectively induce cognitive impairment and can mimic many characters of the natural brain aging process (Cui et al., 2006; Lu et al., 2007; Qu et al., 2016). Thus, these reports indicated that D-galactose can be used as a reliable animal model for mimetic aging.

Furthermore, various therapeutic interventions for brain aging which targeted on several pathways such as mitochondrial function, oxidative stress, apoptosis, inflammation and BDNF deficiency have shown promising results in animal studies (see Tables 2 and 4). This information provides several mechanistic insights and can be beneficial for their clinical applications in elderly patients with brain aging disorders. For examples, as shown in D-galactose-induced aging animal models (Chen et al., 2016), hyperbaric therapy has been used as a method for resuscitation and therapy in elderly patients with acute cerebral and cardio-respiratory dysfunction (Rogatsky and Stambler, 2017). Moreover, anti-oxidant anthocyanin has been shown to improve beneficial effects for brain function and cognitive behavior in older people (Boespflug et al., 2017). In addition, the researchers started lowlevel laser therapy on the D-galactose induced aging animal model and now they observed that trans-cranial low-level laser therapy can restore ATP to delay cognitive decline in aging humans (de la Torre, 2017). All of these findings suggested that the therapeutic approaches used in Dgalactose-induced aging model can be translated to clinical application for prevention and better treatments in the neurodegenerative disorders. This growing evidence suggests that D-galactose-aging model can be used for studies of aging and certain aging-related neurological disorders, including Alzheimer's, Huntington's, and Parkinson's diseases. Moreover, several previous studies demonstrated that D-galactose could induce brain aging by causing oxidative stress and mitochondrial dysfunction (Banji et al., 2014; Kumar et al., 2009; Prakash and Kumar, 2013; Zhang et al., 2010). This will give a better understanding of the pathogenesis of cognitive decline and the nature of mitochondrial dysfunction during normal aging and in the early phases of neurodegenerative diseases for better therapeutic strategies.

#### 2. Conclusion

Aging is a world-wide problem we all are facing every day, which is why the therapeutic approaches to senescence are becoming more and more important. Of all the organs, the brain plays the most critical role in the process of senescence and is the most fragile of all the body organs in this instance. Brain aging encounters cognitive impairment which elevates the rate of dependency of older people worldwide. Dgalactose-induced mimetic aging is associated with the involvement of mitochondrial dysfunction, inflammation and apoptosis and BDNF deficiency and has been shown to mediate cognitive impairment. The effect of D-galactose on mitochondrial dysfunction can be evaluated by determining the activity of respiratory enzymes, oxidative stress markers and ATP synthesis and also measure changes in mitochondria DNA mutations, mitochondrial membrane potential and mitochondrial structures. A variety of treatments which target mitochondria and reducing oxidative stress and inflammation could be the main therapeutic approaches to ameliorate the deterioration of brain aging exerted by Dgalactose. The possible underlying mechanisms involved in D-galactose-induced brain aging and the possible therapeutic approaches utilized to date are summarized in Fig. 1.

Therefore, the findings from this review, which is a comprehensive summary of previous studies investigating the D-galactose-induced aging model, could lead to a better understanding of the underlying aging mechanisms. This increased knowledge could allow researchers to more-effectively manage the socio-economic burden of age-related disorders.

#### Acknowledgements

This work was supported by Thailand Research Fund Grants TRF-RTA6080003 (SCC), MRG5980198 (WP), the Faculty of Medicine, a NSTDA Research Chair Grant from the National Science and Technology Development Agency Thailand (NC), and a Chiang Mai University Center of Excellence Award (NC).

#### **Competing interests**

The authors declare that they have no competing interests.

#### References

- Acosta, P.B., Gross, K.C., 1995. Hidden sources of galactose in the environment. Eur. J. Pediatr. 154, S87–92.
- Ali, T., et al., 2015. Melatonin attenuates D-galactose-induced memory impairment, neuroinflammation and neurodegeneration via RAGE/NF-K B/JNK signaling pathway in aging mouse model. J. Pineal Res. 58, 71–85.
- Ames, B.N., 2004. Delaying the mitochondrial decay of aging. Ann. N. Y. Acad. Sci. 1019, 406–411.
- Ansari, N.A., Dash, D., 2013. Amadori glycated proteins: role in production of autoantibodies in diabetes mellitus and effect of inhibitors on non-enzymatic glycation. Aging Dis. 4, 50–56.
- Aydin, S., et al., 2012. Comparison of oxidative stress biomarkers in renal tissues of D-galactose induced, naturally aged and young rats. Biogerontology 13, 251–260.
- Banji, O.J., Banji, D., Ch, K., 2014. Curcumin and hesperidin improve cognition by suppressing mitochondrial dysfunction and apoptosis induced by D-galactose in rat brain. Food Chem. Toxicol. 74, 51–59.
- Benn, S.C., Woolf, C.J., 2004. Adult neuron survival strategies-slamming on the brakes. Nat. Rev. Neurosci. 5, 686–700.
- Benner, E.J., et al., 2004. Therapeutic immunization protects dopaminergic neurons in a mouse model of Parkinson's disease. Proc. Natl. Acad. Sci. U. S. A. 101, 9435–9440.
- Berry, G.T., 1993. Classic galactosemia and clinical variant galactosemia. In: Pagon, R.A., Adam, M.P., Ardinger, H.H., Wallace, S.E., Amemiya, A., Bean, L.J.H., Bird, T.D., Ledbetter, N., Mefford, H.C., Smith, R.J.H., Stephens, K. (Eds.), GeneReviews(R). University of Washington, Seattle University of Washington, Seattle (GeneReviews is a registered trademark of the University of Washington, Seattle. All rights reserved., Seattle (WA)).
- Bjelakovic, G., et al., 2011. Hypoglycemia as a Pathological Result in Medical Praxis.
   Boespflug, E.L., et al., 2017. Enhanced neural activation with blueberry supplementation in mild cognitive impairment. Nutr. Neurosci. 1–9.
- Çakatay, U., 2010. Protein redox-regulation mechanisms in aging. In: Bondy, S., Maiese, K. (Eds.), Aging and age-related disorders. Humana Press, Totowa, NJ, pp. 3–25.
- Carayon, P., Portier, M., Dussossoy, D., Bord, A., Petitpretre, G., Canat, X., Le Fur, G., Casellas, P., 1996. Involvement of peripheral benzodiazepine receptors in the protection of hematopoietic cells against oxygen radical damage. Blood 87, 3170–3178.
- Cebe, T., et al., 2014. A comprehensive study of myocardial redox homeostasis in naturally and mimetically aged rats. Age (Dordr.) 36, 9728.
- Chen, C., et al., 2008. Treatment with dehydroepiandrosterone increases peripheral benzodiazepine receptors of mitochondria from cerebral cortex in D-galactose-induced aged rats. Basic Clin. Pharmacol. Toxicol. 103, 493–501.
- Chen, B., et al., 2010. Age-related changes in the central auditory system: comparison of D-galactose-induced aging rats and naturally aging rats. Brain Res. 1344, 43–53.
- Chen, B., et al., 2011. Increased mitochondrial DNA damage and decreased base excision repair in the auditory cortex of D-galactose-induced aging rats. Mol. Biol. Rep. 38, 3635–3642.
- Chen, X., et al., 2016. Protective effect of hyperbaric oxygen on cognitive impairment induced by D-galactose in mice. Neurochem. Res. 41, 3032–3041.
- Coelho, A.I., Berry, G.T., Rubio-Gozalbo, M.E., 2015. Galactose metabolism and health. Curr. Opin. Clin. Nutr. Metab. Care 18, 422–427.
- Cui, X., et al., 2006. Chronic systemic D-galactose exposure induces memory loss, neurodegeneration, and oxidative damage in mice: protective effects of R-alpha-lipoic acid. J. Neurosci. Res. 83, 1584–1590.
- Cura, A.J., Carruthers, A., 2012. Role of monosaccharide transport proteins in carbohydrate assimilation, distribution, metabolism, and homeostasis. Compr. Physiol. 2, 863–914.
- Dauer, W., Przedborski, S., 2003. Parkinson's disease: mechanisms and models. Neuron 39, 889–909.
- Du, Z., et al., 2012. NADPH oxidase-dependent oxidative stress and mitochondrial damage in hippocampus of D-galactose-induced aging rats. J. Huazhong Univ. Sci. Technolog. Med. Sci. 32, 466–472.
- Du, Z., et al., 2015. NADPH oxidase 2-dependent oxidative stress, mitochondrial damage and apoptosis in the ventral cochlear nucleus of D-galactose-induced aging rats. Neuroscience 286, 281–292.
- Gao, J., et al., 2015. Salidroside ameliorates cognitive impairment in a d-galactose-induced rat model of Alzheimer's disease. Behav. Brain Res. 293, 27–33.
- van Gelder, B.M., et al., 2007. Coffee consumption is inversely associated with cognitive decline in elderly European men: the FINE Study. Eur. J. Clin. Nutr. 61, 226–232.

- Gillum, R.F., Yorrick, R., Obisesan, T.O., 2011. Population surveillance of dementia mortality. Int. J. Environ. Res. Public Health 8, 1244–1257.
- Golubev, A., Hanson, A.D., Gladyshev, V.N., 2017. Non-enzymatic molecular damage as a prototypic driver of aging. J. Biol. Chem. 292, 6029–6038.
- Grimm, A., Eckert, A., 2017. Brain aging and neurodegeneration: from a mitochondrial point of view. J. Neurochem. http://dx.doi.org/10.1111/jnc.14037.
- Haider, S., et al., 2015. A high dose of short term exogenous D-galactose administration in young male rats produces symptoms simulating the natural aging process. Life Sci. 124. 110–119.
- Hsieh, H.M., Wu, W.M., Hu, M.L., 2009. Soy isoflavones attenuate oxidative stress and improve parameters related to aging and Alzheimer's disease in C57BL/6J mice treated with D-galactose. Food Chem. Toxicol. 47, 625–632.
- Inman, D.M., et al., 2013. Alpha-lipoic acid antioxidant treatment limits glaucoma-related retinal ganglion cell death and dysfunction. PLoS One 8, e65389.
- Kumar, A., Dogra, S., Prakash, A., 2009. Effect of carvedilol on behavioral, mitochondrial dysfunction, and oxidative damage against D-galactose induced senescence in mice. Naunyn Schmiedeberg's Arch. Pharmacol. 380, 431–441.
- Lei, M., et al., 2008. Impairments of astrocytes are involved in the d-galactose-induced brain aging. Biochem. Biophys. Res. Commun. 369, 1082–1087.
- Long, J., et al., 2007. D-galactose toxicity in mice is associated with mitochondrial dysfunction: protecting effects of mitochondrial nutrient R-alpha-lipoic acid. Biogerontology 8, 373–381.
- Lu, J., et al., 2007. Ursolic acid ameliorates cognition deficits and attenuates oxidative damage in the brain of senescent mice induced by D-galactose. Biochem. Pharmacol. 74, 1078–1090.
- Lu, J., et al., 2010a. Chronic administration of troxerutin protects mouse brain against D-galactose-induced impairment of cholinergic system. Neurobiol. Learn. Mem. 93, 157–164.
- Lu, J., et al., 2010b. Ursolic acid attenuates D-galactose-induced inflammatory response in mouse prefrontal cortex through inhibiting AGEs/RAGE/NF-kappaB pathway activation. Cereb. Cortex 20, 2540–2548.
- Morava, E., 2014. Galactose supplementation in phosphoglucomutase-1 deficiency; review and outlook for a novel treatable CDG. Mol. Genet. Metab. 112, 275–279.
- Nagy, G., Pohl, N.L., 2015. Complete hexose isomer identification with mass spectrometry. J. Am. Soc. Mass Spectrom. 26, 677–685.
- Pak, J.W., et al., 2003. Mitochondrial DNA mutations as a fundamental mechanism in physiological declines associated with aging. Aging Cell 2, 1–7.
- Panossian, A., et al., 2014. Mechanism of action of Rhodiola, salidroside, tyrosol and triandrin in isolated neuroglial cells: an interactive pathway analysis of the downstream effects using RNA microarray data. Phytomedicine 21, 1325–1348.
- Prakash, A., Kumar, A., 2013. Pioglitazone alleviates the mitochondrial apoptotic pathway and mito-oxidative damage in the d-galactose-induced mouse model. Clin. Exp. Pharmacol. Physiol. 40, 644–651.
- Qian, Y.F., et al., 2008. Aqueous extract of the Chinese medicine, Danggui-Shaoyao-San, inhibits apoptosis in hydrogen peroxide-induced PC12 cells by preventing cytochrome c release and inactivating of caspase cascade. Cell Biol. Int. 32, 304–311.
- Qu, Z., et al., 2016. Protective effect of tetrahydropalmatine against d-galactose induced memory impairment in rat. Physiol. Behav. 154, 114–125.
- Rehman, S.U., et al., 2017. Anthocyanins reversed D-galactose-induced oxidative stress and Neuroinflammation mediated cognitive impairment in adult rats. Mol. Neurobiol. 54, 255–271.
- Ritchie, K., et al., 2007. The neuroprotective effects of caffeine: a prospective population study (the Three City Study). Neurology 69, 536–545.

  Rogatsky, G.G., Stambler, I., 2017. Hyperbaric oxygenation for resuscitation and therapy
- Rogatsky, G.G., Stambler, I., 2017. Hyperbaric oxygenation for resuscitation and therapy of elderly patients with cerebral and cardio-respiratory dysfunction. Front. Biosci. (Schol, Ed.) 9, 230–243.
- Ronaldson, P.T., Bendayan, R., 2008. HIV-1 viral envelope glycoprotein gp120 produces oxidative stress and regulates the functional expression of multidrug resistance protein-1 (Mrp1) in glial cells. J. Neurochem. 106, 1298–1313.
- Salehpour, F., et al., 2017. Transcranial low-level laser therapy improves brain mitochondrial function and cognitive impairment in D-galactose-induced aging mice. Neurobiol. Aging 58, 140–150.
- Sander, M., et al., 2015. The challenges of human population ageing. Age Ageing 44, 185-187.
- Sanz, A., Stefanatos, R.K., 2008. The mitochondrial free radical theory of aging: a critical view. Curr. Aging Sci. 1, 10-21.
- Schriner, S.E., et al., 2005. Extension of murine life span by overexpression of catalase targeted to mitochondria. Science 308, 1909–1911.
- Takeda, M., Takahashi, M., Matsumoto, S., 2014. Inflammation enhanced brain-derived neurotrophic factor-induced suppression of the voltage-gated potassium currents in small-diameter trigeminal ganglion neurons projecting to the trigeminal nucleus interpolaris/caudalis transition zone. Neuroscience 261, 223–231.
- de la Torre, J.C., 2017. Treating cognitive impairment with transcranial low level laser therapy. J. Photochem. Photobiol. B 168, 149–155.
- Ullah, F., et al., 2015. Caffeine prevents d-galactose-induced cognitive deficits, oxidative stress, neuroinflammation and neurodegeneration in the adult rat brain. Neurochem. Int. 90, 114–124.
- Wortmann, M., 2012. Dementia: a global health priority highlights from an ADI and World Health Organization report. Alzheimers Res. Ther. 4, 40.
- Wright, A.F., et al., 2004. Lifespan and mitochondrial control of neurodegeneration. Nat. Genet. 36, 1153–1158.
- Wu, D.C., et al., 2002. Blockade of microglial activation is neuroprotective in the 1-methyl-4-phenyl-1,2,3,6-tetrahydropyridine mouse model of Parkinson disease. J. Neurosci. 22, 1763–1771.
- Xian, Y.F., et al., 2014. Isorhynchophylline improves learning and memory impairments induced by D-galactose in mice. Neurochem. Int. 76, 42–49.

- Yanar, K., et al., 2011. Protein and DNA oxidation in different anatomic regions of rat brain in a mimetic ageing model. Basic Clin. Pharmacol. Toxicol. 109, 423–433.
- Yang, H., et al., 2016. Ferulic acid ameliorates memory impairment in d-galactose-induced aging mouse model. Int. J. Food Sci. Nutr. 67, 806–817.
- Yu, Y., et al., 2015. Fibroblast growth factor 21 protects mouse brain against D-galactose induced aging via suppression of oxidative stress response and advanced glycation end products formation. Pharmacol. Biochem. Behav. 133, 122–131.
- Zeng, L., et al., 2014. Age-related decrease in the mitochondrial sirtuin deacetylase Sirt3 expression associated with ROS accumulation in the auditory cortex of the mimetic
- aging rat model. PLoS One 9, e88019.
- Zhang, X., et al., 2010. Systemic administration of catalpol prevents d-galactose induced mitochondrial dysfunction in mice. Neurosci. Lett. 473, 224–228.
- Zhang, W.W., et al., 2011. Chronic administration of Liu Wei Dihuang protects rat's brain against D-galactose-induced impairment of cholinergic system. Sheng Li Xue Bao 63, 245–255.
- Zhu, J., et al., 2014. Ginsenoside Rg1 prevents cognitive impairment and hippocampus senescence in a rat model of D-galactose-induced aging. PLoS One 9, e101291.

RESEARCH Open Access



### Decreased microglial activation through gut-brain axis by prebiotics, probiotics, or synbiotics effectively restored cognitive function in obese-insulin resistant rats

Titikorn Chunchai<sup>1,2</sup>, Wannipa Thunapong<sup>1,2</sup>, Sakawdaurn Yasom<sup>3</sup>, Keerati Wanchai<sup>2</sup>, Sathima Eaimworawuthikul<sup>1</sup>, Gabrielle Metzler<sup>1</sup>, Anusorn Lungkaphin<sup>2</sup>, Anchalee Pongchaidecha<sup>2</sup>, Sasithorn Sirilun<sup>4</sup>, Chaiyavat Chaiyasut<sup>4</sup>, Wasana Pratchayasakul<sup>1,2</sup>, Parameth Thiennimitr<sup>3</sup>, Nipon Chattipakorn<sup>1,2</sup> and Siriporn C. Chattipakorn<sup>1,5\*</sup>

#### **Abstract**

**Background:** Chronic high-fat diet (HFD) consumption caused not only obese-insulin resistance, but also cognitive decline and microglial hyperactivity. Modified gut microbiota by prebiotics and probiotics improved obese-insulin resistance. However, the effects of prebiotics, probiotics, and synbiotics on cognition and microglial activity in an obese-insulin resistant condition have not yet been investigated. We aimed to evaluate the effect of prebiotic (Xyloolidosaccharide), probiotic (*Lactobacillus paracasei* HII01), or synbiotics in male obese-insulin resistant rats induced by a HFD.

**Methods:** Male Wistar rats were fed with either a normal diet or a HFD for 12 weeks. At week 13, the rats in each dietary group were randomly divided into four subgroups including vehicle group, prebiotics group, probiotics group, and synbiotics group. Rats received their assigned intervention for an additional 12 weeks. At the end of experimental protocol, the cognitive functioning of each rat was investigated; blood and brain samples were collected to determine metabolic parameters and investigate brain pathology.

**Results:** We found that chronic HFD consumption leads to gut and systemic inflammation and impaired peripheral insulin sensitivity, which were improved by all treatments. Prebiotics, probiotics, or synbiotics also improved hippocampal plasticity and attenuated brain mitochondrial dysfunction in HFD-fed rats. Interestingly, hippocampal oxidative stress and apoptosis were significantly decreased in HFD-fed rats with all therapies, which also decreased microglial activation, leading to restored cognitive function.

**Conclusions:** These findings suggest that consumption of prebiotics, probiotics, and synbiotics restored cognition in obese-insulin resistant subjects through gut-brain axis, leading to improved hippocampal plasticity, brain mitochondrial function, and decreased microglial activation.

**Keywords:** Xyloolidosaccharide, *Lactobacillus paracasei* HII01, Synbiotics, Microglia, Brain mitochondrial function, Cognitive function

<sup>&</sup>lt;sup>5</sup>Department of Oral Biology and Diagnostic Science, Faculty of Dentistry, Chiang Mai University, Chiang Mai 50200, Thailand Full list of author information is available at the end of the article



<sup>\*</sup> Correspondence: scchattipakorn@gmail.com; siriporn.c@cmu.ac.th

Neurophysiology Unit, Cardiac Electrophysiology Research and Training
Center, Faculty of Medicine, Chiang Mai University, Chiang Mai 50200,

#### **Background**

Obesity has reached epidemic proportions in many countries around the world [1]. Obesity is also known to lead to the development of insulin resistance [2, 3] and is associated with learning impairment and memory decline [4]. Growing evidence from our group have clearly demonstrated that obesity in rats, induced by long-term high-fat diet (HFD) consumption, not only caused peripheral insulin resistance, but also brain insulin resistance, dyslipidemia, and increased oxidative stress [3]. Furthermore, chronic HFD-fed rats have been shown to have the hippocampal synaptic dysfunction as indicated by the impairment of long-term potentiation (LTP) and dendritic spine loss, leading to cognitive decline [4-6]. In addition, mitochondrial dysfunction has been associated with a cognitive decline in rats fed chronically with HFD [5, 7-14].

Recently, the role of gut microbiota, a group of beneficial microbes living inside the gastrointestinal tract, has been revealed in several human diseases including obesity [15]. Human and rodents shared the similarity of gut microbiota in the phylum level which composed of the five major phyla including Firmicutes, Bacteroidetes, Actinobacteria, Proteobacteria, and Verrucomicrobia [16, 17]. Prolonged consumption of HFD resulted in an imbalance of gut microbiota termed "gut dysbiosis" by increasing the ratio of Firmicutes to Bacteroidetes (F/B ratio) and promoting the growth of *Proteobacteria* [18, 19]. Cumulative evidence showed that the modulation of gut microbiota by prebiotics and probiotics could be effective therapeutic strategies to improve obesity and insulin resistance [20]. Prebiotics, non-digestible food ingredients which were digested by gut microbiota [21], and probiotics, live microorganisms which, when administered in adequate amount, confer health benefits on the host [22], showed favorable effects by altering the composition and metabolism of gut microbiota and improved metabolic function in various animal models of metabolic syndrome [23]. Previous study also demonstrated that consumption of probiotics had beneficial effects to the brain through gut-brain axis [24]. Although probiotics had been shown to improve cognition and anxiety in hyperammonemia rats and also attenuated depression in humans [25], inconsistent reports exist in which probiotics failed to modulate stress or cognitive performance in healthy male subjects [26]. Furthermore, recent studies demonstrated that consumption of 10% of probiotic xylooligosaccharide (XOS) reduced the body weight, blood glucose, and cholesterol in streptozotozininduced diabetic rats [27]. In addition, a previous study demonstrated that 108 colony-forming unit (cfu) of the Lactobacillus paracasei HII01 could survive in the acidic environment of the gastrointestinal tract and in the presence of gastric enzymes, bile salts, and considered as a safe dose [28].

Microglia, the brain resident macrophage, has been proposed to play a crucial role in neurodegenerative disorders. It has been shown that microglia excessively pruned synapses and increased pro-inflammatory cytokines in models of Alzheimer's disease [29, 30]. Microglia are also associated with cognitive function [31]. Chronic HFD consumption has been shown to trigger microglial activation, leading to cognitive impairment [31-33]. Recent studies also illustrated the communication linking between microglial function and host microbiota [34, 35]. Moreover, it has been shown that gut microbiota could modulate key transcriptional coactivators, transcription factors, and enzymes involved in mitochondrial biogenesis [36]. Since mitochondria are the major producer of reactive oxygen species (ROS) [37], which could cause microglia activation [38, 39], these ROS and pro-inflammatory cytokines released from activated microglia inhibited LTP, resulting in cognitive impairment [40, 41]. In addition, pro-inflammatory cytokines could also activate intrinsic apoptotic pathway [42], which was attenuated by prebiotic and probiotics therapy [43].

Despite these previous findings, the effects of prebiotic XOS, probiotic *L. paracasei* HII01, or its combination, an equal amount of XOS and *L. paracasei* HII01 as a synbiotics, on the modulation of microglia and cognitive functions by altering gut microbiota composition in an obese-insulin resistant model have not been investigated. We tested the hypothesis that prebiotic, probiotic, or synbiotics in obese-insulin resistant rats induced by chronic HFD consumption reduces gut dysbiosis and improves cognitive function by attenuating gut inflammation, peripheral insulin resistance, restoring hippocampal synaptic plasticity, decreasing brain mitochondrial dysfunction and hippocampal oxidative stress and apoptosis, and preserving microglial morphology.

#### **Methods**

#### Animals and diet

All animal studies were approved by the Institutional Animal Care and Use Committee (IACUC) of the Faculty of Medicine, Chiang Mai University (Permit number: 13/2558 on May 12, 2015) and conformed to the Guide for the Care and Use of Laboratory Animals published by the US National Institutes of Health (NIH guide, 8th edition, 2011). Male Wistar rats (180-200 g) were purchased from the National Laboratory Animal Center, Salaya campus, Mahidol University, Bangkok, Thailand. All rats were housed individually in a temperature-controlled environment (25  $\pm$  0.5 °C) with a 12:12 h light-dark cycle. After 1 week of acclimatization, animals were fed with either a normal diet (ND; 19.77% energy from fat) or a high-fat diet (HFD; 59.28% energy from fat) for 12 weeks. All rats received reverse osmosis drinking water ad libitum. Food intake was recorded

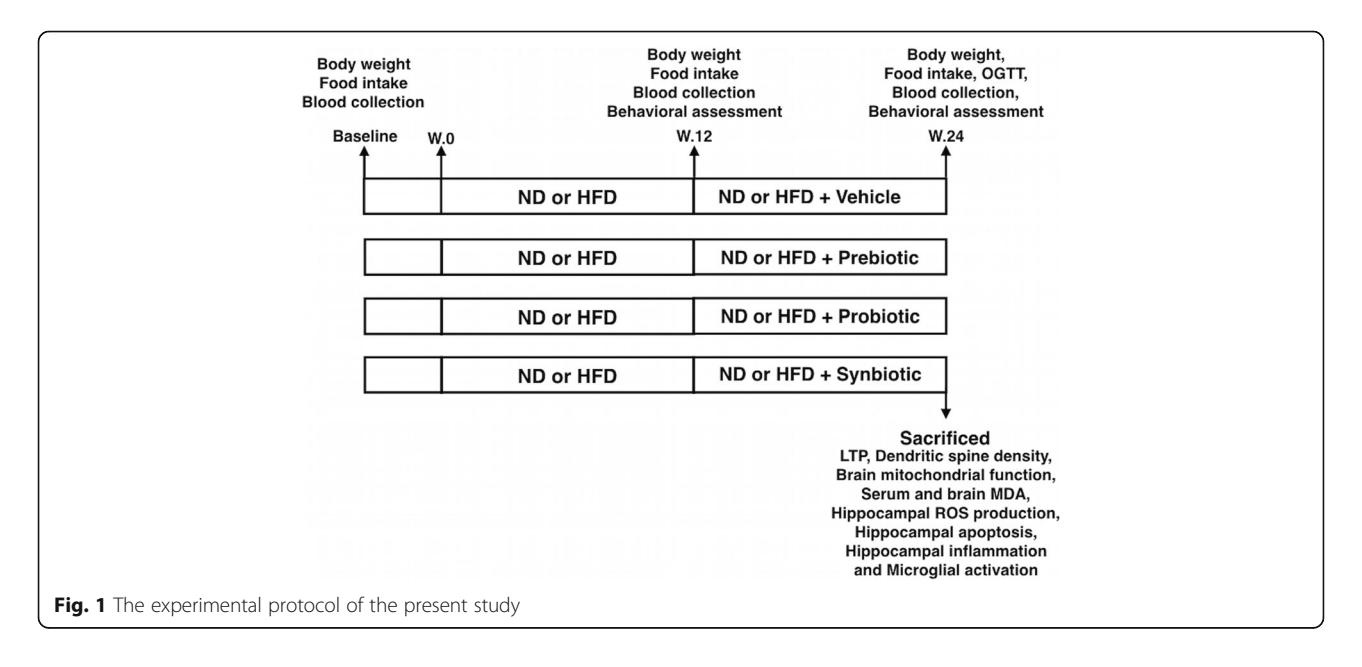
daily and body weight was recorded weekly. After 12 weeks, blood collection and behavioral assessment were measured in all animals. At week 13, the rats in each dietary group were randomly divided into four subgroups including ND- and HFD-fed rats oral feeding with phosphate buffer saline (PBS) as the vehicle group (NDV and HFV); ND- and HFD-fed rats oral feeding with prebiotics (10% XOS in PBS, 1 ml/day; NDPE and HFPE); ND- and HFD-fed rats oral feeding with probiotics  $(1 \times 10^8 \text{ cfu of } L. \text{ paracasei HII01, 1 ml/day; NDPO})$ and HFPO), and ND- and HFD-fed rats oral feeding with 2 ml of synbiotics (a 1:1 mixture of 10% XOS and 108 cfu L. paracasei HII01; NDC and HFC). For prebiotics, 10% of XOS has been shown to reduce the body weight, blood glucose, and cholesterol in streptozotozininduced diabetic rats [27]. For probiotics, a previous study demonstrated that 108 CFU of the L. paracasei HII01, which is a live microorganism, could survive in the acidic environment of the gastrointestinal tract and in the presence of gastric enzymes, bile salts, and considered as a safety dose [28]. The prebiotic XOS was purchased from Shandong Longlive Biotechnology CO., LTD., Shandong, China, and probiotic L. paracasei HII01 was kindly provided by the Department of Pharmaceutical Sciences, Faculty of Pharmacy, Chiang Mai University, Thailand. Rats received their assigned intervention for an additional 12 weeks.

At the end of the experimental protocol, the cognitive functioning of each rat was investigated and the oral glucose tolerance test (OGTT) was performed. Then, rats (n = 6/subgroup) were deeply anesthetized with isoflurane and killed by decapitation. The brain of each rat was quickly removed and carefully sliced in preparation for investigation, including extracellular recording

(electrical-induced LTP) for hippocampal plasticity, brain mitochondrial function, hippocampal ROS production, and hippocampal apoptosis. Another group of rats (n = 6/subgroup) was also deeply anesthetized with isoflurane and subsequently perfused with 4% paraformal-dehyde for determining microglial morphology. The experimental protocol is summarized in Fig. 1.

#### Metabolic parameters determination

Plasma glucose and cholesterol levels were determined via colorimetric assay (Biotech, Bangkok, Thailand). The commercial colorimetric assay kit (Biovision, CA, USA) was used for determining plasma total LDL levels. Plasma insulin levels were also determined using the Sandwich ELISA kit (LINCO Research, MO, USA). Homeostasis Model Assessment (HOMA) was used for assessing the peripheral insulin resistance as described in previous studies [44, 45]. OGTT was performed as described by Pintana et al. [5]. Briefly, rats were fasted overnight before the test and received 2 g/kg of glucose solution via oral gavage feeding. Blood samples were collected from the tail vein at 0, 15, 30, 60, 90, and 120 min after glucose administration. Areas under the curve (AUC) were calculated to evaluate glucose tolerance. To examine the brain oxidative stress, hippocampal malondialdehyde (MDA) level was determined by highperformance liquid chromatography (HPLC), as described in the previous studies [46]. Serum lipopolysaccharide (LPS) levels were measured by colorimetric method using the Pierce® LAL Chromogenic Endotoxin Quantitation Kit (Thermo Fisher Scientific, USA). Serum was diluted (1:10) with sterile endotoxin-free water and inactivated at 70 °C for 15 min. Then, the heat-inactivated serum was incubated with limulus amoebocyte lysate (LAL) at 37° for



 $10~\rm min$  as described previously [19]. Next, substrate solution was added; the development of magenta-colored derivative was detected using the absorbance at 410 nm. The concentrations of serum LPS in the samples were then calculated using the standard curve and reported in EU/mL.

#### Tissue and brain slice preparation

Brain tissue in each rat was removed and immersed in ice-cold artificial cerebrospinal fluid (aCSF) containing high sucrose for 30 min. Brain slices (400  $\mu m$ ) were cut on a vibratome (Vibratome Company, MO, USA). The slices were transferred to a room temperature (22–24 °C) CSF solution for an additional 30 min and subsequently transferred to a recording chamber containing standard aCSF for extracellular recording. Other brain tissue or hippocampi were homogenated in solution buffer containing protease inhibiter for brain mitochondrial function, hippocampal ROS production, and immunoblotting.

#### Quantitative real-time PCR analysis

Transcription levels of pro-inflammatory cytokine genes, IL-1β (5'-CACCTCTCAAGCAGAGCACAG-3' 5'-GGGTTCCATGGTGAAGTCAAC-3'), (5'-TCCTACCCCAACTTCCAATGCTC-3' and 5'-TT GGATGGTCTTGGTCCTTAGCC-3'), and immunosuppressive cytokine IL-10 (5'-AGTCAGCCAGACC CACAT-3' and 5'-GGCAACCCAAGTAACCCT-3') were determined as previously described [47]. In brief, the frozen colon and brain tissues in RNA preservative solution were homogenized by using 1 mm sterile zirconia/silica bead (Biospec Products, Bartlesville, US) and Minibeadbeater (Biospec Products, Bartlesville, US). Next, homogenized tissues were extracted from RNA using TRI reagent (TRIzol® Reagent, Ambion, Life Technologies, CA, US) according to the recommendations of the manufacturer. Then, a DNase treatment was performed by adding the DNA removal and inactivation kit (Ambion, Life Technologies, CA, US). The extracted tissue RNA was converted to complementary DNA (cDNA) using reverse transcription reagents (Tetro cDNA synthesis kit, Bioline, US). SYBR-Green (SensiFAST SYBR Lo-ROX kit, Bioline, US)-based realtime quantitative PCR was conducted using the primers and further analyzed by comparative Ct method. The mRNA expression levels of target genes were normalized with Gapdh (5'-GTATTGGGCGCCTGGT CACC-3' and 5'-CGCTCCTGGAAGATGGTGATGG-3') mRNA levels.

### Extracellular recordings of hippocampal slices long-term potentiation

To determine hippocampal plasticity, the field excitatory postsynaptic potentials (fEPSP) slope of LTP was

measured from CA1 area of hippocampal slices. LTP is a marker of hippocampal synaptic plasticity. [3]. Briefly, brain slices were transferred to a submersion recording chamber and continuously perfused at 3-4 ml/min with standard aCSF warmed to 28-29 °C. Field excitatory postsynaptic potentials (fEPSPs) were evoked by stimulating the Schaffer collateral-commissural pathway with a bipolar tungsten electrode, while the fEPSPs recordings were taken from the stratum radiatum of the hippocampal CA1 region with micropipettes (3 MW) filled with 2M NaCl. LTP was induced by delivering high-frequency tetani [high-frequency stimulation (HFS); four trains at 100 Hz; 0.5 s duration; 20 s interval] at 1.5 times the baseline stimulation intensity. Experiments were performed for at least 40 min after HFS. The amount of potentiation was calculated at 40 min after tetanus. Data were filtered at 3 kHz, digitized at 10 kHz, and stored in a computer using pClamp9.2 software (Axon Instruments, CA, USA). The initial slope of the fEPSPs was measured and plotted against time [3, 8, 9, 11–14, 48].

#### **Brain mitochondrial function**

Brain mitochondria were isolated as described in Pipatpiboon et al. [11]. Mitochondrial protein was determined by the BCA assay as described previously [5], and brain mitochondrial function including brain mitochondrial ROS, mitochondrial membrane potential change ( $\Delta \Psi m$ ), and mitochondrial swelling was determined [13, 14, 48]. Brain mitochondrial ROS were measured using dichlorohydrofluoresceindiacetate (DCFHDA) fluorescent dye. The change in mitochondrial membrane potential ( $\Delta \Psi m$ ) was measured using the fluorescent dye 5, 5¢, 6, 6¢-tetrachloro-1, 1¢, 3, 3¢-tetraethyl benzimidazolcarbocyanine iodide (JC-1), and brain mitochondrial swelling was determined by measuring the change in the absorbance of brain mitochondrial suspension at 540 nm. All were determined by following the methods described previously [13, 14, 48].

#### Immunoblotting of hippocampal apoptotic and antiapoptotic proteins

To investigate the hippocampal apoptosis, homogenate hippocampi were used, as described in the references [13, 14, 48]. Examination of the level of apoptotic and anti-apoptotic protein expression was conducted with homogenates prepared from hippocampus tissue. These proteins were separated and identified by an immunoblot assay conducted with rabbit anti-bax (1:200; Santa Cruz Biotechnology, CA, USA), bcl-2 (1:1000; Cell Signaling Technology, MA, USA). For a loading control, immunoblotting for each membrane was incubated with anti- $\beta$ -actin (1:4000; #4967; Cell Signaling Technology, MA, USA). All membranes were incubated with a secondary goat anti-rabbit antibody conjugated with horseradish peroxidase (1:2000; #7074; Cell Signaling

Technology, MA, USA). The protein bands were visualized on ChemiDocÔ touch imaging system (Bio-Rad, CA, USA) using Amersham ECL Western blot detection reagents (GE Healthcare, Buckinghamshire, UK). The band intensity was measured by Scion Image, and the results were represented as average signal intensity (arbitrary) units.

### Immunofluorescent labeling for hippocampal plasticity, microglial morphology, and image analysis

Animals were transcardially perfused with 4% paraformaldehyde, postfix for an additional 24 h, cryoprotected in 30% sucrose in PBS at 4 °C, and then frozen in isopentane and dry ice, and stored at -80 °C. Then, the brains were cut using cryosection (Leica CM1950, Leica Biosystem Nussloch GmbH, Nussloch, Germany) at 20 µm. Sections were subjected to label immunofluorescence. The sections were quenched with 3% peroxide, blocked with 5% BSA, and incubated overnight at 4 °C with primary antibodies for Iba-1 (ab5076, Abcam, Cambridge, MA) for microglia morphology [32]. After being washed three times in TBS, sections were incubated with AlexaFluor conjugated secondary antibodies; Iba1- AlexaFluor 488 anti-goat, for 1 h at 25 °C then rinsed in TBS. Sections were treated with copper sulfate in ammonium acetate buffer to quench endogenous autofluorescence of the brain tissue. To determine the microglial morphology, the series of z-stacks of microglia images were taken from confocal microscopy (Olympus flouview FV3000) and microglial morphology was measured by Imaris software 7.0 (Bitplane, Oxford instrument company, AG, Zurich, Switzerland). Three microglial cells per brain slice, three brain slices per animal and six animals per group were measured from the CA1 region of the hippocampus. All microglial morphology parameters including soma area, processes length and the number of primary branch projection (ramification) were measured from a 3D constructuring using Imaris. The number of Iba-1 positive cells and the mean fluorescent intensity were also measured. For visualization of dendritic spines, slices were labeled with the carbocyanine dye 1,1'-dioctadecyl-3,3,3',3'-Tetramethylindocarbocyanine Perchlorate (DiI; Invitrogen), as described previously [32, 33]. Slices were incubated with appropriately placed DiI crystals for 48-72 h before being mounted on slides and coverslipped in 0.1 M Tris buffer. Sections were mounted on slides and coverslipped by the anti-fading mounting medium Fluoromount (Sigma-Aldrich Chemie, Steinheim, Germany). To assess the dendritic spine density, a series of 10 optical sections were taken every 0.25 mm in the z-plane, stacked into z-stacks of 2.5 mm, and shown as a z-projection of the total z-stack. For spine analysis, the three tertiary segments, 100-200 µm apart from the soma and  $20-30~\mu m$  in dendritic length, were used to randomly measure dendritic spine density. Three neuronal cells per brain slice and three brain slices per animal were chosen for spine quantitative analysis. The number of spines was counted by double-blind hand counter [48].

#### Cognitive function test

The Morris water maze test was performed to determine cognitive function with two assessments, including five consecutive days of the acquisition test, and the probe test on day sixth. Time to find the platform was recorded in the acquisition test, and the time spent in the target quadrant was also recorded in the probe test [46, 49]. Data analysis of the MWM test was done manually from videotape recordings by the investigators, who were blinded to experimental groups. To determine locomotor activity, all animals were tested by open-field test [50, 51]. In this method, the apparatus consists of a rectangular-based box open from above (70 cm long and wide, and 90 cm in height). Each animal was placed into the box and allowed for 5-min exploration. After 10 mins of exploration time, the animals were taken out. The distance was counted using SMART 3.0 software (Panlab<sup>®</sup>, Harvard Apparatus, Barcelona, Spain).

#### Gut microbiota analysis

Feces of each animal were collected at the end of experimental protocol. Bacterial genomic DNA was extracted from rat fecal pellet using a commercial genomic DNA isolation kit (QIAGEN, Germany). Briefly, the fecal sample (0.25 g) was homogenized in QIAGEN ASL lysis buffer by a Minibeadbeater (BioSpec products, Bartlesville, USA). The extraction of bacterial genomic DNA was done following the manufacturer's instruction. The fractions of bacterial microbiota population (*Firmicutes/Bacteroidetes* ratio) were quantified using real-time quantitative reverse transcription PCR (qRT-PCR) as described previously [52].

#### Statistical analysis

Data from each experiment were expressed as mean  $\pm$  S.E.M. For all multiple comparisons, data were analyzed using a two-way ANOVA, followed by post-hoc Tukey's analysis. Correlations and regression analysis were also conducted to look at relationships between metabolic parameters and behavioral test. For behavioral test, the significance of the difference of acquisition test was calculated using repeated two-way ANOVA, followed by post-hoc Tukey's analysis. The significance of the difference of probe test at week 12 was calculated using an independent t test. A p < 0.05 was considered as statistically significant.

#### **Results**

Long-term HFD consumption induced gut dysbiosis and systemic inflammation, which was attenuated by prebiotic XOS, probiotic *L. paracasei* HIIO1, or synbiotics

Pro-inflammatory cytokine interleukin (IL)-1 and IL-6 mRNA expression levels were significantly increased in the colon of rats fed with a HFD compared to rats fed with a ND, whereas the immunosuppressive cytokine IL-10 mRNA level was not altered (Fig. 2a-c). Diet-induced obese rats also developed the metabolic endotoxemia, the increased LPS in their sera (Fig. 2d), which was ameliorated by consumption of prebiotic XOS, probiotic L. paracasei HIIO1, or the synbiotics (Fig. 2e). Collectively, chronic HFD consumption resulted in both local (colon) and systemic (metabolic endotoxemia) inflammation, and consumption of prebiotic XOS, probiotic L. paracasei HIIO1, or the synbiotics could significantly reduce these low-grade inflammations. In this study, the pro-inflammatory mRNA levels of IL-1β and IL-6 from the whole brain tissues were not different among groups (Table 2). However, the two hippocampi in each animal were sufficient only for protocol of dendritic spine, hippocampal ROS production, and Western blot analysis; therefore, we did not have enough hippocampal tissues for cytokine analysis.

Our findings demonstrated that HFD-induced gut dysbiosis, as indicated by an increased F/B ratio in HFD-fed rats treated with vehicle (0.479  $\pm$  0.174), compared to that of ND-fed rats treated with vehicle (0.159  $\pm$  0.235, p < 0.05). The F/B ratio of HFD-fed rats treated with prebiotic XOS (0.089  $\pm$  0.312), probiotic *L. paracasei HII01* (0.167  $\pm$  0.522), or synbiotics (0.160  $\pm$  0.188) was equally

reduced when compared with the F/B ratio of HFD-fed rats treated with vehicle (0.479  $\pm$  0.174, p < 0.05). These findings indicated that long-term HFD consumption caused gut dysbiosis, and the supplement with prebiotics, probiotics, and synbiotics could attenuate gut dysbiosis, as indicated by decreased F/B ratio.

## Long-term HFD consumption caused peripheral insulin resistance and dyslipidemia, and treatments attenuated these metabolic disturbances

After 12 weeks of HFD consumption, the body weight, plasma insulin level, and HOMA index of HFD-fed rats increased significantly when compared to ND-fed rats without alteration of the plasma glucose level (Table 1). Moreover, rats fed with a HFD had significantly increased plasma total cholesterol and LDL cholesterol when compared to the ND-fed rats (Table 1). Interestingly, 12 weeks of prebiotic XOS, probiotic *L. paracasei* HIIO1 or the synbiotics supplements had significantly decreased plasma insulin level, HOMA index, area under the curve of the oral glucose tolerance test (AUCg), plasma total cholesterol level, and LDL cholesterol level when compared to the HFD-fed rats receiving the vehicle (Table 2). These findings suggested that long-term HFD consumption caused peripheral insulin resistance as indicated by hyperinsulinemia with euglycemia and increased HOMA index as well as dyslipidemia, which were improved by all treatments.

Before treatment, we found a negative correlation between time in target quadrant of probe test with the metabolic parameters including body weight (r = -0.689, p < 0.01), insulin (r = -0.658, p < 0.01),

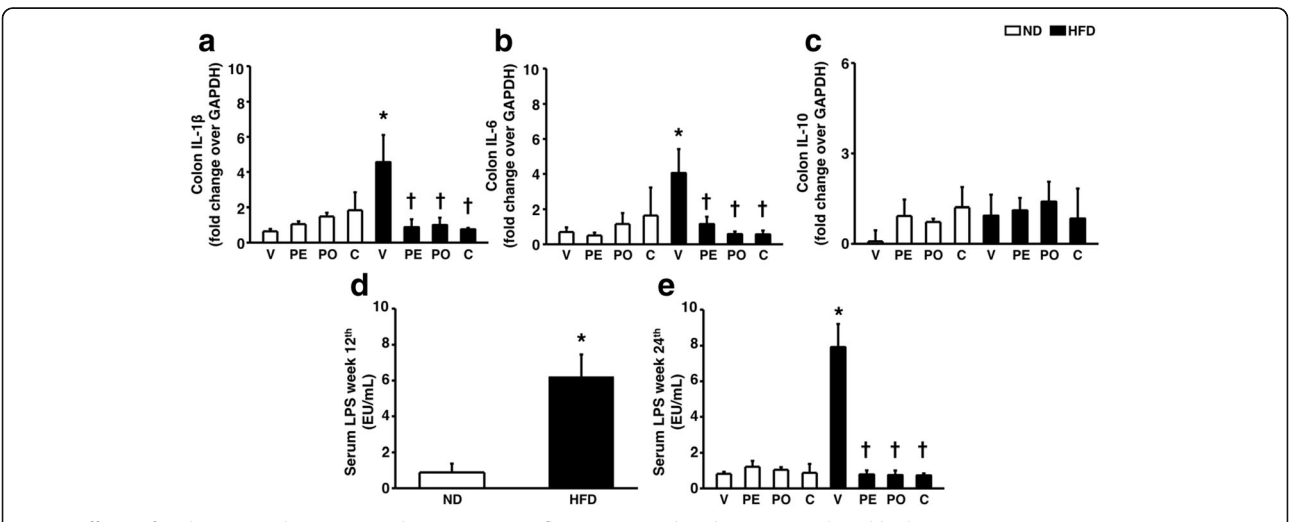


**Fig. 2** Effects of prebiotics, probiotics, or synbiotics on gut inflammation and endotoxemia induced by long-term HFD consumption. **a–c** The pro-inflammatory cytokine including IL-1β expression, IL-6 and IL-10, anti-inflammatory cytokine, expression respectively. **d** Serum LPS level of ND- and HFD-fed rats at 12th week. **e** Serum LPS level of ND- and HFD-fed rats after receiving prebiotics, probiotics, or synbiotics. ND: 12-week-normal diet-fed rats; HFD: 12-week high fat-fed rats; V: rats receiving PBS as vehicle; PE: rats receiving prebiotics; PO: rats receiving probiotics; C: rats receiving combination of prebiotics and probiotics as synbiotics (N = 6 of each group) \*p < 0.05 in comparison with the ND-fed rats; †p < 0.05 in comparison with the HFD-fed rats receiving vehicle

**Table 1** The metabolic parameters at baseline and after 12 weeks of either ND or HFD consumption

| Metabolic parameters              | Baseline      | ND             | HFD             |
|-----------------------------------|---------------|----------------|-----------------|
| Body weight (g)                   | 225 ± 2       | 459 ± 6*       | 540 ± 9*†       |
| Food intake (g/day)               | $21 \pm 0.5$  | $21 \pm 0.2$   | 24 ± 0.2*†      |
| Plasma glucose (mg/dl)            | $132.6 \pm 6$ | $137.7 \pm 4$  | $142.2 \pm 5$   |
| Plasma insulin (ng/ml)            | $2.3 \pm 0.3$ | $4.6 \pm 0.4*$ | $6.0 \pm 0.5*†$ |
| HOMA index                        | $22.4 \pm 5$  | $41.7 \pm 4*$  | 63.4 ± 7*†      |
| Plasma total cholesterol (mg/dl)  | $74.7 \pm 2$  | $72.5 \pm 3$   | 89.4 ± 3*†      |
| Plasma total triglyceride (mg/dl) | $61.1 \pm 5$  | $65.2 \pm 3$   | $66.1 \pm 5$    |
| LDL cholesterol (mg/dl)           | $21.5 \pm 3$  | $21.9 \pm 3$   | 34.1 ± 3*†      |

<sup>\*</sup>P < 0.05 in comparison with baseline group

HOMA index (r = -0.756, p < 0.01), plasma total cholesterol (r = -0.724, p < 0.01), and serum LPS level (r = -0.877, p < 0.01). After treatment with prebiotic, probiotic, or synbiotics, we found the negative correlations between time in target quadrant of probe test with the metabolic parameters and inflammatory markers including body weight (r = -0.387, p < 0.01), plasma total cholesterol (r = -0.388, p < 0.01), LDL cholesterol (r = -0.492, p < 0.01), colon IL-6 mRNA expression (r = -0.355, p < 0.01), fat mass (r = -0.333, p < 0.01), serum LPS level (r = -0.312, p < 0.05), and brain LPS level (r = -0.466, p < 0.01). Taken together, these findings added the potential mechanism regarding the protective effects of prebiotic, probiotic, or synbiotics on cognitive dysfunction in obese-insulin resistant rat that could occur possibly through the modulation of LDL cholesterol level, fat mass, and serum and brain LPS level as well as the level of colon IL-6 mRNA expression.

# Prebiotic XOS, probiotic *L. paracasei* HIIO1, or the synbiotics restored hippocampal plasticity impaired by long-term HFD consumption

To determine hippocampal plasticity, the fEPSP slope of LTP was measured from CA1 area of hippocampal slices. LTP is a marker of hippocampal synaptic plasticity. HFD-fed rats treated with the vehicle showed impaired hippocampal plasticity indicated by a significantly decreased mean fEPSP slopes compared to ND-fed rats, whereas all treatments effectively normalized the fEPSP slopes (n = 2-3 independent slices/animal, n = 6 animals/ group; (Fig. 3a-b)) in these HFD rats. In addition, dendritic spine density was also significantly decreased in HFD rats, which was restored in HFD-fed rats treated with prebiotic XOS, probiotic L. paracasei HIIO1, or synbiotics (Fig. 3c-d). Taken together, long-term HFD consumption demonstrated hippocampal dysplasticity as indicated by impaired LTP and decreased dendritic spine density, and all treatments reversed these impairments.

Prebiotic XOS, probiotic *L. paracasei* HIIO1, or the synbiotics improved brain mitochondrial dysfunction, hippocampal oxidative stress, and hippocampal apoptosis To determine brain mitochondrial function, the whole brain and hippocampus ROS production, brain mitochondrial depolarization, and brain mitochondrial swelling were measured. HFD-fed rats treated with the vehicle had increased brain and hippocampus ROS

**Table 2** The metabolic parameters after 12 weeks of vehicle, prebiotic, probiotic, or synbiotics administration in ND-fed rats and HFD-fed rats

| Metabolic parameters   | ND             |                |                |                | HFD              |                       |                        |                        |
|--|----------------|----------------|----------------|----------------|------------------|-----------------------|------------------------|------------------------|
|  | NDV            | NDPE           | NDPO           | NDC            | HFV              | HFPE                  | HFPO                   | HFC                    |
| Body weight (g)  | 501 ± 9        | 495 ± 11       | 517 ± 14       | 510 ± 13       | 680 ± 24*        | 605 ± 30*†            | 689 ± 33*              | 600 ± 34*†             |
| Food intake (g/day)  | $20 \pm 0.5$   | $19 \pm 0.7$   | $21 \pm 0.9$   | $21 \pm 0.4$   | $25 \pm 0.4*$    | $23 \pm 0.7*$         | $25 \pm 0.5*$          | $24 \pm 0.5*$          |
| Visceral fat (g)   | $25 \pm 2$     | $27 \pm 3$     | $29 \pm 3$     | $33 \pm 2$     | $63 \pm 3*$      | $43 \pm 5*†$          | $65 \pm 3*$            | $48 \pm 5*†$           |
| Plasma glucose (mg/d)  | $132.3 \pm 7$  | $140.5 \pm 8$  | 137.5 ± 8      | $141.6 \pm 12$ | $139.2 \pm 9$    | $142.1 \pm 6$         | $137.8 \pm 4$          | 132.1 ± 14             |
| Plasma insulin (ng/ml)   | $4.8 \pm 0.8$  | $5.5 \pm 1$    | $5.4 \pm 0.8$  | $4.0 \pm 1$    | $7.8 \pm 0.5*$   | 5.5 ± 0.5†            | 5.2 ± 1†               | $5.0 \pm 1 †$          |
| HOMA index   | $40.3 \pm 10$  | $50.0 \pm 14$  | 55.8 ± 11      | $50.9 \pm 12$  | 94.6 ± 12*       | 55.6 ± 6†             | $60.5 \pm 8 †$         | 39.8 ± 5†              |
| Plasma glucose AUC (AUCg) (mg/dl $\times$ min $\times$ 10 <sup>4</sup> ) | $2.1 \pm 0.1$  | $2.0 \pm 0.1$  | $2.2 \pm 1$    | $2.3 \pm 0.1$  | $2.9 \pm 0.1*$   | $2.1 \pm 0.1 \dagger$ | $2.4 \pm 0.1 \dagger$  | $2.2 \pm 0.1 \dagger$  |
| Plasma total cholesterol (mg/dl)   | $74.4 \pm 4$   | $68.7 \pm 4$   | $65.9 \pm 5$   | $58.6 \pm 5$   | 111.1 ± 8*       | 73.9 ± 3†             | $78.8 \pm 4 †$         | 75.2 ± 6†              |
| Plasma total triglyceride (mg/dl)  | $78.3 \pm 13$  | $71.5 \pm 6$   | $68.7 \pm 8$   | $77.7 \pm 7$   | 84.9 ± 10        | $73.3 \pm 6$          | $78.3 \pm 4$           | $74.5 \pm 4$           |
| Plasma LDL cholesterol (mg/dl)   | $24.2 \pm 5$   | $22.3 \pm 2$   | $23.5 \pm 6$   | $22.7 \pm 6$   | 65.7 ± 10*       | 33.1 ± 4†             | 35.3 ± 5†              | 27.1 ± 5†              |
| Serum MDA (µmol/dl)  | $3.72 \pm 0.2$ | $3.92 \pm 0.1$ | $3.91 \pm 0.1$ | $3.64 \pm 0.2$ | $5.76 \pm 0.5$ * | 3.31 ± 0.2†           | $3.23 \pm 0.3 \dagger$ | $3.16 \pm 0.2 \dagger$ |
| Brain MDA (μmol/mg protein)  | $7.59 \pm 1.8$ | $8.10 \pm 1.9$ | $6.58 \pm 1.6$ | 2.01 ± 1.0*    | 15.0 ± 2.1*      | 8.23 ± 1.9†           | 5.59 ± 1.1†            | 1.84 ± 0.7*†           |
| Brain IL-1β (fold change/gapdh)  | 1.39 ± 0.5     | $0.45 \pm 0.1$ | $2.03 \pm 0.1$ | $1.82 \pm 0.4$ | $0.35 \pm 0.1$   | $0.71 \pm 0.3$        | $1.08 \pm 0.6$         | 0.51 ± 0.2             |
| Brain IL-6 (fold change/gapdh)   | $1.27 \pm 0.5$ | $1.30 \pm 0.8$ | 10.68 ± 5.4    | 7.54 ± 1.2     | $1.10 \pm 0.4$   | $1.29 \pm 0.1$        | $3.57 \pm 2.7$         | $0.80 \pm 0.2$         |

<sup>\*</sup>P < 0.05 in comparison with the NDV group

<sup>†</sup>P < 0.05 in comparison with ND group

 $<sup>\</sup>dagger P < 0.05$  in comparison with the HFV group

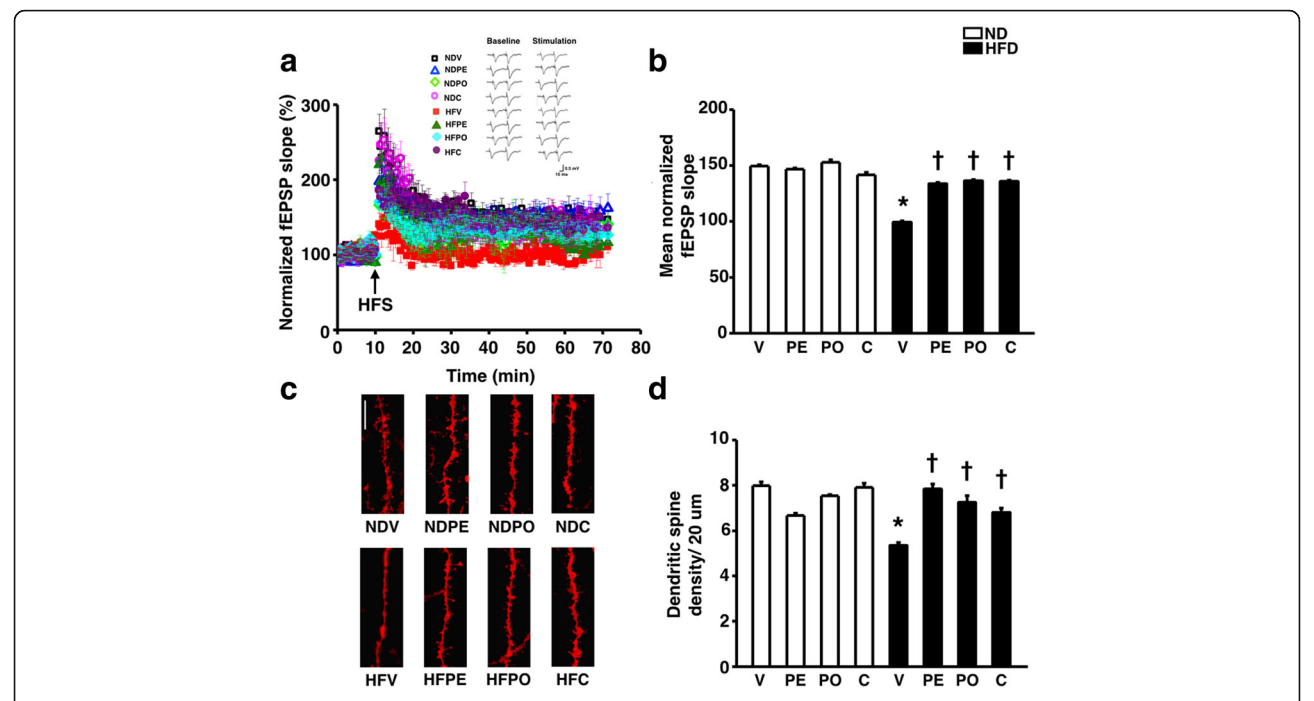


**Fig. 3** Effects of prebiotics, probiotics, or synbiotics on hippocampal plasticity. **a** Percentage normalized fEPSP slope of electrical-induced LTP by extracellular recording. **b** Mean fEPSP slope from 50 to 60 mins of electrical-induced LTP. **c** Representative images of Dil immunofluorescent under confocal microscopy (bar =  $5 \mu m$ ). **d** Mean dendritic spine density. ND: 24-week-normal diet-fed rats; HFD: 24-week high fat-fed rats; V: rats receiving PBS as vehicle; PE: rats receiving prebiotics; PO: rats receiving probiotics; C: rats receiving combination of prebiotics and probiotics as synbiotics (N = 6 of each group) \*p < 0.05 in comparison with the ND-fed rats; †p < 0.05 in comparison with the HFD-fed rats receiving vehicle

production (Fig. 4a–b), brain mitochondrial depolarization (Fig. 4c) as well as decreased brain mitochondrial absorbance indicating brain mitochondrial swelling (Fig. 4d). These impairments were attenuated by all treatments. In addition, to determine hippocampal apoptosis, the expression of apoptotic and anti-apoptotic proteins including bax and bcl-2 was determined. The increase of bax expression and decrease of bcl-2 expression found in HFD-fed rats treated with the vehicle was improved in HFD-fed rats receiving prebiotic XOS, probiotic *L. paracasei* HIIO1, or the synbiotics (Fig. 4e–f). These findings demonstrated that all treatments ameliorated brain mitochondrial dysfunction, decreased hippocampal oxidative stress levels, and exerted anti-apoptotic effects.

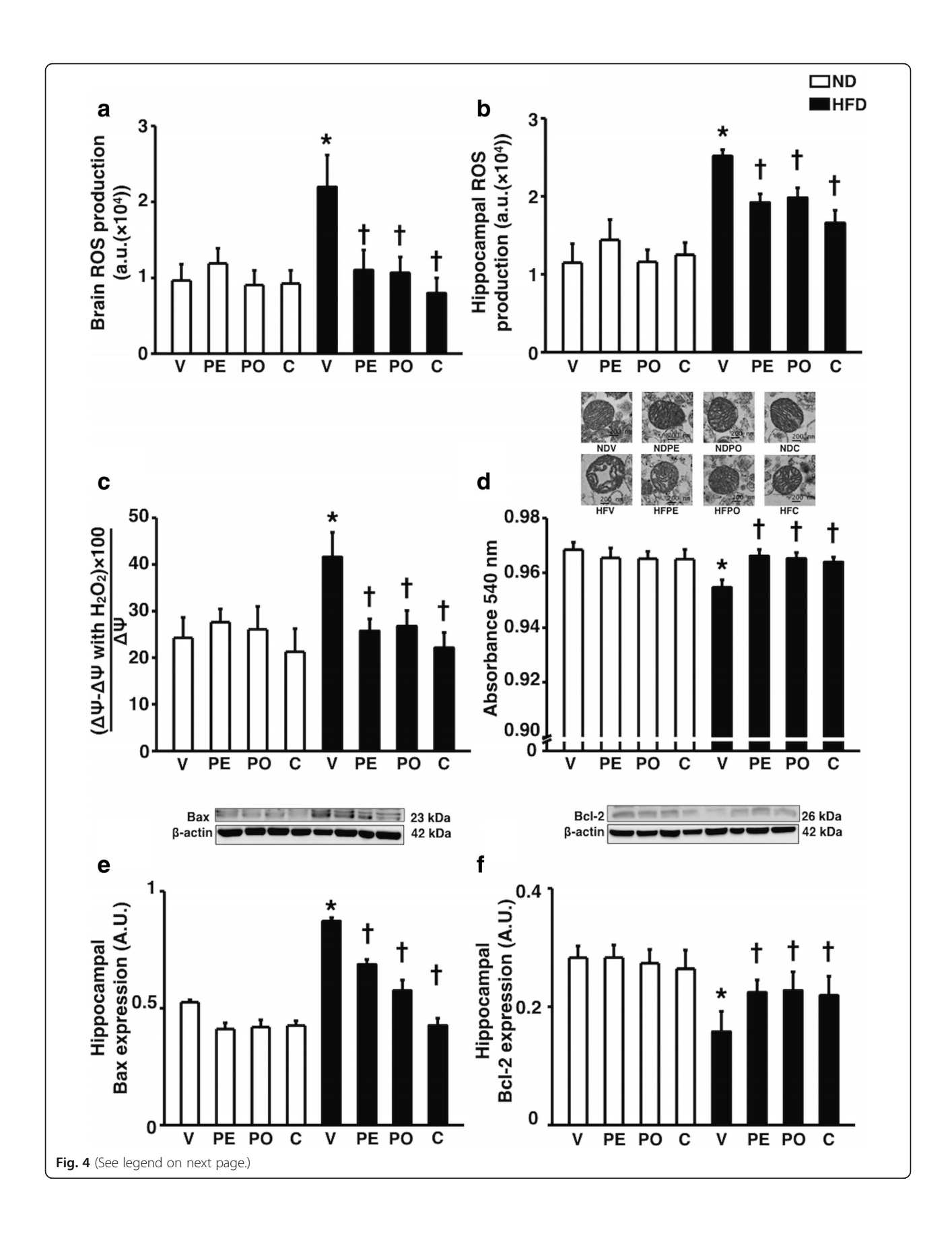
# Microglial activation was attenuated by prebiotic XOS, probiotic *L. paracasei* HIIO1, or the synbiotics in obese-insulin resistant rats

To determine microglia morphology phenotype, soma size, and processes length, ramification number Iba-1 positive cell and mean fluorescent intensity were measured. Three microglial cells per brain slice, three brain slices per animal, and six animals per group were measured from the CA1 region of the hippocampus. The microglial morphology of Iba-1 immunofluorescent under confocal microscopy at CA1 of the hippocampus were demonstrated (Fig. 5a–h). There were no

significant differences in all microglial morphology parameters among the ND-fed groups (Fig. 5a–d). Microglia from HFD-fed rats had amoeboid phenotype (Fig. 5e) as indicated by the significantly increased soma size (Fig. 5i), decreased process length (Fig. 5j), increased major projection and increased Iba-1 positive cell when compared to ND-fed rats (Fig. 5k–m). Prebiotic XOS, probiotic *L. paracasei* HIIO1, or the synbiotics preserved all microglial morphology parameters (Fig. 5i–m). Collectively, HFD consumption led to microglial morphology changes which were attenuated in all treatments.

# Cognitive dysfunction induced by long-term HFD consumption was ameliorated in prebiotic XOS, probiotic *L. paracasei* HIIO1, or the synbiotics consumption

Cognitive function was determined by Morris water maze test. Twelve weeks of HFD consumption caused memory impairment as indicated by the increased time taken to reach the platform (Fig. 6a) and decreased time spent in the target quadrant in these rats, compared to 12-week ND-fed rats (Fig. 6b). After 12 weeks of receiving prebiotic XOS, probiotic *L. paracasei* HIIO1, or the synbiotics in HFD-fed rats, the time to reach the platform was significantly decreased when compared to the vehicle group during the acquisition test (Fig. 6c). In addition, the time spent in the target quadrant during the probe test in HFD-fed rats with prebiotic XOS,



(See figure on previous page.)

**Fig. 4** Effects of prebiotics, probiotics, or synbiotics on brain mitochondrial function, hippocampal oxidative stress, and hippocampal apoptosis. **a** Whole brain isolated mitochondrial ROS production. **b** Hippocampal ROS production. **c** Percent change of whole brain isolated mitochondrial depolarization when incubated with hydrogen peroxide. **d** Upper panel: representative images of brain mitochondrial morphology. Lower panel: whole brain isolated mitochondrial absorbance value. **e** Upper panel: representative immunoblotting images of Bax relative to actin expression. Lower panel: the expression of hippocampal Bax protein relative to actin. **f** Upper panel: representative immunoblotting images of Bcl-2 relative to actin expression. Lower panel: the expression of hippocampal Bcl-2 protein relative to actin. ND: 24-week-normal diet-fed rats; HFD: 24-week high fat-fed rats; V: rats receiving PBS as vehicle; PE: rats receiving prebiotics; PO: rats receiving probiotics; C: rats receiving combination of prebiotics and probiotics as synbiotics (N = 6 of each group) \*p < 0.05 in comparison with the ND-fed rats; tp < 0.05 in comparison with the HFD-fed rats receiving vehicle

probiotic L. paracasei HIIO1, or the synbiotics was also significantly higher than that of the vehicle group (Fig. 6d). All of these findings suggested that all treatments effectively attenuate the impairment of learning and memory behaviors caused by long-term HFD consumption. The locomotor activity was determined by the open-field test. We found that long-term HFD consumption did not alter locomotor activity, indicating by distance (cm/10 min), when compared to ND-fed rats  $(2406 \pm 560 \text{ cm vs.})$ 2423 ± 690 cm for ND-fed rats and HFD-fed rats, respectively). Moreover, the locomotor activity of ND-fed rats and HFD-fed rats treated with prebiotic XOS, probiotics L. HII01, or synbiotics also was not significantly different when compared to ND-fed rats treated with vehicle (NDV 2368 ± 152 cm; NDPE 2658 ± 611 cm; NDPO 3038 ± 340 cm; NDC 2219 ± 444 cm; HFV 2498 ± 707 cm; HFPE 2542 ±646 cm; HFPO 2808 ± 686 cm; and HFC 3135 ± 1389 cm). These findings also indicated that the cognitive impairment during the Morris water maze test did not involve the motor function.

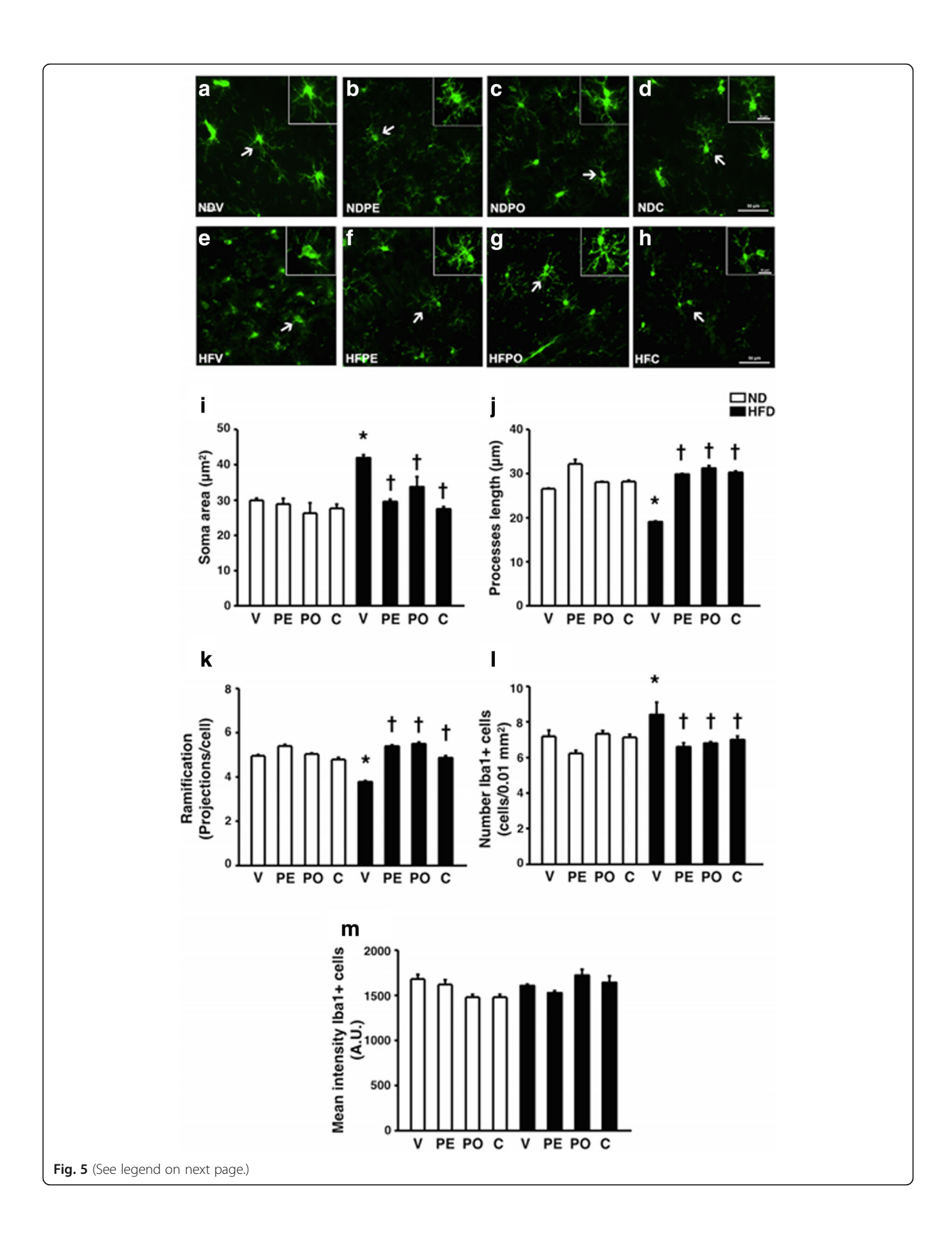
#### Discussion

The major findings of the present study are as follows. The obesity caused by long-term HFD consumption had (1) low-grade inflammation found in both local (gut) and systemic (serum) sites, leading to low-grade systemic inflammation and the development of peripheral insulin resistance; (2) hippocampal dysplasticity; (3) brain mitochondrial dysfunction; and (4) cognitive decline. These impairments are possibly mediated through the induction of gut inflammation, brain and hippocampal oxidative stress, brain inflammation, hippocampal apoptosis, the reduction of dendritic spine density, and microglial dysfunction. Daily consumption of prebiotic XOS, probiotic L. paracasei HIIO1, or the synbiotics for 12 weeks improved the brain function in these obese rats by attenuating gut and systemic inflammations, decreasing brain and hippocampal oxidative stress, increasing dendritic spine density, ameliorating microglial activation, and improving hippocampal dysplasticity and brain mitochondrial dysfunction, leading to restored cognitive function.

Previous studies demonstrated that long-term HFD consumption is known to lead to gut dysbiosis by

enhancing the growth of Proteobacteria, which is mainly composed of Gram-negative LPS containing bacteria, in the gut in the gut content [18, 19] and impaired the gut barrier integrity by inhibition of tight junction proteins [53]. This "leaky gut" found in the obese mice allows the luminal LPS and LPS-containing bacteria translocated from gut lumen to activate the innate immune cells in gut lamina propria, thus triggering the inflammatory response [18, 54]. Consistent with those reports, longterm HFD consumption in this study caused gut inflammation and increased the LPS level, in which it is possible that that amount of Proteobacteria should be increased in our HFD-fed rats. These findings suggested that obesity induced by HFD consumption caused gut inflammation, leading to low-grade systemic inflammation and the development of a peripheral insulin resistance. These undesirable effects were attenuated by consumption of prebiotics, probiotics, or synbiotics. In this study, the pro-inflammatory mRNA levels of IL-1β and IL-6 in the brain were not different among groups. Since this was done in the whole brain tissues, future studies are needed to investigate whether the proinflammatory cytokines in the hippocampal tissues would be different between the treatment groups and the control groups.

Although we found that only prebiotic XOS and synbiotics, not probiotic L. paracasei HIIO1, attenuated adiposity, which was the major source of pro-inflammatory cytokines, by decreasing the body weight and visceral fat, insulin resistance and dyslipidemia were still improved in all treatments. Currently, the beneficial role of probiotics on metabolic syndrome is still debated, at least one part was due to the strain-specific effect. For example, oral supplement of *Lactobacillus acidophilus*, Lactobacillus ingluviei, and Lactobacillus fermentum can cause weight gain [55], whereas Lactobacillus gasseri and Lactobacillus rhamnosus promoted weight loss [56]. Collectively, prebiotic XOS and synbiotics had beneficial effects to metabolic disturbance through systemic inflammation stemming from gut dysbiosis and adiposity, whereas probiotic L. paracasei HIIO1 had beneficial effects through systemic inflammation stemming only from gut dysbiosis. Our findings on probiotic supplement support this hypothesis.



(See figure on previous page.)

**Fig. 5** Effects of prebiotics, probiotics, or synbiotics on brain microglia morphology. **a-h** Representative images of lba-1 immunofluorescent under confocal microscopy at CA1 of the hippocampus (bar = 50 μm). **i** Soma area of lba-1 positive cell. **j** Processes length of lba-1 positive cell. **k** The ramification of lba-1 positive cell. **l** Number lba-1 positive cell. **m** Mean fluorescent intensity of lba-1 positive cell. ND: 24-week-normal diet-fed rats; HFD: 24-week high fat-fed rats; V: rats receiving PBS as vehicle; PE: rats receiving prebiotics; PO: rats receiving probiotics; C: rats receiving combination of prebiotics and probiotics as synbiotics (3 microglial calls/slice, 3 slices/animal and 6 animals/ group) \*p < 0.05 in comparison with the ND-fed rats; †p < 0.05 in comparison with the HFD-fed rats receiving vehicle

In addition, blood-brain barrier (BBB) permeability was increased in a model of obesity-induced by HFD [57] and also aggravated cognitive deficit by increasing the exposure of the brain to various cytokines, including LPS, IL-1β, IL-6, and tumor necrosis factor alpha (TNFα) [58]. These undesirable effects were diminished in rats receiving prebiotic XOS, probiotic L. paracasei HIIO1, or synbiotics and restored cognitive function, possibly modulated through anti-oxidative and antiinflammatory effects. Growing evidence demonstrates that the supplementary XOS decreased oxidative status in white sea bream juvenile [59] and suppressed proinflammatory cytokines including IFNy and IL-1β [60]. Probiotics are also known to exert an anti-inflammatory effect since it has been shown previously that Lactobacillus helveticus decreased inflammatory markers including nitric oxide synthase (NOS), prostaglandin E2 (PGE2), and IL-1β in the brain [25]. In addition, synbiotics, the combination of XOS and Lactobacillus plantarum, had greater antioxidant activity than single therapy, indicating that prebiotics, probiotics, or synbiotics could effectively decrease oxidative stress and inflammation not only in the gut and circulation, but also in the brain [61]. Taken together, prebiotic XOS, probiotic L. paracasei HII01, or synbiotics (the combination of XOS and L. paracasei HII01) exerted an anti-oxidative effect and anti-inflammatory effect, leading to restored cognitive function impaired by HFD. Previous studies also demonstrated that obesity-induced cell apoptosis by increased Bax level, decreased Bcl-2 level, and impaired brain mitochondrial function, which were also seen in the present study [48, 62]. Interestingly, we found that

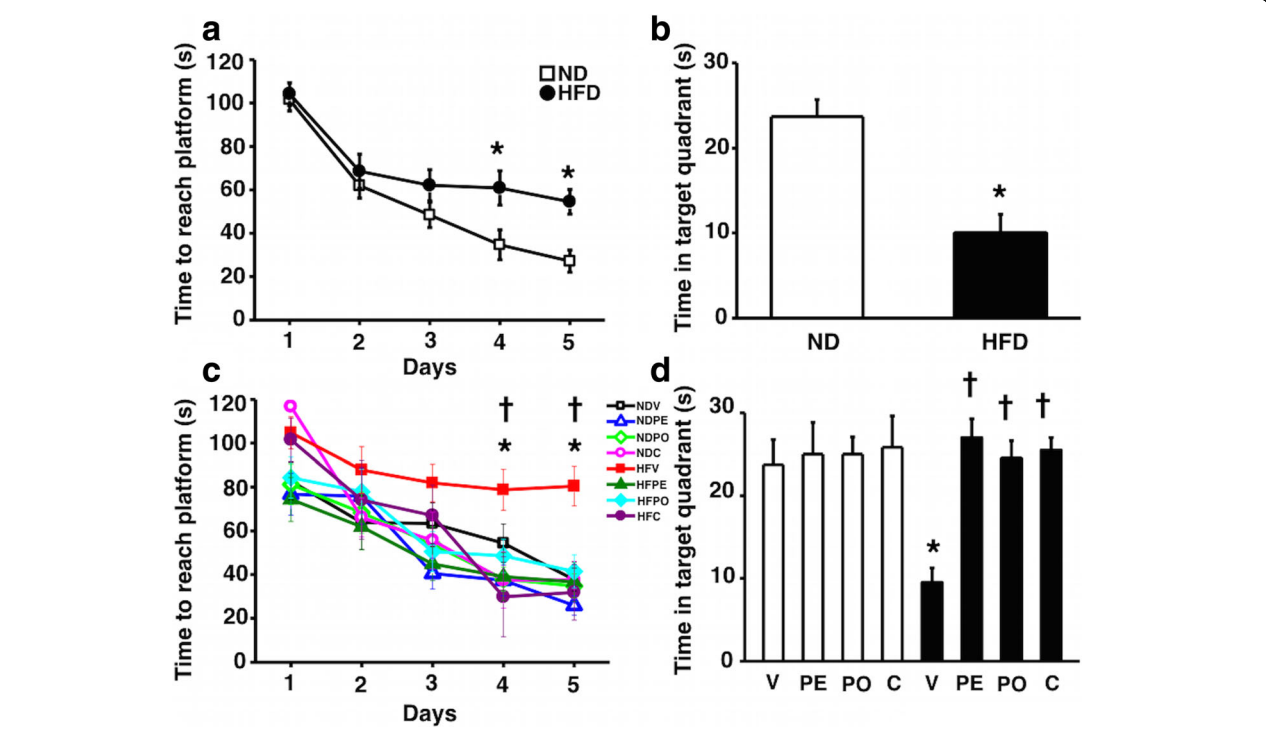


**Fig. 6** Effects of prebiotics, probiotics, or synbiotics on cognitive function. **a** Time to reach the platform in acquisition test of Morris Water maze test of ND- and HFD-fed rats at 12th week. **b** Mean time spent in target quadrant of ND- and HFD-fed rats at 12th week. **c** Time to reach the platform in acquisition test of Morris Water maze test after receiving prebiotics, probiotics, or synbiotics. **d** Mean time spent in target quadrant after receiving prebiotics, probiotics, or synbiotics, or synbiotics, or synbiotics, or synbiotics, or synbiotics, PE: rats receiving prebiotics; PO: rats receiving probiotics; C: rats receiving combination of prebiotics and probiotics as synbiotics (N = 6 of each group) \*p < 0.05 in comparison with the ND-fed rats; †p < 0.05 in comparison with the HFD-fed rats receiving vehicle

prebiotic XOS, probiotic *L. paracasei* HIIO1, or the synbiotics attenuated brain mitochondrial dysfunction, hippocampal ROS production, and hippocampal apoptosis.

Growing evidence has demonstrated the crucial roles of microglia on cognitive dysfunction in neurodegenerative disorders including excessive synaptic pruning of the brain with Alzheimer's disease [29, 30] and robust brain inflammation in obesity [31–33]. Previous studies demonstrated that HFD consumption increased activated microglia, leading to hippocampal dysplasticity including impairment of LTP, decreased dendritic spine density, as well as decreased synaptic protein such as postsynaptic density protein 95 (PSD-95), synaptophysin, and spinophilin, resulting in cognitive dysfunction [31, 33].

Although microglia played a crucial role in cognitive function and prebiotics, probiotics or synbiotics have been shown to exert protective effects on cognition [26, 30]; the link between gut microbiota modulating cognitive function through microglia has never been tested. In the present study, we demonstrated for the first time that long-term consumption of prebiotic XOS, probiotic L. paracasei HIIO1, or the synbiotics ameliorated microglial activation and restored cognitive function in diet-induced obese rats. There are three possible mechanistic explanations for the beneficial effects of the interventions we used in this study with prebiotics, probiotics, and synbiotics on brain cognitive function. First, prebiotics, probiotics, and synbiotics can mediate their effects through vagus nerve activation. It has been shown that consumption of Bifidobacterium longum exerted a vagal pathwaydependent anxiolytic effect in a chemically induced colitis mouse model [63]. Second, prebiotics, probiotics, and synbiotics can attenuate microglial activation which occurs in response to metabolite profiles in diet-induced obesity [18, 19]. Third, the gut microbiota can increase the production of short-chain fatty acids (SCFAs) such as acetate, butyrate, and proprionate, which has been shown to be beneficial in metabolic syndrome [64, 65]. However, the beneficial effects of prebiotics, probiotics, or synbiotics are strain-specific. Further research is needed into the mechanisms behind the role of microglia in cognition and the signaling pathways involved in neuroglia communication.

Surprisingly, the synbiotics did not have the synergistic effect of the attenuation of inflammation, hippocampal oxidative stress, hippocampal apoptosis, mitochondrial dysfunction as well as microglial dysfunction in rats with an obese-insulin resistant condition. These findings suggest that the prebiotic XOS might not effectively promote the probiotic functions of *L. paracasei HII01* in vivo. Moreover, these observations suggest that inconsistent reports regarding the probiotic effect in the

treatment of metabolic syndrome could be due to a strain-specific effect of this probiotic in a combination with a specific prebiotic fiber. This possibility has been supported by previous studies which demonstrated that XOS could not facilitate the growth of *Lactobacillus paracasei* [66, 67].

#### Conclusion

The present study showed that obese-insulin resistant condition, induced by prolonged HFD consumption, causes gut and systemic inflammation, peripheral insulin resistance, hippocampal dysplasticity, hippocampal oxidative stress, brain mitochondrial dysfunction, hippoapoptosis, and microglial morphological changes, resulting in cognitive decline. Moreover, this is the first report to show the possible link between gut microbiota modification by prebiotics, probiotics, or synbiotics supplement and the improvement of cognitive function in obese-insulin resistant rats. These neuroprotective effects may possibly be mediated through the attenuation of inflammation, hippocampal oxidative stress, hippocampal apoptosis, mitochondrial dysfunction as well as microglial dysfunction.

#### **Abbreviations**

aCSF: Artificial cerebrospinal fluid; AUG: Areas under the curve; cDNA: Complementary DNA; cfu: Colony forming unit; fEPSP: Field excitatory postsynaptic potentials; HFD: High-fat diet; HFS: High-frequency stimulation; HOMA: Homeostasis Model Assessment; HPLC: High-performance liquid chromatography; IL-1: Interleukin 1; IL-6: Interleukin 6; LAL: Limulus amoebocyte lysate; LPS: Lipopolysaccharide; LTP: Long-term potentiation; MDA: Malondialdehyde; ND: Normal diet; OGTT: Oral glucose tolerance test; ROS: Reactive oxygen species; XOS: Xylooligosaccharide

#### Acknowledgements

This work was supported by Thailand Research Fund TRF-RTA6080003(SCC), the Royal Golden Jubilee PhD program (PHD/0146/2558 TC&SC), TRG-5980198 (WP), TRG-5880041 (PT), The National Research Council of Thailand (SC), a NSTDA Research Chair Grant from the National Science and Technology Development Agency Thailand (NC) and Chiang Mai University Excellent Center Award (NC). The authors would like to thank Ms. Cicely Proctor, Ms. Thidarat Jaiwongkum, and Ms. Sasiwan Kerdpoo for their technical assistance in this project. A thank also goes to Ms. Maria Love for her editorial assistance of this manuscript.

#### Funding

All sources of funding for the research reported did not have any role in the design of the study and collection, analysis, and interpretation of data and in writing the manuscript.

#### Availability of data and materials

Data sharing is not applicable to this article as no datasets were generated or analyzed during the current study. Please contact author for data requests.

#### Authors' contributions

TC performed the majority of data acquisition, data analysis, writing of the original draft, and revising of the manuscript. WT contributed to the data acquisition and data analysis. SY contributed to the data acquisition and data in the data acquisition. SE contributed to the data acquisition. SE contributed to the data acquisition and data analysis. GM contributed to the data acquisition and data analysis. AL contributed to the data acquisition. SP contributed to the data acquisition. SP contributed to the preparation for probiotics and synbiotics. CC contributed to the preparation for probiotics and synbiotics. WP contributed to the data

acquisition, data analysis, and drafting of the manuscript. PT contributed to the data acquisition for gut and systemic inflammation, data analysis, and drafting of the manuscript. NC contributed to the conception and design and the drafting or revising of the article. SCC contributed to the initial conception and design, data analysis and interpretation, and revision and finalization the manuscript. All authors read and approved the final manuscript.

#### Ethics approval

All animal studies were approved by the Institutional Animal Care and Use Committee (IACUC) of the Faculty of Medicine, Chiang Mai University (Permit number: 13/2558 on May 12, 2015) and conformed to the Guide for the Care and Use of Laboratory Animals published by the US National Institutes of Health (NIH guide, 8th edition, 2011).

#### Consent for publication

Not applicable.

#### Competing interests

The authors declare that there is no conflict of interest that could be perceived as prejudicing the impartiality of the research reported.

#### **Publisher's Note**

Springer Nature remains neutral with regard to jurisdictional claims in published maps and institutional affiliations.

#### **Author details**

<sup>1</sup>Neurophysiology Unit, Cardiac Electrophysiology Research and Training Center, Faculty of Medicine, Chiang Mai University, Chiang Mai 50200, Thailand. <sup>2</sup>Cardiac Electrophysiology Research and Training Center, Department of Physiology, Faculty of Medicine, Chiang Mai University, Chiang Mai 50200, Thailand. <sup>3</sup>Department of Microbiology, Faculty of Medicine, Chiang Mai University, Chiang Mai 50200, Thailand. <sup>4</sup>Faculty of Pharmacy, Chiang Mai University, Chiang Mai 50200, Thailand. <sup>5</sup>Department of Oral Biology and Diagnostic Science, Faculty of Dentistry, Chiang Mai University, Chiang Mai 50200, Thailand.

### Received: 19 November 2017 Accepted: 2 January 2018 Published online: 09 January 2018

#### References

- Collaboration NCDRF. Trends in adult body-mass index in 200 countries from 1975 to 2014: a pooled analysis of 1698 population-based measurement studies with 19.2 million participants. *Lancet*. 2016;387(10026):1377–96.
- Clegg DJ, Gotoh K, Kemp C, Wortman MD, Benoit SC, Brown LM, et al. Consumption of a high-fat diet induces central insulin resistance independent of adiposity. Physiol Behav. 2011;103(1):10–6.
- Pratchayasakul W, Kerdphoo S, Petsophonsakul P, Pongchaidecha A, Chattipakorn N, Chattipakorn SC. Effects of high-fat diet on insulin receptor function in rat hippocampus and the level of neuronal corticosterone. Life Sci. 2011;88(13–14):619–27.
- Stranahan AM, Norman ED, Lee K, Cutler RG, Telljohann RS, Egan JM, et al. Diet-induced insulin resistance impairs hippocampal synaptic plasticity and cognition in middle-aged rats. Hippocampus. 2008;18(11):1085–8.
- Pintana H, Apaijai N, Pratchayasakul W, Chattipakorn N, Chattipakorn SC. Effects of metformin on learning and memory behaviors and brain mitochondrial functions in high fat diet induced insulin resistant rats. Life Sci. 2012;91(11–12):409–14.
- Sripetchwandee J, Pipatpiboon N, Pratchayasakul W, Chattipakorn N, Chattipakorn SC. DPP-4 inhibitor and PPARgamma agonist restore the loss of CA1 dendritic spines in obese insulin-resistant rats. Arch Med Res. 2014; 45(7):547–52.
- Pintana H, Pongkan W, Pratchayasakul W, Chattipakorn N, Chattipakorn SC.
  Testosterone replacement attenuates cognitive decline in testosteronedeprived lean rats, but not in obese rats, by mitigating brain oxidative
  stress. Age (Dordr). 2015;37(5):84.
- Pintana H, Pongkan W, Pratchayasakul W, Chattipakorn N, Chattipakorn SC.
  Dipeptidyl peptidase 4 inhibitor improves brain insulin sensitivity, but fails
  to prevent cognitive impairment in orchiectomy obese rats. J Endocrinol.
  2015;226(2):M1–M11.

- Pintana H, Pratchayasakul W, Sa-nguanmoo P, Pongkan W, Tawinvisan R, Chattipakorn N, et al. Testosterone deprivation has neither additive nor synergistic effects with obesity on the cognitive impairment in orchiectomized and/or obese male rats. Metabolism. 2016;65(2):54–67.
- Pintana H, Sripetchwandee J, Supakul L, Apaijai N, Chattipakorn N, Chattipakorn S. Garlic extract attenuates brain mitochondrial dysfunction and cognitive deficit in obese-insulin resistant rats. Appl Physiol Nutr Metab. 2014;39(12):1373–9
- Pipatpiboon N, Pintana H, Pratchayasakul W, Chattipakorn N, Chattipakorn SC. DPP4-inhibitor improves neuronal insulin receptor function, brain mitochondrial function and cognitive function in rats with insulin resistance induced by high-fat diet consumption. Eur J Neurosci. 2013;37(5):839–49.
- Pipatpiboon N, Pratchayasakul W, Chattipakorn N, Chattipakorn SC.
   PPARgamma agonist improves neuronal insulin receptor function in hippocampus and brain mitochondria function in rats with insulin resistance induced by long term high-fat diets. Endocrinology. 2012;153(1):329–38.
- Pratchayasakul W, Sa-Nguanmoo P, Sivasinprasasn S, Pintana H, Tawinvisan R, Sripetchwandee J, et al. Obesity accelerates cognitive decline by aggravating mitochondrial dysfunction, insulin resistance and synaptic dysfunction under estrogen-deprived conditions. Horm Behav. 2015;72:68–77.
- Sa-Nguanmoo P, Tanajak P, Kerdphoo S, Satjaritanun P, Wang X, Liang G, et al. FGF21 improves cognition by restored synaptic plasticity, dendritic spine density, brain mitochondrial function and cell apoptosis in obese-insulin resistant male rats. Horm Behav. 2016;85:86–95.
- Shen J, Obin MS, Zhao L. The gut microbiota, obesity and insulin resistance. Mol Asp Med. 2013;34(1):39–58.
- Hansen AK, Hansen CH, Krych L, Nielsen DS. Impact of the gut microbiota on rodent models of human disease. World J Gastroenterol. 2014;20(47): 17727–36
- Kostic AD, Howitt MR, Garrett WS. Exploring host-microbiota interactions in animal models and humans. Genes Dev. 2013;27(7):701–18.
- Cani PD, Amar J, Iglesias MA, Poggi M, Knauf C, Bastelica D, et al. Metabolic endotoxemia initiates obesity and insulin resistance. Diabetes. 2007;56(7): 1761–77
- Kim KA, Gu W, Lee IA, Joh EH, Kim DH. High fat diet-induced gut microbiota exacerbates inflammation and obesity in mice via the TLR4 signaling pathway. PLoS One. 2012;7(10):e47713.
- Wu CC, Weng WL, Lai WL, Tsai HP, Liu WH, Lee MH, et al. Effect of Lactobacillus plantarum strain K21 on high-fat diet-fed obese mice. Evid Based Complement Alternat Med. 2015;2015:391767.
- Slavin J. Fiber and prebiotics: mechanisms and health benefits. Nutrients. 2013;5(4):1417–35.
- Sanders ME. Probiotics: definition, sources, selection, and uses. Clin Infect Dis. 2008;46(Supplement 2):S58–61.
- Wang J, Tang H, Zhang C, Zhao Y, Derrien M, Rocher E, et al. Modulation of gut microbiota during probiotic-mediated attenuation of metabolic syndrome in high fat diet-fed mice. ISME J. 2015;9(1):1–15.
- Savignac HM, Tramullas M, Kiely B, Dinan TG, Cryan JF. Bifidobacteria modulate cognitive processes in an anxious mouse strain. Behav Brain Res. 2015;287:59–72.
- Luo J, Wang T, Liang S, Hu X, Li W, Jin F. Ingestion of Lactobacillus strain reduces anxiety and improves cognitive function in the hyperammonemia rat. Sci China Life Sci. 2014;57(3):327–35.
- Kelly JR, Allen AP, Temko A, Hutch W, Kennedy PJ, Farid N, et al. Lost in translation? The potential psychobiotic Lactobacillus rhamnosus (JB-1) fails to modulate stress or cognitive performance in healthy male subjects. Brain Behav Immun. 2017;61:50–9.
- Imaizumi K, Nakatsu Y, Sato M, Sedarnawati Y, Sugano M. Effects of xylooligosaccharides on blood glucose, serum and liver lipids and cecum short-chain fatty acids in diabetic rats. Agric Biol Chem. 1991;55(1):199–205.
- Yamamoto S, Pattananandecha T, Sirilun S, Sivamaruthi BS, Peerajan S, Chaiyasut C. Evaluation of cryoprotective potential of Jerusalem artichoke'lnulin during freeze-drying and storage of lactobacillus paracasei Hll01. J Pure Appl Microbiol. 2016;10(3):1727–34.
- Hong S, Beja-Glasser VF, Nfonoyim BM, Frouin A, Li S, Ramakrishnan S, et al. Complement and microglia mediate early synapse loss in Alzheimer mouse models. Science. 2016;352(6286):712–6.
- Kettenmann H, Kirchhoff F, Verkhratsky A. Microglia: new roles for the synaptic stripper. Neuron. 2013;77(1):10–8.
- 31. Bocarsly ME, Fasolino M, Kane GA, LaMarca EA, Kirschen GW, Karatsoreos IN, et al. Obesity diminishes synaptic markers, alters microglial morphology,

- and impairs cognitive function. Proc Natl Acad Sci U S A. 2015;112(51): 15731–6
- Erion JR, Wosiski-Kuhn M, Dey A, Hao S, Davis CL, Pollock NK, et al. Obesity elicits interleukin 1-mediated deficits in hippocampal synaptic plasticity. J Neurosci. 2014;34(7):2618–31.
- Hao S, Dey A, Yu X, Stranahan AM. Dietary obesity reversibly induces synaptic stripping by microglia and impairs hippocampal plasticity. Brain Behav Immun. 2016;51:230–9.
- Cryan JF, Dinan TG. Gut microbiota: microbiota and neuroimmune signalling—Metchnikoff to microglia. Nat Rev Gastroenterol Hepatol. 2015; 12(9):494–6.
- Erny D, Hrabě de Angelis AL, Jaitin D, Wieghofer P, Staszewski O, David E, et al. Host microbiota constantly control maturation and function of microglia in the CNS. Nat Neurosci. 2015;18(7):965–77.
- Clark A, Mach N. The crosstalk between the gut microbiota and mitochondria during exercise. Front Physiol. 2017;8:319.
- Saint-Georges-Chaumet Y, Edeas M. Microbiota-mitochondria inter-talk: consequence for microbiota-host interaction. *Pathog Dis.* 2016;74(1):ftv096.
- Park J, Min JS, Kim B, Chae UB, Yun JW, Choi MS, et al. Mitochondrial ROS govern the LPS-induced pro-inflammatory response in microglia cells by regulating MAPK and NF-kappaB pathways. Neurosci Lett. 2015;584:191–6.
- Wang T, Qin L, Liu B, Liu Y, Wilson B, Eling TE, et al. Role of reactive oxygen species in LPS-induced production of prostaglandin E2 in microglia. J Neurochem. 2004;88(4):939–47.
- Lee KY, Chung K, Chung JM. Involvement of reactive oxygen species in long-term potentiation in the spinal cord dorsal horn. J Neurophysiol. 2010; 103(1):382–91.
- 41. Massaad CA, Klann E. Reactive oxygen species in the regulation of synaptic plasticity and memory. Antioxid Redox Signal. 2011;14(10):2013–54.
- Grunnet LG, Aikin R, Tonnesen MF, Paraskevas S, Blaabjerg L, Storling J, et al. Proinflammatory cytokines activate the intrinsic apoptotic pathway in betacells. Diabetes. 2009;58(8):1807–15.
- Hardy H, Harris J, Lyon E, Beal J, Foey AD. Probiotics, prebiotics and immunomodulation of gut mucosal defences: homeostasis and immunopathology. Nutrients. 2013;5(6):1869–912.
- Appleton DJ, Rand JS, Sunvold GD. Basal plasma insulin and homeostasis model assessment (HOMA) are indicators of insulin sensitivity in cats. J Feline Med Surg. 2005;7(3):183–93.
- 45. Haffner SM, Miettinen H, Stern MP. The homeostasis model in the San Antonio heart study. Diabetes Care. 1997;20(7):1087–92.
- Pintana H, Apaijai N, Chattipakorn N, Chattipakorn SC. DPP-4 inhibitors improve cognition and brain mitochondrial function of insulin resistant rats. J Endocrinol. 2013;218(1):1–11.
- Peinnequin A, Mouret C, Birot O, Alonso A, Mathieu J, Clarencon D, et al. Rat pro-inflammatory cytokine and cytokine related mRNA quantification by realtime polymerase chain reaction using SYBR green. BMC Immunol. 2004;5:3.
- Chunchai T, Samniang B, Sripetchwandee J, Pintana H, Pongkan W, Kumfu S, et al. Vagus nerve stimulation exerts the neuroprotective effects in obeseinsulin resistant rats, leading to the improvement of cognitive function. Sci Rep. 2016;6:26866.
- Vorhees CV, Williams MT. Morris water maze: procedures for assessing spatial and related forms of learning and memory. Nat Protoc. 2006;1(2): 848–58.
- Stanford SC. The open field test: reinventing the wheel. J Psychopharmacol. 2007;21(2):134–5.
- Denenberg VH. Open-field bheavior in the rat: what does it mean? Ann N Y Acad Sci. 1969:159(3):852–9.
- Winter SE, Thiennimitr P, Winter MG, Butler BP, Huseby DL, Crawford RW, et al. Gut inflammation provides a respiratory electron acceptor for Salmonella. Nature. 2010;467(7314):426–9.
- Murakami Y, Tanabe S, Suzuki T. High-fat diet-induced intestinal hyperpermeability is associated with increased bile acids in the large intestine of mice. J Food Sci. 2016;81(1):H216–22.
- Cani PD, Delzenne NM, Amar J, Burcelin R. Role of gut microflora in the development of obesity and insulin resistance following high-fat diet feeding. Pathol Biol (Paris). 2008;56(5):305–9.
- Million M, Angelakis E, Paul M, Armougom F, Leibovici L, Raoult D. Comparative meta-analysis of the effect of Lactobacillus species on weight gain in humans and animals. Microb Pathog. 2012;53(2):100–8.
- Sanchez M, Darimont C, Drapeau V, Emady-Azar S, Lepage M, Rezzonico E, et al. Effect of Lactobacillus rhamnosus CGMCC1.3724 supplementation on

- weight loss and maintenance in obese men and women. Br J Nutr. 2014; 111(8):1507–19.
- Stranahan AM, Hao S, Dey A, Yu X, Baban B. Blood-brain barrier breakdown promotes macrophage infiltration and cognitive impairment in leptin receptor-deficient mice. J Cereb Blood Flow Metab. 2016;36(12):2108–21.
- Freeman LR, Haley-Zitlin V, Rosenberger DS, Granholm AC. Damaging effects of a high-fat diet to the brain and cognition: a review of proposed mechanisms. Nutr Neurosci. 2014;17(6):241–51.
- Guerreiro I, Couto A, Machado M, Castro C, Pousao-Ferreira P, Oliva-Teles A, et al. Prebiotics effect on immune and hepatic oxidative status and gut morphology of white sea bream (Diplodus sargus). Fish Shellfish Immunol. 2016;50:168–74.
- Hansen CH, Frokiaer H, Christensen AG, Bergstrom A, Licht TR, Hansen AK, et al. Dietary xylooligosaccharide downregulates IFN-gamma and the lowgrade inflammatory cytokine IL-1beta systemically in mice. J Nutr. 2013; 143(4):533–40.
- Yu X, Yin J, Li L, Luan C, Zhang J, Zhao C, et al. Prebiotic potential of xylooligosaccharides derived from corn cobs and their in vitro antioxidant activity when combined with lactobacillus. J Microbiol Biotechnol. 2015; 25(7):1084–92.
- Sinha-Hikim I, Sinha-Hikim AP, Shen R, Kim HJ, French SW, Vaziri ND, et al. A novel cystine based antioxidant attenuates oxidative stress and hepatic steatosis in diet-induced obese mice. Exp Mol Pathol. 2011;91(1):419–28.
- Bercik P, Park AJ, Sinclair D, Khoshdel A, Lu J, Huang X, et al. The anxiolytic effect of Bifidobacterium longum NCC3001 involves vagal pathways for gutbrain communication. Neurogastroenterol Motil. 2011;23(12):1132–9.
- Mollica MP, Mattace Raso G, Cavaliere G, Trinchese G, De Filippo C, Aceto S, et al. Butyrate regulates liver mitochondrial function, efficiency, and dynamics in insulin-resistant obese mice. Diabetes. 2017;66(5):1405–18.
- Perry RJ, Peng L, Barry NA, Cline GW, Zhang D, Cardone RL, et al. Acetate mediates a microbiome-brain-beta-cell axis to promote metabolic syndrome. Nature. 2016;534(7606):213–7.
- Li Z, Summanen PH, Komoriya T, Finegold SM. In vitro study of the prebiotic xylooligosaccharide (XOS) on the growth of Bifidobacterium spp and Lactobacillus spp. Int J Food Sci Nutr. 2015;66(8):919–22.
- Makelainen H, Saarinen M, Stowell J, Rautonen N, Ouwehand AC. Xylooligosaccharides and lactitol promote the growth of Bifidobacterium lactis and Lactobacillus species in pure cultures. Benef Microbes. 2010;1(2):139–48.

### Submit your next manuscript to BioMed Central and we will help you at every step:

- We accept pre-submission inquiries
- Our selector tool helps you to find the most relevant journal
- We provide round the clock customer support
- Convenient online submission
- Thorough peer review
- Inclusion in PubMed and all major indexing services
- Maximum visibility for your research

Submit your manuscript at www.biomedcentral.com/submit

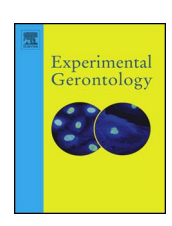


FISEVIER

Contents lists available at ScienceDirect

#### Experimental Gerontology

journal homepage: www.elsevier.com/locate/expgero



### Estrogen deprivation aggravates cardiometabolic dysfunction in obeseinsulin resistant rats through the impairment of cardiac mitochondrial dynamics



Wanitchaya Minta<sup>a,b,c,1</sup>, Siripong Palee<sup>a,c,1</sup>, Duangkamol Mantor<sup>a,b,c</sup>, Wissuta Sutham<sup>a,b,c</sup>, Thidarat Jaiwongkam<sup>a,c</sup>, Sasiwan Kerdphoo<sup>a,c</sup>, Wasana Pratchayasakul<sup>a,b,c</sup>, Sirinart Kumfu<sup>a,b,c</sup>, Siriporn C. Chattipakorn<sup>a,c,d</sup>, Nipon Chattipakorn<sup>a,b,c,\*</sup>

- a Cardiac Electrophysiology Research and Training Center, Faculty of Medicine, Chiang Mai University, Chiang Mai 50200, Thailand
- b Cardiac Electrophysiology Unit, Department of Physiology, Faculty of Medicine, Chiang Mai University, Chiang Mai 50200, Thailand
- <sup>c</sup> Center of Excellence in Cardiac Electrophysiology Research, Chiang Mai University, Chiang Mai 50200, Thailand
- d Department of Oral Biology and Diagnostic Science, Faculty of Dentistry, Chiang Mai University, Chiang Mai, Thailand

#### ARTICLE INFO

# Section Editor: Holly M. Brown-Borg Keywords: Estrogen deprivation Heart Insulin resistance Mitochondrial dynamic

#### ABSTRACT

The incidence of cardiovascular disease and metabolic syndrome increases after the onset of menopause, suggesting estrogen has a vital role in their prevention. Mitochondrial dynamics are known to play an important role in the maintenance of cardiac physiological function. However, the effects of estrogen deprivation on cardiometabolic status and cardiac mitochondrial dynamics under conditions of obese-insulin resistance have never been investigated. We hypothesized that estrogen deprivation aggravates cardiac dysfunction through increased cardiac mitochondrial fission in obese-insulin resistant rats. Female rats were fed on either a high fat (HFD, 57.60% fat) or normal (ND, 19.77% fat) diet for 13 weeks. The rats were then divided into 4 groups. Two sham groups (HFS and NDS) and 2 operated or ovariectomized (HFO and NDO) groups (n = 8/group). Six weeks after surgery, metabolic status, heart rate variability (HRV), left ventricular (LV) function, cardiac mitochondrial function and dynamics, and metabolic parameters were determined. Insulin resistance developed in NDO, HFS and HFO rats as indicated by increased plasma insulin and HOMA index. Although rats in both NDO and HFS groups had markedly impaired LV function indicated by reduced %LVFS and impaired cardiac mitochondrial function, rats in the HFO group had the most severe impairments. Moreover, the estrogen deprived rats (NDO and HFO) had increased cardiac mitochondrial fission through activation of phosphorylation of Drp-1 at serine 616. Our findings indicated that estrogen deprivation caused the worsening of LV dysfunction through increased cardiac mitochondrial fission in obese-insulin resistant rats.

#### 1. Introduction

Obesity

Obese-insulin resistance and estrogen deprivation are major risk factors for cardiovascular diseases (CVDs) due to their impact on the impairment of cardiac autonomic regulation, cardiac function and cardiac mitochondrial function (Apaijai et al., 2013; Ginsberg, 2000; Maas et al., 2011; Sivasinprasasn et al., 2015). It has been shown that the incidence of CVDs in woman is increased after the onset of menopause (Vitale et al., 2009). Moreover, a bilateral ovariectomy (OVX) before the onset of menopause is also associated with increased death involving CVDs in woman, and estrogen treatment has been shown to reduce this risk (Rivera et al., 2009). These findings indicate the

beneficial effects of this female sex hormone on heart diseases.

Mitochondria play an important role in the control of cell survival, especially in the heart (Chan, 2012). The balance of mitochondrial dynamics, namely mitochondrial fission and mitochondrial fusion, is required to maintain normal function and to generate sufficient ATP for cell activity (Chan, 2012). The balance of these two opposing processes in mitochondrial dynamics is regulated by the mitochondrial fission protein, dynamin-related protein 1 (Drp1) and the mitochondrial fusion proteins, mitofusin 1 and 2 (Mfn1 and Mfn2, respectively) and optic atrophy 1 (Opa1) (Chan, 2012). An imbalance in mitochondrial fission and fusion has been shown to be associated with many CVDs (Ding et al., 2017; Knowlton et al., 2014; Vasquez-Trincado et al., 2016).

<sup>\*</sup> Corresponding author at: Cardiac Electrophysiology Research and Training Center, Faculty of Medicine, Chiang Mai University, Chiang Mai 50200, Thailand. E-mail addresses: nchattip@gmail.com, nipon.chat@cmu.ac.th (N. Chattipakorn).

<sup>&</sup>lt;sup>1</sup> Siripong Palee and Wanitchaya Minta contributed equally to this work.

Previous studies have demonstrated that obesity is associated with impaired mitochondrial function and dynamics (Holmstrom et al., 2012; Jheng et al., 2012). Obesity has been shown to induce Drp-1 activation and excessive mitochondrial fragmentation, and this fragmentation was associated with the increased oxidative stress level (Jheng et al., 2012). Moreover, previous studies suggest that estrogen affects cardiac mitochondrial function and mitochondrial dynamics directly (Aurigemma, 2015; Sastre-Serra et al., 2012; Sastre-Serra et al., 2013). In this regard, estrogen plays important regulatory roles in maintaining normal mitochondrial properties by stabilizing the structural assembly of mitochondria as well as attenuating mitochondrial ROS production (Rattanasopa et al., 2015). In addition, it has been shown that cardiac mitochondrial dynamics were altered due to lacking of estrogen as indicated by increased of mitochondrial fission in OVX rats (Aurigemma, 2015). Moreover, previous study demonstrated that 17β-estradiol could alter mitochondrial dynamics by decreasing fission in cancer cell lines (Sastre-Serra et al., 2012). These findings suggest that alteration of estrogen level is associated with changes in mitochondrial dynamics. Despite these previous reports, the effects of estrogen deprivation on cardiometabolic status and cardiac mitochondrial dynamics under conditions of obese-insulin resistance have never been investigated. In this study, we tested the hypothesis that estrogen deprivation aggravates cardiac dysfunction through the increased imbalance of cardiac mitochondrial dynamics in obese-insulin resistant

#### 2. Materials and methods

#### 2.1. Ethical approval

This study was approved by the Institutional Animal Care and Use Committee of the Faculty of Medicine, Chiang Mai University (approval no. 5/2559 on May 5, 2016).

#### 2.2. Animal preparation

Thirty-two female Wistar rats (6 weeks of age, weighing 200–220 g) were obtained from the National animal center (Salaya campus, Mahidol University, Bangkok, Thailand). The rats were given time to acclimatize for 1 week, and were housed in a temperature-controlled room (25 °C) with a 12-h dark/light cycle setting.

#### 2.3. Experimental protocol

Rats were randomly divided into two dietary groups: a normal diet (ND, a diet containing 19.77% energy from fat), and a high fat diet (HFD, a diet containing 52.98% energy from fat) (Pratchayasakul et al., 2011). Thirteen weeks after specific feeding, rats in each dietary group were divided into 2 subgroups to undergo either a sham operation (NDS or HFS) or a bilateral ovariectomy (NDO or HFO). Body weight and food intake of all rats were recorded throughout the experimental period. At the end of the 6th week after surgery, blood samples were collected from the tail vein for determination of metabolic parameters and estrogen levels. An oral glucose tolerance test (OGTT), heart rate variability (HRV) for cardiac autonomic balance, and echocardiography were carried out. At the end of the study protocol, rats were anesthetized with Xylazine (0.15 ml/kg) and Zolitil (50 mg/kg). Cardiac function was determined using a pressure-volume (P-V) loop recording system. Then, the heart was rapidly removed for the determination of cardiac mitochondrial function and biochemical studies.

#### 2.4. Ovariectomy

In the ovariectomized group, rats were anesthetized under a rodent anesthesia machine (2% isoflurane vaporizer and 200 ml/min oxygen flow) and then placed lying on left and right lateral decubitus for left

and right ovariectomy, respectively. After hair shaving and skin cleaning, a bilateral ovariectomy was carried out by initially making a midline dorsal skin incision. The incision was centered between the inferior crest of the rib cage and superior base of the thigh. The abdominal-pelvic cavity was accessed then the uterine tubes and ovaries were identified. Both ovaries were removed and uterine horns were returned into the cavity. In the sham group, all rats received the same anesthesia and also the same surgical preparation procedures as OVX rats. Bilateral ovaries of sham rats were identified and exposed, the ovaries were not excised in these cases. After the operation, rats were individually housed in a clear box with dry bedding for 1 week (Sivasinprasasn et al., 2017).

#### 2.5. Tail-cuff blood pressure measurement and echocardiography

Rats were placed in a restrainer to limit their mobility. Volume-pressure recording sensors (VPR) and occlusion cuffs (O-cuff) were attached to the tails. Systolic blood pressure (SBP) and diastolic blood pressure (DBP) were recorded and analyzed using a CODA2 channel non-invasive blood pressure system (Kent Scientific Corporation, CT, USA) (Tunapong et al., 2017).

Echocardiography was used to determine left ventricular (LV) function as a non-invasive method. Animals were given light anesthesia using 2% isoflurane with oxygen (2 L/min). An echocardiography probe (S12, GE healthcare, CT, USA) was placed on the chest at the parasternal short axis, and connected to an echocardiography machine (GE vivid-i, GE healthcare, CT, USA). An M-mode echocardiogram at LV papillary muscle level was recorded, and %fractional shortening (%FS) was determined. A pulsed-wave Doppler spectrum of mitral flow was recorded from the apical four-chamber view with the guidance of the color Doppler. The mitral E/A ratio were measured.

#### 2.6. Heart rate variability (HRV) measurement

HRV was performed by immobilizing the limbs of rats in a prone position under 2.5% isoflurane inhalation anesthesia. Needle electrodes (27-gauge with 1-inch length) were inserted subcutaneously into the positions for recording of lead II electrocardiogram (ECG). Rats were allowed to gain full consciousness prior to ECG recording. During ECG recording, rats were kept restrained and prohibited from movement. The ECG signals were recorded for 20 min through a signal transducer (PowerLab 4/25 T, ADInstruments, Sydney, Australia), and operated through a Chart 5.0 program (ADInstruments, Sydney, Australia). At least 300 consecutive RR intervals from the section of the tachogram were chosen for HRV analysis. The power spectra of RR intervals were obtained using a fast Fourier transform (FFT) algorithm. Three major oscillatory components were detected as a high-frequency band (HF; 0.6-3 Hz), a low-frequency band (LF; 0.2-0.6 Hz) and a very low-frequency band (VLF; below 0.2 Hz). Each spectral component was calculated as integrals under the respective part of the power spectral density function, and was presented in absolute units (ms<sup>2</sup>). To minimize the effect of changes in total power on the LF and HF bands, LF and HF were expressed as normalized units by dividing them by the total power minus VLF. LF and HF band of HRV were analyzed using an analytical program. Increased LF/HF ratio indicates cardiac sympathovagal imbalance (Tunapong et al., 2017).

#### 2.7. Pressure-volume (P-V) loop study

Rats were anesthetized by intramuscular injection with Zoletil (50 mg/kg, Vibbac Laboratories, Carros, France) and Xylazine (0.15 mg/kg, Laboratories Carlier, SA, Barcelona, Spain), then placed in the supine position. Rats were ventilated with room air via a tracheostomy tube. The right carotid artery was identified and ligated, and then a pressure-volume (P-V) loop catheter (Scisence, Ontario, Canada) was inserted. The catheter tip was directed into the LV chamber to

record LV pressure and volume. A 10-minute period was allowed to get stable PV loop signals. After stable signals were obtained from PV loop catheter, all loops recorded during 20-minute period were used for data analysis. The investigated parameters obtained from the P-V loop study consisted of end-systolic pressure (ESP), end-diastolic pressure (EDP), maximum and minimum dP/dt (dP/dt<sub>max</sub> and dP/dt<sub>min</sub>), cardiac output (CO), % ejection fraction (%EF) and heart rate (HR). All P-V loop parameters were analyzed using Labscribe analytical software (Labscribe, Dover, NH, USA) (Palee et al., 2013; Tunapong et al., 2017).

#### 2.8. Cardiac mitochondrial function study

To study cardiac mitochondrial function, the mitochondrial ROS production, mitochondrial membrane potential changes, and mitochondrial swelling were determined.

using the methods described previously (Palee et al., 2013). Briefly, each rat heart was removed at the end of the study and chopped into small pieces on an ice-cold plate. Then, cardiac tissues were homogenized and centrifuged to isolate cardiac mitochondria. Cardiac mitochondrial ROS production was measured by staining cardiac mitochondria with dichlorohydrofluoresce in diacetate (DCFDA) dye for 25 min, after which a fluorescent microplate reader (Gen5 Microplate Reader, BioTek Instruments, VT, USA) was used to detect the ROS level using the excitation wavelength of 485 nm and emission wavelength at 530 nm (Ding et al., 2017). For mitochondrial membrane potential change. the dye 5,5,6,6-tetrachloro-1,1,3,3ethylbenzimidazolcarbocyanine iodide (JC-1) was used. The green fluorescence (JC-1 monomer) was excited at a wavelength of 485 nm and the emission detected at 590 nm while the red fluorescence (JC-1 aggregates) was excited at a wavelength of 485 nm and the emission detected at 530 nm. A decreased red/green fluorescence intensity ratio indicates depolarization of the mitochondrial membrane (Jheng et al., 2012). Mitochondrial swelling was determined using spectrophotometry at 25 °C as previously described (Di Lisa et al., 2001; Morikawa et al., 2014; Ruiz-Meana et al., 2006; Scorrano et al., 1999). Decreased light absorbance in a mitochondrial suspension at 540 nm indicates mitochondrial swelling (Ruiz-Meana et al., 2006). Mitochondrial swelling is caused by the influx of water to mitochondria. Since major components of mitochondria are protein, lipid and water, the influx of water into mitochondria leads to the decrease in the light absorbance of mitochondria (Morikawa et al., 2014). Cardiac mitochondrial morphology was also studied using a transmission electron microscope (TEM; JEM-1200 EX II, JEOL Ltd., Japan).

#### 2.9. Determination of cardiac mitochondrial dynamics

To determine cardiac mitochondrial dynamics, western blot analysis was used to determine protein expression of the mitochondrial fission protein dynamin-related protein 1(Drp1) and the mitochondrial fusion protein mitofusin 2 (Mfn2) in isolation of crude mitochondrial fraction from hearts. Briefly, isolated cardiac mitochondrial fraction were mixed with a loading buffer consisting of 5% mercaptoethanol, 0.05% bromophenol blue, 75 nM Tris, 2% SDS, and 10% glycerol with pH 6.8), and the mixture was boiled for 5 min and loaded into 10% gradient SDS-polyacrylamide gels. Proteins were then transferred to a nitrocellulose membrane with the presence of a glycine/methanol transfer buffer (containing 20 mM Tris, 0.15 M glycine, and 20% methanol) in a transfer system (Bio-Rad). The membranes were incubated in 5% skim milk in 1 × TBS-T buffer (containing 20 mM Tris (pH 7.6), 137 nM NaCl, and 0.05% Tween-20) for 1 h at room temperature then exposed to anti-phospho-Drp1 (ser616), total-Drp1, Mitofusin 2, and VDAC (Cell Signaling Technology, Danvers, MA, USA) for 12 h. Bound antibody was detected by horseradish peroxidase conjugated with antirabbit IgG. Enhanced chemiluminescence (ECL) detection reagents were administered to visualize peroxidase reaction products.

#### 2.10. Determination of oxidative stress

Malondialdehyde (MDA) concentrations in cardiac tissues were measured using a high-performance liquid chromatography (HPLC) system (Thermo Scientific, Bangkok, Thailand) as described previously (Apaijai et al., 2014). Protein from cardiac tissues were mixed with 10% trichloroacetic acid (TCA) containing BHT then heated at 90 °C for 30 min and cooled to room temperature. The mixture was centrifuged, and the supernatant was mixed with 0.44 M  $\rm H_3PO_4$  and 0.6% thiobarbituric acid (TBA) solution to generate thiobarbituric acid reactive substances (TBARS). The solution was filtered through a syringe filter (polysulfone type membrane, pore size 0.45  $\mu m$ , Whatman International, Maidstone, UK) and analyzed with the HPLC system. Data were analyzed with BDS software (BarSpec Ltd., Rehovot, Israel), and plasma TBARS concentration was determined directly from a standard curve generated from a standard reagent for MDA at different concentrations and reported as MDA equivalent concentration.

#### 2.11. Determination of metabolic parameters and hormone levels

Plasma was prepared from fasted blood samples and was kept frozen at  $-80\,^{\circ}\mathrm{C}$  until analysis of glucose, cholesterol, triglyceride, insulin, and estradiol levels could be completed. Plasma estrogen concentration was measured by using a competitive enzyme immunoassay (EIA) kit (Cayman Chemical Company, MI, USA). Plasma insulin level was detected using a sandwich ELISA kit (Millipore, MI, USA). Plasma glucose and triglyceride levels were determined by colorimetric assay from a commercially available kit (Biotech, Bangkok, Thailand). Fasting plasma HDL and LDL were determined using commercially available kits (ERBA diagnostic, Mannheim, Germany) (Sivasinprasasn et al., 2015).

#### 2.12. Cardiac expression of apoptotic proteins

For determination of cardiac apoptotic protein, Western blot analysis was used for measurement of expression of proteins Bax, Bcl-2, Caspase3, and Cleaved- Caspase3 as described previously (Palee et al., 2013). Anti- Bax, Bcl-2, Caspase3, and Cleaved- Caspase3 (Cell Signaling Technology, Danvers, MA, USA), and anti-actin (Sigma-Aldrich, St. Louis, MO, USA) were used. Bound antibody was detected using horseradish peroxidase conjugated with anti-rabbit or anti-mouse IgG. Enhanced chemiluminescence (ECL) detection reagents were administered to visualize peroxidase reaction products (Palee et al., 2013).

### 2.13. Statistical analysis

Data were expressed as mean  $\pm$  SEM. Comparisons of variables were performed using the one-way ANOVA followed by an LSD post-hoc test. P < 0.05 was considered statistically significant.

#### 3. Results

3.1. Estrogen deprivation aggravated adverse changes in metabolic profiles and oxidative stress in obese-insulin resistant rats

After ingestion of a HFD for 13 weeks, HFD rats developed insulin resistance as indicated by markedly increased body weight (318.20  $\pm$  5.48 vs 272.08  $\pm$  2.69 g) and increased HOMA index (14.28  $\pm$  2.69 vs 7.56  $\pm$  1.34), when compared with ND rats. However, the fasting blood glucose level (143.54  $\pm$  3.47 vs 144.92  $\pm$  4.27 mg/dl) and the amount of daily energy intake (58.85  $\pm$  1.63 vs 62.13  $\pm$  2.21 kcal/day) was not significantly different between the HFD rats and ND rats.

Six weeks after ovariectomy, there was an observable marked increase in body weight in HFO rats when compared with NDS, NDO and HFS rats (Table 1). Moreover, both estradiol levels and uterus weight

Table 1
Effect of estrogen deprivation on metabolic parameters in obese-insulin resistant rats.

| Parameters   | Groups            |                         |                              |                                       |  |  |
|--|-------------------|-------------------------|------------------------------|---------------------------------------|--|--|
|  | NDS               | NDO                     | HFS                          | HFO                                   |  |  |
| Body weight (g)  | 277.22 ± 4.34     | 316.36 ± 5.00*          | 325.94 ± 5.97*               | 371.04 ± 12.87*, <sup>†,‡</sup>       |  |  |
| Visceral fat (g)   | $6.8 \pm 1.08$    | 12.19 ± 1.24*           | $25.89 \pm 1.20^{*,\dagger}$ | $33.71 \pm 1.98^{*,\dagger,\ddagger}$ |  |  |
| Uterus weight (g)  | $0.45 \pm 0.06$   | $0.15 \pm 0.04^{\circ}$ | $0.38 \pm 0.02^{\dagger}$    | $0.14 \pm 0.02^{*,\ddagger}$          |  |  |
| Estradiol level (pg/ml)  | $115.68 \pm 9.10$ | 52.58 ± 3.11*           | $116.44 \pm 16.78$           | 57.62 ± 3.52*                         |  |  |
| Glucose (mg/dl)  | $129.17 \pm 2.69$ | $134.31 \pm 4.46$       | $137.36 \pm 4.68$            | 153.89 ± 6.17*                        |  |  |
| Insulin (ng/ml)  | $0.99 \pm 0.12$   | $2.38 \pm 0.31^{\circ}$ | $2.44 \pm 0.38$ *            | $3.22 \pm 0.30^{*}$                   |  |  |
| HOMA index   | $6.07 \pm 1.41$   | 18.47 ± 4.55*           | 20.32 ± 8.67*                | 18.48 ± 5.44*                         |  |  |
| Plasma glucose AUC (AUCg) (mg/dl $\times$ min $\times$ 10 <sup>4</sup> ) | $1.68 \pm 0.09$   | $1.99 \pm 0.06$ *       | $2.37 \pm 0.12^{*,\dagger}$  | $2.84 \pm 0.15^{*,\dagger,\ddagger}$  |  |  |
| Cholesterol (mg/dl)  | $77.33 \pm 4.64$  | 95.59 ± 7.23            | 106.53 ± 6.80*               | 117.57 ± 10.50*                       |  |  |
| HDL (mg/dl)  | $7.72 \pm 0.20$   | $8.36 \pm 0.23$         | $8.12 \pm 0.35$              | $8.56 \pm 0.29$                       |  |  |
| LDL (mg/dl)  | 67.79 ± 5.64      | $76.49 \pm 2.63$        | 84.40 ± 3.73*                | 85.17 ± 5.88*                         |  |  |
| Triglyceride (mg/dl)   | $70.88 \pm 4.24$  | 67.38 ± 4.49            | 88.51 ± 9.21                 | $90.40 \pm 3.88$                      |  |  |
| Energy intake (kcal/day)   | 57.85 ± 1.73      | $57.20 \pm 1.72$        | $63.13 \pm 2.51$ *,†         | $63.88 \pm 2.24^{*,\dagger}$          |  |  |

Values are mean  $\pm$  SEM (n = 8/group). \*P < 0.05 vs NDS, †P < 0.05 vs NDO, and ‡P < 0.05 vs HFS. NDS, normal-diet fed sham-operated rats; NDO, normal-diet fed ovariectomized rats; HFS, high-fat-diet fed sham-operated rats; HFO, high-fat-diet fed ovariectomized rats; HOMA, Homeostasis model assessment.

showed a significant decrease in NDO, HFS and HFO groups, compared to NDS rats, confirming the endogenous estrogen-deprived condition resulting from the removal of ovaries. Visceral fat deposition was significantly increased in NDO, HFS and HFO rats, compared to the NDS group. Furthermore, plasma cholesterol levels in NDO, HFS and HFO rats were significantly increased when compared with NDS rats (Table 1). Insulin sensitivity was decreased in NDO, HFS and HFO groups when compared with NDS rats (Table 1) indicated by increased area under the curve (AUC) following an OGTT.

#### 3.2. Estrogen deprivation aggravated cardiovascular dysfunction in obeseinsulin resistant rats

After ingestion of a HFD for 13 weeks, HFD rats (HFS and HFO) had significantly increased SBP and DBP, compared to NDS rats (Fig. 1A and B). Moreover, six weeks after ovariectomy, NDO and HFO rats had increased SBP and DBP, compared to NDS and HFS rats, respectively. In all groups, HFO rats had the most severe impairment of BP (Fig. 1A and B). Echocardiograms demonstrated that HFD rats (HFS and HFO) also developed LV systolic dysfunction as indicated by decreased %FS and also LV diastolic dysfunction as indicated by a decreased mitral E/A ratio, when compared to ND rats (Fig. 1C and D). An ovariectomy apparently aggravated LV dysfunction in NDO and HFO rats as shown by both a decreased %FS and mitral E/A ratio, compared to NDS and HFS groups, respectively (Fig. 1C and D). Moreover, an altered of the cardiac morphology as indicated by increased wall thickness and increased chamber size were significantly increased in NDO, HFS and HFO rats. However, HFO rats had the most severe abnormalities of cardiac morphology (Table 2).

The P–V loop analysis was performed at the end of the experimental protocol to determined cardiac function. The LV contractile function including LVESP, dP/dt<sub>max</sub>, CO, and %EF were decreased, whereas LV lusitropy function including LVEDP and dP/dt<sub>min</sub> were increased in the NDO, HFS and HFO groups, compared to NDS rats (Table 3). However, HFO rats had the most severe impairments for both LV contractile function and relaxation (Table 3).

### 3.3. Estrogen deprivation aggravated cardiac sympathovagal imbalance in obese-insulin resistant rats

The LF/HF ratio of the HRV was determined as an index of cardiac sympathovagal balance. Six weeks after ovariectomy, the LF/HF ratio in the NDO, HFS and HFO rats were significantly increased when compared with NDS rats (Fig. 1E). However, HFO rats had the most severe impairment as regards cardiac sympathovagal imbalance.

Furthermore, the cardiac MDA was markedly increased in NDO, HFS and HFO rats when compared with NDS rats (Fig. 1F). Similarly, HFO rats had the most severe impairment in cardiac oxidative stress.

### 3.4. Estrogen deprivation aggravated cardiac mitochondrial dysfunction in obese-insulin resistant rats

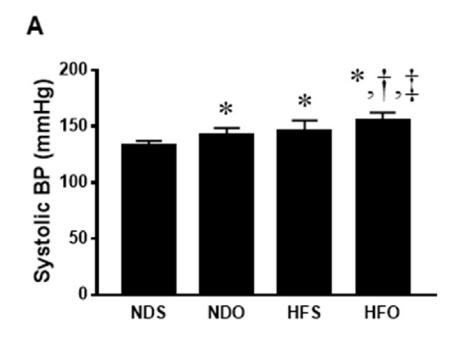
In this study, cardiac mitochondrial ROS production, cardiac mitochondrial membrane potential depolarization, and cardiac mitochondrial swelling were determined to enable the assessment of cardiac mitochondrial function. Six weeks after ovariectomy, NDO, HFS and HFO rats had increased cardiac mitochondrial ROS levels, cardiac mitochondrial membrane depolarization, and mitochondrial swelling, compared to NDS rats (Fig. 2A–C). However, HFO had the most severe cardiac mitochondrial dysfunction as indicated by the highest ROS level, and mitochondrial swelling. Representative transmission electron micrographs of cardiac mitochondria morphology showed unfolding of cristae in the NDO, HFS and HFO groups, compared to the NDS group (Fig. 2D).

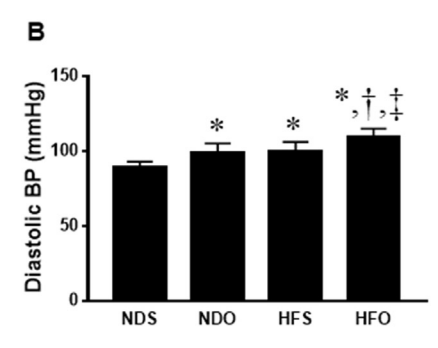
### 3.5. Estrogen deprivation increased cardiac mitochondrial fission in obese-insulin resistant rats

In this study, cardiac expression of mitochondrial fission protein indicated by the phosphorylation of dynamin-related protein 1 (Drp1) at serine 616 and the mitochondrial fusion protein mitofusin 2 (Mfn2) were determined to assess cardiac mitochondrial dynamics. After ingestion of a HFD for 13 weeks, our results demonstrated that the phosphorylation of Drp1 at serine 616 and Mfn2 expression did not alter in HFS rats, when compared to NDS rats. However, 6 weeks after ovariectomy, both NDO and HFO rats had significantly increased levels of phosphorylation of Drp1 at serine 616, compared to NDS and HFS rats (Fig. 2D), whereas cardiac mitochondrial expression of Mfn2 protein was no different among the groups (Fig. 2F).

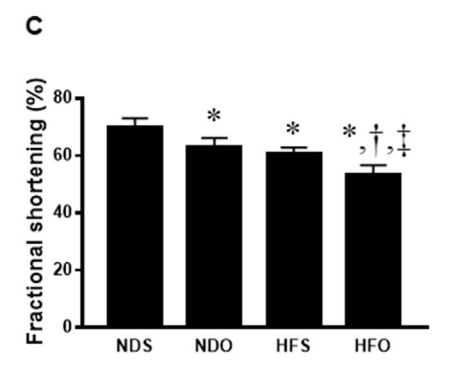
### 3.6. Estrogen deprivation increased cardiac apoptosis in obese-insulin resistant rats

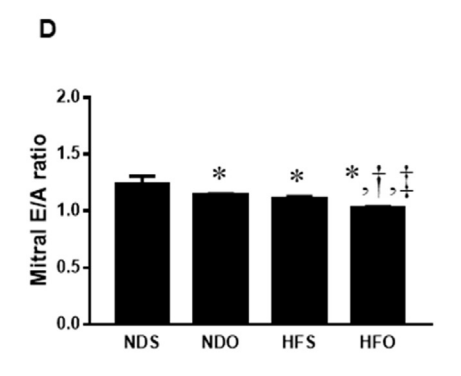
Cardiac expression of apoptotic protein Bax, Caspase 3, and Cleaved-Caspase3, and anti-apoptotic protein Bcl-2 were determined to assess cardiac apoptotic signaling. It was only in HFO rats that the expression of Bax and Cleaved-Caspase 3 was significantly increased, when compared to NDS rats (Fig. 3A and B). However, the expression of Bcl-2 was no different among the groups (Fig. 3C). The representative western blot bands of Bax, Caspase 3, Cleaved-Caspase3, Bcl-2 and actin

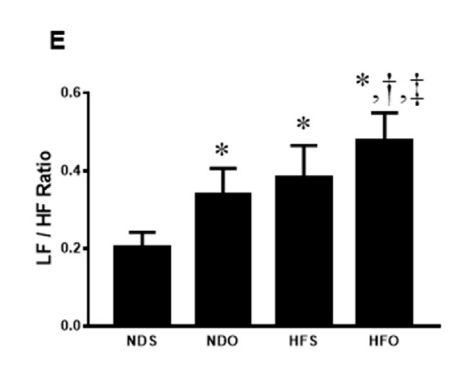


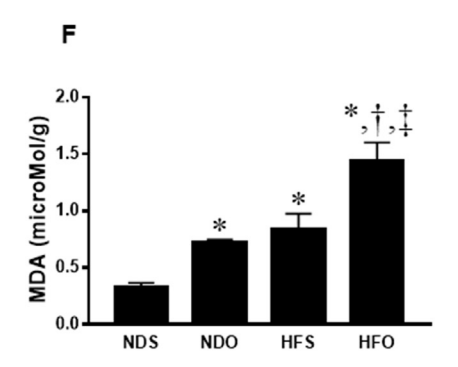


**Fig. 1.** Effects of estrogen-deprivation on blood pressure, echocardiographic parameters, heart rate variability and oxidative stress in obese-insulin resistant rats. (A) Systolic blood pressure; (B) Diastolic blood pressure; (C) % Fractional shortening; (D) Mitral E/A ratio; (E) Heart rate variability; (F) MDA. \*p < 0.05 vs NDO, †p < 0.05 vs NDO, †p < 0.05 vs HFS. NDS, normal-diet fed sham-operated rats; NDO, normal-diet fed ovariectomized rats; HFO, high-fat-diet fed ovariectomized rats; SBP, systolic blood pressure; DBP, diastolic blood pressure; LF/HF ratio, low frequency/high frequency ratio; MDA, malondialdehyde.









are shown in Fig. 3D.

#### 4. Discussion

The major findings from the present study clearly demonstrate that

both estrogen deprivation and obese-insulin resistance independently cause metabolic disturbance, oxidative stress, cardiac autonomic imbalance, LV dysfunction, mitochondrial dysfunction, and increased mitochondrial fission. However, the severity of these metabolic and cardiac adverse effects was increased in obese-insulin resistant rats with

 Table 2

 Effect of estrogen deprivation on M-Mode echocardiographic parameters.

| Parameters | Groups          |                   |                   |                                      |  |
|------------|-----------------|-------------------|-------------------|--------------------------------------|--|
|            | NDS             | NDO               | HFS               | HFO                                  |  |
| IVSd (mm)  | 1.57 ± 0.15     | 1.67 ± 0.07*      | 1.66 ± 0.04*      | 1.73 ± 0.05*,†,‡                     |  |
| IVSs (mm)  | $3.10 \pm 0.13$ | $2.93 \pm 0.12*$  | $2.89 \pm 0.03*$  | 2.75 ± 0.09*,†,‡                     |  |
| LVIDd (mm) | $5.92 \pm 0.13$ | $6.35 \pm 0.04$ * | $6.08 \pm 0.14$ * | 6.60 ± 0.10*,†,‡                     |  |
| LVISs (mm) | $1.94 \pm 0.13$ | $2.59 \pm 0.15$ * | $2.60 \pm 0.28$ * | $2.93 \pm 0.26^*, \dagger, \ddagger$ |  |
| LVPWd (mm) | $1.94 \pm 0.13$ | $1.87 \pm 0.12^*$ | 1.91 ± 0.11*      | $1.77 \pm 0.05^*$                    |  |
| LVPWs (mm) | $3.55 \pm 0.08$ | $3.48 \pm 0.16$   | $3.48 \pm 0.21$   | $3.27 \pm 0.13$                      |  |

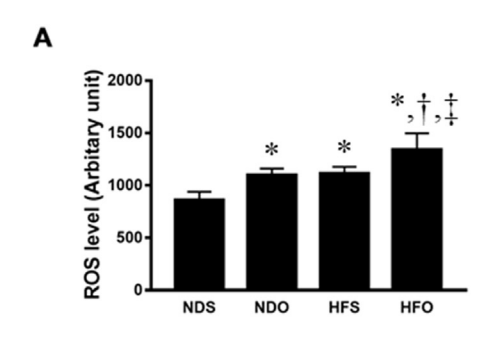
Values are mean  $\pm$  SEM (n = 8/group). \*P < 0.05 vs NDS, †P < 0.05 vs NDO, and ‡P < 0.05 vs HFS. NDS, normal-diet fed sham-operated rats; NDO, normal-diet fed ovariectomized rats; HFS, high-fat-diet fed sham-operated rats; HFO, high-fat-diet fed ovariectomized rats IVSd, interventricular septal thickness at end diastole; IVSs, interventricular septal thickness at end systole; LVIDd, left ventricular internal diameter at end diastole; LVIDs, left ventricular internal diameter at end systole; LVPWd, left ventricular posterior wall end diastole; LVPWs, left ventricular posterior wall thickness at end systole.

 Table 3

 Effect of estrogen deprivation on cardiac function in obese-insulin resistant rats.

| Parameters                     | Groups          |                  |                   |                                      |  |  |
|--------------------------------|-----------------|------------------|-------------------|--------------------------------------|--|--|
|                                | NDS             | NDO              | HFS               | HFO                                  |  |  |
| Heart rate (bpm)               | 257 ± 13        | 282 ± 18         | 283 ± 24          | 333 ± 32*,†,‡                        |  |  |
| LVESP (mm Hg)                  | $127 \pm 11$    | 108 ± 19*        | $100 \pm 11*$     | 95 ± 12*                             |  |  |
| LVEDP (mm Hg)                  | 9 ± 1           | 12 ± 5*          | 16 ± 3*           | 20 ± 5*,†                            |  |  |
| dP/dt <sub>max</sub> (mm Hg/s) | 9959 ± 549      | 6559 ± 866*      | 5273 ± 573*,†     | 4762 ± 611*,†                        |  |  |
| $-dP/dt_{min}$ (mm Hg/s)       | $-6831 \pm 296$ | $-3996 \pm 708*$ | $-3603 \pm 565$ * | $-3365 \pm 626*$                     |  |  |
| CO (ml/min)                    | 78 ± 7          | 68 ± 8*          | 60 ± 8*           | 48 ± 8*,†,‡                          |  |  |
| CO/BW (ml/min/g)               | $0.28 \pm 0.2$  | $0.21 \pm 0.1^*$ | $0.18 \pm 0.3*$   | $0.13 \pm 0.2^*, \uparrow, \ddagger$ |  |  |
| LVEF (%)                       | 71 ± 6          | 63 ± 6*          | 55 ± 9*,†         | 48 ± 4*,†,‡                          |  |  |

Values are mean  $\pm$  SEM (n = 8/group). \*P < 0.05 vs NDS, †P < 0.05 vs NDO, and ‡P < 0.05 vs HFS. NDS, normal-diet fed sham-operated rats; NDO, normal-diet fed ovariectomized rats; HFS, high-fat-diet fed sham-operated rats; HFO, high-fat-diet fed ovariectomized rats; LVESP, left ventricular end systolic pressure; LVEDP, left ventricular end diastolic pressure; dP/dt<sub>max</sub>, maximal slope of the systolic pressure increment; dP/dt<sub>min</sub>, maximal slope of the diastolic pressure decrement; CO, cardiac output; LVEF, left ventricular ejection fraction.



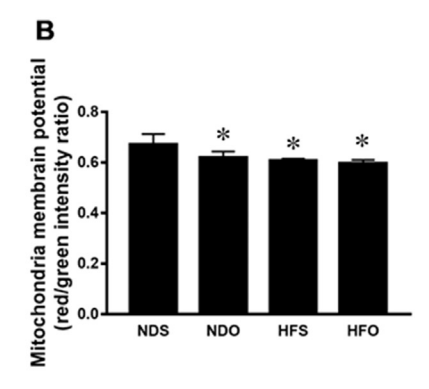
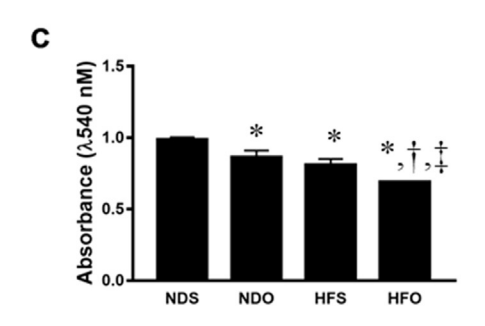
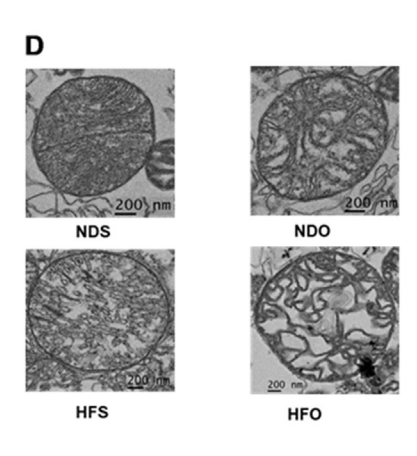
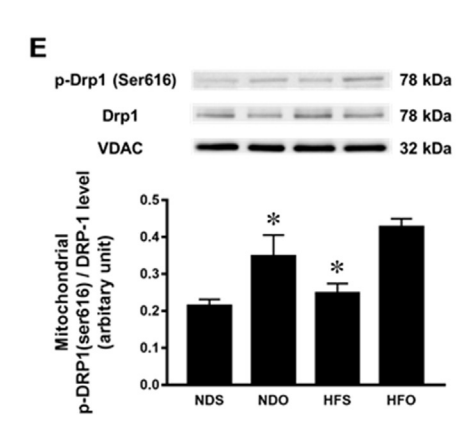
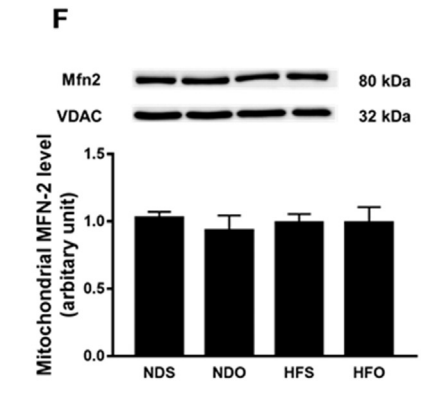


Fig. 2. Effects of estrogen-deprivation on cardiac mitochondrial function and cardiac mitochondrial dynamics in obese-insulin resistant rats. (A) Cardiac mitochondrial ROS production; (B) Cardiac mitochondrial membrane potential; (C) Cardiac mitochondrial swelling; (D) TEM representative images of cardiac mitochondria; (E) Cardiac mitochondrial fusion. \*p < 0.05 vs NDS; †p < 0.05 vs NDO; †p < 0.05 vs NDO, normaldiet fed sham-operated rats; NDO, normaldiet fed ovariectomized rats; HFS, high-fat-diet fed sham-operated rats; HFO, high-fat-diet fed ovariectomized rats; ROS, reactive oxygen species; TEM, transmission electron microscopy; Drp1, dynamin-related protein 1; Mfn2, mitofusin 2; VDAC, voltage-dependent anion channels.









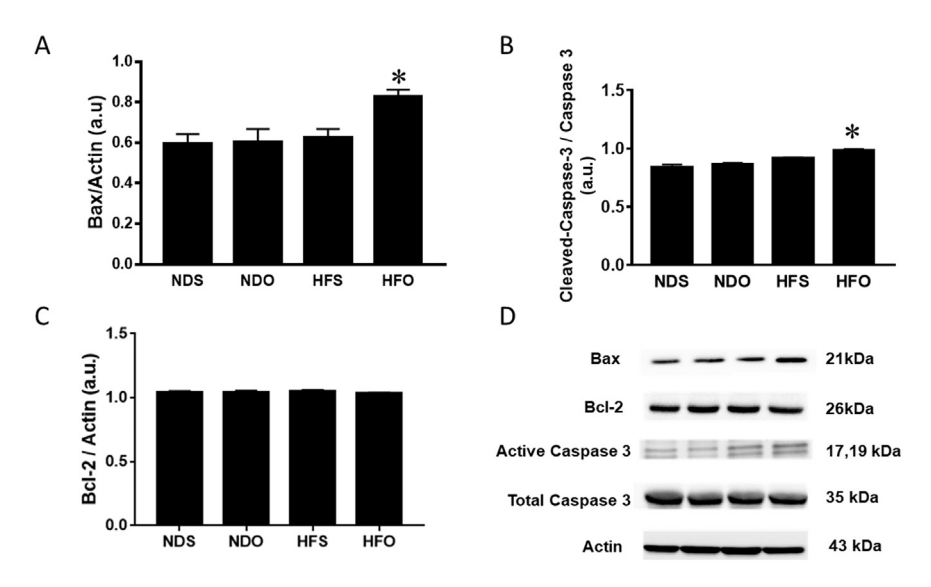


**Fig. 3.** Effects of estrogen-deprivation on cardiac apoptosis in obese-insulin resistant rats. (A) Bax; (B) Cleaved-Caspase3; (C) Bcl-2; (D) Representative images of western blotting band.  $^*p < 0.05$  vs NDS, normal-diet fed sham-operated rats; NDO, normal-diet fed ovariectomized rats; HFS, high-fat-diet fed sham-operated rats; HFO, high-fat-diet fed ovariectomized rats.

Table 4
A summary of cardiometabolic impairment in the experimental groups.

| Impairment                        | Groups            |          |            |             |  |
|-----------------------------------|-------------------|----------|------------|-------------|--|
|                                   | NDS               | NDO      | HFS        | HFO         |  |
| Metabolic disturbance             | $\leftrightarrow$ | 1        | <b>↑</b> ↑ | <b>↑</b> ↑↑ |  |
| LV contractile dysfuction         | $\leftrightarrow$ | 1        | <b>↑</b> ↑ | 111         |  |
| Cardiac autonomic imbalance       | $\leftrightarrow$ | 1        | 1          | 111         |  |
| Oxidative stress                  | $\leftrightarrow$ | 1        | 1          | 111         |  |
| Cardiac mitochondrial dysfunction | $\leftrightarrow$ | 1        | 1          | 111         |  |
| Cardiac mitochondrial fission     | $\leftrightarrow$ | <b>†</b> | ↔          | 1           |  |

NDS, normal-diet fed sham-operated rats; NDO, normal-diet fed ovariectomized rats; HFS, high-fat-diet fed sham-operated rats; HFO, high-fat-diet fed ovariectomized rats; LV, left ventricular.

estrogen deprivation, i.e. when both conditions were present. A summary of these findings is shown in Table 4.

In this study, both estrogen deprivation at the age of adolescence and obese-insulin resistance were associated with metabolic disturbance including obesity, insulin resistance, and dyslipidemia, compared with normal rats. Estrogen is known to promote energy homeostasis, improve body fat distribution, ameliorate insulin resistance (or enhance insulin sensitivity) and improve β-cell function (Mauvais-Jarvis et al., 2013). The prevalence of metabolic syndrome has been shown to increase in women with low levels of estrogen such as those post-menopausal women, and women who have undergone ovariectomy (Carr, 2003; Dorum et al., 2008). Although a previous study found that 8 weeks of estrogen deprivation in very young obese-insulin resistant rats did not aggravate metabolic disturbance (Sivasinprasasn et al., 2015), our findings showed that 7 weeks of estrogen deprivation at the age of adolescence in obese-insulin resistant rats caused the worsening of metabolic disturbance. These findings suggested that an alteration of metabolic function in obese-insulin resistant rats with estrogen deprivation depends upon the onset of estrogen deprivation.

Both oxidative stress and estrogen deprivation have been shown to influence sympathetic hyperactivity (Campese et al., 2005; Ye et al., 2006), leading to cardiac autonomic imbalance and increased BP. Estrogen plays a role in controlling autonomic nervous activity by inhibiting the sympathetic nervous system (Ashraf and Vongpatanasin, 2006). This was confirmed in this study when the HRV was depressed in normal rats with estrogen deprivation, indicating that this inhibitory effect of sympathetic activity had declined due to low estrogen levels in these rats. Furthermore, it has been shown that either estrogen deprivation or obese-insulin resistant rats had increased systemic, cardiac,

and mitochondrial oxidative stress (Sivasinprasasn et al., 2015; Sivasinprasasn et al., 2017). Thus, a combination of oxidative stress and estrogen deprivation greatly provoked cardiac autonomic imbalance as we found in obese-insulin resistant rats with estrogen deprivation, compared with both normal rats with estrogen deprivation and obese-insulin resistant rats without estrogen deprivation.

Our previous studies investigated the effects of obesity-induced insulin resistance and estrogen deprivation on cardiac function in young rats, and showed that cardiac dysfunction was not aggravated after eight weeks of high-fat diet feeding and ovariectomy (Apaijai et al., 2012; Sivasinprasasn et al., 2015). However, this study, using adolescent rats, showed that seven weeks of estrogen deprivation could result in cardiac dysfunction in obese-insulin resistant rats. All of these findings suggest that the age at the onset of estrogen deprivation could be a key determining factor as regards cardiac dysfunction in obese-insulin resistant and estrogen-deprived rats.

Estrogen plays significant regulatory roles in maintaining normal mitochondrial properties by modulating mitochondrial ATP synthesis, stabilizing the structural assembly and dynamics of the mitochondria, and attenuating mitochondrial ROS production (Aurigemma, 2015; Rattanasopa et al., 2015; Sastre-Serra et al., 2012; Sastre-Serra et al., 2013). An impairment in cardiac mitochondrial function including increased cardiac mitochondrial ROS production, mitochondrial membrane depolarization, and mitochondrial swelling were observed in estrogen deprived rats and obese-insulin resistant rats, and these deleterious effects were aggravated in obese-insulin resistant rats with estrogen deprivation. In addition, we demonstrated that only estrogen deprived rats (NDO and HFO) showed increased levels of mitochondrial fission indicated by increased phosphorylation of Drp1 at serine 616, which was activated by oxidative stress (Qi et al., 2011; Zaja et al., 2014). Our results demonstrated that cardiac mitochondrial fusion events were not altered in these models. These data suggest that estrogen deprivation, not chronic consumption of a high fat diet, increased oxidative stress levels, leading to increased cardiac mitochondrial fission. In addition, estrogen is known to play an important role in mitochondrial biogenesis facilitated by estrogen-related receptor (ERR) in mitochondria (Cho et al., 2013). The lack of estrogen in NDO and HFO rats could alter mitochondrial biogenesis and therefore increased mitochondrial fission directly (Klinge, 2008). However, previous studies demonstrated that mice fed on a high fat diet for 40 weeks (Littlejohns et al., 2014), which is much longer than ours, and diabetic mice (Liu et al., 2014) had increased levels of cardiac mitochondrial fission indicated by increased Drp1 expression in skeletal muscle. This discrepancy could be due to the differences in animal models (diabetes vs obese-insulin resistance), duration of high fat diet consumption and the organs susceptible to oxidative stress. Moreover, the predominant shift towards the mitochondrial fission processes without the changes in mitochondrial fusion proteins in high fat diet fed rats (Lionetti et al., 2014) might explain this discrepancy.

In conclusion, our findings demonstrated that the loss of endogenous estrogen by ovariectomy in obese-insulin resistant rats aggravated metabolic and cardiac dysfunction. This could be due to the worsening of cardiac mitochondrial dysfunction caused by estrogen deprivation.

#### 5. Limitation

The limitation of this study is that although we measured mitochondrial ROS production, mitochondrial depolarization and mitochondrial swelling, to assess the mitochondrial function in the heart, the mitochondrial respiratory function was not determined.

#### **Funding**

This work was supported by the Thailand Research Fund grants TRG5980020 (SP), MRG5980198 (WP), and RTA6080003 (SCC); the Faculty of Medicine Chiang Mai University Endowment Fund (SP); the NSTDA Research Chair grant from the National Science and Technology Development Agency Thailand (NC), and the Chiang Mai University Center of Excellence Award (NC).

#### Conflict of interest

None.

#### References

- Apaijai, N., Pintana, H., Chattipakorn, S.C., Chattipakorn, N., 2012. Cardioprotective effects of metformin and vildagliptin in adult rats with insulin resistance induced by a high-fat diet. Endocrinology 153, 3878–3885.
- Apaijai, N., Pintana, H., Chattipakorn, S.C., Chattipakorn, N., 2013. Effects of vildagliptin versus sitagliptin, on cardiac function, heart rate variability and mitochondrial function in obese insulin-resistant rats. Br. J. Pharmacol. 169, 1048–1057.
- Apaijai, N., Chinda, K., Palee, S., Chattipakorn, S., Chattipakorn, N., 2014. Combined vildagliptin and metformin exert better cardioprotection than monotherapy against ischemia-reperfusion injury in obese-insulin resistant rats. PLoS One 9, e102374.
- Ashraf, M.S., Vongpatanasin, W., 2006. Estrogen and hypertension. Curr. Hypertens. Rep
- Aurigemma, N.C., 2015. Alterations in mitochondrial morphology with age-associated estrogen deficiency and ischemia-reperfusion injury. FASEB J. 29, 1047–1049.
- Campese, V.M., Shaohua, Y., Huiquin, Z., 2005. Oxidative stress mediates angiotensin II dependent stimulation of sympathetic nerve activity. Hypertension 46, 533–539.
- Carr, M.C., 2003. The emergence of the metabolic syndrome with menopause. J. Clin. Endocrinol. Metab. 88, 2404–2411.
- Chan, D.C., 2012. Fusion and fission: interlinked processes critical for mitochondrial health. Annu. Rev. Genet. 46, 265–287.
- Cho, Y., Hazen, B.C., Russell, A.P., Kralli, A., 2013. Peroxisome proliferator-activated receptor gamma coactivator 1 (PGC-1)- and estrogen-related receptor (ERR)-induced regulator in muscle 1 (Perm1) is a tissue-specific regulator of oxidative capacity in skeletal muscle cells. J. Biol. Chem. 288, 25207–25218.
- Di Lisa, F., Menabo, R., Canton, M., Barile, M., Bernardi, P., 2001. Opening of the mitochondrial permeability transition pore causes depletion of mitochondrial and cytosolic NAD+ and is a causative event in the death of myocytes in postischemic reperfusion of the heart. J. Biol. Chem. 276, 2571–2575.
- Ding, M., Dong, Q., Liu, Z., Liu, Z., Qu, Y., Li, X., Huo, C., Jia, X., Fu, F., Wang, X., 2017. Inhibition of dynamin-related protein 1 protects against myocardial ischemia–reperfusion injury in diabetic mice. Cardiovasc. Diabetol. 16.
- Dorum, A., Tonstad, S., Liavaag, A.H., Michelsen, T.M., Hildrum, B., Dahl, A.A., 2008. Bilateral oophorectomy before 50 years of age is significantly associated with the metabolic syndrome and Framingham risk score: a controlled, population-based study (HUNT-2). Gynecol. Oncol. 109, 377–383.
- Ginsberg, H.N., 2000. Insulin resistance and cardiovascular disease. J. Clin. Invest. 106, 453–458.
- Holmstrom, M.H., Iglesias-Gutierrez, E., Zierath, J.R., Garcia-Roves, P.M., 2012. Tissue-specific control of mitochondrial respiration in obesity-related insulin resistance and diabetes. Am. J. Physiol. Endocrinol. Metab. 302, E731–739.
- Jheng, H.F., Tsai, P.J., Guo, S.M., Kuo, L.H., Chang, C.S., Su, I.J., Chang, C.R., Tsai, Y.S.,

- 2012. Mitochondrial fission contributes to mitochondrial dysfunction and insulin resistance in skeletal muscle. Mol. Cell. Biol. 32, 309–319.
- Klinge, C.M., 2008. Estrogenic control of mitochondrial function and biogenesis. J. Cell. Biochem. 105, 1342–1351.
- Knowlton, A.A., Chen, L., Malik, Z.A., 2014. Heart failure and mitochondrial dysfunction: the role of mitochondrial fission/fusion abnormalities and new therapeutic strategies. J. Cardiovasc. Pharmacol. 63, 196–206.
- Lionetti, L., Mollica, M.P., Donizzetti, I., Gifuni, G., Sica, R., Pignalosa, A., Cavaliere, G., Gaita, M., De Filippo, C., Zorzano, A., Putti, R., 2014. High-lard and high-fish-oil diets differ in their effects on function and dynamic behaviour of rat hepatic mitochondria. PLoS One 9, e92753.
- Littlejohns, B., Pasdois, P., Duggan, S., Bond, A.R., Heesom, K., Jackson, C.L., Angelini, G.D., Halestrap, A.P., Suleiman, M.S., 2014. Hearts from mice fed a non-obesogenic high-fat diet exhibit changes in their oxidative state, calcium and mitochondria in parallel with increased susceptibility to reperfusion injury. PLoS One 9, e100579.
- Liu, R., Jin, P., Liqun, Yu, Wang, Y., Han, L., Shi, T., Li, X., 2014. Impaired mitochondrial dynamics and bioenergetics in diabetic skeletal muscle. PLoS One 9, e92810.
- Maas, A.H., van der Schouw, Y.T., Regitz-Zagrosek, V., Swahn, E., Appelman, Y.E., Pasterkamp, G., Ten Cate, H., Nilsson, P.M., Huisman, M.V., Stam, H.C., Eizema, K., Stramba-Badiale, M., 2011. Red alert for women's heart: the urgent need for more research and knowledge on cardiovascular disease in women: proceedings of the workshop held in Brussels on gender differences in cardiovascular disease, 29 September 2010. Eur. Heart J. 32, 1362–1368.
- Mauvais-Jarvis, F., Clegg, D.J., Hevener, A.L., 2013. The role of estrogens in control of energy balance and glucose homeostasis. Endocr. Rev. 34, 309–338.
- Morikawa, D., Kanematsu, K., Shibata, T., Haseda, K., Umeda, N., Ohta, Y., 2014. Detection of swelling of single isolated mitochondrion with optical microscopy. Biomed. Opt. Express. 5, 848–857.
- Palee, S., Weerateerangkul, P., Chinda, K., Chattipakorn, S.C., Chattipakorn, N., 2013.
  Mechanisms responsible for beneficial and adverse effects of rosiglitazone in a rat model of acute cardiac ischaemia-reperfusion. Exp. Physiol. 98, 1028–1037.
- Pratchayasakul, W., Chattipakorn, N., Chattipakorn, S.C., 2011. Effects of estrogen in preventing neuronal insulin resistance in hippocampus of obese rats are different between genders. Life Sci. 89, 702–707.
- Qi, X., Disatnik, M.H., Shen, N., Sobel, R.A., Mochly-Rosen, D., 2011. Aberrant mitochondrial fission in neurons induced by protein kinase C{delta} under oxidative stress conditions in vivo. Mol. Biol. Cell 22, 256–265.
- Rattanasopa, C., Phungphong, S., Wattanapermpool, J., Bupha-Intr, T., 2015. Significant role of estrogen in maintaining cardiac mitochondrial functions. J. Steroid Biochem. Mol. Biol. 147, 1–9.
- Rivera, C.M., Grossardt, B.R., Rhodes, D.J., Brown Jr., R.D., Roger, V.L., Melton 3rd, L.J., Rocca, W.A., 2009. Increased cardiovascular mortality after early bilateral oophorectomy. Menopause 16, 15–23.
- Ruiz-Meana, M., Garcia-Dorado, D., Miro-Casas, E., Abellan, A., Soler-Soler, J., 2006. Mitochondrial Ca<sup>2+</sup> uptake during simulated ischemia does not affect permeability transition pore opening upon simulated reperfusion. Cardiovasc. Res. 71, 715–724.
- Sastre-Serra, J., Nadal-Serrano, M., Pons, D.G., Roca, P., Oliver, J., 2012. Mitochondrial dynamics is affected by  $17\beta$ -estradiol in the MCF-7 breast cancer cell line. Effects on fusion and fission related genes. Int. J. Biochem. Cell Biol. 44, 1901–1905.
- Sastre-Serra, J., Nadal-Serrano, M., Pons, D.G., Roca, P., Oliver, J., 2013. The over-expression of ERbeta modifies estradiol effects on mitochondrial dynamics in breast cancer cell line. Int. J. Biochem. Cell Biol. 45, 1509–1515.
- Scorrano, L., Petronilli, V., Di Lisa, F., Bernardi, P., 1999. Commitment to apoptosis by GD3 ganglioside depends on opening of the mitochondrial permeability transition pore. J. Biol. Chem. 274, 22581–22585.
- Sivasinprasasn, S., Sa-Nguanmoo, P., Pratchayasakul, W., Kumfu, S., Chattipakorn, S.C., Chattipakorn, N., 2015. Obese-insulin resistance accelerates and aggravates cardiometabolic disorders and cardiac mitochondrial dysfunction in estrogen-deprived female rats. Age (Dordr.) 37, 28.
- Sivasinprasasn, S., Tanajak, P., Pongkan, W., Pratchayasakul, W., Chattipakorn, S.C., Chattipakorn, N., 2017. DPP-4 inhibitor and estrogen share similar efficacy against cardiac ischemic-reperfusion injury in obese-insulin resistant and estrogen-deprived female rats. Sci. Rep. 7, 44306.
- Tunapong, W., Apaijai, N., Yasom, S., Tanajak, P., Wanchai, K., Chunchai, T., Kerdphoo, S., Eaimworawuthikul, S., Thiennimitr, P., Pongchaidecha, A., Lungkaphin, A., Pratchayasakul, W., Chattipakorn, S.C., Chattipakorn, N., 2017. Chronic treatment with prebiotics, probiotics and synbiotics attenuated cardiac dysfunction by improving cardiac mitochondrial dysfunction in male obese insulin-resistant rats. Eur. J. Nutr..
- Vasquez-Trincado, C., Garcia-Carvajal, I., Pennanen, C., Parra, V., Hill, J.A., Rothermel, B.A., Lavandero, S., 2016. Mitochondrial dynamics, mitophagy and cardiovascular disease. J. Physiol. 594, 509–525.
- Vitale, C., Mendelsohn, M.E., Rosano, G.M., 2009. Gender differences in the cardiovascular effect of sex hormones. Nat. Rev. Cardiol. 6, 532–542.
- Ye, S., Zhong, H., Yanamadala, S., Campese, V.M., 2006. Oxidative stress mediates the stimulation of sympathetic nerve activity in the phenol renal injury model of hypertension. Hypertension 48, 309–315.
- Zaja, I., Bai, X., Liu, Y., Kikuchi, C., Dosenovic, S., Yan, Y., Canfield, S.G., Bosnjak, Z.J., 2014. Cdk1, PKCdelta and calcineurin-mediated Drp1 pathway contributes to mitochondrial fission-induced cardiomyocyte death. Biochem. Biophys. Res. Commun. 453, 710–721.

ELSEVIER

Contents lists available at ScienceDirect

### Toxicology and Applied Pharmacology

journal homepage: www.elsevier.com/locate/taap



### Atorvastatin and insulin equally mitigate brain pathology in diabetic rats



Wasana Pratchayasakul<sup>a,b</sup>, La-ongdao Thongnak<sup>b</sup>, Kenneth Chattipakorn<sup>a</sup>, Anusorn Lungaphin<sup>b</sup>, Anchalee Pongchaidecha<sup>b</sup>, Pattarapong Satjaritanun<sup>a</sup>, Thidarat Jaiwongkam<sup>a</sup>, Sasiwan Kerdphoo<sup>a</sup>, Siriporn C. Chattipakorn<sup>a,c,\*</sup>

- a Neurophysiology Unit, Cardiac Electrophysiology Research and Training Center, Faculty of Medicine, Chiang Mai University, Chiang Mai 50200, Thailand
- <sup>b</sup> Department of Physiology, Faculty of Medicine, Chiang Mai University, Chiang Mai 50200, Thailand
- <sup>c</sup> Department of Oral Biology and Diagnostic Sciences, Faculty of Dentistry, Chiang Mai University, Chiang Mai 50200, Thailand

#### ARTICLE INFO

# Keywords: Atorvastatin Insulin Diabetes mellitus type 1 Brain mitochondrial function Brain apoptosis Amyloid beta

#### ABSTRACT

Although insulin and atorvastatin have been shown to exert glycemic control and could improve brain function, the effects of atorvastatin or insulin as well as the combination of atorvastatin plus insulin on brain pathology in diabetes mellitus type 1 (T1DM) are unclear. Therefore, this study investigated the effect of atorvastatin, insulin or combined drugs on brain pathology in streptozotocin-induced diabetic rats. Thirty-six male rats were divided into two groups, a control group (n = 12) and a diabetic or experimental group (n = 24). Diabetic rats were further divided into four groups (n = 6/group) and the groups received either a vehicle (normal saline), atorvastatin (10 mg/kg/day), insulin (4 U/day) or a combination of the drugs for 4 weeks. The control group rats were divided into two groups (n = 6/group) to receive either just the vehicle or atorvastatin for 4 weeks. We found that streptozotocin-induced diabetic rats developed hyperglycemia, showing evidence of increased brain oxidative stress, impaired brain mitochondrial function, increased brain apoptosis, increased tau protein expression, increased phosphorylation of tau protein expression and amyloid beta levels, and decreased dendritic spine density. Although atorvastatin and insulin therapies led to an equal reduction in plasma glucose level in these diabetic rats, the combined drug therapy showed the greatest efficacy in decreasing plasma glucose level. Interestingly, atorvastatin, insulin and the combined drugs equally mitigated brain pathology. Our findings indicate that the combined drug therapy showed the greatest efficacy in improving metabolic parameters. However, atorvastatin, insulin and the combined drug therapy shared a similar efficacy in preventing brain damage in T1DM rats.

#### 1. Introduction

Diabetes mellitus type 1 (T1DM) is an irreversible disorder with severe complications involving damage to multiple organs, including heart, kidney, nerves and retina (Sochett and Daneman, 1999; Melendez-Ramirez et al., 2010). In addition, impaired cognitive function, increased brain apoptosis, increased tau protein expression, impaired brain mitochondrial function and decreased dendritic spine density have been found in T1DM mice, rats and patients (Kroner, 2009; Ho et al., 2013; Semaming et al., 2015). It has been shown that insulin therapy not only prevents organ damage in T1DM (American Diabetes, 2017), but also improves cognitive function in subjects with comorbid diabetes and Alzheimer's disease (Dhamoon et al., 2009;

Morris and Burns, 2012). Although insulin had beneficial effects as regards the improvement of glycemic control and cognitive function, hypoglycemia can still be a serious adverse effect following insulin therapy (American Diabetes, 2017). Recently, it has been suggested that the combination of insulin therapy with other therapies, including statins, in the treatment of T1DM may be used to decrease cardiovascular risks in diabetic patients (American Diabetes, 2017).

Atorvastatin is one of many lipid-lowering agents which leads to the reduction of cholesterol biosynthesis via the inhibition of 3-hydroxy-3-methylglutaryl coenzyme A (HMG-CoA) reductase enzyme (Stancu and Sima, 2001). Atorvastatin has been shown to exert glycemic control (Suzuki et al., 2005; Tanaka, 2011), reduce oxidative stress (Sugiyama et al., 2005; Kishi et al., 2008; Li et al., 2010), and attenuate brain

Abbreviations: T1DM, diabetes mellitus type 1; HMG-CoA, 3-hydroxy-3-methylglutaryl coenzyme A; T2DM, diabetes mellitus type 2; C, control rats; DM, diabetic rats; DMI, insulintreated diabetic rats; DMS, atorvastatin-treated diabetic rats; DMIS, combined drug-treated diabetic rats; MDA, malondialdehyde; ROS, reactive oxygen species; HPLC, high performance liquid chromatography; TCA, trichloroacetic acid; TBA, thiobarbituric acid solution; BCA, bicinchoninic acid assay; DCFHDA, dichlorohydrofluoresceindiacetate; ECL, enhanced chemiluminescence; Aβ, amyloid beta; STZ, streptozotocin

<sup>\*</sup> Corresponding author at: Department of Oral Biology and Diagnostic Sciences, Faculty of Dentistry, Chiang Mai University, Chiang Mai 50200, Thailand. E-mail address: siriporn.c@cmu.ac.th (S.C. Chattipakorn).

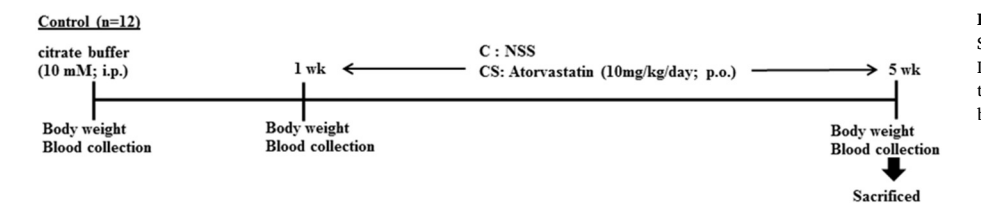
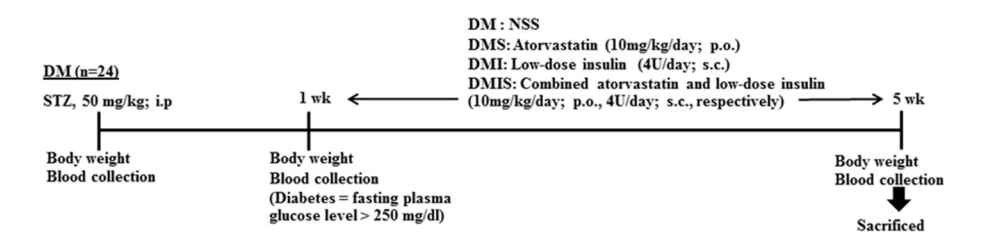


Fig. 1. The experimental protocol of the study. STZ = streptozotocin; C = control rats; DM = diabetic rats; DMI = insulin-treated diabetic rats; DMS = atorvastatin-treated diabetic rats; DMIS = combined drug-treated diabetic rats.



oxidative stress and cognitive impairment in rats with ischemic stroke (Kishi et al., 2008; Yang et al., 2015). Interestingly, it has been reported that the combination of insulin therapy and atorvastatin provided greater benefits than either of the 2 drugs as a monotherapy on the improvement of glycemic control and the reduction of liver oxidative stress in diabetes mellitus type 2 (T2DM) rats (Matafome et al., 2009). There is some evidence that the benefits of atorvastatin may be due to its effects on mitochondrial biogenesis (Bouitbir et al., 2012) and also the restoration of mitochondrial enzyme complex activities in rat and mice brains (Kumar et al., 2012a,b). In addition, a previous study showed that either atorvastatin, insulin or combination of the 2 drugs led to reduced cardiac mitochondrial swelling in T2DM rats with cardiac ischemia/reperfusion injury (Matafome et al., 2008).

Despite these reports on the benefits of atorvastatin and insulin therapies in cases of diabetes, the effects of either atorvastatin or insulin therapy, as well as the combination of atorvastatin and insulin therapy on brain pathology, including brain mitochondrial function, brain apoptosis, brain oxidative stress, tau protein, amyloid beta and dendritic spine density, in the T1DM model have never been investigated. Our hypothesis was that the administration of either atorvastatin or insulin attenuates brain pathology in streptozotocin-induced diabetic rats, and that the combination of these 2 drugs provides the greatest benefits on brain protection in these diabetic rats.

#### 2. Materials and methods

#### 2.1. Animal models and experimental protocols

All experiments were conducted in accordance with the approved protocol from the Faculty of Medicine, Chiang Mai University Institutional Animal Care and Use Committee and were in compliance with NIH guidelines. Thirty-six male Wistar rats weighing 200-220 g (aged ~ 6 weeks old) were obtained from the National Animal Center, Salaya Campus, Mahidol University, Thailand. All animals were individually housed in a temperature-controlled environment with a 12:12 light-dark cycle. Rats were given ad libitum access to food and water. Body weight and food intake were recorded weekly. Rats were divided into a control group (n = 12) and a diabetic or experimental group (n = 24). In the control group, rats were injected intraperitoneally with citrate buffer (10 mM). Then, these control rats were divided into two subgroups (n = 6/subgroup) to receive either a vehicle (normal saline: C) or low-dose atorvastatin (10 mg/kg/day; p.o.; CS) for 4 weeks. In the diabetic group, rats were injected intraperitoneally with streptozotocin to induce diabetes (a single dose of STZ, 50 mg/kg). Diabetes was indicated by hyperglycemia (fasting plasma glucose level > 250 mg/dl) (Semaming et al., 2015). After the development of the diabetic condition, rats were divided into four

subgroups (n = 6/subgroup) to receive either vehicle (normal saline: DM), low-dose atorvastatin (10 mg/kg/day; p.o.: DMS), low-dose insulin (4 U/day; s.c.: DMI) or combined low-dose atorvastatin and lowdose insulin (10 mg/kg/day; p.o., 4 U/day; s.c., respectively; DMIS) for 4 weeks. The reason for using low-dose insulin therapy and low-dose atorvastatin therapy in the study was to prevent hypoglycemia, which is a serious side effect of drug treatment for diabetic patients. At the end of the experimental protocol, animal were fasted for 5 h. After that, the animals were put into deep anesthesia using 2-3% isoflurane. Blood was collected to determine metabolic parameters (insulin, glucose, total cholesterol levels). Then, their brains were rapidly removed and separated to right and left hemispheres. The right hemisphere was used to determine the dendritic spine density using Golgi staining. The left hemisphere was separated to upper and lower parts. The upper part was used to determine brain mitochondrial function by measuring ROS production, membrane potential changes and mitochondrial swelling. The lower part was used to determine levels of brain oxidative stress by measuring MDA levels, brain apoptosis by measuring Bax and Bcl2 protein expressions, Alzheimer's disease markers by measuring Aβ42 level, tau protein expression and phosphorylation tau protein expressions. The experimental protocol is shown in Fig. 1.

### 2.2. Biochemical analysis for assessment of insulin, glucose and cholesterol levels

Fasting plasma glucose and cholesterol concentrations were determined by colorimetric assay using commercially available kits (ERBA diagnostic, Mannheim, Germany). The fasting plasma insulin levels were measured using Sandwich ELISA kits (LINCO Research, Missouri, USA).

#### 2.3. Determination of malondialdehyde (MDA) levels

Malondialdehyde (MDA) level, an indicator of oxidative stress, was determined using a high performance liquid chromatography (HPLC) method (Candan and Tuzmen, 2008). Briefly, brain homogenates were mixed with 10% trichloroacetic acid (TCA) containing butylated hydroxytoluene (BHT), incubated at 90 °C for 30 min, and centrifuged at 6000 rpm for 10 min. The supernatant was mixed with  $\rm H_3PO_4$  and thiobarbituric acid solution (TBA) and incubated at 90 °C for 30 min. MDA levels were measured via absorbance detection at 532 nm by the HPLC system, and were determined directly from the standard curve, and reported as an MDA equivalent concentration (Pratchayasakul et al., 2017).

#### 2.4. The isolation of brain mitochondria

Brain mitochondria were isolated as described in our previous study (Kudin et al., 2004; Pipatpiboon et al., 2012; Pratchayasakul et al., 2015; Pintana et al., 2016). Briefly after decapitation, the brain was removed into 5 ml of ice-cold MSE solution and then the brain was transferred into 10 ml of ice-cold MSE-nagarse solution (0.05% nagarse in MSE solution) and homogenized at 600 rpm/min in an homogenizer. After that the brain homogenate was centrifuged at 2000 g for 4 min and the supernatant was collected and centrifuged at 12,000g for 9 min. Then, the mitochondrial pellets were collected and resuspended in 10 ml of ice-cold MSE-digitonin solution (0.02% digitonin in MSE solution) and further centrifuged at 12,000g for 11 min. Finally, the mitochondrial pellets were resuspended in a respiration buffer (150 mM KCl, 5 mM HEPES, 5 mM K<sub>2</sub>HPO<sub>4</sub>.3H<sub>2</sub>O, 2 mML-glutamate, 5 mM pyruvate sodium salt). Mitochondrial protein concentrations were measured by the bicinchoninic acid assay (BCA) (Thummasorn et al., 2011).

#### 2.5. Brain mitochondrial reactive oxygen species (ROS) assay

ROS in isolated brain mitochondria was measured using a fluorescent probe and dichlorohydrofluoresceindiacetate (DCFHDA). Protein of brain mitochondria (0.4 mg/ml) was incubated with 2  $\mu M$  DCFDA, at 25 °C for 20 min. ROS was evaluated using a fluorescent microplate reader at a wavelength of 485 nm (bandwidth 5 nm) and emission wavelength of 530 nm (bandwidth). The fluorescence was determined using a fluorescent microplate reader (Bio-Tek Instruments, Inc. Winooski, Vermont USA). The increase in fluorescent intensity indicates increased neuronal ROS (Thummasorn et al., 2011).

#### 2.6. The mitochondrial membrane potential ( $\Delta \Psi m$ ) assay

The brain mitochondrial membrane potential ( $\Delta\Psi m$ ) change was measured with fluorescent dye 5, 5′,6,6′-tetrachloro-1, 1′,3,3′-tetraethyl benzimidazolcarbocyanine iodide (JC-1). The JC-1 monomer form (green) fluorescent, excited the wavelength 485-nm and the emission wavelength was detected at 530 nm, and the JC-1 aggregate form (red) fluorescent was excited at a wavelength of 485-nm, and detected at the emission wavelength of 590 nm. The brain mitochondrial protein (0.4 mg/ml) was stained with JC-1 dye at 37 °C for 15 min. The mitochondrial membrane potential was determined as fluorescence intensity using a fluorescent microplate reader. The change in mitochondrial membrane potential was calculated as the ratio of red to green fluorescence intensity (Thummasorn et al., 2011; Pipatpiboon et al., 2012).

#### 2.7. Brain mitochondrial swelling assay

Brain mitochondrial swelling was determined by measuring the change in the absorbance of the brain mitochondrial suspension. The brain mitochondrial protein (0.4 mg/ml) was incubated in 2-ml of a respiration buffer. The suspension was read at 540 nm using a microplate reader. The mitochondrial swelling was indicated by a decrease in the absorbance (Thummasorn et al., 2011; Pipatpiboon et al., 2012).

### 2.8. Immunoblotting

The immunoblot analysis of subsequent brain homogenates was performed as described in our previous study (Pratchayasakul et al., 2011). The brains in each subgroup were homogenized. The cytosol fractions were separated and used for further biochemical analysis of Bax, Bcl2, p-Tau and Tau protein expression. Electrophoresis and immunoblot analysis were carried out on the cytosol fractions with rabbit antibodies for Bax, Bcl2, p-Tau and Tau (1:1000, Cell Signaling Technology, MA, USA). The membranes were then incubated with horseradish peroxidase conjugated anti-rabbit secondary antibody (1:2000;

Cell Signaling Technology, MA, USA) to measure Bax, Bcl2, p-Tau and Tau protein expression. Enhanced chemiluminescence (ECL) detection reagents were used to visualize peroxidase reaction products (Clarity ECL Western blotting substrate, Bio-Rad, CA, USA). The membranes were developed in the ChemiDoc touch imaging system (Bio-Rad Laboratories, CA, USA). Densitometric analysis was done using the image J program.

#### 2.9. Determination of amyloid beta (Aβ42) levels

The brain  $A\beta 42$  levels were measured using Sandwich ELISA kits (Thermo Fisher Scientific, MD, USA).

#### 2.10. Golgi impregnation and analysis

After decapitation, the brains were removed and rinsed with double distilled water and were then processed for Golgi staining using a commercially available kit (FD Neurotechnologies kit, PK 401, Ellicott City, U.S.A.). The details of dendritic spine density analysis have been described previously (Sripetchwandee et al., 2014). Two segments from a pyramidal cell in the CA1 area of the hippocampus were randomly measured. Both segments were located on the tertiary apical dendrites and were viewed through an inverted microscope (IX-81, Olympus, Tokyo, Japan). Three neuronal cells from each brain slice were selected for quantitative analysis (3 slices/animals, n=6 animals/group). The number of spines was counted using a hand counter, and the dendritic length was measured using Xcellence imaging software (Olympus, Tokyo, Japan).

#### 2.11. Statistical analysis

Data were presented as mean  $\pm$  SEM. All statistical analyses were performed using the program SPSS (version 16; SPSS, Chicago, Ill., USA). For all comparisons, the three-way ANOVAs and post-hoc analysis with Fisher's tests were used to test for significant differences. p < 0.05 was considered as a level of statistical significance.

#### 3. Results

### 3.1. The effects of atorvastatin, insulin and combined drugs on metabolic parameters in diabetic rats

Streptozotocin-induced diabetic rats displayed characteristic of diabetes as indicated by decreased body weight, increased fasting plasma glucose levels, and decreased fasting plasma insulin levels, when compared with the control rats (p < 0.05; Table 1). In addition, diabetic (DM) rats showed dyslipidemia as indicated by significantly increased fasting plasma cholesterol level, when compared with control rats (p < 0.05; Table 1). Although diabetic rats treated with either atorvastatin (DMS) or insulin (DMI) had decreased severity of metabolic disorders as indicated by increased body weight and decreased fasting plasma glucose level, when compared with DM rats (Table 1), the combined drugs (DMIS) therapy had greater efficacy on reducing these metabolic disorders in the rats than did the monotherapy (Table 1). Moreover, only these DMIS rats had increased fasting plasma insulin levels and decreased fasting plasma cholesterol, when compared with DM, DMI and DMS rats (p < 0.05, Table 1). These findings suggested that a combination of these drugs exerted a greatest efficacy on reducing metabolic disorder in these diabetic rats.

### 3.2. The effects of atorvastatin, insulin and combined drugs on brain oxidative stress production and brain mitochondria function in diabetic rats

DM rats had increased brain oxidative stress levels as indicated by increased brain MDA levels, when compared with control rats (p < 0.05, Fig. 2A). DM rats also showed evidence of brain

Table 1

Effects of low-dose atorvastatin, low-dose insulin and combined drugs on metabolic parameters.

| Parameters          | С              | CS             | DM              | DMI                           | DMS                           | DMIS                  |
|---------------------|----------------|----------------|-----------------|-------------------------------|-------------------------------|-----------------------|
| Body weight (g)     | 430 ± 5.47     | 407 ± 12.20    | 196 ± 9.41°     | 297 ± 11.13°, <sup>†</sup>    | 248 ± 18.061°, <sup>†</sup>   | 344 ± 13.73°,1,*,#    |
| Glucose (mg/dl)     | 147.10 ± 14.18 | 148.41 ± 11.13 | 503.98 ± 10.95° | 409.23 ± 26.78°, <sup>†</sup> | 401.52 ± 28.98°, <sup>†</sup> | 229.55 ± 25.50°,1,*,# |
| Insulin (U/ml)      | 2.11 ± 0.30    | 2.56 ± 0.36    | 0.34 ± 0.04°    | 0.59 ± 0.09°                  | 0.46 ± 0.10°                  | 1.09 ± 0.17°,1,*,#    |
| Cholesterol (mg/dl) | 56.43 ± 6.55   | 57.97 ± 1.72   | 105.23 ± 6.74°  | 102.12 ± 3.09°                | 97.96 ± 4.78°                 | 76.37 ± 3.36°,1,*,#   |

n = 6/group; C = control rats; DM = diabetic rats; DMI = insulin-treated diabetic rats; DMS = atorvastatin -treated diabetic rats; DMIS = combined drug-treated diabetic rats.

mitochondrial dysfunction, as indicated by increased brain mitochondrial ROS production, increased brain mitochondrial membrane potential change (depolarization) and increased brain mitochondrial swelling, when compared with the control rats (p < 0.05, Fig. 2B-D). DMI, DMS and DMIS rats showed significantly decreased brain oxidative stress level and decreased brain mitochondrial dysfunction as indicated by decreased brain mitochondrial ROS production, brain mitochondrial membrane potential change (depolarization) and brain mitochondrial swelling, when compared with DM rats (p < 0.05, Fig. 2A-D). Interestingly, the level of brain oxidative stress and brain mitochondrial dysfunction in DMI, DMS and DMIS were not significantly different to the control rats. These findings suggested that either atorvastatin, insulin or the combined drug therapy led to an equal restoration of brain oxidative stress and brain mitochondrial dysfunction in diabetic rats.

### 3.3. The effect of atorvastatin, insulin and combined drugs on brain apoptosis in diabetic rats

To investigate brain apoptosis, pro-apoptotic markers (Bax) and anti-apoptotic markers (Bcl2) were determined. DM rats had increased Bax protein expression, when compared with the control rats (p < 0.05, Fig. 3A). DMI, DMS and DMIS rats had significantly decreased Bax protein expression, when compared with DM rats (p < 0.05, Fig. 3A). The level of Bax protein expression in DMI, DMS and DMIS were not significantly different to the control rats. These

findings suggested that either atorvastatin, insulin or the combined drugs led to an equally restored level of brain apoptosis in diabetic rats. Unlike Bax expression, the Bcl2 protein expression between the control and the DM groups was not significantly different, and all treatments did not alter the Bcl2 protein expression (Fig. 3B).

### 3.4. The effects of atorvastatin, insulin and combined drugs on markers of Alzheimer's disease in diabetic rats

To investigate markers of Alzheimer's disease, amyloid- $\beta$  (A $\beta$ 42; a marker of amyloid plaques), tau protein expression and the phosphorylation of tau (p-tau) protein expression (a marker of neurofibrillary tangles) were determined. DM rats had increased tau protein expression, p-tau protein expression and A $\beta$ 42 level in the brain, when compared with the control rats (p < 0.05, Fig. 4A-C). DMI, DMS and DMIS rats had decreased tau protein expression, p-tau protein expression and A $\beta$ 42 level in the brain, when compared with the DM rats (p < 0.05, Fig. 4A-C). Interestingly, the level of tau protein expression, p-tau protein expression and A $\beta$ 42 expression in DMI, DMS and DMIS were not significantly different from the control rats. These findings suggested that either atorvastatin, insulin or the combined drugs led to an equally reduced risk of Alzheimer's disease as indicated by decreased amyloid plaques and neurofibrillary tangles.

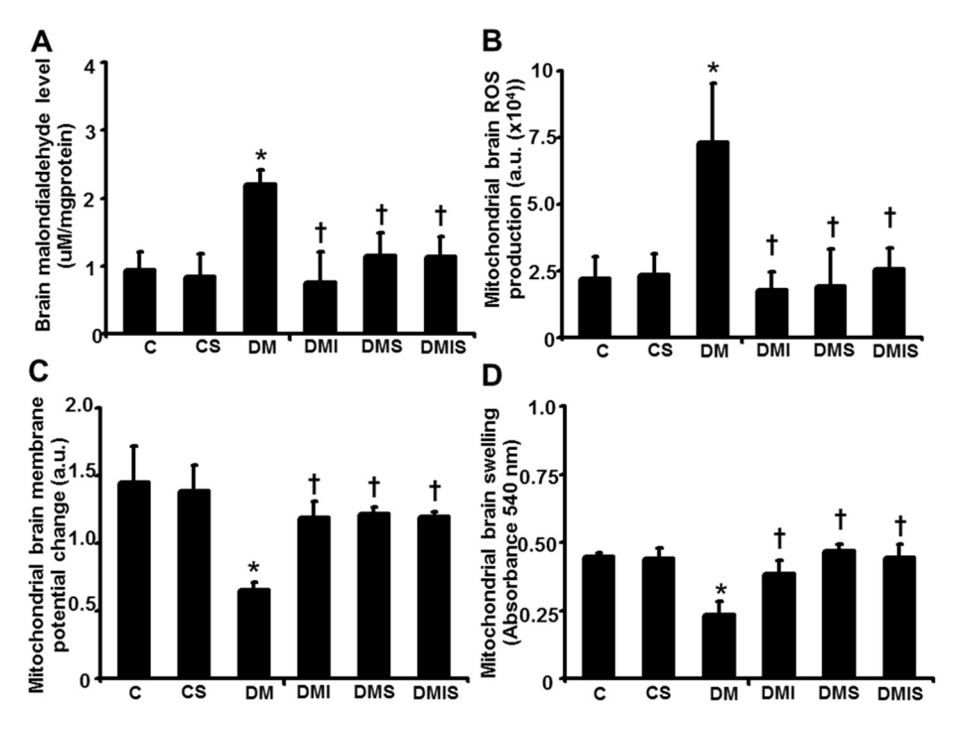


Fig. 2. The effect of low-dose atorvastatin, low-dose insulin and combined drug therapy on brain oxidative stress and brain mitochondrial function in diabetic rats. (A), brain MDA levels (B), brain mitochondrial ROS production (C), brain mitochondrial membrane potential change (D), brain mitochondrial swelling; \*, p < 0.05 compared with control rats; †, p < 0.05 compared with diabetic rats; n = 6/group; C = control rats; DM = diabetic rats; DMI = insulinterated diabetic rats; DMIS = atorvastatin -treated diabetic rats; DMIS = combined drug-treated diabetic rats.

 $<sup>^{*}</sup>$  p < 0.05 compared with C group.

 $<sup>^{\</sup>dagger}$  p < 0.05 compared with DM group.

<sup>\*</sup> p < 0.05 compared with DMI group.

<sup>#</sup> p < 0.05 compared with DMS group.

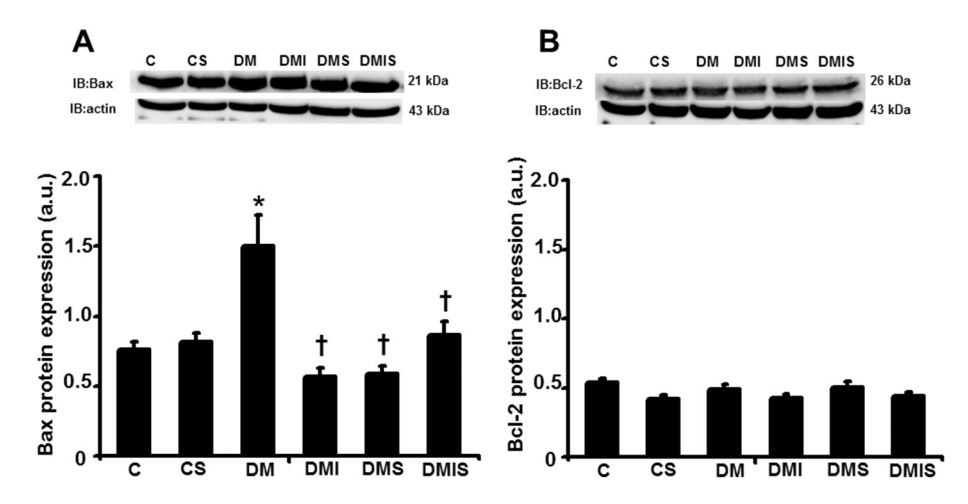


**Fig. 3.** The effect of low-dose atorvastatin, low-dose insulin and combined drug therapy on brain apoptosis in diabetic rats. (A), Bax protein expression (B), Bcl2 protein expression;  $^*$ , p < 0.05 compared with control rats;  $^*$ , p < 0.05 compared with diabetic rats; p = 6/g roup; p = 0.05 compared with diabetic rats; p = 0.05 compared diabetic rats; p = 0.05 control rats; p = 0.05 compared with diabetic rats; p = 0.05 compared diabetic rats.

3.5. The effects of atorvastatin, insulin and combined drugs on dendritic spine density in diabetic rats

To investigate hippocampal synaptic alterations, dendritic spine density was determined. DM rats had a decreased density of dendritic spines in the CA1 area of the hippocampus, when compared with the control rats (p < 0.05, Fig. 5A, B). DMI, DMS and DMIS rats had an increased density of dendritic spines in the CA1 area of the hippocampus, when compared with the DM rats (p < 0.05, Fig. 5A, B). These findings suggested that either atorvastatin, insulin or the combined drugs led to an equal level of prevention of the loss of synaptic spine density in the diabetic condition.

#### 4. Discussion

The major findings of this study are as follows: 1) diabetic rats developed hyperglycemia, increased brain oxidative stress, impaired brain mitochondrial function, increased brain apoptosis, increased amyloid beta and tau protein expression, p-tau protein expression and decreased dendritic spine density; 2) atorvastatin and insulin therapy reduced plasma glucose level in diabetic rats to an equal extent; 3) a

combination of atorvastatin and insulin showed the greatest efficacy in decreasing hyperglycemia and dyslipidemia, when compared to the 2 drugs as a monotherapy; 4) atorvastatin, insulin and the 2 drugs combined equally restored brain oxidative stress, brain mitochondrial dysfunction, brain apoptosis, amyloid beta and tau protein expression, ptau protein expression and prevented dendritic spine loss.

Insulin is an effective drug in the treatment of T1DM. The underlying mechanism of insulin therapy in diabetic condition occurs via the stimulation of glucose and lipid uptake in several organs (Samuel and Shulman, 2016; American Diabetes, 2017). Although the main characteristic of T1DM is hyperglycemia, patients with T1DM also present with dyslipidemia, as indicated by increased plasma triglycerides, plasma cholesterol and plasma low-density lipoprotein (LDL) cholesterol level (Verges, 2009). Atorvastatin is a major lipid-lowering agent. It not only reduces cholesterol biosynthesis (Stancu and Sima, 2001), but also exerts glycemic control (Suzuki et al., 2005; Tanaka, 2011). In this study, in addition to these described effects we also demonstrated that either low-dose insulin alone or atorvastatin alone at a low dosage decreased hyperglycemia without the alteration of plasma insulin level or cholesterol level in these diabetic rats. The possible explanation of these findings could be that the dosages of atorvastatin alone or insulin

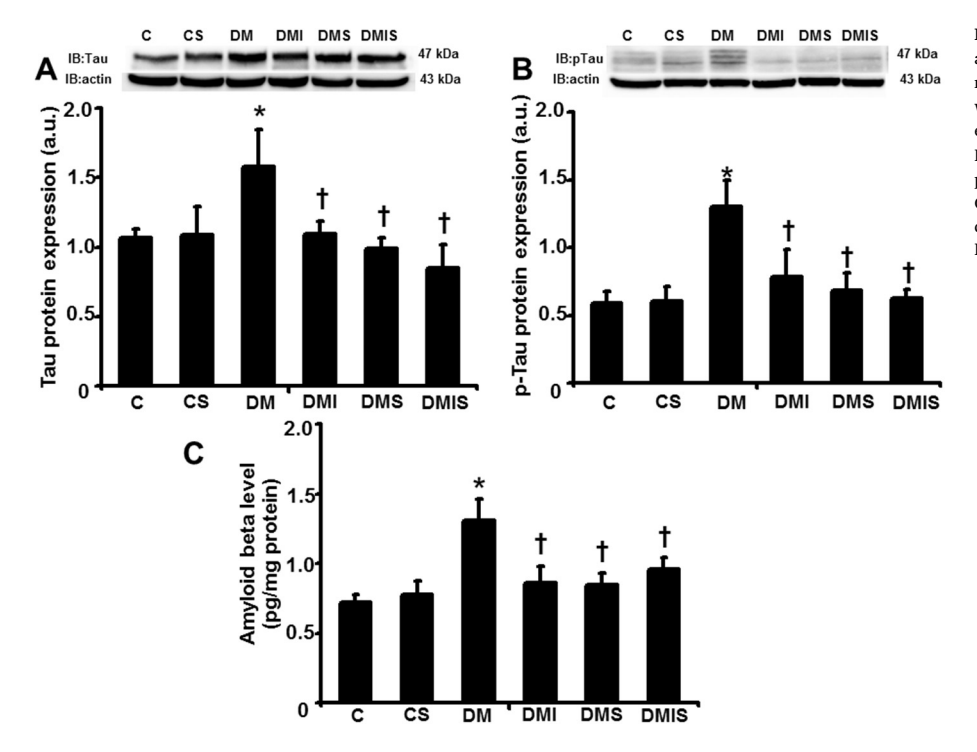


Fig. 4. The effect of low-dose atorvastatin, low-dose insulin and combined drug therapy on brain Alzheimer's disease markers in diabetic rats. (A), tau protein expression by western blot analysis (B), phosphorylation of tau protein expression by western blot analysis (C), A $\beta$ 42 level by ELISA analysis; \*, p < 0.05 compared with control rats; †, p < 0.05 compared with control rats; †, C = control rats; DM = diabetic rats; DMI = insulin-treated diabetic rats; DMS = atorvastatin -treated diabetic rats; DMIS = combined drug-treated diabetic rats.

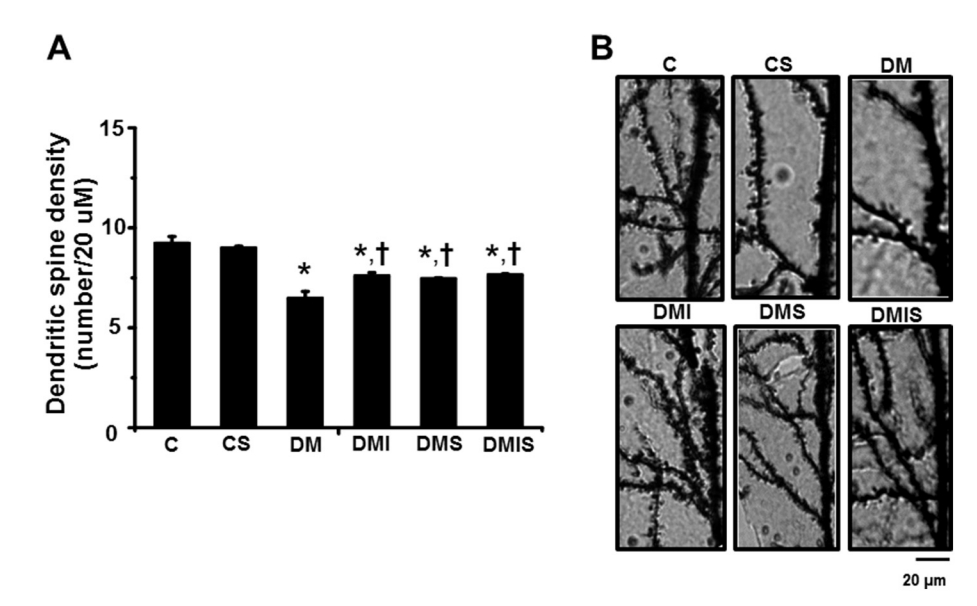


Fig. 5. The effect of low-dose atorvastatin, low-dose insulin and combined drug therapy on dendritic spine density in diabetic rats. (A), the number of dendritic spines on tertiary apical dendrites (B), representative picture of dendritic spine density. \*, p < 0.05 compared with control rats;  $\dot{\eta}$ , p < 0.05 compared with diabetic rats; n = 6/group; C = control rats; DM = diabetic rats; DMI = insulin-treated diabetic rats; DMS = atorvastatin -treated diabetic rats; DMIS = combined drug-treated diabetic rats.

therapy in the study were not a dose which is effective in attenuating hypoinsulinemia and dyslipidemia in the T1DM condition. Interestingly, we found that the combination of the 2 drugs exerted greater efficacy on reducing hyperglycemia and dyslipidemia than did the monotherapies individually. Therefore, these findings suggested that low-dose insulin and atorvastatin have synergistic effects on the glycemic control in diabetic rats. In addition, the circulating insulin level was elevated by combined administration of insulin and atorvastatin, when compared to either single therapy. These findings suggested that the increased lowering effect on glucose level in the combined treatment group might possibly result from an elevation of the insulin level.

Oxidative stress is a driving force for tau hyperphosphorylation, amyloid beta aggregation and synaptic dysfunction. All of these brain pathologies following oxidative stress can lead to cognitive impairment and the development of Alzheimer's disease (Kamat et al., 2016; Tonnies and Trushina, 2017). The findings of this study suggested that diabetic rats had increased brain oxidative stress levels with impaired brain mitochondrial function, increased brain apoptosis as indicated by increased Bax protein expression, increased tau protein expression, increased p-tau protein expression, increased A $\beta$ 42 level, and decreased dendritic spine density in the hippocampal region. To the best of our knowledge, the present study is the first study to demonstrate that atorvastatin, insulin and a combination of these drugs equally decreased brain oxidative stress, brain mitochondrial dysfunction, brain apoptosis, amyloid beta, p-tau protein expression and tau protein expression, and prevented dendritic spine loss in the T1DM model.

It has been known that both atorvastatin and insulin are transported across the blood brain barrier via simple diffusion and transporter proteins, respectively (Shepardson et al., 2011; Banks et al., 2012), indicating that it is feasible that these drugs could have a direct effect on the brain function. In addition, several previous studies found that either atorvastatin and insulin could decrease amyloid production, apoptosis, dendritic spine loss in various models of Alzheimer's disease (Kandiah and Feldman, 2009; Shepardson et al., 2011; Zhang et al., 2014; Bedse et al., 2015). Further support for this can be found in other studies which demonstrated that atorvastatin and insulin had an antioxidant effect on the brain (Duarte et al., 2012; Blazquez et al., 2014; Tu et al., 2014; Martins et al., 2015). In the present study, it has been shown that it is possible that atorvastatin, insulin, and a combination of the drugs can be transported across the blood brain barrier and hence directly affect the brain, the affects being shown by decreased brain mitochondrial dysfunction and brain oxidative stress via their antioxidant effects, thus leading to a reduction of brain apoptosis, tau hyperphosphorylation, amyloid beta aggregation, and prevention of dendritic spine loss. Although all therapies in DM rats effectively reduced brain oxidative stress, brain mitochondrial dysfunction, brain apoptosis, tau hyperphosphorylation and amyloid beta aggregation to the same levels with that of the control rats, none of these therapies could restore the dendritic spine density to the same level as that of the control rats. A possible explanation could be due to the short duration of the administration of these drugs since these drugs might initially have an effect on the oxidative stress, apoptosis and amyloid beta pathway, and the restoration of the dendritic spine density may occur later. As a result, long-term administration of either atorvastatin, insulin or a combination of the drugs may restore dendritic spine density to be the same level as the control. Further studies are needed to give greater evidence to support this possible explanation.

Furthermore, we found that the combinative treatment of atorvastatin and insulin had greater efficacy on reducing the level of plasma glucose and dyslipidemia than the treatments of atorvastatin or insulin alone. However, the combined treatment had similar efficacy as the individual treatments in reducing brain mitochondrial dysfunction, brain apoptosis, tau protein expression, p-tau protein expression and amyloid beta. These findings suggested that hyperglycemia and dyslipidemia might not be mainly responsible for the brain damaged caused by streptozotocin-induced diabetic rats in our study. Moreover, in highfat diet (HFD)-induced cognitive impairment rats, our previous studies demonstrated that alterations in the metabolic parameters could be observed earlier (i.e. 8 weeks after HFD feeding), whereas the changes in the brain function occurred at a later time (i.e. 12 weeks after HFD feeding) (Pratchayasakul et al., 2011; Pratchayasakul et al., 2015; Pintana et al., 2016). Therefore, it is possible that the duration of treatment in the combined group (4 weeks) was long enough to improve metabolic parameters, but not sufficient to demonstrate the synergistic effects in reducing brain mitochondrial dysfunction, brain apoptosis, tau protein expression, and amyloid beta accumulation in these diabetic rats. Longer duration of treatment could have shown the synergistic effect in improving the brain function. Then, future studies are needed to test this hypothesis.

### 5. Conclusion

In summary, our findings demonstrate that low-dose atorvastatin and low-dose insulin had equal effects on the reduction of hyperglycemia in diabetic rats. However, a combination of low-dose atorvastatin and low-dose insulin showed the greatest efficacy on improving metabolic parameters including hyperglycemia and dyslipidemia. Interestingly, low-dose atorvastatin, low-dose insulin and the combined

drugs shared similar efficacy in the prevention of brain damage via decreased brain mitochondrial dysfunction, brain apoptosis, tau protein expression, p-tau protein expression, amyloid beta level, and dendritic spine loss in these streptozotocin-induced diabetic rats.

#### Limitation of the study

Although brain apoptosis markers were determined by western blot analysis in this study, TUNEL staining is still necessary for determining cell apoptosis. Future studies are needed to investigate the effect of atorvastatin and insulin on TUNEL staining in diabetic rats.

#### **Funding**

This work was supported by the Thailand Research FundRTA6080003 (SC); RSA5780029 (AL) and MRG5980198 (WP); a NSTDA Research Chair Grant from the National Science and Technology Development Agency Thailand (NC), and a Chiang Mai University Center of Excellence Award (NC).

#### Conflict of interest statement

The authors declare that there is no conflict of interest and have read and understood the Conflict of Interest Policy from for the journal.

#### References

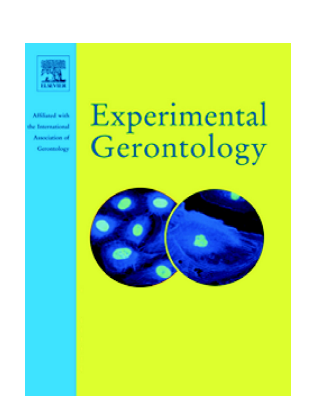
- American Diabetes, A, 2017. Standards of medical care in diabetes-2017 abridged for primary care providers. Clin. Diabetes 35, 5–26.
- Banks, W.A., Owen, J.B., Erickson, M.A., 2012. Insulin in the brain: there and back again. Pharmacol. Ther. 136, 82–93.
- Bedse, G., Di Domenico, F., Serviddio, G., Cassano, T., 2015. Aberrant insulin signaling in Alzheimer's disease: current knowledge. Front. Neurosci. 9, 204.
- Blazquez, E., Velazquez, E., Hurtado-Carneiro, V., Ruiz-Albusac, J.M., 2014. Insulin in the brain: its pathophysiological implications for States related with central insulin resistance, type 2 diabetes and Alzheimer's disease. Front. Endocrinol. 5, 161.
- Bouitbir, J., Charles, A.L., Echaniz-Laguna, A., Kindo, M., Daussin, F., Auwerx, J., Piquard, F., Geny, B., Zoll, J., 2012. Opposite effects of statins on mitochondria of cardiac and skeletal muscles: a 'mitohormesis' mechanism involving reactive oxygen species and PGC-1. Eur. Heart J. 33, 1397–1407.
- Candan, N., Tuzmen, N., 2008. Very rapid quantification of malondialdehyde (MDA) in rat brain exposed to lead, aluminium and phenolic antioxidants by high-performance liquid chromatography-fluorescence detection. Neurotoxicology 29, 708–713.
- Dhamoon, M.S., Noble, J.M., Craft, S., 2009. Intranasal insulin improves cognition and modulates beta-amyloid in early AD. Neurology 72, 292–293.
- Duarte, A.I., Moreira, P.I., Oliveira, C.R., 2012. Insulin in central nervous system: more than just a peripheral hormone. J. Aging Res. 2012, 384017.
- Ho, N., Sommers, M.S., Lucki, I., 2013. Effects of diabetes on hippocampal neurogenesis: links to cognition and depression. Neurosci. Biobehav. Rev. 37, 1346–1362.
- Kamat, P.K., Kalani, A., Rai, S., Swarnkar, S., Tota, S., Nath, C., Tyagi, N., 2016. Mechanism of oxidative stress and synapse dysfunction in the pathogenesis of Alzheimer's disease: understanding the therapeutics strategies. Mol. Neurobiol. 53, 648–661.
- Kandiah, N., Feldman, H.H., 2009. Therapeutic potential of statins in Alzheimer's disease. J. Neurol. Sci. 283, 230–234.
- Kishi, T., Hirooka, Y., Shimokawa, H., Takeshita, A., Sunagawa, K., 2008. Atorvastatin reduces oxidative stress in the rostral ventrolateral medulla of stroke-prone spontaneously hypertensive rats. Clin. Exp. Hypertens. 30, 3–11.
- Kroner, Z., 2009. The relationship between Alzheimer's disease and diabetes: type 3 diabetes? Altern. Med. Rev. 14, 373–379.
- Kudin, A.P., Bimpong-Buta, N.Y., Vielhaber, S., Elger, C.E., Kunz, W.S., 2004. Characterization of superoxide-producing sites in isolated brain mitochondria. J. Biol. Chem. 279, 4127–4135.
- Kumar, A., Sharma, N., Gupta, A., Kalonia, H., Mishra, J., 2012a. Neuroprotective potential of atorvastatin and simvastatin (HMG-CoA reductase inhibitors) against 6-hydroxydopamine (6-OHDA) induced Parkinson-like symptoms. Brain Res. 1471, 13–22.
- Kumar, A., Vashist, A., Kumar, P., Kalonia, H., Mishra, J., 2012b. Protective effect of HMG CoA reductase inhibitors against running wheel activity induced fatigue, anxiety like behavior, oxidative stress and mitochondrial dysfunction in mice. Pharmacol. Rep. 64, 1326–1336.

- Li, J., Sun, Y.M., Wang, L.F., Li, Z.Q., Pan, W., Cao, H.Y., 2010. Comparison of effects of simvastatin versus atorvastatin on oxidative stress in patients with coronary heart disease. Clin. Cardiol. 33, 222–227.
- Martins, W.C., dos Santos, V.V., dos Santos, A.A., Vandresen-Filho, S., Dal-Cim, T.A., de Oliveira, K.A., Mendes-de-Aguiar, C.B., Farina, M., Prediger, R.D., Viola, G.G., Tasca, C.I., 2015. Atorvastatin prevents cognitive deficits induced by Intracerebroventricular amyloid-beta 1-40 Administration in Mice: involvement of glutamatergic and antioxidant systems. Neurotox. Res. 28, 32–42.
- Matafome, P., Monteiro, P., Nunes, E., Louro, T., Amaral, C., Moedas, A.R., Goncalves, L., Providencia, L., Seica, R., 2008. Therapeutic association of atorvastatin and insulin in cardiac ischemia: study in a model of type 2 diabetes with hyperlipidemia. Pharmacol. Res. 58, 208–214.
- Matafome, P., Nunes, E., Louro, T., Amaral, C., Crisostomo, J., Rodrigues, L., Moedas, A.R., Monteiro, P., Cipriano, A., Seica, R., 2009. A role for atorvastatin and insulin combination in protecting from liver injury in a model of type 2 diabetes with hyperlipidemia. Naunyn Schmiedeberg's Arch. Pharmacol. 379, 241–251.
- Melendez-Ramirez, L.Y., Richards, R.J., Cefalu, W.T., 2010. Complications of type 1 diabetes. Endocrinol. Metab. Clin. N. Am. 39, 625–640.
- Morris, J.K., Burns, J.M., 2012. Insulin: an emerging treatment for Alzheimer's disease dementia? Curr. Neurol. Neurosci. Rep. 12, 520–527.
- Pintana, H., Pratchayasakul, W., Sa-nguanmoo, P., Pongkan, W., Tawinvisan, R., Chattipakorn, N., Chattipakorn, S.C., 2016. Testosterone deprivation has neither additive nor synergistic effects with obesity on the cognitive impairment in orchiectomized and/or obese male rats. Metabolism 65, 54–67.
- Pipatpiboon, N., Pratchayasakul, W., Chattipakorn, N., Chattipakorn, S.C., 2012.
  PPARgamma agonist improves neuronal insulin receptor function in hippocampus and brain mitochondria function in rats with insulin resistance induced by long term high-fat diets. Endocrinology 153, 329–338.
- Pratchayasakul, W., Kerdphoo, S., Petsophonsakul, P., Pongchaidecha, A., Chattipakorn, N., Chattipakorn, S.C., 2011. Effects of high-fat diet on insulin receptor function in rat hippocampus and the level of neuronal corticosterone. Life Sci. 88, 619–627.
- Pratchayasakul, W., Sa-Nguanmoo, P., Sivasinprasasn, S., Pintana, H., Tawinvisan, R., Sripetchwandee, J., Kumfu, S., Chattipakorn, N., Chattipakorn, S.C., 2015. Obesity accelerates cognitive decline by aggravating mitochondrial dysfunction, insulin resistance and synaptic dysfunction under estrogen-deprived conditions. Horm. Behav. 72, 68–77.
- Pratchayasakul, W., Sivasinprasasn, S., Sa-Nguanmoo, P., Proctor, C., Kerdphoo, S., Chattipakorn, N., Chattipakorn, S.C., 2017. Estrogen and DPP-4 inhibitor share similar efficacy in reducing brain pathology caused by cardiac ischemia-reperfusion injury in both lean and obese estrogen-deprived rats. Menopause 24, 850–858.
- Samuel, V.T., Shulman, G.I., 2016. The pathogenesis of insulin resistance: integrating signaling pathways and substrate flux. J. Clin. Invest. 126, 12–22.
- Semaming, Y., Sripetchwandee, J., Sa-Nguanmoo, P., Pintana, H., Pannangpetch, P., Chattipakorn, N., Chattipakorn, S.C., 2015. Protocatechuic acid protects brain mitochondrial function in streptozotocin-induced diabetic rats. Appl. Physiol. Nutr. Metab. 40, 1078–1081.
- Shepardson, N.E., Shankar, G.M., Selkoe, D.J., 2011. Cholesterol level and statin use in Alzheimer disease: II. Review of human trials and recommendations. Arch. Neurol. 68, 1385–1392.
- Sochett, E., Daneman, D., 1999. Early diabetes-related complications in children and adolescents with type 1 diabetes. Implications for screening and intervention. Endocrinol. Metab. Clin. N. Am. 28, 865–882.
- Sripetchwandee, J., Pipatpiboon, N., Pratchayasakul, W., Chattipakorn, N., Chattipakorn, S.C., 2014. DPP-4 inhibitor and PPARgamma agonist restore the loss of CA1 dendritic spines in obese insulin-resistant rats. Arch. Med. Res. 45, 547–552.
- Stancu, C., Sima, A., 2001. Statins: mechanism of action and effects. J. Cell. Mol. Med. 5, 378–387.
- Sugiyama, M., Ohashi, M., Takase, H., Sato, K., Ueda, R., Dohi, Y., 2005. Effects of atorvastatin on inflammation and oxidative stress. Heart Vessel. 20, 133–136.
- Suzuki, M., Kakuta, H., Takahashi, A., Shimano, H., Tada-Iida, K., Yokoo, T., Kihara, R., Yamada, N., 2005. Effects of atorvastatin on glucose metabolism and insulin resistance in KK/Ay mice. J. Atheroscler. Thromb. 12, 77–84.
- Tanaka, M., 2011. Beneficial effect of atorvastatin on renal function in patients with type 2 diabetes. J. Int. Med. Res. 39, 1504–1512.
- Thummasorn, S., Kumfu, S., Chattipakorn, S., Chattipakorn, N., 2011. Granulocyte-colony stimulating factor attenuates mitochondrial dysfunction induced by oxidative stress in cardiac mitochondria. Mitochondrion 11, 457–466.
- Tonnies, E., Trushina, E., 2017. Oxidative stress, synaptic dysfunction, and Alzheimer's disease. J. Alzheimers Dis. 57, 1105–1121.
- Tu, Q., Cao, H., Zhong, W., Ding, B., Tang, X., 2014. Atorvastatin protects against cerebral ischemia/reperfusion injury through anti-inflammatory and antioxidant effects. Neural Regen. Res. 9, 268–275.
- Verges, B., 2009. Lipid disorders in type 1 diabetes. Diabete Metab. 35, 353–360.
  Yang, J., Pan, Y., Li, X., Wang, X., 2015. Atorvastatin attenuates cognitive deficits through Akt1/caspase-3 signaling pathway in ischemic stroke. Brain Res. 1629, 231–239.
- Zhang, L.L., Sui, H.J., Liang, B., Wang, H.M., Qu, W.H., Yu, S.X., Jin, Y., 2014. Atorvastatin prevents amyloid-beta peptide oligomer-induced synaptotoxicity and memory dysfunction in rats through a p38 MAPK-dependent pathway. Acta Pharmacol. Sin. 35, 716–726.

### Accepted Manuscript

Both oophorectomy and obesity impaired solely hippocampaldependent memory via increased hippocampal dysfunction

Duangkamol Mantor, Wasana Pratchayasakul, Wanitchaya Minta, Wissuta Sutham, Siripong Palee, Jirapas Sripetchwandee, Sasiwan Kerdphoo, Thidarat Jaiwongkum, Sirawit Sriwichaiin, Warunsorn Krintratun, Nipon Chattipakorn, Siriporn C. Chattipakorn



PII: S0531-5565(17)30894-X

DOI: doi:10.1016/j.exger.2018.04.010

Reference: EXG 10336

To appear in: Experimental Gerontology

Received date: 16 December 2017
Revised date: 18 March 2018
Accepted date: 16 April 2018

Please cite this article as: Duangkamol Mantor, Wasana Pratchayasakul, Wanitchaya Minta, Wissuta Sutham, Siripong Palee, Jirapas Sripetchwandee, Sasiwan Kerdphoo, Thidarat Jaiwongkum, Sirawit Sriwichaiin, Warunsorn Krintratun, Nipon Chattipakorn, Siriporn C. Chattipakorn, Both oophorectomy and obesity impaired solely hippocampal-dependent memory via increased hippocampal dysfunction. The address for the corresponding author was captured as affiliation for all authors. Please check if appropriate. Exg(2017), doi:10.1016/j.exger.2018.04.010

This is a PDF file of an unedited manuscript that has been accepted for publication. As a service to our customers we are providing this early version of the manuscript. The manuscript will undergo copyediting, typesetting, and review of the resulting proof before it is published in its final form. Please note that during the production process errors may be discovered which could affect the content, and all legal disclaimers that apply to the journal pertain.

Both oophorectomy and obesity impaired solely hippocampal-dependent memory via increased hippocampal dysfunction

Duangkamol Mantor<sup>a,b,c\*</sup>, Wasana Pratchayasakul<sup>a,b,c\*</sup>, Wanitchaya Minta<sup>a,b,c</sup>, Wissuta Sutham<sup>a,b,c</sup>, Siripong Palee<sup>a,c</sup>, Jirapas Sripetchwandee<sup>a,b,c</sup>, Sasiwan Kerdphoo<sup>a,c</sup>, Thidarat Jaiwongkum<sup>a,c</sup>, Sirawit Sriwichaiin<sup>a,c</sup>, Warunsorn Krintratun<sup>a,c</sup>, Nipon Chattipakorn<sup>a,b,c</sup>, Siriporn C Chattipakorn<sup>a,c,d</sup>

<sup>a</sup> Cardiac Electrophysiology Research and Training Center, Faculty of Medicine, Chiang Mai University, Chiang Mai 50200, Thailand

<sup>b</sup> Cardiac Electrophysiology Unit, Department of Physiology, Faculty of Medicine,

Chiang Mai University, Chiang Mai 50200, Thailand

<sup>c</sup> Center of Excellence in Cardiac Electrophysiology Research, Chiang Mai University,

Chiang Mai 50200, Thailand

<sup>d</sup> Department of Oral Biology and Diagnostic Science, Faculty of Dentistry,

Chiang Mai University, Chiang Mai 50200, Thailand

\* Duangkamol Mantor and Wasana Pratchayasakul contributed equally to this work.

Corresponding author: Siriporn C Chattipakorn, DDS, PhD

Department of Oral Biology and Diagnostic Sciences, Faculty of Dentistry, Chiang Mai,

University; Neurophysiology Unit, Cardiac Electrophysiology Research and Training Center,

Faculty of Medicine, Chiang Mai University, Chiang Mai, Thailand 50200; Tel: 011-66-53-

944-451; Fax: 011-66-53-222-844; E-mail address:scchattipakorn@gmail.com;

siriporn.c@cmu.ac.th

1

### **Abstract**

Our previous study demonstrated that obesity aggravated peripheral insulin resistance and brain dysfunction in the ovariectomized condition. Conversely, the effect of obesity followed by oophorectomy on brain oxidative stress, brain apoptosis, synaptic function and cognitive function, particularly in hippocampal-dependent and hippocampal-independent memory, has not been investigated. Our hypothesis was that oophorectomy aggravated metabolic impairment, brain dysfunction and cognitive impairment in obese rats. Thirty-two female rats were fed with either a normal diet (ND, n=16) or a high-fat diet (HFD, n=16) for a total of 20 weeks. At week 13, rats in each group were subdivided into sham and ovariectomized subgroups (n=8/subgroup). At week 20, all rats were tested for hippocampaldependent and hippocampal-independent memory by using Morris water maze test (MWM) and Novel objective recognition (NOR) tests, respectively. We found that the obese-insulin resistant condition occurred in sham-HFD-fed rats (HFS), ovariectomized-ND-fed rats (NDO), and ovariectomized-HFD-fed rats (HFO). Increased hippocampal oxidative stress level, increased hippocampal apoptosis, increased hippocampal synaptic dysfunction, decreased hippocampal estrogen level and impaired hippocampal-dependent memory were observed in HFS, NDO, and HFO rats. However, the hippocampal-independent memory, cortical estrogen levels, cortical ROS production, and cortical apoptosis showed no significant difference between groups. These findings suggested that oophorectomy and obesity exclusively impaired hippocampal-dependent memory, possibly via increased hippocampal dysfunction. Nonetheless, oophorectomy did not aggravate these deleterious effects under conditions of obesity

**Keywords:** Oophorectomy; Obesity; Hippocampal-dependent memory; Hippocampal synaptic function; Hippocampal oxidative stress level

### 1. Introduction

Recent evidence reported that obesity during midlife women (35-65 years old: peri-to postmenopausal conditions) increases the relative risk of dementia (RR, 1.33; 95% confidence interval (CI), 1.08–1.63) (Albanese et al., 2017). In addition, several clinical findings reported an increase in the development of obesity, metabolic syndrome, diabetes, and the neurodegenerative disorders occurred during peri-menopausal women and postmenopausal women (Dalal and Agarwal, 2015; Keller et al., 2010). Not only clinical studies, animal studies also demonstrated that the obese-insulin resistant condition can lead to the development of pathophysiological conditions in several organs, including the brain (Craft and Watson, 2004; Greenwood and Winocur, 2005; Winocur and Greenwood, 2005; Zhao et al., 2011). Previous studies found that obese-insulin resistant condition increased brain oxidative stress and increased brain apoptosis as indicated by increased apoptotic protein (Bax) and decreased anti-apoptotic protein (Bcl2), leading to impair cognitive function (FangFang et al., 2017; Hajiluian et al., 2017; Sah et al., 2017). Similarly, our previous studies reported that consumption of a high-fat diet (HFD) over 12-weeks in both male and female rats led to not only obesity and peripheral insulin resistance, but also brain insulin resistance, brain mitochondrial dysfunction, increased brain oxidative stress increased brain apoptosis, leading to impair learning and memory (Chunchai et al., 2018; Pintana et al., 2015; Sa-Nguanmoo et al., 2017). Furthermore, our previous studies and others also found that obese-insulin resistant condition could impair insulin-induced long term depression (LTD), which is related to cognitive decline in this condition (Mielke et al., 2005; Pintana et al., 2015; Pipatpiboon et al., 2013; Pratchayasakul et al., 2011a). Interestingly, our recent study showed that obesity aggravated the conditions of peripheral insulin resistance, brain insulin resistance, brain mitochondrial dysfunction, brain oxidative stress and hippocampal synaptic dysfunction and also impaired learning and memory in rats under the oophorectomy

(Pratchayasakul et al., 2015). However, the effect of oophorectomy after obesity on metabolic changes and brain functions has not been thoroughly investigated.

Although the process of learning and memory can be divided into explicit memory (a hippocampal-dependent process) and implicit memory (a hippocampal-independent process) (Bailey et al., 1996; Dew and Cabeza, 2011), a recent study demonstrated that explicit memory especially episodic memory did not perform only in the hippocampus, but also in other cortical networks such as the parahippocampal cortex and medial entorhinal cortex (Eichenbaum, 2017). Moreover, a recent study reported that the hippocampus was also involved in the acquisition of knowledge during both immediate learning and the memory consolidation with other brain regions (Mack et al., 2017). In an animal study, hippocampaldependent memory can be assessed using the Morris water maze (MWM) test (Vorhees and Williams, 2006) and hippocampal-independent memory can be assessed using the novel object recognition (NOR) test (Antunes and Biala, 2012). Previous studies demonstrated that both HFD-induced obese-insulin resistance and oophorectomy caused the impairment of hippocampal-dependent memory, as indicated by increased time to reach the platform and decreased time spent in the target quadrant in the MWM test (Pintana et al., 2012; Stranahan et al., 2008). However, the impairment of hippocampal-independent memory remains controversial in the case of obesity (Beilharz et al., 2014; Carey et al., 2014; Tran and Westbrook, 2017; Vogel et al., 2017) or oophorectomy (Gervais et al., 2013; Gervais et al., 2016). In addition, the effect of oophorectomy after HFD-induction of an obese-insulin resistant condition on hippocampal-dependent and hippocampal-independent memory and the underlying mechanisms associated with these have not been investigated. Therefore, the hypothesis for this study is that oophorectomy exaggerates metabolic impairment, hippocampal oxidative stress levels, hippocampal synaptic dysfunction and impairment of

learning and memory (both hippocampal-dependent and hippocampal-independent) in HFD-induced obese-insulin resistant female rats.

### 2. Materials and Methods

### 2.1 Ethical approval

This study was approved by the Institutional Animal Care and Use Committee of the Faculty of Medicine, Chiang Mai University (approval no. 5/2559 on May 5, 2016).

### 2.2 Animal models and experimental protocols

Thirty-two female Wistar rats weighing about 200-220 g (about 6 weeks old) were obtained from the National Animal Center, Salaya Campus, Mahidol University, Thailand. All animals were housed (n=2/cage) in a temperature-controlled room and maintained at a light-dark cycle of 12:12 h (lights on at 6 a.m.). One week after arrival, female rats were randomly assigned to either be fed on a normal diet (ND, n=16) or a high-fat diet (HFD, n=16) for a total of 20 weeks. The normal diet was a standard laboratory chow (Mouse Feed Food No. 082, C.P. Company, Bangkok, Thailand), which had an energy content of 4.02 kcal/g, 19.77% of total energy (%E) of the food being from fat. The high-fat diet had an energy content of 5.35 kcal/g (59.28 %E). The source of carbohydrate, fat and protein content in our dietary regiment was from starch, lard and casein, respectively. All animals were given ad libitum access to food and water. The daily amount of food intake and weekly body weight were monitored. In this study, sham animals were housed together as a pair/cage, and oophorectomized animals were housed together as a pair/cage. The daily intake levels were determined in each cage and the averaged value was determined to get the daily intake per animal in that cage. To avoid the repeated number as a pair for each cage, we therefore used only "one n" for each cage for the data comparison for calorie intake. After 13 weeks of either ND or HFD consumption, rats in each diet group were divided into two subgroups: sham-operated (S) and bilateral ovariectomized (O) subgroups. All animals

were finally divided into four subgroups, including sham-ND-fed rats (NDS), ovariectomized-ND-fed rats (NDO), sham-HFD-fed rats (HFS) and ovariectomized-HFD-fed rats (HFO). All animals were continuously fed on either a ND or HFD for 7 weeks.

At week 14 and 20 all animals were tested with several behavioral tests, including the locomotive activity with the open-field test (OFT), the hippocampal-independent learning and memory with the novel object recognition test (NOR), and the hippocampal-dependent learning and memory with the Morris water maze test (MWM). Blood samples were collected from each animal at week 13 and 21 to determine the metabolic parameters. At the end of the experiment protocol (21 weeks), animals were decapitated and the brains removed to enable the hippocampal synaptic plasticity to be investigated by electrical induced long-term potentiation (LTP), brain insulin receptor function (insulin-induced long term depression, LTD), hippocampal and cortical oxidative stress levels, hippocampal and cortical apoptotic levels and hippocampal and cortical estrogen levels.

### 2.3 Ovariectomized procedure

Oophorectomy was performed following our previous study guidelines (Pratchayasakul et al., 2015). Briefly, female rats were anesthetized with 2-3% isoflurane and oxygen support. The ovariectomized groups received bilateral flank incisions, the ovaries were removed and the incisions were closed.

### 2.4 Determination of metabolic parameters and estradiol levels

Fasting plasma glucose, high-density lipoproteins (HDL), low-density lipoproteins (LDL), cholesterol and triglyceride levels were determined using commercially available kits (ERBA diagnostic, Mannheim, Germany). The fasting plasma insulin levels were investigated using the enzyme-linked immunosorbent assay (ELISA) kits (LINCO Research, Missouri, USA). Serum estradiol levels were determined using an enzyme immunoassay (EIA) kit (Cayman chemical, Ann Arbor, Michigan, USA). In addition, the animals were

decapitated and the non-perfused brains were removed to determine hippocampal and cortical estradiol levels by using an EIA kit (Cayman chemical, Ann Arbor, Michigan, USA). All chemical analyses used to identify metabolic parameters were performed in duplicate in the same assay. The coefficient of variation for the intra- and inter-assays were 5.55% and 5.99% for glucose; 4.52% and 8.09% for HDL; 2.32% and 8.93% for cholesterol; 2.14% and 7.57% for triglycerides; 5.76% and 9.04% for insulin, and 4.57% and 8.35% for estradiol, respectively.

### 2.5 Determination of peripheral insulin resistance

Insulin resistance was evaluated by the Homeostasis Model Assessment (HOMA) index (Matthews et al., 1985) and the total area under the curve of the oral glucose tolerance test (OGTT) as described in our previous study (Pratchayasakul et al., 2011b).

### 2.6 Determination of serum malondialdehyde (MDA) levels

The MDA level was determined using a high performance liquid chromatography method following a previous study protocol (Candan and Tuzmen, 2008).

## 2.7 Extracellular recordings of hippocampal slices for insulin-induced long term depression (LTD) and electrical-induced long term potentiation (LTP)

The brain slices for extracellular recordings of insulin-induced LTD and electrical-induced LTP were prepared following the protocol described in our previous study (Chattipakorn and McMahon, 2002; Pratchayasakul et al., 2015). In the LTD protocol, hippocampal slices were perfused with artificial cerebrospinal fluid (aCSF) for ten minutes as a baseline measure. After that, the insulin-induced LTD condition was evaluated by perfusion with aCSF plus 500 nM insulin (Humulin R, Eli Lilly, Giessen, Germany) for an additional ten minutes and then the slices were perfused with aCSF for 50 minutes further. In the LTP protocol, LTP was induced by delivering high-frequency stimulation (HFS: 4 trains

at 100 Hz; 0.5 s duration; 20 s interval). Experiments were performed for at least 50 minutes after HFS.

## 2.8 Protein preparation for the measurement oxidative stress levels in the hippocampus and cortex

The details of protein preparation for hippocampal and cortical oxidative stress have been described in a previous study (Pipatpiboon et al., 2012). Briefly, the hippocampus and cortex were rapidly removed and transferred into 1 ml of ice-cold MSE solution. Then, the supernatant was collected for protein concentration measurement by the bicinchoninic acid assay (BCA assay).

### 2.9 Hippocampal and cortical oxidative stress assay

The details of the measurement of oxidative stress levels have been previously described (Friedman, 2009). Briefly, dichloro-hydrofluoresceindiacetate (DCFH-DA) dye was used to determine hippocampal and cortical oxidative stress levels. Fluorescence was used to determine an excitation wavelength of  $\lambda485$  nm and emission wavelength of  $\lambda530$  nm by a microplate reader (Bio-tek Instrument, Inc. Winooski, Vermont USA). Hippocampal and cortical oxidative stress levels were calculated as a percentage change from the following equation: (oxidative stress with  $H_2O_2$  – oxidative stress)/oxidative stress x 100

### 2.10 Immunoblotting

The brain homogenates for immunoblotting were prepared as described in our previous study (Pratchayasakul et al., 2011b). Electrophoresis and immunoblotting of Bax and Bcl-2 were carried out with rabbit antibodies for the Bax (1:200, Santa Cruz Biotechnology, CA, USA) and Bcl-2 (1:1000, Abcam, MA, USA), respectively. All blots were incubated with a horseradish peroxidase conjugated anti-rabbit secondary antibody (1:2000, Cell Signaling Technology, MA, USA). The membranes were exposed to enhanced

chemiluminescence (ECL) Western blotting substrate, and densitometric analysis was carried out using ChemiDoc Touch Imaging system (Bio-Rad Laboratories, CA, USA).

### 2.11 Morris water maze test (MWM)

The assessment of hippocampal-dependent memory was performed by using MWM, as described in previous studies (Vorhees and Williams, 2006). Before the MWM test, the open-field test (OFT) was used to screen locomotive activity by counting the distance and speed in the area of the open-field during the test (Arakawa, 2005; Pintana et al., 2013). After that, the rats were assessed by the MWM with two different tests, acquisition test (hidden platform) and probe trial test (removal of the platform from the water pool). After testing was completed, times taken to reach the platform, times spent in the target quadrant, and swim speeds were calculated using Smart 3.0 software (Planlab, Harvard Apparatus, Barcelona, Spain).

### 2.12 Novel object recognition test (NOR)

The assessment of hippocampal-independent memory was performed using the NOR, as modified from previous studies (Sanderson et al., 2011; Taglialatela et al., 2009). Briefly, the task procedure consisted of three phases; habituation, familiarization, and test phase. The first 2 days were the habituation phase, each animal was allowed to freely explore the openfield arena without any object for 10 minutes. On the third day, which was the familiarization phase, an animal was allowed to explore two same objects for 10 minutes. Time of exploration was calculated as percent exploration time. After delay time for 2 minutes, during test phase, an animal was allowed to explore two different objects (one object was from the familiarization phase and the other one was a novel object) for 10 minutes. Time spent during exploring the novel object was calculated and presented as a percentage of index preference by comparing to the familiar object. All data were analyzed using Smart 3.0 software (Planlab, Harvard Apparatus, Barcelona, Spain).

### 2.13 Statistical analysis

The data for each experiment was presented as mean  $\pm$  SEM. All statistical analysis was performed using the program SPSS (version 17; SPSS, Chicago, Ill., USA). For all comparisons, the significant differences between the means were calculated using a two-way analysis of variance (ANOVA; diet X surgery) followed by post-hoc the least significant difference (LSD) test. A two-way ANOVA with repeated measurements was used to compare the training trials of the MWM test. P-value < 0.05 was considered as significant.

### 3. Results

## 3.1 Effects of oophorectomy and HFD-induced obese-insulin resistance on metabolic function.

After 13 weeks of HFD consumption, the HFD-fed rats developed obesity, dyslipidemia and peripheral insulin resistance, as indicated by increased body weight and visceral fat weight, increased plasma cholesterol and LDL level, increased plasma insulin level, increased HOMA index and increased total area under the glucose curve (TAUCg) from the OGTT, respectively.

At week 21, oophorectomy was confirmed by determining uterine weight and serum estrogen level. The ovariectomized rats had decreased uterine weight and serum estrogen level when compared with those of sham-operated rats. Moreover, we identified metabolic dysfunction in ovariectomized-ND-fed rats (NDO), sham-HFD-fed rats (HFS) and ovariectomized-HFD-fed rats (HFO), as indicated by increased the body weight, visceral fat weight, cholesterol and LDL level, plasma insulin level, HOMA index and TAUCg when compared with sham-ND-fed rats (NDS). Interestingly, the most severe metabolic dysfunction, as represented by the highest level of obesity, dyslipidemia, insulin resistance and hyperglycemia, was observed in HFO rats (p<0.05; Table 1).

## 3.2 Effect of oophorectomy and HFD-induced obese-insulin resistance on hippocampal-dependent memory and hippocampal-independent memory.

Before testing for learning and memory, the locomotive activity of each rat was determined using the open-field test. We found that the locomotor activity of all rats was not significantly different, as indicated by no significant difference in speed and distance.

In this study, the hippocampal-dependent and hippocampal-independent learning and memory were determined using the Morris water maze test (MWM) and novel object recognition test (NOR), respectively. During the acquisition test of MWM, both time and distance to the platform of the NDO, HFS and HFO rats were significantly increased, when compared with that of NDS rats (Fig. 1A, B). During the probe test of MWM, both time and distance in the target quadrant of the NDO, HFS and HFO rats were significantly decreased, when compared with that of NDS rats (Fig. 1D, E). In addition, the swimming speed of each rat was recorded and there was no significantly difference in the swimming speed among all groups (Fig. 1C). These findings confirmed that the impairment of the cognitive function was due to spatial memory deficit, instead of differences in swimming speed due to the weight and fat content of the animals. In the NOR test, the percentage exploration time as well as index preference were not significantly different among four groups (Fig. 2A, B).

3.3 Effect of oophorectomy and HFD-induced obese-insulin resistance on hippocampal synaptic plasticity and hippocampal insulin receptor function.

Several studies have demonstrated that both hippocampal synaptic plasticity and hippocampal insulin receptor function are involved in the mechanisms involved in hippocampal-dependent learning and memory (Akhondzadeh, 1999; Pratchayasakul et al., 2015). Therefore, hippocampal-synaptic plasticity and hippocampal insulin receptor function were determined by long term potentiation (LTP) and insulin-induced long term depression (LTD), respectively. The electrical-induced LTP observed from hippocampal slices of the

NDO, HFS, HFO rats was significantly decreased, when compared with that of NDS rat (p<0.05; Fig. 3A, C). In addition, the levels of insulin-induced LTD observed from the hippocampal slices of the NDO, HFS and HFO rats were significantly reduced, when compared with that of NDS rats (p<0.05, Fig. 3B, D).

## 3.4 Effect of oophorectomy and HFD-induced obese-insulin resistance on hippocampal and cortical oxidative stress levels.

Several studies found that the underlying mechanisms of impaired learning and memory were influenced by increased oxidative stress level (Chen et al., 2012; Droge and Schipper, 2007). Therefore, both hippocampal and cortical oxidative stress levels were determined for investigation of the hippocampal-dependent process and hippocampal-independent process, respectively. Hippocampal oxidative stress levels of the NDO, HFS and HFO rats were significantly increased when compared with that of NDS rats (p<0.05, Fig. 4A). However, cortical oxidative stress levels were not significantly different between the four groups (Fig. 4B).

## 3.5 Effect of oophorectomy and HFD-induced obese-insulin resistance on hippocampal and cortical apoptosis.

Several studies found that the mechanisms underlying the impairment of learning and memory were influenced by apoptosis (Guo et al., 2014; Tehranian et al., 2008). Therefore, the levels of pro-apoptotic protein (Bax), anti-apoptotic protein (Bcl-2) and the Bax/Bcl-2 ratio in both the hippocampus and cortex were determined for investigating the hippocampal-dependent process and hippocampal-independent process, respectively. We found that Bax protein expression in both hippocampus and cortex was not significantly different between the four groups (Fig. 5A, D). Interestingly, Bcl-2 protein expression in the hippocampus of NDO, HFS and HFO rats were significantly decreased when compared with that of NDS rats (p<0.05, Fig. 5B). In addition, the Bax/Bcl-2 ratios in the hippocampus of NDO, HFS and

HFO rats were significantly increased when compared with that of NDS rats (p<0.05, Fig. 5C). However, Bcl-2 protein expression and Bax/Bcl-2 ratio in the cortex was not significantly different among four groups (Fig. 5E, F).

3.6 Effect of oophorectomy and HFD-induced obese-insulin resistance on hippocampal and cortical estrogen levels.

Previous studies found that estrogen could modulate cognitive function (Brinton, 2009; Daniel et al., 1997; Desmond et al., 2000). Therefore, hippocampal and cortical estrogen levels were determined. We found that estrogen levels in the hippocampus of NDO, HFS and HFO rats were significantly decreased when compared with that of NDS rats (p<0.05, Fig. 6A). However, estrogen levels in the cortex were not significantly different between the four groups (Fig. 6B).

### 4. Discussion

The major findings of the present study are as follows: 1) oophorectomy aggravated the severity of metabolic dysfunction in conditions of HFD-induced obese-insulin resistance; 2) oophorectomy alone, HFD-induced obese-insulin resistance alone and a combination of these conditions impaired solely hippocampal-dependent memory via increased hippocampal dysfunction; 3) oophorectomy did not aggravate these impairments under conditions of HFD-induced obese-insulin resistance.

To study the combined effects of oophorectomy and obesity, many previous studies used the model of oophorectomy followed by obesity. Those studies and our previous study showed that obesity aggravated peripheral insulin resistance in the oophorectomy, as indicated by increased plasma insulin, increased hyperglycemia, increased HOMA index and impaired glucose tolerance, when compared with HFD-fed rats alone or ovariectomized rats alone (Camporez et al., 2013; Feigh et al., 2013; Pratchayasakul et al., 2015; Shen et al.,

2014; Tominaga et al., 2011; Yonezawa et al., 2012). In the present study, we used the model of obesity followed by the oophorectomy and this condition is most likely to occur in menopausal women who suffer from obesity after menopause. We found that not only the highest level of impaired insulin sensitivity, but also the highest level of dyslipidemia was observed in obese-ovariectomized rats, when compared with HFD-fed rats alone or ovariectomized rats alone. These findings suggest that the condition of the obesity followed by oophorectomy could aggravate metabolic disturbance to a greater extent than the condition of oophorectomy followed by obesity, as indicated by the aggravation of both peripheral insulin resistance and dyslipidemia. Furthermore, we found that obese rats had decreased serum estradiol levels when compared with normal rats. This finding is consistent with both animal and clinical studies which showed that the decreased estradiol level was related to visceral fat accumulation in female (Zain and Norman, 2008; Zhang et al., 2017). This action could be related to the alteration of the hypothalamic-pituitary-ovarian (HPO) axis (Broughton and Moley, 2017).

This study was the first to investigate the comparative and cumulative effects of oophorectomy and obesity on hippocampal-dependent and hippocampal-independent memory in the same study. We found that both oophorectomy and obesity impaired hippocampal-dependent memory, but not hippocampal-independent memory. In addition, both oophorectomy and obesity exclusively caused brain pathophysiological changes in the hippocampal region, as indicated by increased synaptic dysfunction, insulin receptor dysfunction, oxidative stress levels and apoptosis. Our findings are consistent with recent reports in animals and humans showing that obesity and/or diet disrupt at least some forms of hippocampal-dependent but not hippocampal-independent learning and memory via impaired the regulation of food intake such as impaired appetite control and inhibited the hypothalamic-pituitary-adrenal stress response (Stevenson and Francis, 2017; Yeomans,

2017). Furthermore, we also found that both oophorectomy and obesity exclusively decreased estrogen level in the hippocampus. Previous studies found that estrogen is synthesized in the brain, especially in the hippocampus (Bian et al., 2014; Fester et al., 2011) and also that hippocampal estrogen plays an important role in cognitive function via moderation of synaptic function (Bian et al., 2014; Foy et al., 2008). In addition, previous studies found that estrogen could have an antioxidant effect, which could reduce brain oxidative stress and apoptosis levels (Moosmann and Behl, 1999; Razmara et al., 2007). Therefore, we speculated that both oophorectomy and obesity caused a decrease in hippocampal estrogen levels and increased hippocampal oxidative stress levels which led to increased hippocampal apoptosis, and as a consequence led to impaired hippocampal synaptic function and also impaired hippocampal insulin receptor function. All of these mechanisms caused the impairment of hippocampal-dependent memory in rats, as indicated by increased time to reach the platform and decreased time in the target quadrant in the MWM test. According to our finding, we speculated that the reduced estradiol level might be causing the observed brain and behavioral changes, therefore estradiol replacement may be rescue this impairment. Our previous study found that estradiol replacement decreased brain oxidative stress and improved the brain insulin sensitivity as indicated by increased insulin-dependent LTD, increased brain Akt phosphorylation and increased brain IR phosphorylation only in ovariectomized rats, but not in ovariectomized rats with obesity (Pratchayasakul et al., 2014). In addition, a previous study found that estradiol treatment significantly improves spatial memory in ovariectomized obese rats via decreased the neuronal cell death, brain oxidative stress level and brain acetylcholinesterase (AChE) activity (Verma and Sharma, 2015). All of these findings suggested that brain estradiol plays an important role on the regulation of brain and behavioral changes under this condition.

Interestingly, we found that oophorectomized rats had higher calorie intake than sham rats, which lead to impair metabolic function in oophorectomized rats. Therefore, all of the observed hippocampal deficits could also be related to metabolic changes. Future studies are needed to elucidate whether oophorectomized rats still have hippocampal deficits when they are pair-fed to match the calorie intake of the sham animals. Previous studies found that metabolic improvements such as exercise training could attenuate the hippocampal deficits and cognitive impairment in either HFD-induced obese-insulin resistant model or oophorectomized model (Habibi et al., 2017; Kaidah et al., 2016; Noble et al., 2014; Woo et al., 2013). Furthermore, other metabolic improvements such as calorie restriction could improve hippocampal function and cognitive function in obese models (Jeon et al., 2016; Kim et al., 2016). However, the effects of calorie restriction on hippocampal function in oophorectomized rats have never been investigated. Therefore, further studies are needed to determine whether exercise or calorie restriction can improve the hippocampal-dependent memory of oophorectomized animals.

However, neither oophorectomy nor obesity impaired hippocampal-independent memory and the brain pathophysiological changes in the cortex region. We speculated that neither oophorectomy nor obesity would decrease cortical estrogen level and cortical oxidative stress level. Therefore, these situations did not cause cortical apoptosis, which therefore did not lead to impaired hippocampal-independent memory, as indicated by no change of percentage exploration time as well as index preference in the NOR test. However, a previous study found that only long-term oophorectomy (12 wks), but not short-term oophorectomy in rats (6 wks), caused the impairment of hippocampal-independent memory, as indicated by a decreased time with novel object in the NOR test (Bastos et al., 2015). Therefore, this short-term oophorectomy (7 wks) in our study could only impair hippocampal-dependent memory, and the impairment of hippocampal-independent memory

may have occurred later. Furthermore, we found that oophorectomy did not aggravate brain pathophysiological changes or cognitive decline in an obese condition. In contrast, our recent studies showed that obesity accelerated and aggravated the increase in brain oxidative stress, hippocampal synaptic dysfunction, brain mitochondrial dysfunction, brain insulin resistance and cognitive impairment in ovariectomized rats (Pratchayasakul et al., 2014; Pratchayasakul et al., 2015). A possible explanation could be the shorter duration of the oophorectomy in this study (7 wks), compared to our previous study (12 wks). As a result, the longer duration of oophorectomy may aggravate aforementioned brain pathophysiological changes and cognitive decline in this obese condition. Further studies are needed to give greater evidence to support this possible explanation.

In summary, our findings demonstrate that oophorectomy aggravated the severity of peripheral insulin resistance and dyslipidemia in the obese condition. In addition, both oophorectomy and obesity impaired solely hippocampal-dependent memory, hippocampal synaptic function, hippocampal insulin receptor function, hippocampal oxidative stress level, hippocampal apoptosis and caused decreased hippocampal estrogen levels. However, oophorectomy did not aggravate these impairments in an obese condition.

### Limitation

Although we detected swim speed in this study which confirmed that the impairment of the cognitive function was likely not due to differences in swimming speed caused by the body composition differences between the two groups, we cannot completely rule out the possibility that differences in performance on the task might have been due to physical ability of the animals. The novel object in context (NOIC) task, which is a hippocampal dependent task that tests episodic and contextual memory, is more closely related to the NOR task is less confounded by exercise ability, therefore future studies comparing performance in the NOIC

task to the NOR task would be highly desirable. Furthermore, since the animals were decapitated and the brains removed immediately to enable the hippocampal synaptic plasticity without perfusion to wash out blood, it is possible that serum estradiol could have contributed in part for hippocampal estradiol levels. Future studies using PCR to measure hippocampal production of estradiol are needed to confirm this hypothesis in ovariectomized-obese rats.

### Potential Clinical Value

In human, learning and memory is divided to the explicit or declarative memory and the implicit or non-declarative memory, which are hippocampal-dependent and hippocampal-independent learning and memory, respectively (Bailey et al., 1996; Dew and Cabeza, 2011). Several studies found that obesity impaired both implicit and explicit memory as indicated by impaired working memory, as well as the associative learning and episodic memory (Cheke et al., 2017; Coppin et al., 2014; Zhang et al., 2014). In addition, loss of ovarian hormones by menopause or oophorectomy impaired mainly explicit memory as indicated by impaired semantic and verbal episodic memory (Kocoska-Maras et al., 2013; Ryan et al., 2012). However, the combined effect of obesity and loss of ovarian hormone on cognitive function has never been investigated. The present study demonstrated that both oophorectomy and obesity impaired solely the hippocampal-dependent memory via hippocampal dysfunction. These findings provide information regarding the role of obesity and oophorectomy on neurodegenerative diseases and offer important insights for future research on interventions that aim to improve quality of life in women who had obesity with or without loss of ovarian hormone.

### **Funding**

This work was supported by the Thailand Research Fund grants: MRG5980198 (WP), TRG5980020 (SP), MRG6080226 (JS), and Senior Research Scholar (RTA6080003 to SCC); Faculty of Medicine Chiang Mai University Endowment Fund (WP), the NSTDA Research Chair grant from the National Science and Technology Development Agency Thailand (NC), and the Chiang Mai University Center of Excellence Award (NC).

### Acknowledgement

The authors would like to thank Ms. Dalila Monica Moisescu for her editorial assistance.

### **Conflict of interest**

None

### References

- Akhondzadeh, S., 1999. Hippocampal synaptic plasticity and cognition. J Clin Pharm Ther. 24, 241-8.
- Albanese, E., Launer, L.J., Egger, M., Prince, M.J., Giannakopoulos, P., Wolters, F.J., Egan, K., 2017. Body mass index in midlife and dementia: Systematic review and meta-regression analysis of 589,649 men and women followed in longitudinal studies.

  Alzheimers Dement (Amst). 8, 165-178.
- Antunes, M., Biala, G., 2012. The novel object recognition memory: neurobiology, test procedure, and its modifications. Cogn Process. 13, 93-110.
- Arakawa, H., 2005. Age dependent effects of space limitation and social tension on open-field behavior in male rats. Physiol Behav. 84, 429-36.
- Bailey, C.H., Bartsch, D., Kandel, E.R., 1996. Toward a molecular definition of long-term memory storage. Proc Natl Acad Sci U S A. 93, 13445-52.
- Bastos, C.P., Pereira, L.M., Ferreira-Vieira, T.H., Drumond, L.E., Massensini, A.R., Moraes, M.F., Pereira, G.S., 2015. Object recognition memory deficit and depressive-like behavior caused by chronic ovariectomy can be transitorially recovered by the acute activation of hippocampal estrogen receptors. Psychoneuroendocrinology. 57, 14-25.
- Beilharz, J.E., Maniam, J., Morris, M.J., 2014. Short exposure to a diet rich in both fat and sugar or sugar alone impairs place, but not object recognition memory in rats. Brain Behav Immun. 37, 134-41.
- Bian, C., Zhu, H., Zhao, Y., Cai, W., Zhang, J., 2014. Intriguing roles of hippocampus-synthesized 17beta-estradiol in the modulation of hippocampal synaptic plasticity. J Mol Neurosci. 54, 271-81.
- Brinton, R.D., 2009. Estrogen-induced plasticity from cells to circuits: predictions for cognitive function. Trends Pharmacol Sci. 30, 212-22.

- Broughton, D.E., Moley, K.H., 2017. Obesity and female infertility: potential mediators of obesity's impact. Fertil Steril. 107, 840-847.
- Camporez, J.P., Jornayvaz, F.R., Lee, H.Y., Kanda, S., Guigni, B.A., Kahn, M., Samuel, V.T., Carvalho, C.R., Petersen, K.F., Jurczak, M.J., Shulman, G.I., 2013. Cellular mechanism by which estradiol protects female ovariectomized mice from high-fat diet-induced hepatic and muscle insulin resistance. Endocrinology. 154, 1021-8.
- Candan, N., Tuzmen, N., 2008. Very rapid quantification of malondialdehyde (MDA) in rat brain exposed to lead, aluminium and phenolic antioxidants by high-performance liquid chromatography-fluorescence detection. Neurotoxicology. 29, 708-13.
- Carey, A.N., Gomes, S.M., Shukitt-Hale, B., 2014. Blueberry supplementation improves memory in middle-aged mice fed a high-fat diet. J Agric Food Chem. 62, 3972-8.
- Chattipakorn, S.C., McMahon, L.L., 2002. Pharmacological characterization of glycine-gated chloride currents recorded in rat hippocampal slices. J Neurophysiol. 87, 1515-25.
- Cheke, L.G., Bonnici, H.M., Clayton, N.S., Simons, J.S., 2017. Obesity and insulin resistance are associated with reduced activity in core memory regions of the brain.

  Neuropsychologia. 96, 137-149.
- Chen, X., Guo, C., Kong, J., 2012. Oxidative stress in neurodegenerative diseases. Neural Regen Res. 7, 376-85.
- Chunchai, T., Thunapong, W., Yasom, S., Wanchai, K., Eaimworawuthikul, S., Metzler, G., Lungkaphin, A., Pongchaidecha, A., Sirilun, S., Chaiyasut, C., Pratchayasakul, W., Thiennimitr, P., Chattipakorn, N., Chattipakorn, S.C., 2018. Decreased microglial activation through gut-brain axis by prebiotics, probiotics, or synbiotics effectively restored cognitive function in obese-insulin resistant rats. J Neuroinflammation. 15, 11.

- Coppin, G., Nolan-Poupart, S., Jones-Gotman, M., Small, D.M., 2014. Working memory and reward association learning impairments in obesity. Neuropsychologia. 65, 146-55.
- Craft, S., Watson, G.S., 2004. Insulin and neurodegenerative disease: shared and specific mechanisms. Lancet Neurol. 3, 169-78.
- Dalal, P.K., Agarwal, M., 2015. Postmenopausal syndrome. Indian J Psychiatry. 57, S222-32.
- Daniel, J.M., Fader, A.J., Spencer, A.L., Dohanich, G.P., 1997. Estrogen enhances performance of female rats during acquisition of a radial arm maze. Horm Behav. 32, 217-25.
- Desmond, N.L., Zhang, D.X., Levy, W.B., 2000. Estradiol enhances the induction of homosynaptic long-term depression in the CA1 region of the adult, ovariectomized rat. Neurobiol Learn Mem. 73, 180-7.
- Dew, I.T., Cabeza, R., 2011. The porous boundaries between explicit and implicit memory: behavioral and neural evidence. Ann N Y Acad Sci. 1224, 174-90.
- Droge, W., Schipper, H.M., 2007. Oxidative stress and aberrant signaling in aging and cognitive decline. Aging Cell. 6, 361-70.
- Eichenbaum, H., 2017. On the Integration of Space, Time, and Memory. Neuron. 95, 1007-1018.
- FangFang, Li, H., Qin, T., Li, M., Ma, S., 2017. Thymol improves high-fat diet-induced cognitive deficits in mice via ameliorating brain insulin resistance and upregulating NRF2/HO-1 pathway. Metab Brain Dis. 32, 385-393.
- Feigh, M., Andreassen, K.V., Hjuler, S.T., Nielsen, R.H., Christiansen, C., Henriksen, K., Karsdal, M.A., 2013. Oral salmon calcitonin protects against impaired fasting glycemia, glucose intolerance, and obesity induced by high-fat diet and ovariectomy in rats. Menopause. 20, 785-94.

- Fester, L., Prange-Kiel, J., Jarry, H., Rune, G.M., 2011. Estrogen synthesis in the hippocampus. Cell Tissue Res. 345, 285-94.
- Foy, M.R., Baudry, M., Diaz Brinton, R., Thompson, R.F., 2008. Estrogen and hippocampal plasticity in rodent models. J Alzheimers Dis. 15, 589-603.
- Friedman, J.M., 2009. Obesity: Causes and control of excess body fat. Nature. 459, 340-342.
- Gervais, N.J., Jacob, S., Brake, W.G., Mumby, D.G., 2013. Systemic and intra-rhinal-cortical 17-beta estradiol administration modulate object-recognition memory in ovariectomized female rats. Horm Behav. 64, 642-52.
- Gervais, N.J., Hamel, L.M., Brake, W.G., Mumby, D.G., 2016. Intra-perirhinal cortex administration of estradiol, but not an ERbeta agonist, modulates object-recognition
- Greenwood, C.E., Winocur, G., 2005. High-fat diets, insulin resistance and declining cognitive function. Neurobiol Aging. 26, 42-5.
- Guo, Y.J., Wang, S.H., Yuan, Y., Li, F.F., Ye, K.P., Huang, Y., Xia, W.Q., Zhou, Y., 2014.

  Vulnerability for apoptosis in the hippocampal dentate gyrus of STZ-induced diabetic rats with cognitive impairment. J Endocrinol Invest. 37, 87-96.
- Habibi, P., Babri, S., Ahmadiasl, N., Yousefi, H., 2017. Effects of genistein and swimming exercise on spatial memory and expression of microRNA 132, BDNF, and IGF-1 genes in the hippocampus of ovariectomized rats. Iran J Basic Med Sci. 20, 856-862.
- Hajiluian, G., Abbasalizad Farhangi, M., Nameni, G., Shahabi, P., Megari-Abbasi, M., 2017.

  Oxidative stress-induced cognitive impairment in obesity can be reversed by vitamin

  D administration in rats. Nutr Neurosci. 1-9.
- Jeon, B.T., Heo, R.W., Jeong, E.A., Yi, C.O., Lee, J.Y., Kim, K.E., Kim, H., Roh, G.S., 2016. Effects of caloric restriction on O-GlcNAcylation, Ca(2+) signaling, and learning impairment in the hippocampus of ob/ob mice. Neurobiol Aging. 44, 127-137.

- Kaidah, S., Soejono, S.K., Partadiredja, G., 2016. Exercise improves hippocampal estrogen and spatial memory of ovariectomized rats. Bratisl Lek Listy. 117, 94-9.
- Keller, C., Larkey, L., Distefano, J.K., Boehm-Smith, E., Records, K., Robillard, A., Veres, S., Al-Zadjali, M., O'Brian, A.M., 2010. Perimenopausal obesity. J Womens Health (Larchmt). 19, 987-96.
- Kim, H., Kang, H., Heo, R.W., Jeon, B.T., Yi, C.O., Shin, H.J., Kim, J., Jeong, S.Y., Kwak, W., Kim, W.H., Kang, S.S., Roh, G.S., 2016. Caloric restriction improves diabetes-induced cognitive deficits by attenuating neurogranin-associated calcium signaling in high-fat diet-fed mice. J Cereb Blood Flow Metab. 36, 1098-110.
- Kocoska-Maras, L., Radestad, A.F., Carlstrom, K., Backstrom, T., von Schoultz, B., Hirschberg, A.L., 2013. Cognitive function in association with sex hormones in postmenopausal women. Gynecol Endocrinol. 29, 59-62.
- Mack, M.L., Love, B.C., Preston, A.R., 2017. Building concepts one episode at a time: The hippocampus and concept formation. Neurosci Lett.
- Matthews, D.R., Hosker, J.P., Rudenski, A.S., Naylor, B.A., Treacher, D.F., Turner, R.C., 1985. Homeostasis model assessment: insulin resistance and beta-cell function from fasting plasma glucose and insulin concentrations in man. Diabetologia. 28, 412-9.
- Mielke, J.G., Taghibiglou, C., Liu, L., Zhang, Y., Jia, Z., Adeli, K., Wang, Y.T., 2005. A biochemical and functional characterization of diet-induced brain insulin resistance. J Neurochem. 93, 1568-78.
- Moosmann, B., Behl, C., 1999. The antioxidant neuroprotective effects of estrogens and phenolic compounds are independent from their estrogenic properties. Proc Natl Acad Sci U S A. 96, 8867-72.

- Noble, E.E., Mavanji, V., Little, M.R., Billington, C.J., Kotz, C.M., Wang, C., 2014. Exercise reduces diet-induced cognitive decline and increases hippocampal brain-derived neurotrophic factor in CA3 neurons. Neurobiol Learn Mem. 114, 40-50.
- Pintana, H., Apaijai, N., Pratchayasakul, W., Chattipakorn, N., Chattipakorn, S.C., 2012. Effects of metformin on learning and memory behaviors and brain mitochondrial functions in high fat diet induced insulin resistant rats. Life Sci. 91, 409-14.
- Pintana, H., Apaijai, N., Chattipakorn, N., Chattipakorn, S.C., 2013. DPP-4 inhibitors improve cognition and brain mitochondrial function of insulin resistant rats. J Endocrinol. 218, 1-11.
- Pintana, H., Pongkan, W., Pratchayasakul, W., Chattipakorn, N., Chattipakorn, S.C., 2015.

  Dipeptidyl peptidase 4 inhibitor improves brain insulin sensitivity, but fails to prevent cognitive impairment in orchiectomy obese rats. J Endocrinol. 226, M1-M11.
- Pipatpiboon, N., Pratchayasakul, W., Chattipakorn, N., Chattipakorn, S.C., 2012.

  PPARgamma agonist improves neuronal insulin receptor function in hippocampus and brain mitochondria function in rats with insulin resistance induced by long term high-fat diets. Endocrinology. 153, 329-38.
- Pipatpiboon, N., Pintana, H., Pratchayasakul, W., Chattipakorn, N., Chattipakorn, S.C., 2013.

  DPP4-inhibitor improves neuronal insulin receptor function, brain mitochondrial function and cognitive function in rats with insulin resistance induced by high-fat diet consumption. Eur J Neurosci. 37, 839-49.
- Pratchayasakul, W., Chattipakorn, N., Chattipakorn, S.C., 2011a. Effects of estrogen in preventing neuronal insulin resistance in hippocampus of obese rats are different between genders. Life Sci. 89, 702-7.

- Pratchayasakul, W., Kerdphoo, S., Petsophonsakul, P., Pongchaidecha, A., Chattipakorn, N., Chattipakorn, S.C., 2011b. Effects of high-fat diet on insulin receptor function in rat hippocampus and the level of neuronal corticosterone. Life Sci. 88, 619-27.
- Pratchayasakul, W., Chattipakorn, N., Chattipakorn, S.C., 2014. Estrogen restores brain insulin sensitivity in ovariectomized non-obese rats, but not in ovariectomized obese rats. Metabolism. 63, 851-9.
- Pratchayasakul, W., Sa-Nguanmoo, P., Sivasinprasasn, S., Pintana, H., Tawinvisan, R., Sripetchwandee, J., Kumfu, S., Chattipakorn, N., Chattipakorn, S.C., 2015. Obesity accelerates cognitive decline by aggravating mitochondrial dysfunction, insulin resistance and synaptic dysfunction under estrogen-deprived conditions. Horm Behav. 72, 68-77.
- Razmara, A., Duckles, S.P., Krause, D.N., Procaccio, V., 2007. Estrogen suppresses brain mitochondrial oxidative stress in female and male rats. Brain Res. 1176, 71-81.
- Ryan, J., Stanczyk, F.Z., Dennerstein, L., Mack, W.J., Clark, M.S., Szoeke, C., Kildea, D., Henderson, V.W., 2012. Hormone levels and cognitive function in postmenopausal midlife women. Neurobiol Aging. 33, 1138-47.
- Sanderson, D.J., Hindley, E., Smeaton, E., Denny, N., Taylor, A., Barkus, C., Sprengel, R., Seeburg, P.H., Bannerman, D.M., 2011. Deletion of the GluA1 AMPA receptor subunit impairs recency-dependent object recognition memory. Learn Mem. 18, 181-90.
- Sa-Nguanmoo, P., Tanajak, P., Kerdphoo, S., Jaiwongkam, T., Pratchayasakul, W., Chattipakorn, N., Chattipakorn, S.C., 2017. SGLT2-inhibitor and DPP-4 inhibitor improve brain function via attenuating mitochondrial dysfunction, insulin resistance, inflammation, and apoptosis in HFD-induced obese rats. Toxicol Appl Pharmacol. 333, 43-50.

- Sah, S.K., Lee, C., Jang, J.H., Park, G.H., 2017. Effect of high-fat diet on cognitive impairment in triple-transgenic mice model of Alzheimer's disease. Biochem Biophys Res Commun. 493, 731-736.
- Shen, M., Kumar, S.P., Shi, H., 2014. Estradiol regulates insulin signaling and inflammation in adipose tissue. Horm Mol Biol Clin Investig. 17, 99-107.
- Stevenson, R.J., Francis, H.M., 2017. The hippocampus and the regulation of human food intake. Psychol Bull. 143, 1011-1032.
- Stranahan, A.M., Norman, E.D., Lee, K., Cutler, R.G., Telljohann, R.S., Egan, J.M., Mattson, M.P., 2008. Diet-induced insulin resistance impairs hippocampal synaptic plasticity and cognition in middle-aged rats. Hippocampus. 18, 1085-8.
- Taglialatela, G., Hogan, D., Zhang, W.R., Dineley, K.T., 2009. Intermediate- and long-term recognition memory deficits in Tg2576 mice are reversed with acute calcineurin inhibition. Behav Brain Res. 200, 95-9.
- Tehranian, R., Rose, M.E., Vagni, V., Pickrell, A.M., Griffith, R.P., Liu, H., Clark, R.S., Dixon, C.E., Kochanek, P.M., Graham, S.H., 2008. Disruption of Bax protein prevents neuronal cell death but produces cognitive impairment in mice following traumatic brain injury. J Neurotrauma. 25, 755-67.
- Tominaga, K., Yamauchi, A., Egawa, T., Tanaka, R., Kawahara, S., Shuto, H., Kataoka, Y., 2011. Vascular dysfunction and impaired insulin signaling in high-fat diet fed ovariectomized mice. Microvasc Res. 82, 171-6.
- Tran, D.M.D., Westbrook, R.F., 2017. A high-fat high-sugar diet-induced impairment in place-recognition memory is reversible and training-dependent. Appetite. 110, 61-71.
- Verma, A., Sharma, S., 2015. Beneficial Effect of Protein Tyrosine Phosphatase Inhibitor and Phytoestrogen in Dyslipidemia-Induced Vascular Dementia in Ovariectomized Rats. J Stroke Cerebrovasc Dis. 24, 2434-46.

- Vogel, H., Kraemer, M., Rabasa, C., Askevik, K., Adan, R.A.H., Dickson, S.L., 2017.

  Genetic predisposition to obesity affects behavioural traits including food reward and anxiety-like behaviour in rats. Behav Brain Res. 328, 95-104.
- Vorhees, C.V., Williams, M.T., 2006. Morris water maze: procedures for assessing spatial and related forms of learning and memory. Nat Protoc. 1, 848-58.
- Winocur, G., Greenwood, C.E., 2005. Studies of the effects of high fat diets on cognitive function in a rat model. Neurobiol Aging. 26 Suppl 1, 46-9.
- Woo, J., Shin, K.O., Park, S.Y., Jang, K.S., Kang, S., 2013. Effects of exercise and diet change on cognition function and synaptic plasticity in high fat diet induced obese rats. Lipids Health Dis. 12, 144.
- Yeomans, M.R., 2017. Adverse effects of consuming high fat-sugar diets on cognition: implications for understanding obesity. Proc Nutr Soc. 76, 455-465.
- Yonezawa, R., Wada, T., Matsumoto, N., Morita, M., Sawakawa, K., Ishii, Y., Sasahara, M., Tsuneki, H., Saito, S., Sasaoka, T., 2012. Central versus peripheral impact of estradiol on the impaired glucose metabolism in ovariectomized mice on a high-fat diet. Am J Physiol Endocrinol Metab. 303, E445-56.
- Zain, M.M., Norman, R.J., 2008. Impact of obesity on female fertility and fertility treatment.

  Womens Health (Lond). 4, 183-94.
- Zhang, Y., Zhang, S.W., Khandekar, N., Tong, S.F., Yang, H.Q., Wang, W.R., Huang, X.F., Song, Z.Y., Lin, S., 2017. Reduced serum levels of oestradiol and brain derived neurotrophic factor in both diabetic women and HFD-feeding female mice.
  Endocrine. 56, 65-72.
- Zhang, Z., Manson, K.F., Schiller, D., Levy, I., 2014. Impaired associative learning with food rewards in obese women. Curr Biol. 24, 1731-6.

Zhao, L., Yao, J., Mao, Z., Chen, S., Wang, Y., Brinton, R.D., 2011. 17beta-Estradiol regulates insulin-degrading enzyme expression via an ERbeta/PI3-K pathway in hippocampus: relevance to Alzheimer's prevention. Neurobiol Aging. 32, 1949-63.



#### **Figure Legends**

- **Fig. 1.** Time to reach platform in acquisition test (A); distance to platform in acquisition test (B); speed to platform in acquisition test (C); time in target quadrant in probe test (D) and distance in target quadrant in probe test (E) in the NDS, NDO, HFS and HFO rats. <sup>a</sup>, p<0.05 compared with NDS; n=8/group; NDS = sham-ND-fed rats; NDO = ovariectomized-ND-fed rats; HFS = sham-HFD-fed rats; HFO = ovariectomized-HFD-fed rats
- **Fig. 2.** Percentage exploration time (A), and index preference (B) from the NDS, NDO, HFS and HFO rats; n=8/group; NDS = sham-ND-fed rats; NDO = ovariectomized-ND-fed rats; HFS = sham-HFD-fed rats; HFO = ovariectomized-HFD-fed rats; Ob1 = object 1; Ob2 = object 2
- **Fig. 3.** The degree of electrical-mediated LTP (A), the degree of insulin-mediated LTD (B), the percentage increment of fEPSP slope (C) and the percentage decrement of fEPSP slope (D) observed from hippocampal slices of NDS, NDO, HFS and HFO rats; <sup>a</sup>, p<0.05 compared with NDS; (n=7-8 independent slices, n=8 animals/group); NDS = sham-ND-fed rats; NDO = ovariectomized-ND-fed rats; HFS = sham-HFD-fed rats; HFO = ovariectomized-HFD-fed rats; Hfs = high frequency stimulation; fEPSPs = field excitatory post synaptic potential
- **Fig. 4.** Hippocampal oxidative stress level (**A**) and cortical oxidative stress level from the NDS, NDO, HFS and HFO rats (**B**); <sup>a</sup>, p<0.05 compared with NDS; n=8/group; NDS = sham-ND-fed rats; NDO = ovariectomized-ND-fed rats; HFS = sham-HFD-fed rats; HFO = ovariectomized-HFD-fed rats

**Fig. 5.** Representative blots of hippocampal Bax protein expression (A), representative blots of hippocampal Bcl-2 protein expression (B), hippocampal Bax/Bcl-2 ratio (C), representative blots of cortical Bax protein expression (D), representative blots of cortical Bcl-2 protein expression (E) and cortical Bax/Bcl-2 ratio (F) from the NDS, NDO, HFS and HFO rats; a, p<0.05 compared with NDS; n=8/group; NDS = sham-ND-fed rats; NDO = ovariectomized-ND-fed rats; HFS = sham-HFD-fed rats; HFO = ovariectomized-HFD-fed rats

**Fig. 6.** Hippocampal estradiol level (A) and cortical estradiol level (B) from the NDS, NDO, HFS and HFO rats; <sup>a</sup>, p<0.05 from NDS; n=8/group; NDS = sham-ND-fed rats; NDO = ovariectomized-ND-fed rats; HFS = sham-HFD-fed rats; HFO = ovariectomized-HFD-fed rats

**TABLE 1:** Effect of estrogen deprivation on metabolic change in obese-insulin resistance rats.

|   | Groups               |                                  |                                    |                                       |
|---|----------------------|----------------------------------|------------------------------------|---------------------------------------|
| Parameters  | NDS                  | NDO                              | HFS                                | HFO                                   |
| Body weight (g)                                       | 279.55±3.90          | 304.21±4.92 <sup>a</sup>         | 325.56±5.33 <sup>a,b</sup>         | 391.19±10.79 <sup>a,b,c</sup>         |
| Visceral fat (g)                                      | 6.82 <u>+</u> 1.42   | 12.29 <u>+</u> 1.53 <sup>a</sup> | 25.98 <u>+</u> 1.30 <sup>a,b</sup> | 33.71 <u>+</u> 2.25 <sup>a,b,c</sup>  |
| Uterus weight (g)                                     | 0.45 <u>+</u> 0.06   | 0.15 <u>+</u> 0.04 <sup>a</sup>  | 0.38 <u>+</u> 0.03                 | 0.13 <u>+</u> 0.02 <sup>a,c</sup>     |
| Plasma glucose (mg/dl)                                | 133.48 <u>+</u> 2.66 | 136.59 <u>+</u> 4.75             | 141.87 <u>+</u> 4.12               | 159.58 <u>+</u> 6.84 <sup>a,b,c</sup> |
| Plasma insulin (ng/ml)                                | 0.99 <u>+</u> 0.12   | 2.38 <u>+</u> 0.31 <sup>a</sup>  | 2.44 <u>+</u> 0.38 <sup>a</sup>    | 3.46 <u>+</u> 0.32 <sup>a,b,c</sup>   |
| HOMA index  | 8.73 <u>+</u> 1.02   | 19.13 <u>+</u> 1.80 <sup>a</sup> | 17.47 <u>+</u> 3.69 <sup>a</sup>   | 29.49 <u>+</u> 3.77 <sup>a,b,c</sup>  |
| Plasma glucose AUC (AUCg)(mg/dl×min×10 <sup>4</sup> ) | 1.85±0.08            | 2.16±0.07 <sup>a</sup>           | 2.26±0.08 <sup>a,b</sup>           | 2.53±0.10 <sup>a,b,c</sup>            |
| Cholesterol (mg/dl)                                   | 77.33 <u>+</u> 4.64  | 95.59 <u>+</u> 7.23              | 106.53 <u>+</u> 6.80 <sup>a</sup>  | 117.57 <u>+</u> 10.50 <sup>a</sup>    |
| HDL (mg/dl)   | 7.72 <u>+</u> 0.21   | 8.34 <u>+</u> 0.25               | 8.12 <u>+</u> 0.39                 | 8.56 <u>+</u> 0.31                    |
| LDL (mg/dl)   | 67.80±4.82           | 76.36± 3.62                      | 84.63± 8.31 <sup>a</sup>           | $85.74\pm5.82^{a}$                    |
| Triglyceride (mg/dl)                                  | 70.99±5.31           | 72.41±4.64                       | 72.84±6.62                         | 91.07±3.92 <sup>a,b,c</sup>           |
| Calorie intake (Kcal/day)                             | 53.98± 2.31          | $60.22 \pm 0.65^{a}$             | $60.35 \pm 1.53^{a}$               | $66.71 \pm 1.24^{a,b,c}$              |
| Estradiol level (pg/ml)                               | 112.37±17.19         | 31.55±3.92 <sup>a</sup>          | 48.49±2.98 <sup>a,b</sup>          | 23.97±2.05 <sup>a,c</sup>             |
| Serum MDA (μM)  | 3.51±0.25            | 4.26±0.20 <sup>a</sup>           | 4.58±0.22 <sup>a</sup>             | 5.22±0.24 <sup>a,b,c</sup>            |

 $<sup>^{\</sup>rm a},$  p <0.05 compared with NDS,  $^{\rm b},$  p <0.05 compared with NDO,  $^{\rm c},$  p <0.05 compared with HFS;

n = 8/group (except calorie intake (n=4/group)); NDS = sham-ND-fed rats; NDO = ovariectomized-ND-fed rats; HFS = sham-HFD-fed rats; HFO = ovariectomized-HFD-fed rats; HOMA= homeostasis model assessment; HDL=

high-density lipoprotein; LDL= low-density lipoprotein, MDA= malondialdehyde



#### **Highlights**

- Oophorectomy impaired only hippocampal-dependent memory via hippocampal dysfunction
- Obesity impaired solely hippocampal-dependent memory via hippocampal dysfunction.
- Oophorectomy did not aggravate these impairments in an obese condition.

